REGIONAL MATURITY AND SOURCE-ROCK POTENTIAL OF PALAEOZOIC AND MESOZOIC STRATA, MELVILLE ISLAND, ARCTIC CANADA

by

Thomas Gentzis

B. Sc. 1981 - University of Calgary - Canada

M. Sc. 1985 - University of Alberta - Canada

A Thesis

Submitted to

The Department of Geology, The University

of Newcastle-upon-Tyne, Great Britain,

For Partial Fulfillment of the Requirements for the Degree

of Doctor of Philosophy

April, 1991

TABLE OF CONTENTS

CHAPTER IV

CHAPTER V

CHAPTER VI

CHAPTER VII

CHAPTER VIII

CHAPTER IX

LIST OF FIGURES

LIST OF TABLES

ABSTRACT

The thermal maturity and source-rock potential of the Palaeozoic and Mesozoic sediments in Melville Island, Arctic Canada were studied using organic petrology and Rock-Eval pyrolysis. A total of 2,000 polished whole-rock samples were examined and their phytoclast reflectances (% Ro random) measured. In addition, selected samples were analyzed qualitatively and quantitatively using ultraviolet excitation.

Hydrogen-rich organic matter was dominated by alginite (Botryococcus and Tasmanites), dinoflagellate cysts and amorphous fluorescing matrix. Sporinite, cutinite, resinite and liptodetrinite formed the lesser hydrogen-rich organic matter. Vitrinite reflectance in Cretaceous sediments ranged from Ro = 0.36 to 0.65%; in Jurassic sediments it ranged from Ro = 0.40 to 1.0% and in Triassic sediments from Ro = 0.45 to 1.30%. Vitrinite showed an overall increase in %Ro with increasing depth of burial but variations do occur, possibly due to the effects of mineral matrix (lithology) and liptinite content. It was observed that when total liptinite percentage was high (20-30%), reflectance was lowered by a magnitude of 0.1 to 0.15%. In addition, the lowering of the reflectance, which was genuine and not experimental, was due to: 1) the effect of bitumen impregnation (staining); and 2) differences in the type of organic matter (hydrogen-rich vitrinite of marine origin).

A large number of shale samples exceeded the worldwide average total organic carbon (TOC) content of 1.05 wt% with the Jurassic-Cretaceous shales and siltstones having higher values than those of Triassic age. The Triassic Schei Point Group shales and siltstones contained organic matter of marine origin, whereas the predominantly plant-derived organic matter present in the Jameson Bay, Ringnes and Deer Bay Formations had a higher TOC.

Among the Schei Point Group sediments, the Cape Richards and Eden Bay Members of the Hoyle Bay Formation were richer in TOC (>2.0 wt%) than the Murray Harbour Formation (Cape Caledonia Member), which may reflect differences in the level of maturity or in the depositional environment (more anoxic conditions for the former). Higher average TOC contents (> 3.0 wt%) were reported in the Cape Richards Member in drillhole Hecla C-32, as well as in the Eden Bay Member in drillholes Hecla C-32, Roche Point J-43 and North Sabine H-49, all located in Sabine Peninsula. The Schei Point Group sediments contained mainly liptinitic organic matter of marine origin, were occasionally bitumen stained and have high potential for the generation of liquid hydrocarbons.

Organic matter in the Palaeozoic strata of the Franklinian miogeosyncline was represented mainly by bitumen in the Silurian and Devonian. Different bitumen types were identified depending on their morphology, reflectance range and association with the enclosing mineral matrix. Thermal maturity of the Palaeozoic strata, based on vitrinite reflectance calculated from bitumen reflectance was high, an indication that the strata were in the overmature stage of hydrocarbon generation and that only dry gas should be expected. There is petrological evidence that hydrocarbons were generated and migrated through the sediments.

Regional variations in the level of thermal maturity of Mesozoic sediments in the Sverdrup Basin are a function of burial depth. The Mesozoic formations thicken towards the basin centre (N-NE direction), reflecting the general pattern of increasing thermal maturity north of the Sabine Peninsula. In addition, periods of high heat flow most likely existed during rifting episodes from Carboniferous to Early Tertiary.

The contour pattern of the regional variation of maturity at the base of

numerous Triassic formations is similar to that of the structural contours of the Sverdrup Basin, indicating that present-day maturation levels are largely controlled by basin subsidence.

ACKNOWLEDGMENTS

I would like to express my sincere acknowledgments to Professor Duncan Murchison, Thesis supervisor, for providing guidance throughout the course of the study, as well as to all the staff of the Organic Geochemistry Unit, University of Newcastle-upon-Tyne for their support.

I am heavily indebted to Dr. Fariborz Goodarzi of the Institute of Sedimentary and Petroleum Geology, Geological Survey of Canada, Thesis co-supervisor, for initiating the study, for continuous financial support and great leadership during the last three years. Fari, you have been a great teacher and mentor for the last eight years and without your help and guidance this thesis would not have been possible.

I would also like to thank Dr. Walter Nassichuk, Director of the Institute of Sedimentary and Petroleum Geology and his staff for providing an excellent environment in which I was able to achieve my goals. I thank Dr. Lloyd Snowdon, Dr. Don Skibo, Dr. Ashton Embry, Dr. Chris Harrison, and Mr. Ross Stewart, all of the ISPG for consultation and fruitful discussions throughout the study.

I am grateful to the Cartography and Word Processing staff of the ISPG and to Mrs. Margaret Goodarzi for providing excellent technical assistance. In addition, my special thanks go to Dr. Arvid Hardin, Head of Coal and Hydrocarbon Processing Department, Alberta Research Council, for encouragement during the latter stage of the thesis and Ms. Joyce Moir for cheerfully typing numerous versions of the thesis. You have done an excellent job Joyce.

Finally, I would like to thank my parents for giving me the opportunity to attend

University and Ms. Jane Butcher for continuous encouragement over the last two years. Janie, you have been a wonderful friend and provided great inspiration.

CHAPTER I

CHAPTER I

1.0 INTRODUCTION AND PREVIOUS WORK

The Canadian Arctic Archipelago is the largest in the world and extends 2,400 km from west to east and 1,900 km from north to south (Harrison et al., 1985).

The Arctic Archipelago contains several distinct regions with contrasting geology and physiography, the result of sedimentation in two different basins and three major orogenies. The two distinct basins are: a) the Lower Palaeozoic Franklinian geosyncline; and b) the Upper Palaeozoic-Cenozoic Sverdrup Basin (Figure 1-1). The three orogenies are: a) the Caledonian Orogeny (Early Devonian) which created the Cornwallis Fold Belt; b) the Late Devonian-Early Carboniferous Ellesmerian Orogeny, which effectively terminated sedimentation in the Franklinian geosyncline and resulted in the development of the Parry Islands and Central Ellesmerian Fold Belts; and c) the Eurekan Orogeny (Tertiary), which resulted in intense compressional folding and thrusting of the previously established Central Ellesmerian Fold Belt (Thorsteinsson and Tozer, 1970; Fox, 1985; Harrison et al., 1985).

The major geological provinces as defined by Thorsteinsson and Tozer (1970) and Balkwill et al., (1982) are: The Canadian Shield, the Arctic Platform, the Franklinian geosyncline (divided into a mio- and a eugeosyncline), the Sverdrup Basin, and the Arctic Coastal Plain (Figure 1-1). Melville Island, which is the focus of the present study, is situated at the margin of the Franklinian geosyncline and the Sverdrup Basin (Figure 1-1). The southern part of Melville Island (Dundas Block) belongs to the Arctic Platform province (Figure 1-1), whereas most of central Melville Island is part of the Parry Islands Fold Belt, a distinctive tract of moderately deformed Devonian and older strata. The Parry

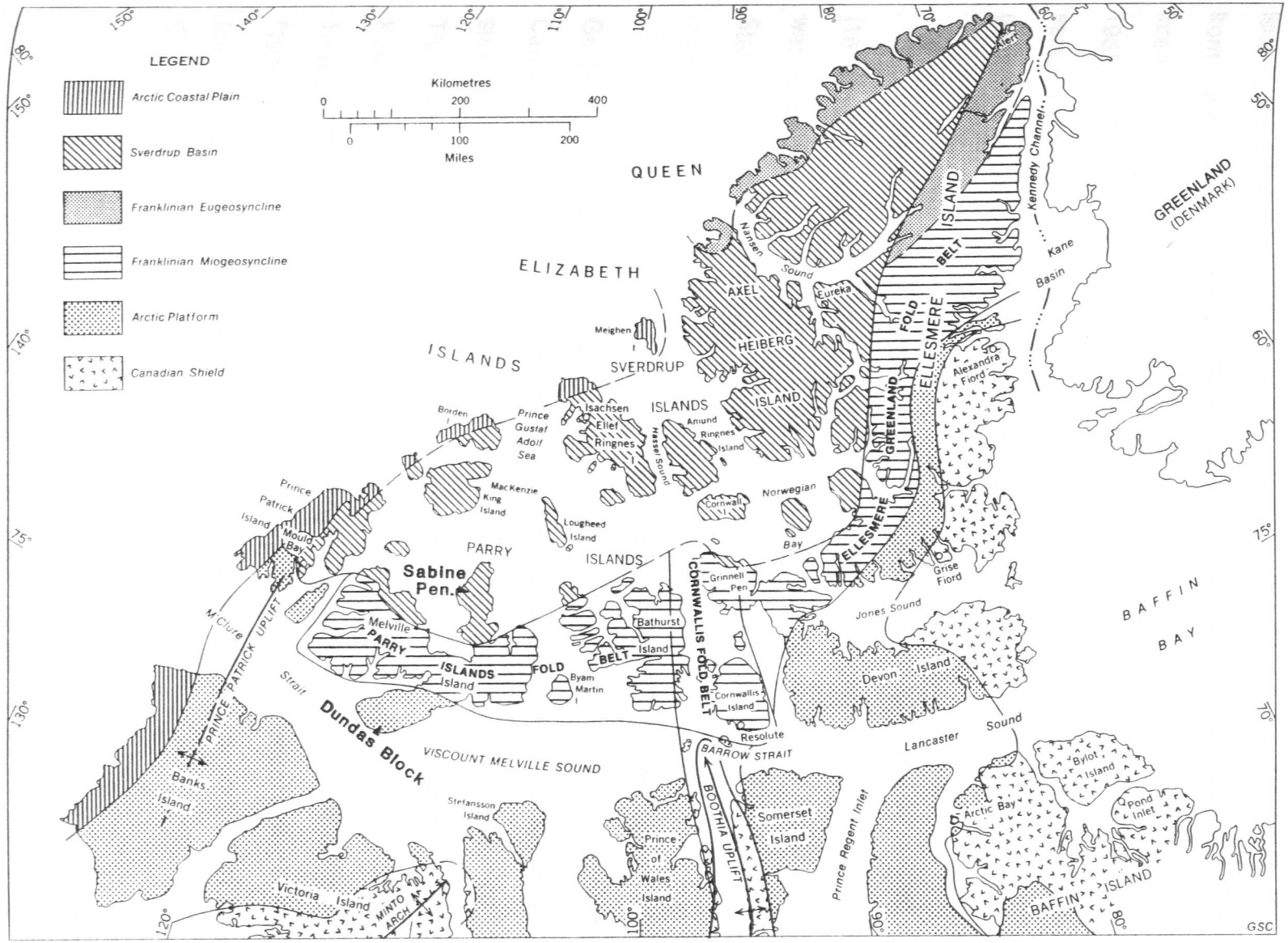

Figure 1-1 Geological provinces, Canadian Arctic Archipelago (modified after Balkwill et al., 1982)

Islands Fold Belt is the southwestern sector of the Ellesmerian Fold Belt, which extends from northern Ellesmere Island southwestwards to northwestern Melville Island, interrupted only by the Cornwallis Fold Belt, a part of the Boothia Uplift (Figure 1-1) (Fox, 1985). Finally, the northern part of Melville Island belongs to the Sverdrup Basin, an episutural basin, which developed due to rifting and collapse of parts of the Franklinian geosyncline following uplift during the Late Devonian Ellesmerian Orogeny.

The earliest exploration in the Canadian Arctic Islands was carried out by Parry (1819) with results published by Konig (1823) and Haughton (1859). Further exploration was carried out by Sverdrup (1898-1902) with results published in 1903 and 1904 and Stefansson (1913-1916) with results published by Stefansson and Bartlett in 1916.

Modern geological field work in the Canadian Arctic began in 1948 by the Geological Survey of Canada (Fortier, 1948). Since that time, the Geological Survey of Canada has been involved in numerous operations involving systematic mapping, stratigraphy, sedimentology, structural geology and regional tectonics (Tozer and Thorsteinsson, 1964; Thorsteinsson and Tozer, 1970; Balkwill et al., 1977; Embry and Klovan, 1976; Mayr, 1980; Balkwill and Fox, 1982; Embry, 1982;1983a; 1984a,b,c; 1985a,b; Fox, 1985; Harrison et al., 1985) to name a few. A more complete list can be found in Christie and Kerr (1981) and some of the most important geological studies, particularly the ones dealing with Melville Island will be described in more detail in Chapter II under Geology.

There are very few systematic regional maturation studies in Arctic Canada, particularly Sverdrup Basin (Figure 1-2) (Baker et al., 1975; Snowdon and Roy, 1975; Henao-Londono, 1977; Powell, 1978; Fisher et al., 1980; Bustin, 1986). These studies have often dealt with limited number of samples collected from wide areas with a focus of

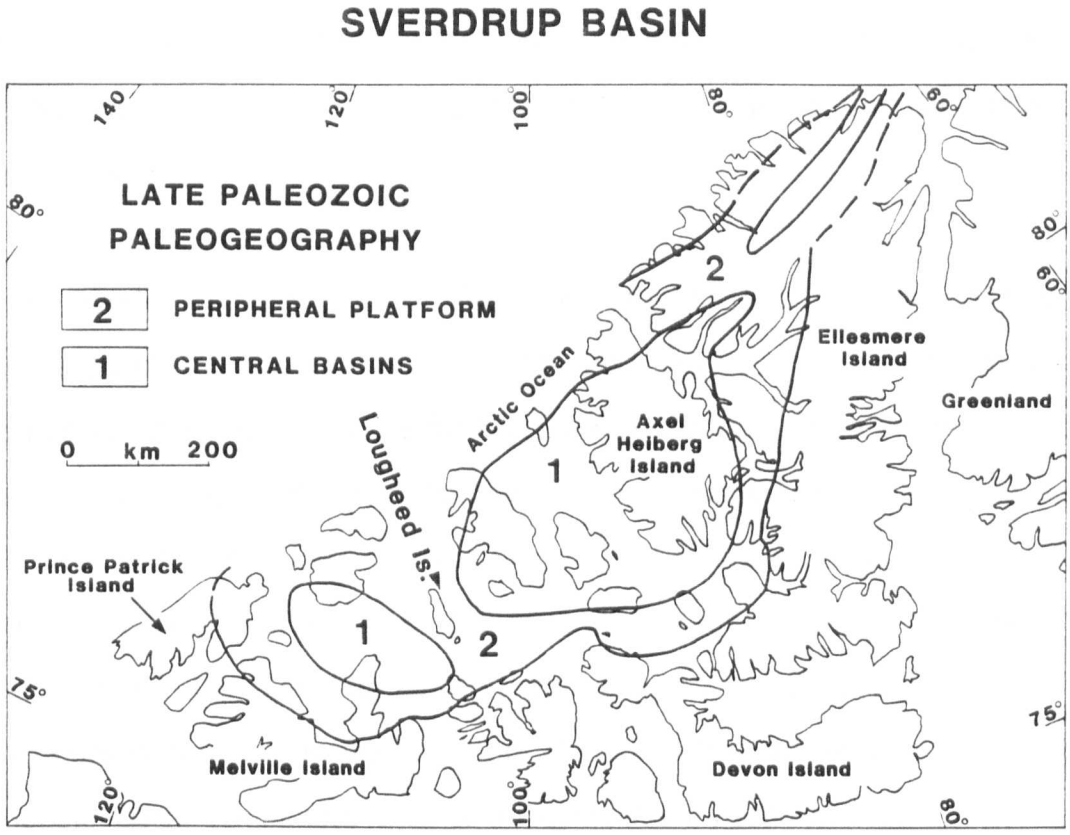

Figure 1-2 Outline of Sverdrup Basin (modified after Beauchamp et al., 1987)

the study being on the regional thermal maturity. Recently, attempts have been made to study, in detail, certain stratigraphical and/or time intervals in the Sverdrup Basin (Goodarzi et al., 1989a).

Early work in the Canadian Arctic Islands, to 1974, consisted mainly of reconnaissance geochemical studies. Snowdon and Roy (1975) studied the levels of organic maturation on a regional scale for the Sverdrup Basin based on the abundance and composition of C_1-C_4 light hydrocarbons. The source-rock potential of specific stratigraphic units within the Mesozoic succession of the Sverdrup Basin has been the focus of research since the mid 1970s. Baker et al., (1975) suggested that the Triassic and Jurassic section in the Sverdrup Basin (Figure 2-3) has good potential for liquid and gaseous hydrocarbons and Henao-Londono (1977) published results indicating the source richness of certain units and maturation levels in the Arctic Islands.

Powell (1978) carried out the most extensive regional organic geochemical study to assess the hydrocarbon potential of the Sverdrup Basin and the Franklinian geosyncline. He defined four organic metamorphic facies, namely immature, marginally mature, mature and overmature, based mainly on the concentration and composition of C_1 to C_4 light hydrocarbons and C_{15+} hydrocarbons. Vitrinite reflectance measurements were also obtained on samples from a few selected drillholes and correlated with the results obtained from the light and heavy hydrocarbon data. In addition, Powell (1978) stated that the Mesozoic strata in the Sverdrup Basin have significant potential for gas generation and that the gas found in the Hecla and Drake hydrocarbon fields, Melville Island, have been formed in the marginally mature zone of hydrocarbon generation. He identified the Triassic Schei Point Group (also referred to as the Blaa Mountain Group, Figure 2-3) as being the only widespread source rock in the Sverdrup Basin, as well as the source of oil in the Sabine Peninsula, Melville Island, and of the Melville Island tar

sands.

Light density oil (47° API) has been encountered in Lower and Middle Triassic rocks in the Sabine Peninsula, Melville Island (Figure 1-1) whereas high density oil (18-22° API) was recovered from the Bjorne sandstone (Figure 2-3) in the Drake L-67 and Hecla P-62 drillholes (Powell, 1978). In addition, the seven gas fields discovered to date in the Sverdrup Basin have total reserves in excess of 280 x $10^9 m^3$, containing almost exclusively dry gas (Drummond, 1973). This figure has been upgraded to 370 x $10^9 m^3$ by Procter et al., (1984) and the ultimate potential has been estimated at 462 x $10^6 m^3$ of oil and 1800 x $10^6 m^3$ of gas. The two large fields that flank the Sabine Peninsula, namely Drake and Hecla, occur in structures draped over ancestral highs (Powell, 1978). Later, Powell and Snowdon (1980) suggested that the occurrence of substantial reserves of dry gas in the marginally mature zone is an indication that overmaturity is not a prerequisite for gas formation. From their study it became apparent that the nature of the source organic matter was variable in both type and level of thermal maturity at which hydrocarbons were generated.

Fisher et al., (1980) studied the maturity and hydrocarbon potential of Mesozoic sediments in the Sverdrup Basin and concluded that generation of hydrocarbons occurred during periods of tectonism and maximum basin infill.

Bustin (1986) studied the maturation of Maastrichtian and Lower Tertiary strata of the Eureka Sound Formation, which includes the major resources of low-rank coals in the Canadian Arctic Archipelago. Maturation gradients measured from Melville Island in the southern part of the Sverdrup Basin were approximately 0.10 log % Ro max/km, and when compared to numerical models suggested paleogeothermal gradients of the order of 15°C/km. He attributed the low paleogeothermal gradients to low heat flow or rapid

Tertiary sedimentation and uplift and estimated a maximum paleodepth of burial of the Eureka Sound Formation to be approximately 4,000 m. This estimate was made by extrapolating vitrinite (huminite) reflectance maturity gradients but it has been disputed recently by the work of Goodarzi et al., (1991) which shows that a maximum of 1,200 m of Tertiary and younger strata has been eroded near the vicinity of Bustin's (1986) study. The work of Goodarzi et al., (in press) has also been substantiated by stratigraphical and structural geological evidence.

Additional studies on the maturity and source-rock potential of Mesozoic sediments in the Sverdrup Basin include those of Goodarzi et al., (1989a), and Goodarzi et al., (1991). Goodarzi et al., (1989a) studied the regional maturity and source-rock potential of organic-rich beds from the Triassic Schei Point Group in the Sverdrup Basin, using reflected light microscopy and maturity parameters determined geochemically (i.e. Rock-Eval and biomarkers). All the samples were from the Eden Bay Member of the Hoyle Bay Formation and contained marine algal organic matter, such as Tasmanites and dinoflagellate cysts mixed with terrestrially-derived organic matter. They concluded that the source rocks became more mature from the Sverdrup Basin margin towards the basin axis due to increase in overburden of sediments in the central part of the basin and also due to the high thermal conductivity of salt which has strongly influenced the maturity of Schei Point source rocks over the crest of salt-cored structures. In addition, Goodarzi et al., (1989a) also observed a good agreement between parameters determined using optical microscopy and geochemically.

Finally, Goodarzi et al., (1991) studied the regional thermal maturity and source-rock potential of the sedimentary successions in Lougheed Island, located in central Sverdrup Basin and approximately 120 km NE of Melville Island (Figure 1-2). They identified good to excellent quality oil-prone source beds in the Murray Harbour and

the Hoyle Bay Formations of the Middle to Upper Triassic Schei Point Group (Figure 2-3). At relatively low levels of thermal maturity (<0.7% Ro), the formations were characterized by high total organic carbon (TOC) content and high hydrogen index (HI) values (>550 mg HC/g Corg). At or near the stage of maximum oil generation (~ 0.9-1.0% Ro) the HI values decreased significantly to <200 mg HC/g Corg. The visible organic matter consisted of marine algae (Tasmanites), dinoflagellate cysts and amorphous fluorescing matrix bituminite. These organic-rich and highly oil-prone source rocks were deposited in a shallow open-marine shelf under highly anoxic, reducing conditions. In addition, Goodarzi et al., (1991) examined the source-rock potential of other Mesozoic formations in the Sverdrup Basin, such as the Jameson Bay, the Ringnes, the Deer Bay and the Christopher (Figure 2-3). The lower part of the Jameson Bay Formation contained moderate to good quality oil-prone source beds in specific localities, while the Ringnes contained mainly gas-prone Type III organic matter. The remaining formations contained an admixture of Types III/IV organic matter and were not considered as potential source-rocks for liquid hydrocarbons.

The present-day geothermal gradients in the Lougheed Island area are between 20 and 45°C/km depending on depth (Skibo et al., 1990). From theoretical models relating vitrinite reflectance gradients and effective paleogeothermal gradient, it is inferred that the present-day reflectance gradients were acquired in geothermal regimes similar to the present, but with episodes of increased heat flow concomitant with increased subsidence rates at Aptian-Albian times, prior to the Eurekan Orogeny. The Paleocene Eurekan Orogeny was marked by tectonic uplift and subsequent erosion of approximately 1,000 m. The amount of eroded section in the Lougheed Island area was determined using the following methods: a) stratigraphic and structural evidence; b) extrapolation of % Ro gradients, c) shale and sandstone compaction systematics; and d) comparison of paleogeothermal gradient to present-day geothermal gradient.

From the work of Balkwill and Roy (1977) and Balkwill et al., (1982), it was possible to infer an upper limit of approximately 700 m of eroded section, whereas using an extrapolation of the maturation gradient above the present surface, to an initial reference Ro value, the amount of eroded section was estimated between 900 - 2,400 m. The upper range (1,400 - 2,400 m) was difficult to justify based on geological evidence (Goodarzi et al., 1991). Shale and sandstone compaction curves gave an estimate of eroded section between 500 and 1,100 m, which is in general agreement with the stratigraphic and structural evidence, whereas the comparison between paleogeothermal and present-day gradients indicated that approximately 750 to 1,050 m of section has been eroded from the Lougheed Island area. The work of Goodarzi et al., (1991) indicated that paleogeothermal gradients were almost 15°C higher than present-day geothermal gradients and that this difference could be explained by either (i) average paleoheat flow about 25 percent higher than present heat flow, and/or (ii) tectonic uplift and erosion of almost 1,000 m of section due to the Eurekan Orogeny with no change in heat flow.

1.1 SCOPE AND PURPOSE OF THE STUDY

The Geological Survey of Canada, as part of its Frontier Geoscience Program (FGP) has undertaken an extensive and systematic study of Fossil Fuel potential and distribution, with particular emphasis on the hydrocarbon potential in Arctic Canada. The program involves a comprehensive geological study and encompasses numerous disciplines of earth sciences, including regional geology (surface and subsurface), seismic geophysics, palynology and micropaleontology, organic petrology and organic geochemistry.

Part of the Frontier Geoscience Program deals with the study of regional

thermal maturity and source-rock potential of sedimentary successions in the Franklinian geosyncline and in the Sverdrup Basin.

As evident from the previous studies dealing with thermal maturity and source-rock potential in the Sverdrup Basin region, outlined and discussed above, the data bank on maturity of sediments and hydrocarbon-generating potential is limited to only the Triassic Schei Point Group. In addition, one study dealt with the Tertiary Eureka Sound Formation and another included a limited organic petrological analysis of selected samples from the Mesozoic of the Sverdrup Basin.

Therefore, this study, which was funded on its entirety by the Ministry of Energy, Mines and Resources, Geological Survey of Canada, aims to achieve a systematic and better understanding of the source-rock potential and maturity of not only the Schei Point Group sediments but also the Upper Palaeozoic sediments of the Franklinian geosyncline and the remaining Triassic, Jurassic and Cretaceous sediments of the Sverdrup Basin. In addition, known Triassic source rocks are limited globally and this area of Arctic Canada is one of the relatively few unexplored areas in the North American continent which may contain mega-hydrocarbon fields. Therefore, such a systematic and regional study in Canada's Arctic is very important not only nationally but also internationally because these unique Triassic source rocks of the Schei Point Group or its equivalent may correlate with possible source rocks in the Arctic regions of Norway and the U.S.S.R.

The purpose of this systematic and regional study, which is based on approximately 2,000 samples from 43 drillholes in Melville Island (drillhole location is shown in Figure 7-1), is multifold:

1) To characterize the type and optical properties of the organic matter in clastic and carbonate sediments in Palaeozoic and Mesozoic strata in Melville Island;
2) To study the level of thermal maturity and hydrocarbon potential of the Melville Island sedimentary succession and produce thermal maturation profiles for all drillholes;
3) To produce maps showing contours of thermal-maturation levels in the study area;
4) To determine zones of oil and gas generation and/or destruction;
5) To provide an outline of source-rock potential for petroleum exploration in the Sverdrup Basin; and
6) To compare and contrast the type of organic matter, level of thermal maturity, depositional environment and type of hydrocarbon products of the Franklinian geosyncline and the Sverdrup Basin to those of other source rocks and potential source rocks of Palaeozoic, Mesozoic and Cenozoic age in known Canadian sedimentary basins.

CHAPTER II

CHAPTER II

2.0 GEOLOGY

Melville Island is a key area in the Arctic Islands for understanding the Middle to Upper Devonian clastic wedge, the Early Carboniferous Ellesmerian Orogeny, the Permian Melvillian Disturbance (a minor orogeny which affected northwestern Melville Island only), the Paleocene Eurekan Orogeny, and the evolution of Carboniferous to Tertiary tectonics and sedimentation of the Sverdrup Basin margin (Harrison et al., 1985).

Melville Island and the nearby offshore region have been the site of considerable petroleum exploration since the early 1960s. Both seismic exploration and drilling have been carried out, with a drillhole spudded as recently as 1983.

Tozer and Thorsteinsson (1964) provided a full account of both early geographical and geological exploration of the Melville Island region. Up until 1964, what was known of the geology of Melville island was mainly due to the work of McMillan (1910), and Tozer (1956, 1963). Tozer and Thorsteinsson's (1964) account and reconnaissance mapping of Melville and other islands of the western Queen Elizabeth Islands has provided a basic stratigraphic and structural framework for the present studies (Harrison et al., 1985).

Geological and geophysical exploration of Melville Island continued throughout the 1960s and 1970s. In 1964, Trettin studied the tar sands of Sproule Peninsula (Trettin and Hills, 1966; 1967) from a geological viewpoint and Nassichuk (1965) studied and collected ammonoids from Permian beds. Nassichuk (1975) made further collections at Barrow Dome, Sabine Peninsula, a site from which a large collection had earlier been

obtained by B.P. Exploration Limited. Stratigraphic sections of Middle Devonian beds were measured in 1968 by McGregor and Uyeno, and samples for microspore studies were collected. The results of this study (McGregor and Camfield, 1982) aimed at both interfacies correlation and correlation of marine and nonmarine biozones. Seismic exploration began on Melville Island in 1968, a year that also saw the announcement of the giant oil strike at Prudhoe Bay, Alaska (Jones, 1981).

Five drillholes were drilled on Melville Island in 1969 and 1970. Two of them were completed in Ordovician and three in Pennsylvanian-Permian strata. In 1970 the first successful drillhole was completed, by Panarctic Oils Limited, in Triassic sandstone. This drillhole, Panarctic Drake Point L-67, blew out of control and Panarctic Oils has since outlined the Drake Point gas field, one of the largest in Canada (Jones, 1981). About 45 exploratory drillholes have been drilled on Melville Island and in the nearby offshore area since 1960.

Seismic surveys were extended to offshore areas in the early 1970s. A considerably improved picture of the subsurface has been obtained from the seismic data, and is reported on and illustrated by Fox (1983; 1985) and Texaco Canada Resources Limited (1983).

Stratigraphic sections of Lower Palaeozoic beds on Melville Island formed a major component of a wide-ranging study by Embry and Klovan (1976) of the Middle and Upper Devonian 'clastic wedge' of the Arctic Islands. This study resulted in refinements of the nomenclatural framework and understanding of the sedimentary environments of the several Middle and Upper Devonian facies. More recently, Embry (1983a,b; 1984a,b,c) erected new stratigraphic divisions for the Middle Triassic to Middle Jurassic beds, based on the extensive subsurface information now available. Finally, Balkwill and

Fox (1982), Fox (1985) and Harrison et al., (1985) studied the tectonic evolution of the western Sverdrup Basin.

2.1 FRANKLINIAN GEOSYNCLINE

The Precambrian basement (Canadian Shield) is overlain to the north by a northward-thickening wedge of Proterozoic and Lower Palaeozoic carbonate and clastic rocks of the Arctic Platform and Franklinian miogeosyncline (Figure 1-1). Layered reflections in southern Melville Island suggest that basement may be at 10 km depth (Balkwill and Fox, 1982). Trettin (1972) identified two major depositional provinces in the geosyncline, a northwesterly clastic province that has the features of an eugeosyncline, and a southeasterly carbonate province that has the characteristics of a miogeosyncline. Two major phases can be distinguished in the terrigenous rocks of the miogeosyncline. During the Upper Proterozoic to Lower Cambrian, clastics were derived from cratonic sources in the southeast and deposited in a basin, the axis of which lay to the northwest (Trettin, 1972). During Middle Cambrian to Upper Devonian, the miogeosyncline was part of a mobile belt that migrated southwestward as a foredeep receiving volumes of synorogenic clastics and carbonates prior to the Ellesmerian Orogeny (Balkwill and Fox, 1982).

Lower Palaeozoic rocks exposed in the western Queen Elizabeth Islands consist of two assemblages (Thorsteinsson and Tozer, 1970); a Lower Ordovician to Eifelian succession of shelf deposits (carbonates and halite) and coeval basinal shales; and a Middle Eifelian to Famennian succession of shales and sandstones that represent synorogenic clastics (referred to as the Devonian clastic wedge), generated and shed in a foredeep in advance of the Ellesmerian Orogeny.

The Ellesmerian Orogeny ended the long history of deposition in the Franklinian geosyncline. The Proterozoic to Devonian rocks were folded, uplifted and eroded creating northeast-to east-trending grabens and half-grabens. These structurally-defined trenches controlled the earliest sedimentation in the embryonic Sverdrup Basin. A subsequent episode of folding and faulting (Melvillian Disturbance) occurred at about the end of Carboniferous times, producing large normal faults, expanding and deepening the axial region of the Sverdrup Basin over the site of the Franklinian miogeosyncline (Balkwill and Fox, 1982).

2.2 SVERDRUP BASIN

The Sverdrup Basin (Figure 1-2) is superimposed on deformed, interior parts of the Ellesmerian orogenic belt (Figure 1-1) and is considered as an episutural basin on continental crust, having persistent eastern and western margins, where some thick wedges of coarse-grained mature clastics accumulated. The Sverdrup Basin also contains Upper Palaeozoic and Mesozoic basalt flows and gabbroic intrusions and has directionally consistent fracture patterns, indicating that the basin was probably generated by episodic, incipient rifting (Balkwill and Fox, 1982).

Clastic sediments filled the basin in three stages creating unconformity-bounded megasequences: Carboniferous-Middle Jurassic; Oxfordian-Neocomian; and Aptian-Maastrichtian. Each of the megasequences was initiated by rejuvenation of thermal subsidence accompanied by regional marine transgression and intra-basin intrusion and volcanism (Balkwill and Fox, 1982).

The Sverdrup Basin contains about 12,000 m of sedimentary rocks at the depocentre region. Of this, approximately 5,000 m are Carboniferous and Permian

shales and evaporites, with the remaining 7,000 m being Mesozoic shales and sandstones (Trettin, 1972).

Carboniferous-Middle Jurassic stratigraphy of the western Sverdrup Basin records a phase of progressive filling of the depocentral region by cratonic-derived clastics. The diapirs of western Sverdrup may have been generated from an evaporite-dominated succession, but evaporite deposition ceased at about the beginning of Upper Carboniferous (Moscovian) (Balkwill and Fox, 1982).

A large delta dominated Lower Triassic sedimentation and the volume of clastics supplied to the delta was greater than tectonic subsidence. From the Norian (Upper Triassic) to Pliensbachian (Lower Jurassic), the deltaic wedge prograded into the basin depositing shallow marine sands and muds. Thereafter, through Callovian time, all of the Sverdrup Basin subsided slowly (Balkwill and Fox, 1982).

Thermal subsidence in the Oxfordian resulted in the deposition of muds and sands and reorganization of the western Sverdrup Basin. The basin lengthened and widened from Oxfordian to Neocomian times, whereas the great supply of Lower Cretaceous clastics filled the basin by Neocomian time (Balkwill and Fox, 1982).

Renewed thermal subsidence in the Sverdrup Basin took place from Aptian through Albian and was accompanied by gabbroic intrusions, basaltic volcanism and marine transgressions. In addition, the presence of Turonian basalts and deep-marine shales indicates the beginning of an Upper Cretaceous episode, followed by fluvial clastics by Middle Maastrichtian. As a result of Cenozoic erosion, the record of Upper Cretaceous stratigraphy is incomplete (Balkwill and Fox, 1982).

Basalt flows, dykes and sills are important constituents of Carboniferous to Upper Cretaceous rocks in the Sverdrup Basin (Blackadar, 1964; Balkwill, 1978). Isotopic ages of the intrusives range from 190 Ma to about 86 Ma (Hettangian to Coniacian). This mafic activity indicates a long-lasting crustal instability in the basin.

Several diapirs in and near the Sabine Peninsula in Melville Island are aligned in a northeast-trending row and their characteristic features are indicative of an episodic growth from Middle Triassic to Upper Cretaceous times.

2.3 STRATIGRAPHY

2.3.1 LOWER PALAEOZOIC FORMATIONS

The Palaeozoic formations of Melville Island (Figure 2-1) can be conveniently subdivided into the following groups:

1. Eleanor River and older beds
2. Bay Fiord evaporites
3. Thumb Mountain carbonates
4. Eids-Cape Phillips fine-grained clastic rocks and their carbonate equivalents (Allen Bay/Read Bay and Blue Fiord), and
5. The Middle to Upper Devonian clastic wedge (Cape de Bray to Griper Bay Formations).

The Eleanor River and older beds are almost entirely unknown in the Franklinian miogeosyncline. A complete section of the Bay Fiord Formation (Figure 2-1), consisting of 524 m of salt and dolomite (Fox, 1985), has been penetrated in the Sabine

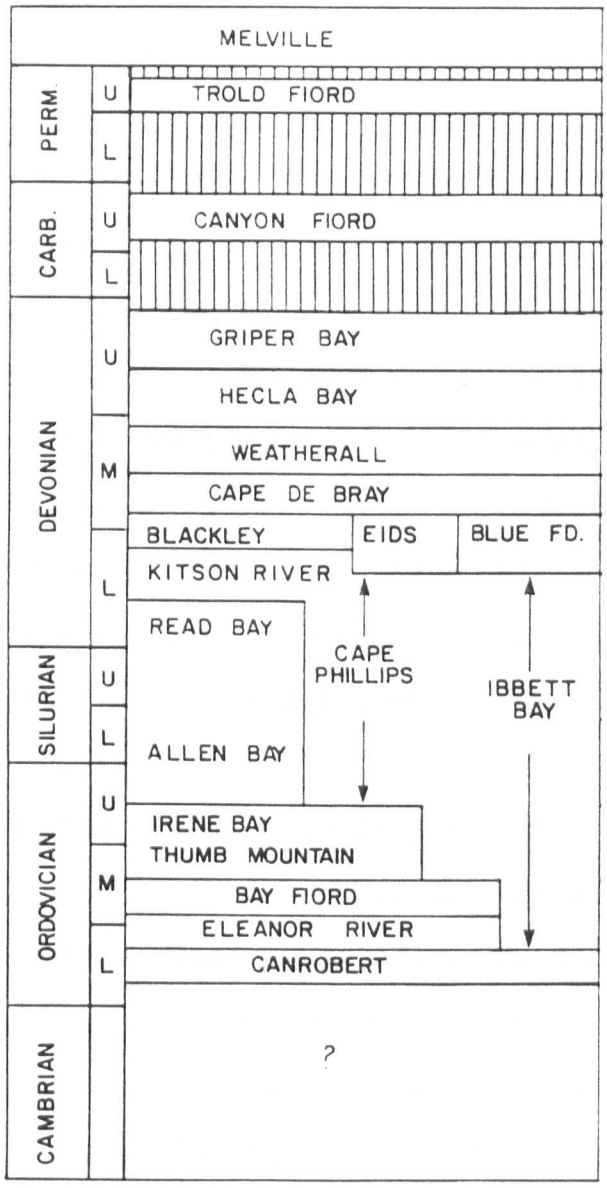

Figure 2-1 Lower Palaeozoic stratigraphy, Melville Island (modified after Fox, 1985)

Bay A-07 drillhole, Melville Island (Figure 7-1).

The Thumb Mountain Formation (Figure 2-1) underlies the Franklinian miogeosyncline with the exception of the Canrobert Hills sector. In the folds of the Canrobert Hills the time interval represented elsewhere in the Franklinian miogeosyncline by the Thumb Mountain Formation is represented in part by the Ibbett Bay Formation (Lower Ordovician to Lower Devonian) (Figure 2-1). The Ibbett Bay Formation is composed mainly of shale, argillite, chert, dolomite and minor limestone. Graptolites indicate the age range of the Ibbett Bay to be Arenigian to Early Devonian. The Ibbett Bay is thus the deep-water equivalent of the Middle Ordovician to Lower Devonian carbonate and clastic rocks of the Franklinian miogeosyncline (Fox, 1985).

The Cape Phillips and Eids shales (Figure 2-1) are both present throughout the greater part of the Franklinian miogeosyncline and have lateral equivalents. The Cape Phillips is the basinal equivalent of the Read Bay/Allen Bay shelf and reefoid limestones and dolomites and the Eids is the equivalent of the Lower and Middle Devonian limestone reefs and shelf carbonates (Blue Fiord Formation) (Fox, 1985). The Eids shale basin overlies the somewhat smaller Cape Phillips basin and both basins include the entire Franklinian miogeosyncline.

The great mass of Middle and Upper Devonian strata, known as the clastic wedge, includes all Devonian beds overlying the Eids-Blue Fiord shale-carbonate complex, such as Cape de Bray, Weatherall, Hecla Bay and Griper Bay Formations (Figure 2-1) (Embry and Klovan, 1976). The total known section composing the wedge comprises 4,000 to 5,000 m of beds in Bathurst and Melville Islands, depending on the locality and depth of the post-Devonian erosion. The top of the Devonian succession is everywhere a major unconformity (Fox, 1985). The lower half of the clastic wedge is

composed of shale, siltstone and very fine to fine-grained sandstone (Blackley, Cape de Bray, and lower Weatherall beds), the upper half comprising fine- to medium-grained sandstone and interbeds of shale (Hecla Bay and Griper Bay beds) (Fox, 1985). The record in Melville Island reveals that continuous sedimentation occurred through Ordovician and Silurian times and the dated rocks range from Arenigian (Lower Ordovician) to Emsian or Eifelian (Lower or Middle Devonian).

Within the Franklinian miogeosyncline, the end of Devonian sedimentation marks the end of a major cycle of deposition. Throughout the miogeosyncline, Devonian and older rocks were folded prior to deposition of the next younger formations, which are of Upper Carboniferous age. Most of the folding of the Franklinian miogeosyncline took place within Frasnian to Middle Pennsylvanian (Ellesmerian Orogeny). Only in northwestern Melville Island is there evidence of later folding within the Franklinian miogeosyncline and these younger folds are superimposed upon the older, mid-Palaeozoic structures (Tozer and Thorsteinsson, 1964).

2.3.2 UPPER PALAEOZOIC FORMATIONS

2.3.2.1 PENNSYLVANIAN

The Pennsylvanian rocks of Melville Island occur in two different structural situations. One is in northwest Melville, where the Pennsylvanian rocks are bounded by angular unconformities. Beneath are folded Ordovician, Silurian and Devonian formations and above are Permian strata. The other situation is displayed in Sabine Peninsula, where the Pennsylvanian rocks rest unconformably on older formations, but are followed concordantly by Permian strata, an indication that they were deposited within the Sverdrup Basin (Tozer and Thorsteinsson, 1964).

In northwestern Melville Island a period of folding took place between Middle Pennsylvanian and Permian times (the Melvillian Disturbance). The Sabine Peninsula area was not affected by the folding. Within the Sverdrup Basin, Middle Pennsylvanian time marks the beginning of a long period of essentially uninterrupted sedimentation which continued through the Mesozoic to Lower Tertiary. On the exposed margins of the basin the Pennsylvanian beds rest with profound angular unconformity on the folded rocks of the Franklinian miogeosyncline. It is suggested that Sverdrup Basin is superimposed on the deformed rocks of the geosyncline (Tozer and Thorsteinsson, 1964).

In Melville Island, the Pennsylvanian Canyon Fiord Formation (Figure 2-2) is resting unconformably on the Upper Devonian Griper Bay Formation (Tozer and Thorsteinsson, 1964; Fox, 1985). The basal beds of the formation contain Pennsylvanian marine fossils, suggesting communication to the north with the Sverdrup Basin. The upper beds are unfossiliferous and consequently there is no evidence to suggest such a connection. The structural relationship of the Pennsylvanian rocks in eastern Melville Island between Weatherall and Sabine Bays is relatively simple. The Canyon Fiord rests with angular unconformity upon most of the Devonian and older formations exposed in the Franklinian miogeosyncline (Tozer and Thorsteinsson, 1964). In northwestern Melville Island the relationship is more complex. Not only was the Canyon Fiord Formation deposited on the folded and eroded Lower Palaeozoic formations, but the Canyon Fiord beds were themselves folded and eroded prior to the deposition of the Permian Assistance Formation (Tozer and Thorsteinsson, 1964).

In several places in the Sverdrup Basin, angular unconformities reflect the important episodes of disturbance. In northwestern Melville Island, Upper Carboniferous strata, uplifted and folded during the Lower Permian Melvillian Disturbance, are

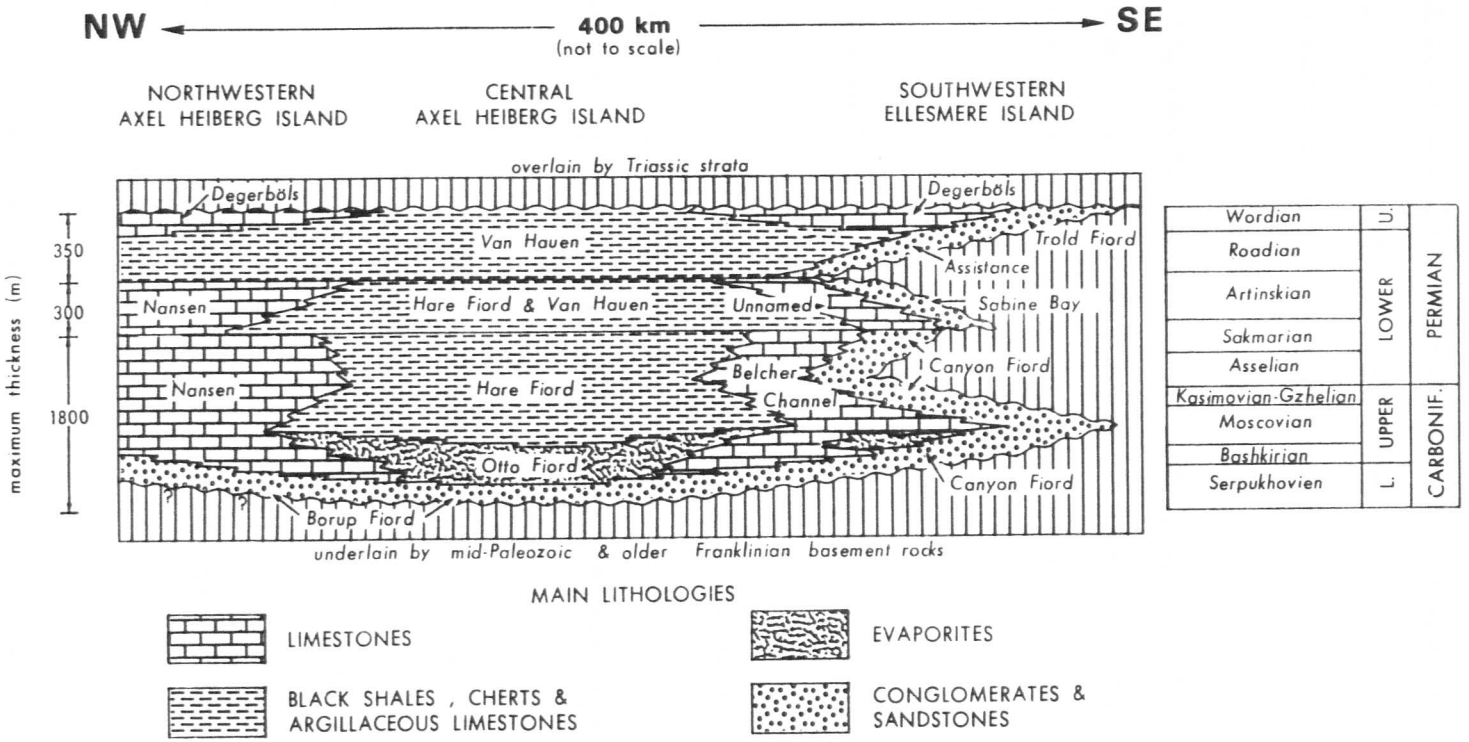

Figure 2-2 Upper Palaeozoic stratigraphy, Sverdrup Basin (modified after Beauchamp et al., 1987)

unconformably overlain by the Upper Permian Trold Fiord Formation (Trettin, 1972). Clastic material in the Canyon Fiord Formation was mainly derived from carbonates and sandstones of the underlying Franklinian miogeosyncline and deposited in a shallow open-marine environment (Trettin, 1972).

The Belcher Channel Formation (Figure 2-2) consists of skeletal and sandy limestones with minor sandstone beds. In Melville Island it is about 180 m thick and its fossil content (oolites, oncolites) indicates deposition in a fairly shallow shelf environment (Trettin, 1972).

2.3.2.2 PERMIAN

Permian rocks are also exposed in Melville Island. Two formations are recognized: the Sabine Bay and the Assistance (Figure 2-2). The Sabine Bay is present near Weatherall and Sabine Bays, where it rests disconformably upon the Pennsylvanian Canyon Fiord Formation. The Assistance beds in Melville Island are transgressive and rest on various older formations (Tozer and Thorsteinsson, 1964). The only good exposures of the Sabine Bay Formation are in the vicinity of Tingmisut Lake. The upper and lower contacts are sharp, they appear to be unconformable, but are probably disconformable. It has been suggested that the Sabine Bay and Belcher Channel Formations are correlative (Tozer and Thorsteinsson, 1964). There are some indications that the Sabine Bay is younger.

In westernmost Melville Island the Permian Assistance Formation (Figure 2-2) rests on Silurian, Devonian, Pennsylvanian and Lower Permian strata (Tozer and Thorsteinsson, 1964). It represents the deposition of a Permian transgression directed east and south from the axial part of the Sverdrup Basin. The Assistance-Bjorne contact

is structurally conformable but may also be a disconformity (Tozer and Thorsteinsson, 1964).

The Assistance Formation grades laterally and basinwards into the Van Hauen Formation (Figure 2-2). The latter includes black shale, siltstone and bedded chert and generally occurs in the axial regions of the Sverdrup Basin (Trettin, 1972). The youngest Permian beds in the Sverdrup Basin are those of the Lower Guadalupian (Wordian) Trold Fiord Formation (Figure 2-2), which includes glauconitic sandstone, limestone and is transgressive. This unit is considered to be equivalent to the Degerbols Formation (Trettin, 1972).

2.3.3 MESOZOIC FORMATIONS

2.3.3.1 TRIASSIC

The Schei Point Group comprises Middle to Upper Triassic (Anisian-Norian) strata in the Sverdrup Basin. The Schei Point encompasses strata deposited on the basin margins and comprises sandstone and bioclastic limestone, along with shale and siltstone.

Although only scattered, poorly exposed outcrops occur in western Sverdrup, the subsurface control is relatively plentiful. For a more detailed summary of the lithologies and stratigraphic relationships of the Middle and Upper Triassic strata in the Sverdrup Basin, the reader is referred to Embry (1982, 1983 a,b; 1984 a,b,c; and 1985 a,b).

The subdivision of the Schei Point into several formations is necessary because

the lithological units are distinct, widespread and each has economic importance as a potential hydrocarbon source. Five new formations are recognized within the group, based on distinct lithological characteristics. They have been named, in ascending order: Murray Harbour, Roche Point, Hoyle Bay, Pat Bay and Barrow Formations (Figure 2-3). The Schei Point Group was deposited on the flanks of the Sverdrup Basin and consists of three shale to siltstone-dominated units separated by two sandstone-dominated units. The lower two shale-dominated units, namely the Murray Harbour and the Hoyle Bay contain organic-rich shales and will be the focus of this study. The Schei Point Group in the southwestern Sverdrup Basin is characterized by five transgressive-regressive cycles and the total thickness is in excess of 750 metres (Embry, 1984a,b).

The sandstone-dominant Roche Point and Pat Bay Formations are recognizable only in the basin margins due to basinward facies change to siltstone and shale. The shale-siltstone units - Murray Harbour, Hoyle Bay and Barrow - can be extended across the basin and comprise the Blaa Mountain Group within the basin centre (Embry, 1984b).

In the North Sabine H-49 drillhole, Sabine Peninsula, the Murray Harbour Formation overlies sandstone of the Bjorne Formation and is conformably overlain by the Roche Point Formation (Embry, 1984b). The formation consists of shale and calcareous siltstone, is Anisian to Ladinian in age (Middle Triassic) based on ammonite and pelecypod studies (Tozer, 1961; 1963) and was deposited in an outer-shelf to slope environment (Embry, 1984b).

The Roche Point Formation is conformably overlain by the Hoyle Bay Formation and consists mainly of calcareous sandstone and bioclastic limestone. Over much of the western Sverdrup Basin the Roche Point is divided into four formal members

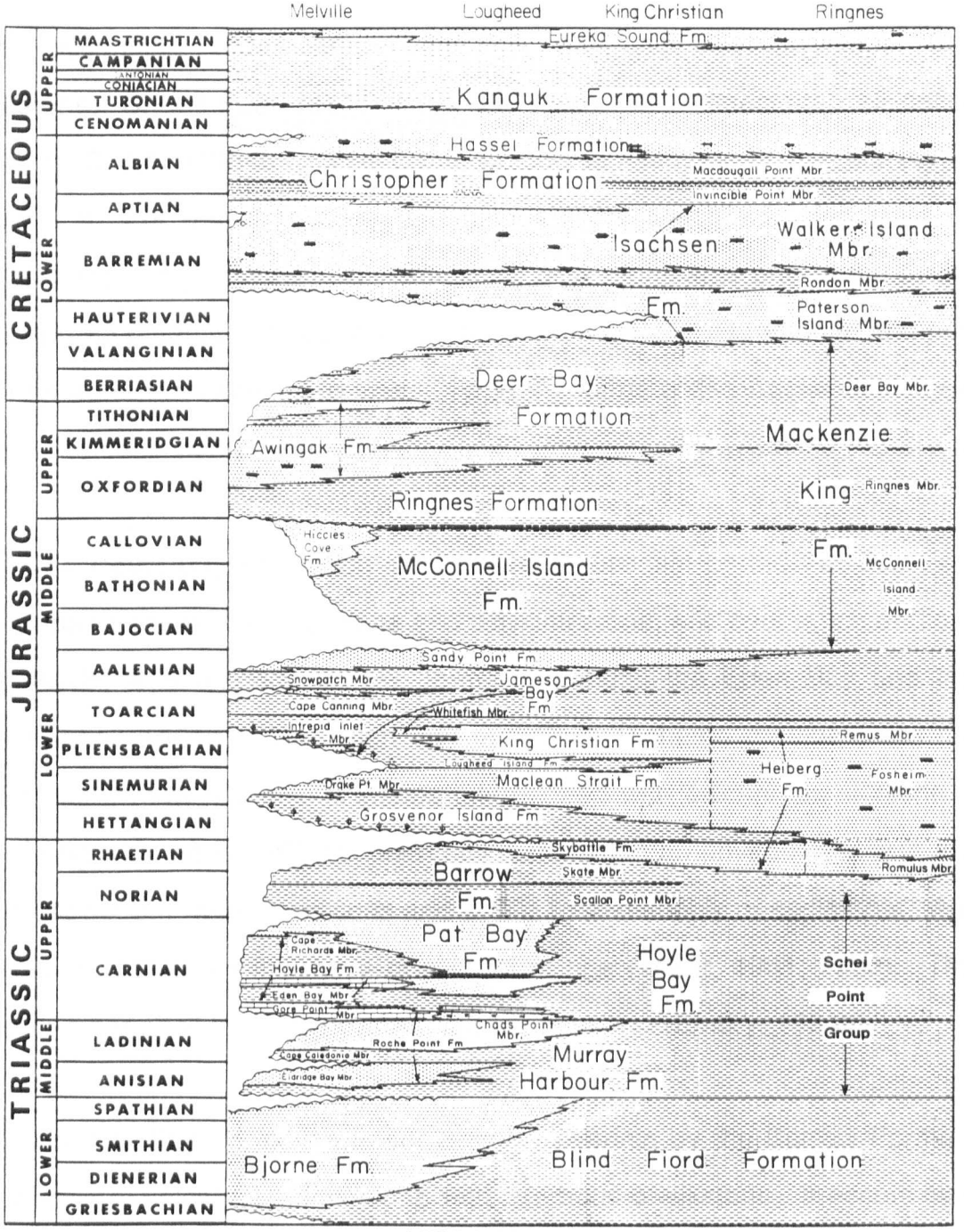

MESOZOIC
STRATIGRAPHIC NOMENCLATURE
WESTERN and CENTRAL SVERDRUP BASIN

A.F.E.
NOV. 1988

Figure 2-3 Mesozoic stratigraphy, Melville Island (modified after Embry, 1984a)

which in ascending order are: Eldridge Bay (sandstone), Cape Caledonia (shale-siltstone), Chads Point (sandstone), and Gore Point (limestone), all defined and described by Embry (1984b). The Cape Caledonia Member of the Murray Harbour Formation is a dark brown to black, bituminous shale which was deposited during a marine transgressive phase (Embry, 1984b). It also represents one of the thickest and most widespread potential source rocks in the Sverdrup Basin. Ammonite and pelecypod data give an age from Ladinian to Carnian and the fauna of the Roche Point indicates a shallow-marine shelf environment of deposition below normal wave-base (Embry, 1984b).

The Hoyle Bay Formation is conformably overlain by the Pat Bay Formation, consists of interbedded shale, siltstone and silty limestone, and over much of the western Sverdrup Basin, it is divided into two formal members, the Eden Bay and the Cape Richards (Embry, 1984b). The Eden Bay and Cape Richards members are thin, dark gray to brown, in part bituminous shales interbedded with calcareous siltstone (Embry, 1984b). Along with the Cape Caledonia they were laid in an environment with anaerobic to dysaerobic bottom water conditions and with a limited supply of sediments. Ammonite and pelecypod fossils are indicative of a Carnian age (Tozer, 1961; 1963). The fauna suggests an outer-shelf to slope environment of deposition (Embry, 1984b).

The Pat Bay Formation is conformably overlain by the Barrow Formation and consists mainly of calcareous sandstone with interbeds of siltstone. It occurs over much of western Sverdrup, is of Carnian age and has been deposited in a nearshore-marine shelf environment (Embry, 1984a).

Finally, the Barrow Formation is overlain conformably by the Skybattle Formation in the western Sverdrup, except near the basin margin where the Grosvenor Island unconformably overlies the Barrow. The lithology is mainly silty shale, siltstone

with minor sandstone. It is dated as Norian (Upper Triassic) on the basis of pelecypods (Balkwill, 1983) and palynomorphs (Balkwill et al., 1982) and is of prodelta and offshore-marine shelf origin (Embry, 1984b).

2.3.3.2 JURASSIC AND CRETACEOUS

The Jameson Bay Formation (Figure 2-3) consists mainly of shale, glauconitic sandstone, siltstone and has been dated as Pliensbachian, Toarcian and Aalenian based on ammonites (Frebold, 1960, 1975; Tozer, 1963; Tozer and Thorsteinsson, 1964; Balkwill, 1983). It is interpreted as an offshore marine-shelf deposit (Embry, 1984c).

The Ringnes Formation (Balkwill et al., 1977) (Figure 2-3) unconformably overlies the McConnell Island Formation and is conformably overlain by the Kimmeridgian Awingak Formation shales with distinctively large and colourful mudstone concretions.

The Deer Bay Formation (Figure 2-3) consists of the dark grey-black, slightly sideritic shales present between the Awingak and Isachsen sandstones. It was named by Heywood (1955) and it is Volgian to Valanginian in age (Balkwill et al., 1982). Shales in the lower part of the Deer Bay Formation contain microfaunas indicative of shallow-marine conditions, probably deposition at the front of delta which grade shoreward into the Awingak sands (Balkwill et al., 1982).

2.4 STRUCTURAL GEOLOGY OF MELVILLE ISLAND

2.4.1 FRANKLINIAN MIOGEOSYNCLINE (PARRY ISLANDS FOLD BELT)

To understand the structural geology of Melville Island, the tectonic evolution of

the Parry Islands Fold Belt must be examined. The name was given in 1953 by Fortier and Thorsteinsson to the part of the Ellesmerian Orogenic Belt that lies in the Bathurst and Melville Islands.

The Parry Islands Fold Belt is the outermost extension of an orogenic system that reached its maximum development far north of the Bathurst and Melville Islands. The northern limit of the fold belt is buried beneath the Sverdrup Basin; the southern limit can be seen in the Dundas Peninsula, Melville Island as well as in Bathurst Island (Fox, 1985). The eastern limit is sharply delineated, where it meets the Cornwallis Fold Belt at an angle of nearly 90°, but its western limit is not to be seen (Fox, 1985). The full length and width of the Fold Belt are not known, although the visible width in central Melville Island is 190 km and in northwest Melville about 60 km. The power of the Ellesmerian Orogeny to deform the Franklinian sediments was not sufficient to reach the Dundas Peninsula block, southern Melville Island (Fox, 1985).

The strata present in the subsurface and surface in the Parry Islands Fold Belt range in age from Lower Ordovician (Arenigian) or older to Cretaceous in parts of the belt. Only strata of Early Ordovician to Late Devonian have been deformed during folding episodes, although, as Fox (1985) points out, based on seismic-reflection evidence, beds older than Early Ordovician were also involved, but they have not been penetrated by any drillhole or seen as outcrops. The total thickness of the sedimentary package in the fold belt is unknown. Balkwill and Fox (1982) have demonstrated that layered reflectors, corresponding to time-depths of approximately 4.5 secs, and indicating a total thickness of about 10,000 m of sedimentary rocks, lie above the basement in southern Melville Island.

The long course of sedimentation in the Franklinian miogeosyncline was ended

by the Ellesmerian Orogeny (Tozer and Thorsteinsson, 1970), which affected Devonian and older rocks. The orogeny terminated Devonian sedimentation and it continued through Lower Carboniferous into Upper Carboniferous (Pennsylvanian) times (Fox, 1985).

The pattern of broad synclines alternating with long and narrow anticlines is characteristic of the greater part of the Parry Islands Fold Belt. The total visible foreshortening is 24 km in the Dundas Block, south Melville Island, and 6 km in the Canrobert Hills area (Fox, 1985). The typical Parry Islands style developed only in those areas where there are Bay Fiord salt, Cape Phillips shale and Eids shale. Where salt is present but the shales are replaced by Blue Fiord and Read Bay/Allen Bay carbonates, the folds are broader and shorter and appear to be detached from the substratum at a much deeper level than the Bay Fiord salt, probably in the Proterozoic (Balkwill and Fox, 1982). In areas where there is no salt and shale, as in the Dundas Block, folding is very broad and the detachment zone must be very deep, most likely in Proterozoic beds (Fox, 1985).

Normal faults are common in the Parry Islands Fold Belt. They are thought to be penecontemporaneous with the folding (Fox, 1985). Thrust faults, on the other hand, are not a major feature of the Parry Islands structures, although seismic studies and deep drilling have shown that at depth faulting played an important role in the erection of the folds.

In spite of its great thickness, the clastic wedge had little influence on structural development in the fold belt. Its role, especially in the upper levels, was essentially passive (Fox, 1985). In addition, the post-Devonian rocks were not involved in the Parry Islands folding, but they suffered deformation in Pennsylvanian time or later (Fox, 1985).

2.4.2 SVERDRUP BASIN

The Sverdrup Basin endured, without tectonic disruption from external stresses, from Lower Carboniferous (Visean) through Upper Cretaceous times. Of the 12,000 m of sedimentary rocks in its depocentre, 5,000 m are Carboniferous and Permian shales and evaporites, and about 7,000 m are Mesozoic shales and sandstones (Balkwill and Fox, 1982).

Evaporite diapirs are the prominent structures in the western Sverdrup Basin, forming part of a broad domain about 150 km wide, trending northeastwards and piercing the entire stratigraphic column. Several diapirs in and near the Sabine Peninsula are aligned in a northeast-trending row. Their surface rocks are mainly anhydrite and gypsum (Balkwill and Fox, 1982).

An array of northeast-striking faults, cutting Cretaceous and older strata in a broad zone between the Sabine Peninsula and Ellef Ringnes Island, has been revealed by offshore seismic and drillhole data. These are normal faults, mappable over distances of a few hundred meters to a few tens of kilometers, and are in co-existence with long, narrow, northeast-striking magnetic anomalies. A graben system east of Drake Point, Sabine Peninsula is in an area of modern earthquakes (Balkwill and Fox, 1982).

The northeast-striking zone acted mainly as a rift, undergoing dilation and extension from Carboniferous to Cretaceous. Fractures associated with the rift acted as conduits for fluids, allowing formation waters and hydrocarbons to migrate from deep to shallow stratigraphic levels (Balkwill and Fox, 1982). Therefore, it is not coincidental that the hydrocarbon-prone belt lies within the long-lasting, northeast-trending, rift domain, expressed by a suite of stratigraphic and structural elements.

Basalt flows, dykes and sills are also important components of Carboniferous to Upper Cretaceous rocks in the Sverdrup Basin (Blackadar, 1964; Balkwill, 1978). An array of nearly vertical gabbro dykes is present in Upper Palaeozoic rocks at Tingmisut Lake, Sabine Peninsula (Balkwill and Haimila, 1978).

The position and trend of the rift zone caused repeated deltaic progradation during Upper Triassic-Lower Jurassic times into parts of the western Sverdrup Basin, thus providing a stack of relatively thick, clean sandstones, that serve as reservoirs, separated by organic-rich marine shales. Organic-maturation levels within these potential source rocks may have been enhanced by diapiric evaporite intrusion (good heat conductors) and magmatic gabbro invasion.

CHAPTER III

CHAPTER III

3.0 ORGANIC PETROLOGY

Organic petrology is the study of the nature and thermal evolution of the organic matter present in coals or dispersed in sedimentary rocks. These organic materials (O.M.) in coal consist of three maceral groups (liptinite or exinite, vitrinite and inertinite) (Teichmuller, 1982) and in sediments consist of four kerogen types (Types I to IV) (Brooks, 1981). Organic matter also includes micro- and macrofossils such as graptolites (Watson, 1976; Combaz, 1980), chitinozoa (Tschudy and Scott, 1969; Combaz, 1980), scolecodonts (Schwab, 1966; Voss-Foucart et al., 1973; Goodarzi and Higgins, 1987), dinoflagellates and acritarchs (Hufnagel, 1977; Combaz, 1980) and bitumen (Robert, 1973; 1980; Jacob, 1975; 1985; Goodarzi et al., 1985). During thermal maturation, organic matter undergoes physical and chemical changes induced by temperature, time and to a minor extent pressure (Murchison, 1987; Teichmuller, 1987). It is believed that pressure may actually retard chemical reactions during thermal maturation with the exception of 'fold pressure' in strongly folded regions (Teichmuller and Teichmuller, 1982).

Chemical changes include an overall increase in the carbon content of the organic matter as a result of condensation and loss of functional groups. Increased aromatization and loss of oxygen, sulphur and nitrogen-bearing functional groups result in the formation of geopolymers enriched in carbon (Murchison, 1987; Teichmuller, 1987). The most important physical change brought in by pressure is a decrease in porosity due to greater compaction (Teichmuller and Teichmuller, 1982).

The reflectance of organic matter increases with maturation because of

irreversible chemical and physical reactions in the molecular structure which leads to increased aromaticity of the organic matter (Teichmuller, 1987). White (1935) was the first to suggest that there is a close relationship between the degree of coalification ('rank') and the occurrence of oil and gas deposits and he successfully applied coalification studies to solve geological problems. Teichmuller (1958) measured the reflectance of the coal maceral vitrinite and related the results to the degree of diagenesis and thermal alteration. Since then, the reflectance of vitrinite particles dispersed in sedimentary rocks has been applied routinely in oil and gas exploration.

3.1 CLASSIFICATION

3.1.1 NATURE OF THE ORGANIC MATTER IN COALS AND DISPERSED IN SEDIMENTS

Coal and bitumen are sedimentary rocks which contain highly concentrated organic matter. Organic matter may also be dispersed in sediments, in concentrations much lower than in coal or bitumen. The insoluble organic residue that remains after a sediment has been extracted by organic solvents and the mineral matter, except pyrite, has been removed by acid treatment is referred to as 'kerogen'. In contrast, the soluble organic matter is termed 'bitumen' by organic geochemists, which is different from the term 'migrabitumen' (ICCP, 1975) used by organic petrologists.

Dispersed organic matter (kerogen) in sediments is primarily derived from organisms such as plants, animals and bacteria, living within the host sediment at the site of deposition or being transported by water and wind action to the depositional site. Petrologically, organic matter is characterized and differentiated based on its reflectance, autofluorescence, morphology and association with the mineral-matrix component of the

sediment.

The classification of organic matter in sedimentary rocks has been made by: 1) coal petrographers, who examine the organic matter of polished blocks under reflected light or ultraviolet excitation; 2) palynologists, from the microscopic examination of mineral-free organic residues under transmitted light; and 3) petroleum geochemists, based on the changes in the elemental composition of organic matter with increased maturity. The interrelationships of these three classification systems is not very clear but sometimes vague and requires further clarification.

All organic matter may be classified into two major groups, sapropelic and humic (Figure 3-1; Hunt, 1979). Sapropelic refers to decomposition and polymerization products of fatty, lipid organic matter such as planktonic algae deposited in subaquatic marine or lacustrine muds, under oxygen-restricted conditions. It also includes spores, waxes, oils and resins, has hydrogen to carbon (H/C) ratios of 1.3-1.7 and organic-rich sapropelic deposits may lead to the formation of boghead coals and oil shales (Hunt, 1979). However, this is a generalization because the end product depends on the environment of deposition. For example, spores are not necessarily sapropelic and cannel coals can be vitrinite-rich as well.

Humic refers to land-plant material deposited in oxygenated, swampy waters. The material is composed of lignin, cellulose and tannins, is mainly derived from plant cell-wall material and has an H/C ratio of only 0.9. Carbonized (fusinitized) organic matter, such as charcoal from fires and oxidized organic matter would fall in this group.

Transmitted light microscopy has been used to study isolated kerogen (kerogen concentrate) (Staplin, 1969; Burgess, 1974; Rogers, 1979; Combaz, 1980). Depending

	SAPROPELIC			HUMIC	
KEROGEN (by transmitted light)	Algal	Amorphous	Herbaceous	Woody	Coaly (Inertinite)
COAL MACERALS	Liptinite (Exinite)			Vitrinite	Inertinite
(by reflected light)	Alginite	Amorphous	Sporinite Cutinite Resinite	Telinite Collinite	Fusinite Micrinite Sclerotinite
KEROGEN (by evolutionary pathway)		Types I,II	Type II	Type III	Type IV
H/C		1.7-0.3	1.4-0.3	1.0-0.3	0.45-0.3
O/C		0.1-0.2	0.2-0.02	0.4-0.02	0.3-0.02
ORGANIC SOURCE		Marine and lacustrine	Terrestrial	Terrestrial	Terrestrial and recycled
FOSSIL FUELS	Predominately oil Oil shales, boghead and cannel coals		Oil and gas	Predominantly gas Humic gas	No oil, trace of gas

Figure 3-1 Classification of organic matter in sedimentary rocks (after Hunt, 1979)

on its origin and morphology, kerogen has been subdivided into four groups, e.g. 'amorphous', 'herbaceous', 'woody' and 'coaly' (Figure 3-1). Amorphous kerogen incorporates degraded products of structured aqueous organic matter (i.e. bituminite from dinoflagellates) and amorphous biodegraded aqueous organic matter, whereas the herbaceous kerogen includes mainly spores, pollen, resins, cuticles and some structured aqueous organic matter. Woody kerogen consists of the structured and biodegraded terrestrial organic matter and coaly kerogen is comprised of charcoal (burnt wood) and fungi.

Coal petrologists classify coal components based on their appearance under microscopic examination in incident-reflected light or under ultraviolet excitation. The three main maceral groups are liptinite (also referred to as exinite), vitrinite and inertinite (Figure 3-1). These same coal macerals found concentrated in coals are also recognized in disseminated form as part of the kerogen in sedimentary rocks, and some petroleum geochemists use these terms (Kendrick et al., 1978; Hunt, 1979). Basically, liptinite (exinite) incorporates the sapropelic organic matter and is subdivided into alginite, amorphous and sporinite, cutinite and resinite. Vitrinite and inertinite comprise the humic organic matter (Figure 3-1).

Apart from the microscopical classification, the most familiar method of classifying organic matter is the Van Krevelen or atomic H/C versus O/C diagram (Tissot et al., 1974). In this diagram (Figure 3-2), kerogen is classified as Type I (very oil-prone), Type II (oil-prone), Type III (gas-prone) and Type IV (inert). The thermal maturation of the kerogen is described by pathways and the most mature kerogen plots near the lower left corner of the diagram. Kerogen may also be classified chemically (based upon Rock-Eval pyrolysis parameters) into four principal groups (Tissot et al., 1974; Harwood, 1977; Murchison, 1987). These groups follow distinct evolutionary pathways on a

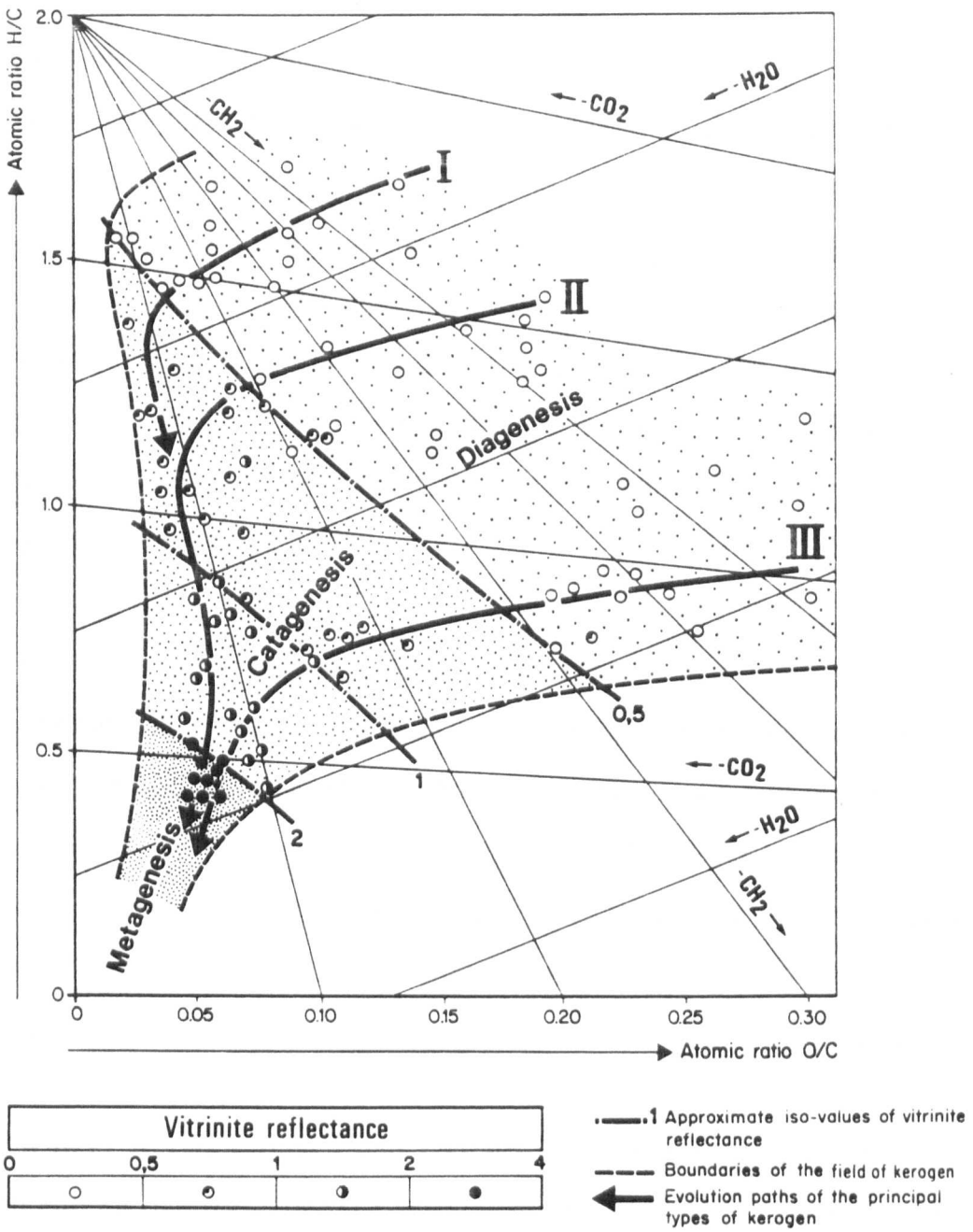

Figure 3-2 Van Krevelen diagram showing the evolutionary pathway of organic matter types (modified after Tissot and Welte, 1984)

pseudo- Van Krevelen diagram, based on their hydrogen index (HI) and oxygen index (OI), which broadly correspond to the thermal maturation tracks (Figure 3-3). The Rock-Eval pyrolysis, developed by the French in the 1970s does not require kerogen isolation and is more rapid and less expensive than elemental analysis. Espitalie et al., (1977) showed that oxygen in the kerogen is proportional to the carbon dioxide liberated during pyrolysis and that the hydrogen content is proportional to the hydrocarbons liberated. Although the pseudo- Van Krevelen diagram can be used to describe the type of organic matter in sediments, the results should be verified by optical microscopy, elemental analysis, or both (Peters, 1986).

Type I kerogen (also referred to as liptinite) (Espitalie et al., 1977) is dominated by algal organic matter and is usually deposited in marine and lacustrine environments. It also has high hydrogen and low oxygen contents due to the presence of aliphatic chains. Type II kerogen, may be subdivided into Type II a (sapropelic) which includes dinoflagellates, acritarchs and their degraded byproducts, and Type II b (exinitic) which includes the exinite macerals in coal. Therefore, Type II kerogen consists of degraded due to bacterial activity, aquatic and herbaceous organic matter and is laid down under reducing conditions in marine and lacustrine environments. It has a lower atomic hydrogen content than kerogen Type I and contains oxygen-bearing functional groups. Kerogen Type III can be deposited under both marine and non-marine environments and originates from terrestrial plants. Type III kerogen is similar to the vitrinite component of coal. It has a relatively low hydrogen and high oxygen content originating from the lignin and cellulose of higher terrestrial plants deposited in basins where suboxic to oxic conditions are achieved but in which no extensive oxidation occurs. Generally it consists of lignin-derived aromatic material, with a small proportion of lipid-derived aliphatic material. Kerogen Type IV, which is normally deposited under non-marine conditions, consists mainly of high-carbon residual organic matter. Type IV kerogen is similar to the

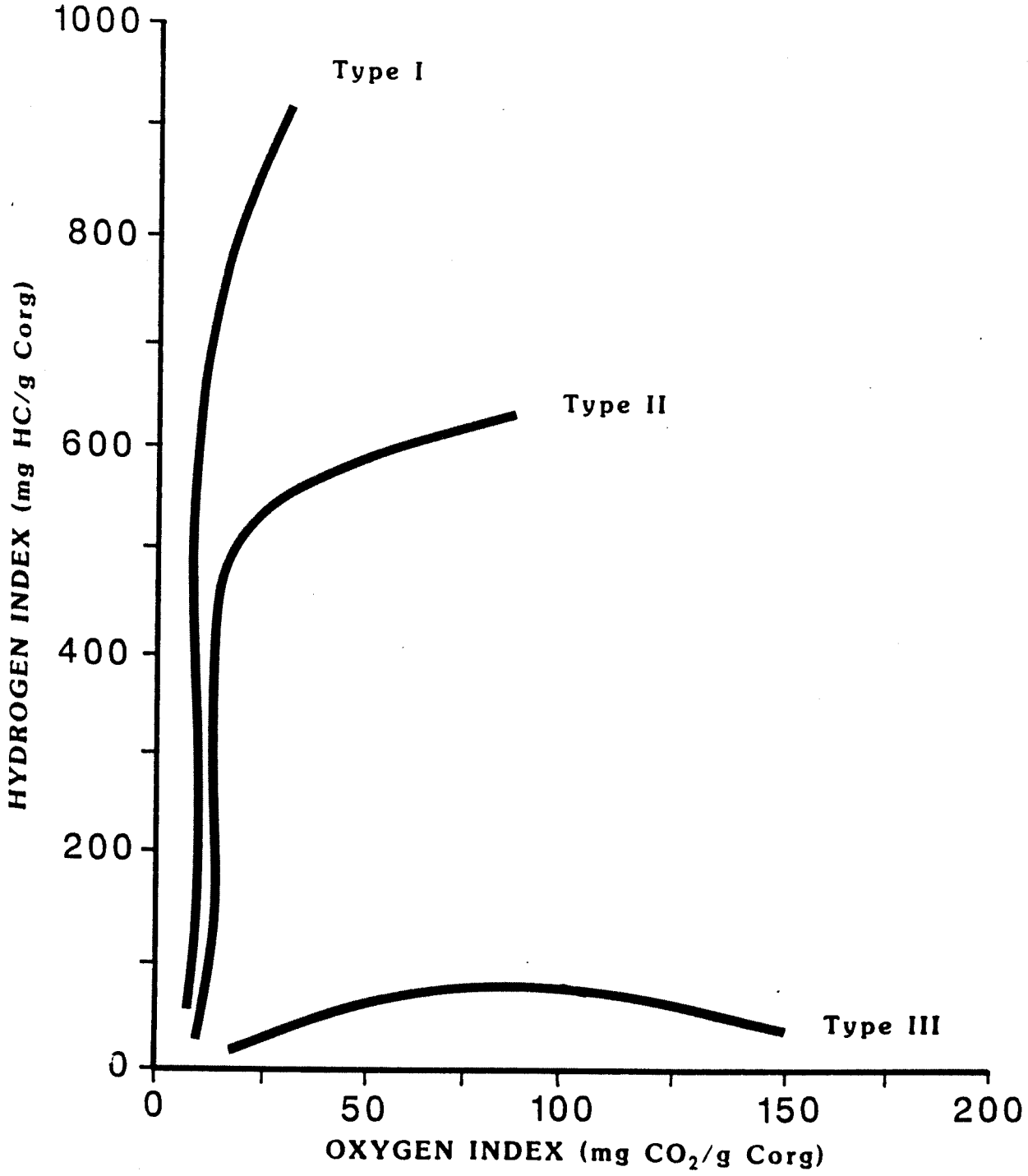

Figure 3-3 Pseudo-van Krevelen diagram showing kerogen evolutionary pathways

maceral inertinite in coal, has very high oxygen and negligible hydrogen content and is derived from carbonized, reworked or oxidized exinite and vitrinite. In addition, mixed kerogen Types II and III may be found in near-shore environments.

Figure 3-1 shows the approximate relationships between the three classification schemes and it should be emphasized that the schemes are not completely and directly analogous to each other. Organic petrologists frequently use the term amorphous kerogen to characterize unstructured sapropelic kerogen and liptinite and exinite to characterize structured algal and herbaceous kerogen (spores, pollen, cuticles, resins) respectively. Kerogen Type I is dominated by algal and amorphous organic matter, with some input of other kerogen types. Type II is dominated mainly by herbaceous organic matter, Type III by woody and Type IV by oxidized and recycled organic matter. Because of the absence of coal seams and the presence of organic matter dispersed in sediments in the study area, the classification scheme which is used throughout this study is based on a combination of organic petrology and Rock-Eval pyrolysis (Tissot et al., 1974; Alpern, 1980; and Tissot and Welte, 1984).

In Lower Palaeozoic (Cambrian to Devonian) sediments, higher plant organic matter is normally absent and maturity must be determined on alternative available and reliable organic matter. Dispersed organic matter identifiable in Lower Palaeozoic sediments consists of:

a) bitumen (Hunt et al., 1954; Abraham, 1960; Hunt, 1963; Jacob, 1976, 1985, 1989; Robert, 1973, 1980; Khavari-Khorasani, 1975; Alpern, 1980; Cornelius, 1984; Jacob and Hiltmann, 1988). In Canada, bitumen has been applied with some degree of success to determine the level of thermal maturity of Lower Palaeozoic successions by Goodarzi et al., (1985; 1989b); Bertrand and Heroux (1987); and Goodarzi and

Macqueen (1990).

b) graptolites (Watson, 1976; Kurylowicz et al., 1976; Teichmuller, 1978; Clausen and Teichmuller, 1982; Goodarzi, 1984; Kemp et al., 1985; Oliver, 1987; and Goodarzi et al., 1988a). In Canada, graptolite reflectance has been used for thermal maturity purposes by Goodarzi and Norford (1985; 1987); Bertrand and Heroux (1987); Bustin et al., (1989); Riediger et al., (1989); Link (1988); and Link et al., (1990).

c) chitinozoa (Eisenack, 1931; Tschudy and Scott, 1969; Jenkins, 1970). Reflectance studies on Ordovician and Silurian chitinozoans carried out recently by Goodarzi (1985a) and Bertrand and Heroux (1987) indicate that this fossil group has potential for use as a maturity and rank parameter.

d) dinoflagellates and acritarchs (Hufnagel, 1977; Erkmen and Bozdogan, 1980; Hutton, 1986; Sherwood and Cook, 1986). In Canada, colour alteration indices of the above fossils have been used for thermal maturity and burial history studies by Legall et al., (1981).

3.1.2 BITUMEN

Bitumen deposits are locally extensive and globally widespread. Extensive bitumen and heavy oil deposits occur in western Canada (Athabasca), Venezuela, the 'Utah Triangle' and California in the United States, Trinidad, the Malagasy Republic, Iran, and Turkey (Goodarzi and Williams, 1986). The Athabasca tar sands are the largest bitumen deposit in the world and they have been studied extensively (Brooks et al., 1988). The bitumen deposits of southwestern Iran were examined by Williams and Goodarzi (1981), Goodarzi and Williams (1986), while the bitumens of the United States

have been studied extensively by Hunt et al., (1954), Curiale (1986), and Khavari-Khorasani (1984). The bitumen deposits of Turkey have also been examined by Lebkuchner et al., (1972) and those from Canada by Khavari-Khorasani (1983); Goodarzi et al., (1985; 1989b) and Kirste et al., (1989).

Bitumen occurs in all sedimentary rocks of geological ages from Precambrian to Recent. Deposits of bitumen are relatively rare and in Quaternary sediments bitumen occurs as seeps or asphalt pools (Williams and Goodarzi, 1981). In contrast, bitumen in older sediments may occur in disseminated or concentrated form (Robert, 1980; Goodarzi et al., 1985; Jacob, 1989; Goodarzi and Macqueen, 1990). These solid oil bitumens ('migrabitumens', Alpern, 1978; Jacob, 1989) are often present in source rocks and reservoir rocks and are indicative of the presence of oil and gas as well as the level of thermal maturity and migration pathways of hydrocarbons (Robert, 1980, 1988; Goodarzi et al., 1985).

Bitumen deposits, besides being geographically widespread, can also be found near mineralization zones, particularly in Mississippi-Valley type ore deposits (i.e. Pine Point Pb-Zn deposit, Canada) (Macqueen and Powell 1983; Goodarzi and Macqueen, 1990) or even in Archaean rocks (Goodarzi et al., 1989b). Some of these bitumen deposits, such as Pine Point, Canada often contain a number of bitumen species including gilsonite, wurtzilite, albertite, glance pitch, grahamite and epi-impsonite (Khavari-Khorasani, 1984; Goodarzi and Macqueen, 1990).

Bitumen is a good indicator of thermal events because its physical (optical properties and density) and chemical properties (solubility, atomic H/C ratio) are affected by temperature, rate of heating, pressure and length of time of exposure to a certain temperature. The irreversible molecular changes in bitumen occur mostly in response to

increased temperatures (Khavari-Khorasani, 1975), and this is similar to changes in coal macerals (Bostick, 1979; Goodarzi and Murchison, 1978; Goodarzi, 1984). However, bitumen should be used with extreme care for thermal maturity interpretations because of the problems of migration, the presence of different bitumen phases and the different maturation path(s) relative to vitrinite.

The nature, properties and classification of bitumens have become of increasing interest to organic petrologists who are concerned with the microscopical evaluation of petroleum source rocks. Classification schemes for bitumen include those of Hunt et al., (1954), Abraham (1960), Hunt (1963), Jacob (1976, 1985), Khavari-Khorasani (1975), Cornelius (1984) and Jacob and Hiltmann (1988) (Figure 3-4). Jacob (1976, 1985) used the term 'migrabitumen' to designate the secondary origin of the bitumens generated from organic matter during diagenesis and catagenesis. The shape of these bitumens is adapted to the form of the cavities they occupy, i.e. interstices, fissures, diffuse distribution (Jacob, 1985).

Contrary to most coal macerals which are primary, bitumens are secondary organic matter derived from the heavier components of crude oil (Jacob, 1989; Kirste et al., 1989). They may be produced by biodegradation, de-asphalting and oxidation/weathering during the earlier stages of maturation or by advanced thermal maturation (Rogers et al., 1974; Kirste et al., 1989).

The study of bitumens is particularly important since carbonate rocks are present in the study area. Carbonates usually contain little or no vitrinite and Robert (1973) used the reflectance of insoluble solid bitumen (asphaltic pyrobitumen) as a substitute for vitrinite reflectance, noting that bitumen reflectance is almost the same as that of vitrinite (in the 1.0 - 2.0% Ro range). He stated (Robert, 1980) that bitumen

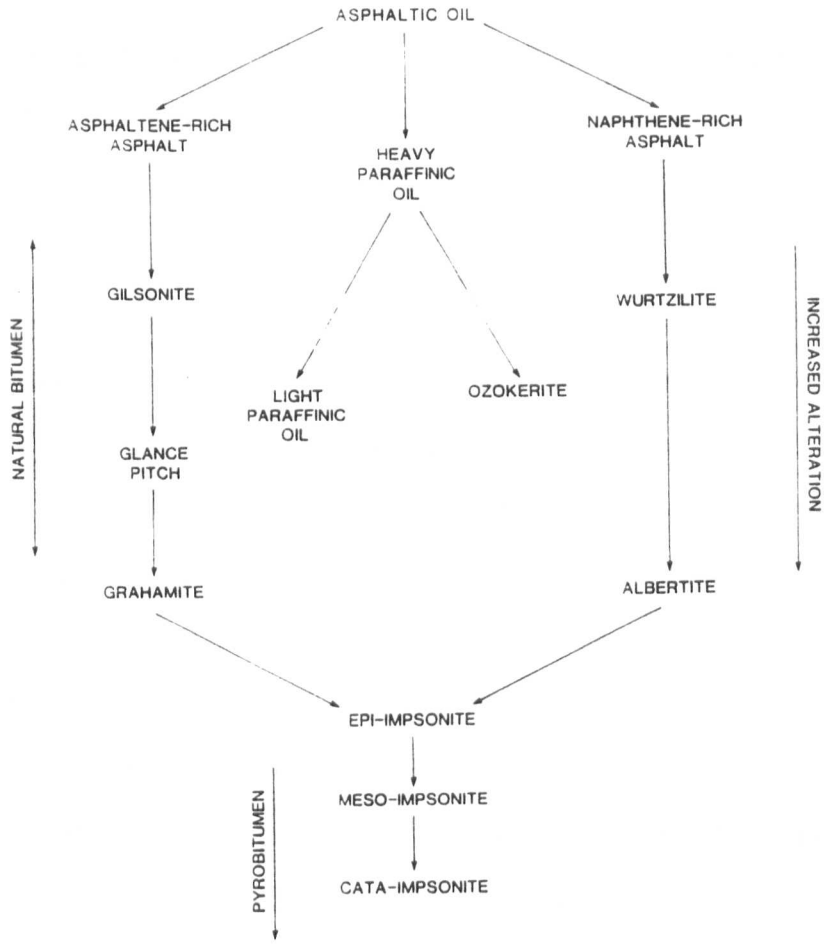

Figure 3-4 Genetic classification scheme of bitumens (modified after Jacob and Hiltmann, 1988)

reflectance shows slight differences when compared with vitrinite reflectance in maturation intervals of high- and medium-volatile bituminous coals (0.5 - 1.5% Ro vitrinite).

Jacob (1967) stated that above a reflectance level of 0.7% it becomes difficult to distinguish between bitumens. Grahamite and albertite can develop to epi- and meso-impsonite and then to cata-impsonite. During this process reflectance and anisotropy increase and very often a granular texture develops. Jacob's cross-plot and equation of solid bitumen reflectance against vitrinite reflectance (Jacob, 1983; 1985) make it possible to compare vitrinite reflectance with that of bitumen. This equation, named Jacob's formula, $R_v = 0.618\ R_b + 0.40$, where R_v is vitrinite reflectance and R_b is bitumen reflectance (Figure 3-5) shows that for vitrinite reflectance lower than 1.0%, bitumen reflectance is lower than that of vitrinite. Because bitumen reflectance increases more rapidly than vitrinite (lines diverge), both reflectances are similar in the Ro = 1.0 to 1.1% range, but disagree significantly when greater than Ro = 1.1%. Above this value solid bitumen reflectance is higher than vitrinite reflectance (e.g. predicted value of 2.6% for a vitrinite reflectance of 2.0%).

If several stages of generation and/or migration of bitumen occur, the generation with the lowest reflectance is representative of the degree of thermal maturity of the hydrocarbons being sought, because its reflectance is closely related to that of the vitrinite present in the same succession. However, the assumption is that the bitumen generation(s) did not occur at greatly different times, for example Palaeozoic and Cenozoic (Robert, 1980; Goodarzi et al., 1985).

Bitumen shows a great range in reflectance depending on type and maturity.

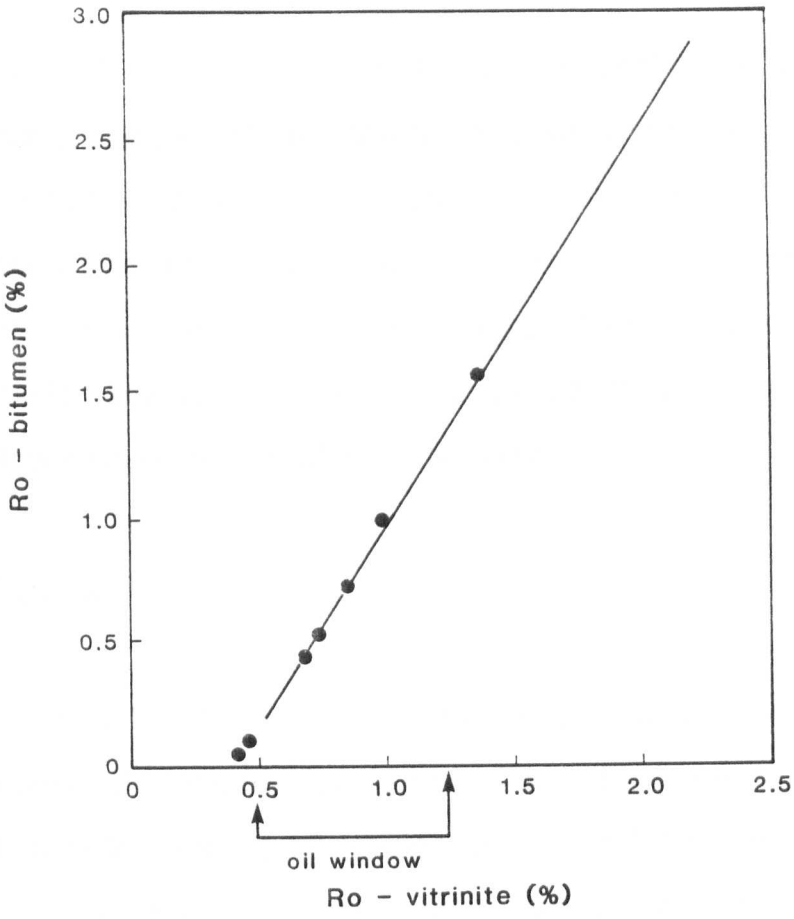

Figure 3-5 Relationship between vitrinite and bitumen reflectance (modified after Goodarzi and Macqueen, 1990)

According to Alpern (1980), many zooclasts (graptolites, chitinozoa, scolecodonts) are similar in appearance to bitumen, especially when present as small fragments making any morphological identification difficult. Consequently, a mixing of the reflectance of zooclasts with those of bitumen may increase the discrepancy between the resulting reflectance and the equivalent vitrinite reflectance (Bertrand and Heroux, 1987). Goodarzi (1984, 1985a) was able to distinguish graptolite and chitinozoa fragments from bitumen without difficulty (see also Goodarzi et al., 1985).

3.1.3 ORGANIC FOSSILS

The potential of using the optical properties of organic material to assess the level of thermal maturity of promising source rocks has been known for at least 25 years or more. According to White's (1935) 'carbon-ratio theory' a close relationship exists between the rank of coal and the occurrence of hydrocarbon deposits. Much later, Teichmuller and Teichmuller (1950) made rank determinations not only on coal seams but also on finely dispersed organic matter in sediments. McCartney (1952) introduced the photomultiplier for reflectance measurements on vitrinite, one of the most common and popular methods used in oil and gas exploration. Since the early 1970s the number of publications dealing with maturation studies has increased dramatically as have the studies applying vitrinite reflectance to solve basin analysis, tectonic history and palaeogeothermic problems. For more information on the recent advances in the field of Organic Petrology, the reader is referred to various reviews, such as Teichmuller and Teichmuller (1981), Stach (1982), Robert (1980), Bustin et al., (1985), Murchison et al., (1985), Murchison (1987) and Teichmuller (1987).

Assessing the thermal maturity of pre-Devonian sedimentary sequences using reflected-light microscopy is hindered by the rarity of vitrinite (van Gijzel, 1975; Goodarzi,

1984). Alternatively, the optical properties of other organic constituents common in Palaeozoic sediments, e.g. graptolites, chitinozoa, scolecodonts and acritarchs, as thermal maturation indices, have recently been investigated by several authors (Kurylowicz et al., 1976; Teichmuller, 1978; Legall et al., 1981; Clausen and Teichmuller, 1982; Goodarzi, 1984, 1985a; Goodarzi and Norford, 1985, 1987, 1989; Goodarzi et al., 1985; Kidwai, 1986; Goodarzi and Higgins, 1987; Bertrand and Heroux, 1987; Goodarzi et al., 1988a; Riediger et al., 1989; Link 1988; and Link et al., 1990).

Unlike solid bitumen, organic fossils are easier to identify, do not migrate and are less affected by degradation processes (Rogers et al., 1974; Goodarzi, 1984; 1985a; Bertrand and Heroux, 1987). Since the optical properties of chitinozoa and scolecodonts were not studied, only graptolites and dinoflagellates will be discussed.

3.1.3.1 GRAPTOLITES

The structure and terminology of the graptolite exoskeleton have been described extensively by Moore et al., (1952) and Crowther (1981). Manskaya and Drozdova (1968) suggest that the graptolite exoskeleton is composed of chitin, while Florkin (1969) suggests a scleroprotein composition.

The graptolite rhabdosome (skeleton of colony) consists of theca, a chitinoid compartment occupied by the zooid; aperture, the external opening of each tube in the skeleton; common cannal, the cavity around the virgella into which the thecae open; and the virgella, a continuous central structure that extends as a spine colony (Figure 3-6).

Recently, graptolite reflectance has been used as an alternative to vitrinite reflectance to assess thermal maturity in Ordovician and Silurian rocks. Although the

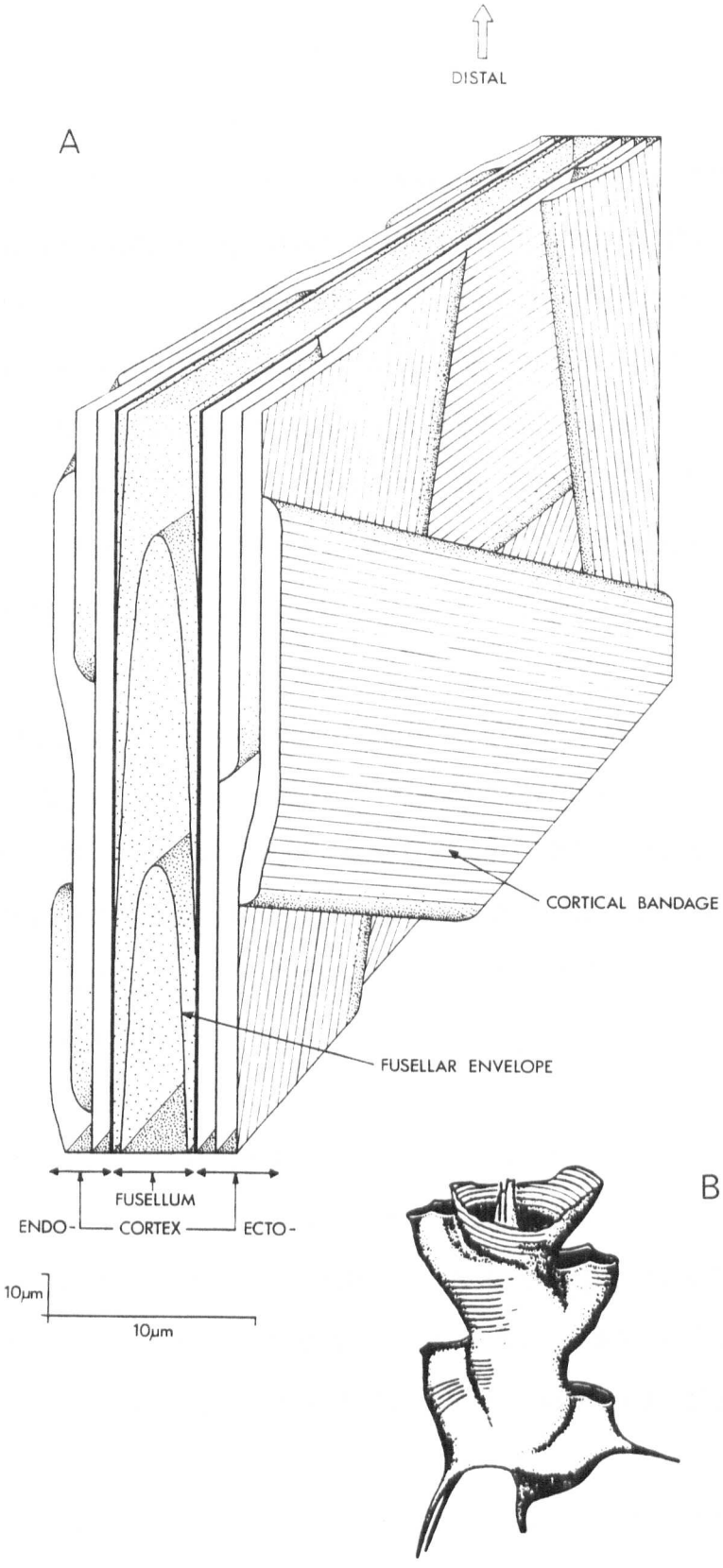

Figure 3-6 Simplified morphology of graptolite (A), and simplified graptolite periderm wall (B) (modified after Goodarzi, 1984)

original idea of using graptolite reflectance was conceived at the University of Newcastle-upon-Tyne, UK in the early 1970s, further studies to test the new method did not materialize until the study of Watson (1976) in Scotland. He observed that graptolite reflectance increased towards dykes and plutons in the southern Uplands. The work of Watson was later followed by Kurylowicz et al., (1976) in Australia, by Teichmuller (1978) and Clausen and Teichmuller (1982) in Germany, by Goodarzi (1984) in Turkey, by Goodarzi and Norford (1985; 1987; 1989) and Bustin et al., (1989) in Canada and by Kemp et al., (1985) and Oliver (1987) in the British Isles.

Kurylowicz et al., (1976) examined beds in the Cambro-Ordovician Larapinta Group of the Amadeus Basin, central Australia. The sediments contained graptolites with a Ro max of 0.80 to 2.37% and a bireflectance of 0.35 to 1.05%. Graptolites appeared as coalified thin and elongated bodies, having a complex skeletal morphology. The above authors stated that the graptolite bireflectance in the Amadeus Basin is higher than that of vitrinite having the same Ro max.

Teichmuller (1978) described the morphology of a suite of graptolites from Germany. The Ro max recorded ranged from 0.80 to 10.0%, and the graptolites consisted of a lamellar cortex, possessing fibrous structure and a central canal. Clausen and Teichmuller (1982) recorded remarkably low Ro max values for Swedish graptolites (0.36 - 0.72%), but values ranging from 0.80 to 12.4% for German graptolites.

Systematic studies of the morphology and optical properties of graptolite fragments have been carried out by Goodarzi (1984, 1985b) and Goodarzi and Norford (1985; 1987; 1989). Goodarzi (1984) studied graptolite fragments from drillholes in southeast Turkey and was able to detect two types of surface morphology, a granular and a non-granular. The non-granular graptolite fragments had higher reflectance and

bireflectance than the granular fragments. Goodarzi (1984) stated that graptolite fragments show true maximum reflectance in sections parallel to bedding and behave as optically biaxial material. Therefore, the Ro max (mean max) is a more consistent criterion than random reflectance and is the true indicator of maturity. Reflectance of natural bitumen present in the same succession was lower than that of graptolites (Goodarzi, 1984; Bustin et al., 1989).

Goodarzi and Norford (1985; 1987; 1989) studied the changes in the optical properties of graptolite skeletal material (reflectance, bireflectance, refractive and absorptive indices) produced by temperature changes related to depth of burial. They stated that the reaction to temperature of graptolite skeletal material appears to be similar to that of bitumen but somewhat different from that of vitrinite and exinite macerals in coal.

Goodarzi (1985b) studied the dispersion of optical properties of graptolite epiderms in Lower Palaeozoic sediments with low to high maturity level (CAI = 1-5) in the visible spectrum (450 - 650 nm). The dispersion follows similar trends to those of coal macerals and bitumen, indicating similar molecular structural changes. In addition, the dispersion of the optical properties of graptolites in low-maturity sediments falls from blue to red, whereas in more mature sediments it rises over the same range. The % Ro of graptolite epiderms increases with the degree of thermal maturation of its host rock, indicating that graptolites are sensitive to rise in temperature and can be useful indicators of the maturity of Early Palaeozoic sediments.

Finally, Goodarzi et al., (1988a) and Goodarzi and Norford (1989) are probably the first studies where an indirect correlation between the optical properties of graptolites and those of vitrinite has been established using conodont alteration indices (CAI). In

general, graptolites show higher reflectance levels than vitrinite for the same conodont indices of thermal maturity (Goodarzi and Norford, 1989).

3.1.3.2 DINOFLAGELLATES-ACRITARCHS

Dinoflagellates are unicellular algae, mostly planktonic and marine, although freshwater and benthonic forms also exist (Sherwood and Cook, 1986). When sinking to the bottom, the outer walls decompose and resistant parts are preserved as dinocysts. In general, thick-walled varieties are characteristic of littoral environments, whereas thin-walled types are found in offshore sediments (Sherwood and Cook, 1986).

Acritarchs are very similar to dinoflagellates in morphology but they have an uncertain origin. They are dominantly marine organisms and forms with long processes are commonly found in quiescent offshore environments, whereas in nearshore turbulent conditions, naked or short-processed forms are prevalent. Bituminous shales containing dinoflagellates and acritarchs are classed as marine (Hutton, 1986; Goodarzi et al., 1989a) because of their content of palynomorphs. Some marine sediments typically contain dinoflagellate-and acritarch-derived amorphous fluorescing matrix.

For further information on the fluorescence of the dinoflagellates and acritarchs the reader is referred to Hufnagel (1977).

3.1.4 SECONDARY ORGANIC MATTER

3.1.4.1 AMORPHOUS FLUORESCING MATRIX (BITUMINITE, LAMALGINITE)

The term 'bituminite' has not become widely accepted even although it has

been extensively described and used by Teichmuller and Ottenjann (1977) and Teichmuller (1982). Although the properties of 'bituminite' are intermediate between those of vitrinite and the strongly fluorescing liptinite macerals, many authors do not use the term 'bituminite' because of the connotation of bitumen in the term. Recognition and classification of 'bituminite' have been a problem for organic petrologists over the years.

Amorphous fluorescing material is a degradation product of hydrogen-rich organic matter, i.e. coal macerals and kerogen (Murchison, 1987; Teichmuller, 1982; 1987) formed under predominantly anoxic conditions. Presumed source materials are algae, faunal plankton and bacterial bodies (Teichmuller and Ottenjann, 1977; Gormly and Mukhopadhyay, 1983; Snowdon et al., 1986). Cook (1980) suggested a genesis of amorphous fluorescing matrix from algal-fungal mats growing on the surface of the sediment near the oxic-anoxic boundary, whereas Gutjahr (1983) considered the amorphous matrix to be of bacterial origin. In the Canadian Arctic Islands, it is found in marine and lacustrine petroleum source rocks (Goodarzi et al., 1987a; Goodarzi et al., 1989a), although in source rocks containing vitrinite, it may have assimilated degradation products of humic origin (Goodarzi and Stasiuk, 1987b).

Amorphous fluorescing material is generally associated with alginite and liptodetrinite (Teichmuller and Ottenjann, 1977; Creaney, 1980a; Sherwood and Cook, 1986) and it has been described by Goodarzi et al., (1987a) in the oil shales of the Emma Fiord Formation, Devon Island, Canadian Arctic Archipelago. It has no definite form, no specific morphology and, in petroleum source rocks commonly occurs as streaks, lenses or as groundmass for other macerals and for minerals (clays, carbonates). With increasing degree of diagenesis the reflectance of amorphous fluorescing material rises and the fluorescence intensity decreases. At a vitrinite reflectance level of 0.8 to 0.9% Ro visible fluorescence of bituminite and lamalginite is usually lost.

3.1.4.2 EXSUDATINITE

This material generally occurs in vein-form or as fillings of bedding-plane joints and also in empty cell lumens. It develops from the lipid components of hydrogen-rich organic matter and its genesis is related to that of liquid petroleum (secondary resinite of Jones and Murchison, 1963; Teichmuller, 1974; 1982; Murchison, 1976; Shibaoka, 1978). In the Canadian Arctic Islands, exsudatinite has been described by Goodarzi et al., (1987b) in Lower Carboniferous oil shales from the Grinnell Peninsula, Devon Island.

Exsudatinite ('eubitumen' of Potonie, 1950) was reported by Hamrla (1956) as cavity-filling 'bituminite' in Eocene bituminous coals from Istria. Later, Jones and Murchison (1963) observed fluorescing organic matter, similar to exsudatinite (secondary resinite) in Tertiary lignites from the Halle-Leipzig area, East Germany and in Carboniferous bituminous coals from the Northumberland and Yorkshire coalfields, UK. Although this organic matter exhibited spectra slightly different than resinite sensu stricto, they classified it as 'secondary resinite'. This 'secondary resinite' of Jones and Murchison (1963), which later on Teichmuller (1974) described as exsudatinite, has been accepted by the International Committee for Coal Petrology.

Exsudatinite, as the name indicates, is an exudate which is given off by macerals and dispersed organic matter during maturation. Its fluorescence intensity and colour vary widely, even in a single crack filling. At low maturation levels exsudatinite appears black in reflected light/oil immersion and is difficult to distinguish from empty fissures and cavities. Its excitation colour is bright yellow to dull orange fluorescence (Teichmuller, 1974).

Generally, exsudatinite has a slightly lower reflectance and higher fluorescence

than the parent liptinite or exinite and usually shows negative alteration after prolonged irradiation. The generation of highly fluorescing exsudatinite has been observed in coals and organic-rich sediments up to 1.0% Ro. Beyond this maturity level the reflectance of exsudatinite is generally greater than that of vitrinite which, according to Kantsler (1980), is probably due to better plasticity and more condensation of the aliphatic molecular complexes compared with the more rigid ring systems of vitrinite.

CHAPTER IV

CHAPTER IV

4.0 HYDROCARBON-GENERATING POTENTIAL OF ORGANIC MATTER

Organic matter can conveniently be classified into three groups according to its H/C and O/C atomic ratios (Tissot et al., 1974; Harwood, 1977). Type I organic matter has an initial H/C ratio of >1.3, Type II has an initial H/C ratio of 1.0 to 1.3, and Type III a H/C ratio of 0.8 to 1.0. In addition, Harwood (1977) introduced Type IV with initial H/C ratio of <0.8. The atomic H/C and O/C ratios decrease with increasing maturation and different organic matter types have different maturation thresholds for hydrocarbon generation. As Tissot et al., (1980) have indicated, Type I organic matter does not begin to generate hydrocarbons until a reflectance level of 0.70%, compared with 0.50% Ro for Type II organic matter (Powell and Snowdon, 1983).

Organic matter with a high H/C ratio generates primarily oil, whereas organic matter with initially lower H/C ratio (Type III) generates more gas and less oil upon burial than the more hydrogen-rich Types I and II, although as Brooks et al., (1969) and Powell and McKirdy (1975) have shown, many Australian oils have been generated from terrestrially-derived organic matter.

The oil-source potential of terrestrial organic matter is related to the proportion of hydrogen-rich components present and, in terms of coal petrological description, the liptinite (or exinite) group of macerals is enriched in hydrogen relative to vitrinite. Type II terrestrial organic matter usually produces waxy oils at reflectance levels of 0.50% Ro. Lacustrine Type I organic matter which has undergone extensive microbial degradation can generate highly-waxy oils (Tissot and Welte, 1984).

Highly euxinic marine-source rocks from carbonate-evaporite or phosphatic regions generate oil at lower levels of maturation than do clastic marine source rocks (Powell and Snowdon, 1983). Differences in maturation threshold are attributed to differences in activation energy associated with the dominant chemical structural type of the organic matter present. Tissot et al., (1980) indicated that Type I organic matter requires more time and/or temperature for petroleum generation than Type II organic matter. When terrestrial organic matter is rich in resinite, less time and lower temperatures are required to generate liquid hydrocarbons than Type II organic matter devoid in resinite.

4.1 HYDROCARBON GENERATION OF ORGANIC MATTER AS APPLICABLE TO THE CANADIAN ARCTIC

Powell and Snowdon (1983) reviewed the hydrocarbon-generating potential in the Canadian Arctic Basins and concluded that the pre-oil generation stage is indicated by reflectance values below 0.50% Ro. When the organic matter is hydrogen-rich (Type II), liquid hydrocarbons are generated in the catagenetic stage and the hydrocarbon yield reaches its maximum at a vitrinite reflectance level of 0.70% Ro. Terrestrial organic matter (Type III) shows no significant liquid hydrocarbon potential unless plant resins are present. Since resinite makes up 10-15% of the total organic matter in the Upper Cretaceous-Tertiary sediments in the Beaufort-Mackenzie delta, Powell et al., (1978) and Snowdon (1980) have suggested that resinite is the source of hydrocarbons in the area and that they have been generated at reflectance levels below 0.60% Ro. Resinite can also be the source of gas-condensate at reflectance levels of >0.55% Ro (Snowdon and Powell, 1982). The gas in the Beaufort-Mackenzie is thermogenic and has been generated at an early stage (Ro = 0.45-0.60%) (Powell and Snowdon, 1983). Other authors have also suggested that an early thermogenic phase of gas generation, which is

separate from the formation of biogenic gas, may be significant in forming accumulations of gas at low maturity levels (Hitchon, 1963; Stroganov, 1973; Stahl, 1977; Connan and Cassou, 1980; Monnier et al., 1983). Monnier et al., (1983) have shown that there is a five-fold increase in gas yield, per unit weight of organic carbon, in the reflectance range of 0.55-0.65% Ro, from terrestrial organic matter (Type III), reaching a maximum at the onset of liquid hydrocarbon generation. The amounts of gas generated from Type II organic matter at the marginally mature to mature stage of hydrocarbon generation is one-third of that generated from Type III organic matter and the main phase of gas generation from Type II organic matter takes place in the overmature stage due to extensive cracking of the liquid hydrocarbons (Powell and Snowdon, 1983). According to Powell and Snowdon (1983), in the Canadian Arctic the threshold of liquid hydrocarbons generation is delayed in Type III organic matter relative to Type II organic matter but the peak of oil generation is approximately coincidental.

Terrestrial organic matter is the source of hydrocarbons not only in the Beaufort-Mackenzie Basin, but also in the Labrador and Scotian Shelves (Snowdon and Powell 1982) and in the Cretaceous Deep Basin of Alberta (Welte et al., 1982). The major difference is the level at which the hydrocarbons were generated. The terrestrial organic matter in the Beaufort-Mackenzie is rich in resinite and has yielded a naphthenic oil and gas-condensate at relatively low maturity levels. In the Scotian Shelf the product is mainly gas-condensate and minor amounts of oil forming in the main stage of hydrocarbon generation. To the contrary, gas-condensate in the Labrador Shelf was generated in the mature to overmature stages of hydrocarbon generation, whereas in the Alberta Basin, gas is a product of organic matter overmaturity (Powell and Snowdon, 1983).

CHAPTER V

CHAPTER V

5.0 DEVELOPMENT OF FLUORESCENCE MICROSCOPY, ROCK-EVAL PYROLYSIS AND CORRELATION BETWEEN MATURATION PARAMETERS

INTRODUCTION

Fluorescence microscopy and Rock-Eval pyrolysis are extensively used in determining the level of thermal maturity and source-rock potential of sedimentary rocks, in conjunction with vitrinite reflectance. In addition, biological marker geochemistry has been used in oil to oil and oil to source rock correlations at vitrinite reflectance levels below 0.70% (Murchison, 1987; Kirste et al., 1989). In this chapter the development of fluorescence microscopy, Rock-Eval pyrolysis and correlations between vitrinite reflectance, fluorescence and Rock-Eval parameters will be discussed.

5.1 FLUORESCENCE MICROSCOPY

The liptinite constituents show greater liquid-hydrocarbon potential than vitrinite which is considered principally as gas producer. The fluorescence properties of exinite macerals are used to determine the maturity and source-rock potential of sediments (Teichmuller and Durand, 1983; Goodarzi et al., 1987a). A more clean differentiation of the various exinite macerals can also be achieved using fluorescence because macerals of this group are difficult to identify in reflected light due to their low reflectances. Van Gijzel (1966; 1967; 1971) was one of the first workers to study the fluorescence of fossil spores and pollen. He extended his studies to cuticles, wood and a range of sedimentary organic matter (van Gijzel, 1975). He plotted the shift of the spectral maximum of the emission spectrum of microspores and the percentage of 'fading' of the entire

fluorescence intensity after 30 min. of irradiation. The parameters that are most commonly used at present are:

(a) the wavelength (λmax) between 400 and 700 nm at which peak relative intensity of fluorescence emission occurs;

(b) the spectral quotient (Q) being the ratio of the relative fluorescence intensity at 650 nm compared with that at 500 nm;

(c) the spectral quotient (Q max), which is the ratio of the relative fluorescence intensity at λmax compared with that at 500 nm; and

(d) A_I, the alteration of intensity ('fading' of van Gijzel, 1975) at 546 nm recorded 30 min. after irradiation of the field had begun.

Ottenjann et al., (1975) produced a sequence of spectra from sporinites in the range between peat and medium-volatile bituminous coal. They showed a satisfactory correlation between carbon content and fluorescence parameters (λmax and Q) for sporinites and soon after correlations were established between vitrinite reflectance on the one hand and fluorescence parameters of sporinite, cutinite and fluorinite (essential plant oil) (Teichmuller, 1982) on the other (Teichmuller and Durand, 1983). In general, the fluorescence intensity of exinite macerals decreases with increasing rank. As rank increases a shift in fluorescence occurs from blue to red end of the spectrum. At low rank, the fluorescence intensity of huminite (the precursor of vitrinite) can be as high as that of some exinite macerals (Kantsler, 1980). The fluorescence of exinite macerals may change following short or prolonged irradiation. This change may be either a positive or a negative shift in both spectrum and intensity and is dependent on type and rank of the enclosing coal maceral. Fluorescence is generally lost at 1.35 to 1.4% Ro max (the oil 'deadline'). Cook (1980) was able to place members of a series of organic-rich rocks in different order of maturity depending on the ranking parameter used. Fluorescence microscopy allows a more detailed and accurate petrographic assessment of both coals

and source rocks than reflected-light microscopy despite the fact that at any particular rank-level fluorescence parameters may vary widely. The wide use of fluorescence microscopy has largely contributed to a more precise identification of exinite macerals.

5.2 ROCK-EVAL PYROLYSIS IN COALS AND OF TYPES I AND II ORGANIC MATTER IN SEDIMENTS

The best known, by far, analytical development of bulk-flow pyrolysis systems is the "Rock-Eval" system (Espitalie et al., 1977). Information, such as level of thermal maturity of the organic matter and quantity of distillable material which the organic matter can generate, may be obtained and the system's usefulness to petroleum organic geochemistry is still being assessed. The pyrolysis data were pivotal regarding conclusions on the level of maturity and source-rock potential of Mesozoic sediments in Sverdrup Basin.

The way in which the Rock-Eval system operates is that the crushed rock (mainly cuttings but also core) is heated over a temperature range from ambient to 550°C. The products of pyrolysis develop three chromatographic peaks, namely S_1, S_2, and S_3. The first two peaks are subsequently analyzed by a flame-ionization detector, the gas-producing S_3 peak by a thermal conductivity detector. The series of parameters that can be determined is given in Table 1. For definition of the parameters and interpretive guidelines the reader is referred to Chapter VI, Section 6.5.

Over the years, correlations between Rock-Eval parameters and other maturity parameters have been attempted. Teichmuller and Durand (1983) observed a close relationship between the temperature of maximum hydrocarbon release (referred to as

TABLE 1

Geochemical Parameters Describing Source Rock Generative Potential

Quantity	TOC (wt.%)	S1*	S2*
Poor	0 - 5	0 - 0.5	0 - 2.5
Fair	0.5 - 1	0.5 - 1	2.5 - 5
Good	1 - 2	1 - 2	5 - 10
Very good	2+	2+	10+

* Nomenclature:
S1 = mg HC/g rock
S2 = mg HC/g rock

Type	HI (mg HC/g C_{org})*	S2/S3*
Gas	0 - 150	0 - 3
Gas and oil	150 - 300	3 - 5
Oil	300+	5+

* Assumes a level of thermal maturation equivalent to R_o = 0.6%

Maturation	PI [S1/(S1 + S2)]	T_{max} (°C)	R_o (%)
Top oil window (birthline)	~ 0.1	~ 435-445*	~ 0.6
Bottom oil window (deadline)	~ 0.4	~ 470	~ 1.4

* Many maturation parameters (particularly T_{max}) depend on type of OM. (from Peters, 1986)

Tmax in °C) and vitrinite reflectance in coal, concluding that Tmax could be used as a rank parameter for coals. They also showed that there was a considerable variation in the amount of hydrocarbons released by pyrolysis at any given rank, this variation being due to variations in the petrographic composition of the coals.

Powell and Snowdon (1983) and Mukhopadhyay et al., (1985) developed classification schemes of dispersed organic matter based on maceral composition, fluorescence properties, atomic H/C ratio, range of hydrogen index from Rock-Eval pyrolysis, types of hydrocarbons generated and environment of deposition (Figure 5-1). Other critical information, such as the production index (PI) $[S_1/(S_1 + S_2)]$ can also be determined using Rock-Eval. For detailed discussions the reader is referred to Leventhal (1982), Katz (1983), Teichmuller and Durand (1983) and Tissot (1984). One of the major problems associated with Rock-Eval is that mineral-matrix effects can influence both the quantity and the composition of pyrolysates (Larter, 1984), particularly when the samples are very rich in carbonates, clays (catalytic effect) or when the total organic-carbon content is too high (i.e. coals). For a more detailed analysis of the effect of organic matter types on Rock-Eval results, effect of minerals, migrated oil and others, the reader is referred to Chapter VI, section 6.5.

5.3 CORRELATION AMONG MATURATION PARAMETERS

Vitrinite is composed mainly of clusters of condensed aromatic rings linked with chains and stacked on top of one another. Increasing maturity results in the clusters fusing into larger, condensed aromatic ring structures which increase in size causing increased reflectivity. Changes in the molecular structure of vitrinite are caused by irreversible chemical reactions, the rate of which increases with temperature. As a result, reflectance, which detects these maturation changes, increases exponentially with a

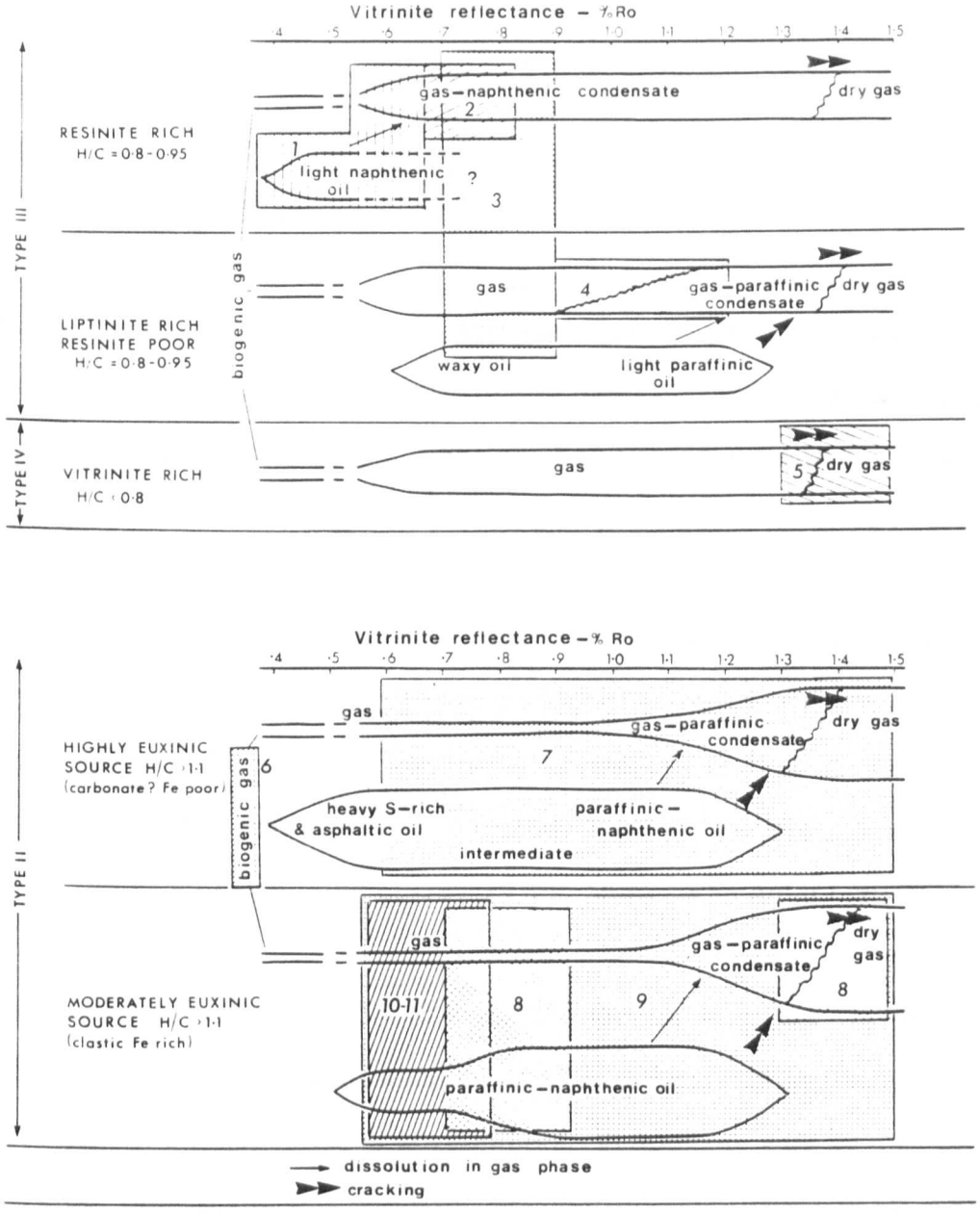

1 - Tertiary, Beaufort-Mackenzie Basin, 2 - Lower Cretaceous, Beaufort-Mackenzie Basin, 3 - Scotian Shelf, 4 - Labrador Shelf, 5 - Mesozoic Deep Basin, Alberta, 6 - Cretaceous, South Eastern Alberta, 7 - Middle Devonian, Northern Alberta/British Columbia, 8 - Sverdrup Basin, 9 - Upper Devonian, Mississippian, Alberta, 10 - Upper Cretaceous, Alberta, 11 - Jeanne D'Arc Sub-basin, E. Newfoundland

Figure 5-1 Hydrocarbon generation models for Types II and III organic matter in different depositional environments (modified after Powell and Snowdon, 1983)

linear increase in temperature (Hunt, 1979).

Vitrinite reflectance is the most common maturation index used in geological studies (Jones and Edison, 1979). Its validity has been challenged (Powell et al., 1982; Price and Barker, 1985; Durand et al., 1985) pointing to weaknesses of the method and recommending their own alternatives.

Vitrinite reflectance defines the zone of catagenesis within which liquid and gaseous hydrocarbons are formed and may be used to interpret the sedimentary and tectonic history of basins. It is less applicable in defining the oil- and gas-generating capability of sedimentary rocks and to studies related to the origin of biogenic hydrocarbon accumulations occurring in shallow immature sedimentary strata.

Vitrinite reflectance may be affected by factors such as: 1) mineral matrix (lithology), 2) bitumen impregnation (staining), and 3) differences in the type of vitrinite, which is a reflection of the depositional environment. In addition, vitrinite may be oxidized in the subsurface, particularly along major, regional unconformities or in sedimentary strata in contact with meteoric waters. Nevertheless, vitrinite reflectance has the advantage over other maturation techniques (fluorometry, Rock-Eval pyrolysis, organic geochemistry) because it covers the entire temperature range from early diagenesis through catagenesis into metamorphism.

Vitrinite reflectance has also been correlated to kerogen thermal alteration index (TAI), which is based on colour changes of kerogen, and elemental analysis of kerogen. Most importantly, vitrinite reflectance values have been compared and contrasted with spectra fluorescence analysis and Rock-Eval pyrolysis, particularly over the last 15 years. Therefore, this correlation is the subject of the subsequent discussion

because all three techniques were used extensively in the present study.

The temperature index, Tmax, obtained from Rock-Eval pyrolysis has also become a widely used maturation index (Tissot and Welte, 1984). The value of Tmax increases in response to increasing maturation of the organic matter. Espitalie et al., (1985) showed that the range of variation of Tmax is narrow for marine Type I organic matter (algae only), wider for Type II organic matter (dinoflagellates, bituminite, resinite, sporinite) and still wider for Type III organic matter (vitrinite). The consequence is that Tmax is not recommended as a maturation parameter in Type I organic matter because of its small variation with maturity but provides a better maturation index for Types II and III organic matter (Tissot et al., 1987). Further, the Rock-Eval parameters should be used with extreme caution in the determination of maturity and source-rock potential of outcrop samples because weathering and oxidation are most likely in surface samples. In contrast, vitrinite reflectance and fluorescence properties can be used with care, although when oxidation is severe, the use of fluorescence is more risky than reflectance.

Teichmuller and Durand (1983) showed an excellent relationship between Tmax and vitrinite Ro for coals. The onset of the 'oil window' for Type III organic matter in sediments (~0.5% Ro) corresponds to a Tmax value of approximately 430°C (Espitalie et al., 1985) (Figure 5-2), whereas the main gas generation phase for Type II organic matter in sediments occurs at Tmax values of 450-455°C, and for Type III organic matter at 465-470°C. The oil 'death line' is indicated by a Tmax of approximately 465°C and values greater than 520°C indicate the dry gas zone (Figure 5-2).

Ottenjann et al., (1974), Teichmuller and Ottenjann (1977), and Teichmuller and Durand (1983) have studied extensively the fluorescence of exinite macerals during coalification. The results of Teichmuller and Durand (1983) show a good relationship

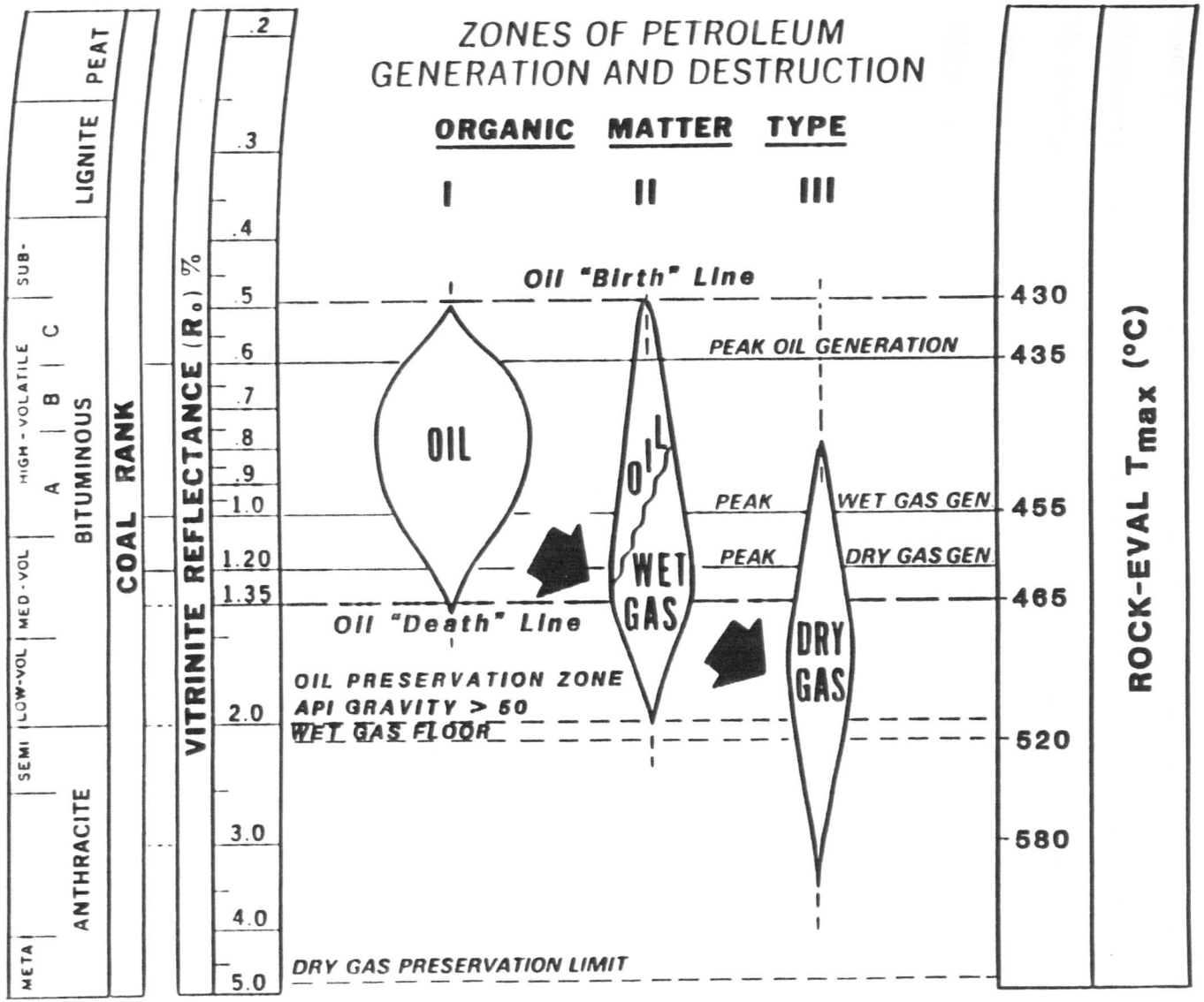

Figure 5-2 A comparison of vitrinite reflectance, hydrocarbon generation zones and Rock-Eval (Tmax) (modified after Dow, 1977 and Teichmuller and Durand, 1983)

between fluorescence parameters, vitrinite reflectance and Rock-Eval parameters, thus confirming that fluorescence is a useful tool for determining the rank of coal and maturity level of source rocks. Relative to vitrinite reflectance, the changes in fluorescence are somewhat irregular. Fluorescence changes rapidly (increase in λmax and R/G Q) at an Ro vitrinite level of 0.35-0.5%, followed by a rapid shift of λmax to higher wavelengths and loss of fluorescence intensity at an Ro level of 0.8-0.9% (Teichmuller and Durand, 1983). Above 1.2% Ro fluorescence intensities are so low that they cannot be measured.

CHAPTER VI

CHAPTER VI

6.0 EXPERIMENTAL

6.1 SAMPLE COLLECTION AND PREPARATION

A total of approximately 2,000 core and cuttings samples taken from Palaeozoic and Mesozoic sediments in 43 drillholes were collected at the core depository of the Institute of Sedimentary and Petroleum Geology in Calgary, Alberta. The depth of the samples is listed in Appendix I. Samples were collected from lithological intervals in the Mesozoic known to be rich in organic matter (shales). The vertical distance was kept to a maximum of 50 m, but in organic-rich sediments (source rocks) a much smaller sampling interval (~10 m) was employed. The thickness of rocks covered by each sample is approximately 3 to 5 metres. Cutting samples were also collected from other lithologies (carbonate, sandstone) from the Palaeozoic of Melville Island.

All samples were hand-picked and consultation was made using the available well logs (resistivity, gamma-ray, density) in order to identify the lithology and eliminate possible contamination from cavings. Contaminated organic matter was identified optically (using both incident white light and ultra-violet excitation).

The followed procedure in preparing the samples for microscopical examination is similar to that used in coal petrology (Mackowsky, 1982). The cuttings were placed in plastic "Teflon" moulds, mixed with epoxy resin and hardener, and let cure overnight. Then, they were ground using isopropyl alcohol and paper (250 and 600 grit respectively). Isopropyl alcohol, instead of distilled water, was used to polish those samples having high mineral matter content in order to minimize the swelling of the clays and reduce the relief

of the sample. Polishing was performed using two grades of alumina powder (0.3 and 0.05 μm) and silk cloth. Core samples were hand polished using the procedure outlined above. The graptolite samples were polished following the method described by Goodarzi and Stasiuk (1987a). This is a modification of the coal/dispersed organic matter polishing method in that the graptolite samples were polished on wet blocks of wood using the same two grades of alumina powder.

6.2 EQUIPMENT USED

Reflectance analysis of the dispersed organic matter was primarily carried out at the Institute of Sedimentary and Petroleum Geology, using a reflected light Zeiss MPM II microscope equipped with both halogen (12V, 100W) and mercury vapour (HBO, 100) light sources. In addition, a Leitz MPV II compact microscope was used at the Organic Geochemistry Unit, the University of Newcastle. The microscope was attached to a Zonax microcomputer and Epson printer. Epiplan-"Neofluor" oil immersion objectives were used, with the oil having a refractive index equal to 1.518 at 546 nm. The magnification power of the objective is X 40 (N.A. X 0.90), of the ocular is X 10 and of the lens in the direct path of the light source is X 1.6, for a combined magnification of X 640.

A series of six glass standards was used for standardizing the microscope prior to reflectance measurements. Each glass standard has its own refractive index and calculated reflectance. The diameter of the measuring aperture (field diaphragm) used for vitrinite reflectance determinations is 0.32.

Vitrinite reflectance in the Mesozoic succession was generally <1.0%, therefore random reflectance was recorded. This is achieved by not inserting the polarizer in the light's direct path and by not rotating the microscope's stage. In addition, the vitrinite

fragments were so small in numerous samples that any rotation of the stage would have been time-consuming and have resulted in erroneous values since it is very easy for the aperture to deviate from the phytoclast fragment towards the mineral matrix or binding medium (epoxy).

Although it is not known precisely when anisotropy becomes significant in rank determination, reflectance on all vitrinite and bitumen fragments in the Palaeozoic of Melville Island beyond 1.0% Ro is recorded as Ro, max because of the degree of anisotropy present. In this case, the polarizer was inserted into the light's path, the microscope's stage was rotated 360° and the Ro, max was measured for the bitumen fragments. In addition, Ro, max of bitumens was needed to construct the evolutionary pathway of bitumen and vitrinite, the bituminization curves as well as the relationship between vitrinite and graptolite reflectance using the colour alteration index of conodonts as an intermediate step.

A high pressure mercury arc lamp (100W, 10V) was used for ultra-violet excitation. For observation of the liptinite macerals the filters used were: excitation 450-490 nm, beam splitter 510 nm and barrier filter 520 nm. For measurement of the λmax and R/G Quotient the filters used were: excitation 365 nm, beam splitter 395 nm and barrier filter 420 nm. Approximately five measurements were taken on each liptinite and exinite fragment and the values recorded represent the mean of all five measurements. The size of the field diaphragm used to measure the fluorescence parameters was 0.32, the shutters were controlled electronically by a 'Zonax' microcomputer connected to an 'Epson' printer and the estimated depth of penetration is 5 microns.

All photomicrographs under ultra-violet excitation were taken using an Epiplan

water-immersion objective (N.A. 0.90 x 40). This was done in order to increase the contrast and, therefore, the clarity of the fluorescing organic matter relative to the non-fluorescing background.

6.3 SURFACE SAMPLES

A series of Middle to Upper Devonian coals, taken from outcrops of the Weatherall, Hecla Bay and Beverley Inlet formations in western Melville Island was also examined. The coals are very rich in spores (up to 80% by volume), megaspores being the dominant, and were classified as cannel coals. They have been described petrologically by Gentzis and Goodarzi (in press) and their sedimentological setting and depositional environment have been the focus of a separate study by Goodarzi and Goodbody (1990). Although the coals shown in Plates 2A and 2B are samples taken from surface exposures, their inclusion in the description is deemed necessary because of their peculiarities regarding age and petrological composition.

6.4 PROBLEMS ENCOUNTERED DURING ANALYSIS

One of the major problems encountered while examining the cuttings was the presence of 'roasted' fragments. The samples had been artificially heated at the well site and the organic particles had developed devolatilization vacuoles and increased reflectance. Extra care was taken to ensure that no reflectance measurements were made on 'roasted' fragments, a relatively easy task because of the non-problematic identification of these fragments. The problem was more pronounced in the top 1,000 m of the successions and appeared to diminish with increasing depth.

Another problem regarding sample quality was the presence of cavings in the

cuttings, as well as drilling mud additives. Additives included lignite fragments, walnut shells and gilsonite bitumen. Therefore, caution had to be used in order to ensure that reflectance was measured on organic matter which was indigenous to the particular depth interval, it was not measured on 'roasted' fragments and that periodical controls were performed when the presence of casings was known.

The whole-rock technique employed in the present study has an advantage over the kerogen concentrate technique because the former gives the opportunity to determine the relationship between the phytoclasts and the mineral matrix. This, in turn, aids in determining any bitumen staining effect which usually suppresses the reflectance. In addition, the whole-rock technique allows for better differentiation among phytoclasts and is particularly helpful when different types of vitrinite, recycled and oxidized vitrinite and inertinite are present in the same sample.

Fluorescence was used as a supplemental to reflectance mainly for two reasons: 1) a large percentage of the liptinite and exinite organic matter was oxidized and corroded, thus diminishing drastically the usefulness of fluorescence analysis, and 2) since caving of uphole material was a major problem, it would have been relatively difficult to identify with certainty whether the liptinite and exinite organic matter was part of the interval under study or material which caved from intervals further above.

The type of organic matter present in the samples was observed under both white and fluorescent light. Furthermore, quantitative information on the amount of organic matter using the point counting method was thought not to be necessary because of the availability of total organic carbon (TOC) data from Rock-Eval pyrolysis. Rock-Eval parameters are more accurate because they are less subjective and are run on duplicates, whereas point counting besides being time-consuming can often be less

accurate.

There was very little material available in the cuttings vials stored at the ISPG repository in Calgary. Permission was not given to sample the same vials for both Rock-Eval and organic petrology due to the very limited volume of the sample. Samples for reflectance measurements were prepared first, followed by Rock-Eval analysis which was performed at the ISPG.

6.5 ROCK-EVAL

The Rock-Eval instrument at the Institute of Sedimentary and Petroleum Geology was calibrated by analysis of a synthetic standard (n - $C_{20}H_{42}$) and solid CO_2. S_1 (Table 1) is the integral of the first hydrocarbon peak detected after heating the powdered sample in flowing helium at 250°C for 15 min. This peak represents the free or adsorbed hydrocarbons in the rock and is roughly proportional to the content of organic matter that can be extracted from the rock with organic solvents.

S_2 (Table 1) is the integral of the second hydrocarbon peak, produced mainly by cracking of solid organic matter when the rock is heated from 250°C to 550°C at a rate of 25°C/min. These hydrocarbons are probably produced by thermal cracking of the organic matter and to a small degree by the cracking of resins and asphaltenes (Espitalie et al., 1977).

S_3 is the integral of the carbon dioxide peak measured on a split of the gas trapped during the heating interval from 250°C to 390°C. This temperature range is lower than the temperature of thermal dissociation for carbonate minerals under most circumstances. Therefore, S_3 is considered to be a measure of the CO_2 produced by

pyrolysis of the organic matter in the rock. S_1 and S_2 are reported in milligrams of hydrocarbons per gram of dry rock and S_3 in milligrams of CO_2 per gram of dry rock.

The hydrogen index (HI) (Table 1) is defined as S_2 divided by the organic carbon content of the rock (S_2/C_{org}) and is reported in milligrams of hydrocarbons per gram of organic carbon. The oxygen index (OI) is defined as S_3 divided by the organic carbon of the rock (S_3/C_{org}) and is reported in milligrams of CO_2 per gram of organic carbon.

Thermal maturity is interpreted from the temperature of maximum yield of pyrolytic hydrocarbons [Tmax (S_2)] and the transformation ratio or production index [$S_1/(S_1 + S_2)$]. In general, the transition from immature to mature petroleum source rocks is indicated by Tmax values of about 430-435°C and production indices of about 0.1 (Tissot and Welte, 1984).

The reliability of Rock-Eval parameters is affected by numerous factors which include: 1) Variations in organic matter type; 2) contamination by drillhole additives; 3) bitumen and migrated oil; 4) interference by mineral matrix; and 5) problems associated with the Tmax. Coals and organic-rich samples are a problem simply because a 100 mg sample (recommended weight for shaley cuttings) may overload (saturate) the FID (Flame Ionization Detector). As a result, it is recommended that coal is diluted with inert pure carbonate, followed by pyrolysis of 100 mg of the mixture (Peters, 1986).

One of the problems is that coals of higher-plant origin and dispersed Type III organic matter do not respond to pyrolysis in the same way. Some coals plot between Types II and III organic matter on a pseudo-Van Krevelen diagram, resulting in an overestimation of their liquid-hydrocarbon generative potential. The reasons for this

anomalous behaviour of some coals may be due to differences in procedure and product detection between Rock-Eval pyrolysis and elemental analysis (Peters, 1986). For example, while the atomic H/C ratio is determined on kerogen, the FID responds only to carbon-hydrogen bonds and carbon mass, thus not including common by-products of pyrolysis such as water and diatomic hydrogen in the HI, which are measured by the H/C analysis.

There is also a problem with the OI, particularly in mature coals (>0.60% Ro), because at higher levels of maturity more pyrolytic oxygen is released as carbon monoxide, which is not analyzed by the Rock-Eval. As a result, the coals show OI values lower than expected based on the atomic O/C ratio. This problem is negligible in coals at low maturity (Ro = <0.60%) (Peters, 1986).

Oxidation of organic matter during transportation, deposition and diagenesis tends to remove hydrogen and add oxygen to the kerogen, thus changing the HI versus OI diagrams (Durand and Monin, 1980). In addition, outcrop samples tend to show a depletion in the S_1 and S_2 and an increase in the S_3 values due to weathering. Drying or heating of cuttings samples can reduce the S_1 peak (Peters, 1986).

The S_1, S_2, and S_3 and Tmax values can also be affected by oil-based and water-based drilling mud additives and lubricants. Tmax is generally lowered by the above-mentioned contaminants. Migrated oil and bitumen can create similar problems (Clemenz, 1979). An anomalously high PI (>0.4), a low Tmax (compared to adjacent samples), a bimodal S_2 peak and an S_1 peak greater than 2 mg HC/g rock are indicative of contamination by bitumen and migrated oil (Peters, 1986).

Another problem associated with Rock-Eval is the interference by the mineral

matrix, particularly on the HI and Tmax values due to adsorption of pyrolytic organic compounds onto the mineral matrix. Espitalie et al., (1980) stated that the degree of adsorption generally increases in the following order: illite, montmorillonite, calcite, kaolinite. Both the S_1 and S_2 peak sizes depend on (1) type of mineral matrix; (2) ratio of organic matter (OM) to matrix; and (3) type of organic matter (Peters, 1986). It is generally accepted that for argillaceous rocks containing less than 0.5 wt % TOC, HI values tend to be low and Tmax high.

There are also problems associated with the Tmax because variations in organic matter type affect the Tmax, especially in rocks that are in the immature and marginally mature stage of hydrocarbon generation. For example, recycled organic matter may show variations in Tmax up to almost 10°C at low maturity (Ro <0.6%) and this variation decreases as the 'oil window' is approached. As a result, differences in mature or overmature organic matter are generally less than 5°C (Peters, 1986). It has also been shown (Tissot et al., 1978) that the threshold of oil generation for Type I organic matter is higher than for Types II and III. Strong cross-linkage of long aliphatic chains and a scarcity of thermally labile heteroatomic bonds are believed to be the cause of the resistance of Type I organic matter to thermal degradation. In addition, oil-prone Type II organic matter does not always show higher Tmax values than Type III organic matter and significant amounts of primary (indigenous) or secondary (migrated) resinite in a rock may severely reduce Tmax (Peters, 1986). If soluble resinite is present in the samples, solvent extraction prior to pyrolysis is recommended.

Finally, rocks which are organically lean (<0.5 wt % TOC) are most likely to be affected by adsorption of pyrolysate by the mineral matrix resulting in reduced S_2, HI, and increased OI and Tmax (Peters, 1986).

6.6 CALCULATION OF GEOTHERMAL GRADIENT

Geothermal gradient is the rate of temperature increase through the sediments in the subsurface. It is influenced by many factors such as heat input at the base of the rock column under study, hydrodynamic regime, thermal conductivity, and amount of radiogenic heat generated in the section. The geothermal gradient is proportional to the heat flow and inversely proportional to the thermal conductivity, the latter varying depending on lithology, temperature, porosity and degree of compaction (Pitt, 1986).

Basement rocks are typically better thermal conductors than sedimentary rocks of overlying basins (Gretener, 1981). Porosity has the effect of decreasing conductivity while pore-filling fluids are very poor conductors (Pitt, 1986). Within a basinal sequence, and given a constant heat input, the geothermal gradient will be greater in soft shale, coal or porous, poorly lithified sandstone, and less in indurated siltstone and carbonate (Sass et al., 1971; Zierfus, 1969). A world 'average' geothermal gradient is considered to be 25°C/km (Lee and Uyeda, 1965). The normal range in geothermal gradient is 15 to 50°C/km (Tissot et al., 1980) or 20 to 40°C/km (Gretener, 1981) for typical basins. Those of shield or stable cratonic areas vary from 8 to 15°C/km (Gretener, 1981; Pitt, 1986). In addition, geothermal gradients as low as 5°C/km and as high as 77°C/km have been observed (Tissot and Welte, 1984).

Geothermal gradients are not always linear and the irregularities are caused mainly by variations in thermal conductivity of lithologic units, by proximity to the surface and by subsurface water flow (Tissot and Welte, 1984). Rocks with poor thermal conductivities act as barriers to heat flow, causing a rise in temperature when compared to average gradients not by being hotter than the beds above but by merely preventing a decrease in the temperature. When highly conductive salt diapirs and poorly conductive

shales are present in the same succession, high geothermal gradients are created above the diapirs.

Conductivity differences result in higher basin and lower basement gradients. As the basement shallows towards the basin margin, the accompanying lower gradients will also be at shallower depths. However, the gradient within a thinner basinal sequence will be greater than the gradient of an equivalent thicker basinwards sequence since geothermal gradients are dependent on the thickness of sediments in a basin (Pitt, 1986).

Geothermal gradients are calculated by simply dividing the temperature change over a vertical section by the length of that section:

$$\text{Grad.} = {}^{\circ}\text{C}/100\text{ m}, \qquad \frac{T_1 - T_2}{D_1 - D_2}$$

where T_1 is the formation temperature at depth D_1, and
T_2 is the formation temperature at depth D_2.

For 'overall' gradients from ground surface to the base of the sequence under consideration, T_1 is the formation temperature at D_1, the total depth of the drillhole while T_2 is the ambient temperature at ground surface where $D_2 = 0$.

There is a problem of deciding the value of the surface temperature and many authors (Pitt, 1986) argue that the 'base line' temperature to which the most meaningful overall thermal gradient is drawn is not the temperature at the ground surface but the rock temperature some metres or tens of metres below the surface. Having established such a surface temperature, formation temperatures must be determined to provide values for

T_2 and/or T_1. Subsurface temperature observations may be made in a variety of ways with the following technique being the most commonly used for temperature measurement in petroleum drillholes.

The most preferential method of recording bottom-hole temperatures (BHT) is wireline logging. The recorded temperature is not the true formation temperature but must be correlated to an estimated formation temperature due to cooling of the formation by mud circulation prior to logging. Some 30 hours after cessation of circulation, the measured temperature probably approaches by a few percent the true formation temperature (Pitt, 1982). Equilibrium is probably attained after 50 to 100 days.

Other techniques include drill stem tests, static pressure surveys and temperature surveys. The most productive approach is believed to be the use of corrected wireline logging with a drill stem test providing added resolution and a check on the accuracy of extrapolation of wireline log temperatures to estimated formation temperatures (Pitt, 1986).

RESULTS AND DISCUSSION

GENERAL INTRODUCTION

The study area covers three different geological provinces, each with a unique geological evolution and organic-matter types. These geological provinces are: 1) the Arctic Platform (Dundas Block) in southern Melville Island; 2) the Franklinian miogeosyncline (part of the Parry Islands Fold Belt); and 3) the Sverdrup Basin (Figure 1-1). A total of 43 drillholes were studied, one in the Dundas Block, nine in the Franklinian miogeosyncline and thirty three in the Sverdrup Basin.

The flat-lying Ordovician to Devonian strata of the Dundas Peninsula have not been affected by the Ellesmerian Orogeny. In contrast, the Lower Palaeozoic strata of the Franklinian miogeosyncline have undergone extensive deformation during the Upper Devonian Ellesmerian Orogeny. The characteristic anticlines and synclines typical of the Parry Islands Fold Belt in Melville Island are the result of flexural-flow deformation of evaporites in the Middle Ordovician Bay Fiord Formation and coincident thrust faulting in the overlying Ordovician to Devonian strata (Fox, 1983; Harrison et al., 1985). There are a few isolated patches of Cretaceous strata present in the southern part of the Franklinian miogeosyncline in Melville Island directly overlying Devonian strata. Strata belonging to the Sverdrup Basin have been superimposed on earlier folded and faulted Franklinian strata and these have been further folded by the Tertiary Eurekan Orogeny.

The Lower Palaeozoic strata in Melville Island contain numerous bitumen types and graptolites, whereas the Upper Palaeozoic strata near the Sverdrup Basin margin and the entire Mesozoic sequence in Sverdrup Basin are dominated by phytoclasts.

The following Chapters, VII, VIII and IX deal specifically with the maturity and source-rock potential of sedimentary strata in the above mentioned regions. The burial history of selected drillholes is discussed in Chapter X. Finally, Chapter XI compares and contrasts the study area to other sedimentary basins in Canada in terms of organic-matter type, level of thermal maturity and hydrocarbon products.

CHAPTER VII

CHAPTER VII

7.0 DUNDAS BLOCK

INTRODUCTION

The southwestern part of the Dundas Peninsula contains Lower Palaeozoic rocks which have not been affected by the Ellesmerian Orogeny and at present are flat-lying forming a plateau (Tozer and Thorsteinsson, 1964). There are only two drillholes drilled in the Dundas Block (longitude 111°-114°30', latitude 74°30'-75°) and because of their proximity, only one, Panarctic Dundas C-80 (Figure 7-1) (Table 2) will be discussed in detail.

PANARCTIC DUNDAS C-80

A succession, approximately 3,980 m thick, was penetrated. The formations range in age from Late Middle Ordovician to Devonian. The Ordovician and Lower Devonian formations are mainly creamy-grey dolomites, whereas the Middle to Upper Devonian rocks comprise alternating shales, siltstones and sandstones. The latter are slightly calcareous with carbonaceous streaks.

Three different sections can be identified based on the type of organic matter and its optical properties (Figure 7-2). The top section (A) contains higher-plant remains (vitrinite) with very little bitumen (Plate 1A). The organic-rich samples of the Hecla Bay Formation contain coal particles rich in exinite. Organic matter in this section is similar to that described by Goodarzi and Goodbody (1990) in a suite of Devonian coals from the

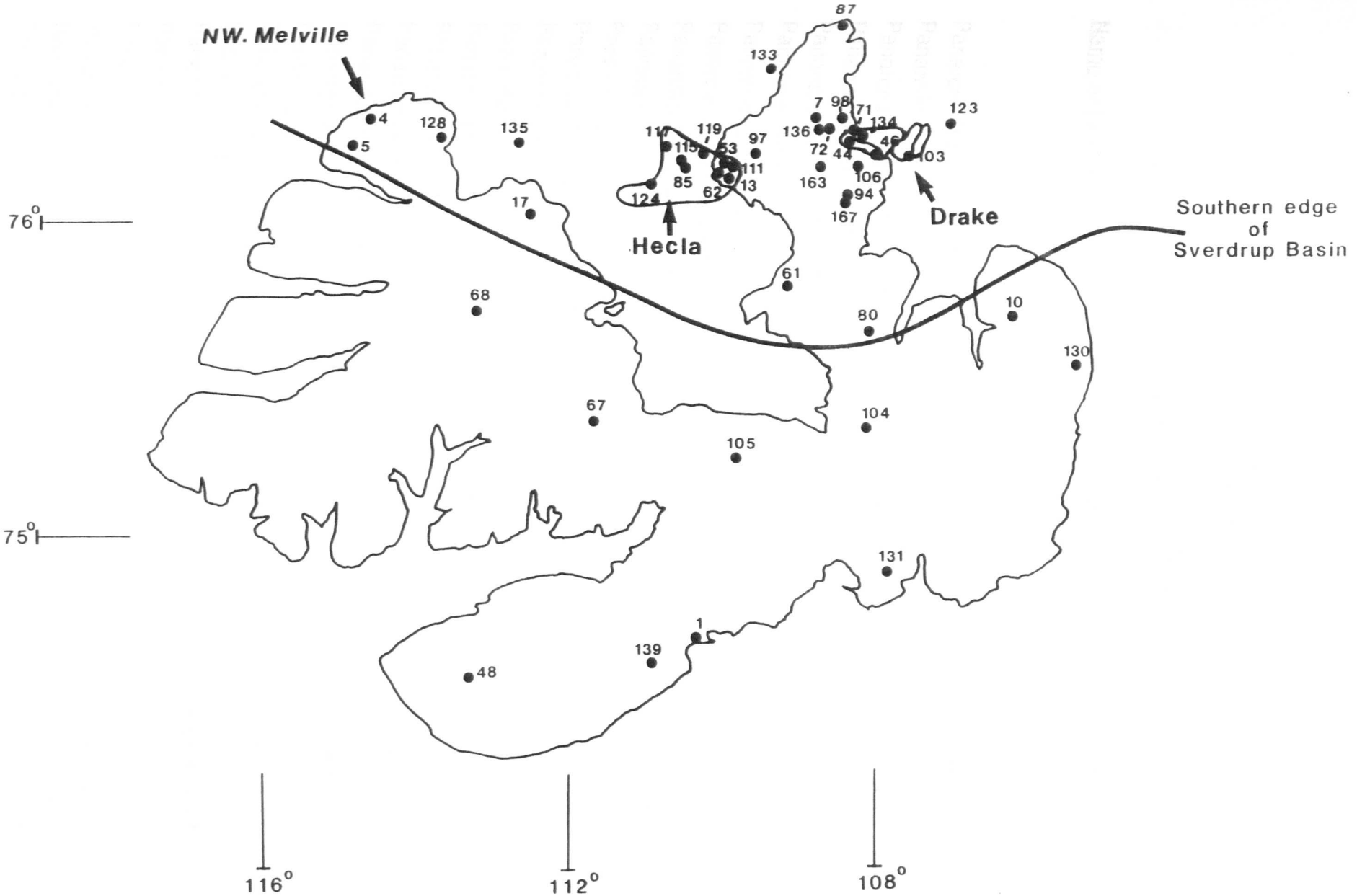

Figure 7-1 Map of Melville Island showing drillhole location. For drillhole identification number and corresponding name refer to Table 2

TABLE 2

Drillhole Identification Number

Name of Drillhole	Panarctic's Reference Number	Figure in Text
Panarctic Dundas C-80	48	Figure 7-2
Panarctic Apollo C-73	67	Figure 8-1
Panarctic Hearne Point F-85	139	Figure 8-2
Panarctic Winter Harbour #1	1	Figure 8-3
Panarctic Beverley Inlet G-13	131	Figure 8-4
Panarctic Zeus F-11	68	Figure 8-5
Panarctic Sabine Bay A-07	105	Figure 8-6
Panarctic King Point West B-53	104	Figure 8-7
Panarctic Towson Point F-63	10	Figure 8-8
Panarctic Richardson G-12	130	Figure 8-9
Panarctic Drake Point D-68	72	Figure 9-1
Panarctic Chads Creek B-64	97	Figure 9-2
Panarctic Hecla J-60	13	Figure 9-3
Panarctic Depot Island C-44	128	Figure 9-4
Panarctic Roche Point J-43	133	Figure 9-5
Panarctic North Sabine H-49	87	Figure 9-6
Panarctic Weatherall O-10	80	Figure 9-7
Panarctic Eldridge Bay E-79	61	Figure 9-8
Panarctic Kitson River C-71	17	Figure 9-9
Panarctic Sherard Bay F-34	167	Figure 9-10
Panarctic Sherard Bay F-14	94	Figure 9-11
Panarctic Marryatt K-71	163	Figure 9-12
Panarctic Collingwood K-33	98	Figure 9-13
Panarctic Drake L-67	7	Figure 9-14
Panarctic Drake Point K-79	136	Figure 9-15
Panarctic Drake F-76	134	Figure 9-16
Panarctic Drake E-78	71	Figure 9-17
Panarctic Drake B-44	46	Figure 9-18
Panarctic Drake D-73	106	Figure 9-19
Panarctic Drake F-16	44	Figure 9-20

TABLE 2 (continued)

Name of Drillhole	Panarctic's Reference Number	Figure in Text
Panarctic Drake P-40	123	Figure 9-21
Panarctic East Drake I-55	103	Figure 9-22
Panarctic Hecla South West C-58	124	Figure 9-23
Panarctic Hecla West P-62	115	Figure 9-24
Panarctic North West Hecla M-25	117	Figure 9-25
Panarctic Hecla West N-52	85	Figure 9-26
Panarctic Hecla West C-05	119	Figure 9-27
Panarctic Hecla I-69	62	Figure 9-28
Panarctic Hecla F-62	53	Figure 9-29
Panarctic Hecla C-32	111	Figure 9-30
Panarctic Marie Bay D-02	5	Figure 9-31
Panarctic Sandy Point L-46	4	Figure 9-32
Panarctic Grassy I-34	135	Figure 9-33

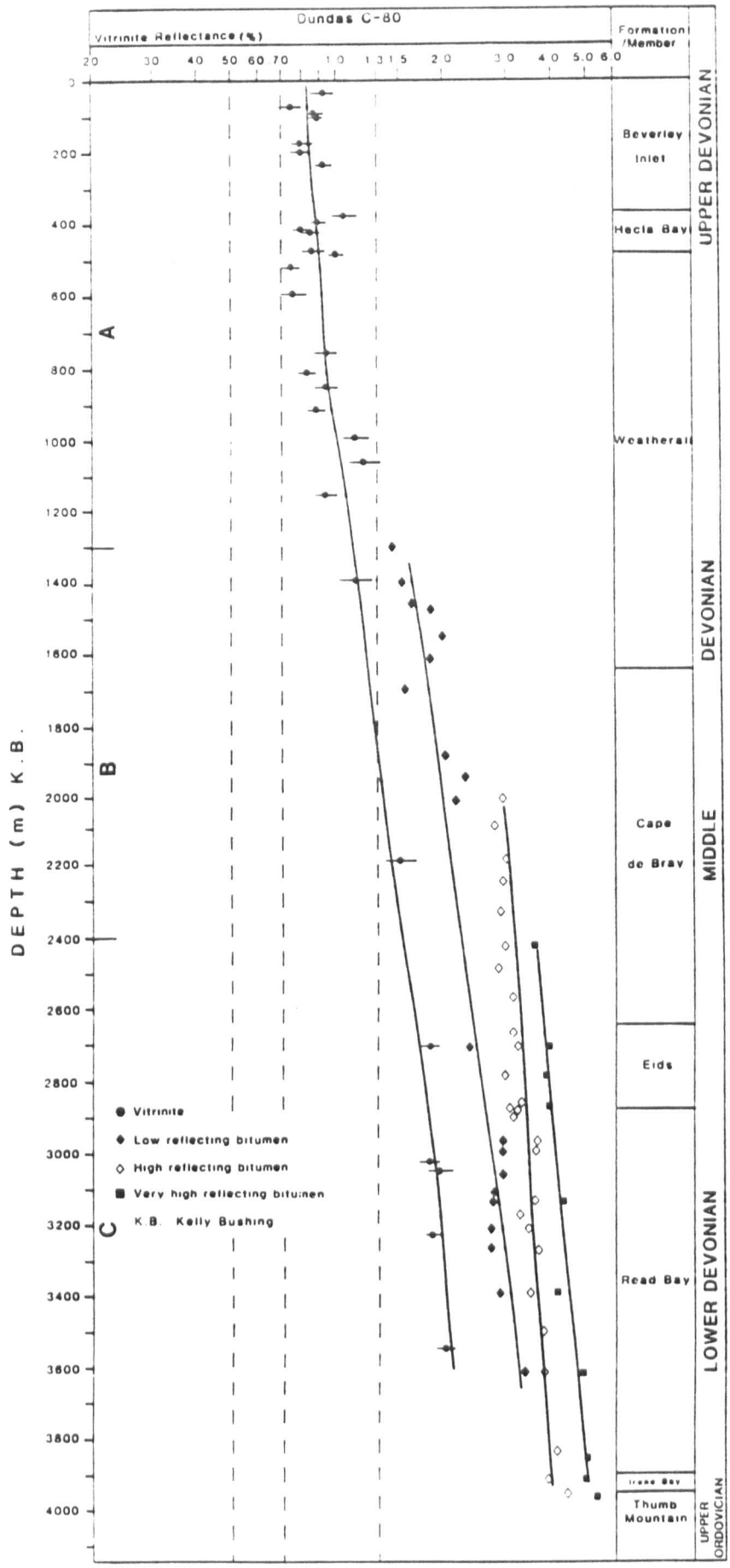

— — indicates 'bottom' 0.5% Ro for Type III and 0.7% Ro for Type I kerogen and 'top' of the oil window.

Figure 7-2 Vitrinite reflectance versus depth profile, Panarctic Dundas C-80

PLATE 1A. Organic matter in the Lower Palaeozoic rocks, Melville Island

All photomicrographs taken in colour under plane polarized light, oil immersion. The long axis of each photomicrograph is 180 μm.

a) Vitrinite bands (V) enclosing microspores (Mi) and megaspores (Mg) showing internal reflection, King Point West B-53, 275 m.

b) A concentration of spores (sporangia, S) between vitrinite bands (V), Dundas C-80, 480 m.

c) A band of vitrinite (V) in association with shaley intervals and framboidal pyrite (P), Apollo C-73, 510 m.

d) Angular and rounded fragments of vitrinite (V), inertinite (I) and low-reflecting bitumen (B) in shaley matrix, King Point West B-53, 245 m.

e) Vitrinite (V) in Dundas C-80, 2185 m (% Ro, max ~ 1.50).

f) Angular metabituminite (MB) occupying the interstitial spaces among carbonate grains (C). Same sample as e) above.

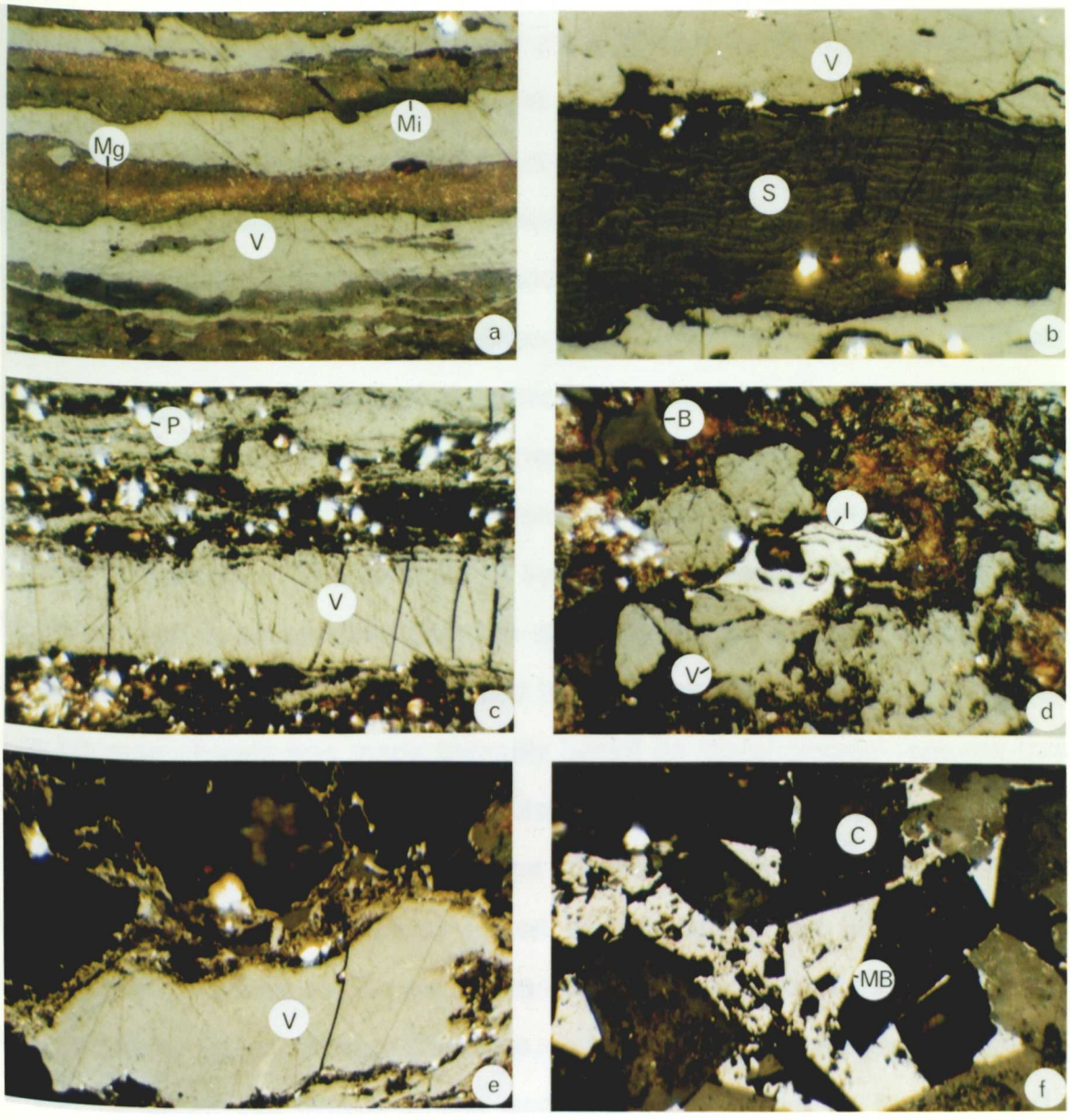
Mg
Mi
V
a
V
S
b
P
V
c
B
I
V
d
V
e
C
MB
f

Hecla Bay Formation in the western part of Melville Island, shown in Plates 2A and 2B. The coals contain a high percentage of microspores and megaspores (up to 80%) with minor cutinite, fluorinite, exsudatinite, resinite, amorphous fluorescing matrix, and fluorescing vitrinite and were classified by the above authors as cannel coals.

Section B includes the lower half of the Weatherall Formation and contains very little vitrinite suitable for determining thermal maturation. It commonly contains solid black and bituminous material which downhole in section C occurs as coatings and as fillings among carbonate grains. This material resembles bitumen and microscopic examination shows that it is insoluble in immersion oil and shows no fluorescence under UV excitation. Numerous samples in sections B and C contain one or more phases of bitumen, which may indicate multiple hydrocarbon generation or multiple oil migration episodes through the sediment (Robert, 1980). The bitumen was most likely formed from the thermal degradation of hydrocarbons generated from the organic matter in these sediments due to thermal maturation. The amount of hydrocarbons generated may not have been sufficient enough to be expelled from the shales and the bitumen observed most likely represents the remnants of the generated hydrocarbons ('dead oil'). The differentiation among bitumen phases was made primarily based on morphological features (presence of mosaic, elongate versus highly angular shape), matrix association (shale versus carbonate matrix) and reflectance. The distinction between low-, high- and very high-reflecting bitumens was made based on reflectance but other factors such as morphology and mineral matrix association were also considered in differentiating the numerous bitumen populations. Therefore, distinction is not subjective but is as objective as it can be under the circumstances and was made based on features and optical properties of bitumens as observed under the microscope.

The reflectance versus depth profile can be seen in Figure 7-2. The bar lines

on the individual data points correspond to the limits of the reflectance measurements. Organic matter is moderate throughout the succession but is more abundant in the Devonian Hecla Bay and Griper Bay Formations. Vitrinite (Plate 1B) was identified in all formations with the exception of Irene Bay and Thumb Mountain. It consists of the higher-reflecting, hydrogen-poorer vitrinite and the lower-reflecting, hydrogen-richer vitrinite types (Goodarzi et al., 1987a,b; Goodarzi et al., 1988b) (Plate 2A). Exinite is mainly composed of microspores and megaspores, resinite, amorphous fluorescing matrix and exsudatinite, similar to the organic matter shown in Plates 2A and 2B. This type of organic matter is common in the Hecla Bay and in the upper part of the Weatherall Formations which contain a considerable amount of coaly particles. Palyniferous, marine-liptinitic, organic matter (Tasmanites algae) was observed at 803 m (Plate 1B).

Random vitrinite reflectance at the top of the drillhole averages about 0.80% Ro. Reflectance increases with depth to show a gentle gradient that reaches the upper limit of the hydrocarbon generation zone (1.25% Ro) at about 1,800 m. The interval between 1,300 m and total depth (Middle-Upper Ordovician) is rich in bitumen and three types can be identified, all of which are anisotropic. The interval between 1,212 to 2,626 m contains two types of bitumen and sparse vitrinite. The low-reflecting bitumen type has an irregular morphology, a 'pitted' surface and a reflectance range from 1.50 to 3.05% Ro, max (epi- to meso-impsonite maturity stage) (Jacob, 1985; Goodarzi et al., 1985) (Plate 1B), whereas the high-reflecting bitumen has a reflectance ranging from 2.60 to 3.20% Ro, max with increasing depth. The latter is angular, granular under crossed polars, and is associated with carbonate grains, closely resembling metabitumen (Plate 1B).

The interval between 2,626 m to total depth (3,939 m) also contains three types of bitumen. Maximum reflectance of the low bitumen ranges from 2.45 to 3.05% and of the high bitumen from 3.05 to 4.10%. The strongly-reflecting bitumen is in the

PLATE 1B. Organic matter in the Lower Palaeozoic rocks, Melville Island

All photomicrographs taken in black and white under plane polarized light, oil immersion. The long axis of each photomicrograph is 180 μm.

a) Vitrinitized Tasmanites showing characteristic suture, Dundas C-80, 803 m.

b) Phytoclasts (PH) in shale, Dundas C-80, 3050 m.

c) Low-reflecting bitumen (LB) in shaley matrix, Dundas C-80, 3220 m.

d) Highly-angular metabitumen (MB) in carbonate matrix, Dundas C-80, 3220 m.

e) Bitumen of the cata-impsonite level showing granular anisotropy (medium-grained mosaic - Mm), Dundas C-80, 3615 m.

f) Same as above but under crossed-polars to show anisotropy.

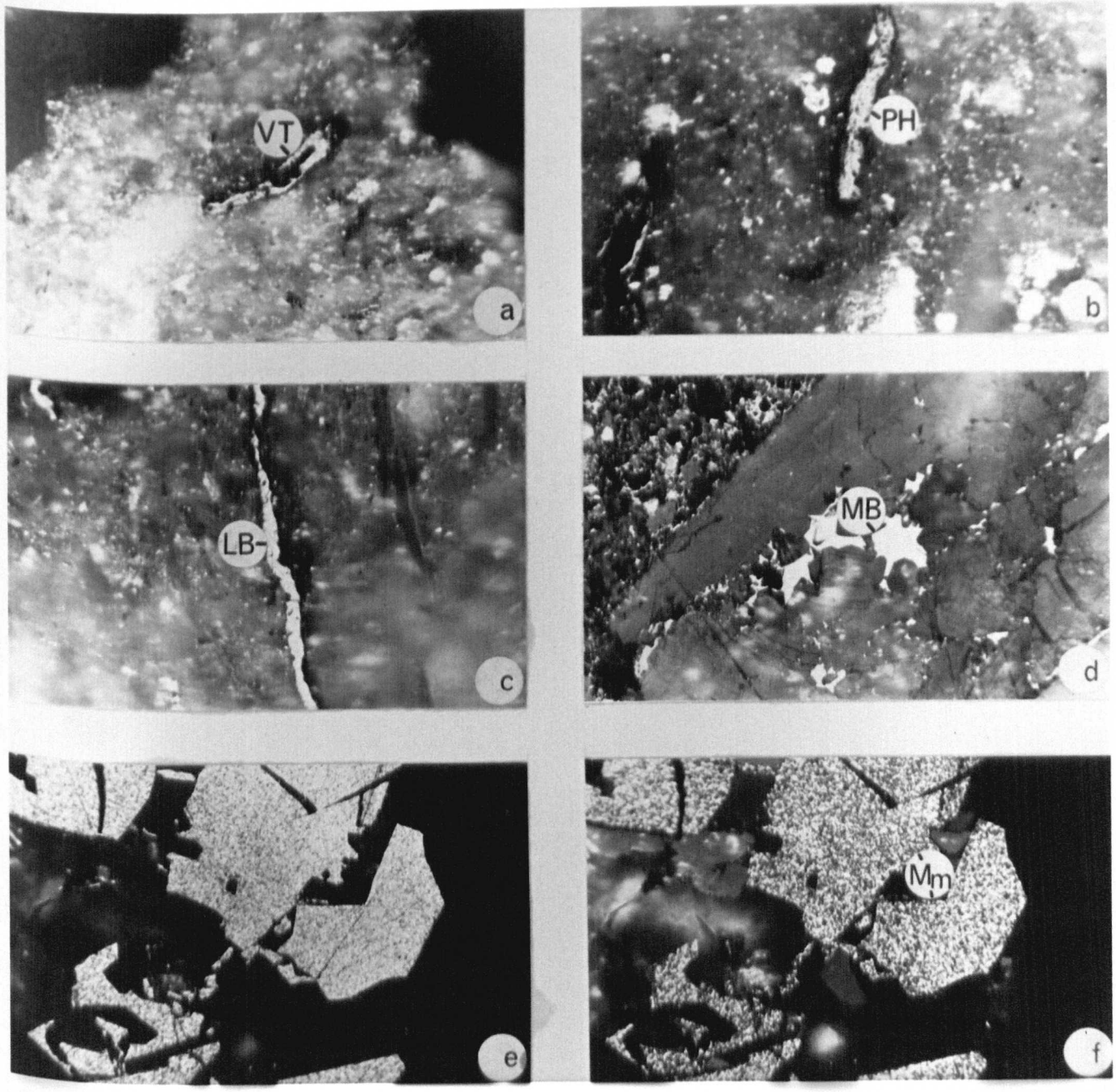
VT
a
PH
b
LB
c
MB
d
e
Mm
f

PLATE 2A. Middle to Upper Devonian cannel coals.

All photomicrographs taken under ultraviolet excitation, water immersion (excitation 400 - 440 nm, barrier filter 470 nm). The long axis of each photomicrograph is 180 μm.

a) Resinite globules (R), megaspore and microspores, Beverley Inlet Formation, 91 m above base. Note the absence of visible fluorescence in the vitrinite matrix.

b) A megaspore showing ornamentation associated with microspores, Hecla Bay Formation, 85 m above base.

c) Fluorescing vitrinite (VA) and microspores, Hecla Bay Formation, 85 m above base. Telocollinite and desmocollinite do not fluoresce (hydrogen-poor).

d) Exsudatinite (EX) and sporinite, Beverley Inlet Formation, 91 m above base.

e) Thin-walled cutinite (CU), fluorinite (FL) and megaspores, Weatherall Formation, 120 m above base.

f) Resinite globules in a fluorescing matrix, consisiting of hydrogen-rich (perhydrous) vitrinite, Weatherall Formation, 120 m above base.

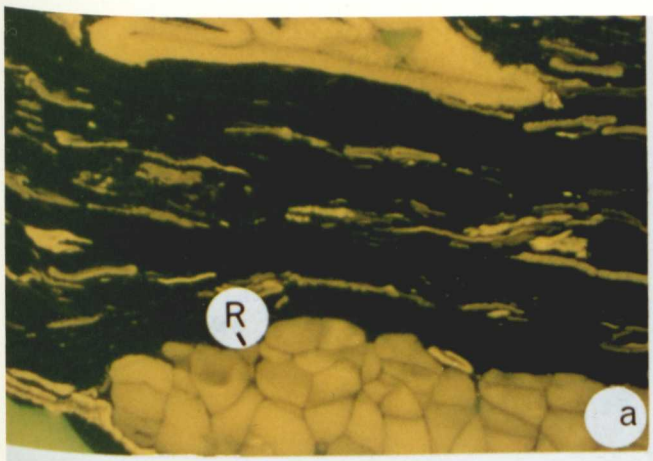
R
a

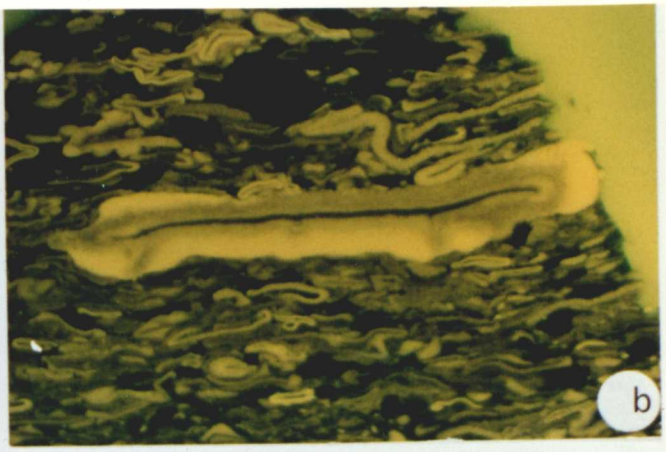
b

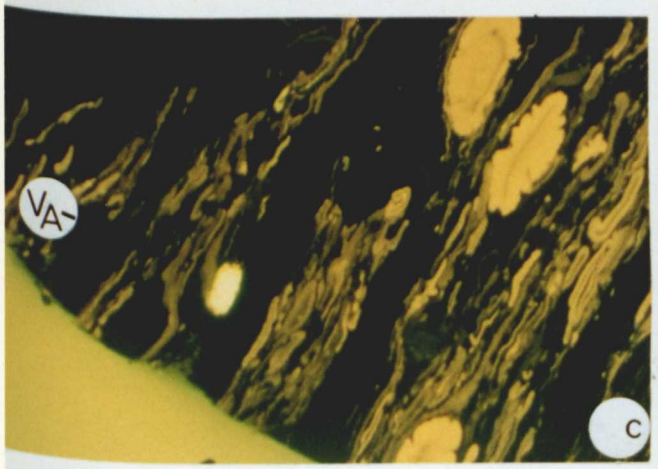
VA
c


EX
d

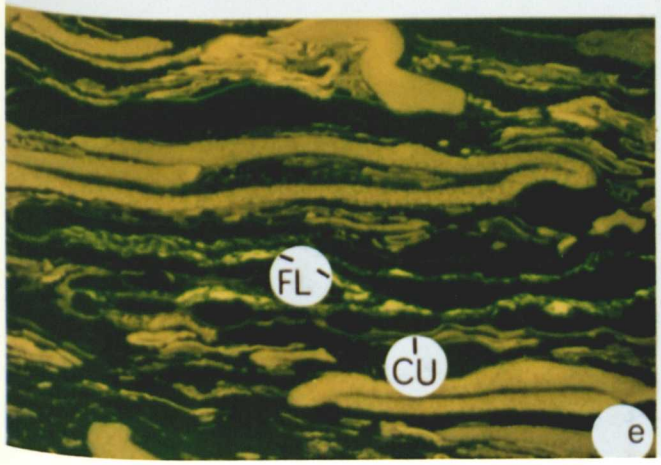
FL
CU
e

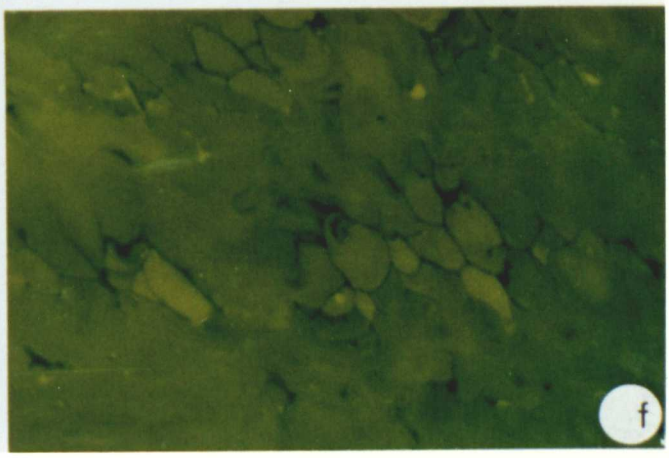
f

PLATE 2B. Middle to Upper Devonian cannel coals.

All photomicrographs taken under ultraviolet excitation, water immersion (excitation 400 - 440 nm, barrier filter 470 nm). The long axis of each photomicrograph is 180 μm.

a) A concentration of megaspores (MG) and microspores (MC) in a sporoclarite band. Note the ornamentation of the megaspores, Weatherall Formation, 33 m above base.

b) Thin-walled microspores (MC) in association with heavily-ornamented megaspores. Note the higher fluorescence intensity of the microspore, Beverley Inlet Formation, 40 m above base.

c) A megaspore with a low fluorescence intensity. The darker fluorescing rim may be due to oxidation (OX) or weathering, Beverley Inlet, 91 m above base.

d) Thin-walled untoothed cuticles (CU), fluorescing brighter than associated microspores, Hecla Bay Formation, 85 m above base.

e) Exsudatinite (EX) within he internal structure of a megaspore, Beverley Inlet Formation, 40 m above base.

f) A highly-fluorescing algal body (A) cut perpendicular to bedding enclosed by mega- and microspores, Weatherall Formation, 120 m above base.

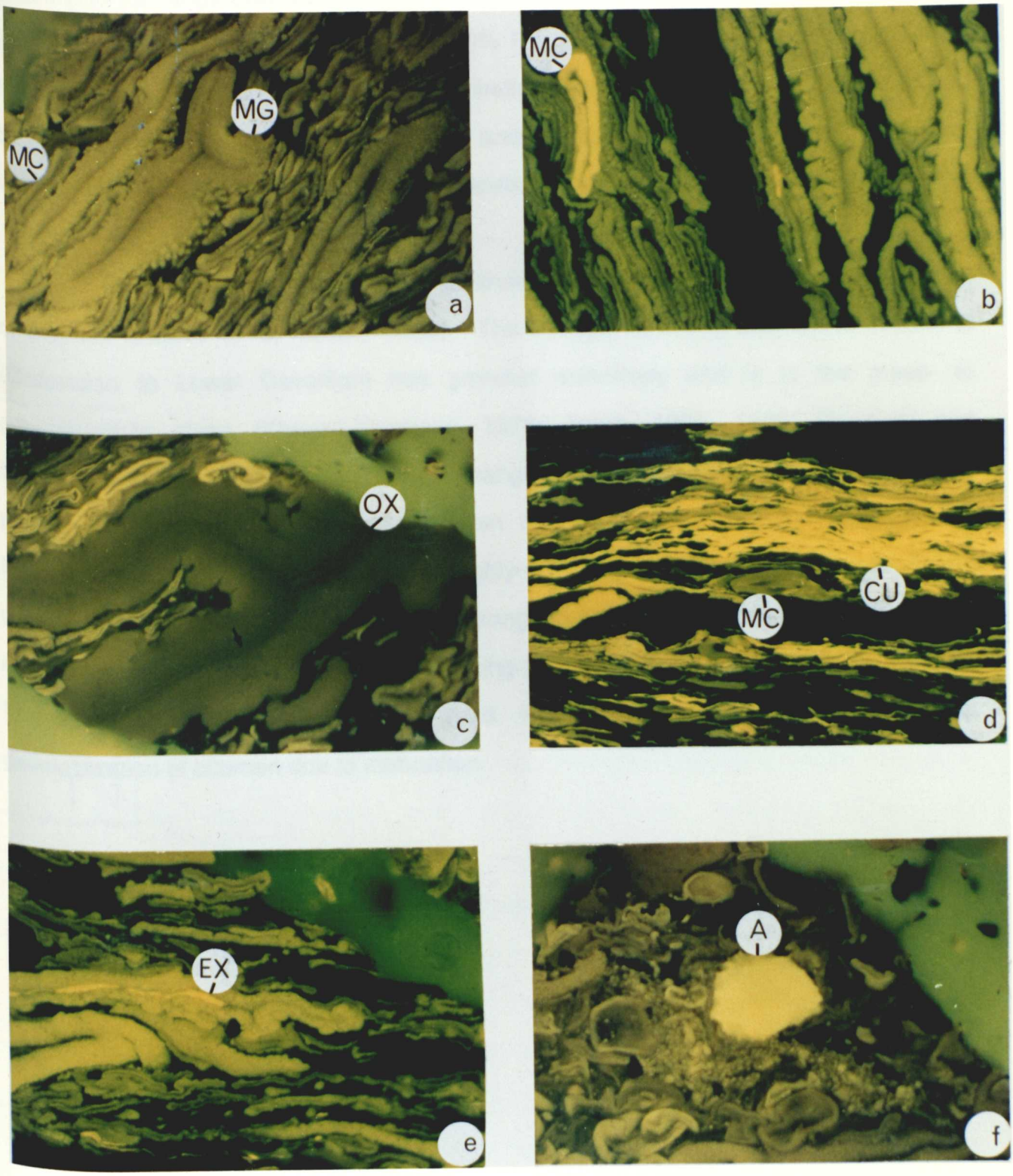
MC
MG
a
MC
b
OX
c
MC
CU
d
EX
e
A
f

cata-impsonite range (Jacob, 1985), shows granular anisotropy (mosaic) (Plate 1B) and its reflectance increases from 3.55 to 5.10% Ro, max. The latter bitumen occurs as massive, sub-angular fragments and has a bireflectance of almost 2.0%. Finally, it should be noted that the reflectance of low-, high-, and strongly-reflecting bitumen as well as of vitrinite (Figure 7-2) increases with depth following almost subparallel trends.

Bitumen covers a range of reflectance depending on the degree of maturation of bitumen (Jacob, 1976; Robert, 1980). The strongly-reflecting bitumen in section C (Ordovician to Lower Devonian) has granular anisotropy and is in the meso- to cata-impsonite stage (Khavari-Khorasani 1975; Jacob, 1975, 1983; Goodarzi and Macqueen, 1990). There is a lithology change from section B to section C and it is possible that porosity and lithology or even the depositional environment played an important role in the occurrence of this highly-reflecting bitumen, which may represent de-asphalted bitumen. Some of the strongly-reflecting bitumens have developed microbrecciation, pores and vesicles, ranging in diameter from a few to 50 microns. These pores are either empty or filled with mineral matter, indicating partial devolatilization of bitumen due to maturation.

CHAPTER VIII

CHAPTER VIII

8.0 FRANKLINIAN MIOGEOSYNCLINE

INTRODUCTION

There are nine drillholes (Figure 7-1) (Table 2) present in the Franklinian miogeosyncline, Melville Island, (105°-107° longitude and 74°30' - 76° latitude) with the deepest being Sabine Bay A-07 (~5,200 m). The drillholes penetrate strata of Lower and Upper Palaeozoic age. Most of them spud in the Weatherall and Beverley Inlet Formations of the clastic wedge with one in the Blue Fiord Formation.

King Point West B-53 has the lowest random reflectance in the Weatherall Formation (~ 0.60% Ro) as opposed to Sabine Bay A-07 which has the highest (> 0.90% Ro) at the same stratigraphic level. In addition, Richardson G-12 has the lowest reflectance in the Beverley Inlet Formation (0.55%) and Winter Harbour #1 has the highest (0.70%) at the same stratigraphic level. The most noticeable observation when constructing the vertical reflectance profiles for the Franklinian miogeosyncline drillholes is the consistent occurrence of phytoclasts in the Middle to Upper Devonian part of the succession comprising the clastic wedge, followed by the occurrence of various bitumen types in the Ordovician and Silurian.

Because of the similarity in organic matter content and thermal maturity only one of the drillholes (Panarctic Apollo C-73) (Figure 8-1) (Table 2) will be discussed in detail and the discussion will be supplemented with observations from the remaining drillholes (Figures 8-2 to 8-9).

8.1 PANARCTIC APOLLO C-73

The drillhole penetrates a 3,644 m thick succession consisting of Lower-Middle Ordovician to Middle Devonian strata. The Eleanor River, Bay Fiord and Thumb Mountain Formations are rich in limestone, dolomite and minor anhydrite (Bay Fiord evaporites), the Eids and Cape Phillips are micaceous shales and the Weatherall is an alternating siltstone-shale unit with minor sandstone.

Satisfactory organic matter contents are preserved throughout the drilled section and the maturity level was confirmed by examining samples from cored intervals. The maturity pattern is fairly clear (Figure 8-1). The Weatherall Formation contains vitrinite and exinite consisting of spores (microspores and megaspores), cuticles and possibly resin bodies (Plate 3). Spores fluoresce dark yellow-orange, whereas cuticles fluoresce yellow.

The average reflectance measured on phytoclasts is 0.80% at the top and 1.50% at the base of the Weatherall. Small quantities of bitumen are present, having always a higher reflectance than phytoclasts. The interval below 1,700 m is rich in bitumen. It occurs in association with finely crystalline, limey dolomite and in vugs. The Cape Phillips shales contain two bitumen types. The bitumen having a wispy to rounded form with an Ro, max between 1.85 and 2.30% is less abundant than the bitumen having an Ro, max range from 2.40 to 2.80%. The latter is granular, angular, and is associated with the carbonate-rich intervals of the succession. It appears that the bitumen forms may be related to lithological facies. The Cape Phillips shales also contain scattered graptolite fragments identified under the microscope as well as in hand specimen. Graptolite periderm is non-granular and anisotropic (Plates 4A and 4B) and most of the particles have a reflectance range between 2.50 and 2.80% Ro, max. The Thumb

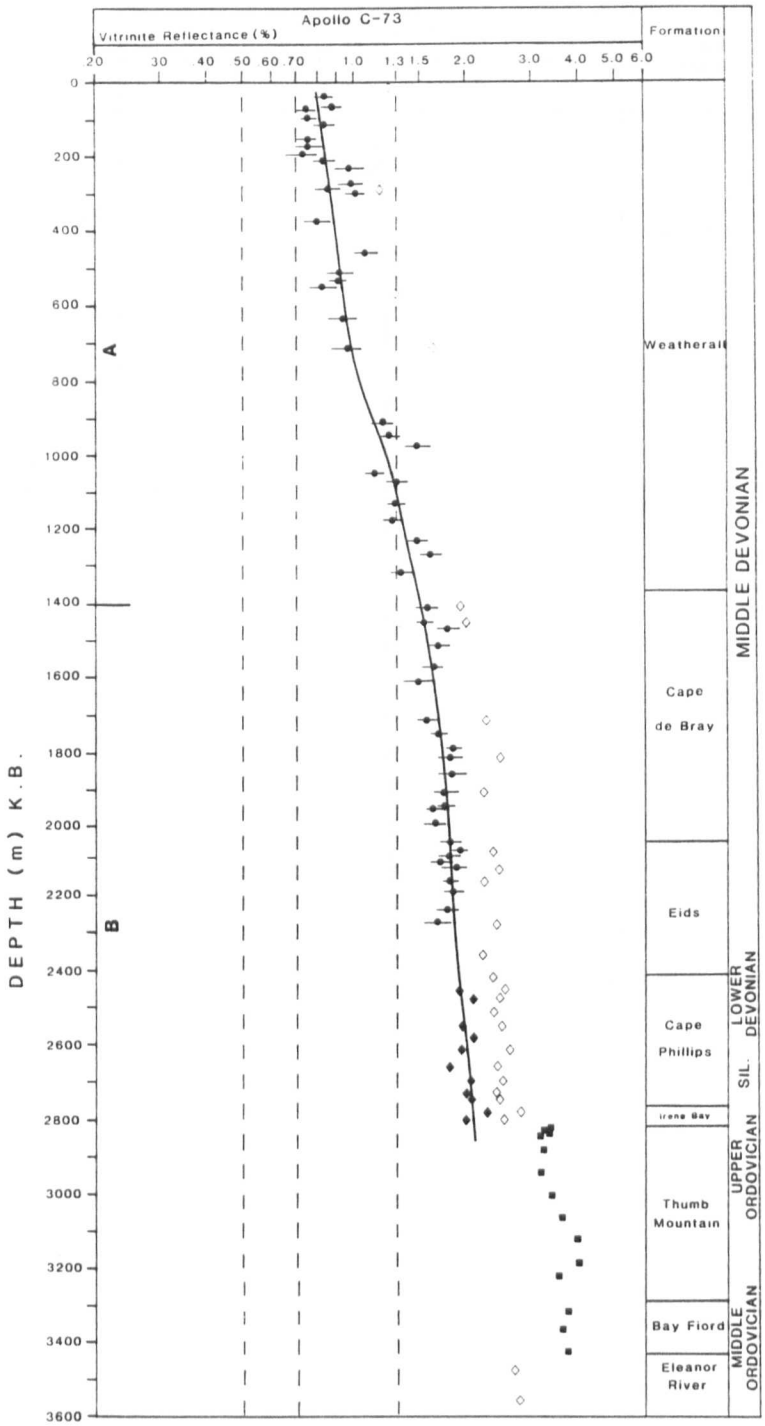

Figure 8-1 Vitrinite reflectance versus depth profile, Panarctic Apollo C-73

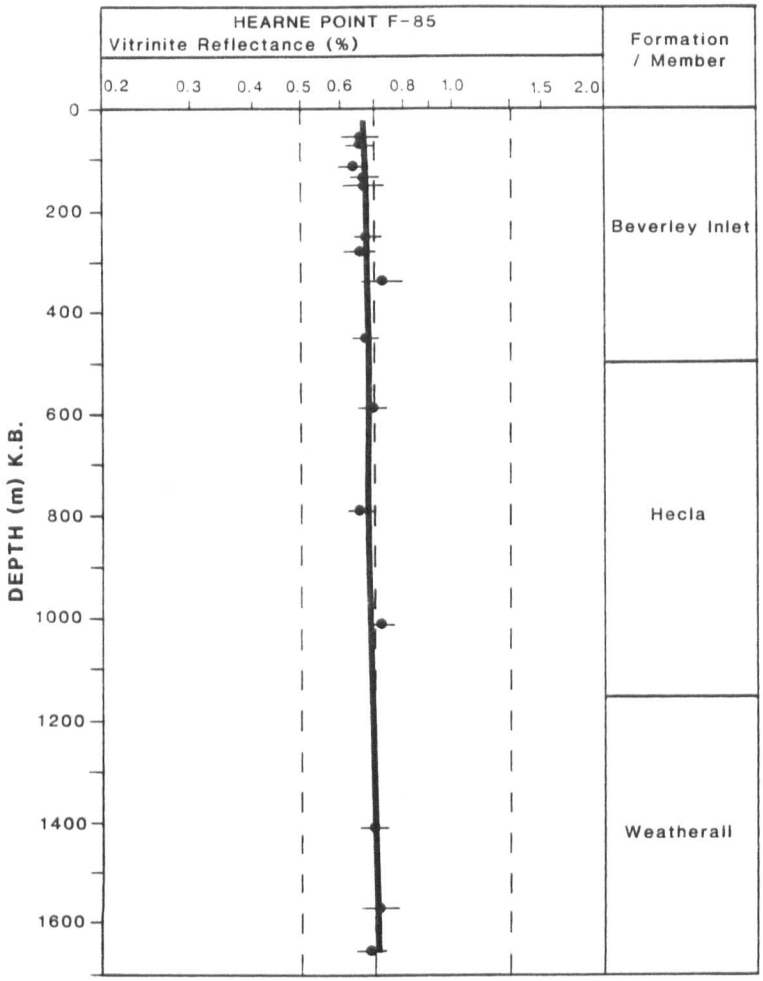

Figure 8-2 Vitrinite reflectance versus depth profile, Panarctic Hearne Point F-85

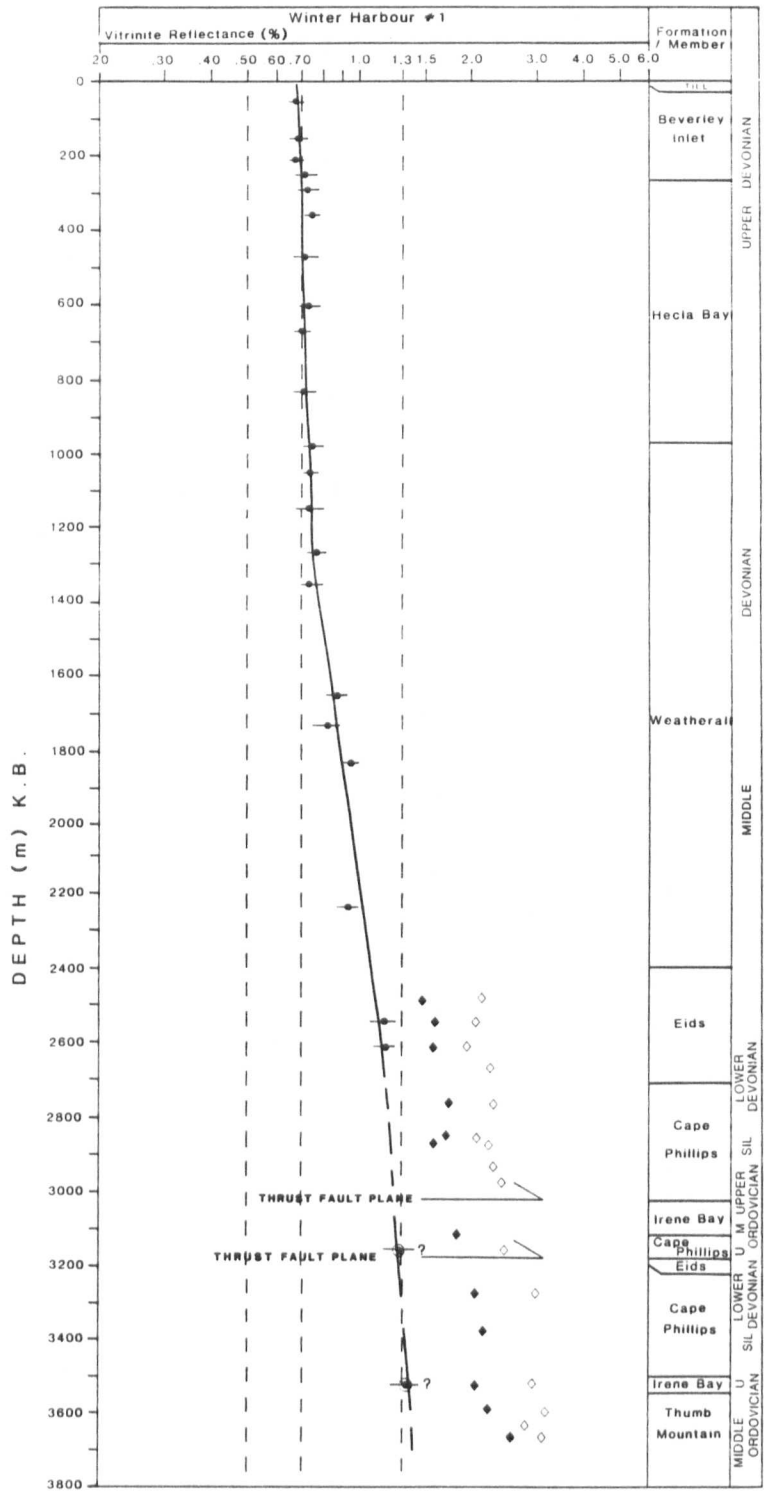

Figure 8-3 Vitrinite reflectance versus depth profile, Panarctic Winter Harbour #1

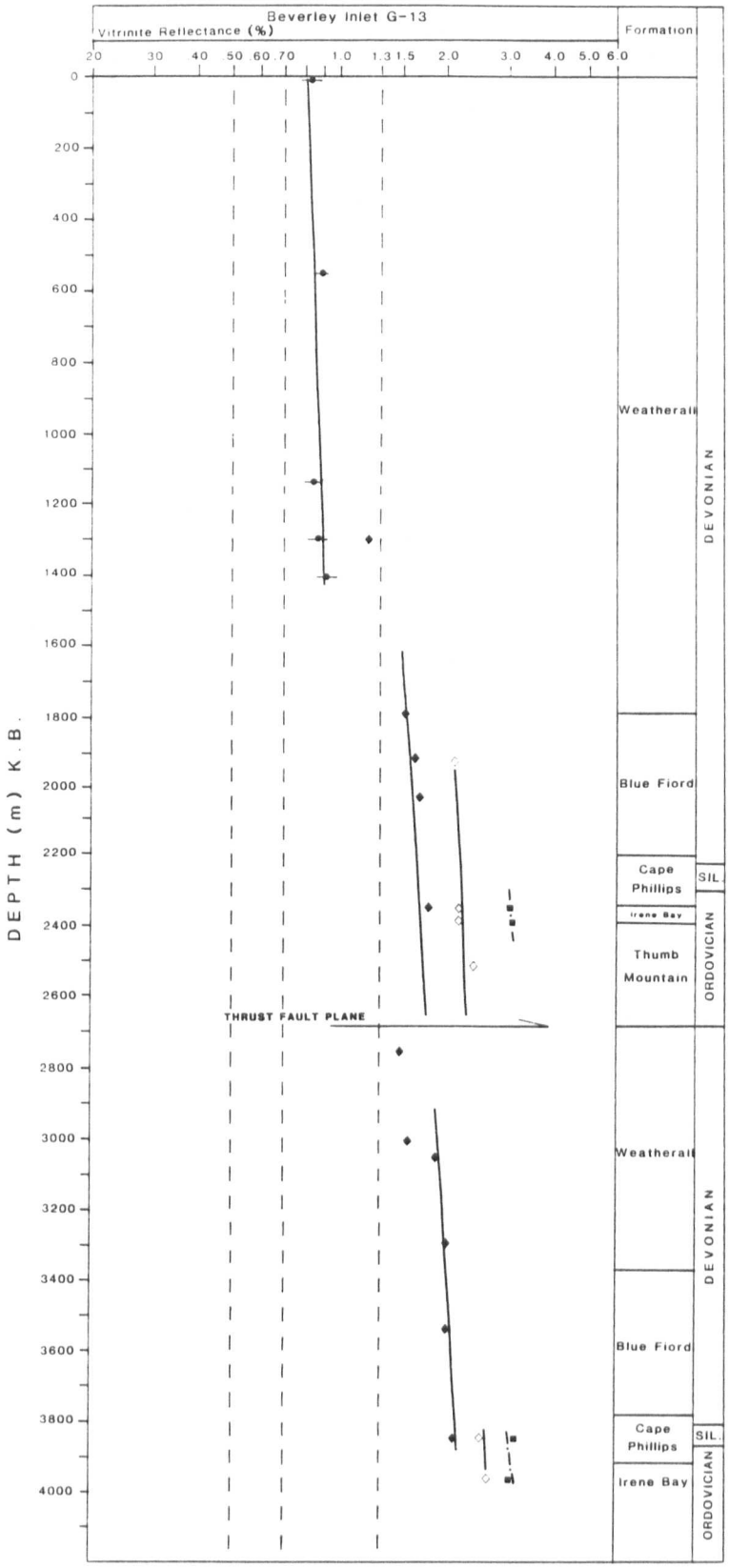

Figure 8-4 Vitrinite reflectance versus depth profile, Panarctic Beverley Inlet G-13

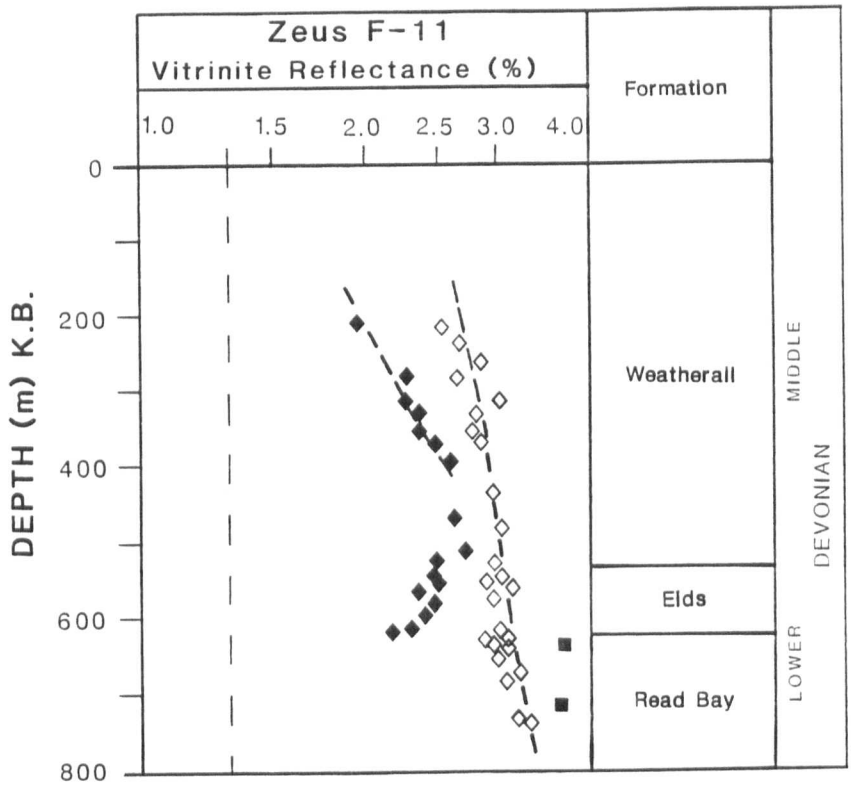

Figure 8-5 Vitrinite reflectance versus depth profile, Panarctic Zeus F-11

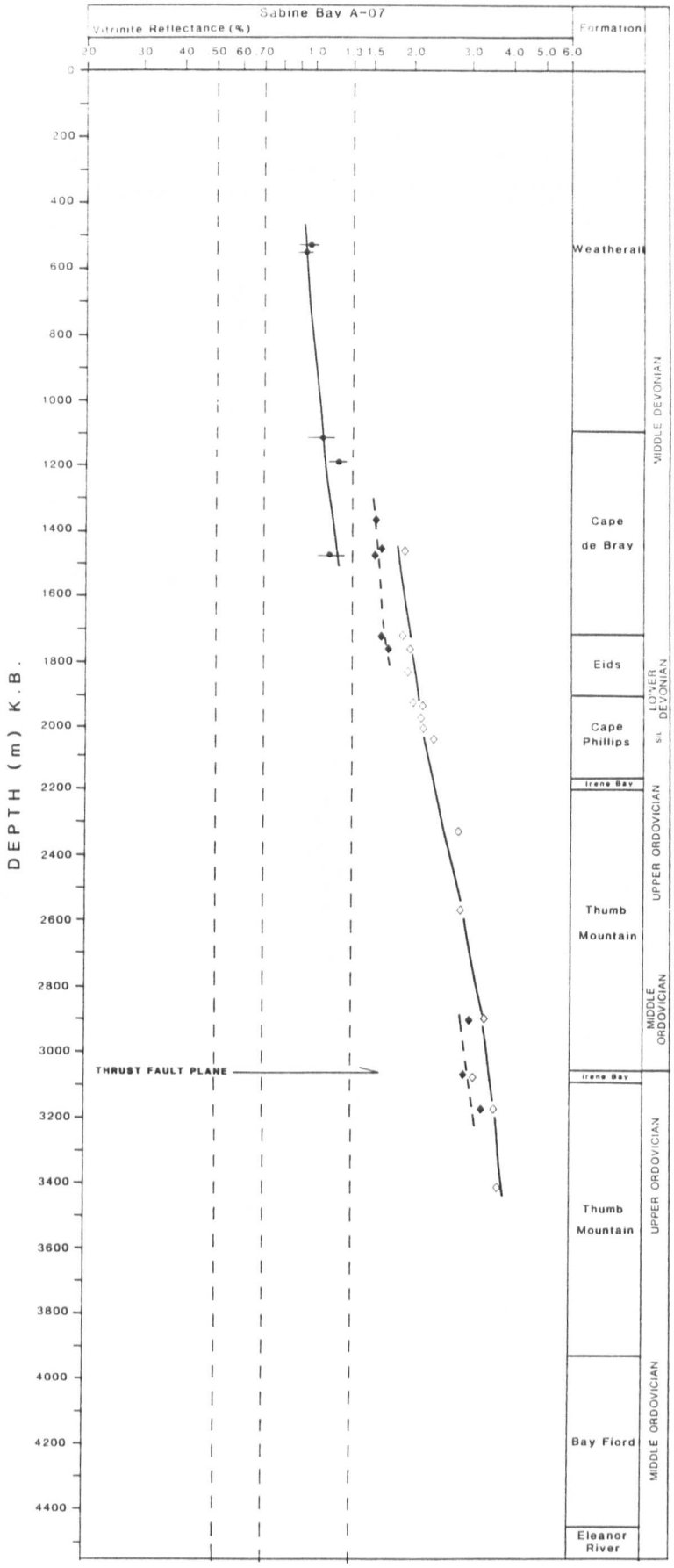

Figure 8-6 Vitrinite reflectance versus depth profile, Panarctic Sabine Bay A-07

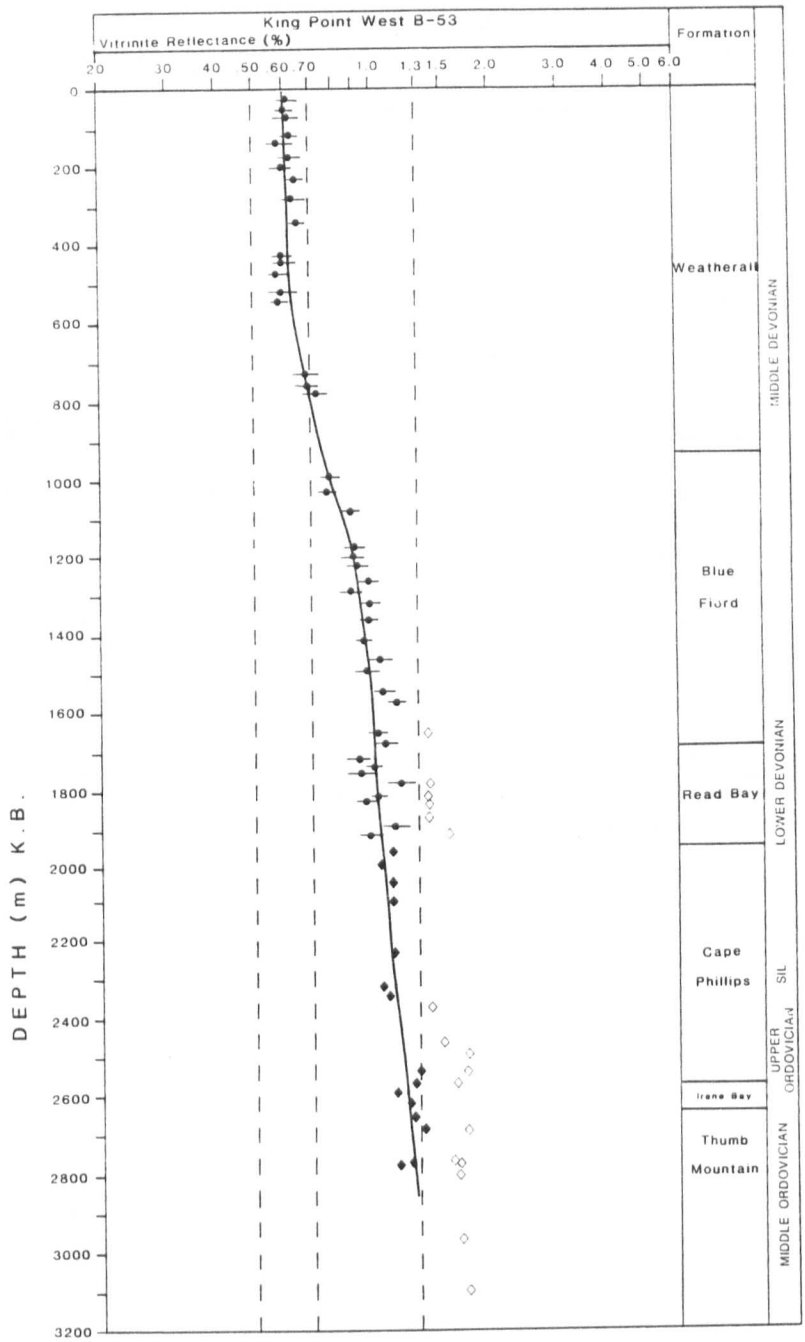

Figure 8-7 Vitrinite reflectance versus depth profile, Panarctic King Point West B-53

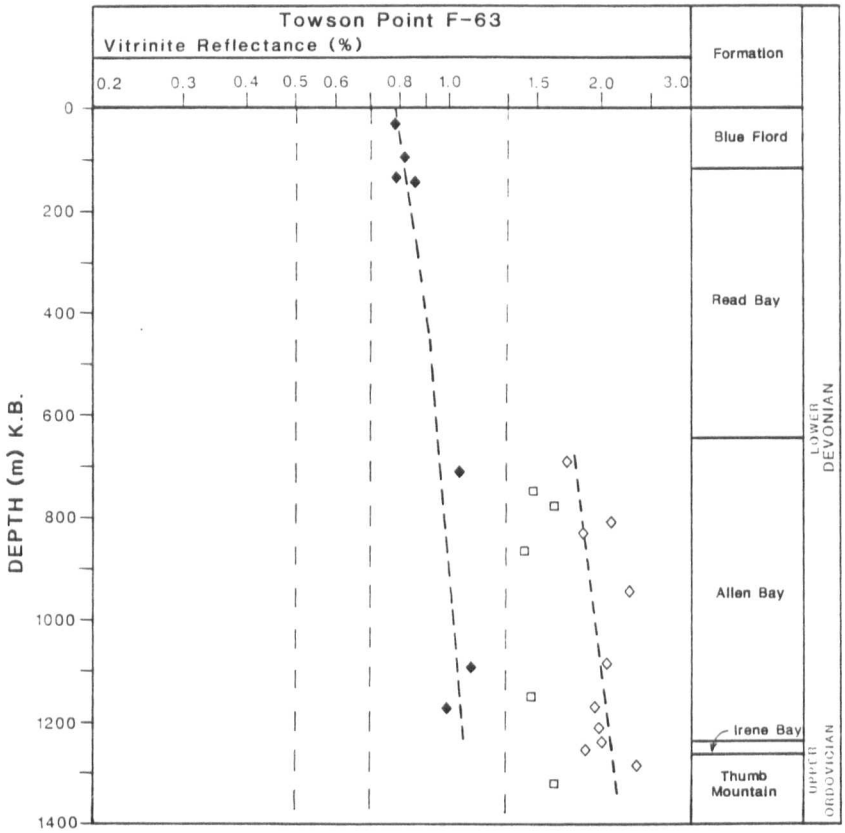

Figure 8-8 Vitrinite reflectance versus depth profile, Panarctic Towson Point F-63

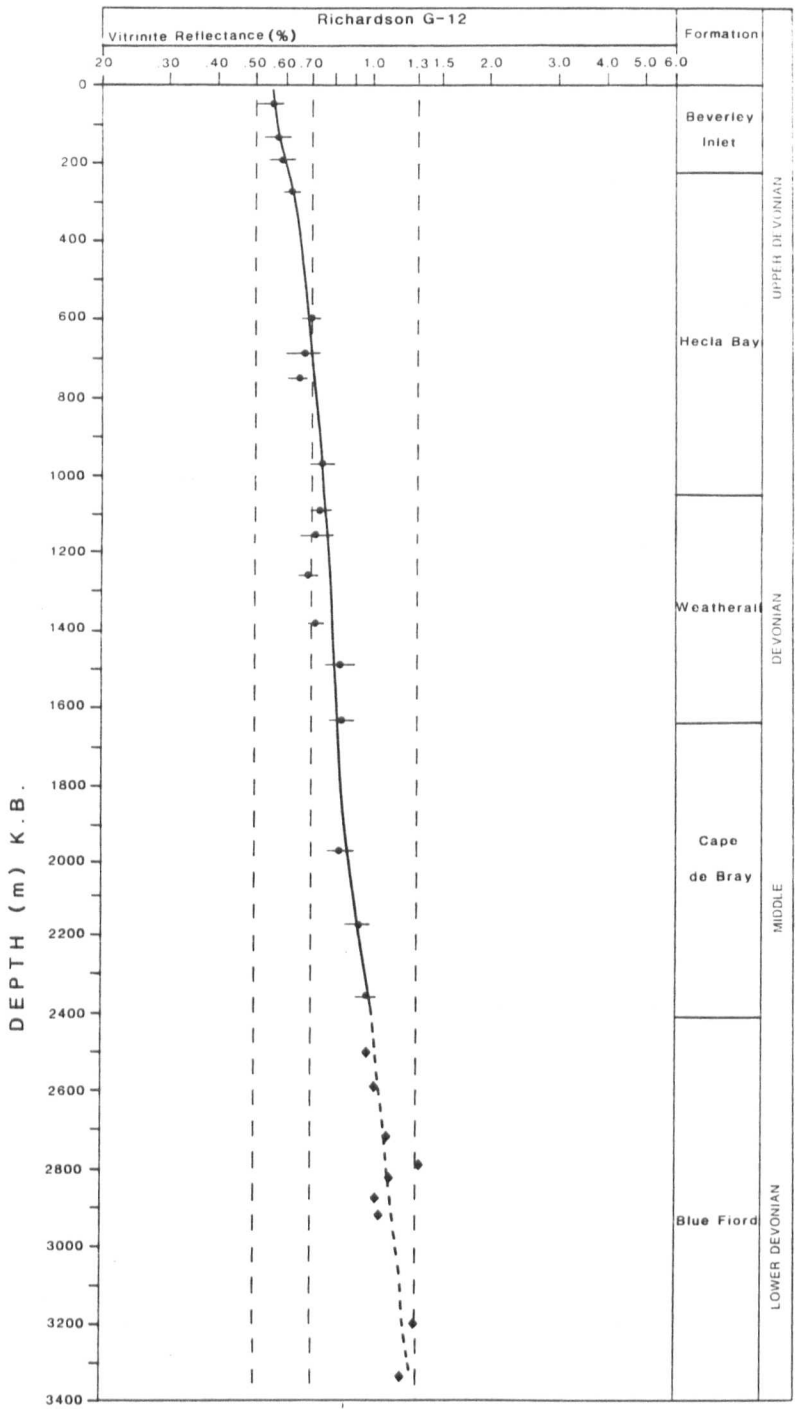

Figure 8-9 Vitrinite reflectance versus depth profile, Panarctic Richardson G-12

PLATE 3

All photomicrographs taken under ultraviolet excitation, water immersion (excitation 400 - 440 nm, barrier filter 470 nm). The long axis of each photomicrograph is 240 μm.

a) A concentration of microspores, Apollo C-73, 40 m.

b) Megaspores showing processes (P) and variable fluorescence intensities, Apollo C-73, 40 m.

c) A brown-fluorescing megaspore (MG) surrounded by brightly-fluorescing cutinite layers (CU) Apollo C-73, 40 m.

d) A massive resinite body showing what appears to be the effect of degradation, Apollo C-73, 40 m.

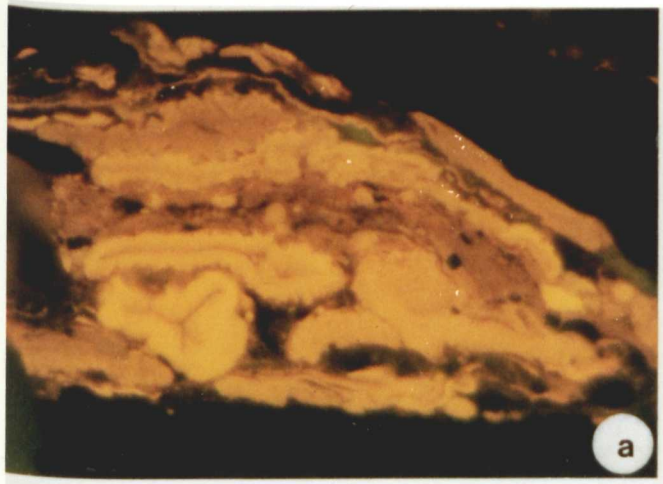
a

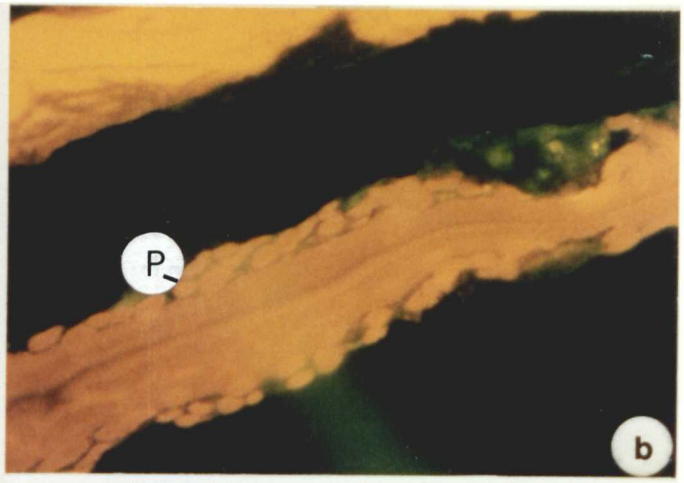
P
b

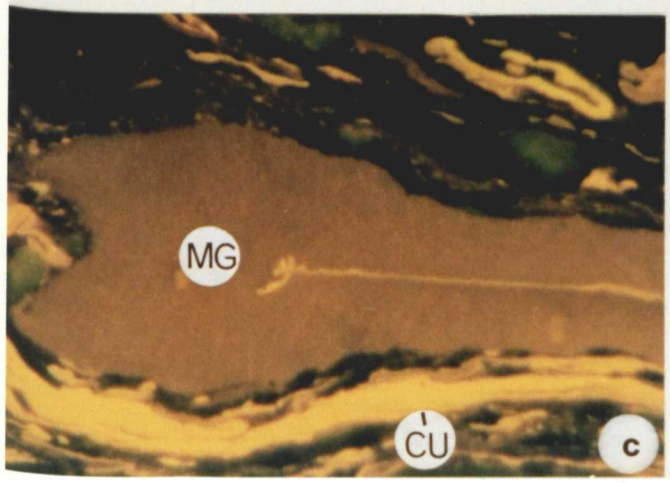
MG
CU
c

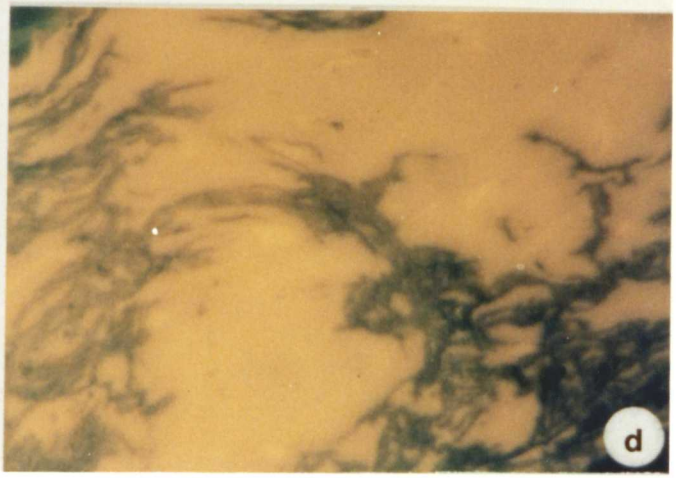
d

PLATE 4A Graptolite fragments in the Cape Phillips shales

All photomicrographs taken in black and white under plane polarized light, oil immersion. The long axis of each photomicrograph is 200 μm.

a) Graptolite fragment showing fusselar layers (L), Apollo C-73, 2455 m.

b) Subtangential graptolite fragment showing traces of U-shaped fusellar layers (L) Apollo C-73, 2455 m.

c) Graptolite fragment showing almost horizontal or broad U-shaped fusellar layer (L), Apollo C-73, 2720 m.

d) Subtangential graptolite fragment showing V-shaped fusellar layers (L), Apollo C-73, 2600 m.

e) Non-structured fragment of graptolite (NS), Eldridge Bay E-79, 1550 m.

f) Same as d) above but rotated 90° to show anisotropy of fragment.

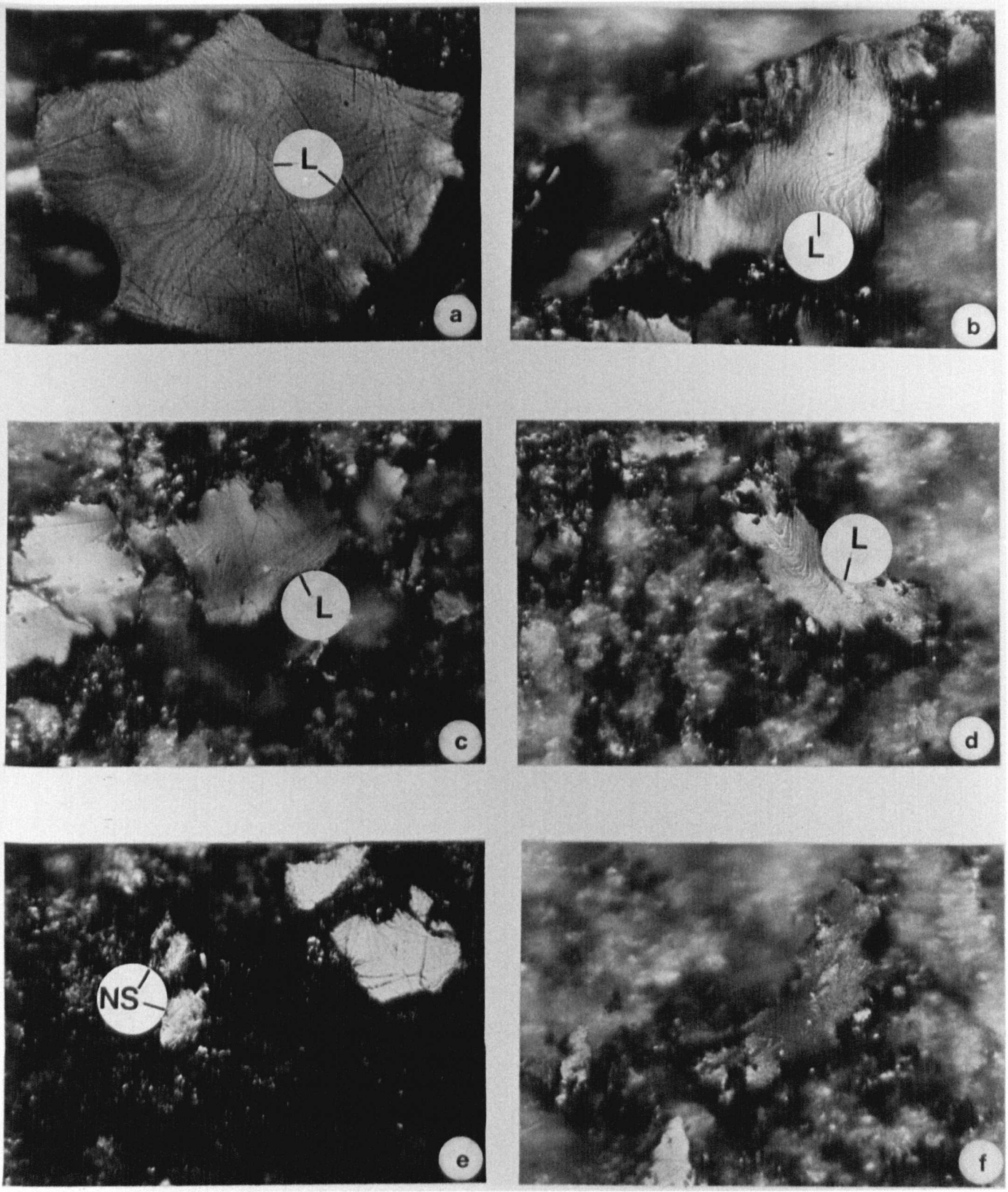
L
a
L
b
L
c
L
d
NS
e
f

PLATE 4B

All photomicrographs taken in black and white under plane polarized light, oil immersion. The long axis of each photomicrograph is 240 μm.

a) A subtangential section of graptolite through the layered wall (periderm) (PD). Thecae (TH) and common canal are clearly visible, Marie Bay D-02, 1060 m.

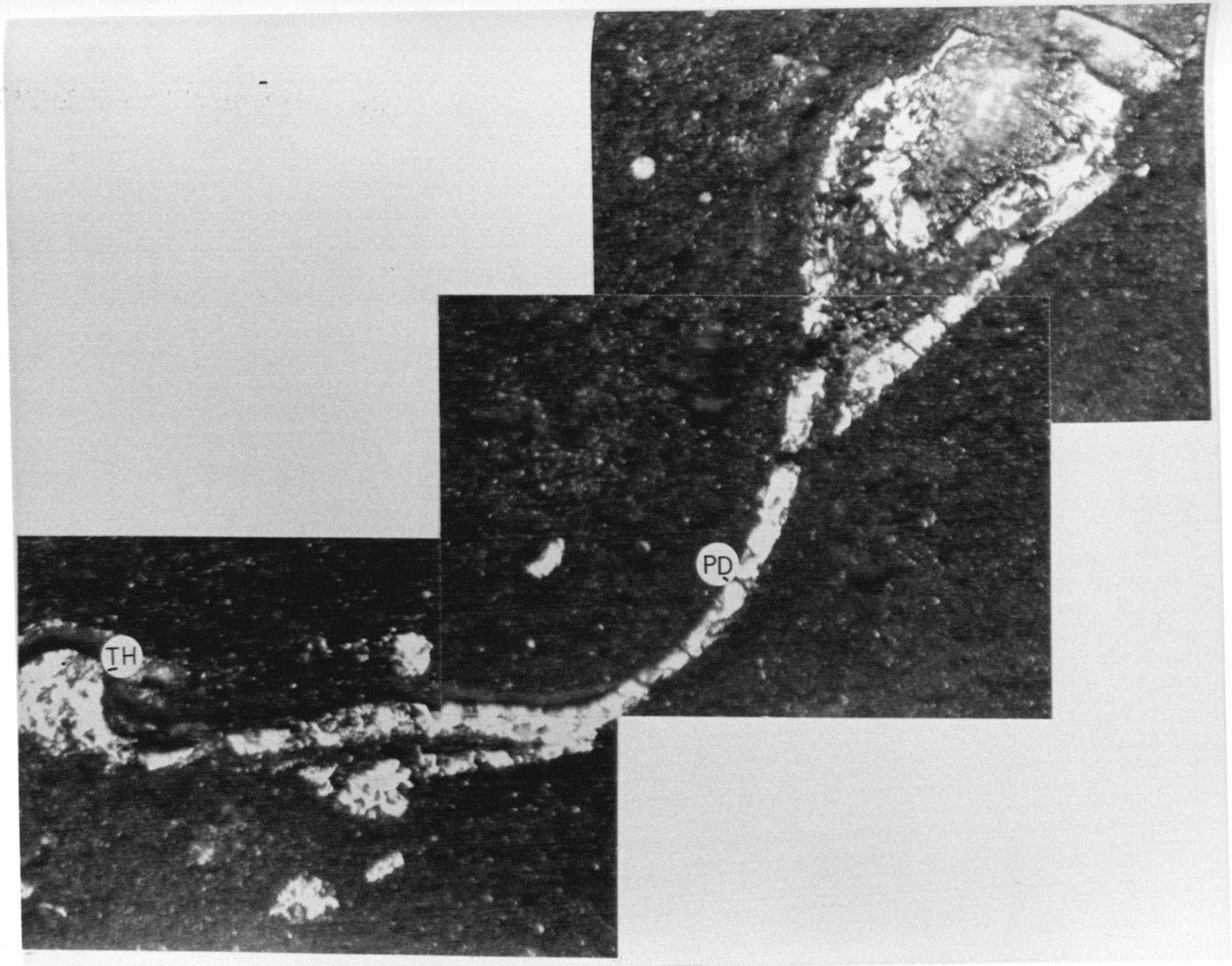
TH
PD

Mountain carbonates and Bay Fiord evaporites contain strongly-reflecting bitumen, which reflects from 3.10 to 4.05% Ro, max and is angular, non-granular to slightly granular, anisotropic metabitumen. The Eleanor River Formation contains only traces of bitumen with maximum reflectance of 2.60 to 2.70%.

This drillhole offers the opportunity to use bitumen reflectance as an indicator of thermal maturation because of the absence of vitrinite in the Lower Palaeozoic sediments. Two different sections can be distinguished based on the type of organic matter, its optical properties and enclosing matrix. The top section (A) contains higher-plant remains with very little bitumen. Organic-rich samples of the Weatherall Formation contain vitrinite and exinite particles. The reflectance trends of vitrinite and bitumen are sub-parallel with bitumen following a higher trend (Figure 8-1). At least three bitumen types are present in section B. Bitumen is more abundant in the Lower Palaeozoic carbonates than in the Middle-Upper Devonian Weatherall sandstones. The low-reflecting solid bitumen with a wispy to rounded form appears to be primary and autochthonous. This material is morphologically similar to vitrinite and could have been derived from algae present in the Upper Ordovician to Lower Devonian strata. The second type of solid bitumen shows a pore-filling shape and its relationship to the source organic matter is unknown. Where this latter bitumen type is associated with fossils (graptolites), as in the Cape Phillips Formation, it appears autochthonous.

All bitumen types in section B increase non-linearly with depth (Figure 8-1). Even at depths of 3,000 m, the criteria of distinction among the bitumen types (reflectance, morphology) can be applied, an indication that each type follows its own trend. Increased burial has affected the bitumens differently. The reflectance of all bitumen types increases with depth.

Although graptolites coexist with at least two low-reflecting bitumen types in the Cape Phillips Formation (Figure 8-1), it is difficult to envisage the reflectance trend of the graptolites due to their narrow vertical distribution.

8.2 SOURCE - ROCK POTENTIAL

8.2.1 LOWER PALAEOZOIC

The drillholes that penetrate strata belonging to the Parry Islands Fold Belt are confined to the Melville and Cameron Islands. The strata penetrated in Melville Island belong to the Middle to Upper Devonian clastic wedge (Embry and Klovan, 1976) and terminate in either Silurian or Upper Ordovician strata. Gas logs of Melville Island drillholes show that wet gas was penetrated near the surface (Powell, 1978). The same author also observed a decline in the percentage of wet gas with depth in the following drillholes: Zeus F-11, Apollo C-73, Dundas C-80 and Sabine Bay A-07. This decline indicates the onset to the overmature zone and atomic hydrogen to carbon ratios measured on bitumen from the Blue Fiord Formation fall in the range of 0.55 to 0.60 (Powell, 1978) which indicates their overmaturity (Rogers et al., 1974).

All of the Palaeozoic Melville Island drillholes spud in the mature zone. The mature to overmature transition occurs in the lower part of the Weatherall Formation at Apollo C-73, Zeus F-11, Dundas C-80 and Sabine Bay A-07. Generally, the Palaeozoic limestones have a very low organic carbon content and the transition between the mature and overmature zone must be determined from bitumen reflectance.

The Hecla Bay Formation consists mainly of fine- to medium-grained sandstone with thin intervals of dark grey carbonaceous shale, siltstone and occasional thin coal

seams. Organic carbon content is low (0.2 - 0.5 wt%) apart from the relatively high values represented by the thin coals (Powell, 1978). Organic-matter examination indicates a land-plant origin and the hydrogen to carbon atomic ratios are low.

The Weatherall Formation is characterized by repetitive coarsening-upward cycles of shale, siltstone and sandstone (Embry and Klovan, 1976), whereas the Bird Fiord Formation contains a higher proportion of calcareous sediments. These formations, along with the Eids, tend to be overmature in the following drillholes: Apollo C-73, Zeus F-11, and below 1,300 m in Dundas C-80. The hydrocarbon product expected would be gas condensate since examination of the organic matter indicates a predominance of herbaceous material with coaly organic matter being the next dominant component. The latter fluoresces slightly and has become darkened (gray to black) during hydrocarbon generation.

The Blue Fiord Formation is a resistant limestone with lesser dolomite, shale and siltstone and is largely correlative with the Eids and Cape de Bray Formations in the subsurface of Melville Island (Thorsteinsson and Tozer, 1970). The Formation has a low organic carbon content (0.1 - 0.2 wt%) and organic matter resembles that of the Weatherall Formation.

According to Powell (1978) the shale facies of the Cape Phillips are characterized by very high organic carbon values (3 - 5 wt%), accompanied by high gas yields (in excess of 54,000 ppm). The above sequence is overmature in the Apollo C-73, Zeus F-11, Sabine Bay A-07 and Dundas C-80 drillholes and the hydrocarbons expected would be dry gas or gas condensate. The carbonates of the Allen Bay and Read Bay Formations generally have a low organic carbon content (<0.2 wt%) (i.e. Dundas C-80; Powell, 1978) and the hydrocarbon yields are low. The Thumb Mountain carbonates are

overmature in Dundas C-80 and yielded no hydrocarbons. The Bay Fiord evaporites in Sabine Bay A-07 are also overmature. The source-rock potential of these formations is nil.

From the foregoing discussion it is evident that the Weatherall, Cape de Bray and Cape Phillips Formations can have some source potential for hydrocarbons, particularly in eastern Melville Island. The governing factor is the transformation from mature to overmature, in which case the hydrocarbon product changes from oil to gas-condensate or dry gas. The Weatherall and Bird Fiord Formations have low organic carbon contents (Powell, 1978) which downgrades their potential relative to the Cape Phillips Formation. Drainage of oil should be highly effective because these formations have well developed sandstone bodies which may act as reservoirs.

Within the Parry Islands Fold Belt, the Cape Phillips shales are generally overmature. According to Powell (1978) the Bent Horn oil is most likely to have been derived from the Bird Fiord Formation. The Bent Horn oil pool in Cameron Island is located in the upper part of the Blue Fiord Formation and is overlain by the lower part of the Devonian clastic wedge which contains good source-quality organic matter but in low quantities.

There is ample evidence (in the form of bitumen) that a great deal of oil was trapped in pores in the Ordovician-Middle Devonian carbonate-shelf edges and reefs during Late Devonian times when the regional dip was to the south (Hamilton and Varney, 1982). As mentioned earlier, the most likely source of the hydrocarbons is the Upper Ordovician to Lower Devonian Cape Phillips Formation. The Ellesmerian Orogeny and subsequent development of the Sverdrup Basin by collapse resulted in a reversal of the regional dip and the destruction of most of these traps. Large hydrocarbon accumulations

developed during the Late Devonian, but was converted to bitumen when uplift and a consequent reduction in pressure during the Ellesmerian Orogeny resulted in de-asphalting (Hamilton and Varney, 1982).

All original matrix porosity is now plugged with bitumen and calcite, although some of the original vadose porosity is preserved (i.e. Bent Horn Oil Field) and reservoirs now a second accumulation of oil. Unfortunately, the distribution of this type of porosity is difficult to predict and drilling has failed to establish economic reservoirs.

8.3 REGIONAL THERMAL MATURITY

In this section the isoreflectance and structural contour maps of the Devonian Weatherall Formation will be discussed. A discussion of two cross-sections constructed through the Lower Palaeozoic of Melville Island will follow.

The isoreflectance-contour map for the base of the Palaeozoic Weatherall Formation (Figure 8-10) shows that the Ro variation of the Formation ranges from 0.65% near the Franklinian miogeosyncline-Sverdrup Basin margin to >1.50% in the vicinity of Apollo C-73 (Figure 8-10). The base of the Weatherall Formation was chosen because the formation is penetrated by most drillholes in the Franklinian miogeosyncline. The reflectance increase is gradual in a south to southwesterly direction which coincides with the direction of migration of the foredeep from Cambrian to Late Devonian (Balkwill and Fox, 1982). Although all available drillholes were used, the control of the isoreflectance contour lines is not great because of the limited number of drillholes present in the Franklinian geosyncline and the Dundas Block.

Contrary to the Mesozoic of the Sverdrup Basin, there appears to be little

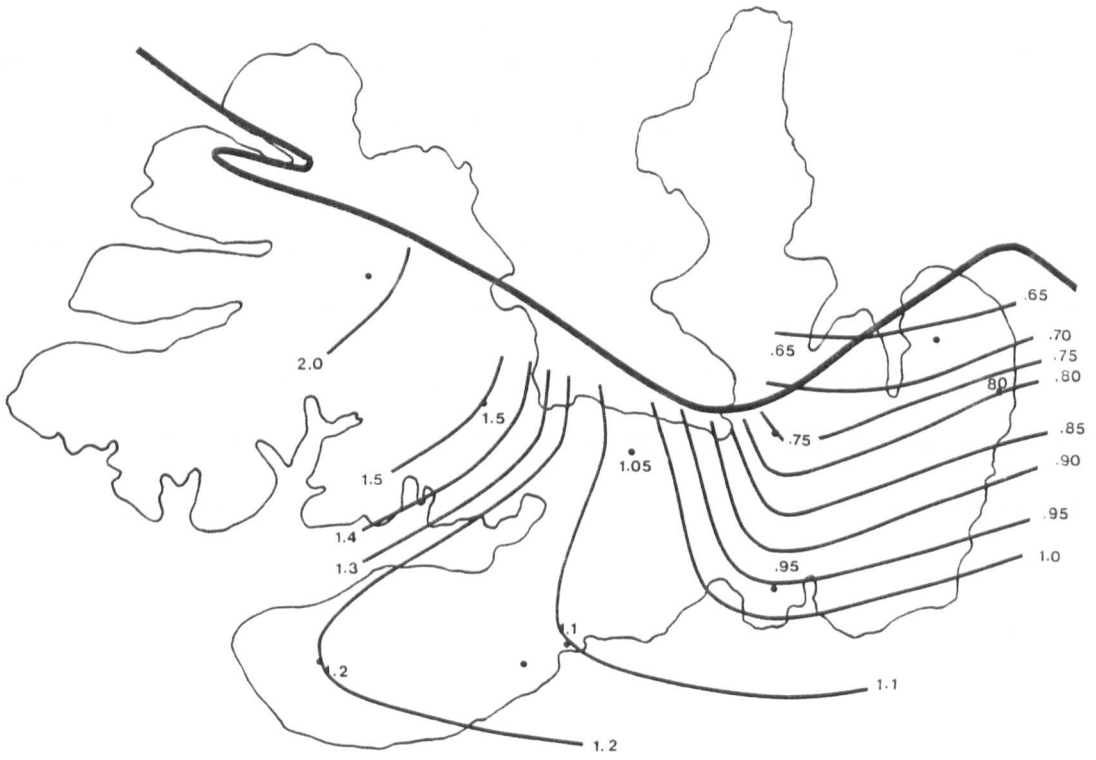

Figure 8-10 Isoreflectance contour map (% Ro), Weatherall Formation

correspondence between the isoreflectance and structural contour maps of the Weatherall Formation in the Franklinian miogeosyncline. The structural contour map (Figure 8-11) shows an increase in present-day burial depth from <500 m near the Sverdrup Basin - Franklinian miogeosyncline margin to >2000 m in southern Melville Island. The isoreflectance contour map has its highest value in the vicinity of Zeus F-11 in west-central Melville (2.10% Ro calculated from bitumen reflectance), yet it has the shallowest burial depth (540 m). This suggests much deeper burial prior to the Ellesmerian Orogeny and subsequent erosion. The amount of section eroded in Zeus F-11 is estimated at >3.0 km based on sedimentological and structural data (Embry, pers. commun., 1989) which would explain the discrepancy between the two sets of contour maps.

Two cross sections (Figure 8-12) were constructed and boundaries between lithostratigraphic units and isoreflectance lines have been drawn. The first cross section A-A^1 (Figure 8-13) connects Dundas C-80 in Dundas Peninsula to Richardson G-12 in eastern Melville Island. The formations penetrated are Devonian and older and are all within the mature stage of hydrocarbon generation. Both Dundas C-80 and Beverley Inlet G-13 have a surface Ro of 0.80%, Winter Harbour #1 and Hearne Point F-85 an Ro of 0.70% and Richardson G-12 a surface Ro of 0.60%. The remainder of the succession falls within the overmature stage based on vitrinite reflectance calculated from bitumen reflectance using Jacob's formula (Jacob, 1983).

In the cross section through the Franklinian miogeosyncline B-B^1 (Figure 8-14), the Middle-Upper Devonian clastic wedge formations are also within the mature stage of hydrocarbon generation (%Ro >0.60). The cross section connects Zeus F-11 in western Melville to Towson Point F-63 in eastern Melville. The King Point West B-53 drillhole has the lowest Ro at the surface (0.60%), Apollo C-73 has a surface Ro of 0.80%, and Sabine

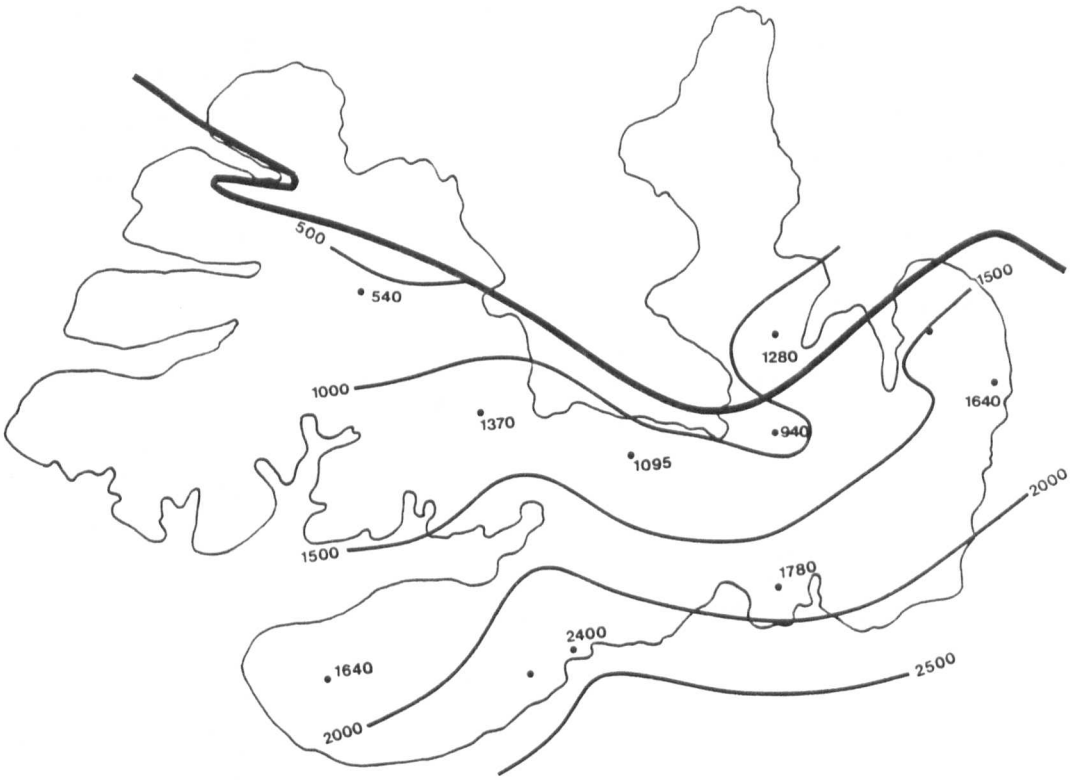

Figure 8-11 Structural contour map (m), Weatherall Formation

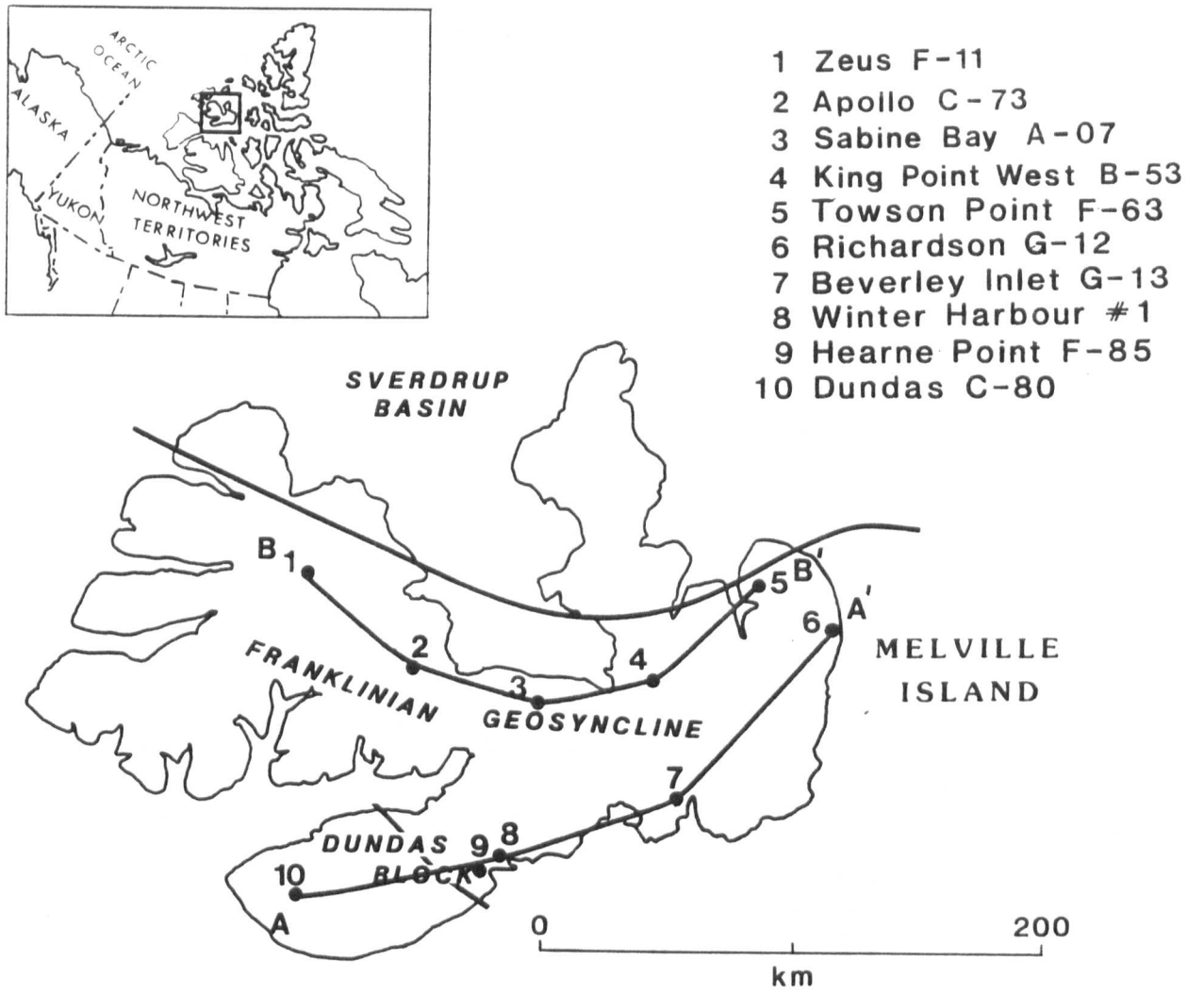

Figure 8-12 Map of Melville Island showing the lines of cross sections

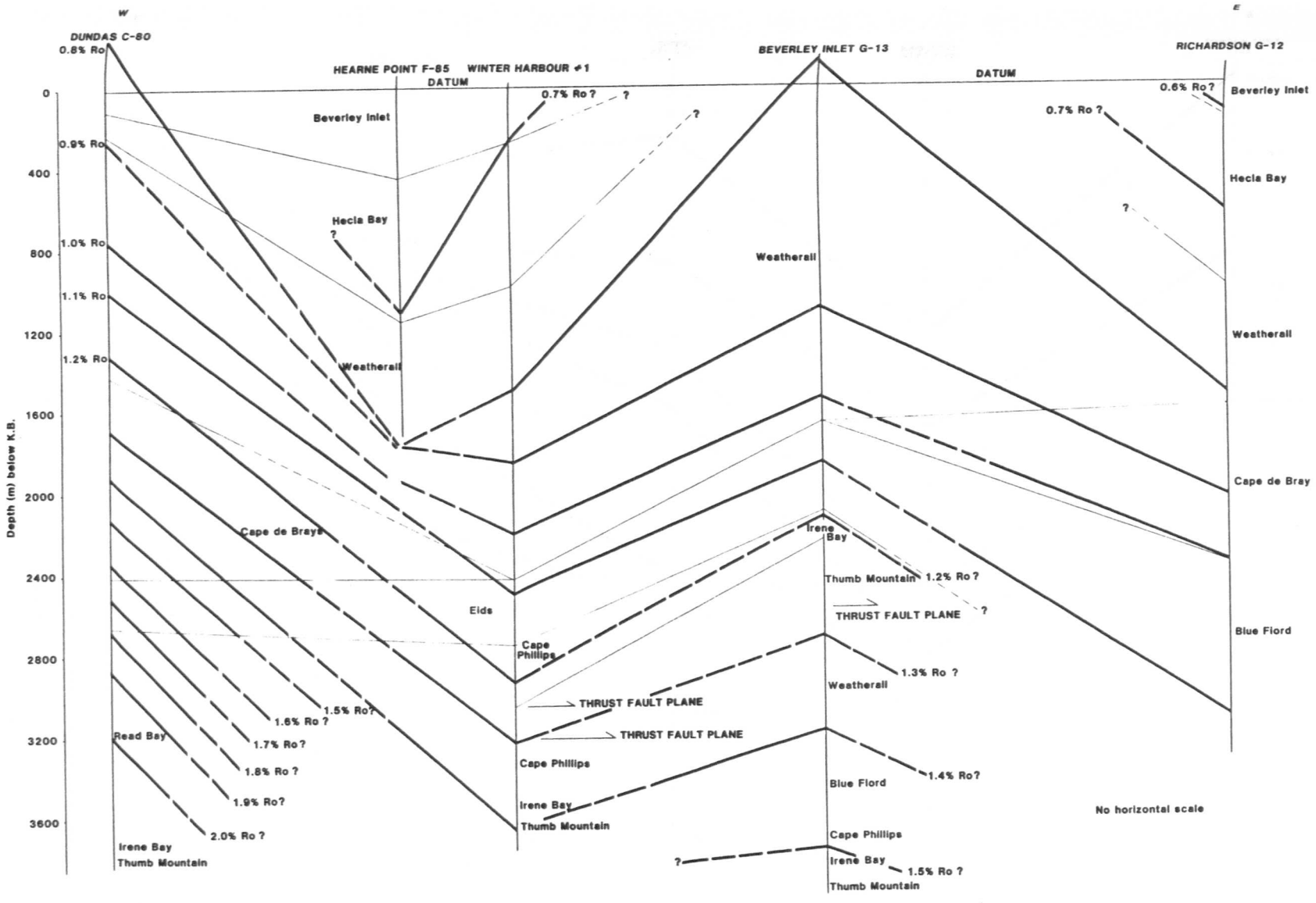

Figure 8-13 Cross section A-A[1], Franklinian miogeosyncline

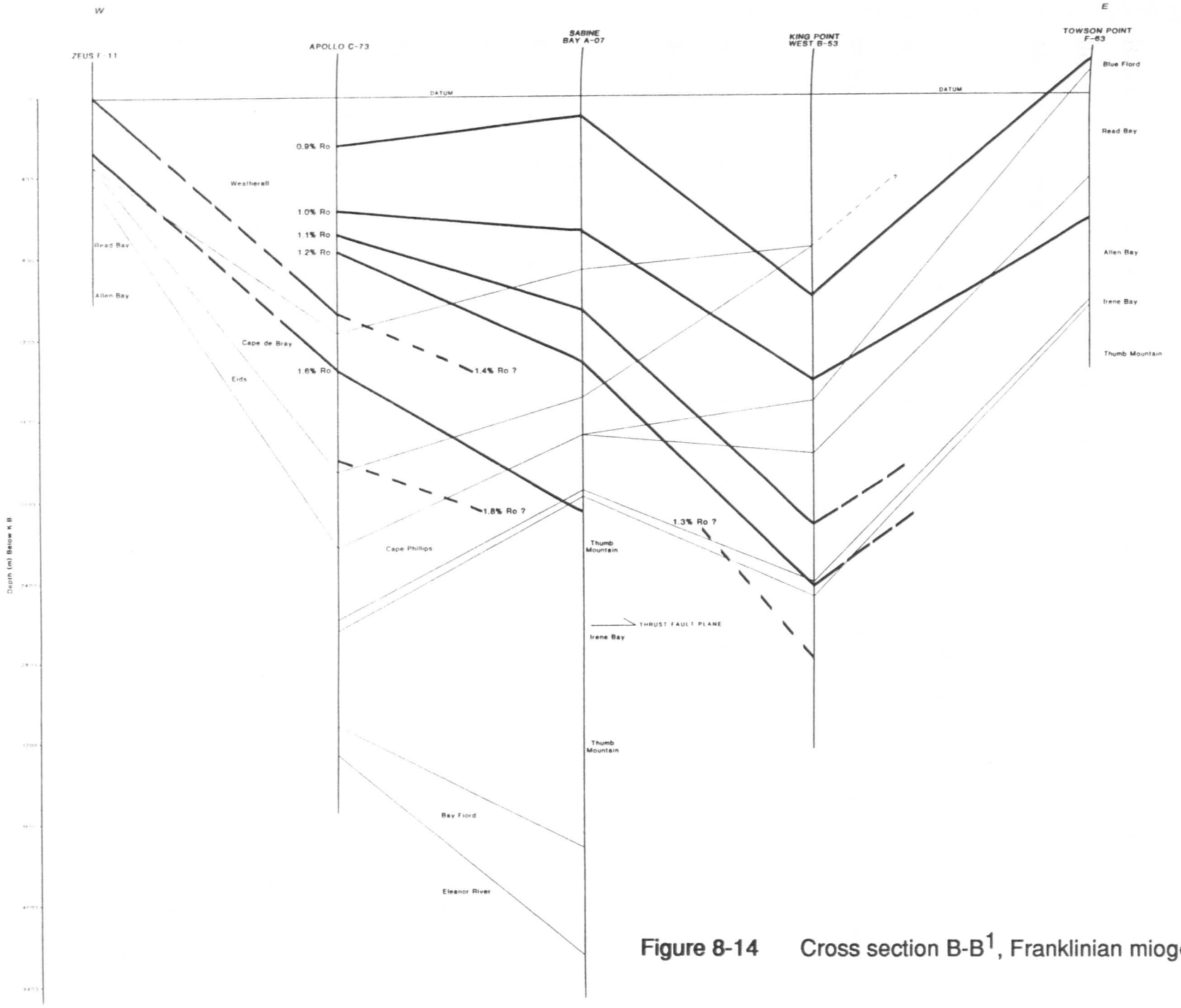

Figure 8-14 Cross section B-B[1], Franklinian miogeosyncline

Bay A-07 an Ro of <0.90%. Towson Point F-63 and Zeus F-11 contain only bitumen and the surface Ro vitrinite of the former is 0.90% whereas of the latter is 1.50%, as calculated from bitumen reflectance.

The differences in maturity of the Weatherall Formation at similar present-day burial depths in section B-B[1] (Figure 8-14) are most likely attributable to differential erosion after maximum depth of burial and variations in the geothermal gradients between the western and eastern parts of Melville Island.

8.4 RELATIONSHIP BETWEEN BITUMEN AND VITRINITE REFLECTANCE IN MELVILLE ISLAND

Figure 8-15 shows the evolutionary path of low-reflecting bitumen in the Palaeozoic and Mesozoic successions studied in Melville Island. The reason for choosing the low-reflecting bitumen from a population of two or three is that there are complexities in the application of bitumen reflectance for maturation studies because of differentiation between primary and reservoir or migrated bitumen. Among various bitumen types, the one with the lowest reflectance correlates well with vitrinite and is most likely to be representative of the most recent generation or migration (Robert, 1980; Goodarzi et al., 1985). The optical properties of bitumen (at 546 nm) follow trends similar to those of vitrinite (Goodarzi and Macqueen, 1990), however, the following differences exist: 1) Bitumen has lower reflectance than vitrinite up to the 'onset' of oil generation, as determined by vitrinite reflectance; and 2) Bitumen reflectance follows a higher trend than that of vitrinite at an Ro level of >1.0% (peak of oil generation).

The reflectance of primary (syngenetic) bitumen increases with increasing burial depth, whereas the reflectance of migrated (epigenetic) bitumen remains

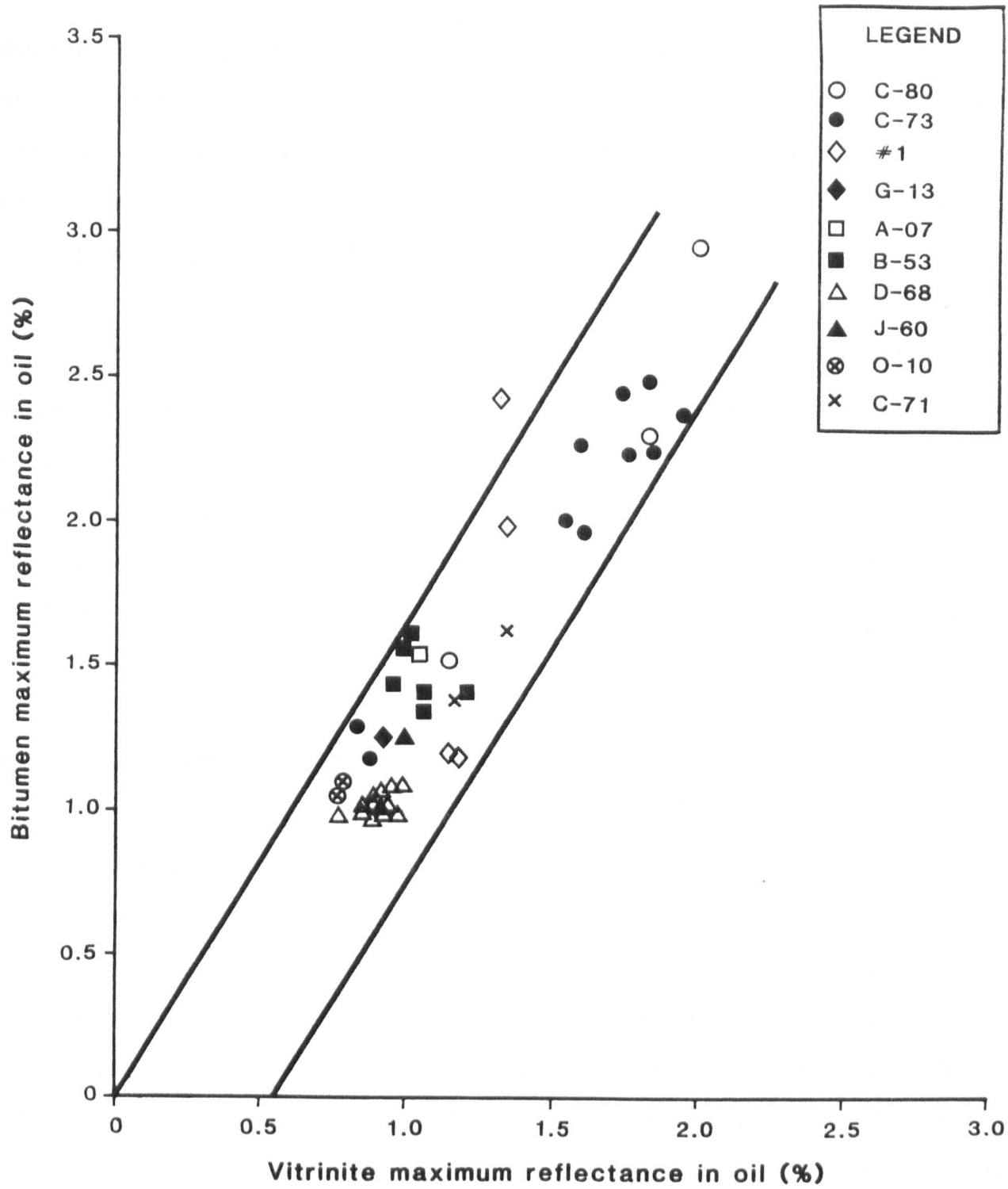

Figure 8-15 Evolutionary pathway of low-reflecting bitumen versus vitrinite reflectance in Palaeozoic and Mesozoic strata, Melville Island

unchanged within the depth intervals it is found. Primary bitumen in the Mesozoic of Melville Island has an Ro range between 0.30-1.50% indicating that it is in the grahamite to epi-impsonite stage (Jacob, 1989). On the other hand primary bitumen in the Palaeozoic carbonates has an Ro, max range between 1.50-2.50% indicating an epi- to meso-impsonite stage (Jacob, 1989).

Bitumen and vitrinite display a linear relationship in the range of 0.10-2.50% Ro, max as shown in Figure 8-15, in agreement with results by Jacob and Hiltmann (1985) and Jacob (1989). Despite the fact that the primary bitumens used in Figure 8-15 have been generated at greatly different times, i.e. in the Palaeozoic and Mesozoic, there is a linear correlation between the lowest-reflecting of the primary bitumens and vitrinite reflectance. This relationship indicates that bitumen reflectance can be used as a maturity parameter for hydrocarbon exploration.

8.4.1 BITUMINIZATION CURVES

When plotting maximum versus minimum bitumen reflectance (Figure 8-16) a linear relationship with some deviations becomes apparent. Despite the different age of the bitumens (Palaeozoic and Mesozoic), there appears to be a relationship in the 0.10-3.0% Ro range. Above this level, the anisotropic bitumens of Dundas C-80 (cata-impsonite) which show mosaic texture deviate towards the region of heat-affected organic matter (Figure 8-16) (Goodarzi, 1984). The non-granular bitumens of Apollo C-73 do not deviate from the broadly linear path, even at Ro, max levels of >3.0% (Figure 8-16).

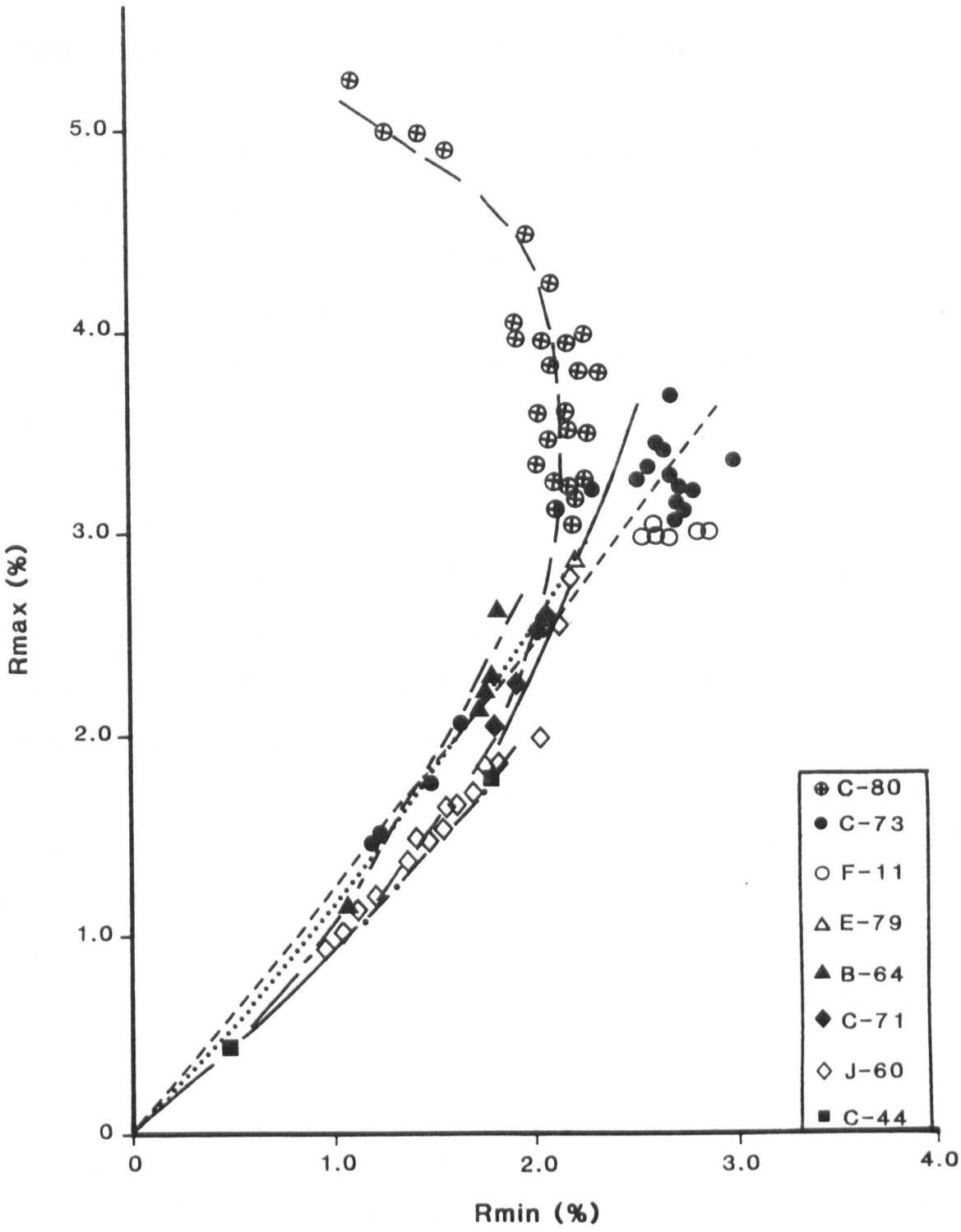

Figure 8-16 Bituminization curves (maximum versus minimum reflectance) of Melville Island bitumen

8.5 THERMAL MATURITY USING GRAPTOLITE REFLECTANCE

Goodarzi (1984) and Goodarzi and Norford (1985; 1987; 1989) compared graptolite reflectance with that of vitrinite, heat-affected organic matter, and natural bitumen. Reflectance in oil of graptolites increases with depth similarly to vitrinite (Goodarzi and Norford, 1985; 1987; 1989) and the dispersion of the optical properties of graptolite periderms follows similar trends to those of vitrinite with increasing coalification (Goodarzi, 1985b).

Figure 8-17 shows the comparison between minimum and maximum graptolite reflectance and the coalification series. Graptolites in Melville Island were identified in Lower Palaeozoic rocks in the following drillholes: Eldridge Bay E-79, Marie Bay D-02 and Apollo C-73. The graptolites have a maximum reflectance range from 1.05-4.0%, with the Eldridge E-79 graptolites having the lowest reflectance (1.10-1.70% Ro, max) and the Apollo C-73 graptolites having the highest (2.50-4.0% Ro, max). Graptolites indicate a maturation stage equivalent to bituminous-anthracite rank (Figure 8-17). Most of the fragments observed were non-granular, parallel to the bedding and highly anisotropic (Plate 4A). Maximum reflectance in oil rather than random should be used because graptolites may behave optically as biaxial material (Clausen and Teichmuller, 1982; Goodarzi, 1984).

Because of the narrow depth distribution of graptolites in Melville Island (Ibbett Bay, Cape Phillips Formations), no definite correlations with bitumen were possible. A direct comparison of graptolite and vitrinite reflectances was not possible due to the absence of phytoclasts in the Ibbett Bay and Cape Phillips basinal shales. Goodarzi and Norford (1989) demonstrated that graptolites generally show higher reflectance trend than primary natural bitumen and were able to correlate graptolite and vitrinite reflectances

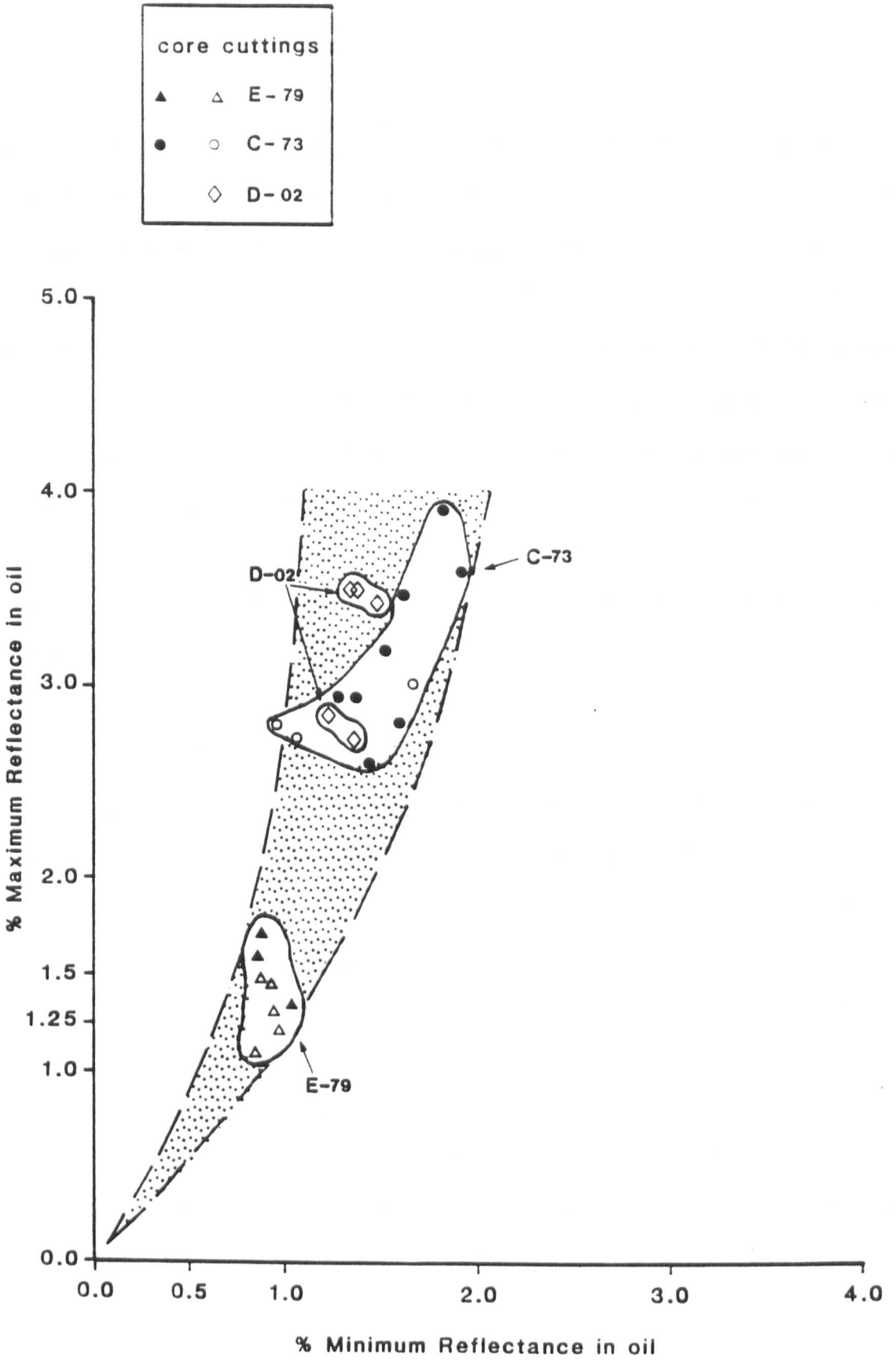

Figure 8-17 Relationship between maximum and minimum graptolite reflectance

using the colour alteration index (C.A.I.) of conodonts which are associated with both. Figure 8-18 shows the comparison between % Ro, max of graptolites versus conodont alteration index (Epstein et al., 1977) superimposed on the stages of hydrocarbon generation (Legall et al., 1981). The thermal maturity of sediments may be estimated using Figure 8-18 by extrapolation of the hydrocarbon generation zone boundaries, based on conodont alteration indices to graptolite and vitrinite reflectance curves. The main hydrocarbon generation zone ('oil window'), corresponding to % Ro, random of 0.5 and 1.3% intersects the graptolite reflectance lines at % Ro, max 1.1 and 2.2 respectively. Goodarzi and Norford (1989) warn that this correlation should be treated with caution because often a C.A.I. value may represent a range of vitrinite reflectance (Epstein et al., 1977) and graptolite reflectance.

When plotting the % Ro, max of graptolites present in drillholes Eldridge Bay E-79, Marie Bay D-02 and Apollo C-73 on Goodarzi and Norford's graph, it is observed that the graptolite reflectance corresponds to 0.7 - 1.0%, 1.5 - 1.9% and 1.6 - 2.0% Ro, max vitrinite respectively. This is in good agreement with the vitrinite reflectance values obtained when converting the low-reflecting bitumen present in the shales to vitrinite using Jacob's (1983) formula. The above values indicate that only the sediments in Eldridge Bay E-79 are within the 'oil window', while the sediments in the other two drillholes are in the overmature ('wet gas') zone of hydrocarbon generation. They also show that for the same level of thermal maturity, graptolite reflectance (% Ro, max) is higher than vitrinite reflectance (% Ro, max), in agreement with the results of Goodarzi and Norford (1989).

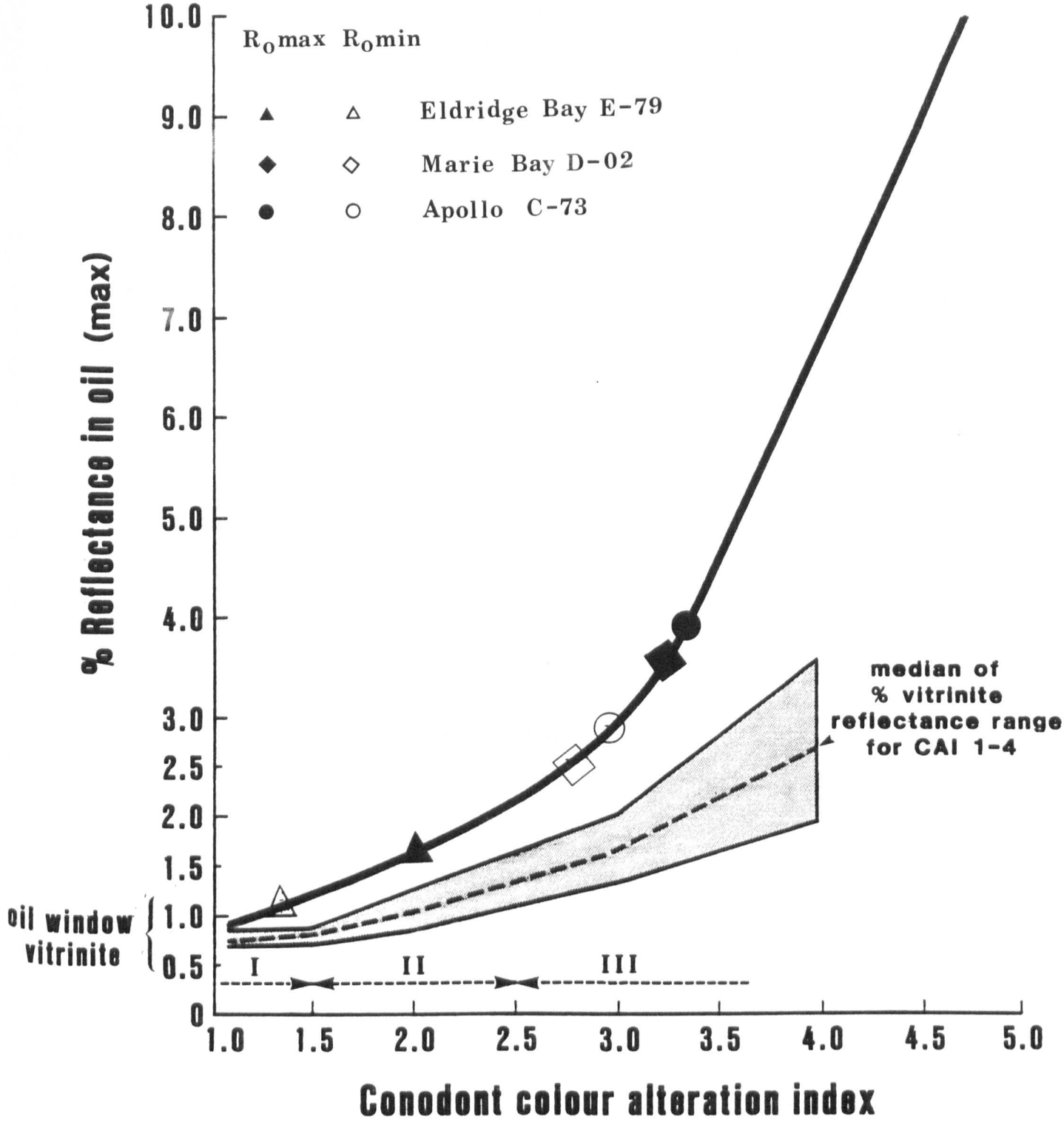

Figure 8-18 Relationship between maximum vitrinite reflectance, graptolite reflectance, conodont alteration index (CAI) and hydrocarbon generation (modified after Goodarzi and Norford, 1989)

CHAPTER IX

CHAPTER IX

9.0 INTRODUCTION

The Sverdrup Basin in Melville Island (longitude 106°-117°, latitude 75° 30'-77°) (Figure 1-2) contains some of the most prolific source rocks found anywhere in the Canadian Arctic Archipelago. This chapter is structured as follows:

a) Description of the type of organic matter and level of thermal maturity of the source rocks and potential source rocks in the Sverdrup Basin, Melville Island; and
b) Description of representative drillholes, supplemented by additional data from other drillholes in the hydrocarbon fields or regions.

9.1 ORGANIC PETROLOGY AND THERMAL MATURITY

Organic-rich shales and siltstones in the Sverdrup Basin occur at four stratigraphic intervals. From the base upwards they are: the Schei Point Group (Middle to Upper Triassic), the Jameson Bay Formation (Lower Jurassic), the Ringnes Formation (Upper Jurassic) and the Deer Bay Formation (Upper Jurassic to Lower Cretaceous) (Figure 2-3).

Organic matter in the Schei Point beds is liptinitic and of marine origin, dominated by Tasmanites algae, dinoflagellate cysts and amorphous fluorescing matrix. In the Jameson Bay and Ringnes Formations terrestrial organic matter dominates, although there are intervals containing Botryococcus algae and amorphous fluorescing matrix. The Deer Bay is dominated by woody and herbaceous organic matter. All reflectance profiles are shown in Figures 9-1 to 9-33.

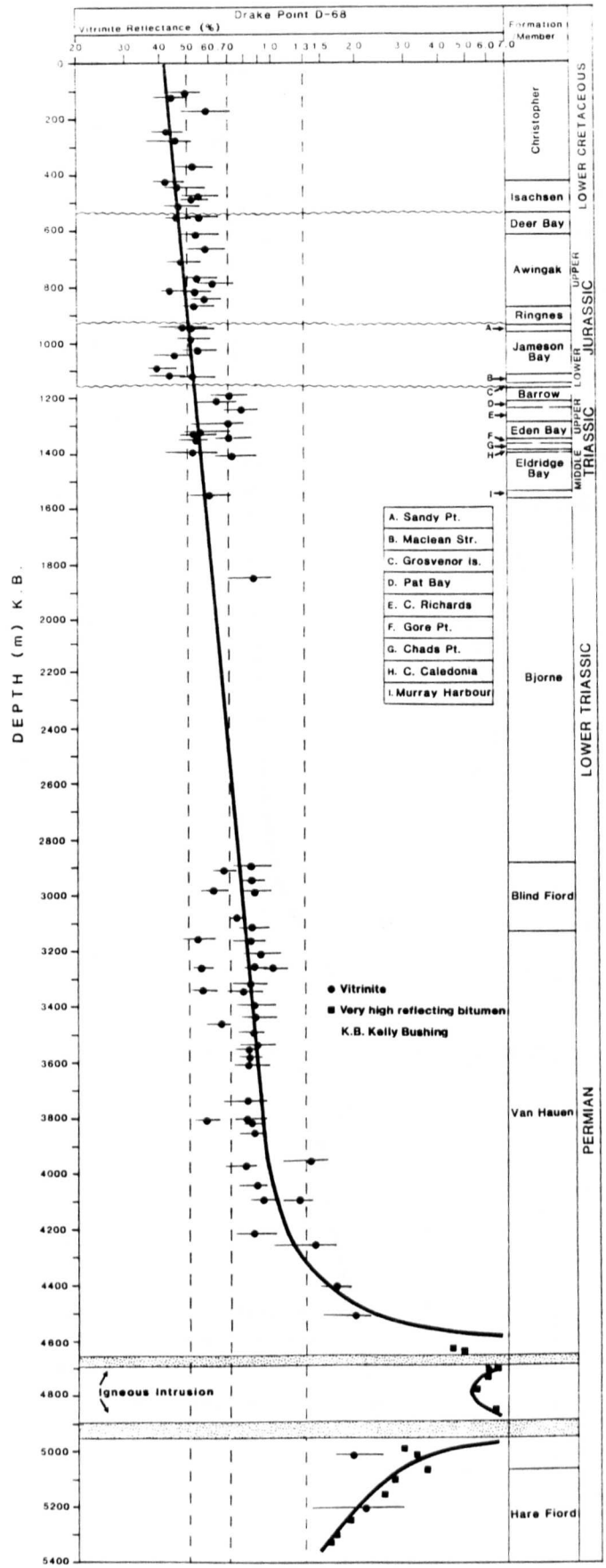

Figure 9-1 Vitrinite reflectance versus depth profile, Panarctic Drake Point D-68

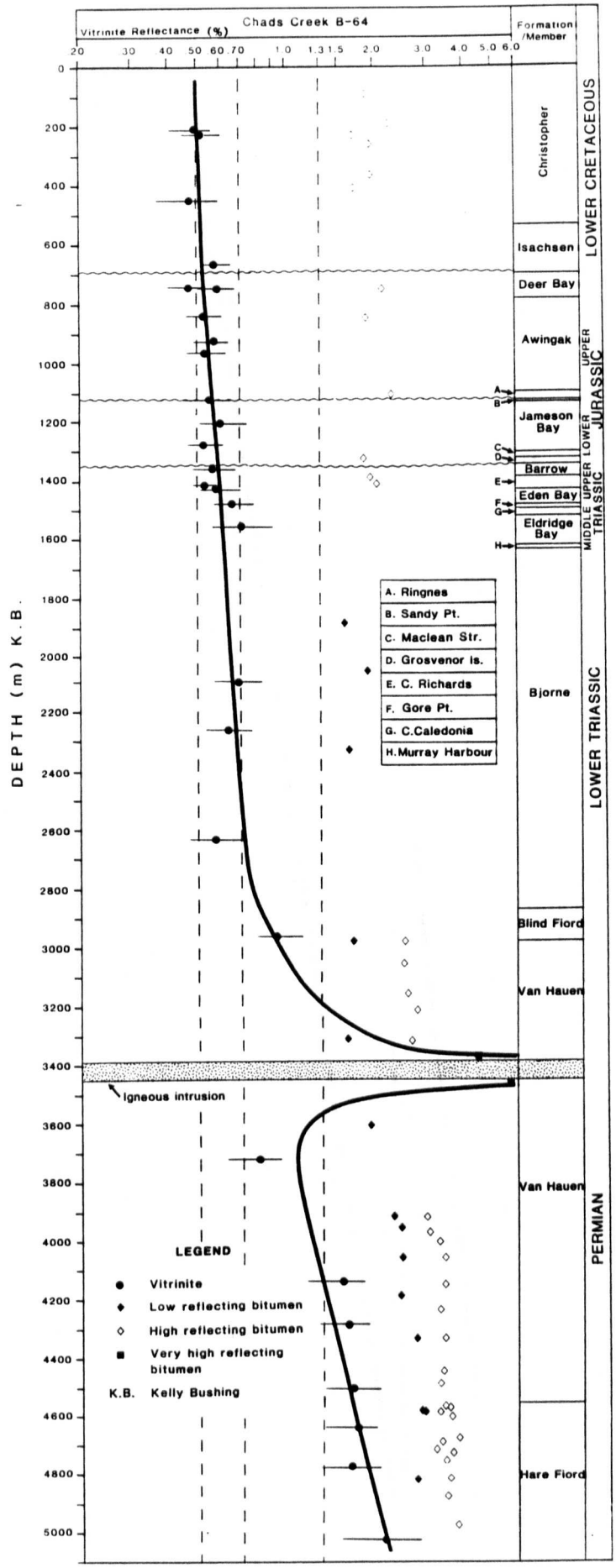

Figure 9-2 Vitrinite reflectance versus depth profile, Panarctic Chads Creek B-64

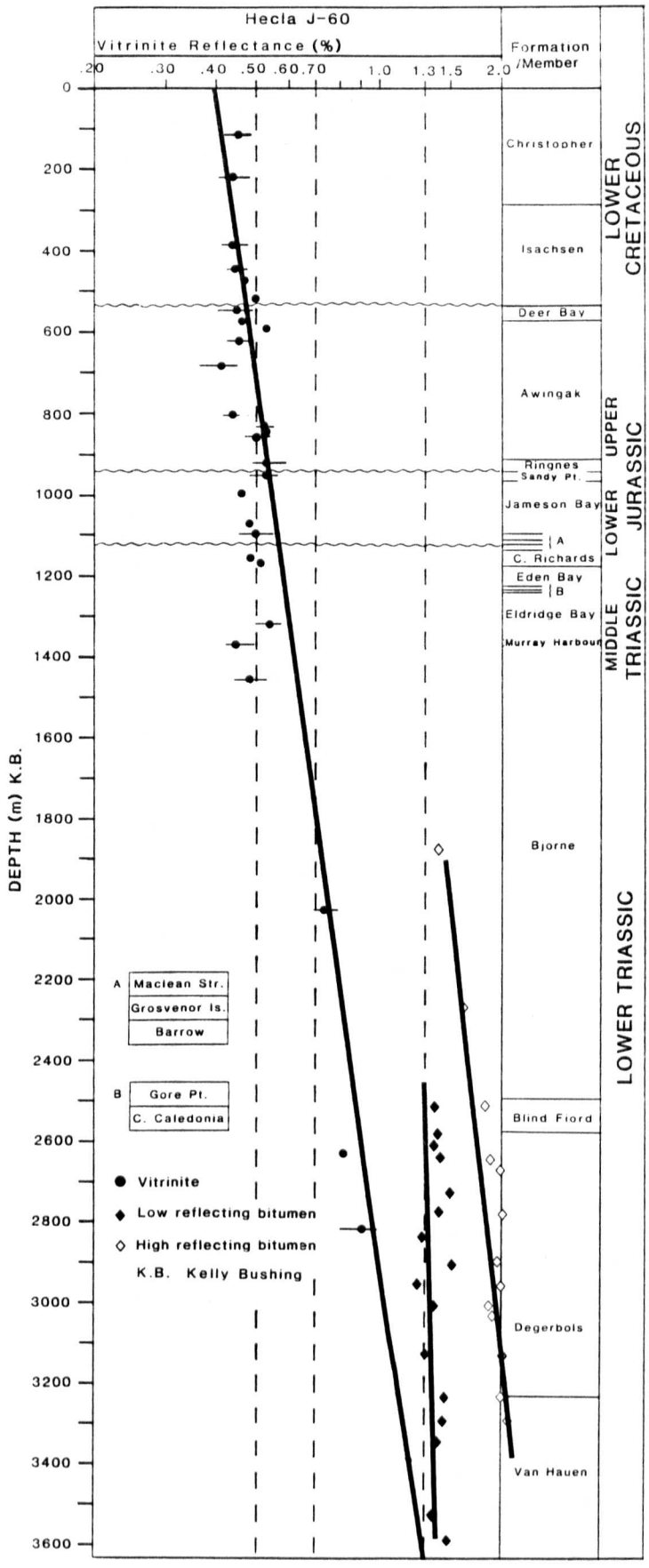

Figure 9-3 Vitrinite reflectance versus depth profile, Panarctic Hecla J-60

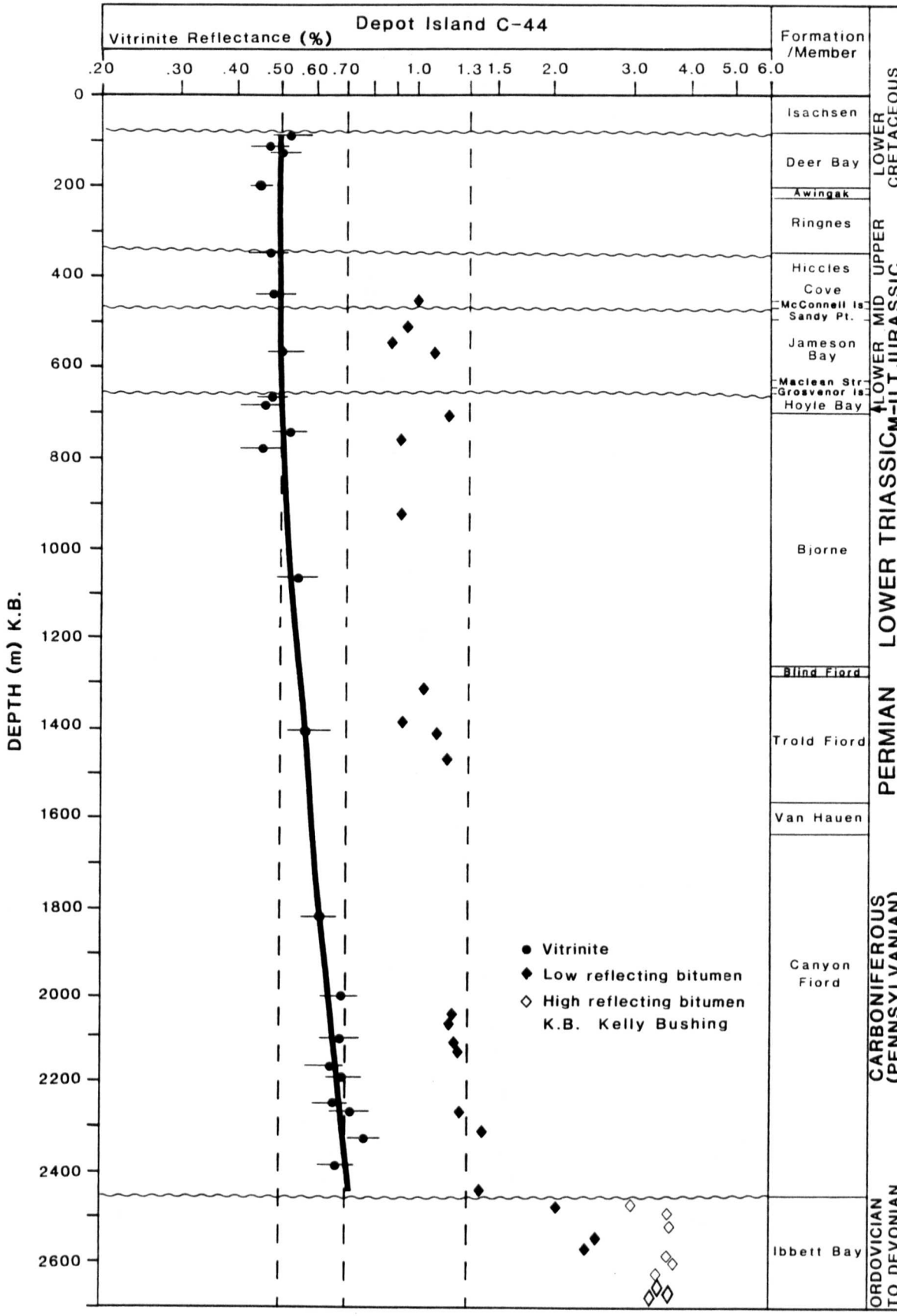

Figure 9-4 Vitrinite reflectance versus depth profile, Panarctic Depot Island C-44

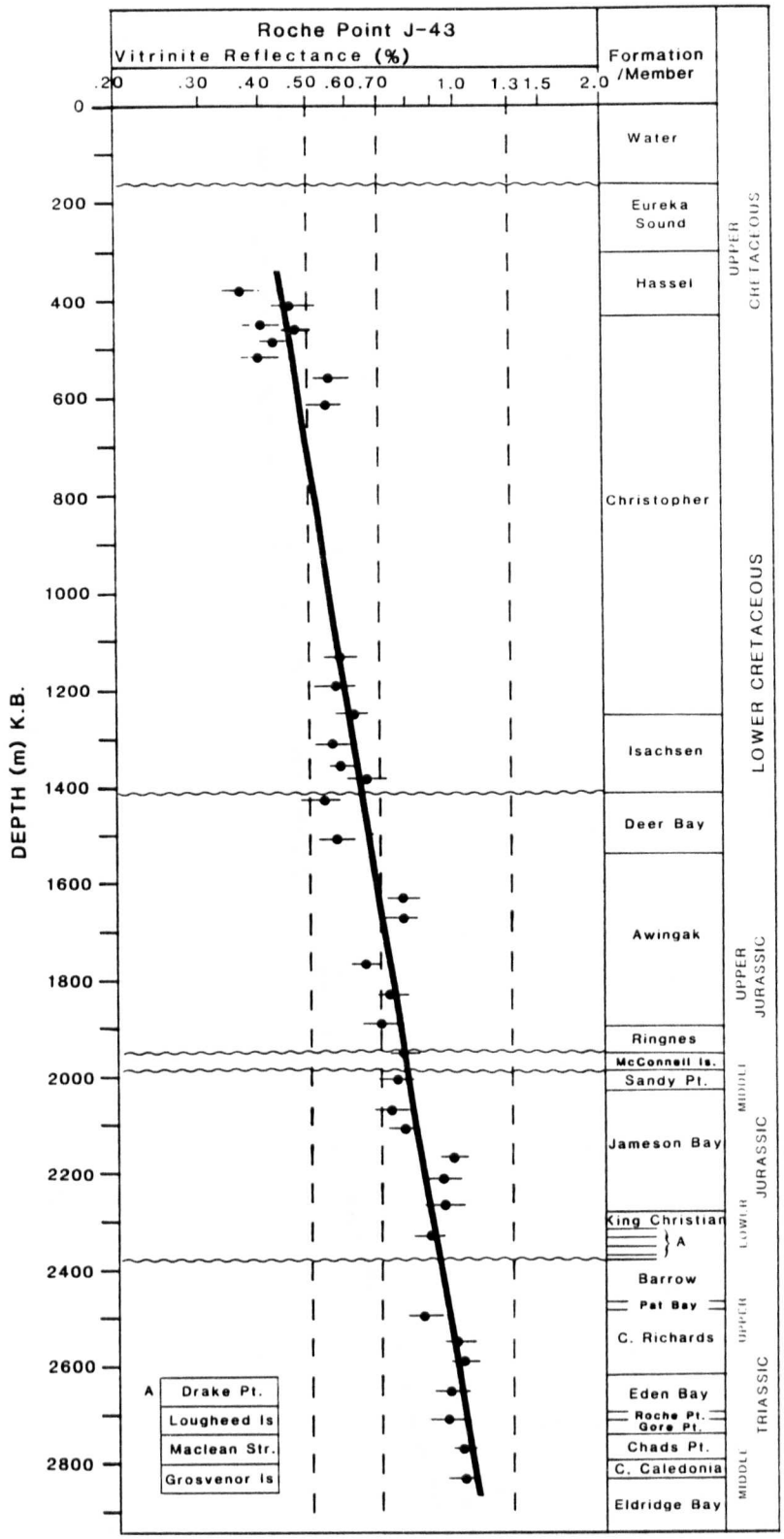

Figure 9-5 Vitrinite reflectance versus depth profile, Panarctic Roche Point J-43

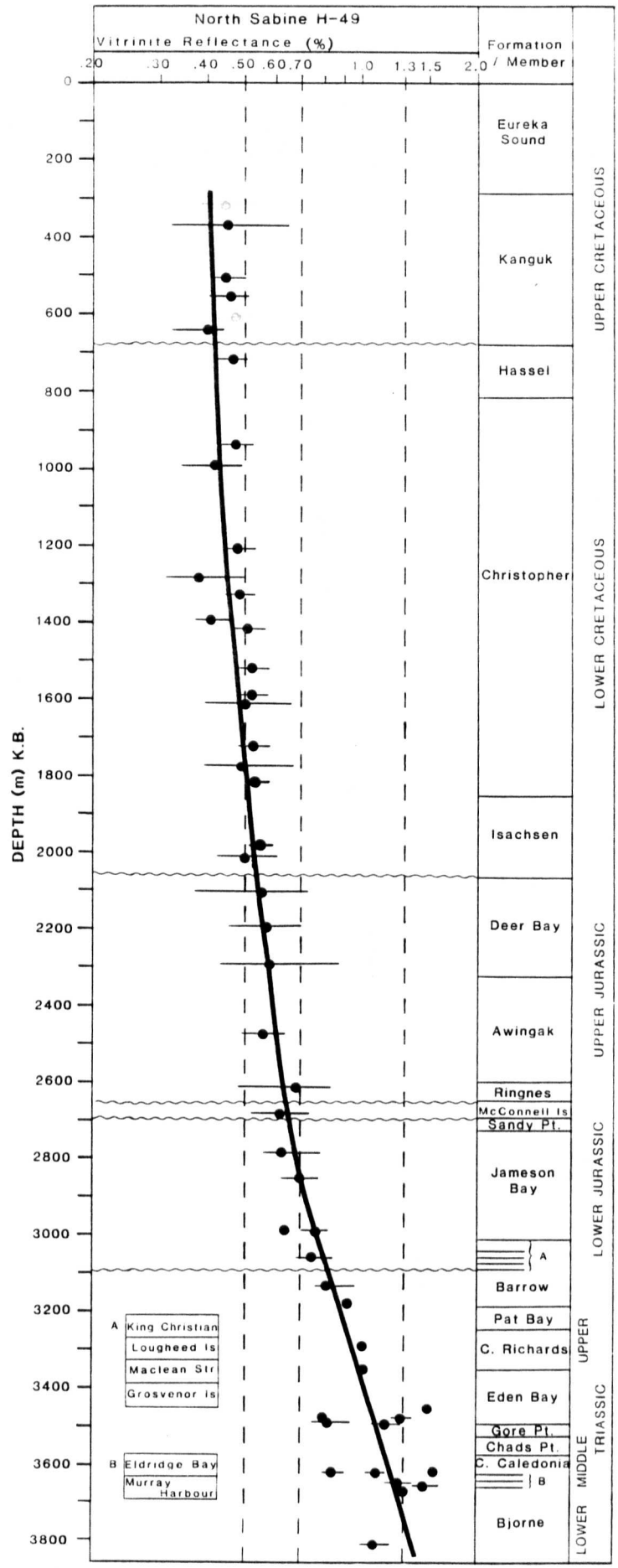

Figure 9-6 Vitrinite reflectance versus depth profile, Panarctic North Sabine H-49

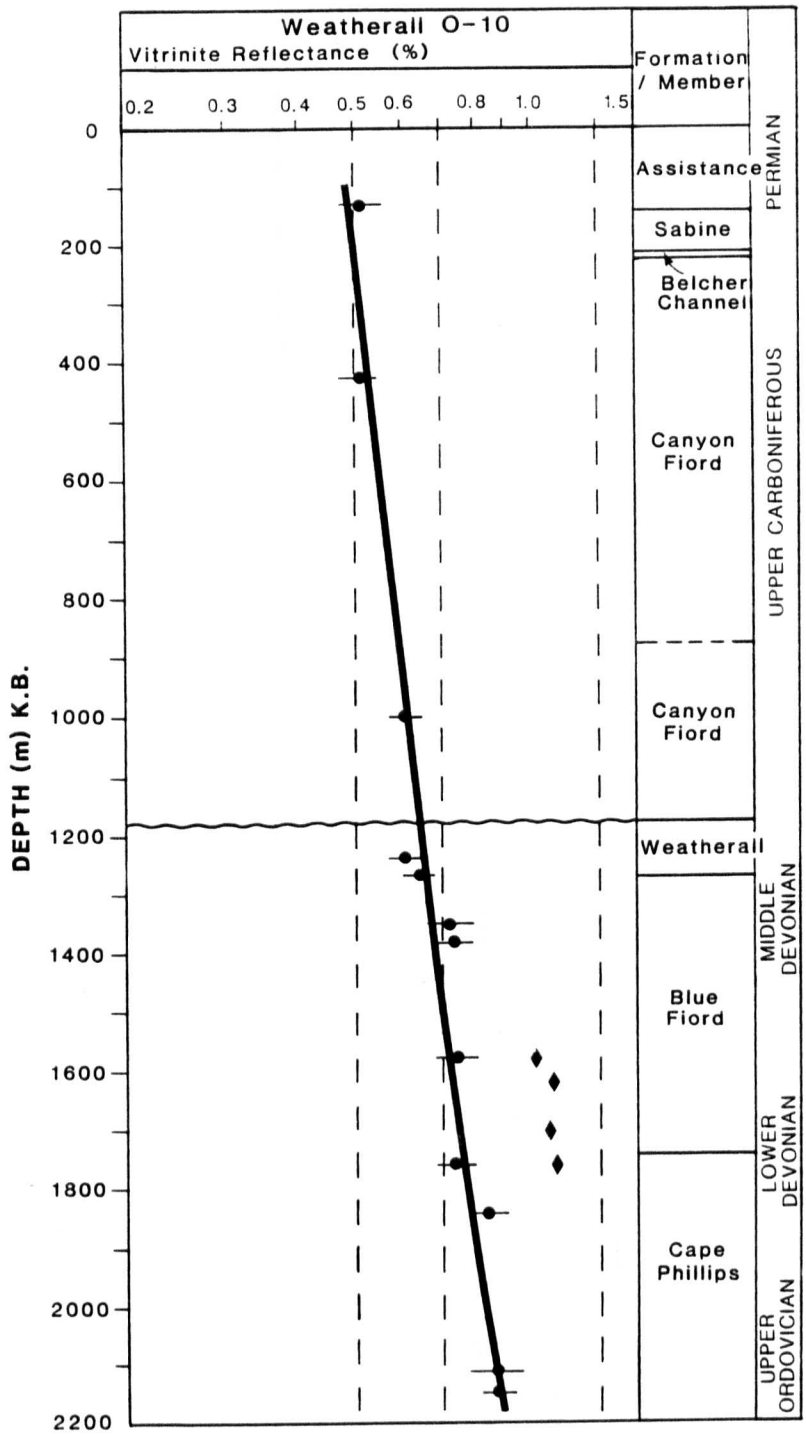

Figure 9-7 Vitrinite reflectance versus depth profile, Panarctic Weatherall 0-10

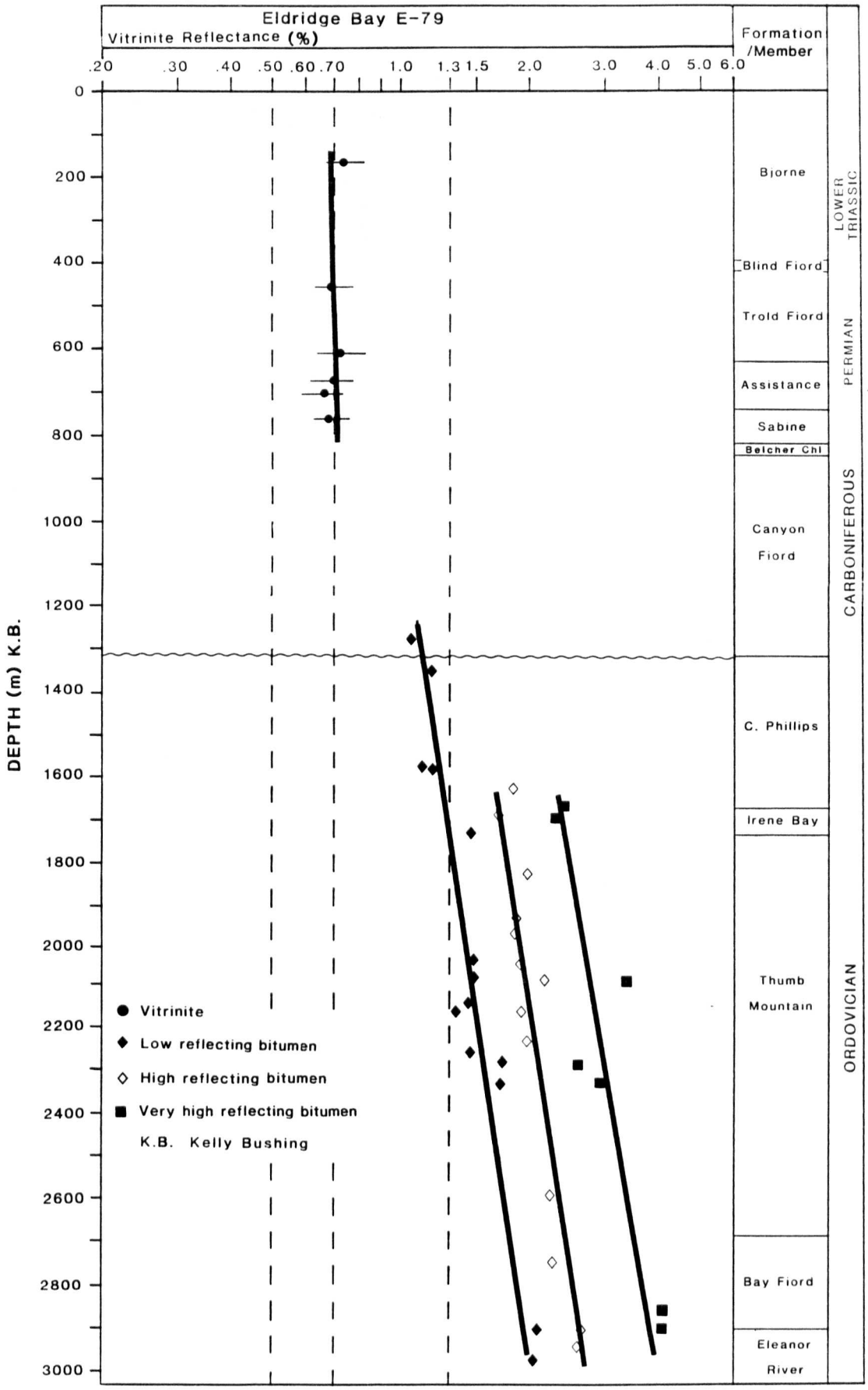

Figure 9-8 Vitrinite reflectance versus depth profile, Panarctic Eldridge Bay E-79

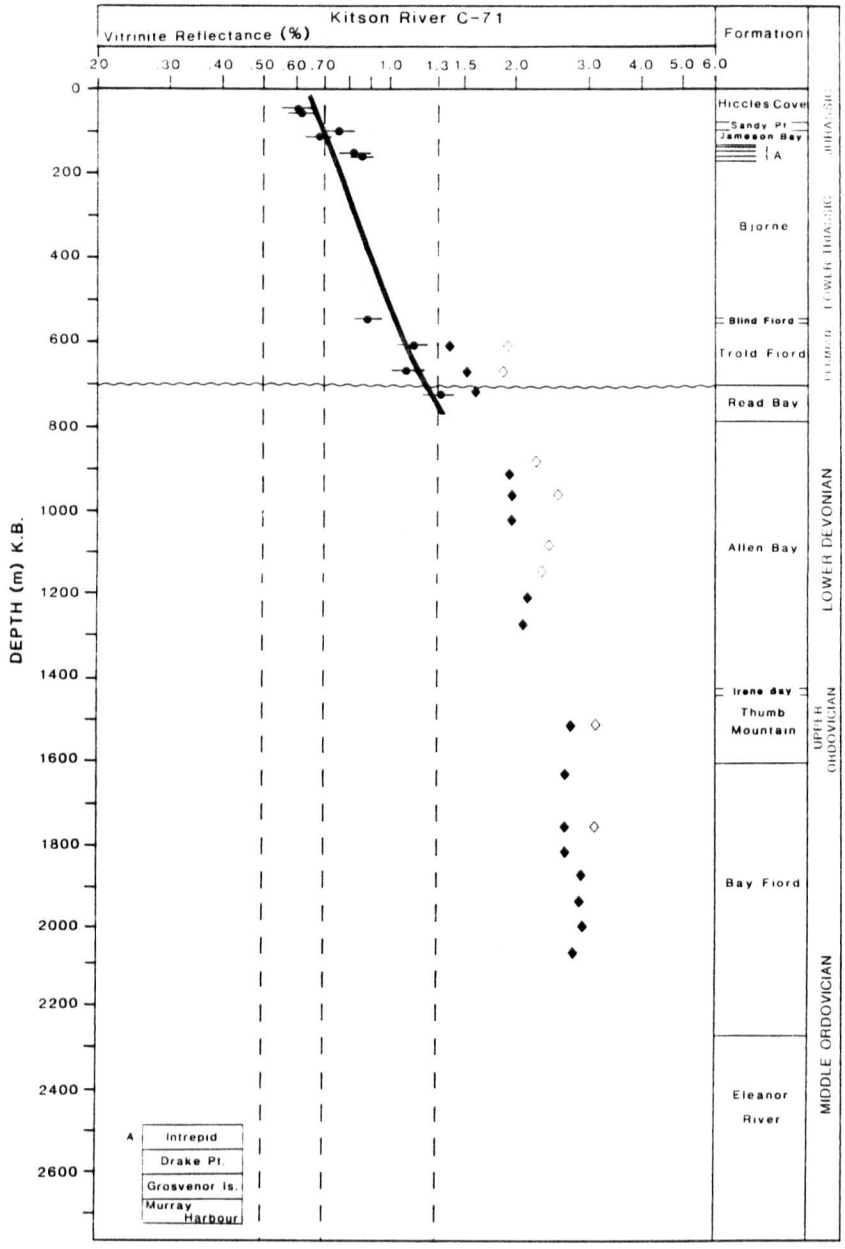

Figure 9-9 Vitrinite reflectance versus depth profile, Panarctic Kitson River C-71

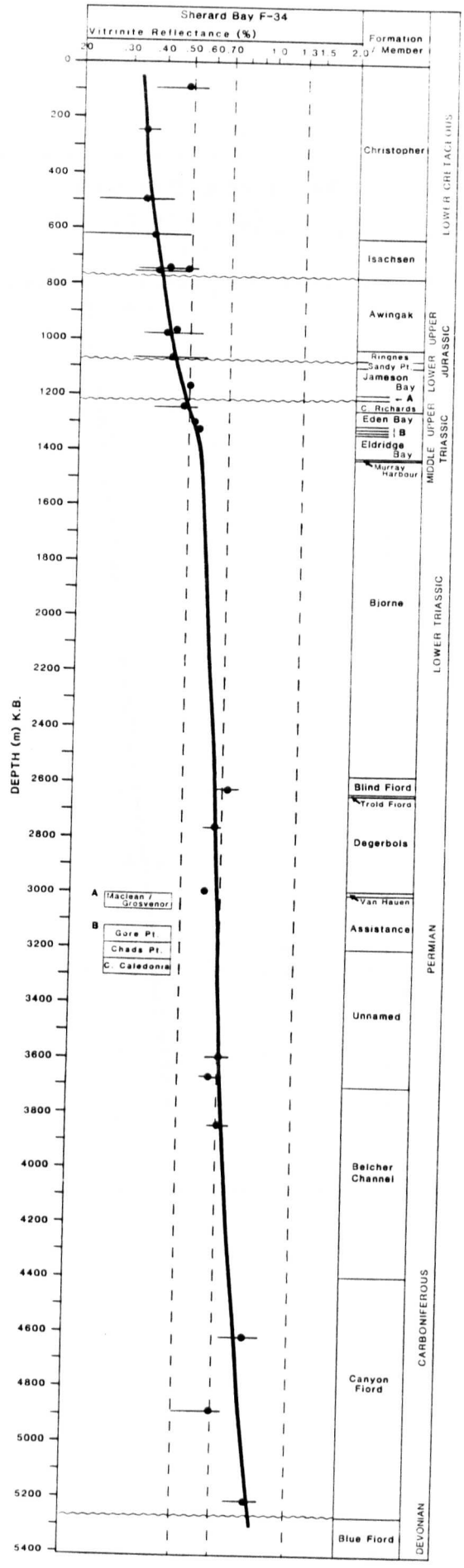

Figure 9-10 Vitrinite reflectance versus depth profile, Panarctic Sherard Bay F-34

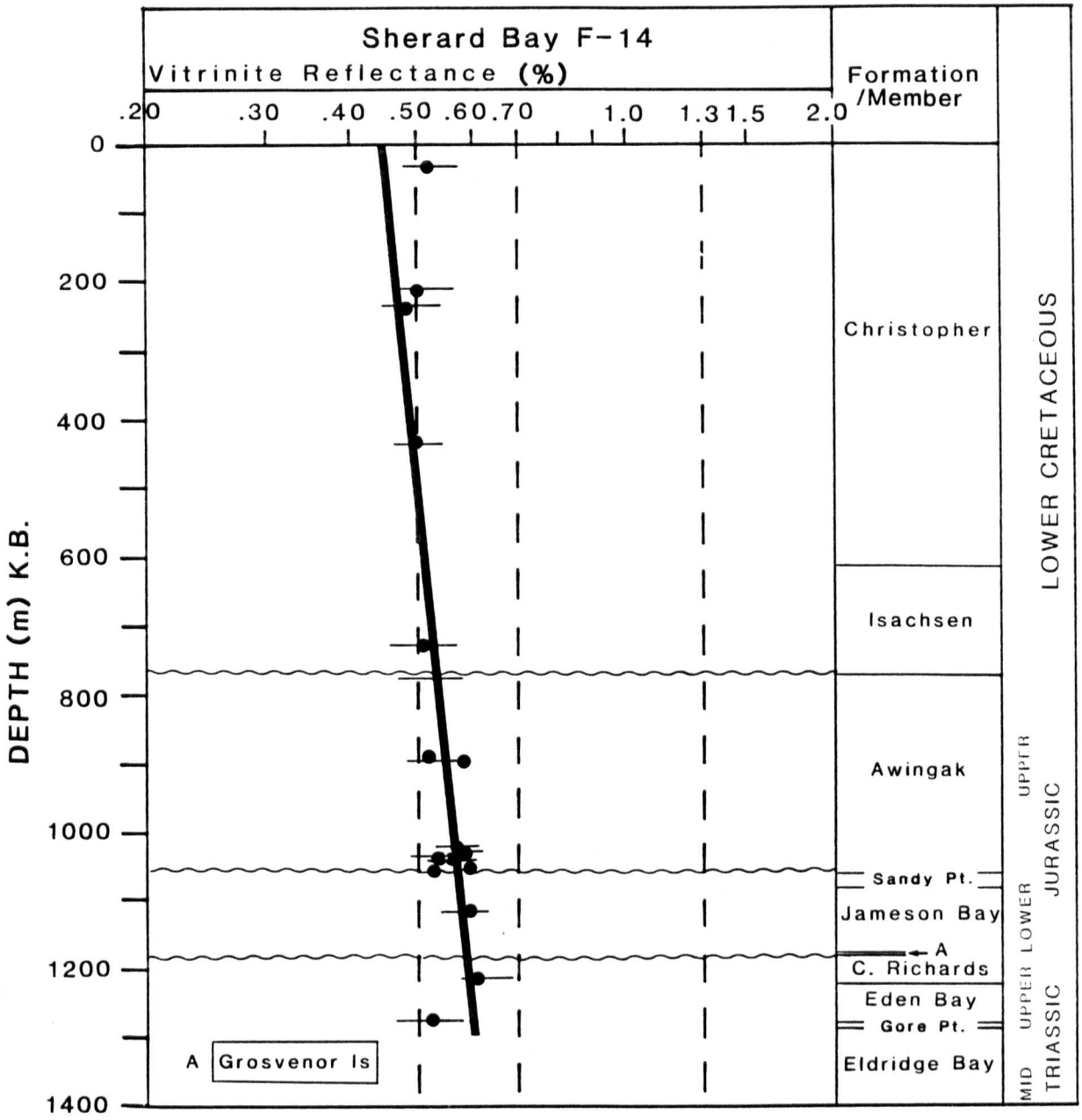

Figure 9-11 Vitrinite reflectance versus depth profile, Panarctic Sherard Bay F-14

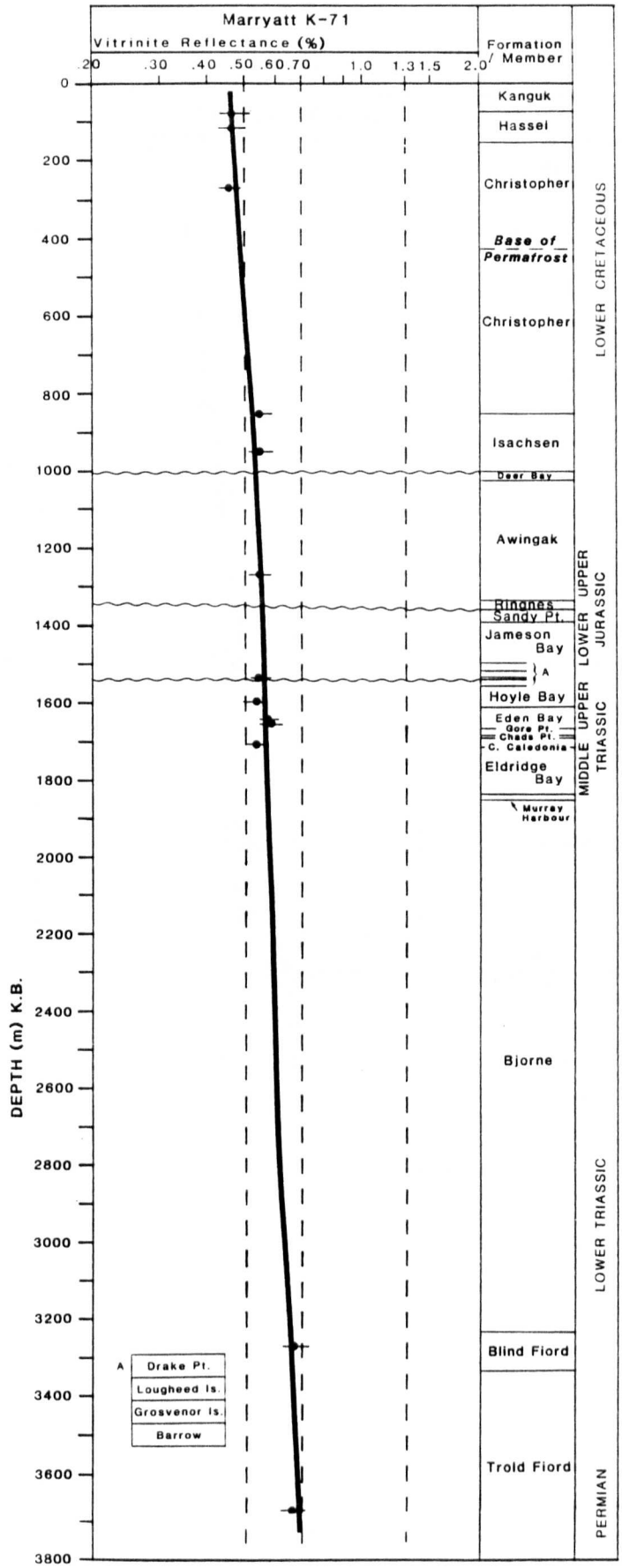

Figure 9-12 Vitrinite reflectance versus depth profile, Panarctic Marryatt K-71

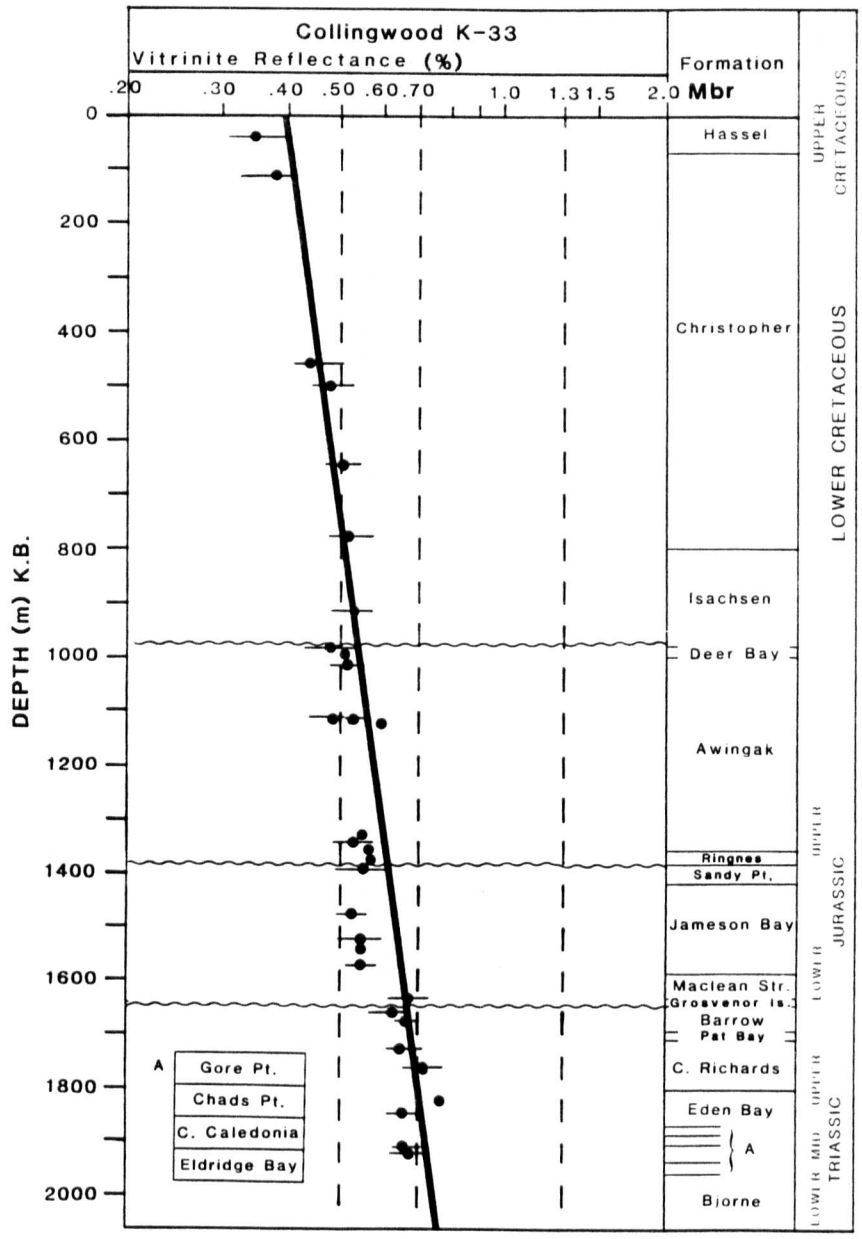

Figure 9-13 Vitrinite reflectance versus depth profile, Panarctic Collingwood K-33

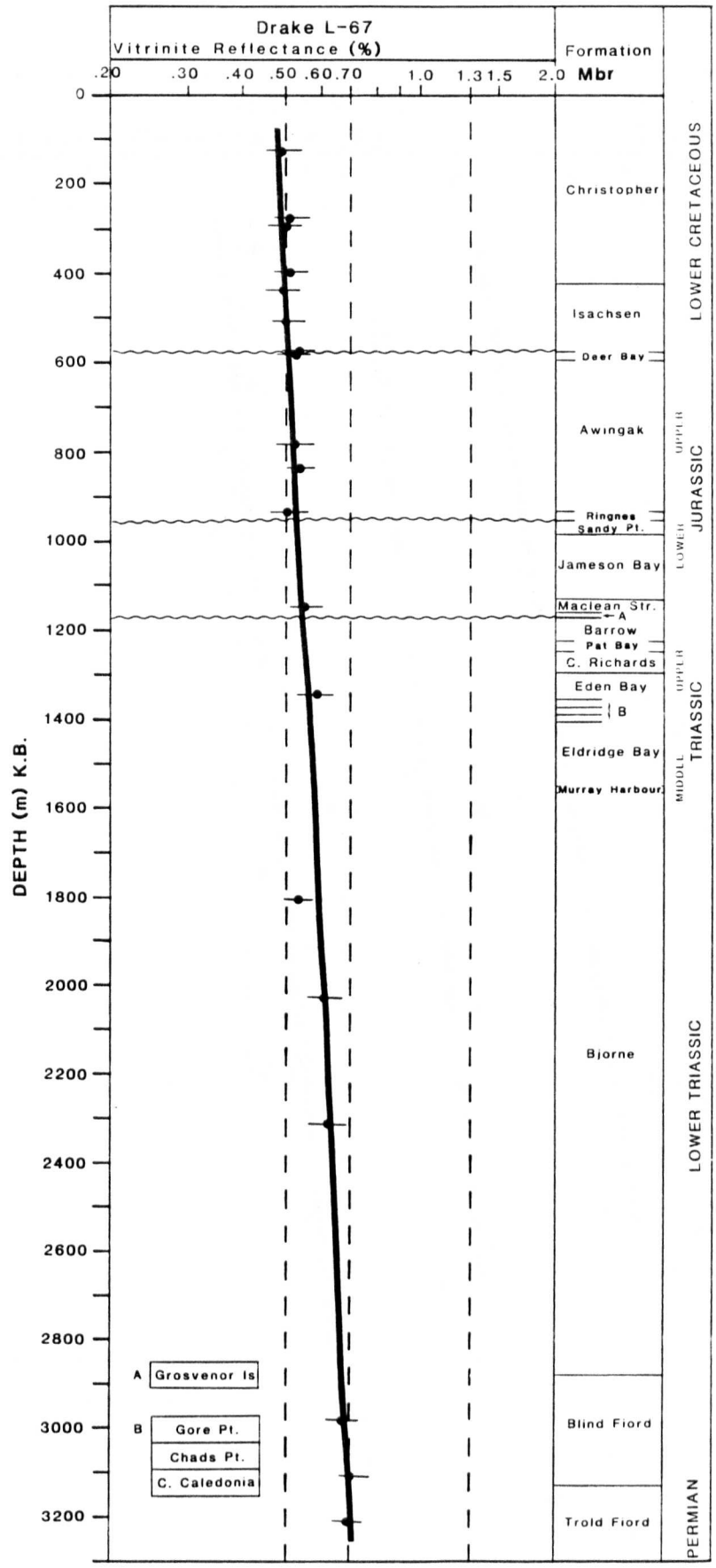

Figure 9-14 Vitrinite reflectance versus depth profile, Panarctic Drake L-67

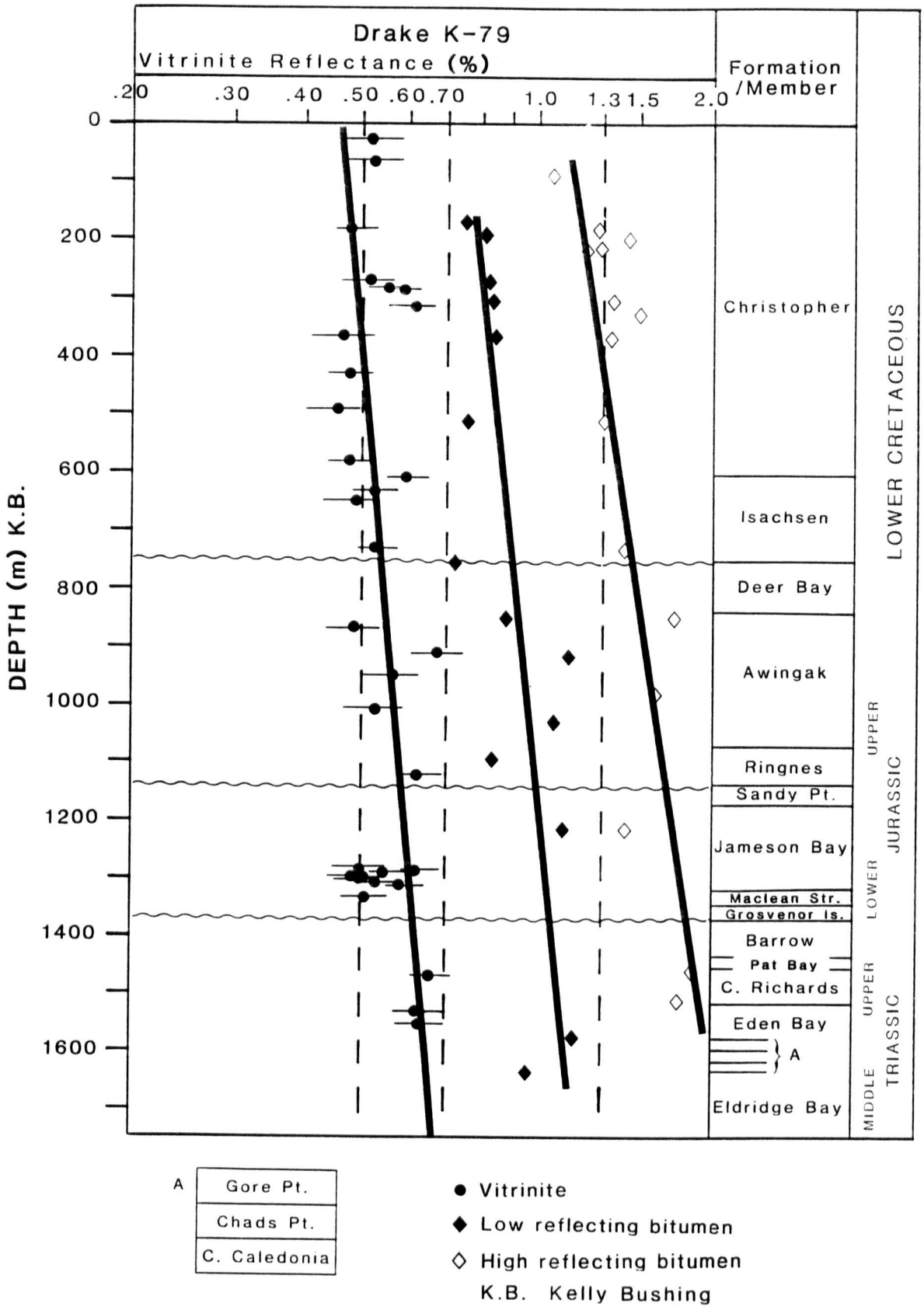

Figure 9-15 Vitrinite reflectance versus depth profile, Panarctic Drake K-79

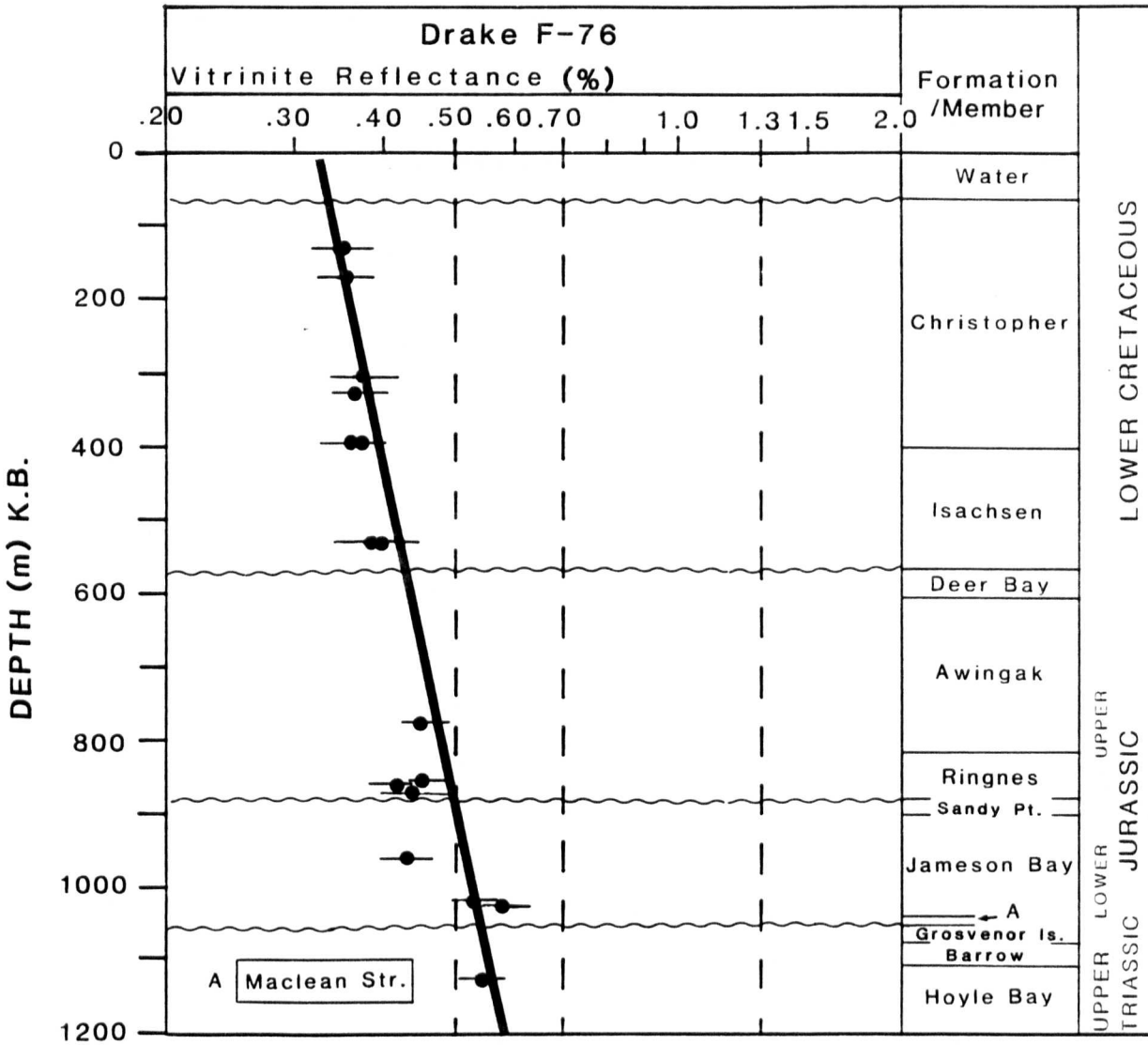

Figure 9-16 Vitrinite reflectance versus depth profile, Panarctic Drake F-76

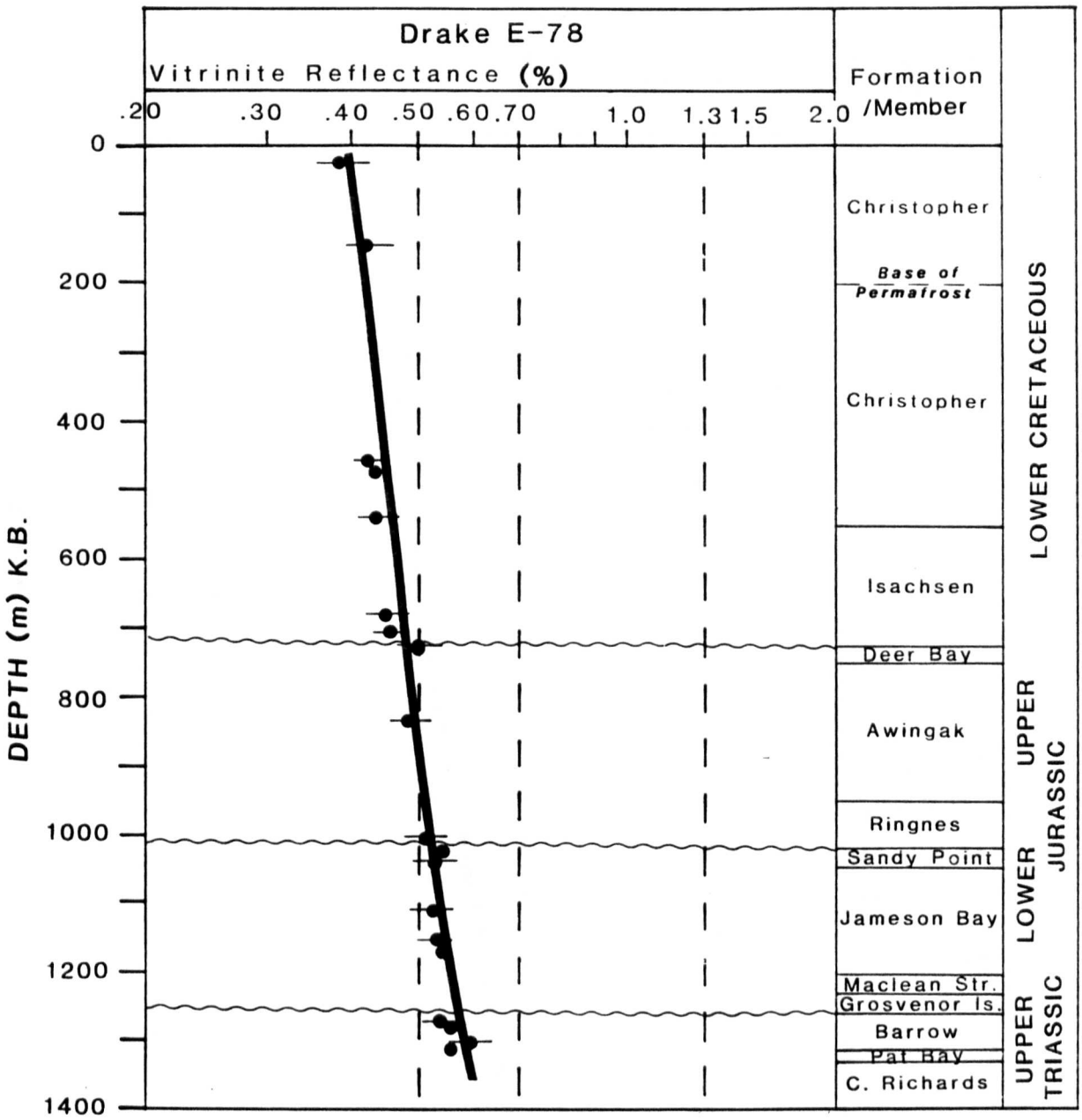

Figure 9-17 Vitrinite reflectance versus depth profile, Panarctic Drake E-78

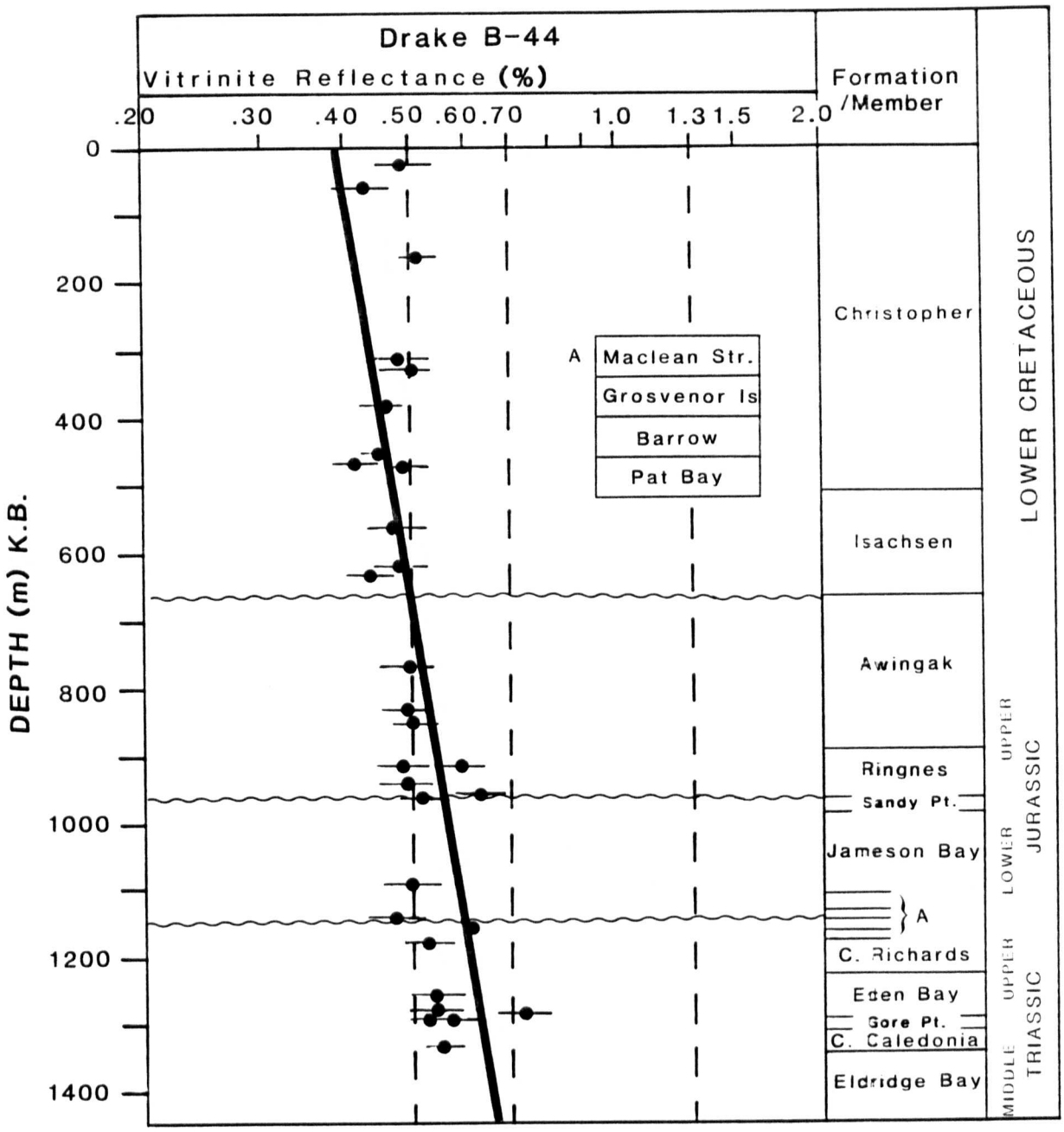

Figure 9-18 Vitrinite reflectance versus depth profile, Panarctic Drake B-44

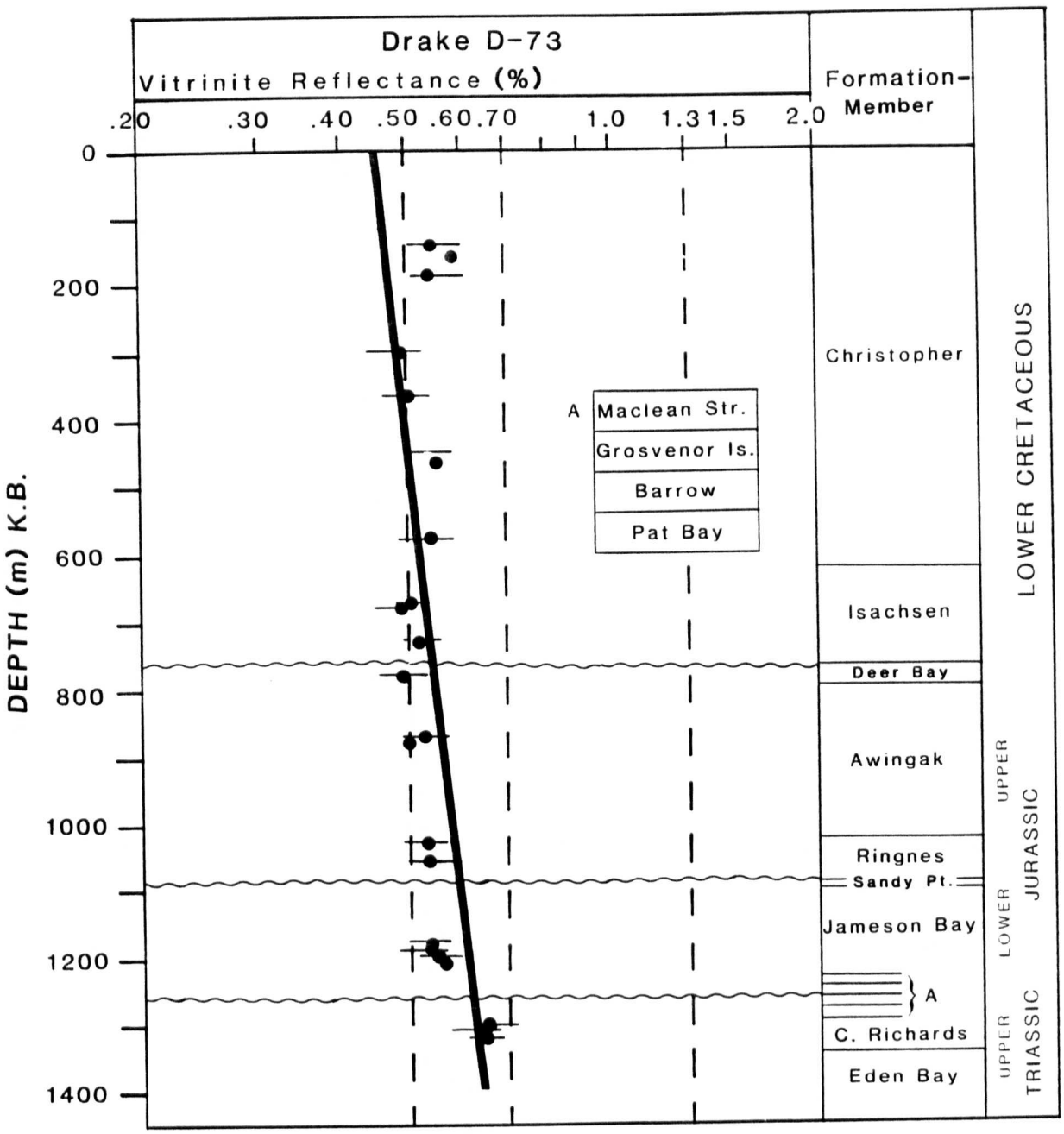

Figure 9-19 Vitrinite reflectance versus depth profile, Panarctic Drake D-73

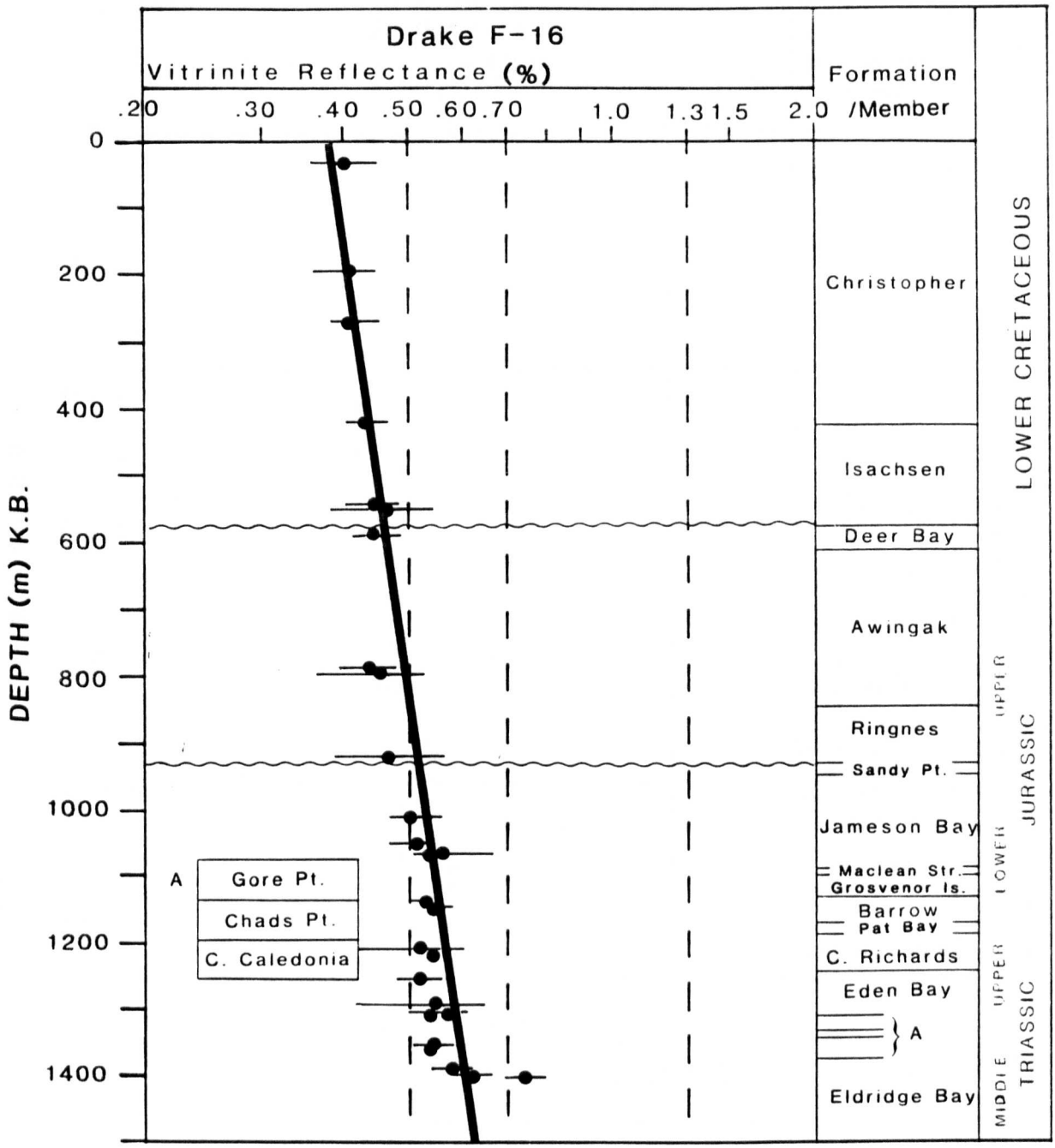

Figure 9-20 Vitrinite reflectance versus depth profile, Panarctic Drake F-16

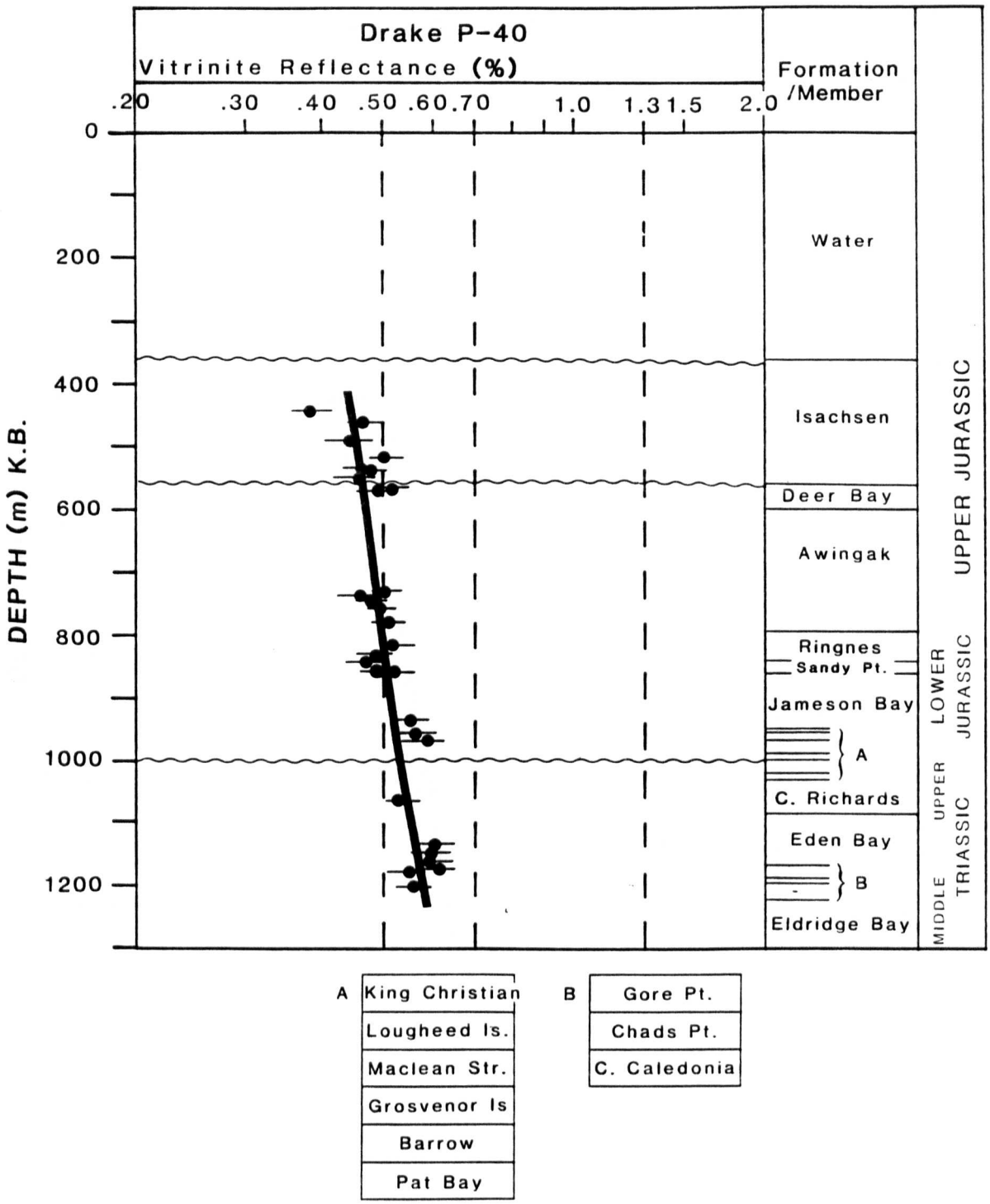

Figure 9-21 Vitrinite reflectance versus depth profile, Panarctic Drake P-40

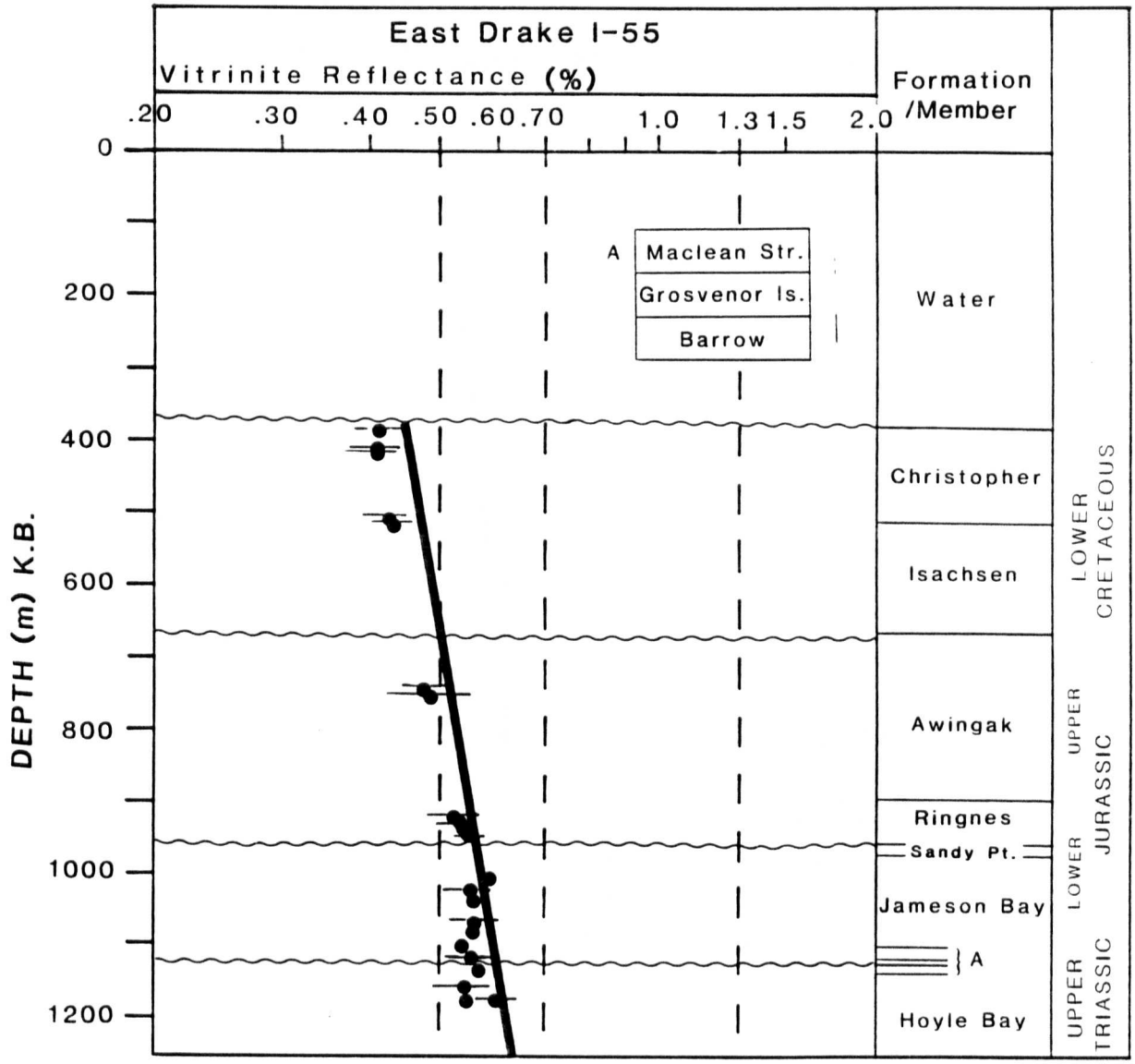

Figure 9-22 Vitrinite reflectance versus depth profile, Panarctic Drake East I-55

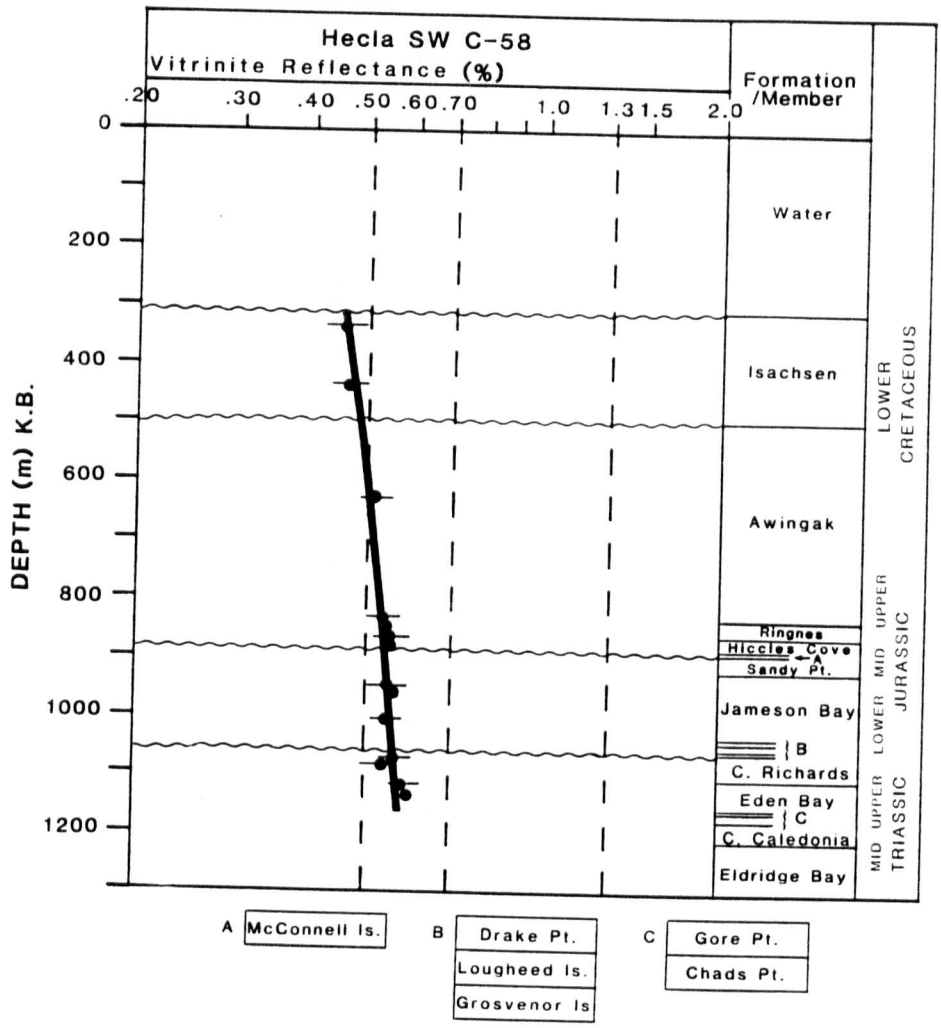

Figure 9-23 Vitrinite reflectance versus depth profile, Panarctic Hecla South West C-58

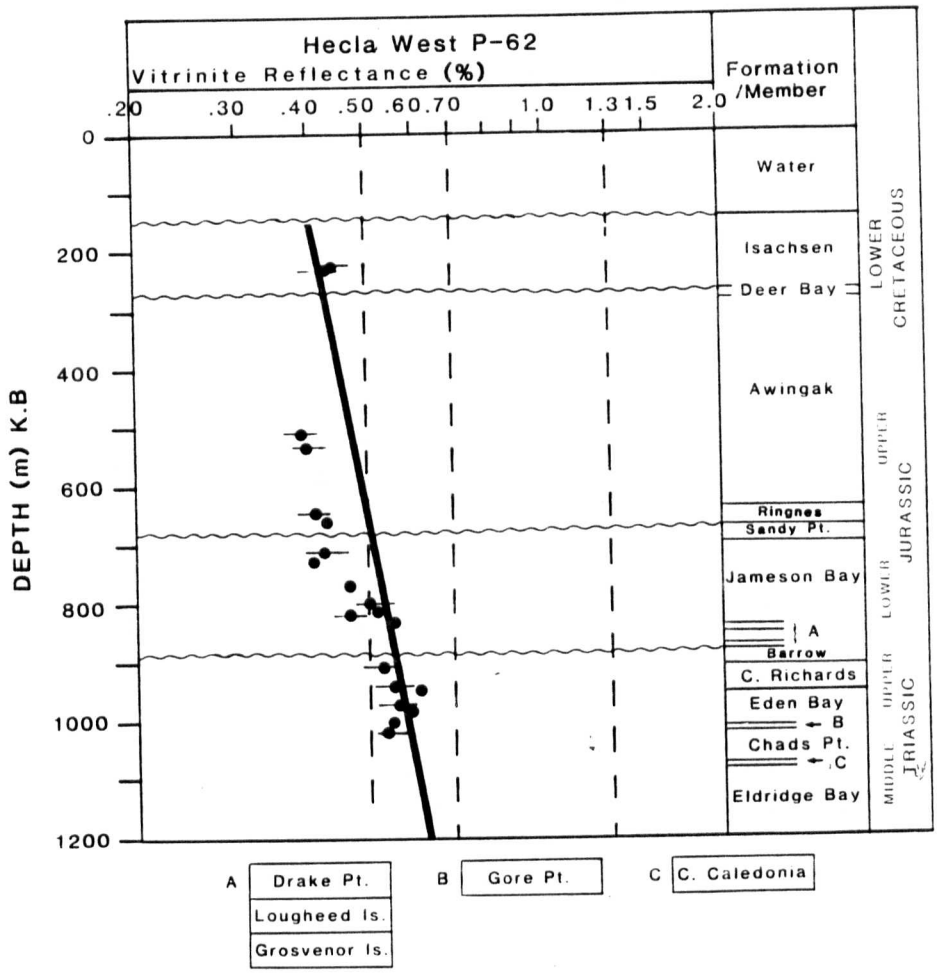

Figure 9-24 Vitrinite reflectance versus depth profile, Panarctic Hecla West P-62

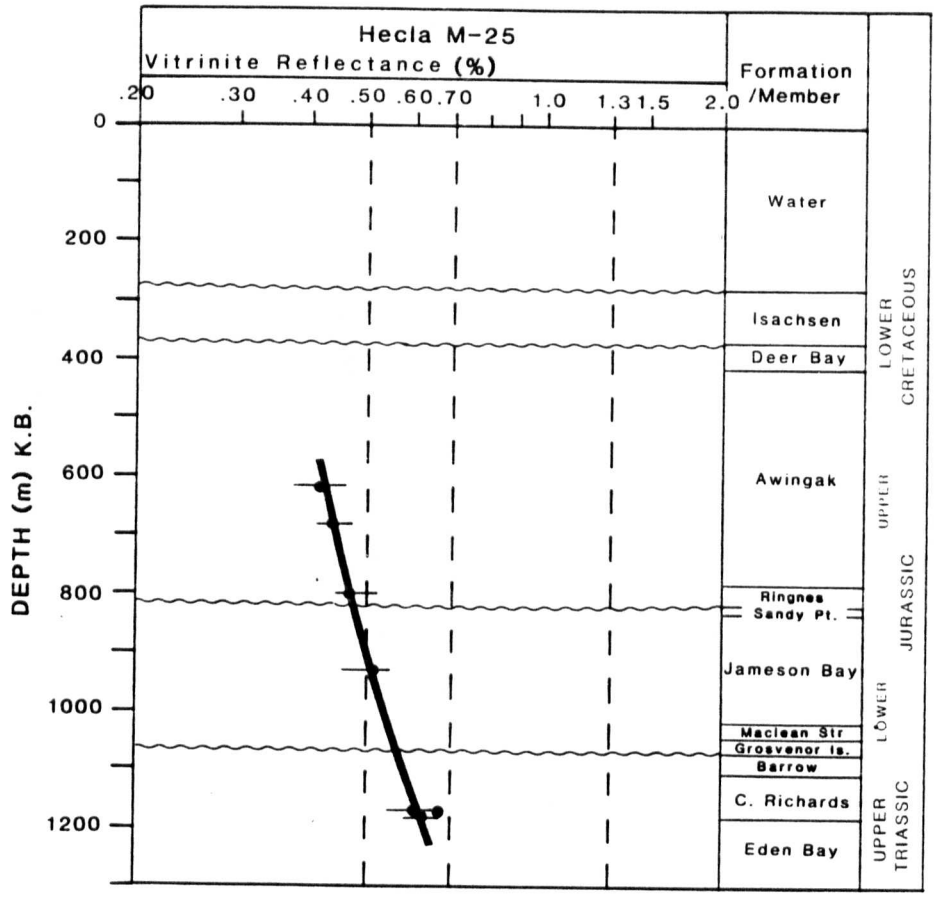

Figure 9-25 Vitrinite reflectance versus depth profile, Panarctic Hecla North West M-25

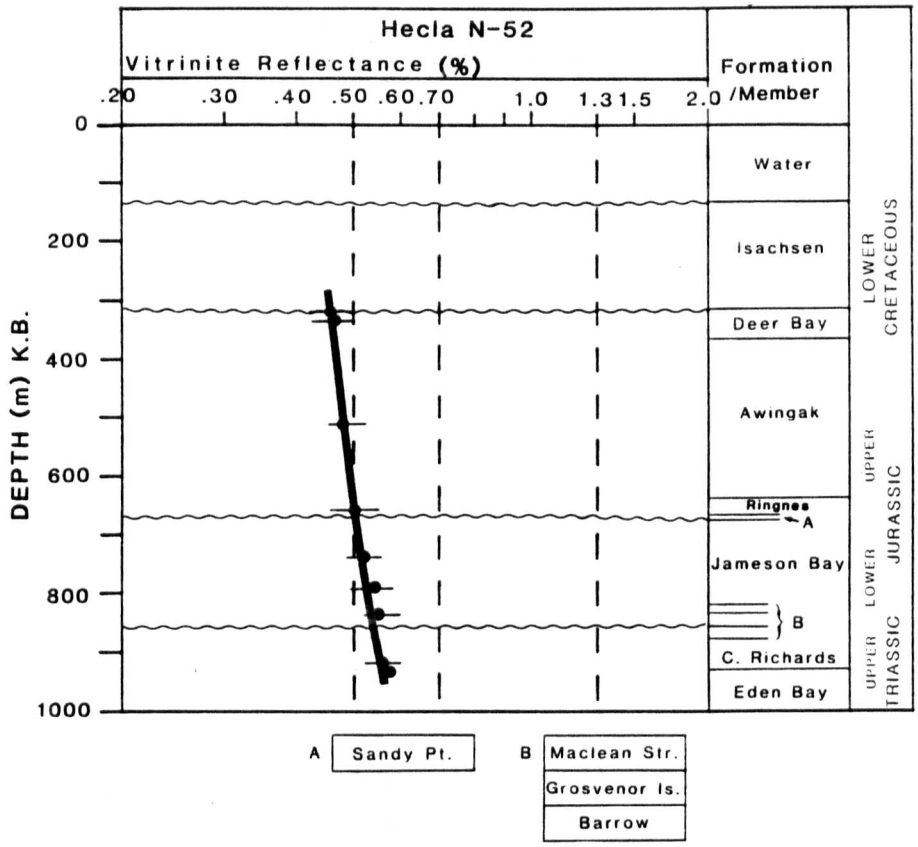

Figure 9-26 Vitrinite reflectance versus depth profile, Panarctic Hecla West N-52

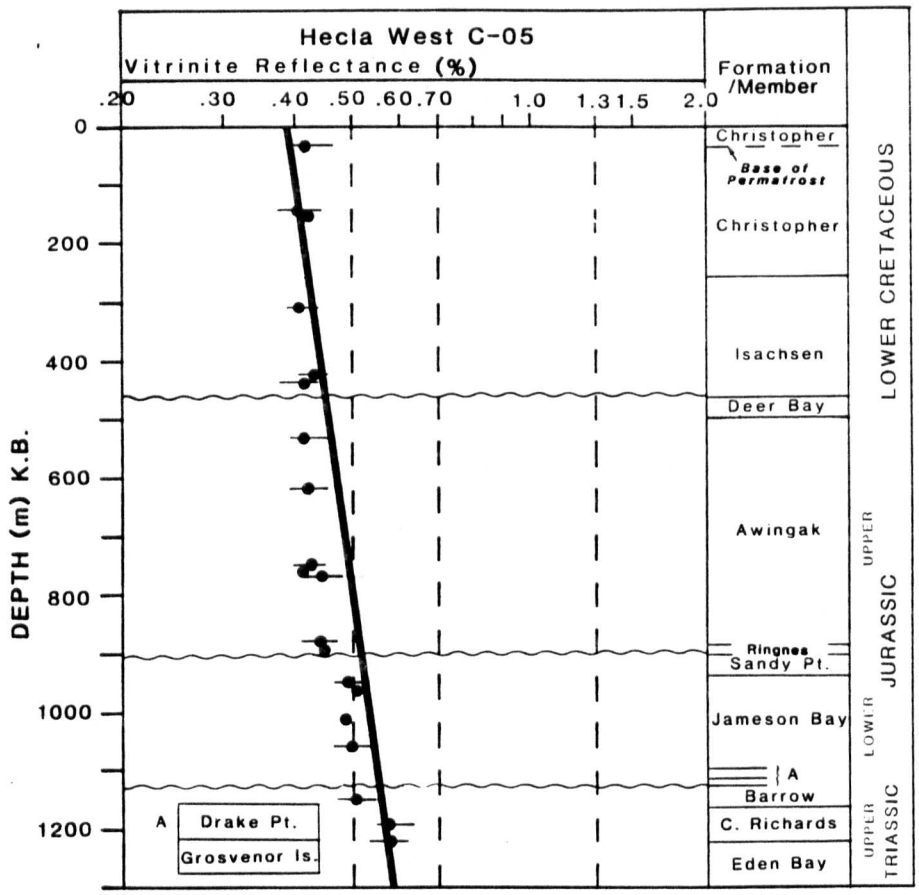

Figure 9-27 Vitrinite reflectance versus depth profile, Panarctic Hecla West C-05

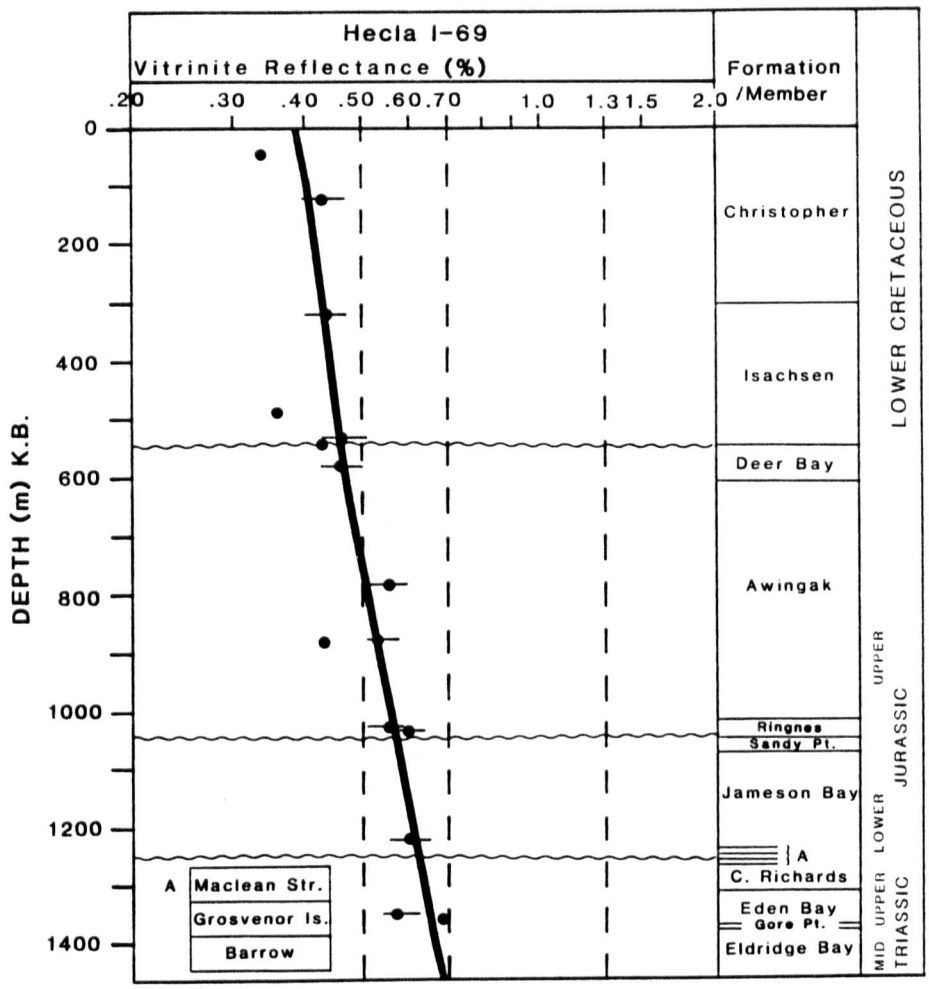

Figure 9-28 Vitrinite reflectance versus depth profile, Panarctic Hecla I-69

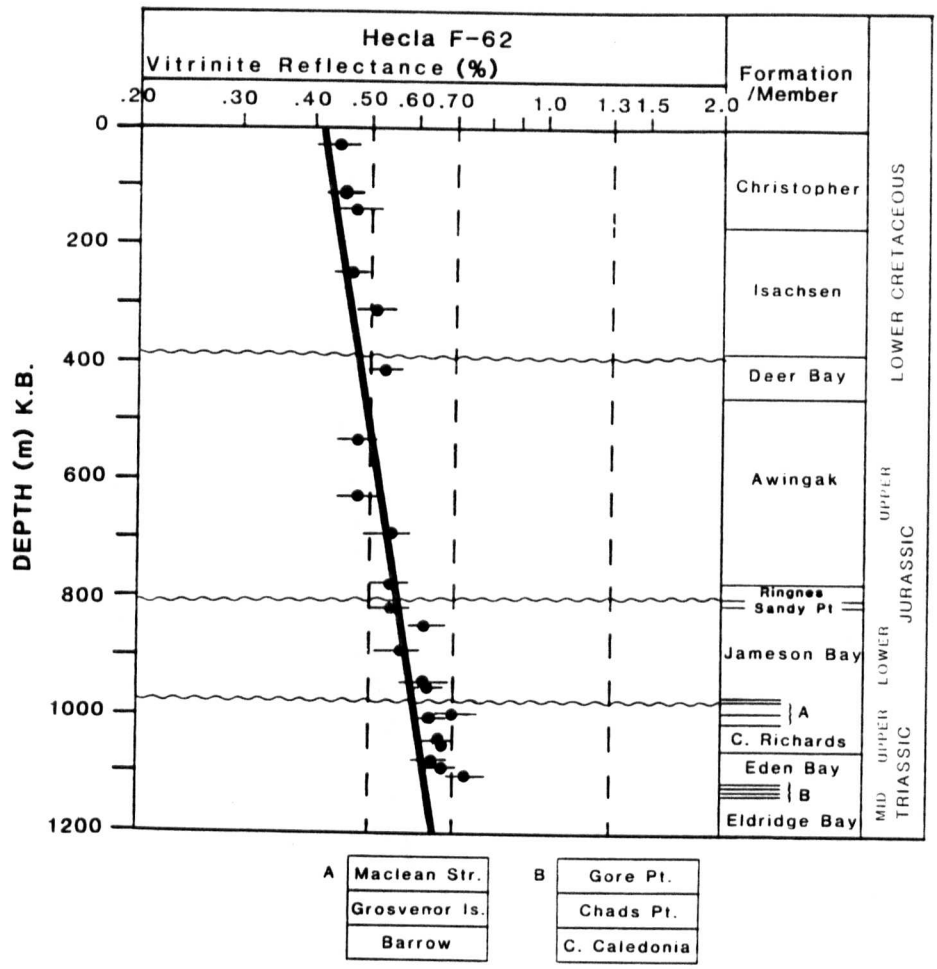

Figure 9-29 Vitrintie reflectance versus depth profile, Panarctic Hecla F-62

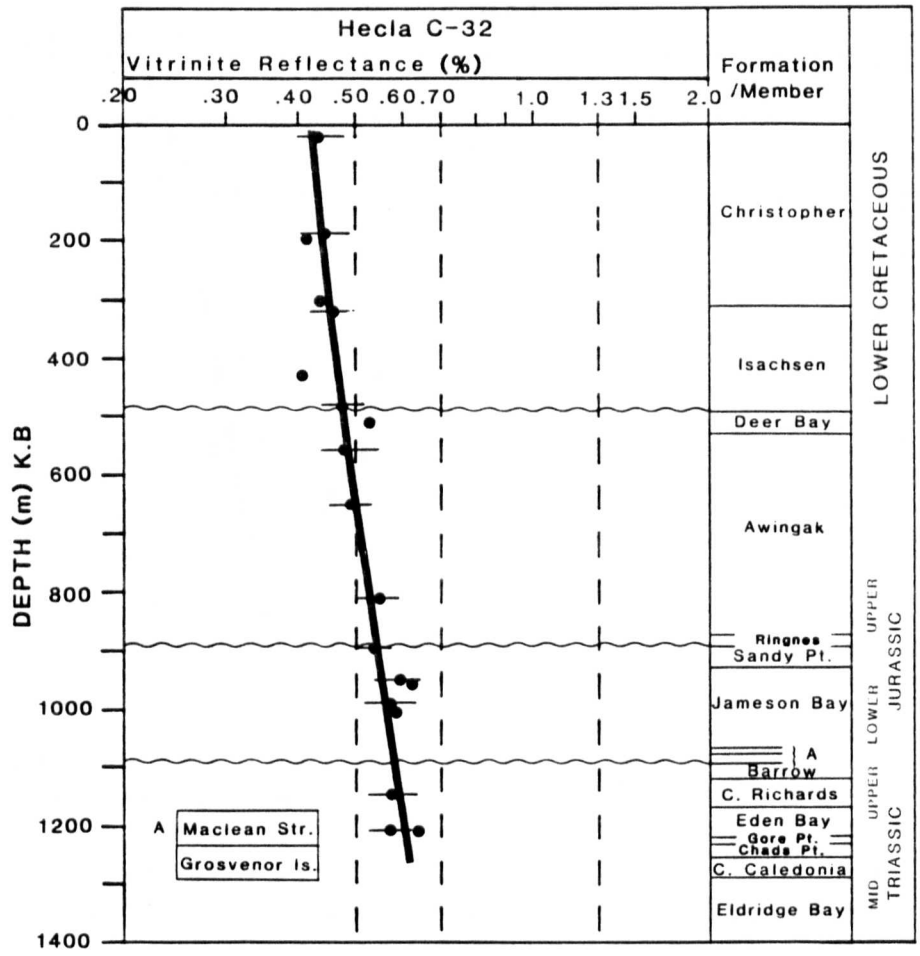

Figure 9-30 Vitrinite reflectance versus depth profile, Panarctic Hecla C-32

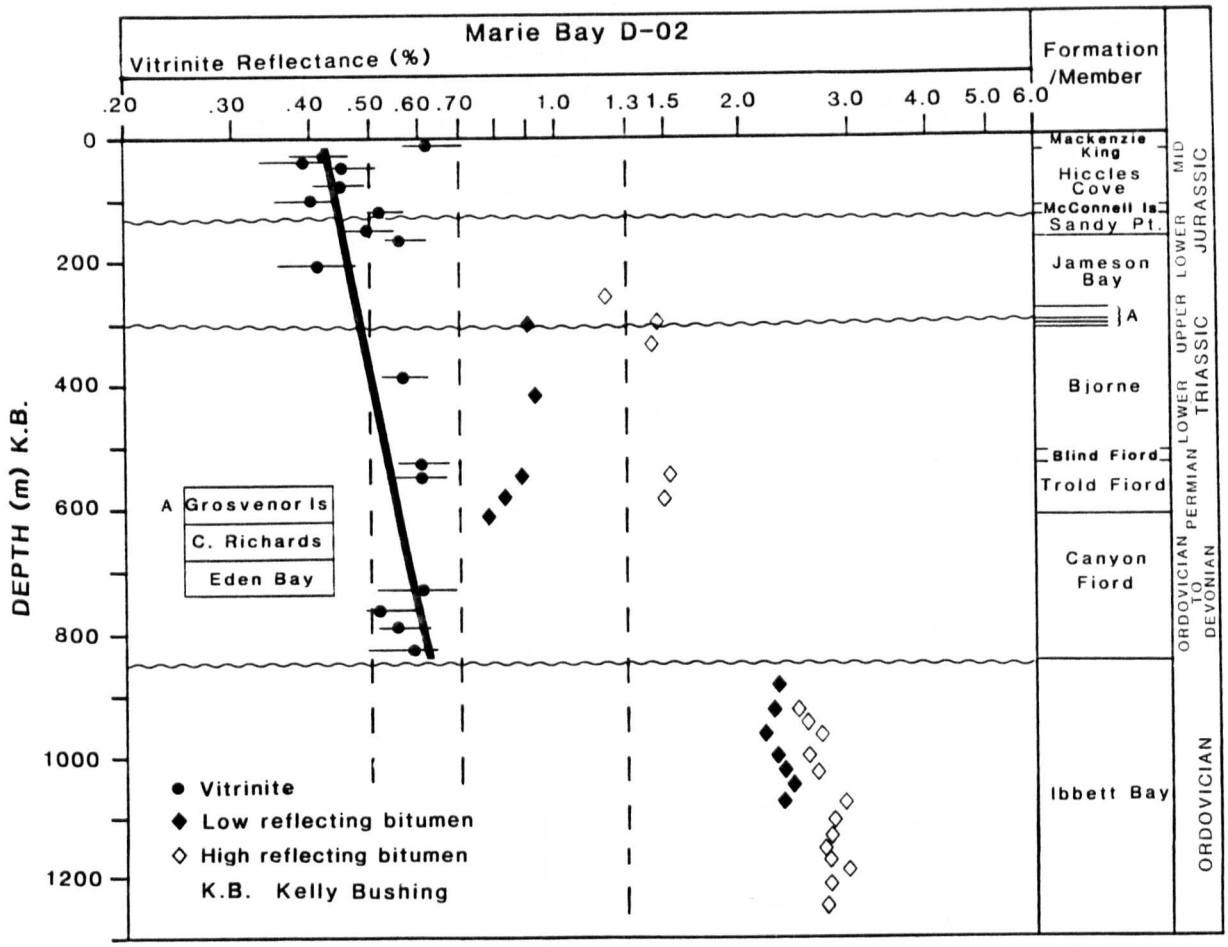

Figure 9-31 Vitrinite reflectance versus depth profile, Panarctic Marie Bay D-02

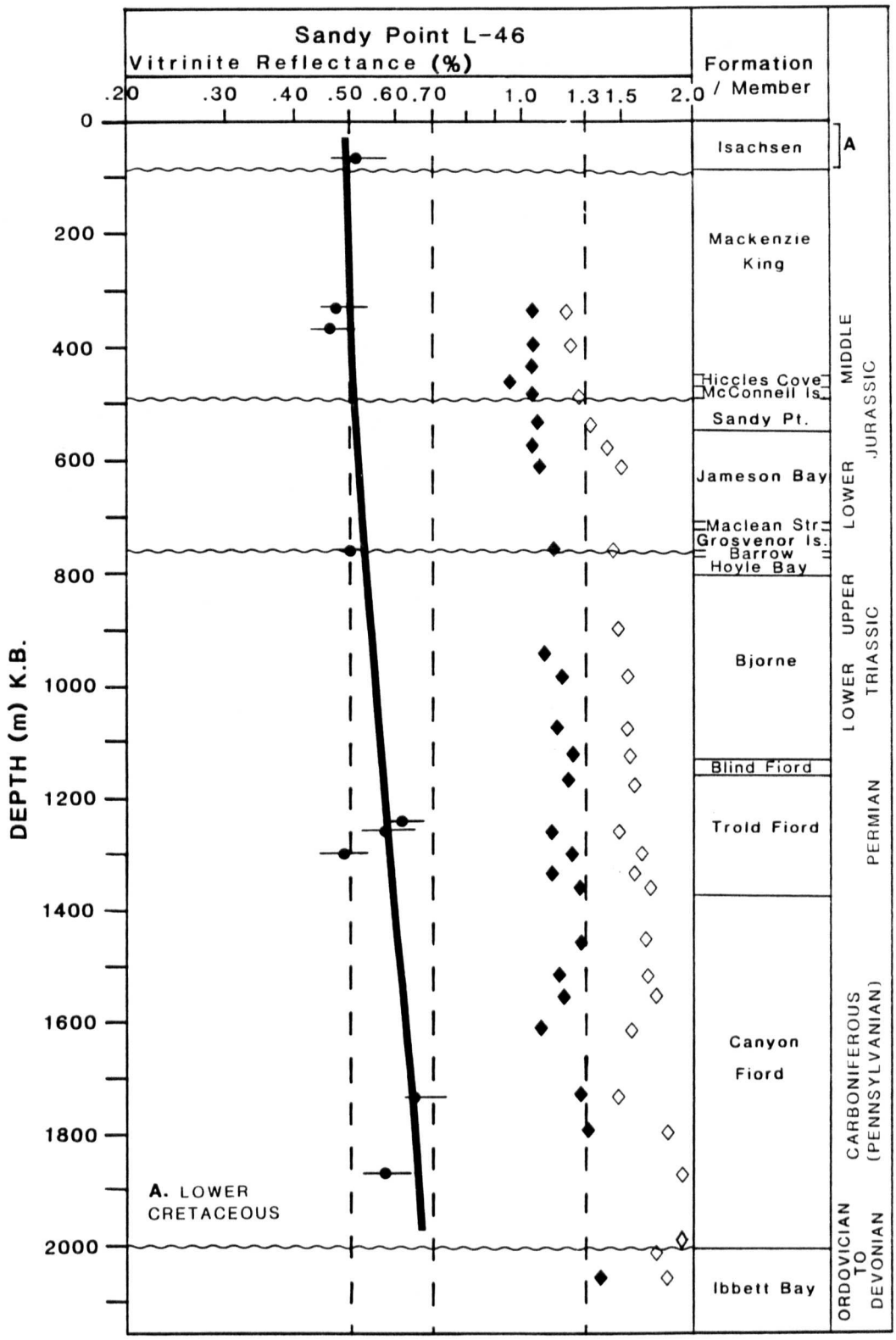

Figure 9-32 Vitrinite reflectance versus depth profile, Panarctic Sandy Point L-46

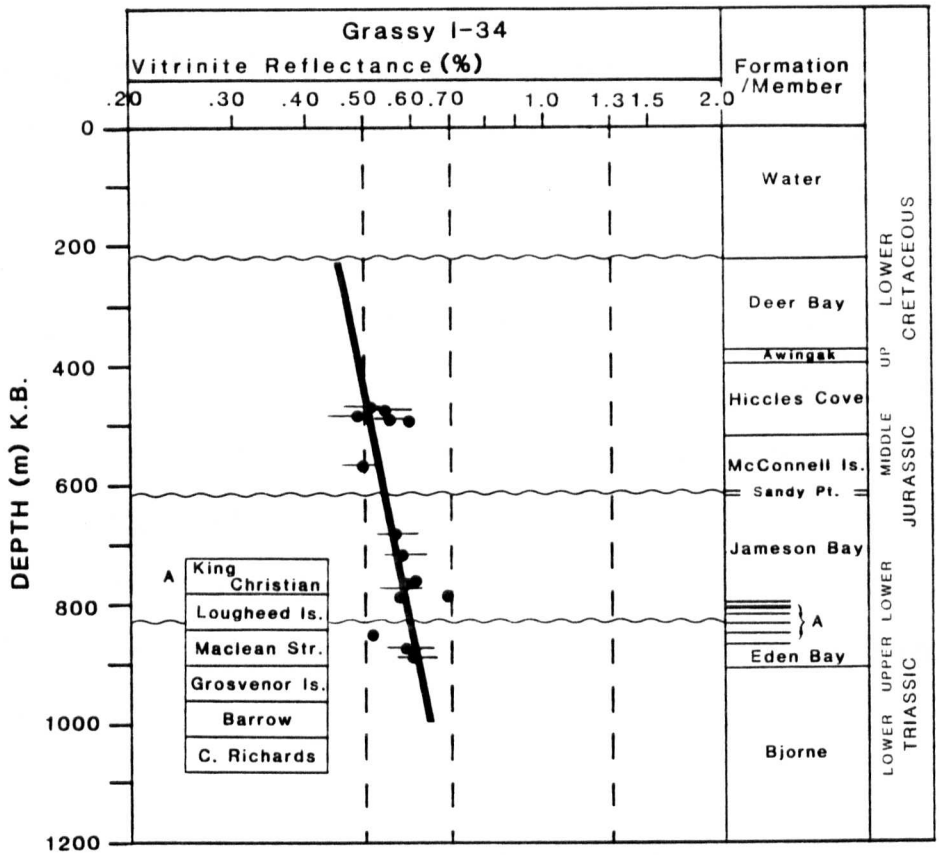

Figure 9-33 Vitrinite reflectance versus depth profile, Panarctic Grassy I-34

The maturity of the Schei Point Group ranges from 0.55 to >1.3% Ro indicating that the formations fall in the marginally mature to overmature stage of hydrocarbon generation. The onset of maturity for Type I organic matter (0.7% Ro) is reached at depths as shallow as 1,200m in drillhole Drake Point D-68 (Figure 9-1) or as deep as 2,850m in drillhole North Sabine H-49 (Figure 9-6). The floor of the 'oil window' (Ro ~ 1.3%) is reached at 3,600 m in drillhole North Sabine H-49 (Figure 9-6). The depth limits of the hydrocarbon-generation zone appear to vary regionally with depth and they are a function of the amount of burial and uplift, at least in the non-intrusive igneous areas of Melville Island. Where there are intrusives, for example in the vicinity of Drake Point D-68 and Chads Creek B-64, the heat generated has resulted in localized steep maturity gradients relative to the country rock gradients (Figures 9-1 and 9-2).

The total thickness of these potential source beds varies from 25 m in the Hecla P-62 drillhole (Figure 9-24) to almost 400 m at the North Sabine H-49 drillhole (Figure 9-6). Hydrogen-index values in excess of 600 mg HC/g Corg and as high as 850 mg HC/g Corg have been measured in the Eden Bay and Cape Richards Members at the locality of Chads Creek B-64 (Figures 9-34 and 9-35).

Most of the remaining Mesozoic potential source rocks, for example the Jameson Bay, Ringnes and Deer Bay Formations, are immature to marginally mature and they have lower HI and higher OI values than the Schei Point Group rocks (Figures 9-34 and 9-35). As maturation increases, the hydrogen index of the same formations (or members) progressively decrease (Appendix II).

9.1.1 SCHEI POINT GROUP

The group comprises the Middle to Upper Triassic succession of the Sverdrup

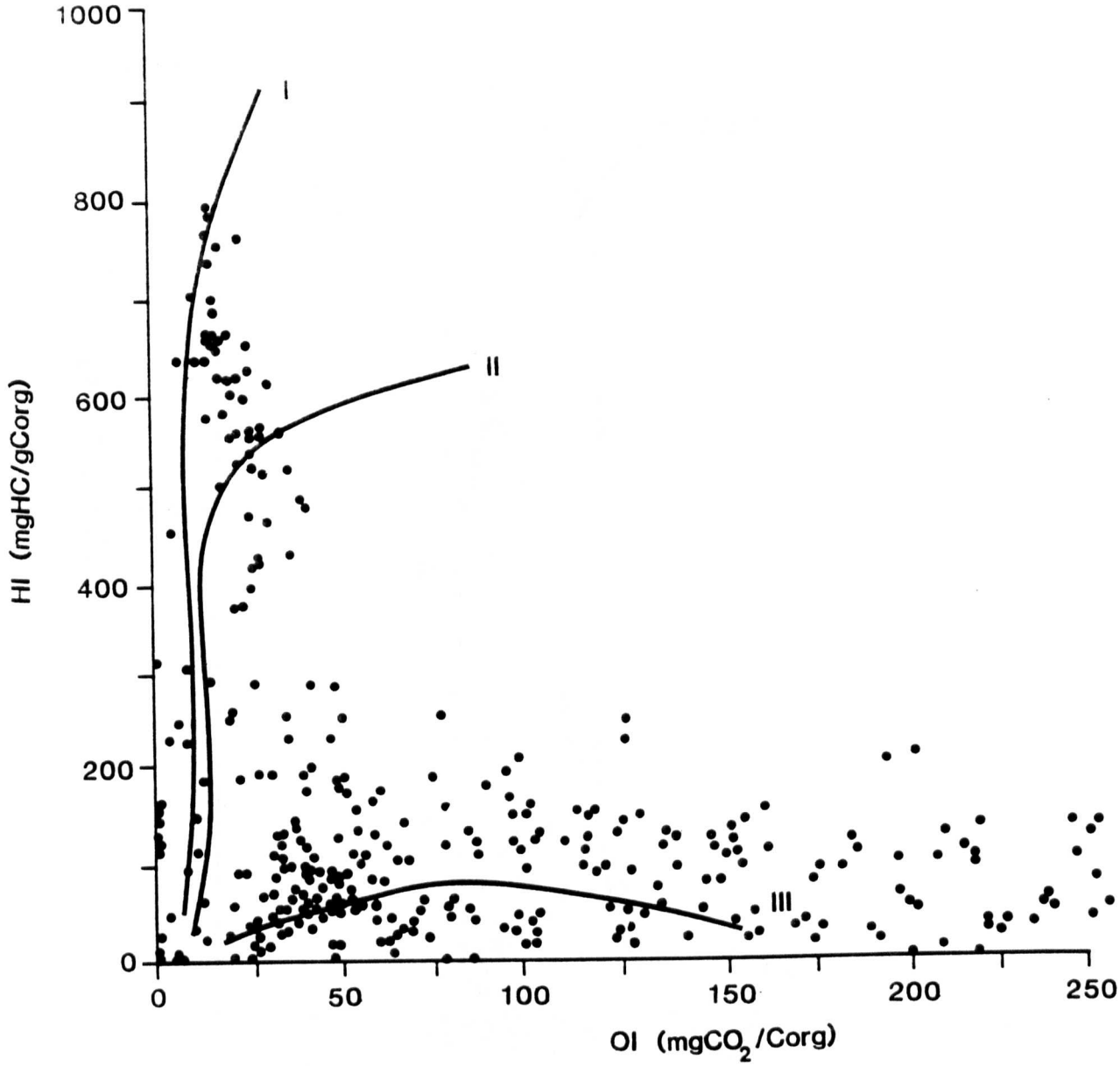

Figure 9-34 Pseudo-van Krevelen diagram of the samples studied

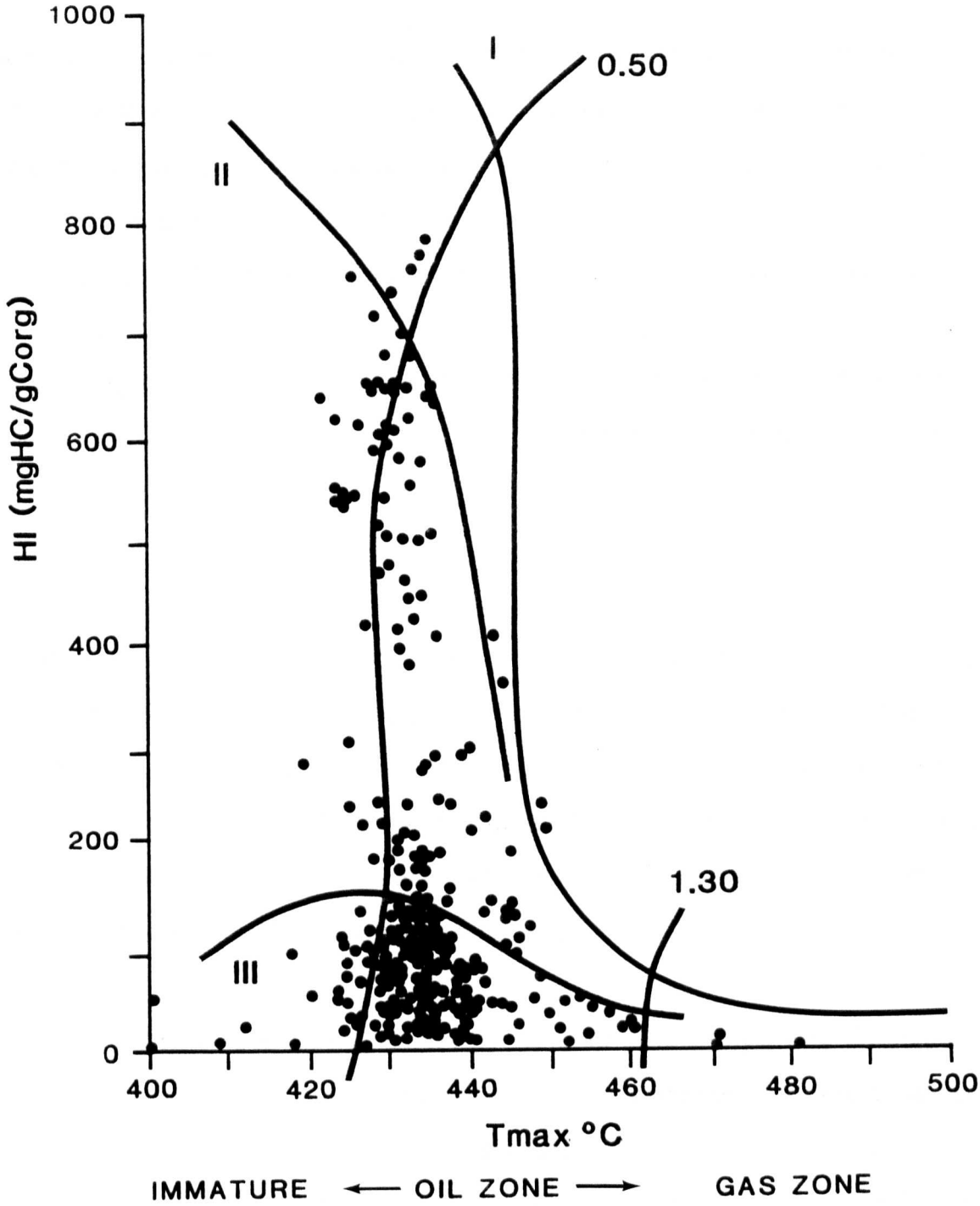

Figure 9-35 Plot of hydrogen index versus Tmax (°C) of the samples studied

Basin and consists of interbedded shales, siltstones, sandstones, and limestone. The thickness of the beds is variable from one area to another and the highly interbedded nature of these prolific source rocks has resulted in a high expulsion efficiency (Stewart, pers. commun., 1988). An attempt has been made to estimate the accumulated thickness of good quality source rocks from the logs of drillholes which penetrated the Schei Point Group. Most of the sections examined have an effective source-rock thickness ranging from 60 m to >300 m. (Figures 9-33 and 9-6). Most of the drillholes were drilled on structural highs where the Schei Point is thin, but there is an increase in the effective thickness of potential source rocks in the large synclinal areas adjacent to the structural highs.

Most of the samples contain an admixture of Type I and Type II organic matter (Plates 5 and 6). The aliphatic nature of the Schei Point organic matter thus gives it a good to excellent petroleum generating potential. In the Murray Harbour Formation of Middle Triassic age (Figure 2-3), there is a general trend of improving organic-matter quality, as determined by Rock-Eval and petrology, from the basin edge towards the basin centre, where restored HI values exceed 600 mg HC/g Corg.

Restored HI values for the Eden Bay Member of the Hoyle Bay Formation are in excess of 700 mg HC/g Corg in marginally mature sediments, indicating excellent quality source rocks. Restored HI values of the Cape Richards Member are lower than those of Eden Bay. This is achieved by shifting the measured HI values parallel to the kerogen evolutionary pathways. The reason for restoring HI values to maturity levels below the 'onset' of hydrocarbon generation is to estimate the maximum potential of the source rocks. Once source rocks start generating hydrocarbons, the HI values drop considerably depending on organic matter type (Orr, 1981). In the locality of the Sproule Peninsula, Melville Island, good quality source rocks are lacking in the Murray Harbour

PLATE 5. Organic matter in the Triassic Schei Point Group.

All photomicrographs taken under ultraviolet excitation, water immersion (excitation 400 - 440 nm, barrier filter 470 nm). The long axis of each photomicrograph is 240 μm.

a) A section of Tasmanites (T) perpendicular to bedding showing large suture in the middle, Barrow Formation, Drake D-68.

b) Thick-walled leiospheres of Tasmanites algae (T) along with fluorescing matrix (FM), Cape Caledonia Member, Chads Creek B-64.

c) Two bodies of Tasmanites algae, Cape Caledonia Member, Chads Creek B-64.

d) Compressed leiospheres of Tasmanites enclosed in fluorescing matrix, Cape Caledonia Member, Drake D-68.

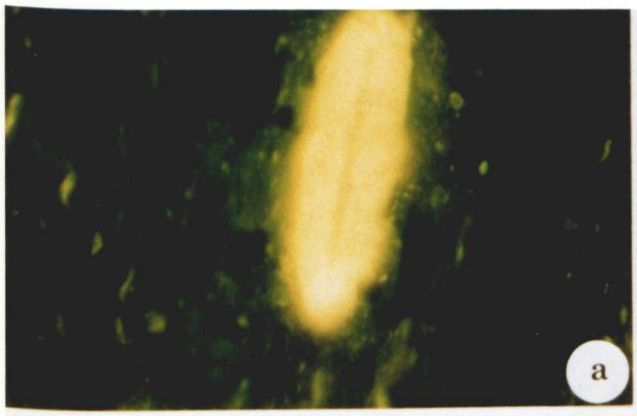
a

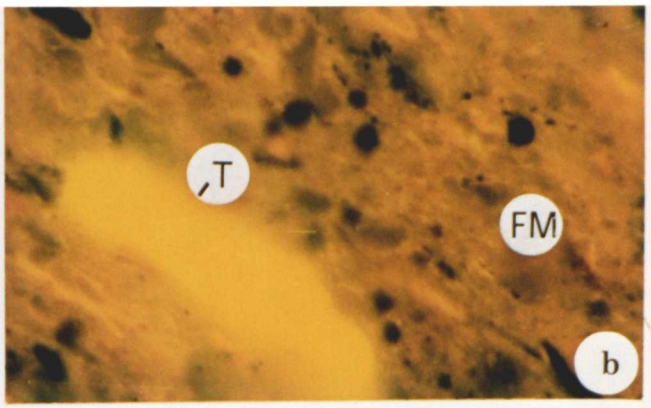
T
FM
b

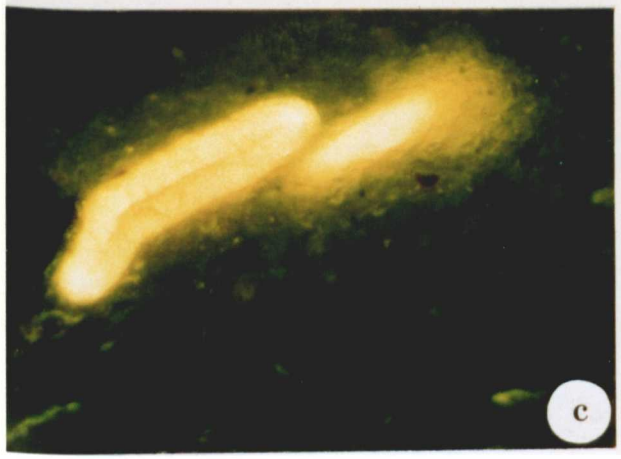
c

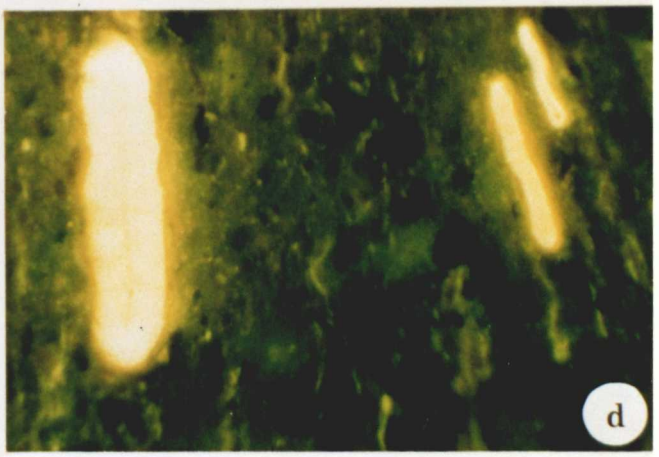
d

PLATE 6. Organic matter in the Triassic Schei Point Group.

All photomicrographs taken under ultraviolet excitation, water immersion (excitation 400 - 440 nm, barrier filter 470 nm). The long axis of each photomicrograph is 240 μm.

a) Dinoflagellate cyst (D) showing characteristic spines enclosed in fluorescing matrix, Eden Bay Member, Chads Creek B-64.

b) A large spineless dinoflagellate cyst, Eden Bay Member, Chads Creek B-64.

c) Dinoflagellate cyst, Cape Richards Member, Hecla J-60.

d) Same as above, Hoyle Bay Formation, Depot Island C-44.

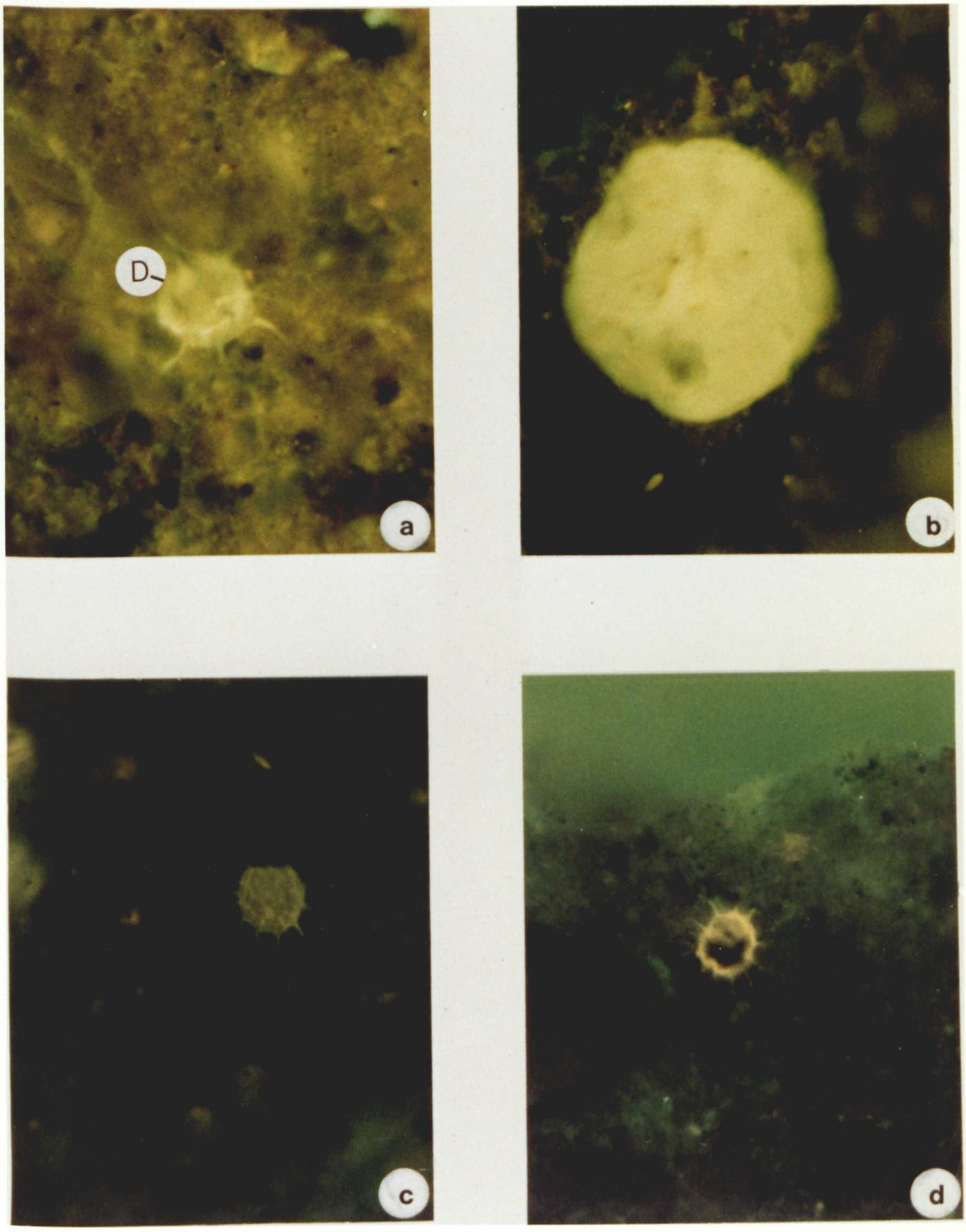
D
a
b
c
d

Formation, but they are present in the overlying Eden Bay and Cape Richards Members.

The Schei Point beds are in the marginally mature to overmature stage of hydrocarbon generation. In the areas in which the Schei Point source strata have attained adequate maturity levels for hydrocarbon generation to occur, the present hydrogen index (HI) values can be expected to be lower than the initial hydrogen indices prior to the onset of oil generation. A similar trend is observed for the total organic carbon (TOC) values with TOC of the Schei Point samples being up to 14.0 wt% where the Schei Point is marginally mature and <4.0 wt% where it is fully mature (Appendix II).

Increasing rates of petroleum generation with increasing maturity are clearly evident from electrical logs. The resistivity of the Eden Bay Shale increases progressively as a result of increasing maturity, from less than 40 Ohms/m at Chads Creek B-64 (0.55% Ro) to approximately 1,700 Ohms/m at Roche Point J-43 (1.05% Ro). The increase in resistivity may also be due to a decrease in porosity, therefore, a pressure phenomenon rather than thermal. In addition, the Eden Bay also exhibits high resistivities at North Sabine H-49 where it has attained maturation levels greater than 1.25% Ro. Thus, the Cape Caledonia Member of the Murray Harbour Formation and the Eden Bay Member of the Hoyle Bay Formation, as indicated by petrology and Rock-Eval (TOC up to 14.0 wt%, HI up to 800 mg HC/g Corg), are good to excellent quality source rocks (Appendices I and II).

There is geochemical evidence that the Schei Point source rocks where they are mature (i.e. North Sabine H-49 drillhole in Melville Island and other parts of Sverdrup Basin), and at peak generation (0.9 - 1.0% Ro) have effectively expelled hydrocarbons (Brooks et al., 1991). The timing of hydrocarbon generation and migration and their relation to structural history and trap formation in the Sverdrup Basin are important.

Burial history diagrams have been prepared for a selected number of the Melville Island drillholes and will be discussed later in more detail.

9.1.2 JAMESON BAY FORMATION

The Lower Jurassic Jameson Bay Formation consists of medium to dark-gray shales and silty shales deposited under marine conditions. Organic matter consists of land-plant remains, mainly spores along with alginite, dinoflagellates (Plate 7), partially degraded during sediment transport, liptodetrinite, vitrinite and inertinite embedded in a weakly fluorescing groundmass.

The Jameson Bay Formation has its minimum thickness (<100 m) in drillhole Sherard F-14 (Figure 9-11) and its maximum thickness (>250 m) in drillhole North Sabine H-49 (Figure 9-6). The locally developed source intervals containing vitrinitic to mixed exinitic/vitrinitic or sapropelic liptinitic organic matter are still immature (<0.6%Ro) in the Drake and Hecla hydrocarbon fields, except in drillhole Roche Point J-43 where the Jameson Bay Formation is in the mature stage of hydrocarbon generation (0.75-0.88% Ro).

The HI values for the Jameson Bay shales range from 24 in Grassy I-34 to 250 in Drake E-78, with most samples having values between 100-180 mg HC/g Corg. The Jameson Bay Formation was deposited during a period of maximum water depth at a peak of a major transgression (Goodarzi et al., 1991). The marine transgression over a broad shelf resulted in the development of favourable conditions for the accumulation and preservation of Types II and III organic matter leading to the formation of mainly gas and to a minor extent oil-prone source beds.

PLATE 7. Organic matter in the Jameson Bay Formation.

All photomicrographs taken under ultraviolet excitation, water immersion (excitation 400 - 440 nm, barrier filter 470 nm). The long axis of each photomicrograph is 240 μm.

a) Botryococcus algae showing characteristic cup-like structure, 1200 m, Drake D-68.

b) Same as above, 1210 m, Chads Creek B-64.

c) Numerous dinoflagellate cysts (D) in fluorescing matrix, 1070 m, Drake D-68.

d) Same as above, 970 m, Hecla C-32.

e) Compressed Tasmanites (T) 1095 m, Hecla J-60.

f) Densely-packed lamellae (lamalginite) possibly of Nostocaceae-genus origin 1200 m, Drake D-73.

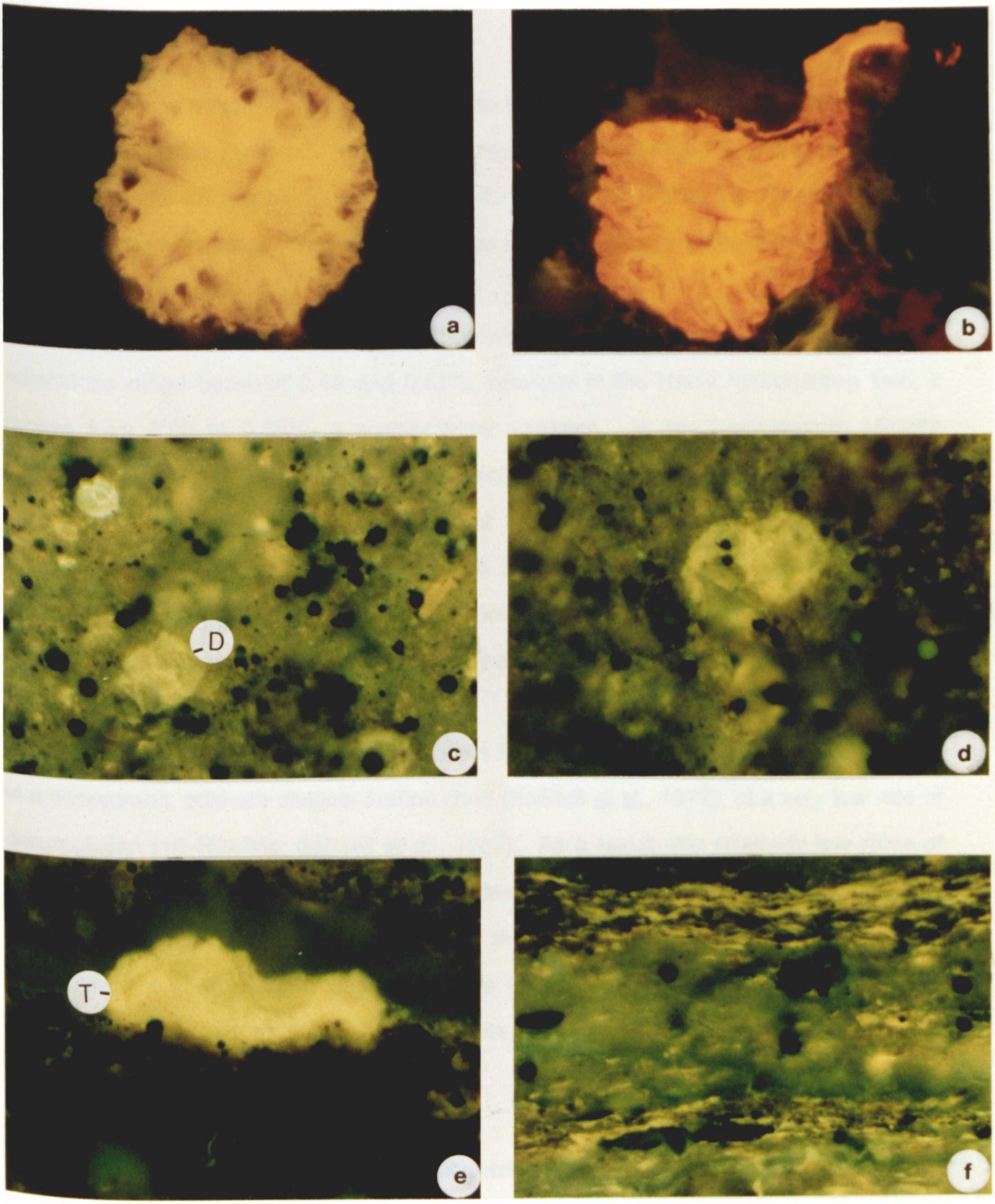
a
b
D
c
d
T
e
f

9.1.3 RINGNES FORMATION

The Jurassic Ringnes Formation also thins towards the Sverdrup Basin margin, from 50m in Sabine Peninsula to 20m in Marryatt K-71 (Figure 9-12) and in most of the Hecla and Drake drillholes (Figures 9-14 to 9-22 and 9-28 to 9-30). The sediments in this formation are immature to marginally mature as is evident from the above figures.

The base of the Ringnes Formation in the Drake hydrocarbon field has a reflectance range between 0.48 and 0.55%, whereas in the Hecla hydrocarbon field, it ranges from 0.43 to 0.58%, a slightly wider variation. In the northwestern Melville hydrocarbon field the Ringnes is very consistent, reflecting at 0.46-0.50% Ro. The Ringnes Formation in the two south-central Sverdrup region drillholes is marginally mature to mature (% Ro 0.6-0.75) (Figures 9-5 and 9-6). Ringnes samples contain mainly fluorescing organic matter Type II (cutinite, resinite, sporinite) and unrecognizable organic matter with variable amounts of woody and herbaceous components (Plate 8).

Sedimentological evidence indicates that the Ringnes Formation was deposited in a widespread, offshore shallow-marine shelf (Balkwill et al., 1977), at a very low rate of accumulation (10-15m/Ma; Balkwill et al., 1982). As a result, the relatively low rates of sedimentation compared to other Sverdrup Basin shales and the shallow oxic to mildly anoxic marine-shelf environment resulted in the formation of an organically-rich shale which contains predominantly gas-prone Type III organic matter. The organic matter in the Ringnes shale was protected from complete destruction by aerobic bacteria, resulting in the relatively high TOC content.

There is a basinward trend of increasing organic-matter quality for the Ringnes shales from a minimum HI of 60 to 150 along the basin margin to a maximum HI of 250 to

PLATE 8. Organic Matter in the Ringnes Formation

All photomicrographs, with the exception of 8b, taken under ultraviolet excitation, water immersion (excitation 400 - 440 nm, barrier filter 470 nm). Photomicrograph 8b taken under reflected plane-polarized light, oil immersion (colour film). The long axis of each photomicrograph is 260 μm.

a) Thin-walled cutinite, resinite and sporinite, 940 m, Drake D-68, 930 m.

b) Inertinite (I) and finely dispersed bitumen, 930 m, Drake L-67.

c) Folded cutinite, 1130 m, Drake K-79.

d) Botryococcus algae in a section parallel to bedding, 940 m, Drake D-68.

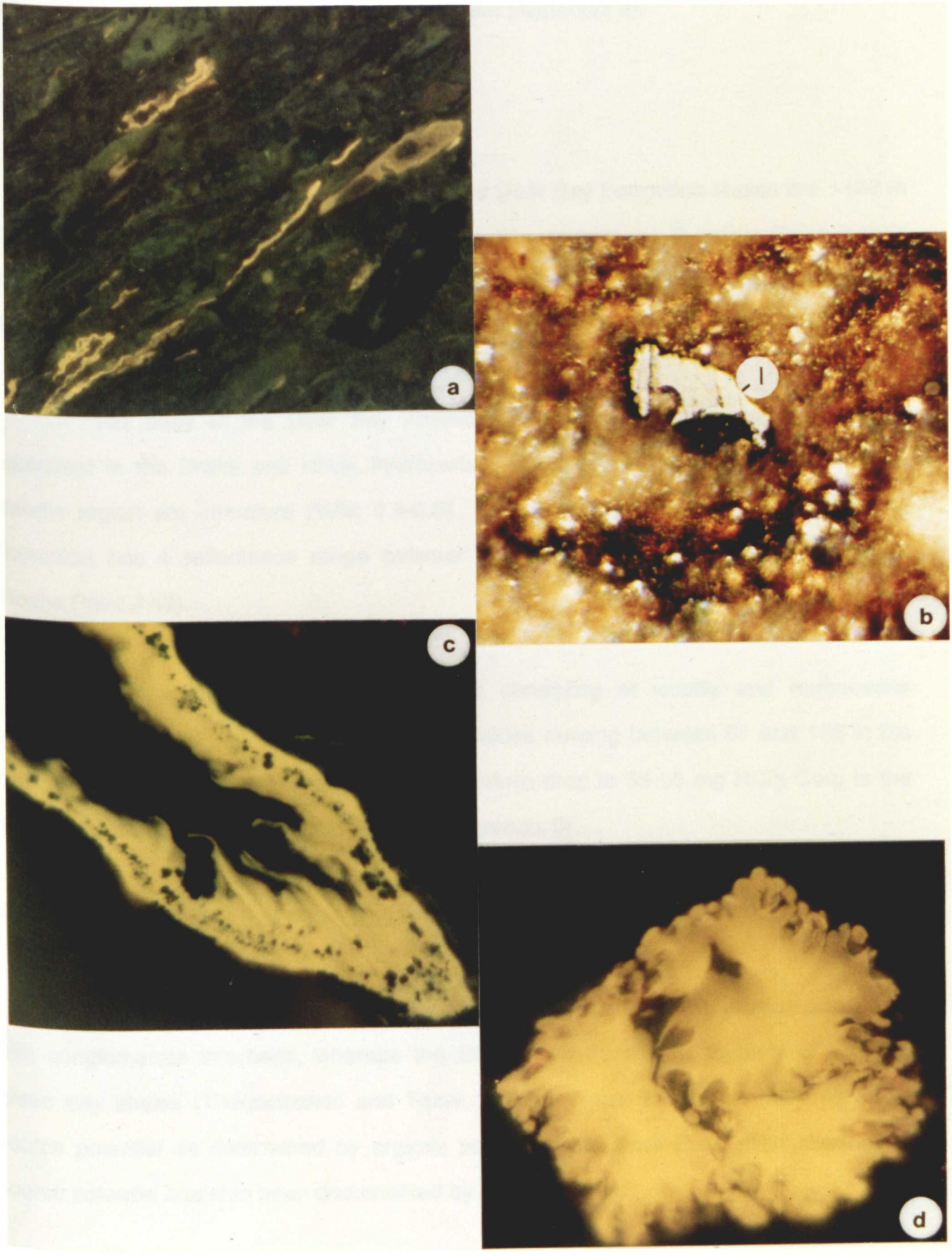
a
b
l
c
d

300 mg HC/g Corg in the centre of Sverdrup Basin (Appendix II).

9.1.4 DEER BAY FORMATION

The Upper Jurassic-Lower Cretaceous Deer Bay Formation shales are >100 m thick in North Sabine H-49 (Figure 9-6) but they thin towards the Sverdrup Basin margin in the locality of Collingwood K-33 and they are completely absent in Sherard Bay F-14 (Figure 9-11).

The base of the Deer Bay Formation and its (the base's) stratigraphically equivalent in the Drake and Hecla hydrocarbon fields, as well as in the northwestern Melville region are immature (%Ro 0.4-0.5). In the south-central Sverdrup region the Formation has a reflectance range between 0.56% (North Sabine H-49) and 0.66% (Roche Point J-43).

Organic matter is mainly terrestrial consisting of woody and herbaceous components (Plate 9). The Deer Bay has HI values ranging between 91 and 168 in the Drake and Hecla hydrocarbon fields, and the values drop to 55-80 mg HC/g Corg in the more mature south-central Sverdrup region (Appendix II).

9.1.5 BJORNE AND BLIND FIORD FORMATIONS

The Lower Triassic Bjorne Formation consists mainly of quartzose sandstone with conglomerate interbeds, whereas the Blind Fiord Formation consists of red and green silty shales (Thorsteinsson and Tozer, 1970). These formations have very little source potential as determined by organic petrology and Rock-Eval. The absence of source potential has also been documented by Powell (1978).

PLATE 9. Organic Matter in the Deer Bay Formation

All photomicrographs, with the exception of 9a, taken under ultraviolet excitation, water immersion (excitation 400 - 440 nm, barrier filter 470 nm). Photomicrograph 9a taken under reflected, plane-polarized light, oil immersion (colour film). The long axis of each photomicrograph is 260 μm.

a) Huminite fragment (PH) associated with finely-dispersed bitumen (B) in a shaley matrix, 540 m, Drake D-68.
b) Sporinite, 535 m, Hecla J-60.
c) A slightly biodegraded resinite body, 110 m, Depot Island C-44.
d) Section of Botryococcus algae parallel to bedding showing colony of unicellular algae, 120 m, Depot Island C-44.

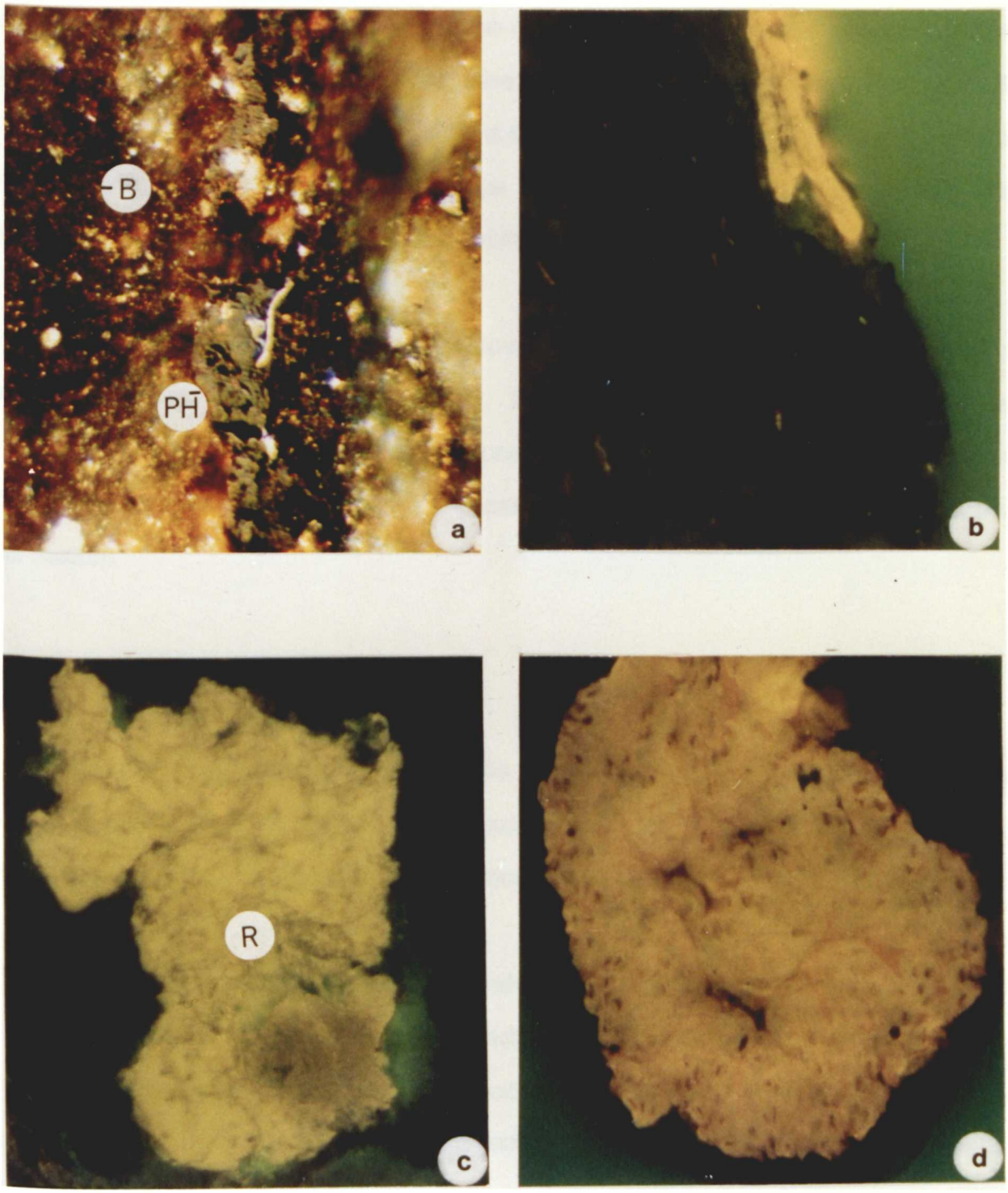
B
PH̄
a
b
R
c
d

The Permo-Pennsylvanian section is in the mature stage of hydrocarbon generation, but both Rock-Eval and petrological data (reflectance and kerogen types) (Appendices I and II) indicate a poor source-rock potential. The total organic carbon (TOC) values obtained from several Van Hauen Formation samples range from 0.55 to 1.23 wt%, the hydrogen index values (HI) are low (13-97) and so are the S_2 peaks (0.10-2.89). Powell (1978) states that gas yields and organic carbon values are extremely low, except from drillholes in the Sabine Peninsula.

In the Sabine Peninsula, the organic-carbon content of the clastic sediments is in the order of 1.0 to 1.5 wt% (Powell, 1978). In both the Chads Creek B-64 and Drake Point D-68 the main phase of oil generation occurs above 4,000 m. Visual examination of the organic matter and atomic hydrogen and carbon ratios confirm the poor source of the organic matter.

9.1.6 TROLD FIORD FORMATION

The Permian formations in Melville Island are generally characterized by terrestrially-derived organic matter. An exception may be the Botryococcus-rich, sapropelic coal found in the Trold Fiord Formation in drillhole Sandy Point L-46 (Plate 10).

The existence of large gas fields (Drake and Hecla) at relatively shallow depths (900 - 1,200 m), close to the onset of the mature zone, indicates that an overmature facies is not a necessary prerequisite for the occurrence of reservoired gas in Sverdrup Basin. It appears that accumulation of gas is mostly dependent on the availability of traps for early generated gas.

9.2 DESCRIPTION OF REPRESENTATIVE DRILLHOLES IN THE MELVILLE ISLAND

PLATE 10 Organic matter in the Permian Trold Fiord Formation

All photomicrographs taken under ultraviolet excitation, water immersion (excitation 400 - 440 nm, barrier filter 470 nm). The long axis of each photomicrograph is 240 μm.

a) Boghead coal showing brightly fluorescing Botryococcus algae, Trold Fiord Formation, Sandy Point L-46.

b) Botryococcus algae (A), section parallel to bedding showing a colony of unicellular algae, Trold Fiord Formation, Sandy Point L-46.

c) A megaspore (MG) showing brown fluorescence colour enclosing brightly fluorescing fluorinite (FL), Trold Fiord Formation, Sandy Point L-46.

d) Thick-walled cutinite (CU) showing the characteristic tooth-like structure, Trold Fiord Formation, Sandy Point L-46.

e) A mixed boghead-cannel coal sample, Trold Fiord Formation, Sandy Point L-46. Note the presence of highly-fluorescing Botryococcus algae (A) and the microstratification of spores.

f) Folded cutinite (CU) enclosing an algal body (A). Note the difference in fluorescence intensity between the two maceral types, Trold Fiord Formation, Sandy Point L-46.

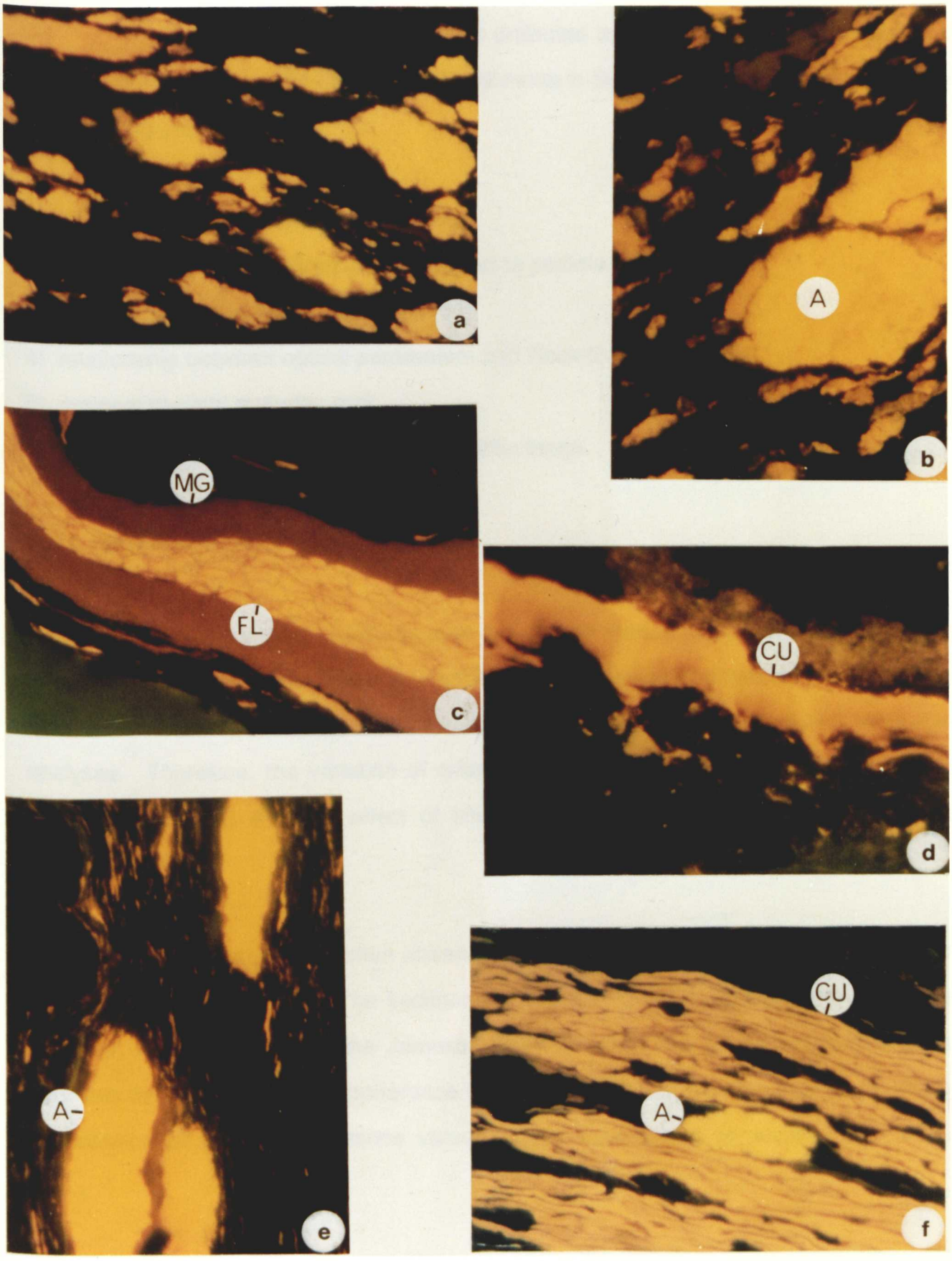
a
A
b
MG
FL
c
CU
d
A
e
CU
A
f

HYDROCARBON FIELDS AND PROMISING REGIONS

The description of representative drillholes and the subsequent discussion of the maturity and source-rock potential of sediments in Sverdrup Basin will be presented in the following order:

1) bitumen staining in Melville Island strata,
2) variation of thermal indicators with respect to sediment lithology,
3) maturity and source-rock potential,
4) relationship between optical parameters and Rock-Eval,
5) regional thermal maturity, and
6) effect of igneous intrusions on bitumen reflectance.

9.2.1 BITUMEN STAINING

The sediments in the study area are of both marine and non-marine origin and are often bitumen-stained. These two factors (i.e. environmental differences and staining) have some impact on the determined level of maturity based on optical and Rock-Eval analyses. Therefore, the variation of reflectance (% Ro) versus Rock-Eval parameters (HI, Tmax, S_2, PI) and the effect of bitumen staining on measured reflectance are discussed initially.

Bitumen staining is often observed throughout the sedimentary successions of the Drake and Hecla fields. The sedimentary strata in Drake K-79 (Figure 9-15) are an example. The sediments of the Jameson Bay Formation are bitumen-stained and the core has an oily and greasy appearance (Plate 11). Bitumen staining causes significant suppression of vitrinite reflectance values. This suppression is possibly due to the

PLATE 11 Bitumen staining in the Mesozoic formations

All photomicrographs taken under reflected, plane-polarized light, oil immersion (using a colour film). The long axis of each photomicrograph is 240 μm.

a) Finely-dispersed bitumen (B) in silty shale, Hassel Formation, 400 m, Roche Point J-43.

b) Low-reflecting bitumen (LB), Eden Bay Member, Drake K-79.

c) Wispy bitumen staining (BS) in shale, Jameson Bay Formation, Drake K-79.

d) Phytoclast fragments showing bitumen staining (BS) near the edges, Hoyle Bay Formation, Depot Island C-44.

e) Inertinite with bitumen staining, Ringnes Formation, Hecla M-25.

f) Same as above.

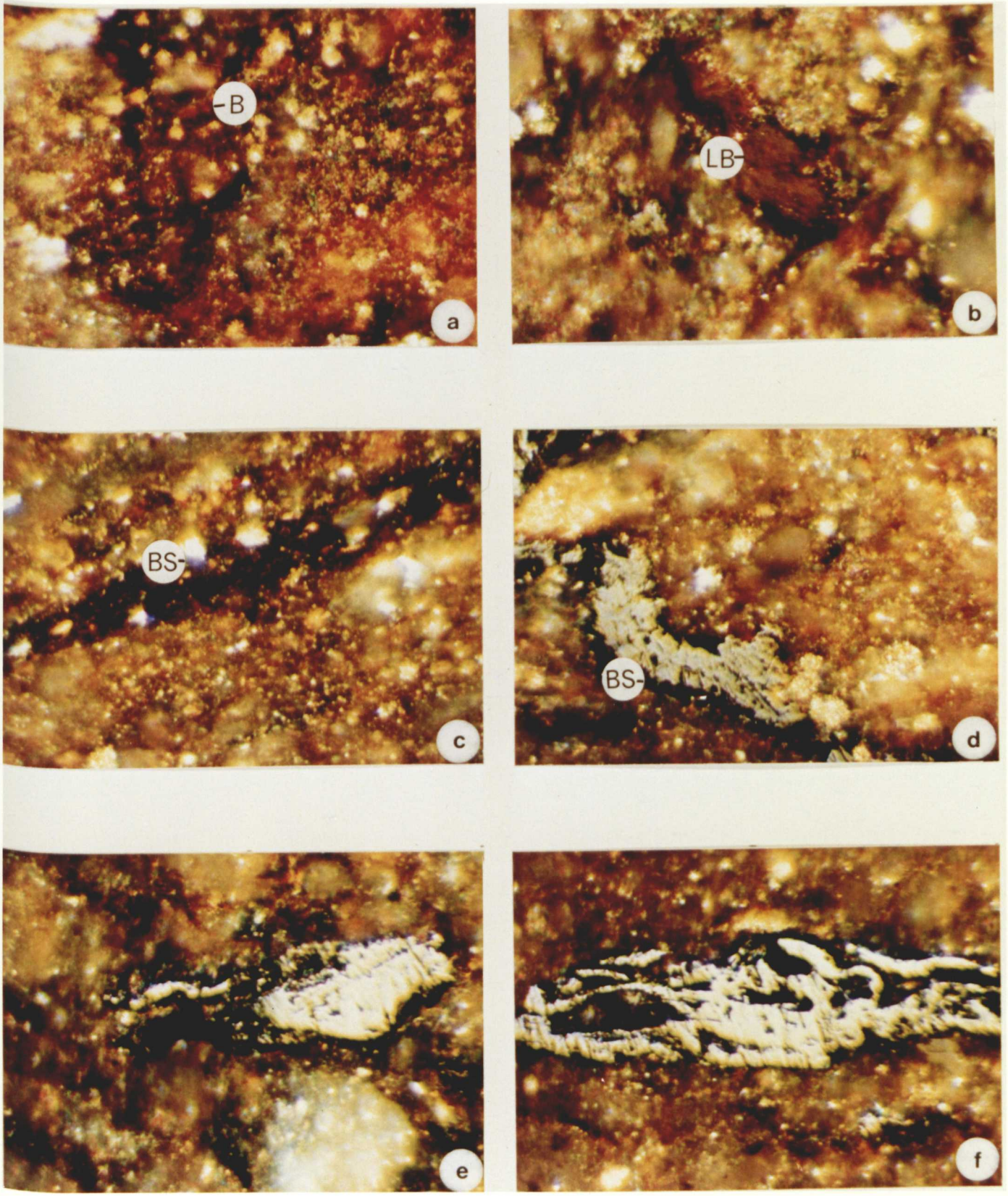
B
a
LB
b
BS
c
BS
d
e
f

localized diffusion of aliphatic compounds into vitrinite, as for example in the Eden Bay Member in which the marine shales are rich in liptinite, particularly in dinoflagellates, Tasmanites and other marine algae and amorphous fluorescing matrix (Goodarzi et al., 1989a). The suppression of organic matter reflectance near the base of the Jameson Bay Formation is presumed to be 0.1% Ro (Figure 9-15). The suppression of reflectance for the Eden Bay sediments is estimated by extrapolating the trend for vitrinite (Figure 9-15).

The occurrence of solid bitumen in the Drake K-79 drillhole (Figure 9-15) indicates the paths of oil migration. There are two migration paths, the oldest migration evidenced by the occurrence of high-reflecting bitumen throughout the strata. The reflectance of both bitumen phases increases with depth. The first oil migration affected the stratigraphic interval between the Eden Bay Member (Carnian) and the Christopher Formation (Albian) and the second migration affected the interval between the Eldridge Bay Member (Anisian) and the Christopher Formation (Figure 9-15). The path of both bitumen types indicates that migration took place after deposition of the Christopher Formation.

9.2.2 VARIATION OF THERMAL INDICATORS AND LITHOLOGY OF SEDIMENTS

The alternating intervals of marine shales/siltstones of the Jurassic Schei Point Group, non-marine to marginally marine shales/siltstones and sandstone and coaly intervals of Cretaceous age, offer the rare opportunity to compare Tmax values obtained from all the above lithologies. A good agreement between Tmax and Ro could help further interpretations of Tmax in marine to non-marine sequences.

With respect to marine and non-marine lithologies of the Mesozoic, the following observations can be made:

1) Tmax values for the marine shales and siltstones increase slowly with increasing maturation (Figure 9-36), and

2) Non-marine formations are generally characterized by higher Tmax values at the same or similar rank levels (Figure 9-36), indicating that the non-marine sediments mature at a lower reflectance level. The higher Tmax in the non-marine samples is most likely due to the presence of inertinite and degraded organic matter which pyrolyzes at higher temperatures. Leckie et al., (1988) made similar observations in Lower Cretaceous strata of the Monkman Pass area, British Columbia, Canada. Tmax values may be affected by the type of organic matter present in shallow marine and non-marine sediments. Fundamental differences in the chemical properties of terrestrial versus marine organic matter are thus believed to be responsible for the variation in Tmax values with lithology and maturation. Espitalie et al., (1985) show a wider temperature range of Tmax for vitrinite compared with exinite. Differences in thermal conductivities of the lithologies and different hydrodynamic properties that have controlled temperatures cannot be discounted.

Despite the limited number of coal samples studied, it is apparent that the Tmax values of coals are generally higher than those of both marine and non-marine shales (Appendix II). Coal seams, because of their low conductivity and great heat capacity, act as thermal 'blankets' over long periods of time, which results in higher reflectance values for vitrinite in coals compared to vitrinite in shales. Variations in vitrinite reflectance have been reported from sediments of different lithology and depositional environment.

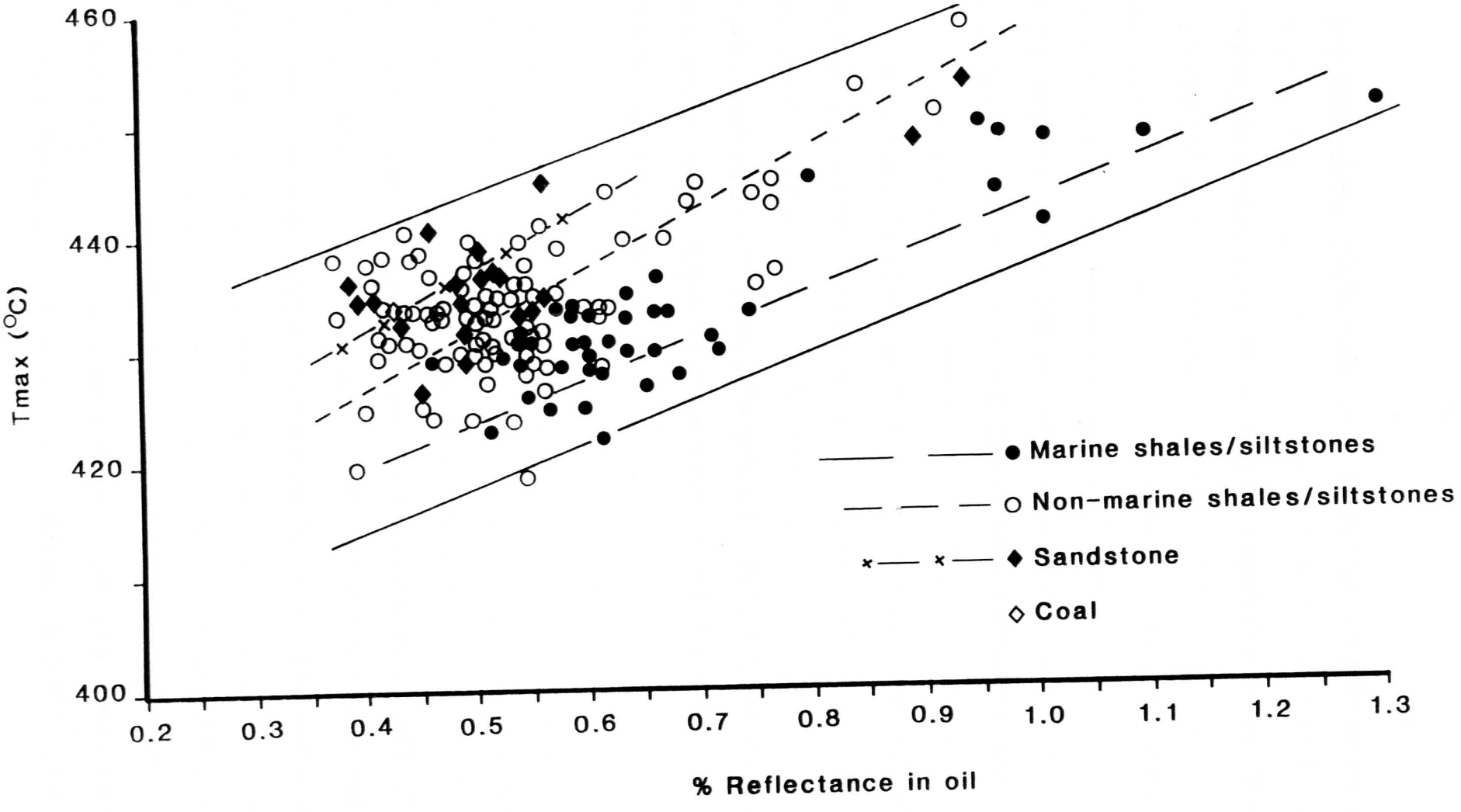

Figure 9-36 Relationship between vitrinite reflectance and Tmax according to matrix lithology

Timofeev and Bogolyubova (1975) consistently found that coaly inclusions in shale, siltstone and sandstone had lower reflectance than coal. In addition, Bostick and Foster (1975), examining the behaviour of vitrinite reflectance in sandstone, shale, limestone and coal seams from a drillhole in the Illinois Basin, observed that vitrinite in all three lithology matrices had generally lower reflectance than in coal seams. In a similar study, Jones et al., (1971) examining vitrinite reflectance distribution in the Northumberland and Durham coalfields (NE England) noticed that vitrinite in coal seams covered by sandstones generally displayed lower mean maximum and minimum reflectance than vitrinite in shale-covered coal seams at equivalent depths in the same succession. Recently, Pearson and Murchison (1990) made similar observations in coal seams of Westphalian B age in County Durham, UK. Coal seams overlain by sandstone had a lower rank than coal seams overlain by mudstone and shale units. Differences in thermal conductivities and rock permeabilities, early oxidation of the coal and differing degrees of degradation of the organic matter at the diagenetic stage were thought to be responsible for the observed reflectance variations.

Goodarzi et al., (1988b) studied in detail the effect of maceral subtypes and mineral matrix on measured reflectance of subbituminous coals and dispersed organic matter in a 515-metre thick coal and interbedded sediment succession in the Hat Creek No. 2 deposit, south-central British Columbia. They observed that eu-ulminite reflectance recorded from carbonate matrix was higher, reflectance from shale matrix was lower and reflectance from coaly matrix had intermediate values. In addition, Goodarzi et al., (in prep) examined the variation of vitrinite reflectance with respect to mineral matrix (lithology), thickness of coal seams and coal lenses as well as type of organic matter in two cores of a 550-metre sedimentary succession from the Upper Jurassic to Lower Cretaceous Kootenay Group. The data obtained indicate that reflectance in high- to low-volatile bituminous coals (% Ro max = 0.80 - 1.35) with depth of burial is affected by

the percentage of organic matter in the samples. A positive correlation between the % Ro and the % organic matter and a negative correlation with the % mineral matter were shown to exist and it was also observed that the thicker the coal interval, the higher was the reflectance. Thick coal seams (>1.0 m) with mineral content of <20.0% generally exhibited higher vitrinite reflectance than thin coaly lenses (15-30 cm thick) with mineral content of >20.0%. Vitrinite dispersed in sandstone and to a lesser extent siltstone and carbonaceous shale had the lowest reflectance.

Variations in the reflectance of vitrinite in association with different matrices have been widely recognized (e.g. Teichmuller and Teichmuller, 1968; Jones et al., 1971; Bostick and Foster, 1975; Goodarzi et al., 1988b). A mechanism by which matrix affects vitrinite reflectance is at present uncertain. Among the mechanisms commonly proposed are differential thermo-catalytic effect and thermal conductivity of the hosting matrices (Brooks, 1948; Teichmuller and Teichmuller, 1968; Galwey, 1970; Jones et al., 1971; Johns and Shimoyama, 1972, Karweil, 1975; and Goldstein, 1983).

The potential of mineral matrix to catalyze organic maturation was mainly attributed to clay minerals, in particular montmorillonite-like expandable minerals with a relatively high cation exchange capacity (Galwey, 1970; Johns and Shimoyama, 1972; Goldstein, 1983, Tannenbaum et al., 1986; Huizinga et al., 1987). In contrast, Timofeev and Bogolyubova (1975) suggested that during diagenesis clay minerals slow down the process of transformation of organic matter rather than accelerate it. Along with this suggestion, recent studies (Goodarzi, 1987; Eglinton et al., 1986; Goodarzi et al., 1988b) suggest that maturation of organic matter is suppressed when it is associated with shaley matrix (a relatively clay-rich rock) and increases in association with carbonate (clay-poor) matrix when compared to coaly matrix. The lower reflectance of organic matter in sandstones may be explained either by the small differences in temperature present in

sandstone bodies due to the good heat conductivity (high transmission rate of heat of siliciclastic rocks) (Damberger, 1968; Bostick and Foster, 1975; Teichmuller and Teichmuller, 1982) or due to the cooling effect of fluids which may circulate through the open spaces of a porous sandstone. The thermal conductivity effect is likely to be more pronounced in organic matter overlain by the thick Triassic Bjorne Formation sandstone and to a lesser extent by the sandy Awingak Formation. Therefore, a matrix 'effect' was identified but it is not known whether differences in reflectance of organic matter in various lithologies are due to differential retention, efficiency of reaction products removed, thermal conductivity or the existence of a catalyst.

Although the main factors governing the level of vitrinite reflectance are maximum temperature and time of exposure to maximum temperature, other physical and chemical processes such as tectonic stress and bituminization of marine organic matter may have a significant influence on the establishment of vitrinite reflectance (Leckie et al., 1988; Goodarzi et al., 1988b). The possibility that the matrix has an effect on the reflectance of organic matter and therefore, on maturation may have an important implication to oil exploration, because the stage at which hydrocarbons are being released from organic matter is dependent on the lithology of the host rock. Experimental data of Goodarzi et al., (in prep) indicate that up to the first coalification 'jump' (~0.50% Ro) or during late diagenesis, the difference in reflectance of organic matter in various lithologies such as thick coal seams, thin coaly layers, carbonaceous shales, sandstones and argillaceous shales is small but it increases during early catagenesis and continues into late catagenesis and early metagenesis.

The reason for this behaviour is at present uncertain, although it may reflect the effect of relative retention or expulsion of early diagenetic products from the vicinity of macerals (Goodarzi et al., 1988b). Jones et al., (1971) also stated that retention of any

decomposition products of coalification may influence the vitrinite properties, especially if retention is in close contact with organic matter. It has been shown by a large number of dry and hydrous pyrolysis experiments (Espitalie, et al., 1980; Orr, 1981; Katz, 1983; Espitalie et al., 1984; Hunt and McNichol, 1984; Eglinton et al., 1986; Tannenbaum et al., 1986; Goodarzi et al., 1988b) that clay minerals, particularly the montmorillonite group, effectively retain a relatively large proportion of high molecular weight compounds, which may be subjected to further thermal cracking.

Variations in the composition of the organic matter associated with the various lithologies and/or differential degradation and oxidation have been suggested to account for diverging reflectance (Goodarzi et al., 1988b). Diverse reflectance of organic materials is caused by changes in the chemistry of the organic matter itself, which can be penecontemporaneous and post-depositional. Optical differences in vitrinites associated with sandstone bodies have been attributed to chemical oxidation of the organic matter (Kunstner, 1974). The reason is that thin organic matter in coals present under sandy intervals is more severely biodegraded during early diagenesis, whereas organic matter in mudstones has not been degraded to a large extent because of the relatively stagnant-water conditions.

The relationship between HI and Ro shows a considerable difference between the non-marine samples and the marine shales and siltstones which are richer in Type I and Type II kerogen. The regression line for the marine samples of the Schei Point Group mainly shows a regular and rapid decrease of HI with increasing Ro (Figure 9-37), whereas the regression line through the HI values of the non-marine or marginally marine samples has a more gentle slope, showing a slight decrease only with increasing maturity. The marine samples in Figure 9-37 have higher hydrogen indices because they are initially richer in hydrogen-rich components than the other samples, but at a

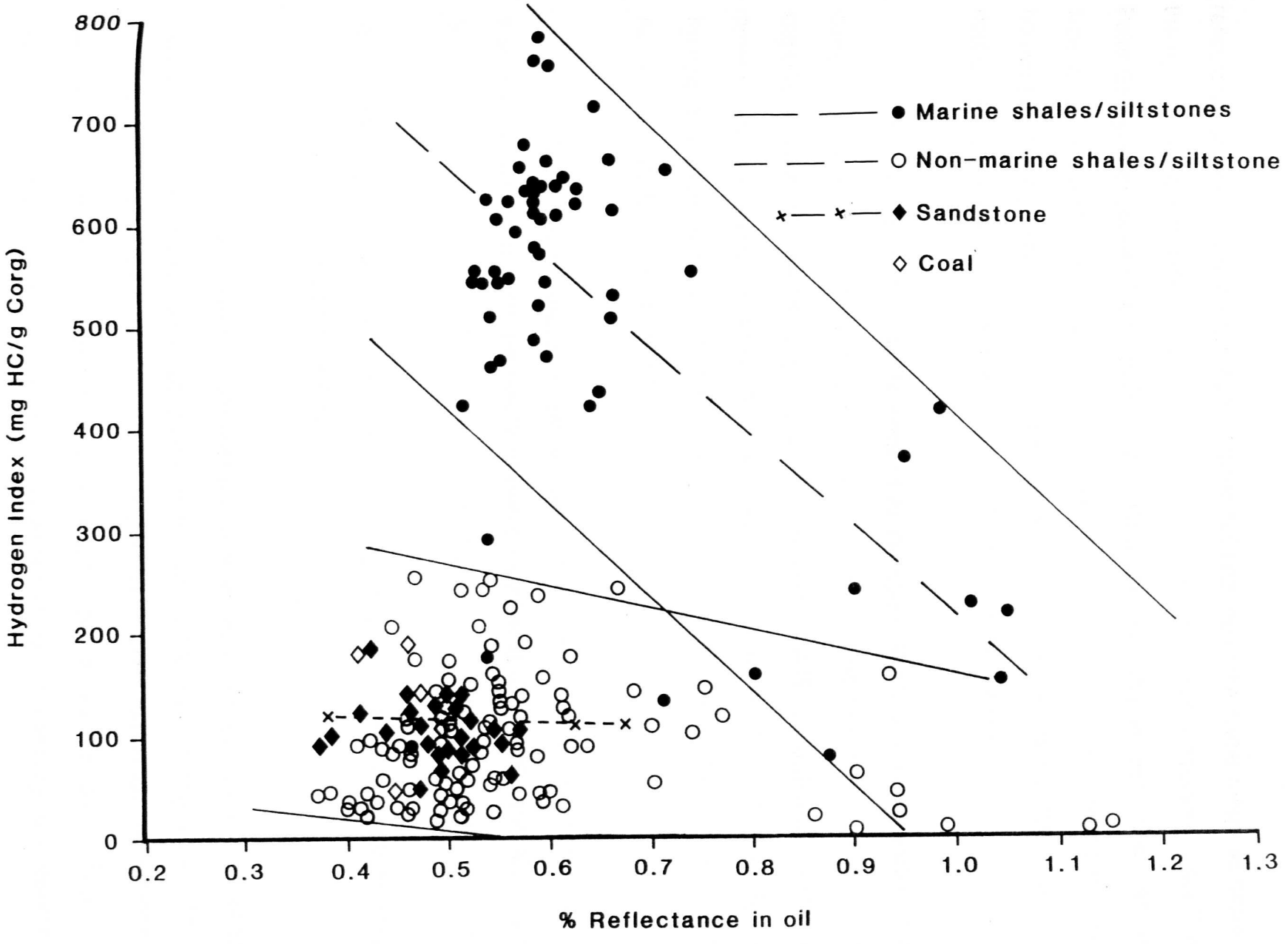

Figure 9-37 Correlation between hydrogen index (HI) and vitrinite reflectance for marine and non-marine samples

reflectance level of 1.0% the hydrogen indices fall and are in the same range as those of the non-marine and sandstone samples. Also, vitrinite in the marine samples of the Schei Point Group is associated with greater amounts of liptinitic material and, hence, exhibits suppressed reflectances. The regression line through the sandstone samples is almost horizontal showing very little if any correlation at all, while the regression line through the coal samples follows a trend similar to that of the non-marine samples.

According to the results presented in Figure 9-37, the steep slope of the correlation between the HI values of marine sediments and reflectance indicates that organic matter of marine origin (i.e. dinoflagellate cysts, Tasmanites algae and amorphous fluorescing matrix) is much more sensitive to thermal maturity and hydrocarbon generation than terrestrial and also marine organic matter characteristic of nearshore or deltaic environments.

The present results show a more clear distinction between marine and non-marine sediments than the results shown by Leckie et al., (1988), and also indicate that the reflectance versus HI and Tmax of organic matter in sandstones changes little.

9.2.3 MATURITY AND SOURCE-ROCK POTENTIAL OF HYDROCARBON FIELDS AND PROMISING REGIONS

There are numerous hydrocarbon fields in the Sverdrup Basin. Two of these fields, Hecla and Drake, are located on and/or offshore Melville Island (Figure 7-1). The majority of the drillholes in Melville Island were drilled in these two fields, except for five in the northwestern part and two in the north-eastern part of Melville Island (Figure 7-1), (Table 2). The maturation and source-rock potential of the sedimentary succession in this area will be discussed as follows:

1. Drake hydrocarbon field,
2. Hecla hydrocarbon field,
3. Northwest Melville region, and
4. Southwest Sverdrup Basin region.

9.2.3.1 DRAKE HYDROCARBON FIELD

The Drake hydrocarbon field occurs between 108° to 110° longitude and 76° to 76°30' latitude (Figure 7-1). Fourteen drillholes were drilled in this field and five more were drilled close to it. The five are: Marryatt K-71, Sherard Bay F-14, Collingwood K-33, North Sabine H-49 and Roche Point J-43 (Figure 7-1). Only two drillholes, Drake P-40 and Drake I-55, are situated offshore and to the east of Sabine Peninsula.

Most of the drillholes are relatively shallow and penetrate the Lower Triassic Schei Point Group. The total depth ranges from 1,000m in Drake F-76 (Figure 9-16), which penetrates into the Lower Triassic Schei Point Group, to 5,400m in Drake Point D-68 (Figure 9-1), which penetrates into the Permian Hare Fiord Formation.

Vitrinite-reflectance trends are not affected by the presence of unconformities, except in one drillhole, Drake Point D-68 (Figure 9-1). The sediments at the top are immature in Drake E-78 (%Ro - 0.35) to marginally mature in Drake D-73 (%Ro - 0.55). Reflectance increases with depth to reach a value of 0.65% in the Cape Caledonia Member (Collingwood K-33) indicating that the Mesozoic sedimentary succession in all Drake field drillholes lies in the immature to marginally mature stage of oil generation (Powell, 1978).

The maturity and the type of organic matter in the sedimentary succession for

any specific unit, for example the Schei Point Group, is very similar for all drillholes in the Drake field. As a result, only the drillhole Drake Point D-68 is discussed in detail.

PANARCTIC DRAKE POINT D-68

Drake Point D-68 is the deepest drillhole in Melville Island with a total depth of approximately 5,384 m (Figure 9-1). Formations range in age from Pennsylvanian to Lower Cretaceous, covering a wide range of lithologies. The Jurassic-Cretaceous interval is dominated by shale, siltstone and minor limestone, whereas the thick Triassic Bjorne Formation is composed of sandstone with a good porosity. Siltstone and shale with minor limestone and sandstone make up the Permo-Pennsylvanian part of the succession, with the exception of two intervals at 4,675 m and 4,810 m, which is a contact metamorphic zone produced by the intrusion of granodiorite sills (Balkwill and Haimila, 1978).

The phytoclast content in Drake Point D-68 is low to moderate and consists of higher-plant remains (coal) in the Jurassic Awingak and the Cretaceous Isachsen Formations. Most of the Triassic interval, due to its arenaceous nature, is relatively barren of organic matter. The Schei Point Group is often rich in marine algae, i.e. dinoflagellate and Tasmanites in Drake Point D-68 and other drillholes, such as Drake F-16 and Drake B-44 (Plates 5 and 6).

The maturation pattern established (Figure 9-1) is relatively clear to a depth of about 1,200m, with an increase in reflectance from 0.45% to 0.56% indicating a continuously subsiding basin. The sediments at the base of the Jurassic are marginally mature. The Schei Point sediments containing alginite are marginally mature (%Ro ~ 0.55) but the actual level of maturity may be represented by a reflectance level of 0.10 to 0.15% higher than the measured value, hence they most likely have generated some oil,

which accounts for the lower reflectance (Hutton and Cook, 1980; Goodarzi et al., 1989a). An intense 'background' orange-light brown fluorescence is observed in numerous Schei Point samples. Teichmuller and Ottenjann (1977), Creaney (1980a), and Goodarzi et al., (1987a) respectively describe a similar matrix effect from the Posidonia oil shale of West Germany, the Upper Cretaceous Boundary Creek Formation in the Beaufort-Mackenzie Basin, and the Carboniferous Grinnel Peninsula in Sverdrup Basin, Canada, and attribute it to absorption of lipoid substances on the mineral matrix.

The reflectance trend is not affected by the presence of two minor unconformities in this section (Figure 9-1), neither is it affected by the unconformity at the top of the Upper Triassic Schei Point Group (Figure 9-1), indicating that this is a minor erosional unconformity (Dow, 1977). Following a 1,000m organic-barren interval, the Lower Triassic Blind Fiord in Drake Point D-68 contains both vitrinite and bitumen. The vitrinite has a reflectance of 0.80% and the bitumen 1.0-1.10% indicating that this section is in the mature zone of oil generation (Figure 9-1).

The thermal history of Permo-Pennsylvanian strata in the drillhole has been influenced by high paleoheat flows associated with periods of igneous intrusion. The two igneous intrusions have thermally altered both bitumen and vitrinite, and at such high reflectance level (>5.0% Ro, max) it is difficult to differentiate between bitumen and vitrinite. Bitumen became thermally altered and is in the form of rounded to subangular fragments with a %Ro, max of 5.8-6.8 (cata-impsonite) (Khavari-Khorasani, 1975). The reflectance of bitumen below the lower sill decreases gradually to a value to 1.53% at the base of the drillhole. The trend above the upper sill, from unaffected bitumen at approximately 4,242 m to a depth of 4,636 m, can only be inferred. The thermal alteration of bitumen in this drillhole is similar to those described by Creaney (1980b).

Bitumen fragments in proximity to the sills have developed granular anisotropy (mosaic) indicating that the bitumen has gone through molecular re-arrangement (Khavari-Khorasani and Murchison, 1978). The thermal alteration of bitumen by the two sills shows that the bitumen had migrated into the sediment before intrusion occurred. The results of Balkwill and Haimila (1978), based on K/Ar isotopic technique, indicate that the upper sill was intruded at 152±6Ma and the lower sill at 131±Ma into the Permian strata.

The sedimentary successions are immature to marginally mature for most of the Mesozoic strata penetrated in this field. The oil-prone source rocks of the Schei Point Group are characterized by the presence of marine-liptinite organic matter, are immature in the southern part of the Sabine Peninsula, but they progressively become mature towards the basin centre. As a result they are overmature in the northern part of Sabine Peninsula (Goodarzi et al., 1989a).

OTHER DRILLHOLES IN THE DRAKE HYDROCARBON FIELD

The good to excellent source-rock potential of the Schei Point Group sediments is evident from Rock-Eval data. The southern part of the Drake field, in the vicinity of the Sherard Bay and Collingwood drillholes, contains sediments with some of the highest HI values encountered anywhere in Sverdrup Basin. Among the highest values in Sherard Bay F-34 and F-14 are the Cape Richards Member (474-553) and the Eden Bay Member (480-548). The Eden Bay in Collingwood K-33 has an HI as high as 700 (mg HC/g Corg) and the Cape Caledonia Member as high as 506. In Drake L-67, the Eden Bay has an HI value of 630 (Appendix II).

Moving towards the vicinity of Drake Point D-68 and K-79, the Eden Bay

Member still has high HI values (428-682),a TOC of 4.2-5.7 wt%, a Tmax is 428-431 °C and Ro <0.70%. The Cape Caledonia is next with an HI of 281-559, a TOC 1.1-3.8, and Tmax = 433-436 °C, followed by the Cape Richards (HI= 129-508), (TOC = 1.3-3.0), Tmax = (432-436 °C), and Ro <0.70% (Appendix II). The immature Eden Bay marine shales are organic-rich throughout the Drake field with an average TOC of 3.5-6.0 wt% and a Tmax of 423-432 °C. The Eden Bay Member has an HI of 622 in the Drake F-16 drillhole, 508 in Drake B-44, and 623-642 in Drake P-40. The Cape Richards shales have an HI value of 392 in Drake F-16, while the Eldridge Bay Member has an HI of 419 in the same drillhole. The Cape Caledonia has an HI value of 462 in Drake B-44 and the Cape Richards a value of 433 in Drake D-73.

Based on the % Ro and Rock-Eval analysis (Appendices I and II), the Schei Point organic-rich marine shales and siltstones are marginally mature and have not begun to generate any significant amounts of hydrocarbons in the Drake field.

9.2.3.2 HECLA HYDROCARBON FIELD

This hydrocarbon field occurs between 110° - 112° longitude, and 76° to 76°30' latitude (Figure 7-1): ten drillholes were drilled. Most of the drillholes are relatively shallow with their total depth ranging between 1,000m (Hecla West P-62) (Figure 9-24) and 1,200m (Hecla C-32) (Figure 9-30). There are two deep drillholes, Chads Creek B-64 and Hecla J-60 (Figures 9-2 and 9-3). Hecla J-60 has a total depth of 3,594m and penetrates to the Permian Van Hauen Formation (Figure 9-3), while Chads Creek B-64 has a total depth of 5,000m, penetrating to the Permian Hare Fiord Formation (Figure 9-2). Five of the drillholes under study were drilled offshore. The reflectance versus depth profiles for drillholes drilled on Sabine Peninsula show gentle maturity trends (Figures 9-1 and 9-2), while a slightly steeper maturity trend is evident for some drilled

offshore (Figures 9-5 and 9-33).

The inland drillholes have penetrated a succession of 800m (Hecla F-62) (Figure 9-29) to 2,900m (Chads Creek B-64) of Lower Triassic to Lower Cretaceous age. The sediments at the top are immature (%Ro = 0.45 - 0.52). Reflectance increases with depth to reach a value of 0.68% in the marine shales of the Eden Bay Member, indicating that the sedimentary successions in all Hecla hydrocarbon-field drillholes are in an immature to marginally mature stage for liquid hydrocarbon generation (Powell, 1978), although the above value may be slightly suppressed. The maturity determination for the Eden Bay Member is consistent with the organic geochemical results of Brooks et al., (1991) and the organic petrological study of Goodarzi et al., (1989a) on the Schei Point shales. Because of the similarity in range of maturity and type of organic matter occurring in the sedimentary succession of all drillholes in this field, only the two deepest drillholes, Hecla J-60 and Chads Creek B-64 will be discussed in detail.

PANARCTIC CHADS CREEK B-64

This drillhole penetrates a succession 5,000m thick that ranges in age from Permian to Cretaceous. The top 3,370m consist mainly of alternating shales, siltstones and calcareous sandstones with carbonaceous streaks. From 3,380m to 3,697m the dominant lithology is a dark grey to black chert, very argillaceous and slightly calcareous. Beyond this depth a medium to dark grey siliceous, slightly glauconitic shale dominates, showing black carbonaceous inclusions.

The reflectance versus depth profile is shown in Figure 9-2. Organic matter is generally low to moderate, except in the interval between 3,900m and total depth (Permian Van Hauen Formation), where it is moderate to high. The organic matter

dispersed in the Permian sediments is mainly composed of bitumen, thermally-altered bitumen, inertinite, high-reflecting Tasmanites algae with some input from vitrinite. The occurrence of mature Tasmanites at depths of 3,606m, 4,000m, 4,333m and 4,878m points to a reducing marine environment for these sediments.

The most promising interval for the generation of liquid hydrocarbons is the Schei Point Group. The organic matter content in these sediments consists mainly of dinoflagellates and Tasmanites algae. The highest HI values are present in the Schei Point Group (310-659 mg HC/g Corg) (Appendix II). The TOC for this interval is between 1.43-4.88 wt%, but the maturity as indicated by Tmax (432-439°C) and reflectance (0.58-0.60% Ro), points only to marginally mature sediments which have not fully generated hydrocarbons.

The Jameson Bay samples have moderate HI values (106-142), but their TOC and S_2 values are generally low (TOC 0.47-0.49 wt% and S_2 between 0.5 to 0.7). Tmax ranges from 433-434°C and the reflectance is 0.57%, indicating marginal maturity for the Jameson Bay. Botryococcus algae with well-defined internal structure and a yellow fluorescing colour are present in this Formation (Plate 7).

The Ringnes Shale, which has high input of terrestrial organic matter, also has the highest TOC of all samples in this drillhole (8.12 wt%). The source-rock potential is low as shown by HI (144), Tmax (435°C) and % Ro (0.53). The other younger shales (i.e. Deer Bay, Christopher) are immature and have very limited hydrocarbon potential (Appendix II). The mature sediments in this drillhole are represented by the Permian Van Hauen and Hare Fiord Formations, but these formations have very limited hydrocarbon potential.

The sediments at the top of this drillhole are marginally mature (%Ro = 0.50) and become fully mature (%Ro = 1.35) at a depth of 4,800m. The reflectance versus depth shows a gentle maturity profile for vitrinite (Figure 9-2).

Variation of bitumen reflectance

Bitumen occurs throughout this drillhole (Figure 9-2), but it shows higher concentrations in the Lower Triassic and Permian successions. There are two populations of bitumen, a low reflecting (%Ro, max = 1.1 - 1.9) and a high reflecting (%Ro, max = 1.6 - 2.5), which is granular and is often found in carbonates. Both these bitumens are at the epi-impsonite maturity level (Jacob, 1983) and have higher reflectance than vitrinite at the same depth, which confirms that for the same level of thermal maturity, bitumen has higher reflectance and higher aromaticity than vitrinite in the mid-catagenesis stage of hydrocarbon generation (Jacob, 1983). The reflectance of both low-and high-reflecting bitumen increases with depth, with the low-reflecting bitumen showing a trend subparallel to that of the high-reflecting population (Figure 9-2). Bitumens in the Lower Triassic-Permian were most likely generated from the primary phytoclasts in these sediments and, therefore, were subjected to thermal stress similar to that of vitrinite. Bitumens are more sensitive to thermal stress than is vitrinite (Khavari-Khorasani and Murchison, 1978; Goodarzi and Macqueen, 1990) and can attain higher aromaticity and higher reflectance than vitrinite due to their structural mobility during heat treatment (Khavari-Khorasani and Murchison, 1978).

The maturity of phytoclasts at a depth of 3,300m is elevated to many times that of the country rocks due to an igneous intrusion which is an undated diabase sill (Balkwill and Haimila, 1978). The reflectance of high-reflecting bitumen increases rapidly from 1.8% to 3.0% near the contact (see also Creaney, 1980b) who reported a similar increase

in reflectance of bitumen in close proximity to an intrusion in northern England). At a depth of 4,000m and greater, bitumen reflectance once again follows the extrapolated trend of bitumen for the country rocks (Figure 9-2), demonstrating that thermal stress generated by this intrusion has had only a limited effect on the sedimentary succession in the area. Creaney (1980b) also found a similar trend in his study.

In contrast to the bitumen in the Lower Triassic-Permian section, bitumen in the Upper Triassic-Upper Cretaceous has a similar reflectance for about 1,000m, while reflectance of vitrinite has increased over this depth (Figure 9-2). This bitumen is thus a residue of migration of hydrocarbons into these sediments. The migrated bitumen has probably originated from organic matter which underwent a thermal stress much higher than its thermal stability, thus resulting in thermal cracking and migration of hydrocarbons. These hydrocarbons were subsequently trapped in this section and formed a residual high-reflecting bitumen.

The maturity of the Permian sedimentary succession in both the Chads Creek B-64 and Drake Point D-68 drillholes has been significantly affected by igneous intrusions (Figures 9-1 and 9-2). The thermal alteration, as determined by reflectance, is higher in Drake D-68. The maximum reflectance of bitumen in proximity to a granodiorite sill is 5.8-6.8% for Drake D-68: in contrast, the maximum reflectance of bitumen is 3.0% in proximity to the diabase sill in Chads Creek B-64 (Figures 9-1 and 9-2). The granodiorite sills are approximately 45-75m thick and the diabase sill is almost 120m. A diabase sill has higher temperature of implacement (~1,000°C) than a granodiorite sill (~850°C) (Kostopoulos, pers. commun., 1990), yet organic matter affected by the thinner, cooler granodiorite sill has developed higher reflectance and granular anisotropy. Numerous factors, such as the pulsation of sill implacement, the lithology of the host rock, the thermal conductivity and the type and level of organic-matter maturity (initial maturation

level) prior to sill implacement may have influenced the effect of the intrusion on organic matter.

Recently, Raymond and Murchison (1988), examining the development of organic maturation in the thermal aureoles of sills in the Midland Valley of Scotland, arrived at the conclusion that the physical state of the sediments, such as the degree of sediment compaction and the volume of pore water in the sediments at the time of the magma invasion are also significant factors influencing organic matter behaviour during igneous intrusions.

The bitumen near the intrusion zone in Drake Point D-68 (Figure 9-1) has been carbonized and produced granular mosaic, similar to that produced by carbonized vitrinite. This implies that the sediments in the above drillhole were likely consolidated before the magmatic invasion. The sediments in Chads Creek B-64 (Figure 9-12) may have been less consolidated and contained greater pore water volume than sediments in Drake Point D-68, although this cannot be completely justified because the precise age of the diabase sill is unknown. This would result in an increase in the rate of cooling and in preventing heat conduction through the sediments. Although it may be difficult to prove, this could be a possible explanation for the contrasting reflectance pattern (presence of mosaic on the Drake Point D-68 bitumens) and absence of mosaic on the Chads Creek B-64 bitumens.

PANARCTIC HECLA J-60

A succession approximately 3,595m thick was penetrated with the formations ranging in age from Lower Cretaceous to Permian. The undifferentiated Permian strata grade from limestone at the top to siliceous shale with chert at the base. The thick

Triassic Bjorne is a quartzose sandstone with good porosity but also containing caved material. The Jurassic section consists mainly of shale with minor siltstone, whereas the Cretaceous section contains sandstone, siltstone, shale and coal.

Organic matter throughout the succession is moderate with the exception of the Bjorne sandstone where it is sparse. Vitrinite and coaly fragments are the dominant components of the dispersed organic matter in the top 900 m from the Ringnes to the Christopher Formations, indicating the terrestrial origin of the organic matter (Plates 8 and 9). Terrestrial organic matter has high TOC (4.70 - 74 wt%) and low HI content (70 -181 mg HC/g Corg).

The thermal maturity of Mesozoic sediments in this section is low and the section has experienced little thermal stress. Reflectance of vitrinite increases from 0.45% Ro at the top in the Lower Cretaceous Christopher Formation to 0.58% Ro in the Middle Triassic Eldridge Bay Member. The hydrocarbon potential of the sedimentary succession in this drillhole is limited to biogenic gases, due to the low thermal maturity of the Upper Cretaceous to Lower Triassic (Eden Bay Member) strata and lack of source rocks in more mature sediments, for example, parts of the Lower Triassic Blind Fjord and Permian Degerbols Formations. The highest HI values are recorded from the Eden Bay (547), the Tmax is 429°C, the TOC is 3.90 wt% and the Ro 0.55% (Appendices I and II).

Bitumen is relatively abundant in the Lower Triassic Blind Fiord Formation and in the Permian Degerbols Formation (Figure 9-3) showing that the sediments have been in the path of hydrocarbon migration (Robert 1980; Goodarzi et al., 1985). There are two generations of bitumen in these formations (Figure 9-3), indicating multiple paths of hydrocarbon generation/migration. The oldest generation/migration path is evidenced by the occurrence of high-reflecting bitumen, the reflectance of which increases over a depth

interval of nearly 1,400m (Figure 9-3). This migration path covers the interval between the Bjorne and Van Hauen Formations. The most recent migration path covers nearly 1,100m of sedimentary strata between the top of the Blind Fiord and the Van Hauen Formations. The reflectance of this lower-reflecting bitumen is almost the same for the entire thickness of the interval (Figure 9-3).

9.2.3.3 NORTHWEST MELVILLE REGION

This hydrocarbon field is situated between 113°-116° longitude and 76°-76°30' latitude, near the edge of the Sverdrup Basin (Figure 7-1). It covers the Sproule Peninsula and there are four drillholes present, three of them inland and one offshore (Figure 7-1). The maximum depth penetrated is 2,651m in Depot Island C-44 and this drillhole has penetrated into the Ibbett Bay Formation of Ordovician to Devonian age (Figure 9-4). The drillholes, namely Marie Bay D-02, Sandy Point L-46 and Depot Island C-44 are located onshore and penetrate almost similar geological formations. Depot Island C-44, which is the deepest drillhole, will be discussed in detail.

The Devonian Ibbett Bay Formation is a basinal shale, black, very carbonaceous, and micro-micaceous, while Permo-Pennsylvanian strata are composed mainly of shale with minor sandstone. The Triassic Bjorne Formation is dominated by sandstone and has a very poor organic matter content. The Hoyle Bay and Grosvenor Island Formations are dominated by silty shale, whereas the Isachsen Formation is a shale-sandstone unit with carbonaceous and coaly fragments. The Schei Point Group in Depot Island C-44, represented by the Hoyle Bay Formation, is relatively thin (60 m) and silty. The microspores fluoresce with a yellow colour and appear oxidized. The phytoclast content is generally low, apart from some organic-rich intervals, i.e. an algal-rich shale (Plate 10) of Permian age from the Trold Fiord Formation in Sandy Point

L-46 (Figure 9-32) and graptolitic shales of the Ibbett Bay Formation in Marie Bay D-02. Organic matter consists of Botryococcus algae (Plate 10), sporinite, with some input from vitrinite and graptolites (in the Palaeozoic only). Bitumen is often present throughout the sedimentary successions (Figures 9-4 and 9-32).

Mesozoic

The Mesozoic sediments throughout these drillholes are marginally mature (%Ro = 0.50-0.60) and have not reached the peak of oil generation for Type I organic matter (~ 0.90% Ro). The sediments of the Hoyle Bay Formation, which is the major source rock in the area (Brooks et al., 1991), are immature (%Ro =0.48 - 0.52) in this field.

The Eden Bay Member of the Hoyle Bay Formation (% Ro = 0.48 - 0.52) has an HI value of 421 in Sandy Point L-46, TOC of 2.10 wt%, a Tmax of 436 and an S_2 of almost 9.0, indicating that it is a good potential source rock. The same member in the Depot Island C-44 drillhole (% Ro = 0.50) has a lower source-rock potential: (HI = 93; TOC ~ 3.50 wt%; S_2 ~ 3.3; Tmax ~ 429°C) (Appendices I and II). The Cape Richards Member in Grassy I-34 has an excellent source potential (HI 620; TOC >8.0 wt%, S_2 >50.0), but it is immature (Tmax 429°C). The Eden Bay Member has similar pyrolysis data (HI = 625; TOC ~ 7.0 wt%; S_2 ~ 42.5; Tmax = 430°C). Reflectance values indicate that the Eden Bay and Cape Richards Members are still in the marginally mature stage of hydrocarbon generation (<0.70% Ro) for liptinitic marine organic matter. Core samples taken from the Jameson Bay shales are poor source rocks (HI= 185; TOC >1.0%; low S_2 ~2.2; Tmax = 430°C. One sample from the Ringnes Formation has a low HI (50) despite its relatively high TOC content (almost 4.0 wt%) (Appendix II). It appears, therefore, that the Cape Richards and the Eden Bay Members in Grassy I-34 have an organic richness

which is very similar to that of the same members in the subsurface of the Hecla and Drake hydrocarbon fields (Appendix II), but quite different from the remainder of the northwest Melville region (i.e. Depot Island C-44, Marie Bay D-02 and Sandy Point L-46).

Both the Jameson Bay and Ringnes Formations are immature (Tmax between 429 and 433°C and Ro <0.55%) and have limited source potential (HI < 100). The Ringnes has higher TOC values than the Jameson Bay (3.5 - 6.5 vs <1.0 wt%): both have low S_2 values.

The Lower Cretaceous Deer Bay Formation is immature and has low source-rock potential (HI <100; TOC <3.0%), with the exception of a sample in Sandy Point L-46 (59. wt%) which is attributed to coal cavings from the overlying coal-bearing Isachsen Formation.

Palaeozoic

The Upper Palaeozoic (Permian) organic-rich interval in the Trold Fiord Formation is algal-rich and contains Botryococcus algae, has a TOC of 47.0 wt%, an HI of 305, a Tmax of 438°C and a high S_2 peak (143.0), thus having good potential for hydrocarbon generation. The upper 606 m of Permian strata in Depot Island C-44 are moderately to heavy bitumen-stained, the bitumen having a wispy form indicating possible migration paths of hydrocarbons.

The Lower Palaeozoic Ibbett Bay Formation is a poor source-rock (HI <65), despite its high TOC content (6.7 wt%) in a number of samples from the Marie Bay D-02 drillhole (Figure 9-31) (Appendix II).

Variation of reflectance with depth

The vitrinite reflectance of phytoclasts ranges from 0.45 to 0.65 Ro and follows a gentle gradient. Wispy bitumen-staining of low to moderate degree is also present. Bitumen appears below the sub-Cretaceous disconformity and is also present in the Devonian Ibbett Bay. Above the major regional unconformity between the Upper Devonian and Pennsylvanian, this bitumen occurs mainly in the sandy Canyon Fiord, Trold Fiord and Bjorne Formations and has reflectance values between 0.90 and 1.35%. Below the unconformity it reflects much higher (2.0 - 2.45% Ro, max) and shows a gradient parallel to that above the unconformity. The bitumen occurs in shaley matrix and in the form of elongated bodies enclosing pyrite grains while the extremely high-reflecting bitumen is associated with carbonate grains, shows angularity and reflectances between 3.0 and 3.65%. The high-reflecting appears below 2,460 m and is present only in the Ibbett Bay.

The unconformities throughout the Mesozoic are minor and do not affect the reflectance trend of either vitrinite or bitumen but the major unconformity at the boundary between the Ordovician to Devonian Ibbett Bay and the Carboniferous Canyon Fiord in Marie Bay D-02, Sandy Point L-46 and Depot Island C-44 is an erosional unconformity caused by the Ellesmerian Orogeny (Balkwill and Fox, 1982). The deep erosional event is clear from the presence of both vitrinite and bitumen above the unconformity and bitumen only below the unconformity i.e. the presence of vitrinite in the Permo-Carboniferous and bitumen only in Ordovician to Devonian strata of the Ibbett Bay Formation in Depot Island C-44 (Figure 9-4).

The use of bitumen in estimating the amount of eroded section

The magnitude of erosion involved can be estimated based on the % Ro versus depth profile recorded in Depot Island C-44 (Figure 9-4). Dow (1977) estimated the erosion by extrapolating the sub-unconformity maturation profile to the maturation level immediately above the unconformity. The assumption here is that the measured log-linear maturation gradient in the preserved section is representative of the maturation gradient in the eroded section. This may not be true because the % Ro increases faster in the post-unconformity section than in the pre-unconformity section in response to the new sediment load. As a result, the magnitude of the extrapolation (and, therefore, the estimated amount of erosion) is underestimated (Feinstein, 1985; Katz et al., 1988). The Depot Island C-44 drillhole (Figure 9-4) offers the opportunity to estimate the amount of erosion based on bitumen reflectance because vitrinite reflectance in the post-unconformity section is well established and also maturation characteristics of bitumen below and above the unconformity are available.

The low-reflecting primary bitumen in the Ibbett Bay Formation in Depot Island C-44 has an Ro, max of 2.0-2.2% which means that the equivalent Ro for vitrinite in the Ibbett Bay/Canyon Fiord contact would be 1.6% (using Jacob's formula of Rv = Rb x 0.618 + 0.4) (Jacob, 1983). The vitrinite in the Canyon Fiord has an Ro of 0.7% and the only primary bitumen present has an Ro of 1.3%, a difference of 0.6% Ro. If the relationship between vitrinite and bitumen in the post-unconformity section is similar to that in the pre-unconformity section, then the Ro equivalent of vitrinite in the Ibbett Bay would be approximately 1.5% (2.1 - 0.6), a value very close to that calculated by Jacob's formula.

The specific temperature under which a certain temperature level is attained is dependent on the effective heating time, i.e. the residence time in the range (15°C) of the maximum temperature (Hood et al., 1975). Although the control available on the

residence time near the maximum temperature and on the surface temperature involved is not great, it is known that sedimentation in the area did not cease until the Upper Devonian-Lower Carboniferous. Therefore, with an estimated maximum heating timespan of at least 20 Ma and an estimated vitrinite Ro max of 1.6%, a maximum paleotemperature of approximately 170-175°C is obtained using the method of Hood et al., (1975) and Bostick et al., (1978). Assuming that: 1) the average paleogradient geothermal was similar to the present-day geothermal gradient (~20°C/km), 2) the surface temperature was approximately 20°C, and 3) that the paleogeothermal gradients and rate of subsidence both above and below the unconformity were similar, then a corresponding amount of erosion of the order of approximately 7.0 km is estimated.

Stratigraphic and structural evidence (Harrison, pers. commun., 1989) indicates that a minimum of 6.2 and a maximum of 7.2 km were deposited above the Ibbett Bay and beneath the Canyon Fiord. The estimated section missing is calculated as follows: Blackley Formation (700 m), Cape de Bray Formation (900 m), Weatherall Formation (1,400 m), Hecla Bay Formation (1,200 m), Beverley Inlet Formation (500 m) and unknown Mississippian strata (1,500 m), for a total of 6.2 km ±1.0 km.

The gentle maturity gradients in all three drillholes examined in northwestern Melville Island (Depot Island C-44, Sandy Point L-46 and Marie Bay D-02) most likely indicates a relatively fast rate of sedimentation in the Mesozoic and temperatures of the order of 50-80°C. Reflectance at the surface (Isachsen Formation) is approximately 0.50% in Depot Island C-44 and Sandy Point L-46. Assuming that huminite (precursor of vitrinite) reflectance at the surface is 0.20%, a surface temperature of 20°C and an average geothermal gradient of 20°C/km, then the amount of section lost above the Isachsen is estimated at 2.0 km. This section includes the remaining of the Isachsen and Christopher Formations as well as possibly the Hassel and Kanguk Formations. The

upper range of the linear extrapolation (Dow's method) is difficult to justify based on geological evidence which indicates that approximately 1.0-1.2 km have been eroded due to the Eurekan Orogeny.

The % Ro versus depth profile recorded for the Lower Palaeozoic section in Depot Island C-44 reflects higher temperatures but not necessarily higher thermal gradients compared to the Upper Palaeozoic and Mesozoic sections. The similarity of the maturation gradients in the Mesozoic of Depot Island C-44 and Sandy Point L-46 suggests similar thermal conditions for the two drillholes during the time of the post-Ellesmerian maturation. In addition, bitumen reflectance in the pre-unconformity section suggests similar thermal conditions during the pre-Ellesmerian maturation for drillholes Depot Island C-44 and Marie Bay D-02. Although the data control on bitumen reflectance in the pre-unconformity section in Sandy Point L-46 is very limited, it appears that thermal conditions in the Sandy Point L-46 were not as pronounced as in the two other drillholes.

The vitrinite reflectance versus depth profiles for Marie Bay D-02 and Sandy Point L-46 (Figures 9-31 and 9-32) show a gentle maturity gradient increase for the Mesozoic, pointing to a fast sedimentation rate. Bitumen is present almost uniformly in these drillholes except in the top 200 - 1,200m. The bitumen is mainly found in an argillaceous matrix where it has a lower reflectance than when it occasionally occurs in a carbonate matrix. This relationship is similar to the relationship between the reflectance of vitrinite in argillaceous and carbonate matrix of sediments associated with coal-bearing strata (Bostick and Foster, 1975; Goodarzi et al., 1988).

Similarities between the maturity trends of vitrinite and bitumen observed in Figures 9-4 and 9-32 indicate that the formations above the major unconformity contain

mainly vitrinite and the Palaeozoic sediments contain only bitumen (Figure 9-4). There are often two generations of bitumen, a low-reflecting type which contains pyrite and coats the carbonate grains as a thin film and a higher-reflecting, de-asphalted bitumen which is angular and is present in vugs and intercrystalline porosity of carbonates.

There are certain differences between Permian samples from Sandy Point L-46 and other drillholes such as Drake K-79 and Chads Creek B-64. Both Drake K-79 and Chads Creek B-64 contain more terrestrial organic material, such as exinite and vitrinite, while the Sandy Point L-46 contain more marine organic material. The algal shale (Plate 10) present at 1240m in Sandy Point L-46 indicates an anaerobic terrestrial to lacustrine environment, having an excellent source-rock potential (Tissot and Welte, 1984).

9.2.3.4 SOUTHWEST SVERDRUP BASIN REGION

This field occurs between 108°-110° longitude and 76°30'-77° latitude. Two drillholes have been examined in detail, namely Roche Point J-43 and North Sabine H-49 (Figure 7-1). The phytoclast content in both drillholes is moderate and consists of higher-plant remains (coal) in the Jurassic Awingak and the Cretaceous Isachsen Formations, with a considerable input of marine-liptinite organic matter (Tasmanites, dinoflagellates and amorphous fluorescing matrix) in the Schei Point Group sediments. The samples in both drillholes are heavily bitumen-stained and thus a suppression of vitrinite reflectance is expected (Hutton, and Cook 1980; Price and Barker, 1985). A low-reflecting bitumen (0.20% Ro) is present in Roche Point J-43 (not shown in Figure 9-5). This bitumen does not show any increase in reflectance with depth and appears to represent the most recent product of hydrocarbon migration through the Jurassic and Cretaceous sediments.

In Roche Point J-43 all the organic-rich shales and siltstones below 700 metres

are in the mature stage of hydrocarbon generation (Figure 9-5). Parts of the Lower Jurassic Jameson Bay Formation are organic-rich and along with the Ringnes Formation bear a mixed exinitic/vitrinitic organic matter with occasional Botryococcus colonial algae. The majority of the samples in the above formations contain organic matter dominated by high land-plant remains (mainly spores). Roche Point J-43 is the only drillhole in Melville Island in which the Upper Jurassic-Lower Cretaceous Deer Bay Formation is mature.

The Cape Richards Member of the Hoyle Bay Formation in the Roche Point J-43 drillhole has an HI of 227, a TOC of <1.0 wt% and a low S_2 value (2.1). The Eden Bay Member has HI values ranging between 368 and 417, a Tmax of 441 °C: TOC values are higher than 3.0 wt% and S_2 varies from 13-20. The Cape Caledonia Member of the Murray Harbour Formation has an HI of 152, a Tmax of 442°C, the TOC is >1.0 wt%, but the S_2 is low (<2.0). The Tmax values (441-442°C) of the above Members indicate that they are in the mature stage of hydrocarbon generation, which is also evident from the relatively high Ro value (>1.0%) for the Schei Point Group in Roche Point J-43. The Cape Richards Member has a thickness of approximately 100m and the Eden Bay 150m. These are the only two areas in Melville Island (Roche Point J-43 and North Sabine H-49) in which hydrocarbons have been expelled from mature Schei Point source rocks. In addition, the Jameson Bay has HI values between 100-150, but a very low TOC (<1.0 wt%) with S_2 <1.0. One sample from the Ringnes shale has a very high TOC content (~9.0 wt%), a HI value of 178 and an S_2 of 15.7. Also, one sample from the Christopher shale has a high HI value (254), accompanied by a high TOC (7.5 wt%) and an S_2 of 19.0 (Appendix II).

The North Sabine H-49 drillhole (Figure 9-6) contains some of the most prolific organic-rich, marine shales and siltstones of the Schei Point Group which are within the mature stage of hydrocarbon generation. The Cape Richards and the Eden May

Members of the Hoyle Bay Formation are organic-rich (TOC >3.0 wt%), contain marine organic matter and have an Ro of 0.90 - 1.10%. Rock-Eval pyrolysis data demonstrate the richness of these source beds and the fact that they have generated and expelled hydrocarbons (Appendix II). In this drillhole, the Cape Richards Member has much lower HI values (126-162), low TOC (<1.0 wt%), low S_2 (<2.0) and Tmax values of 445-447°C. In addition, the Eden Bay Member has HI values of 216-242, a TOC of 3.8-4.0 wt%, S_2 values between 8.5 and 9.2 and a Tmax of 448°C (Appendix II). The Barrow Formation shales have low hydrocarbon potential, an HI of 142-152,a TOC generally <1.0 wt% and low S_2 values (<1.0). The Jameson Bay shales also have low TOC content (<1.0 wt%), HI values ranging from 98-191 and S_2 values that are also low (<2.0). One sample from the Ringnes shales has a high TOC content (6.4 wt%), a high HI value (224),a low OI (6), and an S_2 of almost 15.0. Finally, the Deer Bay shales have TOC values between 2.0-3.0 wt%, but their HI values are less than 100, the OI values are relatively high and the S_2 values are low (<2.0) (Appendix II).

Comparison of maturity and source-potential of sediments

When comparing the pyrolysis data from North Sabine H-49 with those from Roche Point J-43 and the other Drake, Hecla and northwestern Melville drillholes, it becomes apparent that:

1) there is a drastic decrease in the HI values of the Schei Point samples (mainly Cape Richards and Eden Bay), from the Hecla (HI 310-659), Drake fields (HI 129-682) and the northwest region (HI 421-620) towards the south-central Sverdrup region (HI 227-417) (Appendix II), indicating an increased maturity of sediments. HI values for the Cape Richards and Eden Bay change from the 500-650 range to <250 in North Sabine H-49. This decrease is also evident when comparing Roche Point

J-43 (227 for Cape Richards, 368-417 for Eden Bay) to North Sabine H-49 (126-162 for Cape Richards, 216-242 for Eden Bay).

2) The above strongly indicate that hydrocarbon generation has begun from the two formations and that the sudden decrease in HI value is due to hydrocarbon generation and expulsion. The high Tmax values, along with the high Ro values (1.25% for the Cape Caledonia and 1.0% for the Eden Bay), support the opinion that the two formations have already generated hydrocarbons. Oil would be the main hydrocarbon product expected when the Schei Point is mature (>0.7% Ro), as in North Sabine H-49 and Roche Point J-43. Gas and immature condensate would be the anticipated product where the Schei Point is marginally mature <0.7% but >0.5% Ro.

3) There is a rapid change in the Ro gradient in North Sabine H-49 at the top of the Schei Point Group. This increase may be attributed to overpressuring of the organic-rich Schei Point beds. Overpressuring can be generated by a) rapid loading (sedimentation); b) generation of oil and gas from organic matter; c) thermal expansion of fluids; and d) compression by tectonic forces (Hunt, 1979). When organic matter generates hydrocarbons as in North Sabine H-49, thermal conductivity decreases resulting in an increase of geothermal gradient which, in turn, causes a high maturation gradient. The change in gradient is most likely not related to the unconformity at the top of the Barrow Formation because the unconformity is only a minor one.

The main event which triggered hydrocarbon generation in the Schei Point source beds was the drastic increase in the rate of subsidence about 107 million years ago, during Albian times, which resulted in the deposition of the shales and siltstones of the Christopher Formation and which led to the maturation of the Cape Richards, Eden Bay and Cape Caledonia Members.

9.2.4 RELATIONSHIP BETWEEN OPTICAL PARAMETERS AND ROCK-EVAL

The changes in fluorescence properties of exinite macerals during coalification have been investigated (Teichmuller and Durand, 1983). Cutinite shows some variations in fluorescence properties, even at the same or similar coal rank, whereas resinite is characterized by broad variations of fluorescence properties even in one and the same coal. As a result, resinite fluorescence properties should be used with extreme caution for maturity estimations (Teichmuller and Durand, 1983).

The sedimentary succession of Melville Island offers the opportunity to compare vitrinite reflectance (% Ro) and fluorescence properties of liptinite and exinite macerals in numerous drillholes. The variation of % Ro with λmax and R/G Q for Botryococcus and Tasmanites algae as well as dinoflagellates, sporinite, cutinite and resinite is shown in Figures 9-38 and 9-39 and Table 3. The fluorescence properties of all types of organic matter increase with increasing vitrinite reflectance, with groups of materials following different trends. Liptinitic organic matter of marine origin (e.g. Tasmanites, dinoflagellates and fluorescing matrix) shows a slower rise in both λmax and Q with increasing reflectance (steeper curves) in the 0.6 - 0.8% Ro range, while the other types show a faster rate of increase with rank (flatter curves). Sporinite and cutinite (terrestrially-derived organic matter) span the entire range for λmax and follow a trend similar to Botryococcus algae in the Q vs %Ro graph. The increase in both λmax and Q is connected to the formation and expulsion of 'petroleum-like' products of Teichmuller (1974,1982) from the marine liptinites. In contrast to most exinites of herbaceous origin, fluorescing matrix (matrix bituminite) behaves in a similar fashion to marine liptinite by showing a slower rate of increase with reflectance (Figures 9-38 and 9-39). This is in general agreement with the observations of Teichmuller and Durand (1983) who showed that the λmax of fluorescing huminite/vitrinite increased at a fast

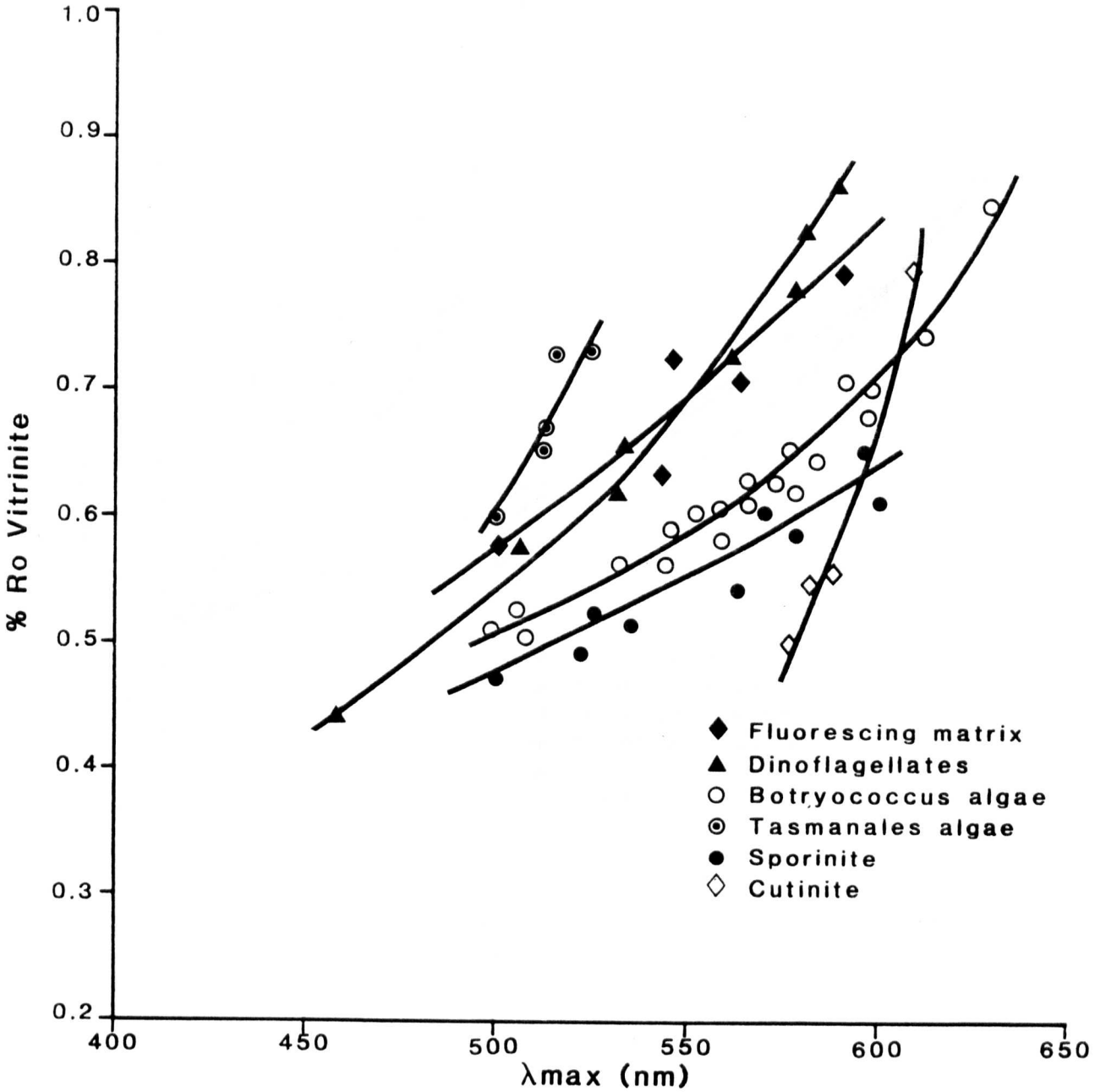

Figure 9-38 Variation of λmax of exinite with vitrinite reflectance

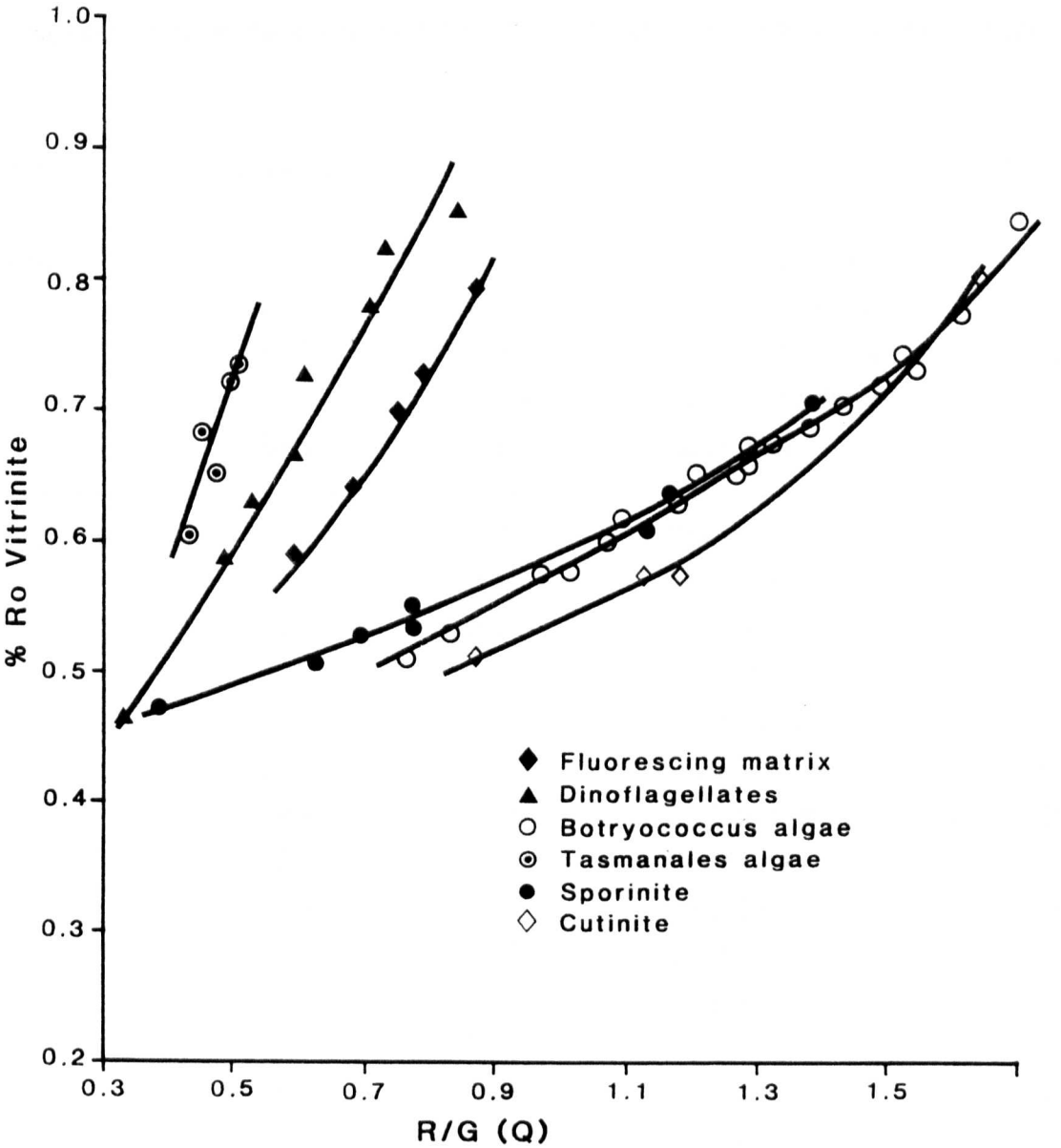

Figure 9-39 Variation of R/G Quotient of exinite with vitrinite reflectance

TABLE 3

Spectral fluorescence parameters of macerals in the Melville Island drillholes

Maceral	λmax (nm)	R/G Q	Formation/Mbr.	% Ro, vit.
Tasmanites	500	0.42	Cape Richards	0.59
	510	0.48	Cape Richards	0.65
	510	0.45	Cape Caledonia	0.67
	515	0.50	Cape Caledonia	0.72
	525	0.51	Eden Bay	0.73
Botryococcus	500	0.77	Christopher	0.49
	510	0.75	Christopher	0.50
	510	0.87	Christopher	0.52
	530	0.98	Christopher	0.55
	540	0.96	Christopher	0.55
	560	1.05	Christopher	0.57
	545	1.08	Christopher	0.58
	550	1.10	Deer Bay	0.59
	555	1.12	Deer Bay	0.59
	565	1.10	Deer Bay	0.59
	575	1.18	Deer Bay	0.60
	570	1.17	Deer Bay	0.61
	565	1.20	Deer Bay	0.62
	580	1.30	Jameson Bay	0.63
	575	1.38	Jameson Bay	0.64
	590	1.42	Jameson Bay	0.66
	585	1.47	Jameson Bay	0.67
	600	1.50	Jameson Bay	0.69
	585	1.53	Jameson Bay	0.70
	615	1.60	Jameson Bay	0.73
	630	1.65	Jameson Bay	0.84

TABLE 3 (continued)

Maceral	λmax (nm)	R/G Q	Formation/Mbr.	% Ro, vit.
Dinoflagellates	460	0.34	Christopher	0.44
	510	0.49	Ringnes	0.57
	530	0.53	Ringnes	0.60
	535	0.60	Ringnes	0.63
	560	0.61	Eden Bay	0.71
	575	0.70	Eden Bay	0.76
	580	0.73	Jameson Bay	0.82
	585	0.83	Jameson Bay	0.85
Sporinite	500	0.39	Christopher	0.46
	525	0.62	Christopher	0.48
	535	0.70	Christopher	0.50
	525	0.76	Deer Bay	0.52
	560	0.76	Deer Bay	0.53
	575	1.12	Deer Bay	0.57
	565	1.15	Jameson Bay	0.59
	595	1.27	Jameson Bay	0.60
	590	1.40	Jameson Bay	0.64
Cutinite	575	0.87	Christopher	0.48
	580	1.17	Christopher	0.53
	585	1.13	Christopher	0.54
	610	1.60	Jameson Bay	0.78
Fluorescing matrix	500	0.60	Jameson Bay	0.57
	540	0.68	Jameson Bay	0.62
	560	0.74	Deer Bay	0.70
	545	0.80	Deer Bay	0.72
	580	0.87	Jameson Bay	0.78

rate up to an Ro of 0.5%, then it flattened showing a slow rate of increase up to 1.1% Ro. Almost all the curves are 'concave up', that is the trend is for a decreasing rate of fluorescence property change with increasing rank. These correlations are strong and indicate that there is rather little scatter in the %Ro (or the fluorescence) and allow one to conclude that the measured %Ro values are correct, that is, not affected by oxidation or suppression or other unknown factors. Therefore, it appears that the %Ro is the independent parameter and the Tmax data are scattered in response to oxidation, bitumen staining, organic matter type differences, contamination, etc. In addition, Rock-Eval is a bulk analysis (i.e. the whole organic fraction is characterized), whereas reflectance is done on carefully-selected organic particles, and thus not as susceptible to variation other than thermal stress.

Figure 9-40 shows a plot of Tmax values against vitrinite reflectance for all samples irrespective of lithology. The Tmax increases gradually with increasing Ro from <400°C in the diagenetic stage (<0.5% Ro) to approximately 450°C in the mature stage of hydrocarbon generation (~1.0% Ro). Figure 9-40 is a modification of a graph by Teichmuller and Durand (1983) who stated that a fairly linear correlation exists between Tmax of 425°C-475°C (0.5-1.5% Ro), but before and after these values Tmax increases more quickly than Ro. Figure 9-36, mentioned previously in section 9.2.2, shows the correlation between vitrinite reflectance and Tmax obtained from marine, non-marine shales and siltstones, sandstones and coals. Due to the wide scatter of Tmax values at any given maturation level (Figure 9-36), Tmax must be interpreted in terms of trends rather than absolute values. Tmax and Ro correlate reasonably well in marine sediments, but may not correlate to a satisfactory degree in non-marine sediments. Espitalie et al., (1985) state that terrestrial organic matter of plant origin (i.e. vitrinite) has a more complex chemical structure than other types of organic matter of plant origin (i.e. spores, pollen, cuticles, resins) and a wider temperature range for Tmax is observed

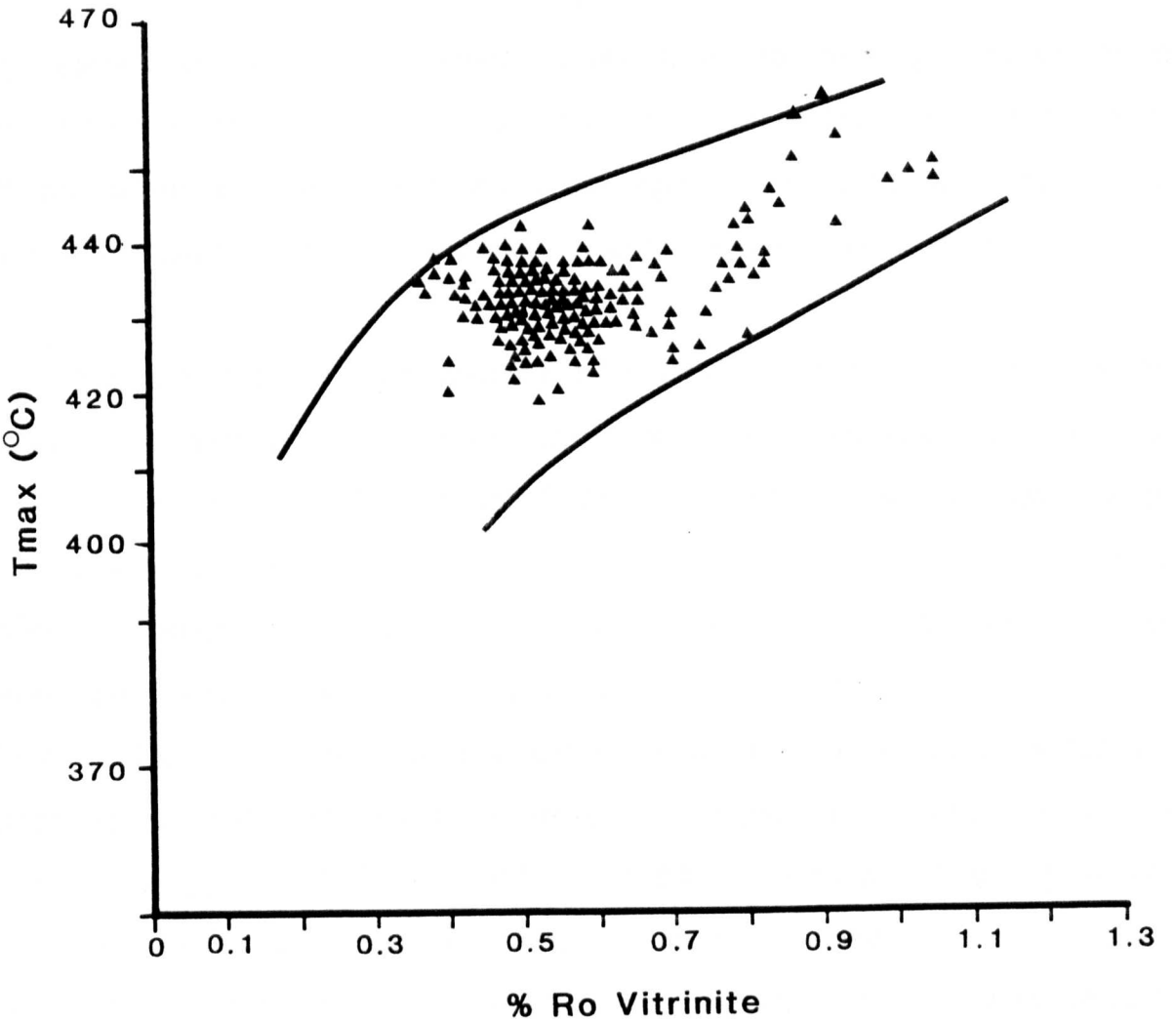

Figure 9-40 Relationship between vitrinite reflectance and Tmax for all samples

during thermal cracking. This observation is also true when relating Tmax and Ro for the non-marine Sverdrup Basin samples (Figure 9-36). In addition, Ro is measured on vitrinite only whereas Tmax is measured on the organic matter of the whole rock, thus it is influenced by organic-matter composition (Teichmuller and Durand, 1983).

Figure 9-41 shows the relationship between vitrinite reflectance, Tmax, S_1 and S_2 peaks for the Melville Island samples, superimposed on a coal-data graph taken from Teichmuller and Durand (1983). Previous Rock-Eval pyrolysis studies on coals covering a large range in rank (Teichmuller and Durand, 1983) show a very clear correlation between coalification (Ro) and S_2 (Figure 9-43). S_2 maximum values (up to 150) occur between 0.5-0.7% Ro and 425-435°C Tmax and they decrease to a minimum of <25 at an Ro level of 0.9-1.0%. Such a decrease in S_2, which corresponds to hydrocarbon generation during maturation, has been observed in organic-rich sediments other than coals (Espitalie et al., 1977; Tissot and Welte, 1984). The present data (Figure 9-41) indicate that there is a small variation in the maturity of the sediments. A decrease of S_2, with increasing Tmax and Ro, is not clearly evident due to the narrow range of the level of thermal maturity. Samples from mature areas (North Sabine H-49), which have generated hydrocarbons, show such a decrease in S_2 with increasing Tmax and Ro (Figure 9-41).

The relationship between reflectance and the S_2 peak for organic matter in different lithologies (i.e. marine and non-marine shales and siltstones and sandstones) is shown in Figure 9-42. S_2 values decrease with increasing maturity for marine sediments, a trend expected because of depletion of hydrocarbon-generating potential of these sediments at 0.6% Ro. As a result, the low S_2 values beyond 0.60% Ro level are believed to have been caused by hydrocarbon generation and expulsion. The wide range of S_2 values (1-110) in the 0.5-0.6% Ro range is merely an indication of

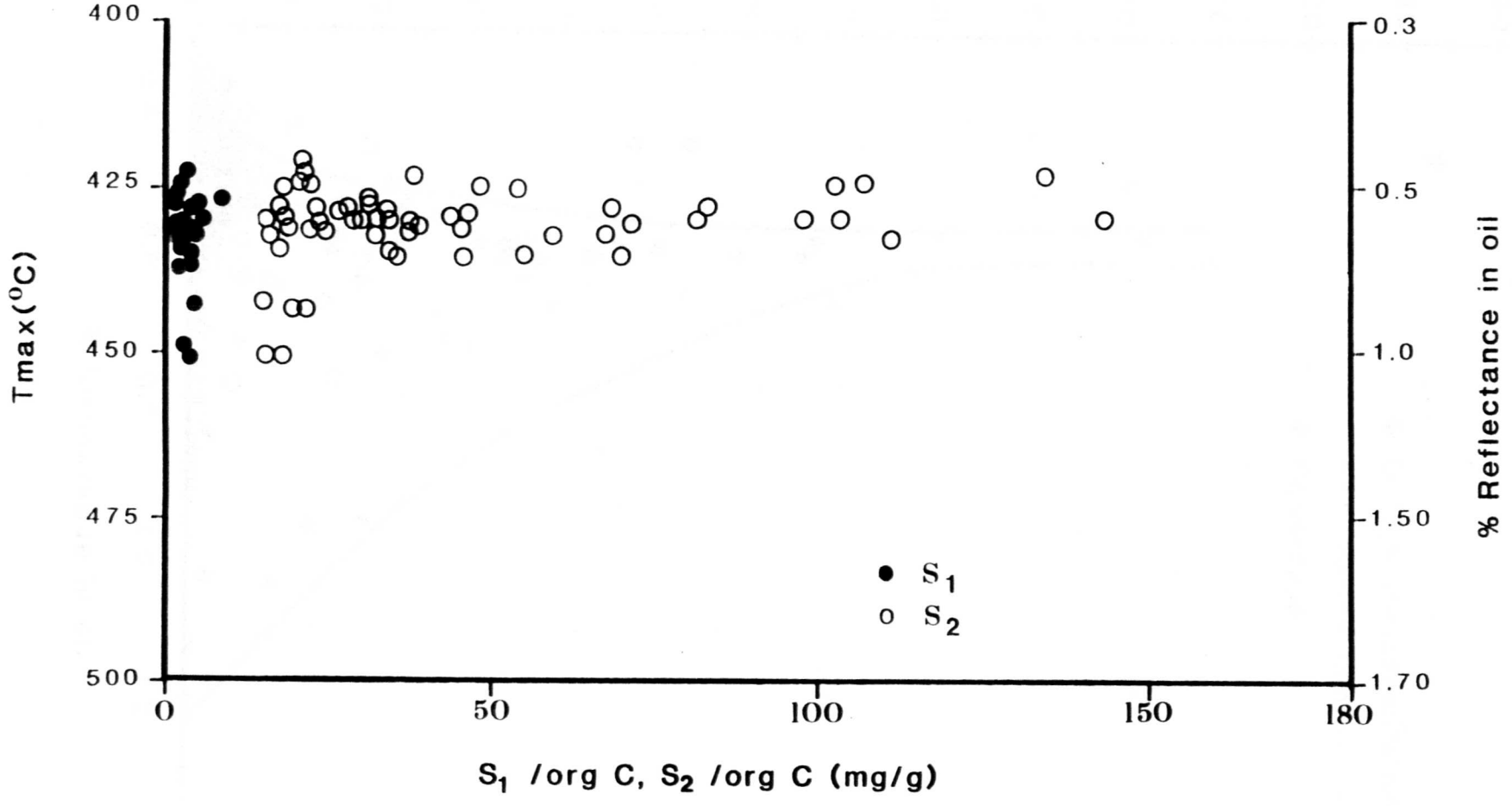

Figure 9-41 Relationship among vitrinite reflectance, Tmax, S_1 and S_2

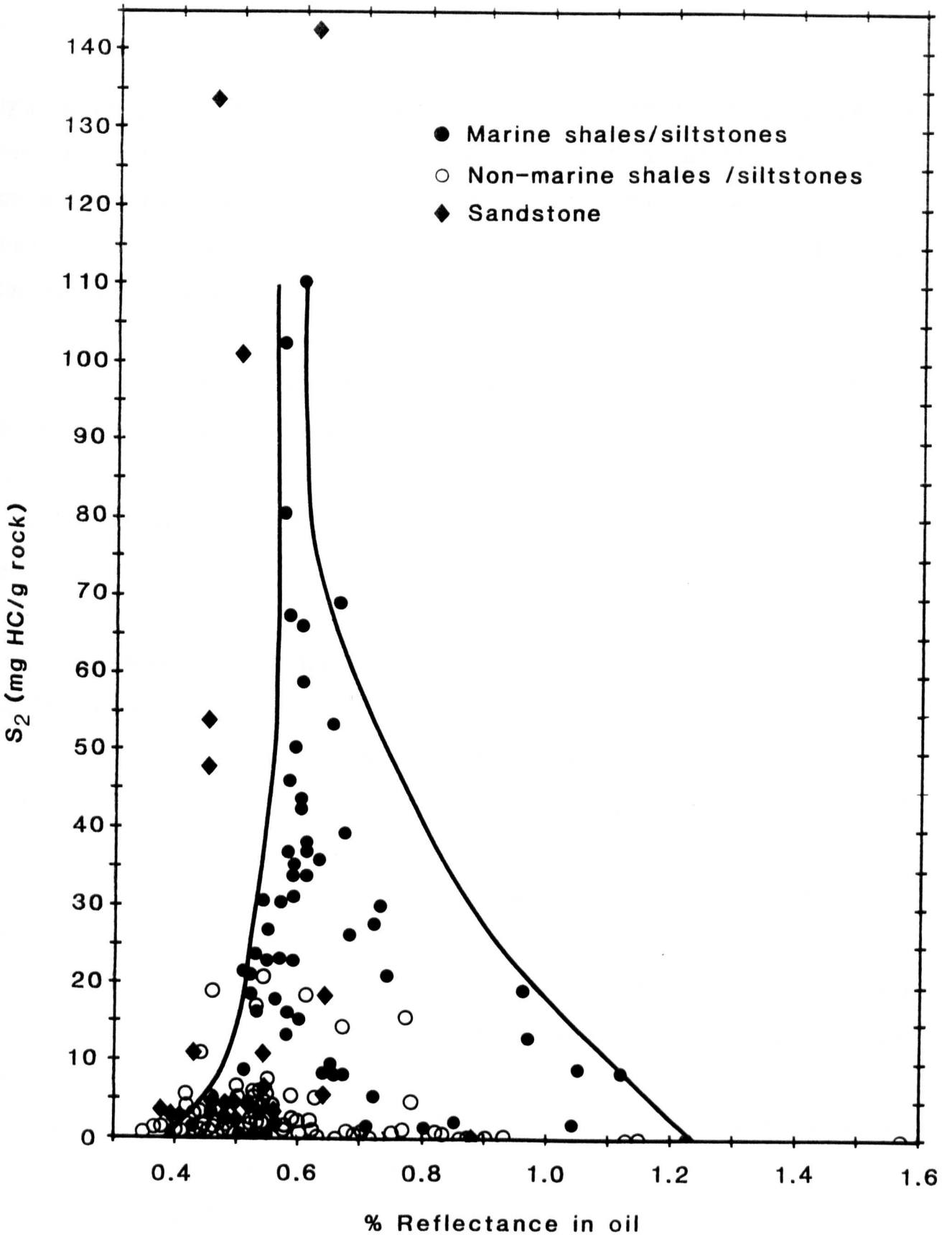

Figure 9-42 Relationship between S_2 and vitrinite reflectance

hydrocarbon-generating potential of some Schei Point sediments. An S_2 of over 10 represents a good source-rock potential (Table 1). The S_2 values of the non-marine formations range between 1 and 22 and there is no noticeable trend with Ro. Organic matter in sandstones has an S_2 range of 1 to 143 and there appears to be a slight decrease with increasing maturity (Figure 9-42).

The production index (PI) increases with increasing maturity in both the marine and non-marine shales and siltstones (Figure 9-43), although the trend is clearer among the marine samples. There is no apparent trend for the sandstone samples. Production index values above 0.4 are believed to be due to migrated oil (Peters, 1986) and, as a result, are not reliable.

9.2.5 REGIONAL THERMAL MATURITY

INTRODUCTION

An attempt has been made to evaluate the regional variation in organic-matter quality of sediments with potential for generation of hydrocarbons. As discussed previously, the Schei Point Group and other formations (Jameson Bay, Ringnes and Deer Bay) fall within this category. For this reason a series of isoreflectance and structural contour maps for the most prolific source rocks in Melville Island has been constructed. Source potential is also related to changes in organic facies and depositional environment. Therefore, contour maps showing the regional variation of the hydrogen index (HI) and the S_2 peak of Schei Point source rocks have also been constructed. Finally, a series of structural cross-sections showing isoreflectance lines superimposed on lithostratigraphic units will be discussed.

9.2.5.1 ISOREFLECTANCE MAPS

Isoreflectance maps were constructed for the following lithostratigraphic

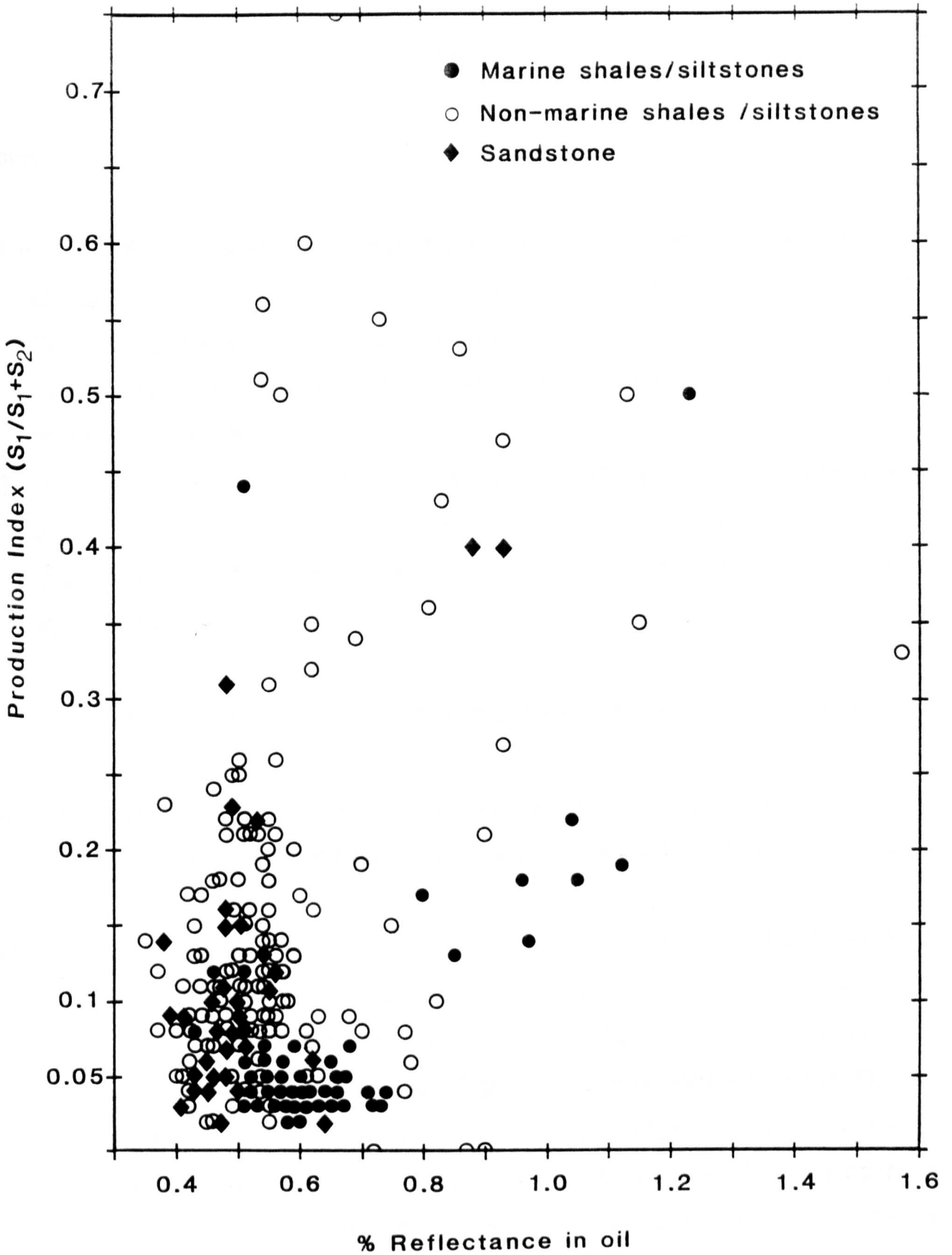

Figure 9-43 Relationship between production index (PI) and vitrinite reflectance

boundaries:

1) the top of the Barrow Formation (Figure 9-44), which is also the top of the Schei Point Group (isoreflectance contour maps of other potential Schei Point source rocks i.e. Cape Caledonia, Eden Bay and Cape Richards Members) were not constructed because not all drillholes penetrating Mesozoic strata in Melville Island encountered all the above members, and
2) the base of the Jurassic Jameson Bay Formation (Figure 9-44), the base of the Jurassic Ringnes Formation (Figure 9-44), the base of the Jurassic-Cretaceous Deer Bay Formation (Figure 9-44), and the base of the Cretaceous Isachsen Formation (Figure 9-44).

The main features of the isoreflectance maps of the Mesozoic formations are:

1) an increase in reflectance from approximately 0.4-0.5% near the Sverdrup Basin margin for all lithostratigraphic units to approximately 1.0% towards the basin centre, and
2) a reflectance increase that is greater for the older formations than for the younger formations. For example, the top of the Triassic Barrow Formation changes from an Ro of approximately 0.55% near the basin edge in the Sabine Peninsula to almost 1.0% north of the Sabine Peninsula (Figure 9-44), a difference of 0.45% Ro. In contrast, the Ro of the Cretaceous Isachsen Formation changes from approximately 0.35% near the basin edge in the Sabine Peninsula to almost 0.65% in the northern part of the Sabine Peninsula (Figure 9-44), a difference of only 0.3% Ro. The Ro variation for the Jameson Bay Formation over the same area is from 0.50% at the basin margin to 0.90% near the basin centre (Figure 9-44) a difference of 0.4%. For the Ringnes Formation the variation is from 0.50% to 0.75% (Figure 9-44) (a

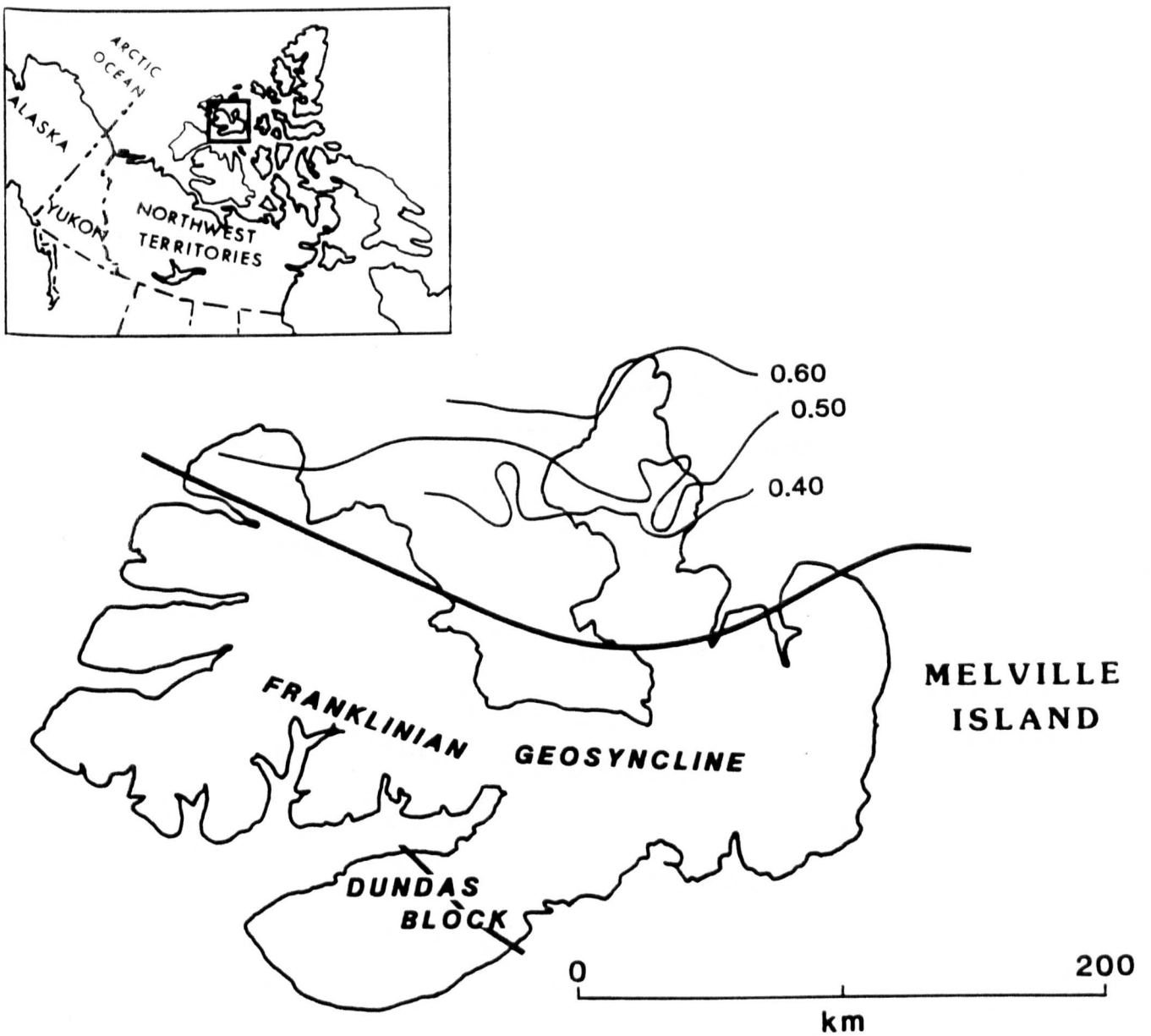

Figure 9-44 Isoreflectance contour map (% Ro) of selected Mesozoic formations
a) Isachsen Formation

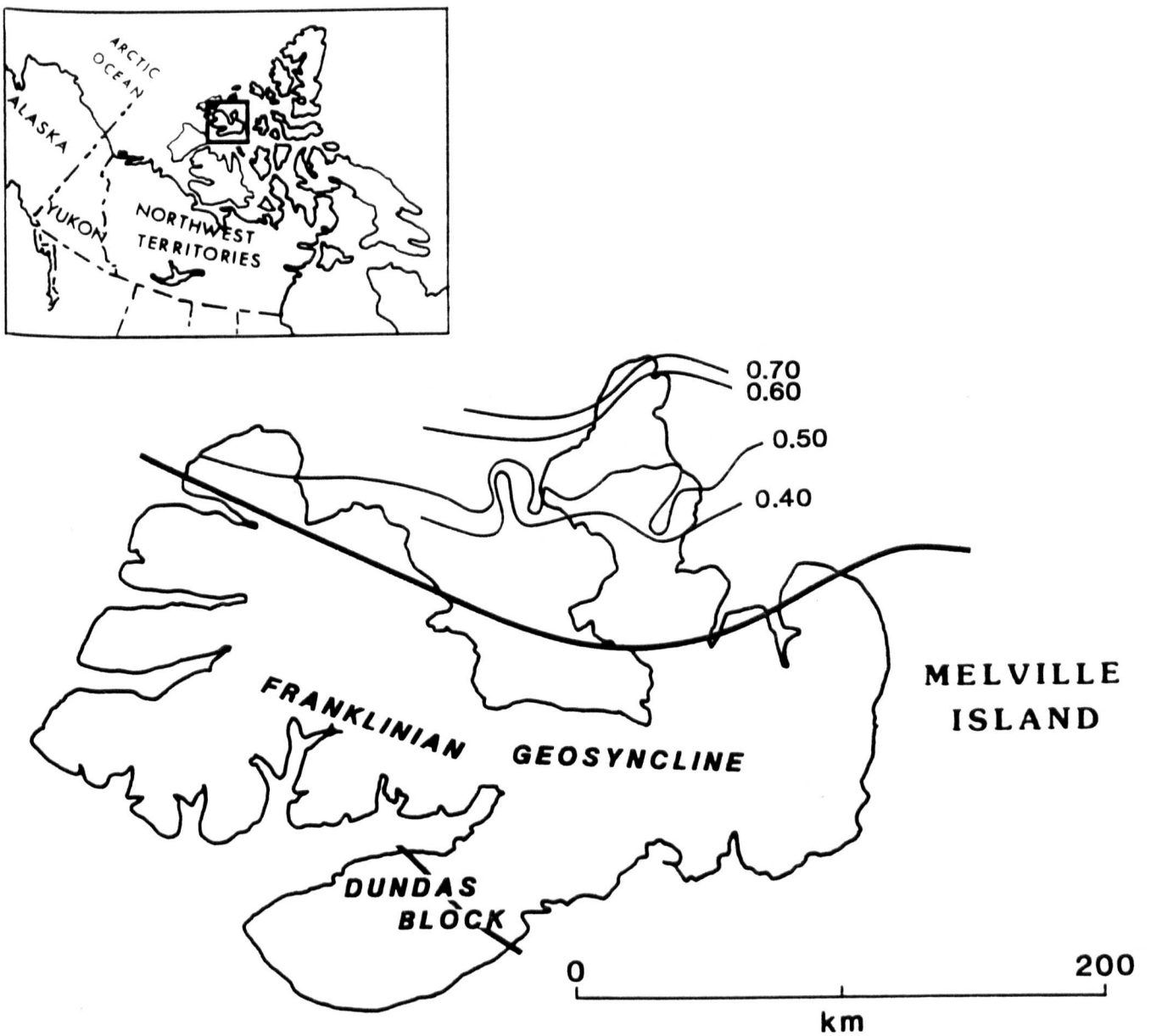

b) Deer Bay Formation

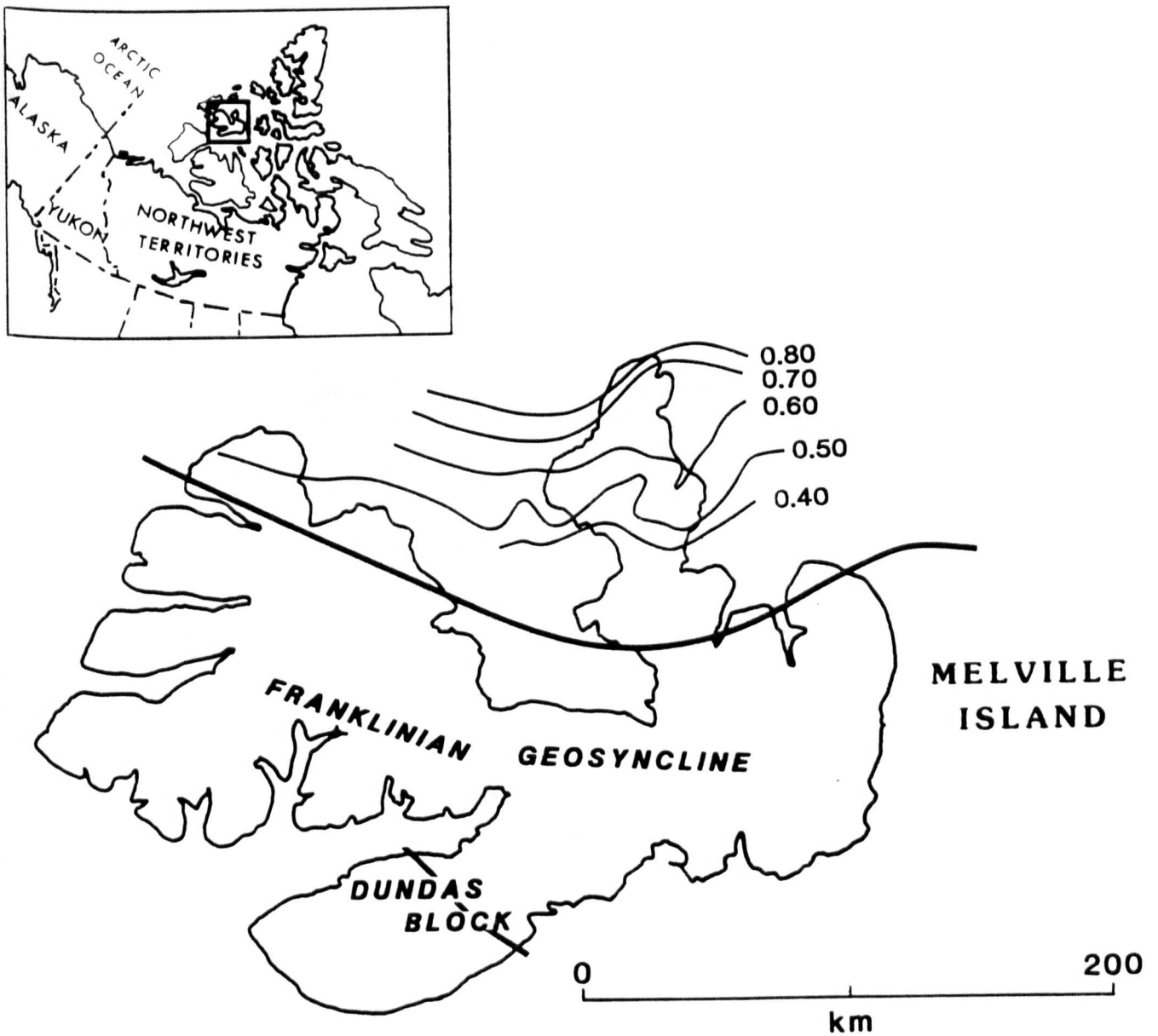

c) Ringnes Formation

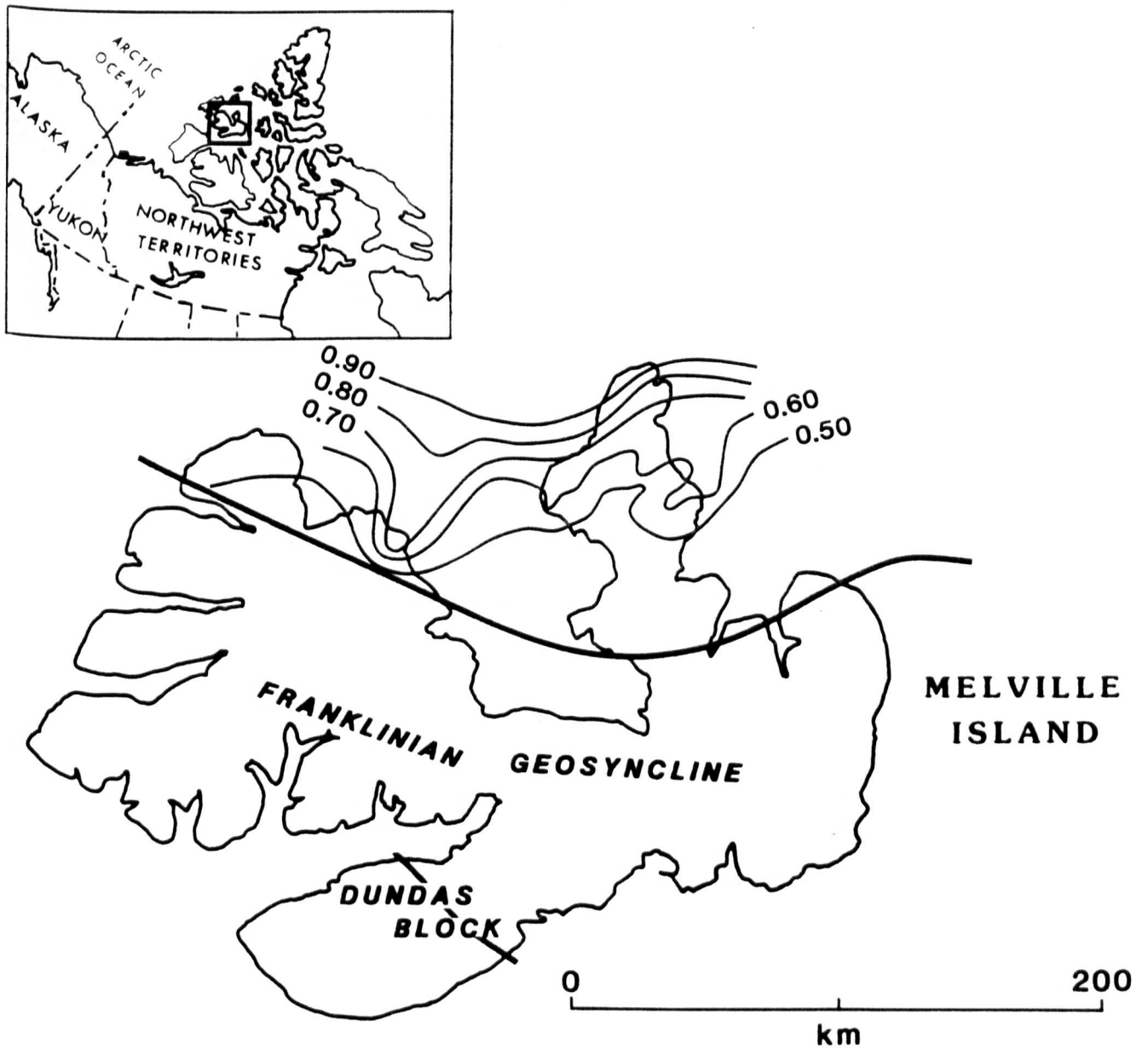

d) Jameson Bay Formation

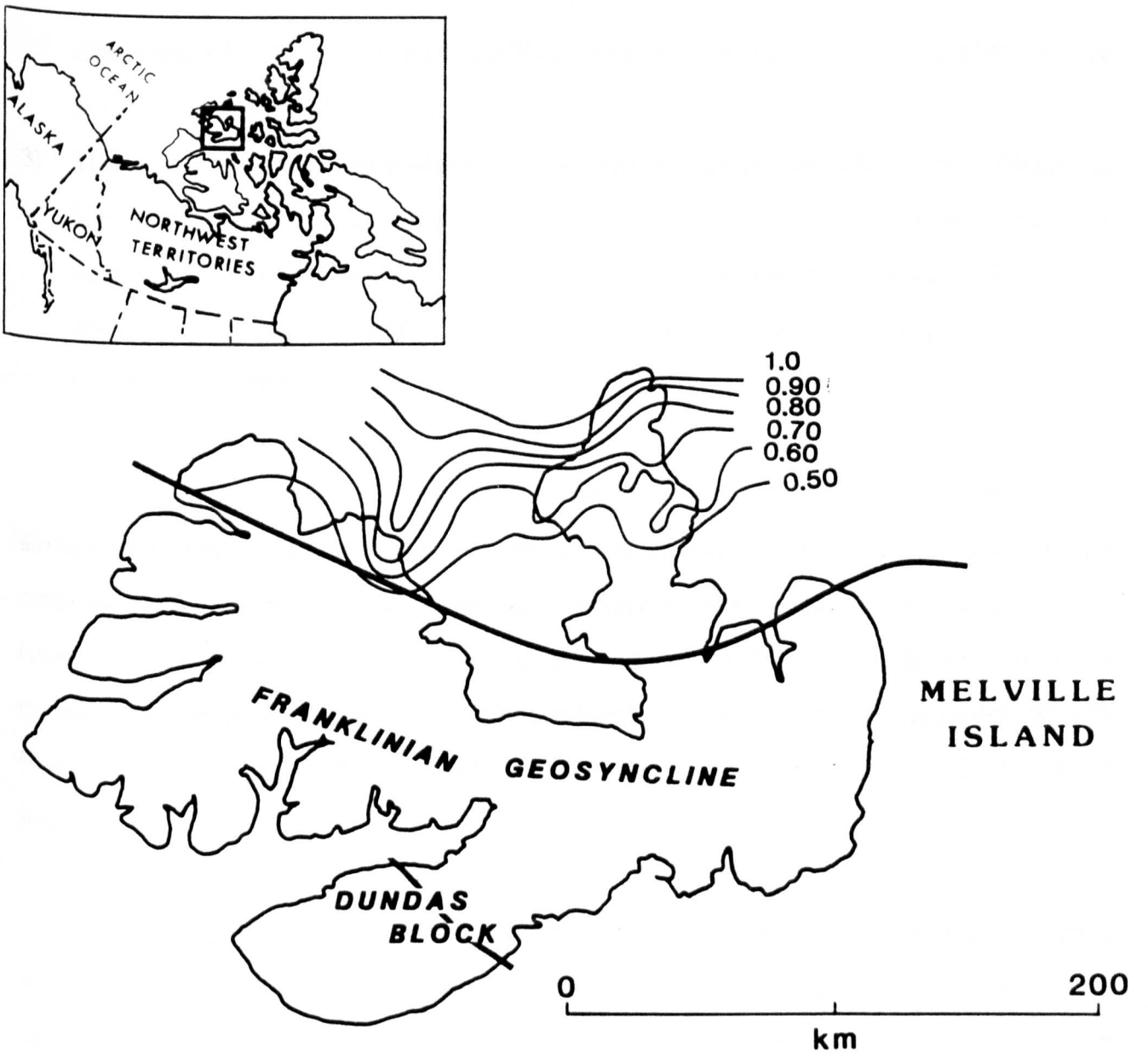

e) Barrow Formation

difference of 0.25%), for the Deer Bay Formation is from 0.45% to 0.65% (Figure 9-44) (a difference of 0.2%).

3) There is a strong parallelism in the isoreflectance trends of the Mesozoic formations. In particular, there is an obvious similarity between the isoreflectance contour maps of the Barrow and the Jameson Bay Formations (Figure 9-44), as well as among the isoreflectance contour maps of the Ringnes, Deer Bay and Isachsen Formations (Figure 9-44).

The isoreflectance maps of the Barrow and Jameson Bay Formations are very similar and show a curvature of the lines in the vicinity of the Kitson River C-71, the offshore Hecla hydrocarbon field and southeastern Sabine Peninsula. The isoreflectance maps of the Ringnes, Deer Bay and Isachsen Formations also show the curvature of the contour lines in the offshore Hecla field and in the southeastern Sabine Peninsula but the above three formations are absent in the Kitson River C-71 (Figure 9-44).

Figure 9-44 indicates that it is most likely the depth of burial that is mainly responsible for the maturity of these sediments, providing it coincides with maximum temperatures. This observation is in agreement with geological observations (Harrison pers. commun., 1989) which shows that <100 m of Cretaceous and younger sediments were deposited near the basin margin and >1.0 km towards the basin centre north of the Sabine Peninsula.

Not all isoreflectance contour maps follow the same trend. For example, isoreflectance maps of the Barrow and Jameson Bay Formations are very similar and show a curvature in the contour lines near the vicinity of Kitson River C-71 (Figure 9-44), which is probably due to the presence of >500 m of carbonates. Carbonates have a

higher thermal conductivity than shales (Pitt, 1986) and have the ability to transmit the heat to overlying strata (Figure 9-9). These strata, therefore, have a higher thermal maturity in this location which causes the curvature of the contour lines. In contrast, the curvature of the contour lines for the offshore Hecla drillholes appears to be due to the amount of eroded section and not due to thermal conductivity.

9.2.5.2 STRUCTURAL CONTOUR MAPS

Structural contour maps were prepared for the same lithostratigraphic boundaries and compared with the isoreflectance maps.

The structural contour map of the top of the Barrow Formation (Figure 9-45) shows an increase of burial depth from approximately 1,200 m in the southern part of the Sabine Peninsula and <500 m in northwestern Melville Island to almost 3,200 m in North Sabine H-49 (Table 4). The base of the Jameson Bay is encountered at approximately 1,200 m in the southern Sabine Peninsula and 3,000 m in North Sabine H-49 (Figure 9-45). For the base of the Ringnes the depths are 1,060 m and 2,620 m respectively (Figure 9-45) for the Deer Bay 1,020 m and 2,330 m (Figure 9-45), and for the Isachsen 1,000 m and 2,060 m (Figure 9-45) (Table 4).

The structural contour map for all formations (Figure 9-45) indicates an increase in overburden and burial depth, similar to the isoreflectance map. The formations follow an almost similar trend, indicating that the burial depth increases from basin margin to basin centre.

For the Mesozoic formations, areas of deep burial coincide with areas of high reflectance (Figures 9-5 and 9-6). The isopach and isoreflectance contour maps show

TABLE 4

Depth relative to datum (sea level) and Vitrinite Reflectance at the base of selected Mesozoic Formations

	Base of Isachsen Fm		Base of Deer Bay Fm		Base of Ringnes Fm		Base of Jameson Bay Fm		Base of Barrow Fm	
Drillhole	Drilled Depth (m)	(Ro)	Drilled Depth (m)	(Ro)	Drilled Depth (m)	(Ro)	Drilled Depth (m)	(Ro)	Drilled Depth (m)	(Ro)
H-49	2000	0.53	2270	0.58	2560	0.63	2950	0.78	3130	0.86
J-43	1403	0.63	1533	0.68	1943	0.77	2273	0.85	2463	0.95
P-40	560	0.48	-	0.48	840	0.50	950	0.52	1020	0.53
I-55	655	0.50	-	(0.50)	945	0.56	1085	0.60	1125	0.61
D-73	722	0.54	752	0.55	988	0.58	1128	0.60	1178	0.62
B-44	670	0.50	-	(0.50)	975	0.56	1110	0.61	1170	0.52
F-76	580	0.42	610	0.44	880	0.50	1040	0.54	1110	0.56
K-33	970	0.53	990	0.53	1370	0.60	1580	0.66	1690	0.69
F-16	580	0.47	-	0.48	920	0.52	1090	0.54	1170	0.56
K-79	658	0.55	748	0.58	1048	0.57	1228	0.60	1338	0.62
C-32	480	0.48	520	0.50	890	0.55	1060	0.59	1120	0.60
F-62	380	0.48	450	0.50	800	0.55	960	0.59	1010	0.62
I-69	550	0.46	610	0.48	1040	0.56	1230	0.60	1260	0.63
C-05	460	0.44	500	0.45	900	0.51	1090	0.55	1160	0.55
N-52	310	0.46	330	0.47	660	0.50	820	0.54	880	0.56
P-62	270	0.42	280	0.43	670	0.50	840	0.55	910	0.55
M-25	365	(0.35)	425	(0.36)	815	0.47	1015	0.54	1105	0.57
C-58	545	0.49	-	(0.49)	845	0.54	1025	0.55	(1145)	0.55
D-68	496	0.47	576	0.49	896	0.51	1076	0.53	1126	0.54
L-67	580	0.51	620	0.51	950	0.53	1130	0.56	1180	0.57
B-64	700	0.52	710	0.54	1050	0.55	1230	0.58	1310	0.60
J-60	525	0.47	545	0.48	925	0.55	1085	0.58	1125	0.60
K-71	1000	0.53	1020	0.54	1350	0.55	1490	0.55	1550	0.56
F-34	780	0.40	-	(0.40)	1070	0.45	1180	0.50	(1220)	0.50
C-44	43	0.50	173	0.50	313	0.50	593	0.50	(623)	0.50
I-34	-	-	365	0.50	505	0.50	785	0.60	835	0.62
E-78	680	0.48	-	0.49	940	0.52	1110	0.55	1190	0.59
F-14	720	0.53	-	(0.53)	(1010)	(0.56)	1130	0.58	(1140)	(0.59)

TABLE 4 (continued)

C-71	-	-	-	-	-	-	76	0.72	(86)	0.75
L-46	50	0.50	-	(0.50)	-	0.50	675	0.53	735	0.53
D-02	-	-	-	-	-	0.46	263	0.49	(273)	(0.50)

( ) estimated Ro

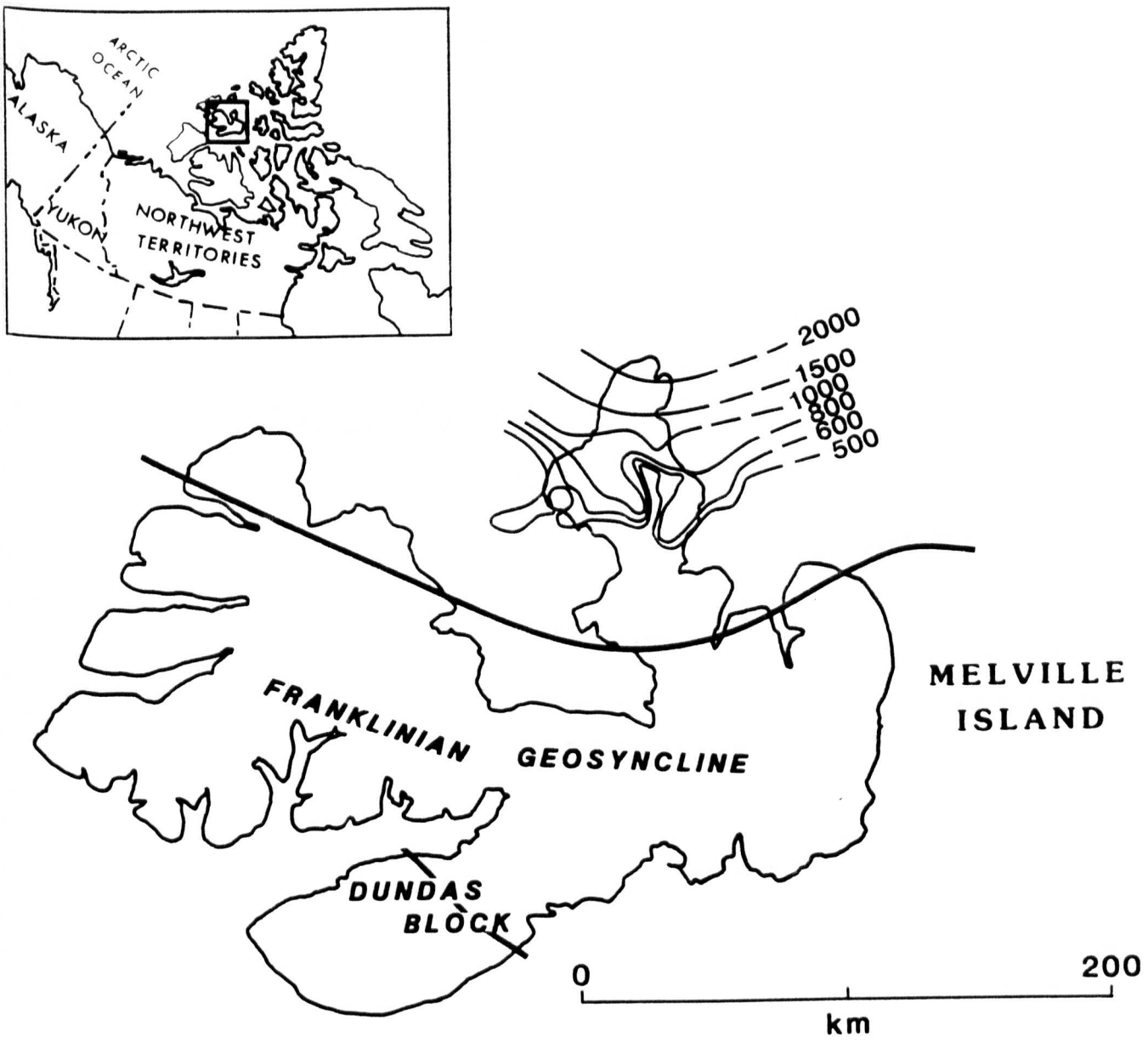

Figure 9-45 Structural contour map (m) of selected Mesozoic formations
a) Isachsen Formation

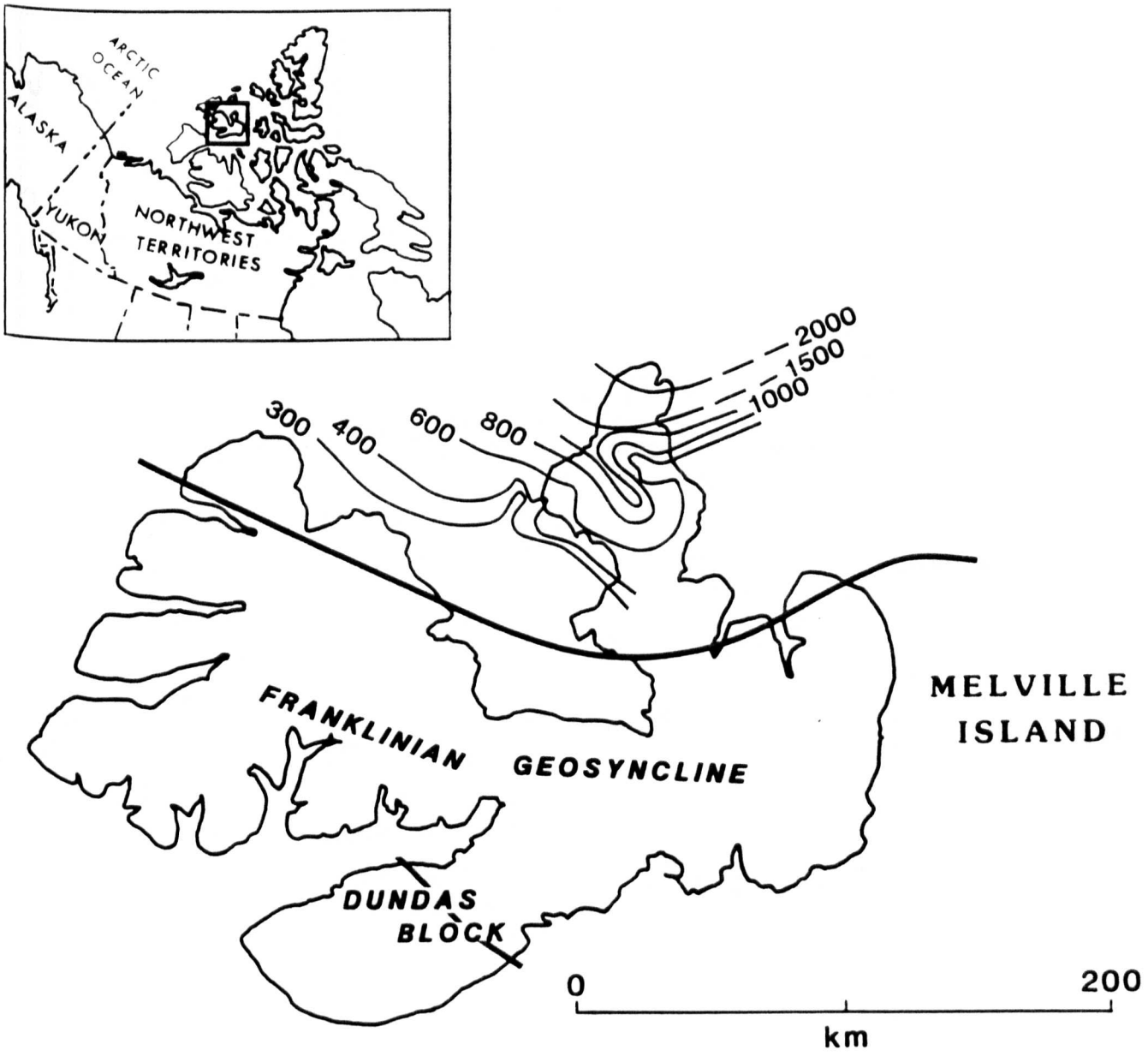

b) Deer Bay Formation

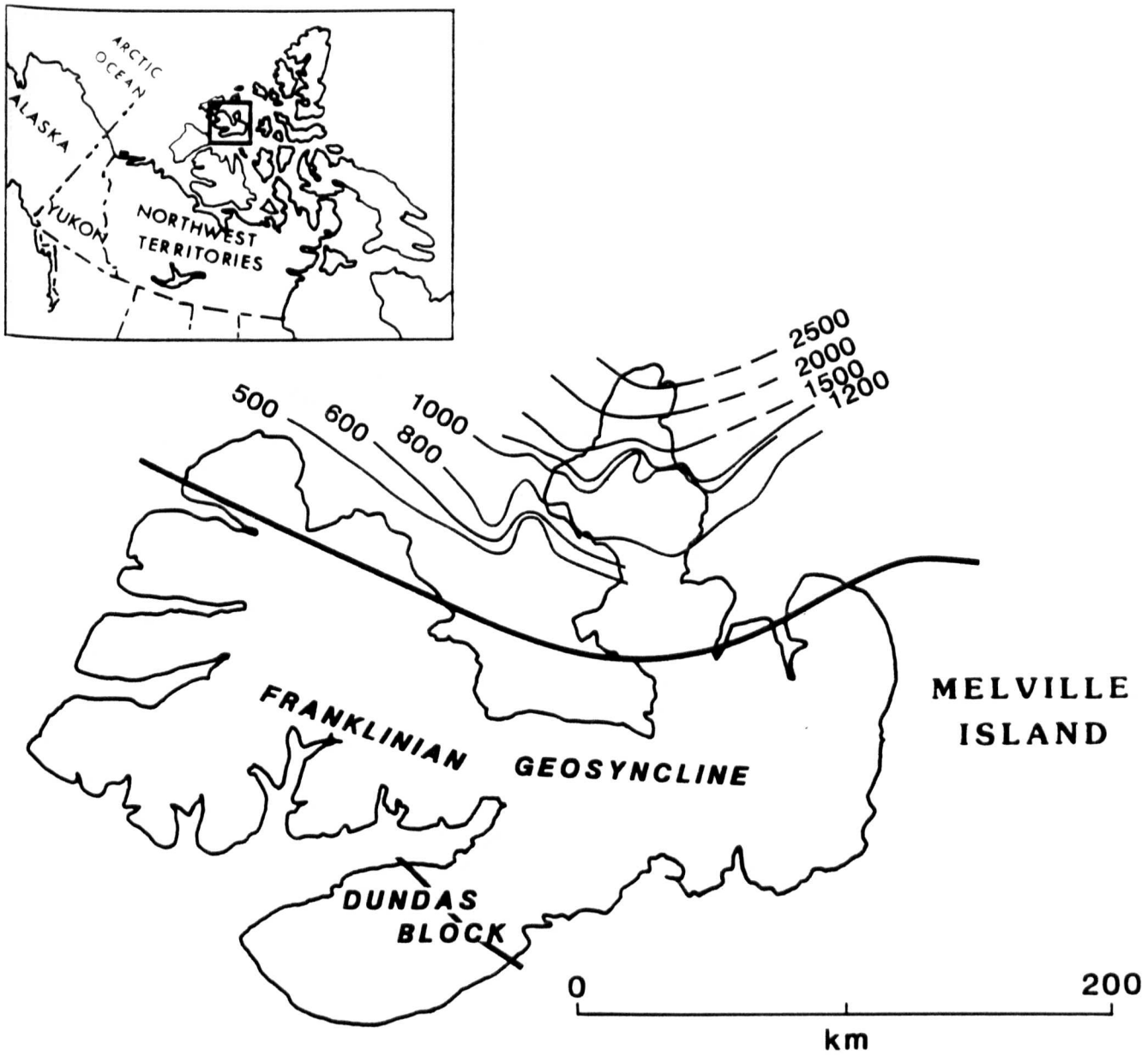

c) Ringnes Formation

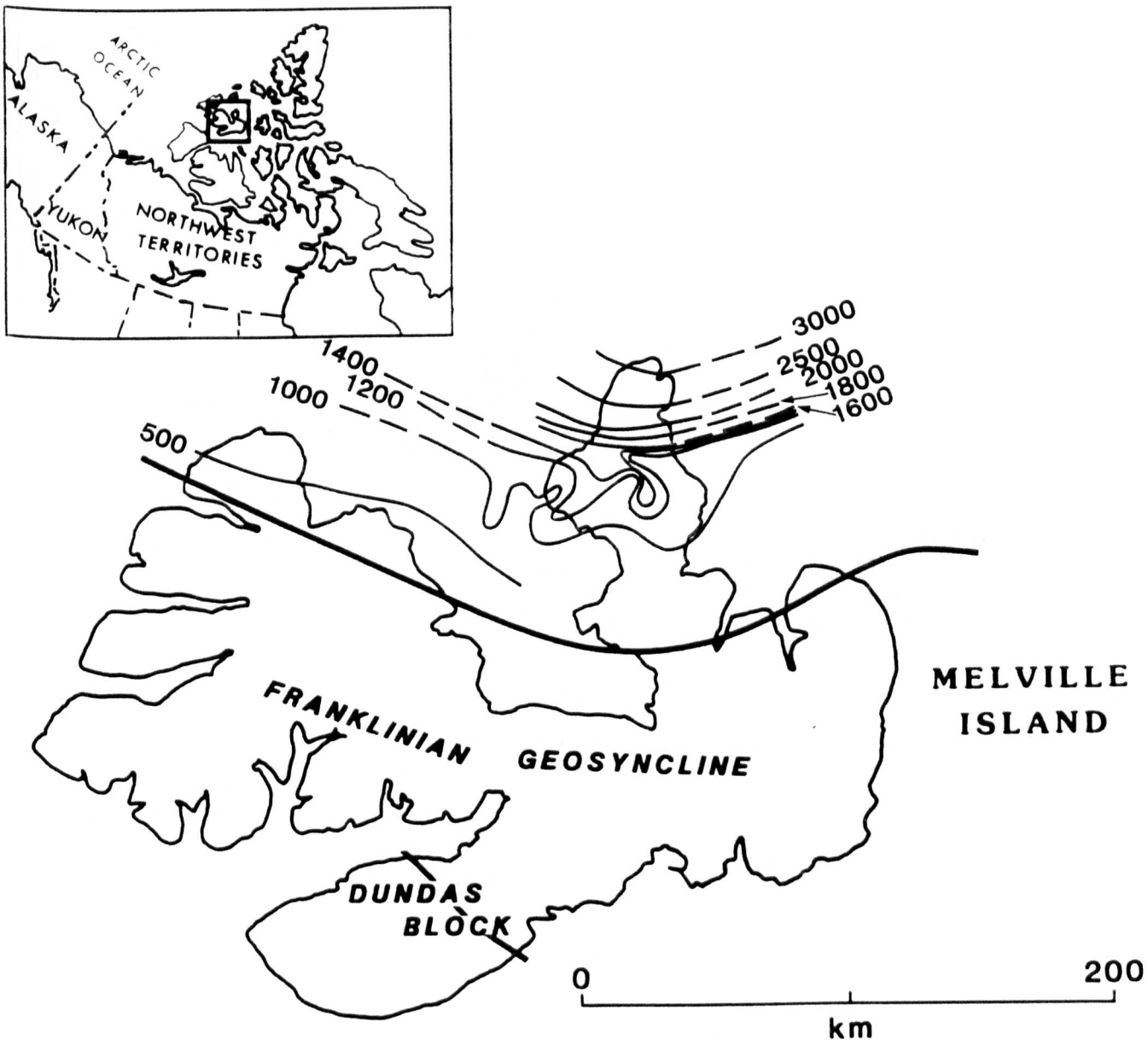

d) Jameson Bay Formation

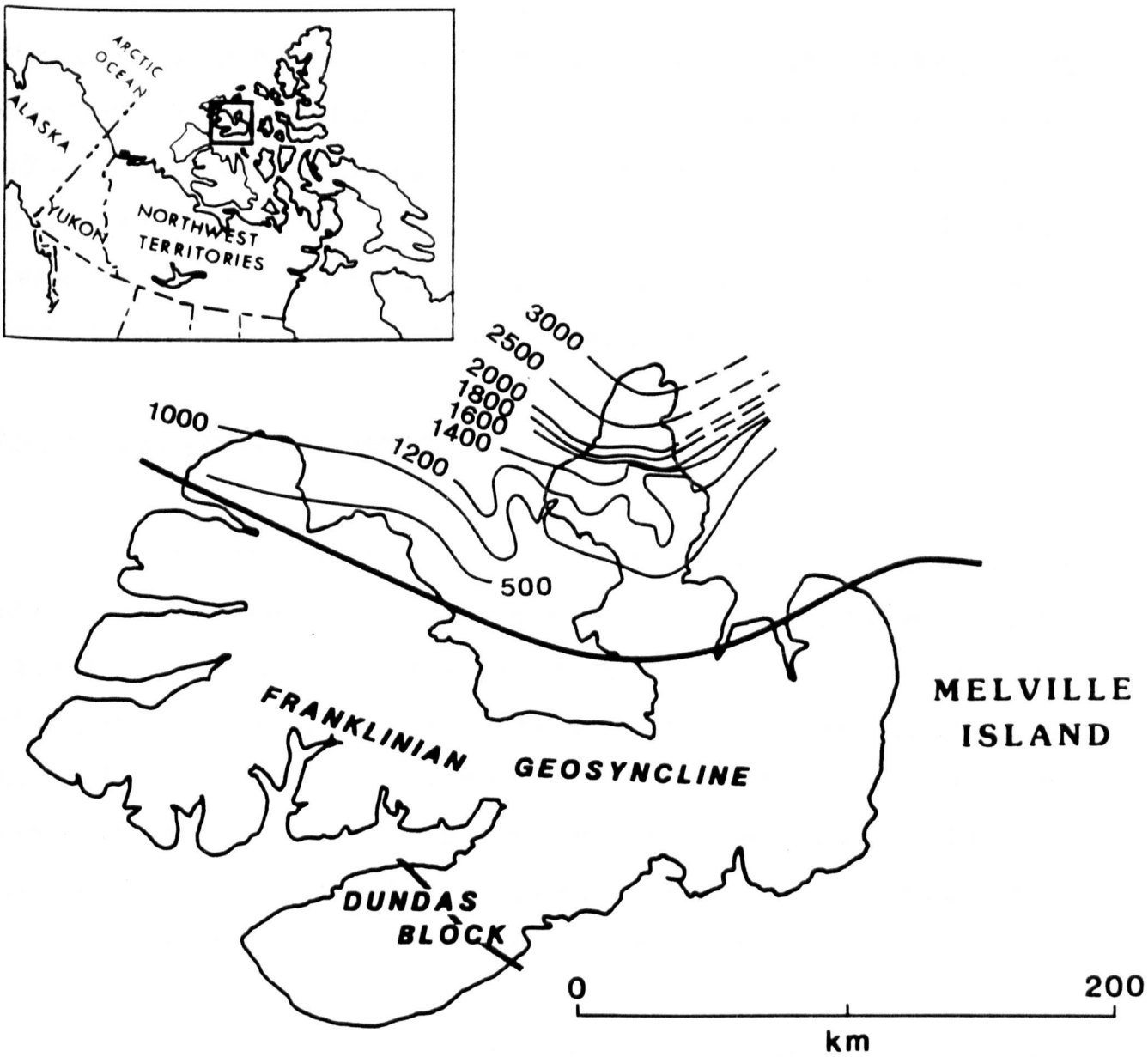

e) Barrow Formation

tighter curvatures of the contour lines in the vicinity of the southeastern part of the Sabine Peninsula and the offshore Hecla and Drake hydrocarbon fields (Figures 9-44 and 9-45). The contours are generally smoother towards the northern part of the Sabine Peninsula for both structural and isoreflectance contour maps. The good correspondence between the two sets of contour maps suggests that maturation in the Sverdrup Basin is largely a function of present-day burial depths.

9.2.5.3 HI and S_2 CONTOUR MAPS

For immature to marginally mature sediments the evaluation of the source-rock potential is easier than overmature sediments, but in areas where the Schei Point sediments are mature a correction was applied to restore HI values at a maturity level of 0.5% Ro. The correction was made according to Orr (1981) by shifting the measured HI values parallel to the kerogen evolution pathways, the reason being that the HI of the organic matter decreases when hydrocarbons are being generated. As a result, the HI values recorded within the 'oil window' are not truly representative of the initial potential, which is just prior to any hydrocarbon generation.

The regional variation of the highest HI values for Schei Point source rocks is shown in Figure 9-46. The contour map shows a general trend of improved organic-matter quality from the basin margin towards the basin centre. HI values in the immature to marginally mature source rocks in the Sabine Peninsula range from 430 to approximately 800 mg HC/g Corg and the restored HI values in the northern part of the Sabine Peninsula exceed 600 mg HC/g Corg (Figure 9-46). This reflects a trend towards more anoxic conditions basinwards (Stewart, pers. commun., 1989), a decrease in the influx of terrestrially-derived organic matter away from the paleoshoreline and an increase in maturation.

Figure 9-46 HI contour map of the Schei Point Group samples

The regional variation of the highest S_2 values for the Schei Point source rocks is shown in Figure 9-47. The contour map shows a good similarity to the iso-HI contour map (Figures 9-46 and 9-47). S_2 values range from 10 to >100 mg HC/g rock and are highest in the offshore drillholes of the Hecla hydrocarbon field. The S_2 values in the Sabine Peninsula range from 10 to 90 mg HC/g rock with the majority being near 30-40 mg HC/g rock (Figure 9-47). The S_2 values decrease to <10 mg HC/g rock in the northern part of the Sabine Peninsula and in northwestern Melville, indicating that the Schei Point source rocks in North Sabine H-49 and Roche Point J-43 have already generated hydrocarbons. Since an S_2 of >10 mg HC/g rock is considered to be very good (Peters, 1986) the Rock-Eval pyrolysis data point to good quality, potential source rocks in the Schei Point Group of Melville Island.

Despite the fact that there are differences in the aerial distribution of hydrogen-rich organic matter in the southern part of the Sverdrup Basin, the overall pattern, as shown in Figures 9-46 and 9-47, is of widespread occurrence of good quality source rocks within the Murray Harbour and Hoyle Bay Formations.

9.2.5.4 CROSS SECTIONS

A series of six cross sections has been constructed through the Mesozoic of Melville Island (Figure 9-48).

A significant lateral variation in section C-C^1 (Figure 9-49) occurs between drillholes Eldridge Bay E-79 and Roche Point J-43 in the Sabine Peninsula. The formations dip from the margin towards the depocentre of the Sverdrup Basin and this is reflected in the behaviour of the isoreflectance lines as well. The only exception is the convergence of isoreflectance lines in and around drillhole Kitson River C-71, where the

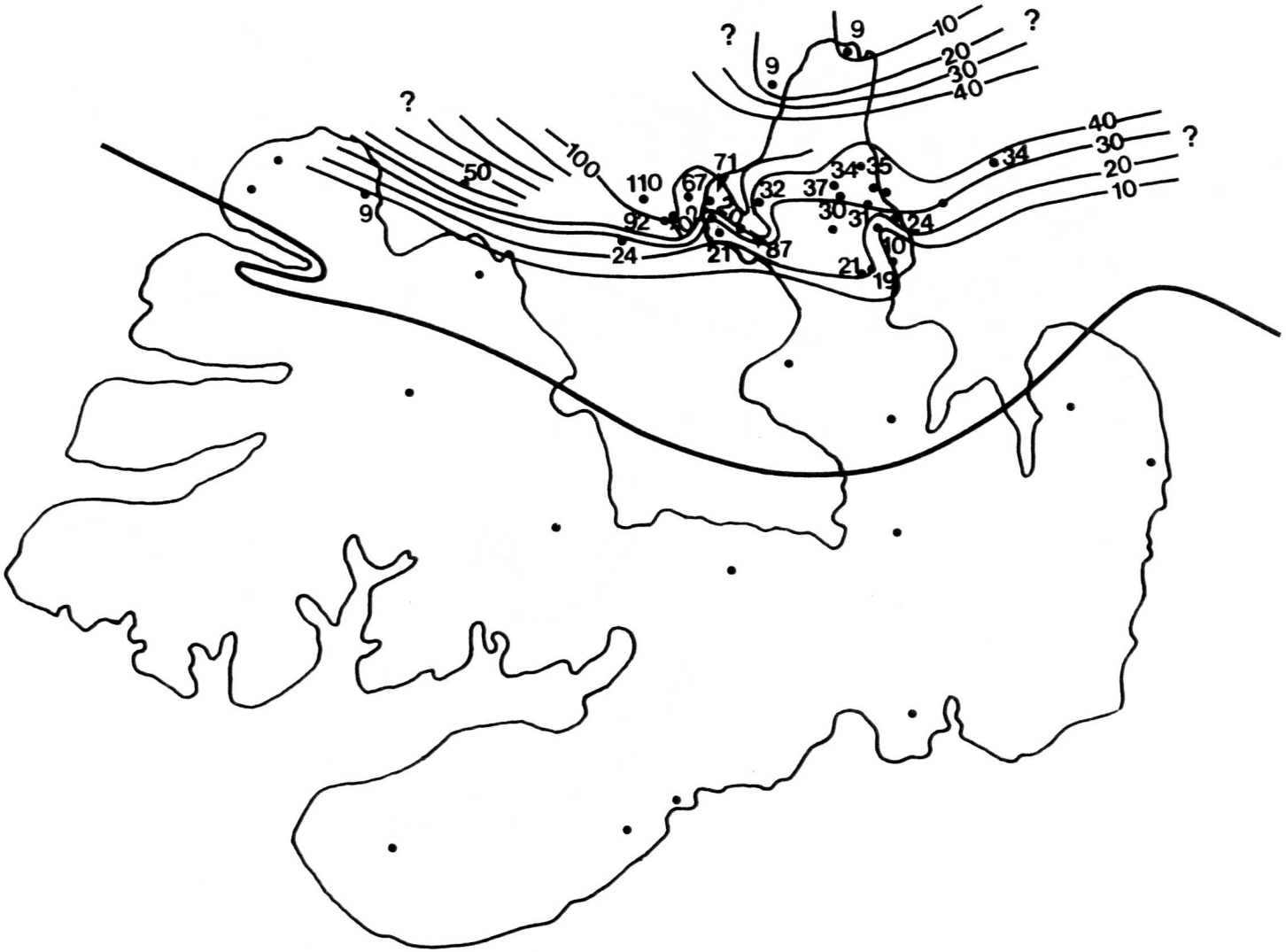

Figure 9-47 S_2 contour map of the Schei Point Group samples

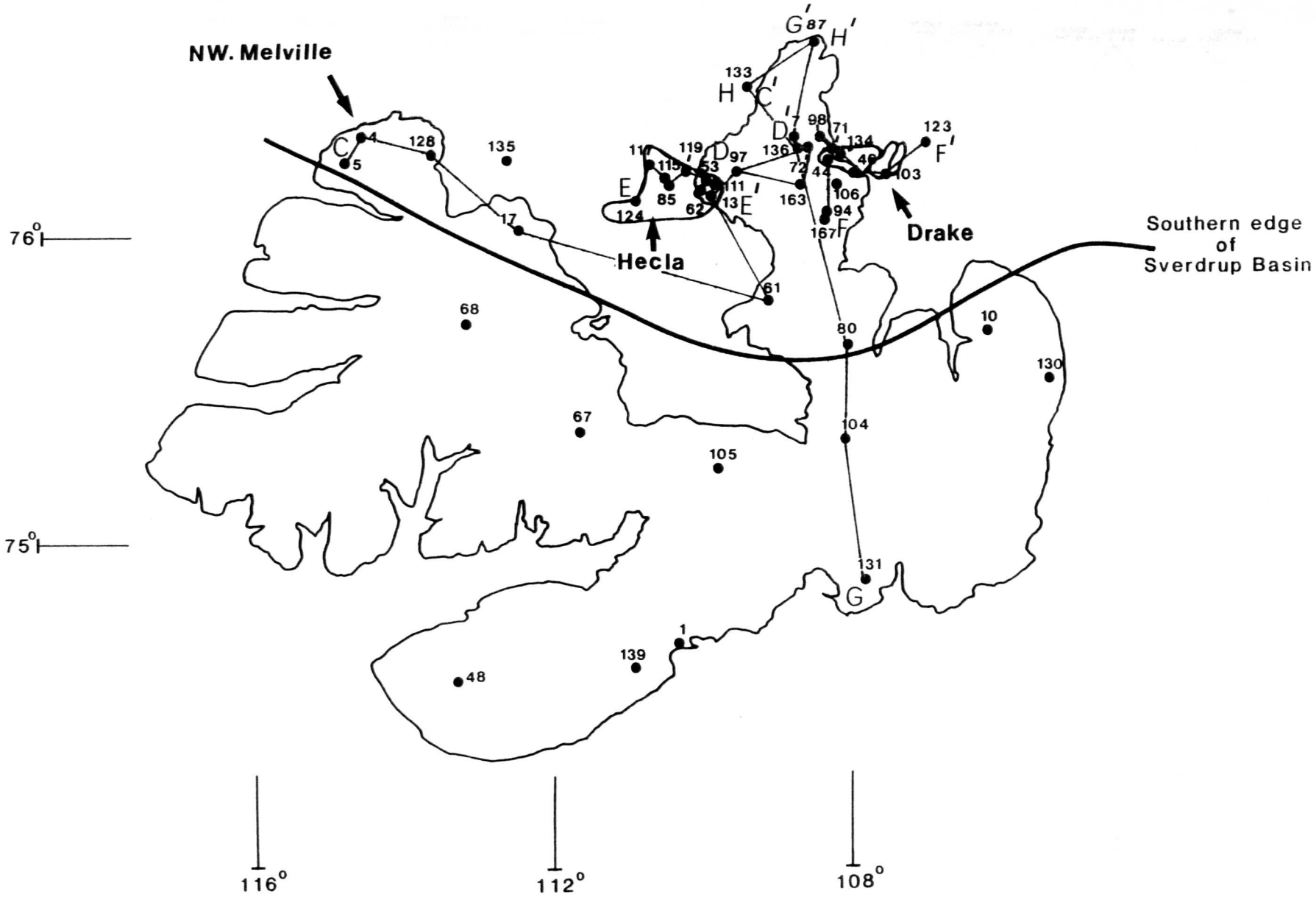

Figure 9-48 Map of Melville Island showing the lines of cross sections

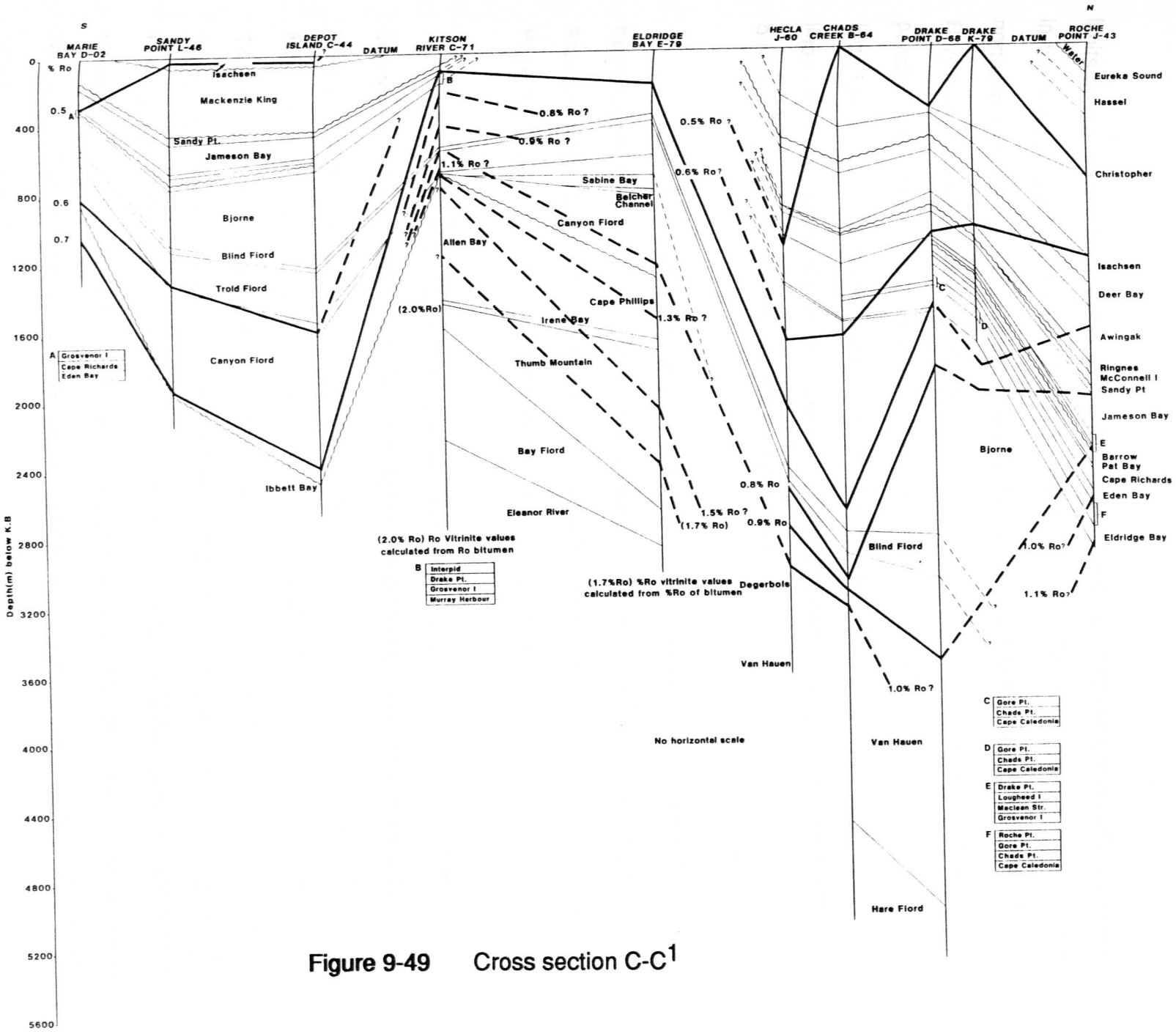

Figure 9-49 Cross section C-C[1]

limits of the mature zone occur at much shallower depths when compared with drillholes in the western part (Marie Bay D-02, Sandy Point L-46, Depot Island C-44) and in the northern part (Hecla J-60, Chads Creek B-64, Drake Point D-68, Drake Point K-79 and Roche Point J-43) of the Sverdrup Basin. The 0.6 and 0.7% isoreflectance lines are parallel to the stratigraphic boundaries in the western part, as is the 0.7% line between Eldridge Bay E-79 and Hecla J-60. In the northern part of the section the isoreflectance lines cross the stratigraphic boundaries. Varying geothermal gradients and depth of burial are believed to be responsible for such a pattern.

Cross section D-D^1 (Figure 9-50) connects Chads Creek B-64 in the Hecla hydrocarbon field to Drake L-67 in the Drake hydrocarbon field. The strata penetrated are mainly Mesozoic with the exception of Chads Creek B-64, Marryatt K-71 and Drake Point D-68 in which the oldest formations are Pennsylvanian.

The 0.5% Ro isoreflectance line lies parallel to the lithostratigraphic boundaries whereas the 0.6% Ro line crosses the boundaries in the eastern part of the section, as well as in the western part due to the low thermal-maturation gradient in Marryatt K-71. The Cretaceous sediments are mostly immature and the Jurassic and Triassic sediments are between the marginally mature and the mature zone of hydrocarbon generation (% Ro >0.55) (Drake Point D-68) (Figure 9-1). The highest Ro recorded is 1.4% in the Hare Fiord Formation (Chads Creek B-64), and any correlation between the drillholes of section D-D^1 beyond an Ro level of 0.8% is not possible because of either the shallow depth penetrated by a few of them or lack of reliable reflectance control.

Similar observations to section D-D^1 are made in cross section E-E^1 (Figure 9-51) which connects Hecla C-58 to Hecla J-60 in the Hecla hydrocarbon field. The

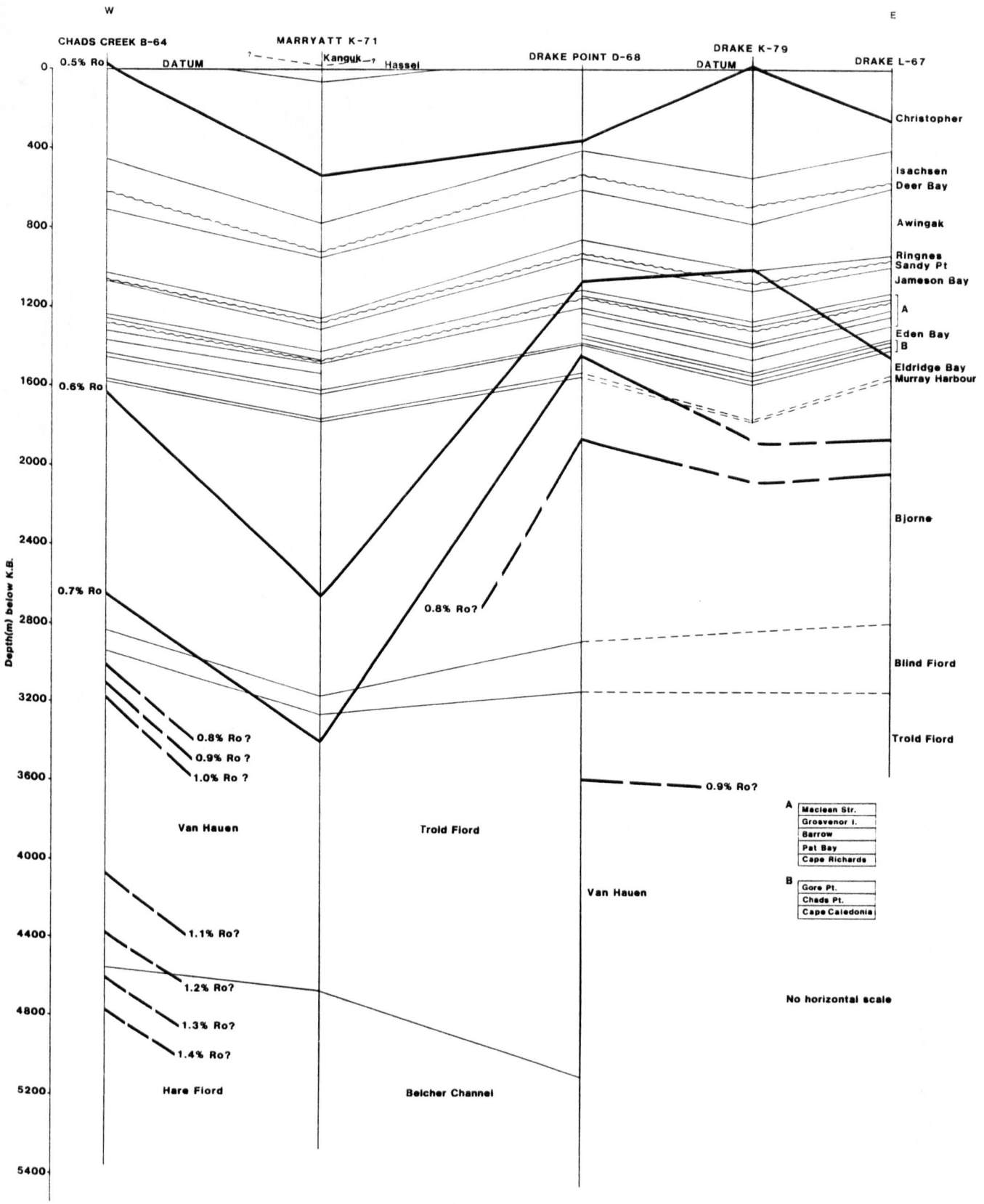

Figure 9-50 Cross section D-D[1]

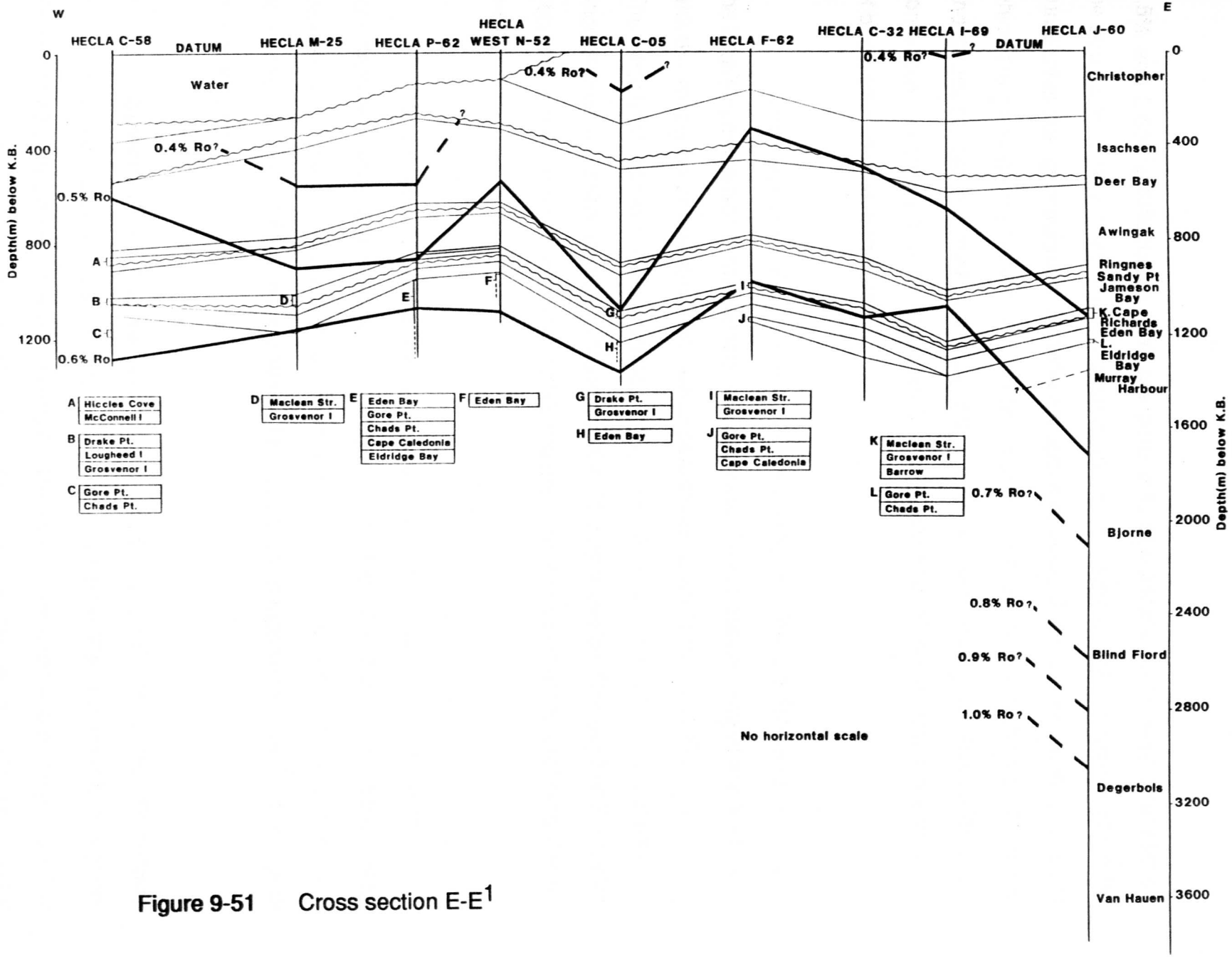

Figure 9-51 Cross section E-E[1]

0.5% and 0.6% isoreflectance lines are parallel to sub-parallel when superimposed on the structural contour lines which suggests uniform subsidence of the basin and similar burial rates during maturation, with the exception of Hecla F-62 and Hecla West N-52 in which the maturation gradients are slightly higher. The behaviour of the isoreflectance and structural contour lines indicates that maturation was mainly syndepositional but some local variations may be attributed to the effects of geothermal gradient and depth of burial prior to uplift and erosion.

Cross section F-F^1 (Figure 9-52) correlates the Sherard drillholes to those in the Drake hydrocarbon field, onshore and offshore. The strata penetrated are Mesozoic, with the exception of Sherard F-34, which penetrates down to the Blue Fiord Formation. The structural contour lines correlate very well and the Mesozoic formations are encountered at similar depths. Collingwood K-33 has a thicker Christopher Formation section, so the formation tops are slightly deeper than in the rest of the drillholes (Figure 9-52).

When superimposed on the structural contours, the 0.50 and 0.60% isoreflectance lines are parallel to subparallel. In fact, the 0.6% line shows better parallelism to the structural contours than the 0.5% isoreflectance line, indicating that maturation in the Drake hydrocarbon field was syndepositional, as in the Hecla hydrocarbon field.

Section G-G^1 (Figure 9-53) runs south to north from the Franklinian miogeosyncline (Beverley Inlet G-13) through the Sverdrup Basin margin to the North Sabine H-49 drillhole near the basin centre. The oldest formation in the miogeosyncline drillholes is the Ordovician Thumb Mountain, in which the % Ro vitrinite is >1.8 (calculated from bitumen reflectance) and the youngest is the Permian Assistance

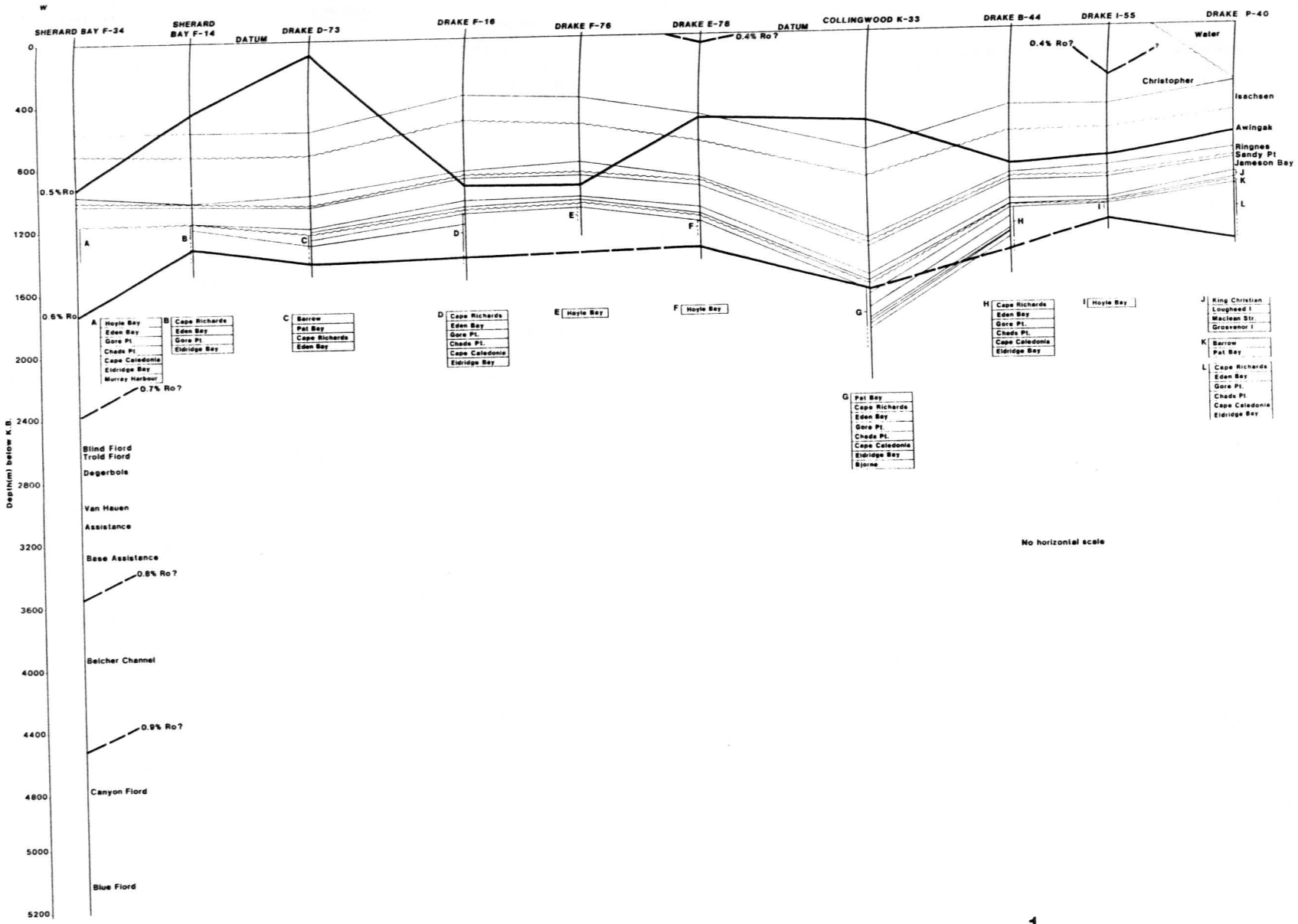

Figure 9-52 Cross section F-F[1]

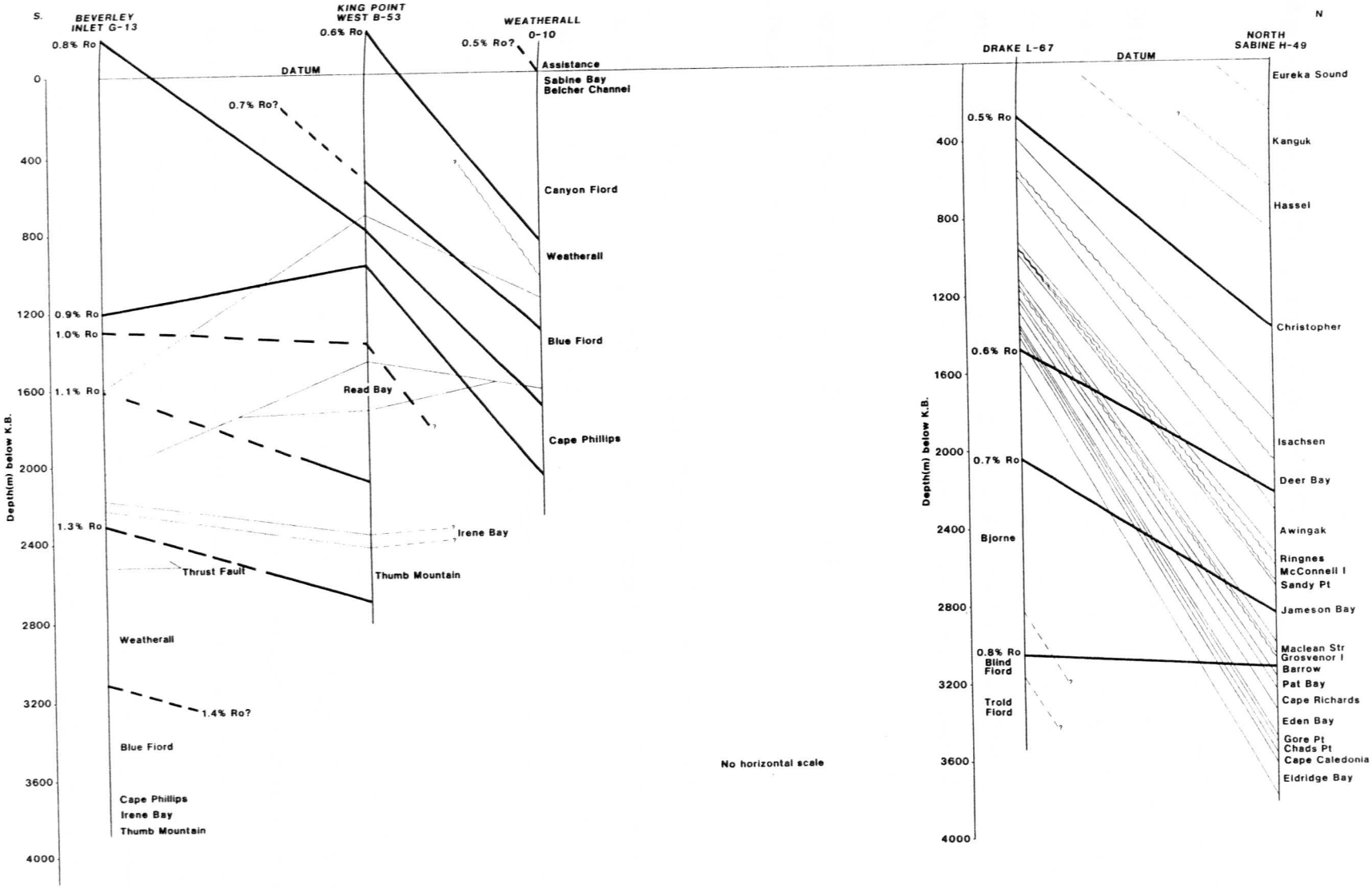

Figure 9-53 Cross section G-G[1]

Formation with an Ro of 0.5% (Figure 9-53).

The two Sverdrup Basin drillholes show a good correlation of their formations, but the structural contour lines are very steep due to the deeper lithostratigraphic boundaries in North Sabine H-49. Despite this, the 0.5% isoreflectance line is parallel to the structural lines and the 0.6 and 0.7% isoreflectance lines are subparallel to the structural-contour lines, again indicating syndepositional maturation. The youngest formation in Drake L-67 is the Christopher, whereas in North Sabine H-49 it is the Tertiary Eureka Sound Formation. The correlation in the Franklinian miogeosyncline drillholes is poor between Beverley Inlet G-13 and King Point West B-53, but it is better between the latter and Weatherall O-10.

Section H-H^1 (Figure 9-54) correlates Roche Point J-43 to North Sabine H-49 and the correlation of the formation tops is very good. The isoreflectance lines, when superimposed on the structural contour lines, are parallel to subparallel, indicating syndepositional maturation which seems to be the case in almost all the Sverdrup Basin drillholes.

Vitrinite reflectance for all major packages of rocks show a gradual increase from the margin towards the centre of the Sverdrup Basin. The shallow parts of the basin correspond to milder organic diagenesis, whereas the deeper parts reflect more severe thermal conditions. When isoreflectance maps are superimposed on structural (isopach) maps, a good correlation results between thermal maturation and depth. The only exception appears to be the behaviour of the isoreflectance contours in the locality of drillhole Kitson River C-71, in the Raglan Range area of Melville Island.

Most Melville Island maturation profiles are characterized by a relatively

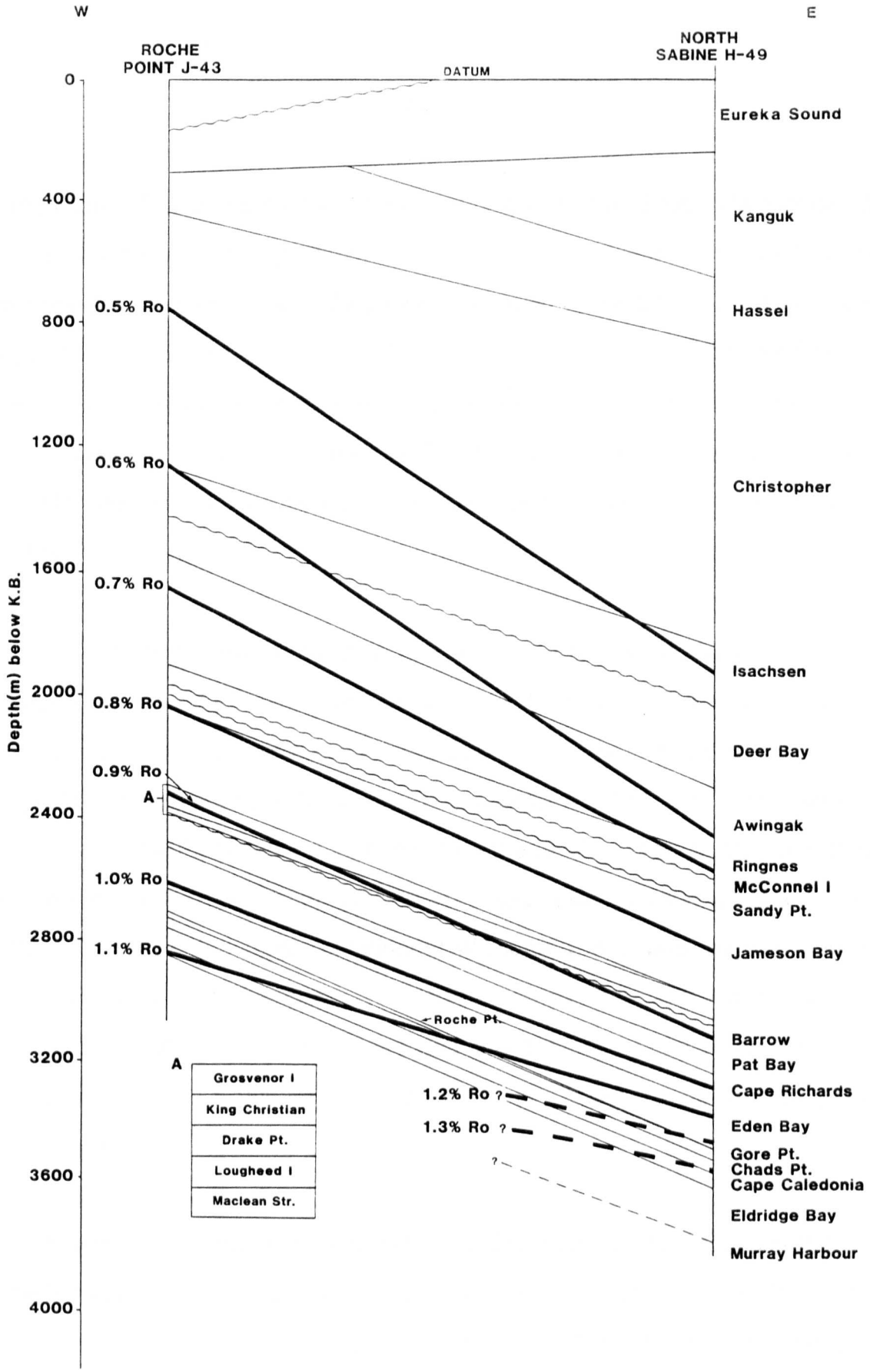

Figure 9-54 Cross section H-H[1]

uniform increase of reflectance with depth throughout the Upper Palaeozoic and Mesozoic sequences suggesting stable heat-flow conditions over much of the basin throughout the above time period. By plotting the level of maturity for the Palaeozoic and Mesozoic formations (isoreflectance lines) above the structural cross-sections, the relative effects of geothermal gradient and depth of burial on maturity can be observed. The depth of burial is a significant factor in determining the level of maturity of source rocks in Melville Island, providing maximum depth coincides with maximum temperatures.

The level of organic maturation at the top of the Triassic Barrow Formation and the base of the Jurassic Jameson Bay and Lower Cretaceous Isachsen and Deer Bay Formations appears to mimic closely the paleogeometry of the basin as outlined from the geology interpreted by Tozer and Thorsteinsson (1964) and Fox (1985). In deformed strata of the Franklinian miogeosyncline the level of organic maturity reflects the stratigraphic level rather than the present structural position of the samples suggesting that at least the major component of maturity was pre-orogenic and thus pre-Late Devonian to Carboniferous. The isoreflectance lines are almost parallel to subparallel to the stratigraphic boundaries and the only exception is in the area of drillhole Kitson River C-71, where the maturity levels appear to follow the present structural position.

Because the maturation gradients in Sverdrup Basin are different, the paleoisopach maps are not a replica of the isoreflectance maps although the general trends are similar. The paleoisopach maps define a north-northeast to south-southwest-trending basin with a major depocentre to the northeast, towards Ellef Ringnes Island. All paleoisopach maps suggest the strata thickened in this direction and that the isoreflectance surfaces are relatively planar and dip in a direction slightly east of

north. The dip of the isoreflectance surfaces is slightly less than that of the strata so that for any given stratigraphic horizon the reflectance increases to the north and east.

9.2.6 THE EFFECT OF IGNEOUS INTRUSIONS ON BITUMEN REFLECTANCE

Sabine Peninsula, Melville Island is an ideal area in which to study the effects of igneous intrusions upon organic matter in sediments. Thick sequences of Permo-Pennsylvanian strata have been intersected by two such igneous intrusions in drillholes Drake Point D-68 and Chads Creek B-64 (Figures 9-1 and 9-2).

The intrusives in Drake Point D-68 are granodiorite sills that were emplaced (~850°C emplacement temperature) during the Upper Jurassic (152 Ma) and Lower Cretaceous (131 Ma) based on k/Ar dating (Balkwill and Haimila, 1978). The intrusive in Chads Creek B-64 is a diabase sill (~1,000°C emplacement temperature) which has not yet been dated. An attempt will be made to compare and contrast the effects of the two sets of intrusions on the organic matter dispersed in the sediments above and below the intrusion zones. Raymond and Murchison (1989) state that the pore-water volume, the degree of sediment compaction and the background reflectance of the organic matter prior to the intrusion are significant factors in the development of thermal aureoles. Additional factors are the nature of the intrusive body which would determine the temperature of intrusion and the heat flow pattern from the intrusion which may be in one or multiple phases.

When organic matter is exposed to high temperatures over a short period of time, certain changes take place which can be observed microscopically. These include primary and secondary vesiculation, microbrecciation and granular anisotropy (Chandra and Taylor, 1982). Phytoclasts near the intrusion zone in both drillholes have been

altered varyingly. Bitumen in Drake Point D-68 has developed microbrecciation and mosaic texture within the aureoles, but in Chads Creek B-64 the bitumen has not developed this texture, which means that the bitumen in Chads Creek B-64 is non-graphitizable whereas the bitumen in Drake Point D-68 is. It is also expected that bitumen, due to its higher hydrogen content compared to most vitrinites, would react more easily to high temperatures than vitrinite.

The rank gradient prior to sill emplacement can be determined with reasonable certainty because of the satisfactory data above and below the intrusions. Prior to sill emplacement in Drake Point D-68, the Ro of organic matter near the intrusive zones was ~0.8% for vitrinite which indicates a caking rank, the sediments were well lithified and the bitumen underwent carbonization after being exposed to high temperatures (~600°C or more at the contact).

In Drake Point D-68 the metamorphic effects of the sill, as determined by reflectance trend, can be observed up to seven times its thickness. The upper, older sill is approximately 45 m and the aureole zone above it has a width of 330 m. The width of the aureole below the sill is difficult to establish because it has been obliterated by the effect of the lower, younger sill. The thickness of the lower sill is 75 m and the contact metamorphic zone below appears to be at least seven times and, possibly, as much as eight times the width of the sill (485 m). These aureole thicknesses are of no surprise bearing in mind the differences between the age of the sills and the age of the intruded strata. It is noted (Figures 9-1 and 9-2) that the form of the reflectance curves above and below the two sills appears to be symmetrical despite the superimposition of the effects of one sill on the other.

CHAPTER X

CHAPTER X

10.0 BURIAL HISTORY

INTRODUCTION

Burial-history models are widely used to estimate levels of thermal maturity within sedimentary basins. The model estimates and the computer graphs the burial history curves of a stratigraphic section, establishes an inferred thermal maturity for the section and assists in the evaluation of potential petroleum-source rocks. There are numerous models available at present, e.g. Lopatin (1971), Waples (1980), Wright (1980) and Falvey and Deighton (1982). Recently more complex burial models have been developed (Sclater and Christie, 1980; Stainforth, 1984), using decompaction, and variations in thermal conductivity and lithology.

Thermal conductivity of porous rocks increases with compaction and decompacted burial paths follow higher temperatures (Cook, 1986). Whenever the heat-flow history of a basin and the porosity-reduction functions for various lithologies are not firmly established, the burial model can only be an approximation.

For further discussions on the construction of burial models and their application to thermal maturation the reader is referred to van Hinte (1978); Feinstein (1981); Nunn et al., (1984) and Guidish et al., (1985). Further details of the model used in the construction of the burial plots can be found in Appendix III.

This chapter will be discussed in the following order:

1) geothermal gradients in Melville Island,
2) maturation gradients in Melville Island,
3) geothermal versus maturation gradients,
4) estimation of the amount of eroded section, and
5) burial history plots based on modelling techniques

10.1 GEOTHERMAL GRADIENTS

The average present-day geothermal gradients for the Sverdrup Basin in the Sabine Peninsula vicinity are approximately 13°C-40°C/km, with the majority being about 25°C/km (Bustin, 1986) which is at the low end of the 'normal' geothermal-gradient range (Gretener, 1981). The low geothermal gradients of the Sverdrup Basin are probably caused by the thick sedimentary-rock section (Balkwill et al., 1982). Discrepancies occur when determining the present-day geothermal gradient if bottom-hole temperatures are taken before thermal equilibrium is reached. Temperatures will be lower owing to the cooling effects of circulation (Hunt, 1979; Price et al., 1981; Barker, 1983; Cardott and Lambert, 1985). Present-day temperatures would be expected to be maximal only if maximum depth of burial alone produced the level of thermal maturity. But because of high heat flow associated with rifting episodes and evaporite intrusions, it is unlikely that present-day temperatures are maximal and it is possible that maximum temperatures were not strictly due to depth of burial in the Sverdrup Basin. Also, evaporite (salt) diapirs enhance maturation levels due to the anomalously high geothermal gradients (up to 100°C/km) (Issler, 1985) that have been measured in localities adjacent to diapirs (Gretener, 1981).

Bustin (1986) estimated the paleoheat flow on Melville Island to be 30mw/m^2, assuming a constant thermal conductivity of 2.0w/m°C. He also approximated

paleogeothermal gradients in Melville Island (West Sverdrup Basin) for the Eureka Sound Formation by modelling the measured maturation gradients using an integral form of the Lopatin equation (MacKenzie, 1981; Bustin, 1984). The model solves for maturation gradients, assuming a constant burial history but varying geothermal gradient, and compares the calculated with measured maturation gradients. The palaeogeothermal gradient of Melville Island that Bustin (1986) suggested is in the order of 15°C/km, a relatively low value, but similar to gradients reported from the Western Canadian Sedimentary Basin (8° to 15°C/km) (England and Bustin, 1986; Hughes and Cameron, 1985; Osadetz et al., 1989), and the Gippsland Basin in Australia (Shibaoka and Bennett, 1977).

The low present-day geothermal gradients obtained for the Mesozoic of drillholes Chads Creek B-64 and Drake Point K-79 from bottom-hole temperature (BHT) readings (Figure 10-1) are in good agreement with Bustin's results, but the question that remains to be answered is how similar are the present-day geothermal gradients to the palaeogeothermal gradients? Figure 10-2 shows the relationship between reflectance and present-day geothermal gradient.

The present-day, low, geothermal gradients observed in the Sverdrup Basin (20-25°C/km) (Figure 10-1) may at least partially be the result of meteoric water recharge over that region. Majorowicz and Jessop (1981) observed a similar effect in the Prairies Basin, Western Canada. Recent studies in the Western Canadian Sedimentary Basin (Majorowicz and Jessop, 1981; Hitchon, 1984) have documented that heat carried by moving groundwater has had a significant effect on organic maturation. Those authors state that there is a genetic link between hydrocarbon occurrence and fluid regime with the latter being controlled by present topography. There appears to be little doubt that gravity-induced, cross-formational flow does control

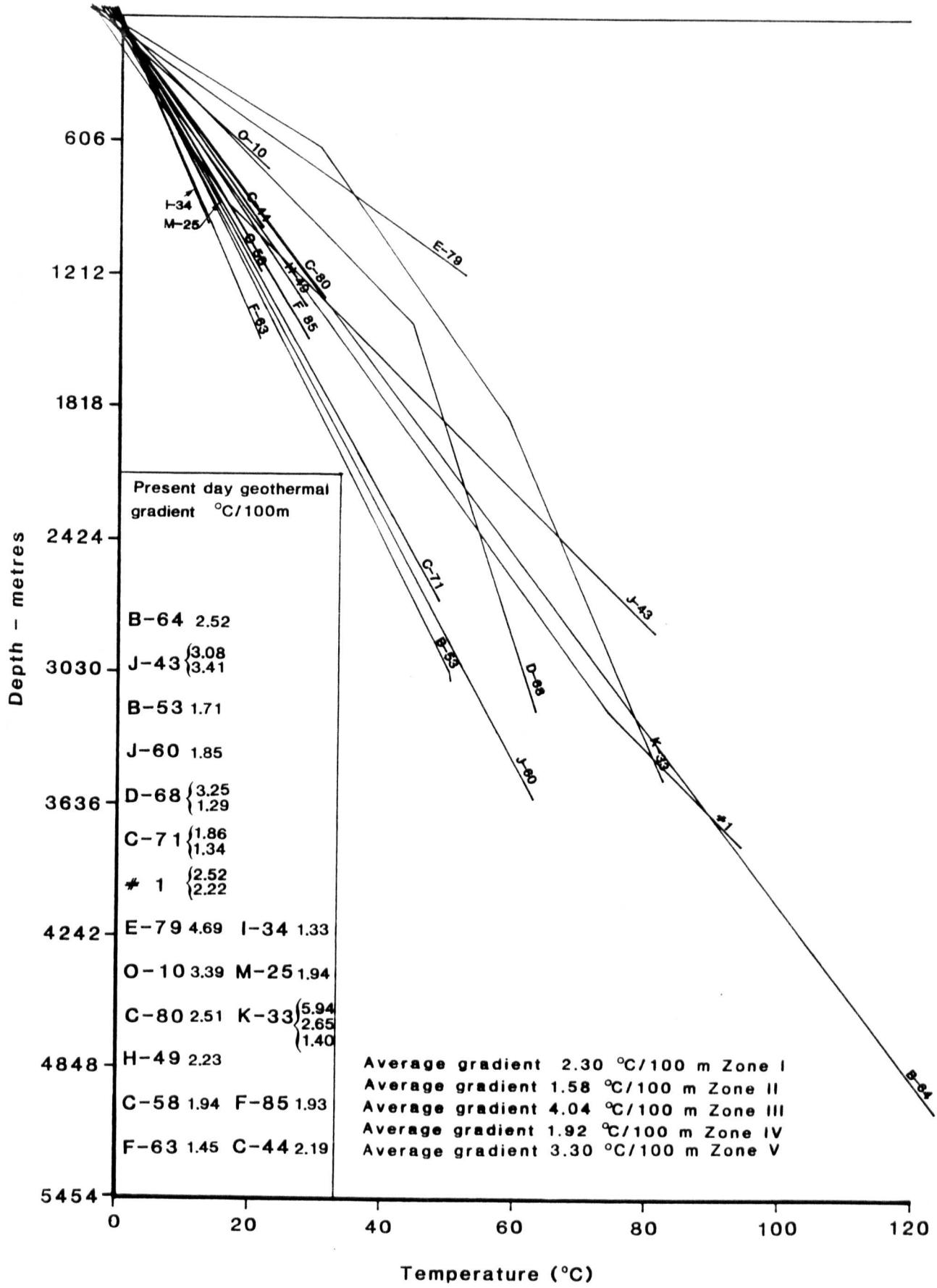

Figure 10-1 Present-day geothermal gradients, Melville Island (°C/100m)

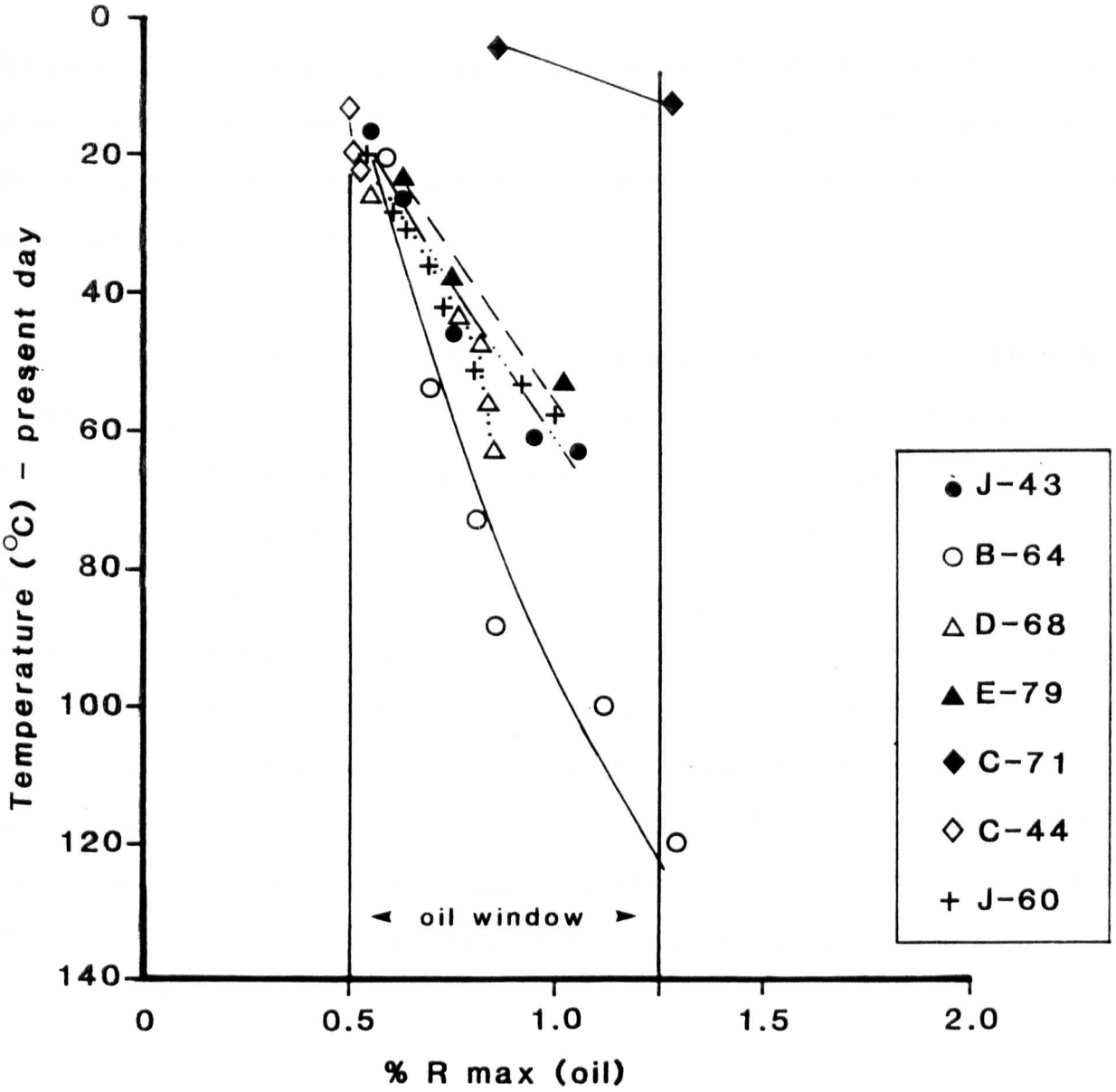

Figure 10-2 Relationship between vitrinite reflectance and present-day geothermal gradients

the hydrodynamic regime, which in turn influences the geothermal-gradient pattern and the accumulation of hydrocarbons (Hitchon, 1984). In addition, fault planes can be active as conduits that bring heated water to the surface, thereby increasing the local geothermal gradient (Lam et al., 1982).

It appears that maximum paleotemperatures in the Sverdrup Basin were reached during the final stage of development, which is Cretaceous and Tertiary. Besides variations in depth of burial, another factor which must be considered in any model of basin development is the variation in heat flux which may be related to large-scale tectonics, e.g. plate collision, sea-floor spreading or to more localized activity, e.g. compaction of sediments leading to movement of connate waters from deeply buried shales. If migration of heated water is persistent, it will locally affect maturation indices so that maturation discontinuities or changes in gradient will be seen, usually at junctions of porous with non-porous lithologies (Skibo, pers. commun., 1989). The change in Ro gradient at the boundary between the Schei Point shales (non-porous) and the Skybattle Formation sandstone (porous) in North Sabine H-49 is such (Figure 9-6) may be explained by a combination of overpressuring and hot connate water flow.

10.2 MATURATION GRADIENTS

The lack of measured maturation gradients throughout much of the Canadian Arctic Archipelago introduces considerable doubt about the paleothickness of the Sverdrup Basin formations. In the Sabine Peninsula area, depths of burial, as indicated on the basis of maturity levels, can only be considered as first approximations.

Coal or coaly material dispersed in sedimentary rocks can be found throughout most of the Sverdrup Basin succession. It is generally possible to obtain

reliable information about the vertical maturation gradient where samples can be obtained over a stratigraphic interval of about 500 m or more. Maturation gradients (expressed as % Ro vitrinite/km) have been determined for all exploration drillholes used in this study and these data are shown in Table 5. The maturation gradients range from 0.03% log Ro/km to 0.70% log Ro/km with most of the drillholes having a gradient of about 0.15 to 0.20% log Ro/km. The highest gradient is present near the basin margin (Kitson River C-71) and the gradients decrease to the north and east of this area. The range of vitrinite reflectance in the drillholes is similar for the Mesozoic succession, being in the range of 0.4 to 0.7% Ro, random, with the exception of Roche Point J-43 and North Sabine H-49.

The low maturation gradients observed in the Sverdrup Basin have resulted from the imposition of very low palaeogeothermal gradients during maturation. The low maturation gradients measured in the Mesozoic of Melville Island (Table 5) may also be attributed to rapid sedimentation and uplift in the Tertiary (Eurekan Orogeny) so that an equilibrium geothermal gradient may never have existed.

Similar observations have also been made in other sedimentary basins. For example, the relatively low reflectance gradient of the Gippsland Basin in Australia (0.08 to 0.15% log Ro/km) is related to very rapid subsidence and sedimentation since Early Tertiary or Cretaceous times (Shibaoka and Bennett, 1977). Low maturation gradients have been reported by Bostick et al., (1978) from the Los Angeles and Ventura Basins where sedimentation rates have been up to 1.82 mm/yr (1.82 km/Ma) in the last 3 Ma.

Alternatively, the low maturation gradients may reflect low heat flow. One of the effects of a low maturation gradient is that a great thickness of strata now lies within the hydrocarbon-generation zone. The regional maturity pattern and depth to the

TABLE 5

Maturation Gradients (% log Ro/Km)

Drillhole Name	Maturation gradients % Ro/Km	
Dundas C-80	0.25	
Apollo C-73	0.40	
Hearne Pt. F-85	0.03	
Winter Harbour #1	0.07	
Beverley Inlet G-13	0.07	
Zeus F-11	-	
Sabine Bay A-07	0.20	
King Point West B-53	0.20	
Towson Point F-63	-	
Richardson G-12	0.19	
Drake Point D-68	0.10	
Chads Creek B-64	0.08	
Hecla J-60	0.17	
Depot Island C-44	0.09	
Roche Point J-43	0.20	
North Sabine H-49	0.33 *	0.06 Two gradients, above 0.6 and below major unconformity
Weatherall O-10	0.14	
Eldridge Bay E-79	0.08	
Kitson River C-71	0.71	
Sherard Bay F-34	0.10	
Sherard Bay F-14	0.12	
Marryatt K-71	0.08	
Collingwood K-33	0.14	
Drake L-67	0.07	
Drake Point K-79	0.11	
Drake F-76	0.20	
Drake E-78	0.13	
Drake B-44	0.06	

TABLE 5 (continued)

Drake D-73	0.12
Drake F-16	0.17
Drake P-40	0.16
East Drake I-55	0.12
Hecla Southwest C-58	0.15
Hecla P-62	0.20
Northwest Hecla M-25	0.33
Hecla West N-52	0.17
Hecla West C-05	0.14
Hecla I-69	0.16
Hecla F-62	0.20
Hecla C-32	0.17
Marie Bay D-02	0.25
Sandy Point L-46	0.10
Grassy I-34	0.20

* Average maturation gradient

hydrocarbon generation zone is shown in Figure 10-3 (the oil generation threshold taken at 0.60% Ro) (Waples, 1980), but it can vary between 0.50 and 0.70% Ro depending on organic matter type. From south to north the depth to the oil window increases from 1,000 m to 2,500 m. In the Sproule Peninsula area to the west, the depth to the oil window is from 900 m to 1,650 m, and in the Raglan Range it is as shallow as 50 m (Figure 10-3).

Vitrinite-reflectance, gradient-data points were measured over a similar maturation range. The drillholes in the central part of Sabine Peninsula i.e. Drake Point D-68, Chads Creek B-64, Hecla J-60 (Figures 9-1, 9-2 and 9-3) passed through thick Permian and Triassic strata compared with those in the southern part of the basin. It is unlikely that differences in the age of the intervals or the time over which they were deposited would significantly affect the use of maturation gradients as indicators of palaeogeothermal gradients. The uplift and removal of cover may have occurred at different times between the south and more central parts of the basin because orogenies affected parts of the basin differently (Tozer and Thorsteinsson, 1964). As a result the effective period of maturation may have been different. Such a difference would influence the relationship between maturation gradient and palaeogeothermal gradient, but it seems unlikely that the effect is large enough to invalidate conclusions based upon the considerable differences observed in the maturation gradients.

The increase in rank from south to north in the Sverdrup Basin is probably related to the increase in cover which allowed the temperature to build up to higher values in the northern part of the basin, i.e. Roche Point J-43 (Figure 9-5). A further significant factor may be the development of relatively thick units of fine clastic rocks in the Triassic of Drake Point D-68 and Chads Creek B-64 (Figures 9-1 and 9-2) having low thermal conductivity.

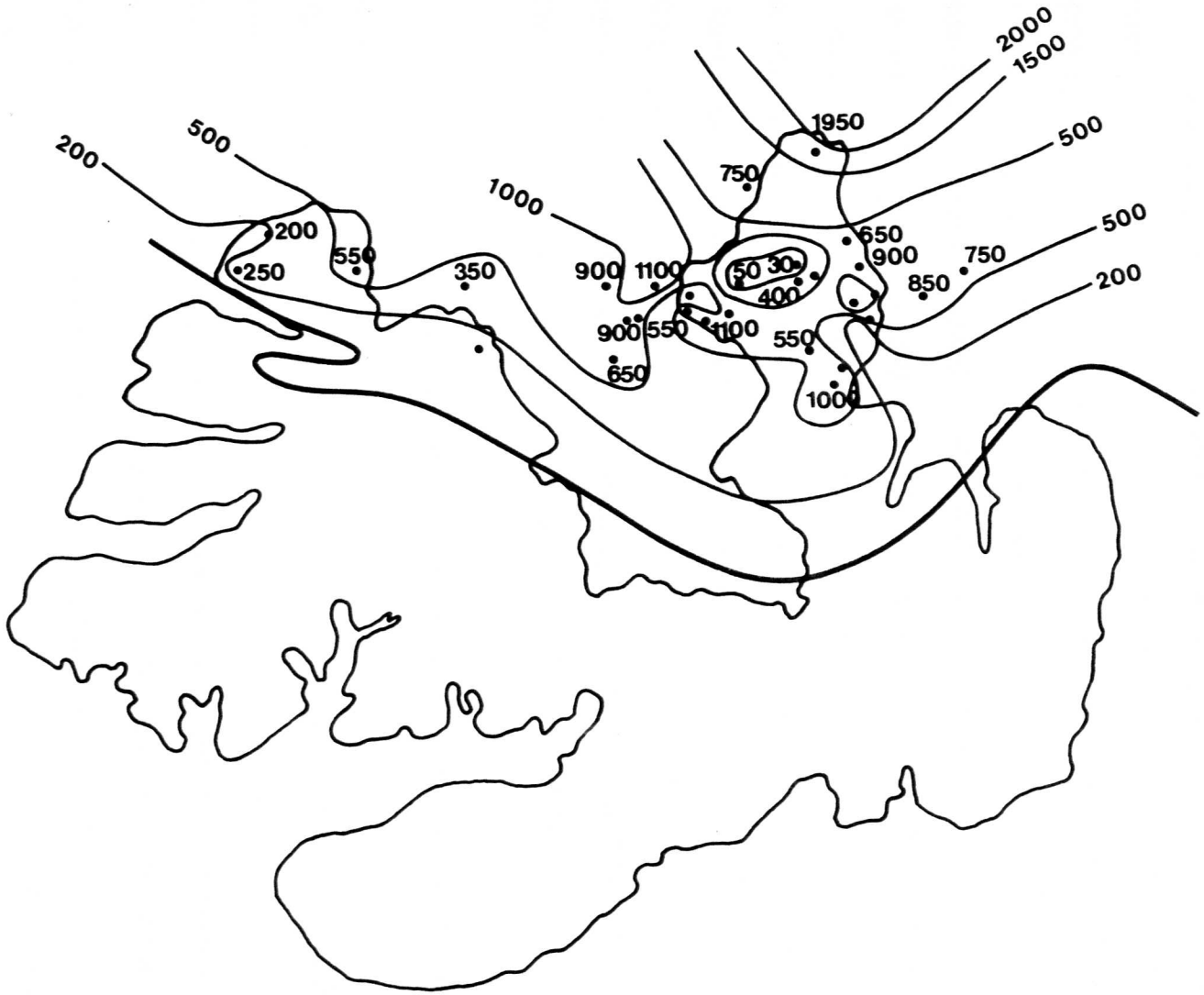

Figure 10-3 Contour map (m) showing depth to the 'oil window'

10.3 GEOTHERMAL VERSUS MATURATION GRADIENTS

Log-heading information was gathered from several Melville Island drillholes. Pertinent data such as the maximum bottom-hole temperature and the depth of the logging run from the surface or from the sea floor was obtained. Often essential information, such as the time the tool was at bottom and the time drilling and circulation stopped was missing, measurements were of poor quality or data was incorrectly recorded. Unfortunately only a limited number of the 43 drillholes had sufficient information to permit several temperature corrections at various depth intervals. These are: Roche Point J-43, Kitson River C-71, and Drake Point D-68. Because the duration of fluid circulation and the time that temperatures were measured after circulation of drilling fluids were not available, no correction of formation temperatures was made. Bottom-hole temperatures were corrected using a Horner temperature plot (Dowdle and Cobb, 1975), as determined from petroleum-exploration well logs.

Figure 10-4 is a geothermal gradient map of the Sverdrup Basin, Melville Island. Geothermal gradient may vary with depth because of such factors as lithology, reflecting variations in the thermal conductivity of rocks, subsurface fluid movement, porosity and the rate of heat production in basement and overlying sedimentary rocks (Pitt, 1986). Average gradients computed from the deepest bottom-hole temperature in each drillhole were used in constructing the map. Because of problems with permafrost in Arctic Canada, the base of the permafrost, considered as the 0°C surface, was taken at a minimum depth of 100 m. This value is arbitrary, but the depth to the permafrost zone may as well vary from one part of the island to another. It is at 420 m in Marryatt K-71, 180 m in Hecla C-32, 200 m in Drake E-78, and Drake B-44 and only 40 m in Hecla West C-05. It is assumed that the heat flow from the basement is uniform throughout the study area, but the basement rocks may be variable sources of

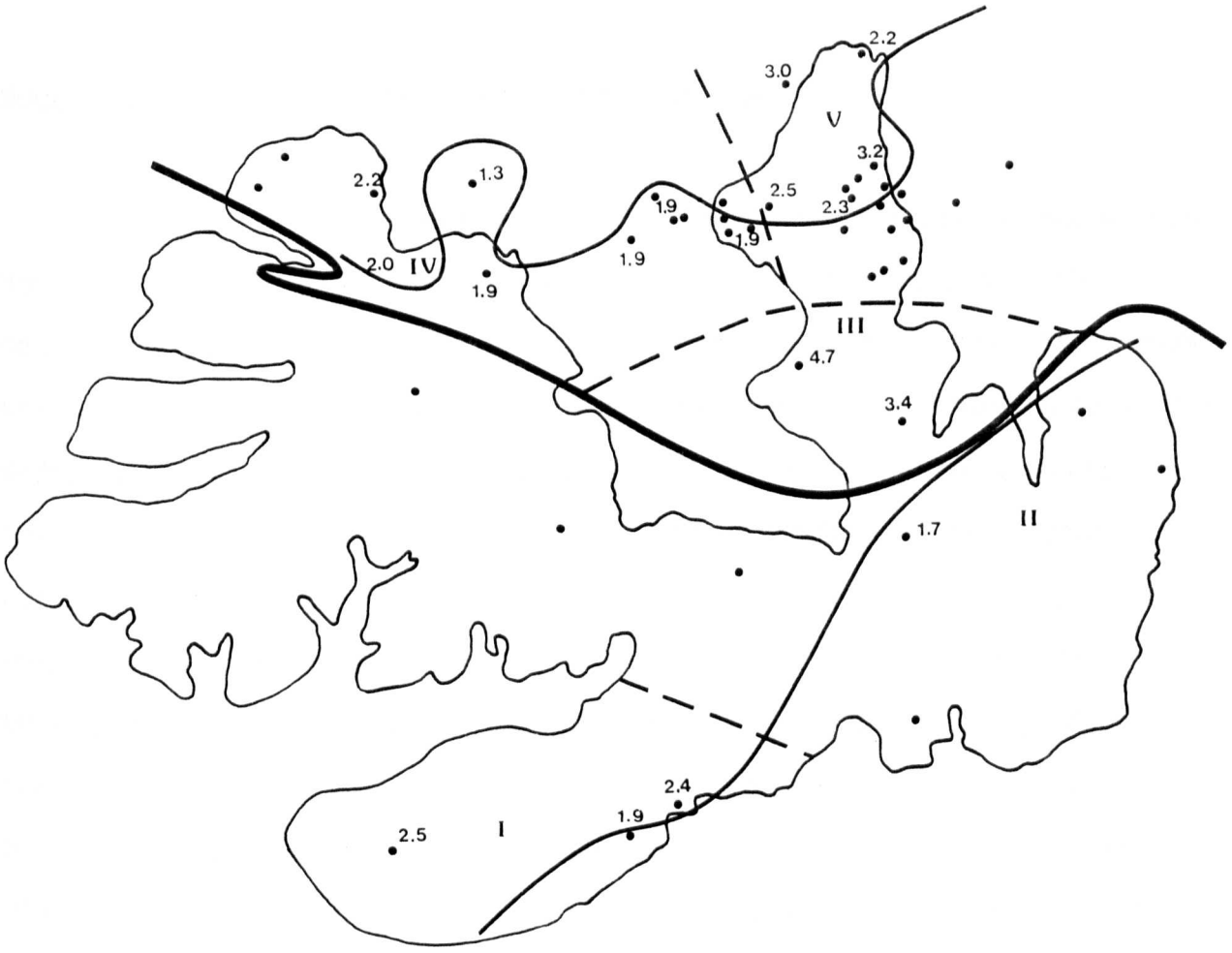

Figure 10-4 Contour map of present-day geothermal gradients (°C/100m)

radiogenic heat production in proportion to their thickness.

If spatial variation in heat production within basement rocks is not a major factor in affecting the geothermal gradient distribution, then variations in the thermal conductivity of the overlying sediment must be considered. It has been documented (Nassichuk, 1972) that a larger proportion of shale exists in the deeper parts of the Sverdrup Basin than in the marginal areas. The higher thermal conductivity of sandstone in comparison with shale means that thermal gradients in areas dominated by sandstone lithology will be lower than in those dominated by shale (Sass et al., 1971; Zierfus, 1969; Teichmuller and Teichmuller, 1982). Drake Point D-68 (Figure 9-1) is a good example illustrating the effect of thermal conductivity on geothermal gradient. The interval between 1,424 to 3,106 m is dominated by the Lower Triassic Bjorne sandstone which contributes to a present-day geothermal gradient of less than 20°C/km (~ 13°C/km), whereas the geothermal gradient of the interval above is 32°C/km, an interval dominated by shale, siltstone and only minor limestone and sandstone.

Higher thermal gradients within the Sverdrup Basin may be due to high-conductivity salt and anhydrite at depth and overall low conductivity of the overlying sedimentary succession. An example is drillhole Eldridge Bay E-79, located in the southern part of Sabine Peninsula. One of the highest present-day geothermal gradients (47°C/km) may be due to high-conductivity salt at depth and the overall low conductivity of the overlying shaley sediments. The Ordovician Bay Fiord Formation, a 250 m-thick salt and anhydrite unit, is present at 2,636 m and may be responsible for the high gradient of drillhole Eldridge Bay E-79 (Figure 9-8). In addition, the greater the proportion of shale the higher the thermal maturation of the sediments. An example is the relatively high geothermal gradient of Roche Point J-43 in which the proportion of the silty and shaley-dominated intervals is high (Figure 9-5).

The present-day geothermal gradient range in the Sverdrup Basin is 13 to 40°C/km, although some extreme values outside these limits do occur. High gradients (greater than 40°C/km) occur in the southern part of the Sabine Peninsula (Zone III) (Figure 10-4), whereas lower gradients (~ 20°C/km) are very common and occur in Zone IV in the northern Sabine Peninsula and the northern Sproule Peninsula (Figure 10-4). Even lower gradients (15°C/km) are characteristic of the Raglan Range area and of the central-east part of Melville Island (Zone II) (Figure 10-4).

The maturation-gradient map (Figure 10-5) does not show a high correlation with the present-day geothermal gradient map (Figures 10-4 and 10-5). The low geothermal gradient anomaly in the vicinity of the Kitson River C-71 is not reflected in its maturation gradient (the highest of all drillholes). To the contrary, the high geothermal gradient in Eldridge Bay E-79 is not reflected and has not resulted in a very high maturation gradient. The fact that there is no one-to-one correspondence of present geothermal anomalies to maturation-gradient anomalies suggests that the palaeogeothermal gradients were different from the gradients observed today, at least for some localities, for example the Raglan Range and the southern Sabine Peninsula. In geothermal problems both the regional maturity variation of a specific horizon or horizons and the maturation gradients should be determined.

Paleogeothermal conditions may be reconstructed by comparing the geothermal gradient (°C/km) and the maturation gradient (% log Ro/km). For instance, Kitson River C-71 and Apollo C-73, which lie in a geothermal 'high' have maturation gradients of 0.70% and 0.50% log Ro/km (Table 5), which are considerably higher than for most drillholes in Melville Island (0.15 - 0.20% log Ro/km) if a comparison is made over the same maturation range (0.7 - 1.5% Ro). These findings suggest a high palaeogeothermal gradient and a possible heat source at depth in the area of the two

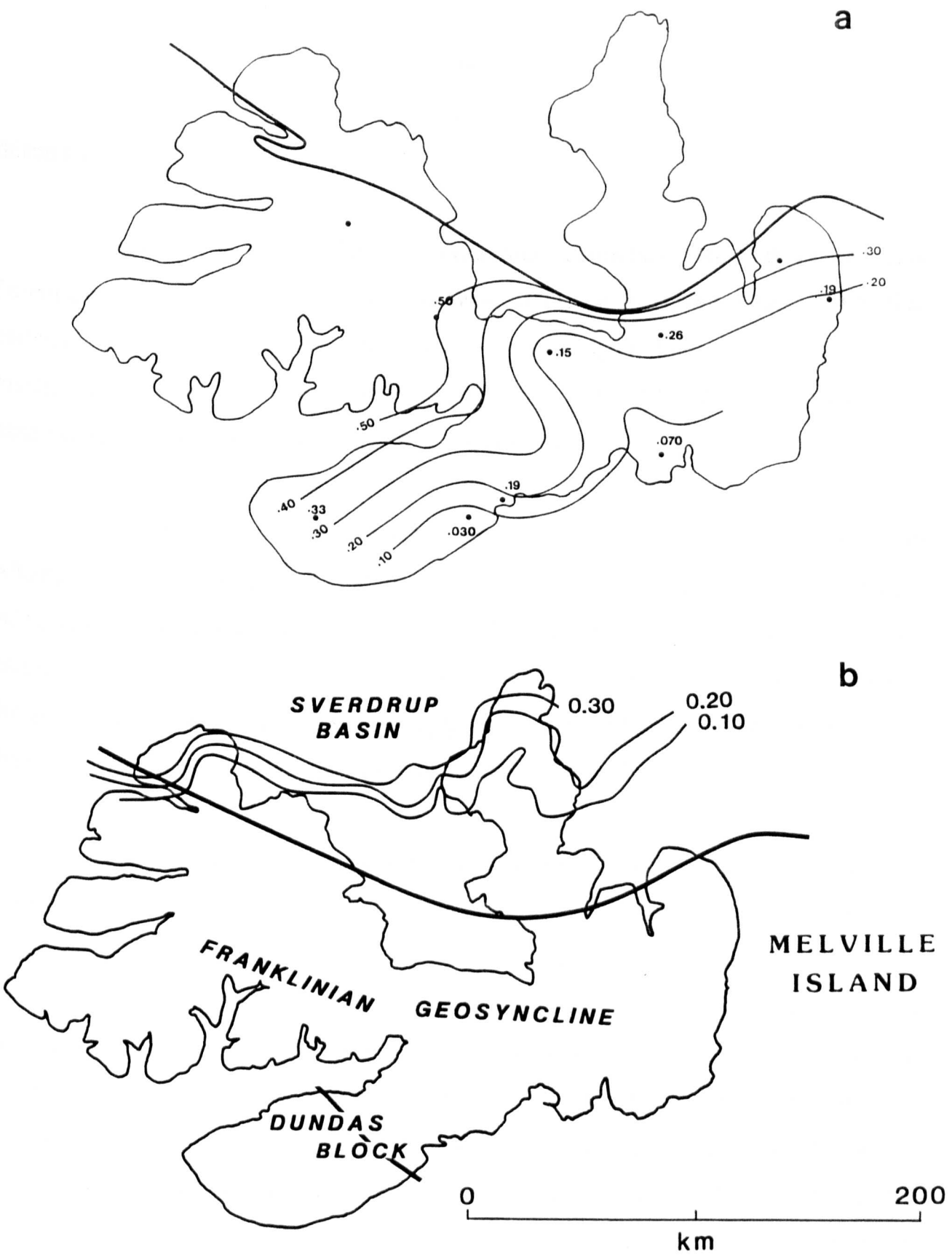

Figure 10-5 Maturation gradient contour map (% log Ro/km)

a) Palaeozoic Franklinian Geosyncline

b) Mesozoic Sverdrup Basin

drillholes.

There is a thick (>500 m) carbonate sequence (Allen Bay/Read Bay Formations) in the subsurface of Kitson River C-71. It is known (Clark, 1966) that carbonate rocks have thermal conductivity 3-4 times higher than clastic rocks. As a result, the high maturation observed in Kitson River C-71 in the sediments above the carbonates may be due to the presence of the carbonates.

There are distinct anomalies between present-day geothermal gradients and reflectance. One example is Eldridge Bay E-79 which has a high geothermal gradient (47°C/km) and a maturation gradient of 0.45% log Ro/km in the Ordovician to Devonian part of the succession and a 0.08% log Ro/km in the Pennsylvanian to Triassic part of the succession. These discrepancies suggest that the maturation pattern is not solely determined by the present-day geothermal conditions.

The strongly-matured Upper Palaeozoic and Triassic rocks of Eldridge Bay E-79, Roche Point J-43, and North Sabine H-49 point to maximum heating during the lower part of the Carboniferous. This maximum corresponds to the initiation of rifting in the western Sverdrup Basin. Balkwill and Fox (1982) indicate that the basin was initiated by episodic, incipient rifting that took place in three stages, the first being between the Carboniferous and Middle Jurassic. During periods of rifting, basins receive large volumes of sediment, thus increasing the sedimentation rate and the heat connected with it. Teichmuller and Teichmuller (1979) made similar observations in the Upper Rhine graben and attributed the maximum heat and high rate of sedimentation to an increase in rifting and spreading of the graben in recent times. Since there is no evidence of a shallow basement in the subsurface of Melville Island (Balkwill and Fox, 1982; Fox, 1985), then the possibility of the occurrence of deep-seated faults in the

subsurface of the above drillholes, which may act as conduits for hot fluids, should be considered. Furthermore, it appears that the correlation between burial depth and reflectance is closer than between present-day formation temperature and reflectance in some drillholes (i.e. Eldridge Bay E-79), whereas the converse seems to be true for other drillholes (i.e. Kitson River C-71).

When comparing drillholes Kitson River C-71 and Eldridge Bay E-79 it is noticeable that the thermal regime that existed in the Upper Palaeozoic and Mesozoic strata must have been quite different. For example, the Permian Trold Fiord at a depth of only 606 m has a reflectance in excess of 1.0% Ro in Kitson River C-71, whereas the same formation at a depth of 450 m has a reflectance of only 0.70% Ro in Eldridge Bay E-79. In both cases the effective maturation time was more or less the same, but the thermal and maturation gradients are very different (16°C/km and 0.70% log Ro/km for C-71 and 47°C/km and 0.08% log Ro/km for E-79), which shows that the high present-day geothermal gradient in Eldridge E-79 is most likely to be a relatively recent phenomenon (younger than Lower Triassic), although high heat due to the first phase of rifting cannot be excluded.

The thermal history of the Mesozoic succession in Melville Island may have been influenced by factors other than increased temperatures due to depth of burial. Previously, the principal factors that control geothermal gradient were discussed, namely differences in the primary heat flow related to tectonic phenomena, differences in the thermal conductivity of lithologic units and subsurface water flow.

To summarize, heat flux tends to be low in stable cratonic parts of the crust and high in orogenic areas and active rift zones (Balkwill and Fox, 1982). Salt is a very good heat conductor and salt domes rising from a 'mother' salt bed transfer heat rapidly

into overlying strata in a basin. High conductivity results in a low geothermal gradient for the salt but in a high geothermal gradient (low thermal conductivity) for the adjacent sediments. Shales have a poorer thermal conductivity when compared to sandstones: they impede heat flow and cause an increase in the geothermal gradient. Circulation of water has a strong influence on subsurface temperatures, usually as a warming agents.

10.4 ESTIMATION OF AMOUNT OF ERODED SECTION

The amount of eroded section in the Melville Island area was determined using the following methods:

a) stratigraphic and structural evidence;
b) extrapolation of % Ro gradients; and
c) comparison of paleogeothermal gradient to present-day thermal gradient.

a) From the work of Balkwill and Roy (1977) and Balkwill et al., (1982) on the nearby Lougheed Island, it is possible to infer an upper limit of about 1,300 m of eroded section on Melville Island with the average being approximately 1,000 m.

b) The thickness of the eroded section can be estimated by using the Dow (1977) method or the Middleton (1982) methodology. The thickness of eroded section is calculated under the assumption that the measured log-linear maturation gradient in the preserved section is representative of the maturation gradient in the eroded section. However, this assumption may not be valid because the strata may not have reached thermal equilibrium or because of differences in thermal conductivity of the two sections. Assuming a linear maturation gradient for the section with reflectance values less than 0.40% Ro may not closely approximate the gradient in the eroded section. A

non-exponential increase of maturity with depth at reflectances less than 0.4% Ro, which has been observed in some Melville Island drillholes, has also been shown by Bustin et al., (1977). Extrapolation of the maturation gradient above the present surface to an initial, reference Ro value may be made to estimate the thickness of the missing section. Using Dow's method the amount of eroded section varies considerably from drillhole to drillhole ranging between 700 and 2,000m (Table 6 and Appendix III). The upper range of Dow's method (1,400-2,400 m) is difficult to justify based on geological evidence. Knowledge of stratigraphy and geologic evidence from the study area is essential and provides important constraints upon such estimates.

c) A relationship between Ro and effective paleogeothermal gradient was given by Middleton (1982) as

$$dT/dZ = 194.8 \times d[\log (\% Ro)]/dz$$

where T is in °C and depth Z is in km. From the observed % Ro versus depth profiles, an effective paleogeothermal gradient can be calculated using the above relationship or that of Falvey and Deighton (1982). This calculated paleogeothermal gradient is then used as input to the computer program which calculates the time-temperature index (TTI) and vitrinite reflectance according to the Waples-Lopatin correlation (Waples, 1980). For further details on the computer program which calculates TTI versus Ro and paleogeothermal gradients using kerogen conversion kinetics, the reader is referred to Skibo et al., (1990). Solutions were iterated for choices of surface temperatures until satisfactory agreement between calculated and observed % Ro values was obtained. The calculated paleotemperatures are only slightly higher (~5°C) than present temperatures and at depth, within the uncertainties of the two methods of gradient calculation, both present and paleotemperature gradients (°C/km) are similar.

TABLE 6

Estimated Amount of Eroded Section (m)

Drillhole name	Estimated eroded section (m)
Dundas C-80	3,550 ± 500
Apollo C-73	3,300 ± 550
Hearne Point F-85	ndp
Winter Harbour #1	ndp
Beverley Inlet G-13	ndp
Zeus F-11	3,450 ± 500
Sabine Bay A-07	ndp
King Point West B-53	3,654 ± 460
Towson Point F-63	ndp
Richardson G-12	3,519 ± 600
Drake Point D-68	2,900 ± 570
Chads Creek B-64	3,050 ± 425
Hecla J-60	2,600 ± 750
Depot Island C-44	3,200 ± 250
Roche Point J-43	1,616 ± 425
North Sabine H-49	1,211 ± 740
Weatherall O-10	2,803 ± 920
Eldridge Bay E-79	ndp
Kitson River C-71	1,076 ± 430
Sharard Bay F-34	ndp
Sherard Bay F-14	ndp
Marryatt K-71	ndp
Collingwood K-33	ndp
Drake L-67	ndp
Drake Point K-79	ndp
Drake F-76	1,060 ± 625
Drake E-78	2,164 ± 460
Drake B-44	ndp
Drake D-73	ndp
Drake F-16	1,909 ± 550
Drake P-40	1,940 ± 575
East Drake I-55	1,358 ± 510

TABLE 6 (continued)

Drillhole name	Estimated eroded section (m)
Hecla South West C-58	2,100 ± 520
Hecla West P-62	258 ± 170
North West Hecla M-25	477 ± 180
Hecla West N-52	1,875 ± 650
Hecla West C-05	1,812 ± 180
Hecla I-69	1,375 ± 750
Hecla F-62	2,250 ± 400
Hecla C-32	2,080 ± 540
Marie Bay D-02	2,158 ± 840
Sandy Point L-46	ndp
Grassy I-34	90 ± 625

ndp The amount of eroded section estimated was considered unrealistic based on stratigraphic and structural evidence and not recorded.

10.5 BURIAL HISTORY PLOTS

10.5.1 INTRODUCTION

The method of Waples (1980), as modified by Wood (1988) is used for estimation of organic maturity level. The thickness of the eroded Tertiary strata was estimated in terms of the timing of the Eurekan Orogeny (Mid-Eocene to Oligocene), obtained from the work of Riediger et al., (1984). The magnitude and timing of heat flow of the previous rifting interval (Early Cretaceous, Valanginian - Upper Deer Bay to earliest Late Cretaceous, Cenomanian - top of the Hassel Formation) are obtained from Stephenson et al., (1987). In this work, estimation of the eroded Tertiary section made by Balkwill et al., (1982) in the adjacent Lougheed Island was used. The rate of uplift/erosion was assumed to be continuous, occurring between 27.5 and 5 Ma.

The present day temperature gradients obtained from corrected bottom-hole temperatures, calculated equilibrium bottom hole temperatures (from well logs) and drillstem testing vary considerably, ranging between about 15 and 34°C/Km. Jones et al., (1989) determined gradients between 24 and 34°C/Km for three drillholes in the study area. Further, they also observed that geothermal gradient is not constant with depth.

10.5.2 THERMAL HISTORY OF MELVILLE ISLAND (MODELLING)

A computer program was used which calculates and draws the burial history curves of a stratigraphic section as determined from lithostratigraphic and biostratigraphic analyses of drillhole data. Burial history diagrams, showing depth of stratigraphic units below the active surface of deposition as a function of time, were

generated for selected drillholes in the Melville Island area (Figure 10-6 to 10-13). The variation of the 'oil window' as a function of depth and geologic age is plotted on these diagrams. Inferred thermal maturity in terms of Ro is calculated for the stratigraphic section throughout the burial history. The burial histories were iterated until calculated Ro profiles agreed, within statistical uncertainty, with the observed Ro. Similarly, broad agreement was obtained between calculated transformation ratios from the thermal models and transformation ratios calculated from Rock-Eval measurements. To assist in the evaluation of petroleum potential of source rocks and to better understand the timing of significant oil generation, burial history plots were constructed for eight drillholes, five from the Sverdrup Basin, one from northwestern Melville Island and two from the Franklinian miogeosyncline, based on geographical distribution and the availability of complete geological and geothermal data.

The plots of the North Sabine H-49 and Roche Point J-43 drillholes are similar (Figures 10-6 and 10-7). Sedimentation for all formations appears to have been continuous from approximately 250 Ma to 120 Ma. In the case of H-49 a short period of rapid uplift and erosion took place between 120-110 Ma and the formations were buried at a very fast rate from 110-100 Ma. Finally, sedimentation was normal from 100-30 Ma, but it was terminated by an uplift during the last 25-30 Ma. The fast rate of sedimentation at 110-100 Ma is correlated with the deposition of the Christopher Formation shales: the uplift in the last 25-30 Ma is due to the Eurekan Orogeny. It can be seen (Figure 10-6) that the deepest formation of the Schei Point Group (Murray Harbour) entered the oil-generation zone (0.7% Ro) at approximately 80 Ma and the gas-generation zone at 42 Ma. The youngest formation within the 'oil window' (Ringnes) entered it at approximately 30 Ma, whereas the youngest member to exit from the 'oil window' (Chads Point) left at <10 Ma.

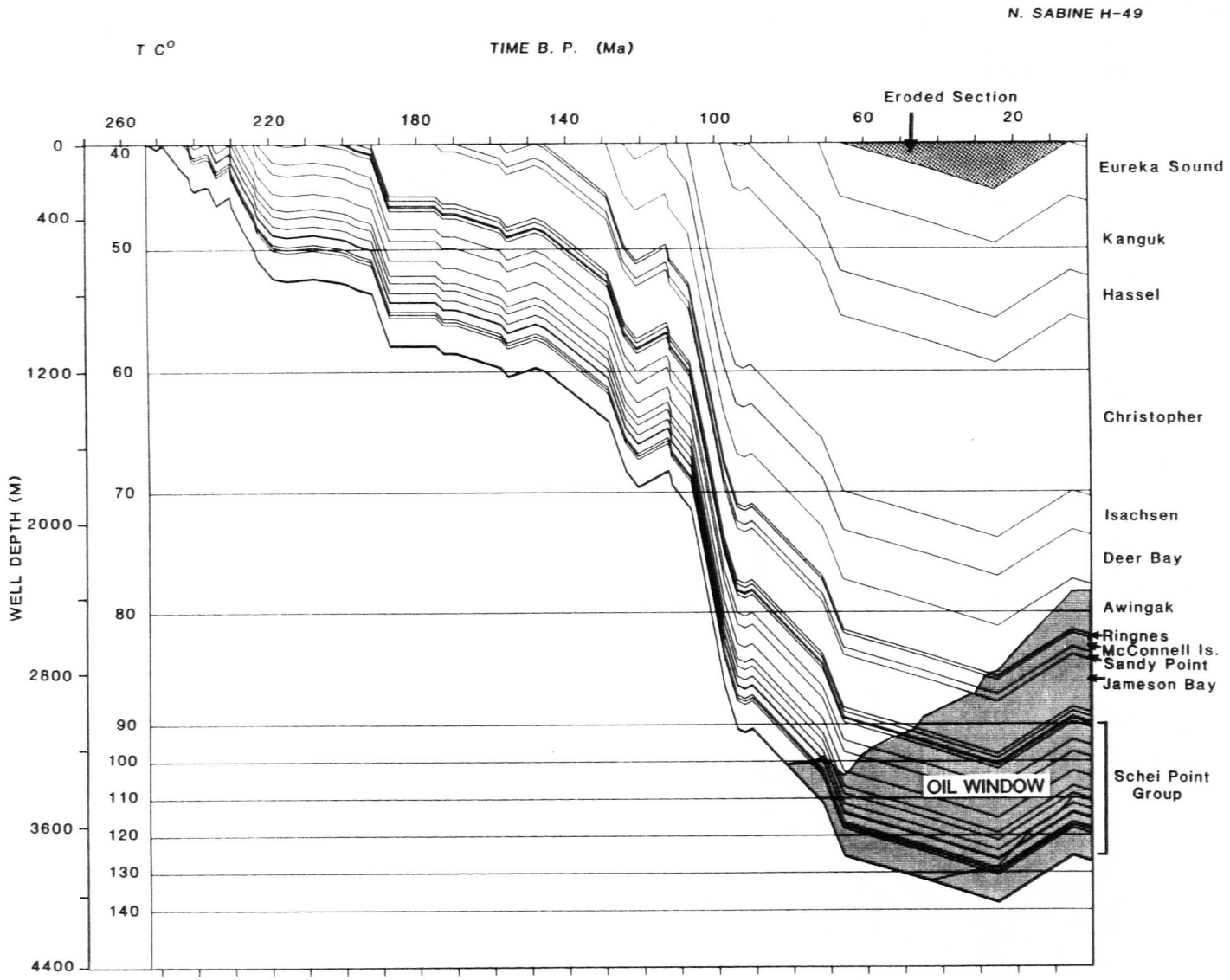

Figure 10-6 Burial history plot of Panarctic North Sabine H-49. Hatched area represents the 'oil window'

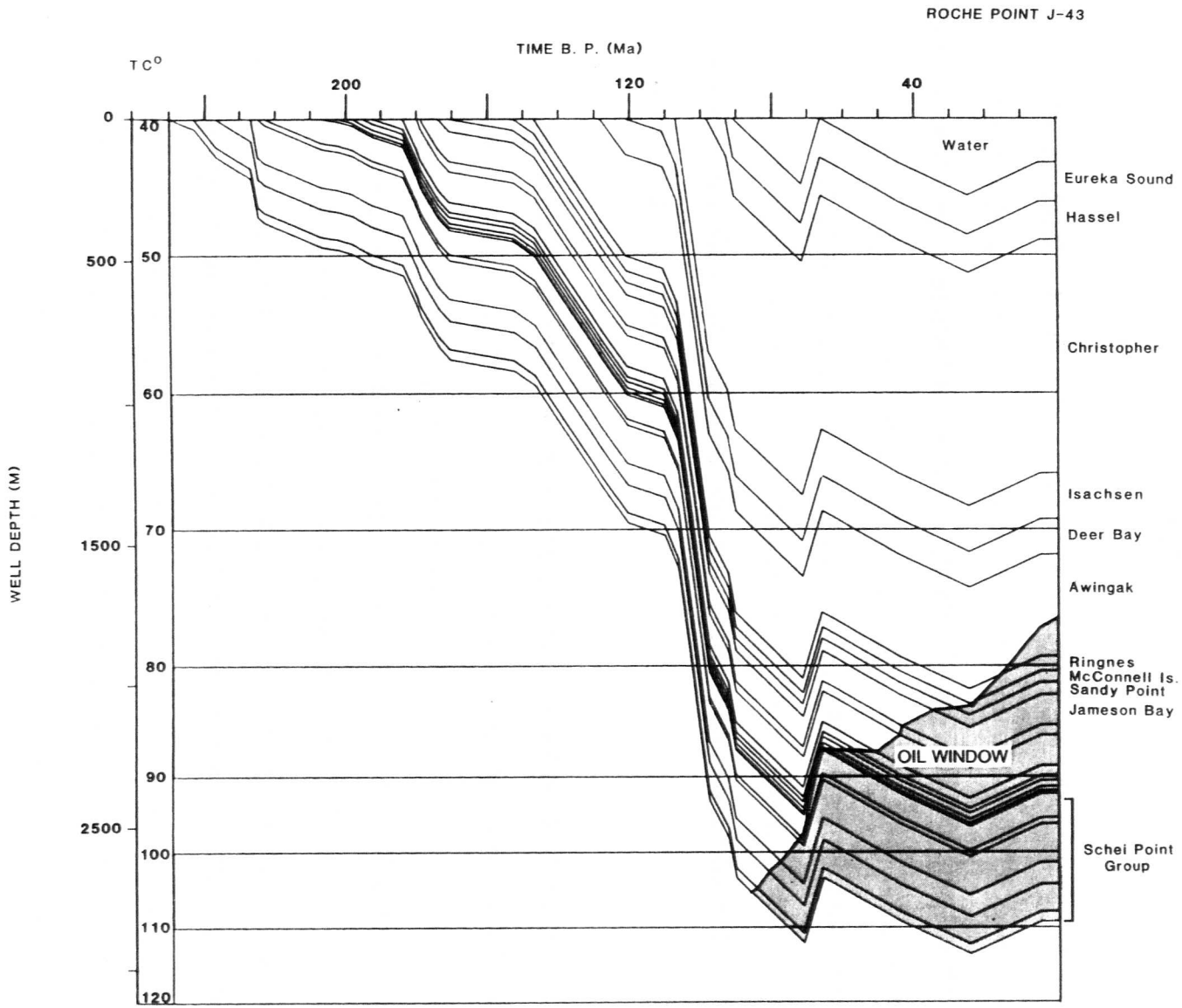

Figure 10-7 Burial history plot of Panarctic Roche Point J-43

In the Roche Point J-43 case, an even more pronounced burial has taken place between 110-100 Ma, due to the rapid sedimentation of the Christopher shales. In addition, a relatively rapid uplift and erosion followed from 75-65 Ma, then the formations were buried again slightly deeper than before the uplift. Finally, they were uplifted and eroded in the last 30 Ma due to the Eurekan Orogeny. The oldest member to enter the 'oil window' is Eldridge Bay (at approximately 95 Ma). The youngest formation within the 'oil window' is the Ringnes. None of the formations penetrated has exited from the hydrocarbon-generation zone.

The burial curves for the Hecla J-60 and Chads Creek B-64 drillholes are very similar (Figures 10-8 and 10-9). Both curves are dominated by rapid sedimentation and burial between 260-250 Ma at the boundary between the Upper Palaeozoic and Mesozoic. Sedimentation was continuous until 110-100 Ma, followed by a steep increase in burial due to the fast deposition rate of the Christopher shales. The noticeable feature of the burial curves is the great similarity in the burial history during the last 100 Ma. There has been relatively little uplift in the last 20 Ma. The oldest formation to enter the oil-generation zone in Hecla J-60 (Van Hauen) entered at approximately 180 Ma and the youngest Formation (Bjorne) at 85 Ma. In Chads Creek B-64, the oldest formation (Hare Fiord) entered the 'oil window' at approximately 215 Ma, the youngest Bjorne at 95 Ma. In addition, the oldest formation to exit from the above zone (Blind Fiord) left at 95 Ma. The present-day 'death' of the oil zone is located at approximately 3,800 m within the Van Hauen Formation.

The burial plot of the Drake D-68 drillhole (Figure 10-10) appears different from those described. The burial of the Upper Palaeozoic succession in Drake D-68 is comparable with that of the same succession in Chads Creek B-64. A similar observation can be made for the Mesozoic strata which have been exposed to

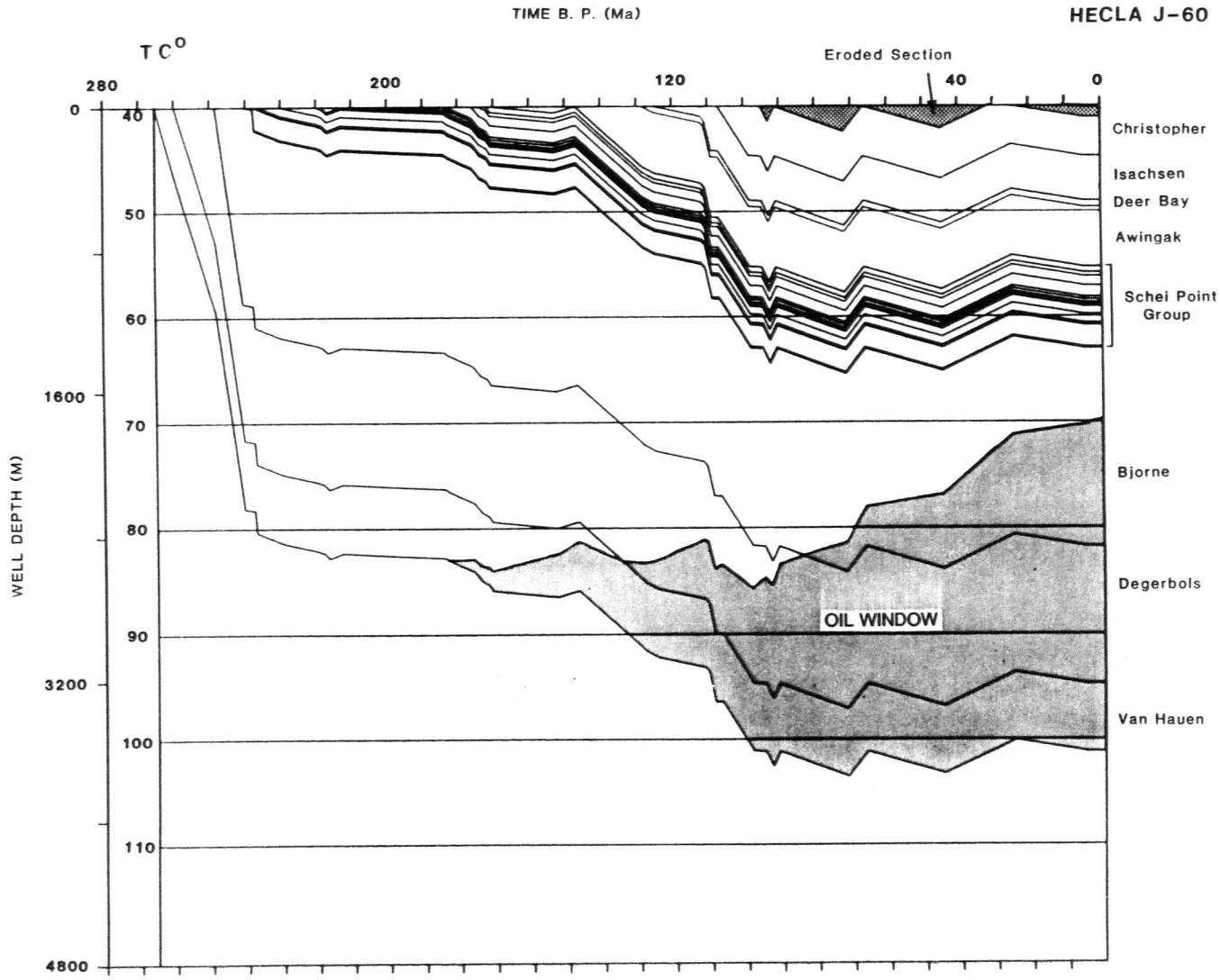

Figure 10-8 Burial history plot of Panarctic Hecla J-60

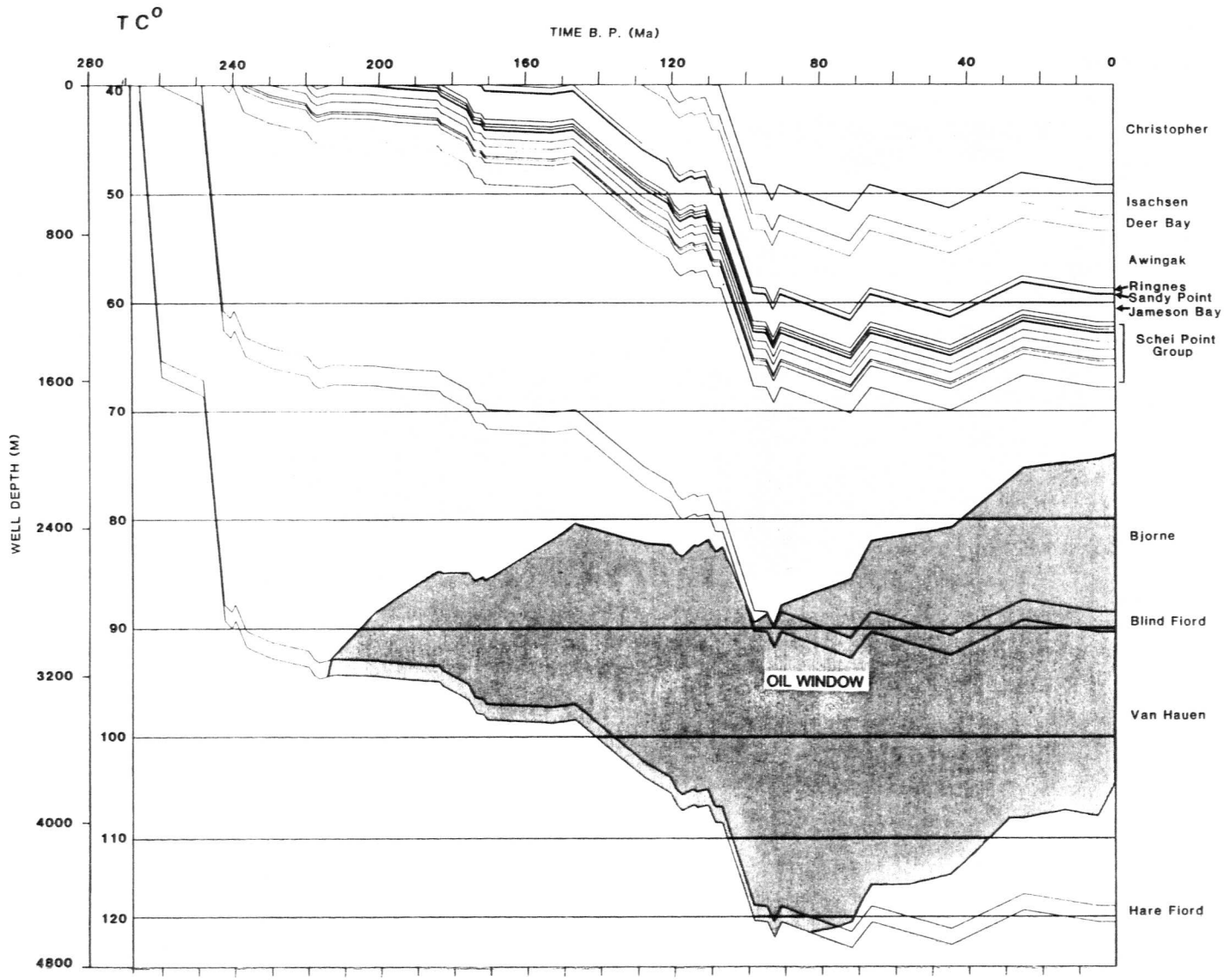

Figure 10-9 Burial history plot of Panarctic Chads Creek B-64

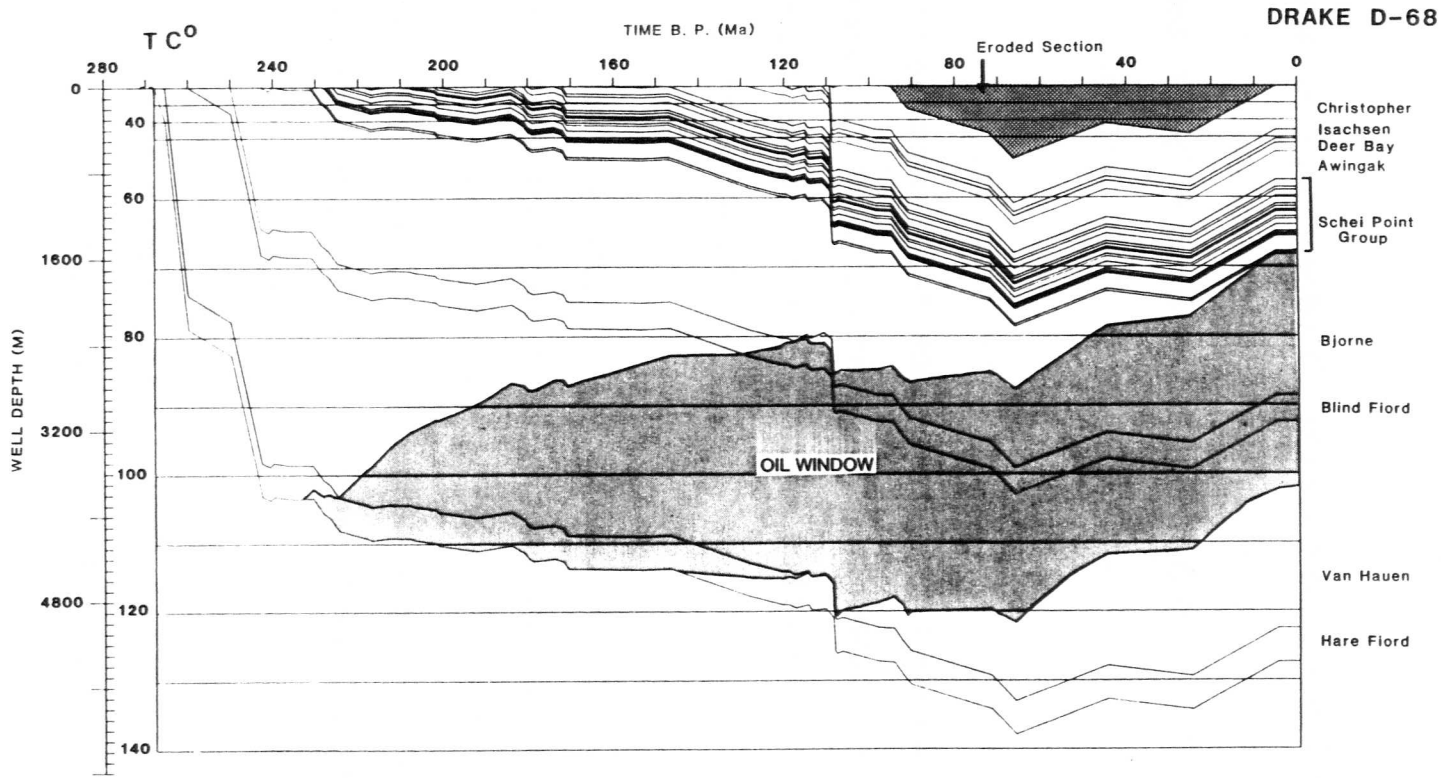

Figure 10-10 Burial history plot of Panarctic Drake Point D-68

temperatures higher that 80°C. The same strata in both Hecla J-60 and Chads Creek B-64 have also experienced temperatures less than 80°C at different time intervals, whereas in Roche Point J-43 and North Sabine H-49, the formations were exposed to much higher temperatures, of the order of 120-140°C.

The burial plot of Drake D-68 shows the rapid burial due to deposition of the Christopher shales. The oldest formation to enter the oil window is Hare Fiord at approximately 230 Ma, the 'onset' to the 'oil window' is estimated at about 1,100 m, at the base of the Jameson Bay Formation, and the oil 'deathline' is located within the Van Hauen shales at 3,700 m.

The burial plot of Depot Island C-44 (Figure 10-11) reflects the deep burial (>6,000 m) that the Lower Palaeozoic formations experienced prior to the uplift and erosion resulting from the Ellesmerian Orogeny. The top of the 'oil window' was near the surface (<800 m) by 320 Ma. Subsequently, the Upper Palaeozoic and Mesozoic formations subsided continuously and the Canyon Fiord was buried at >3,000 m by 50 Ma, experiencing temperatures around 75-80°C. At approximately this time, the formations were uplifted and eroded due to the Eurekan Orogeny, resulting in their present-day drilled depth. The oldest formation from the succession above the major unconformity to enter the 'oil window' is the Pennsylvanian Canyon Fiord at 70 Ma.

The burial plot of Apollo C-73 and Dundas C-80 are similar (Figures 10-12 and 10-13). They both show a rapid burial starting at approximately 380-390 Ma and continuing until 280-290 Ma. At this time the deepest formation in Apollo C-73 (Eleanor River) was buried to more than 5,000 m and experienced temperatures of the order of 140C. In addition, the deepest formation in Dundas C-80 (Thumb Mountain) was buried more than 5,500 m and experienced temperatures of about 130°C.

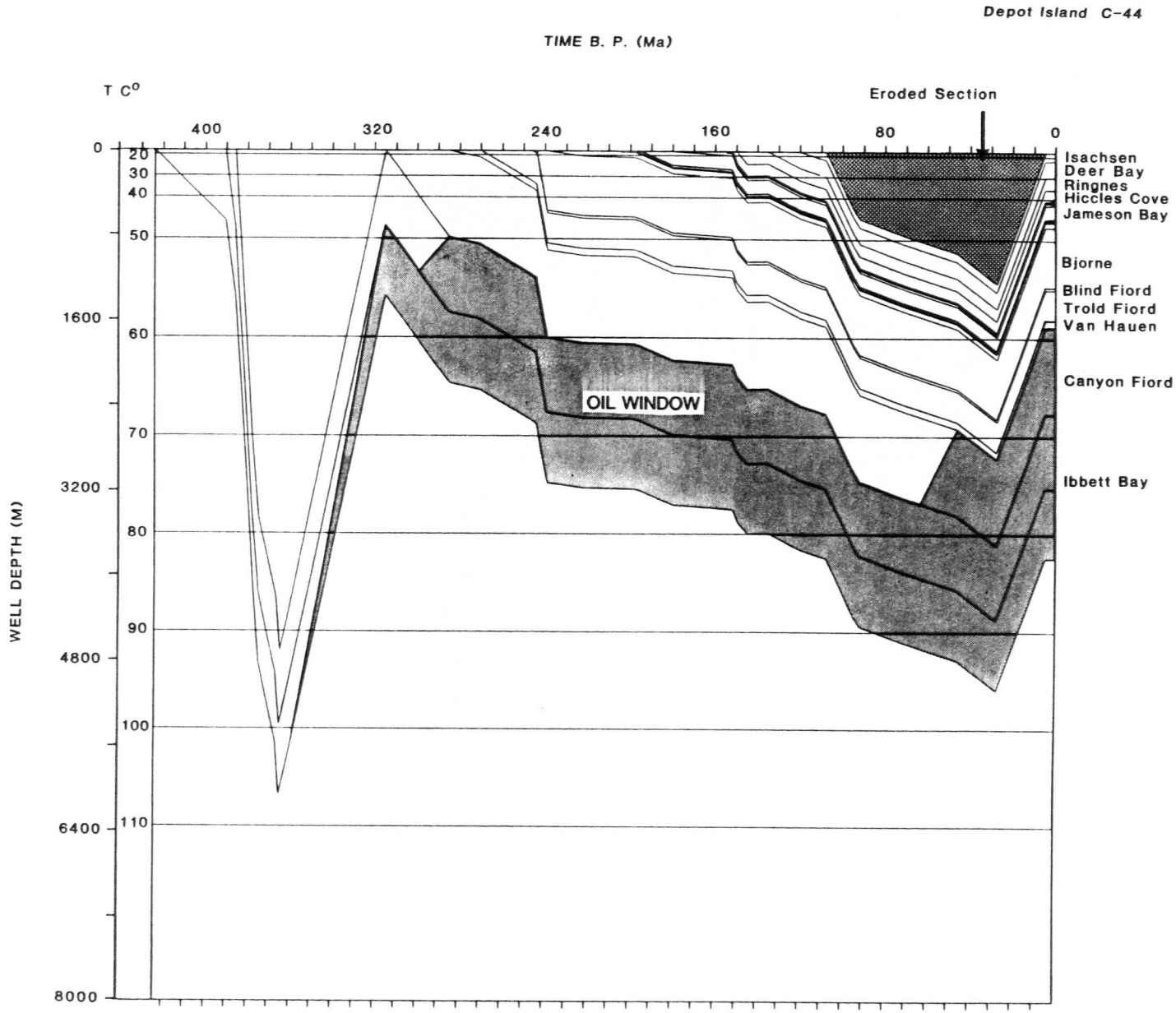

Figure 10-11 Burial history plot of Panarctic Depot Island C-44

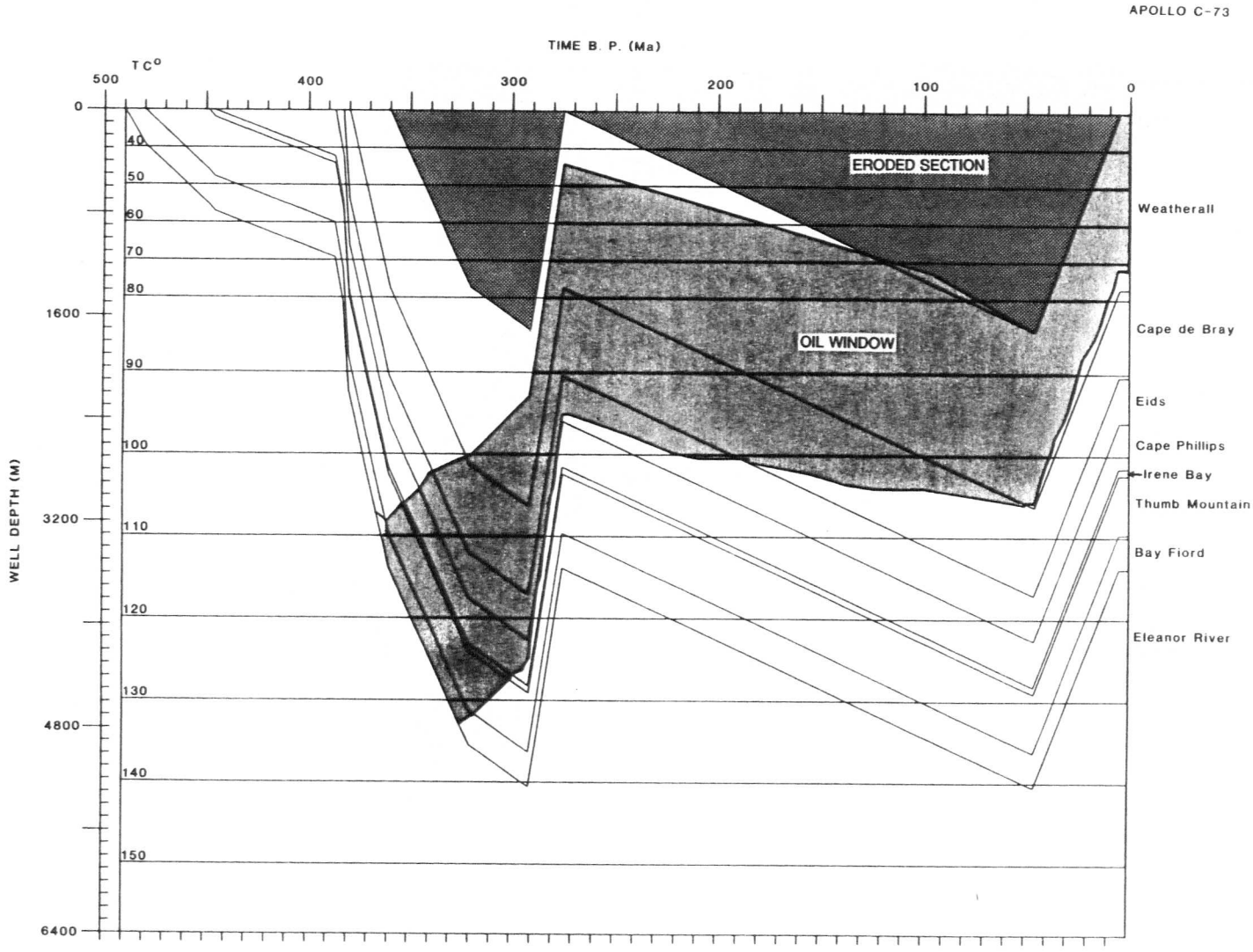

Figure 10-12 Burial history plot of Panarctic Apollo C-73

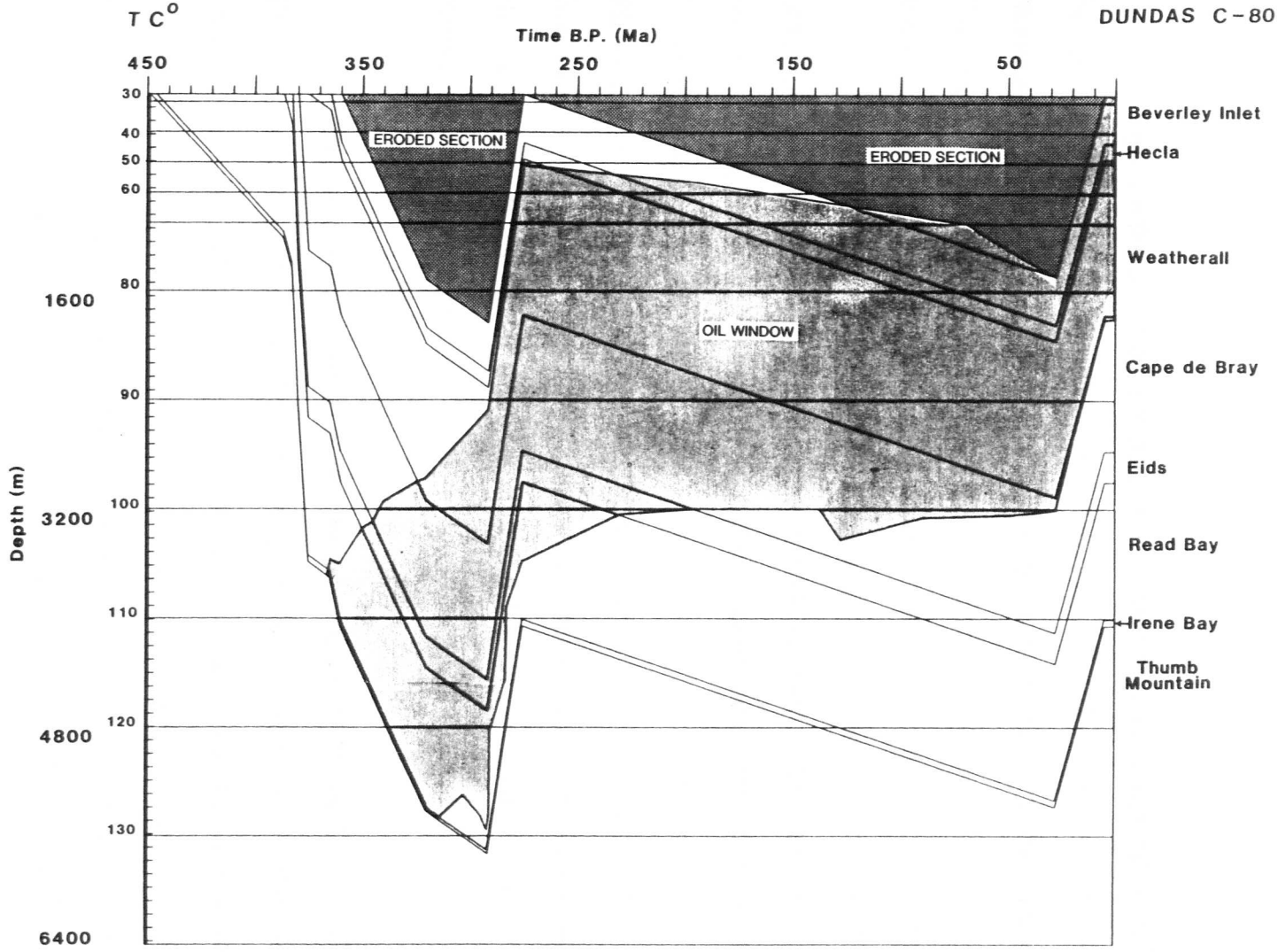

Figure 10-13 Burial history plot of Panarctic Dundas C-80

Both drillholes were affected by the Ellesmerian Orogeny at 270-280 Ma and the uplift and subsequent erosion are estimated at 2,000 m. Following the orogeny, the Palaeozoic formations continued to subside at a rate lower than that before the orogeny. The Eleanor River in Apollo C-73 was subsequently buried at >5,000 m and experienced temperatures of 130°C before being uplifted, along with the younger formations, to its present day depth by the Eurekan Orogeny at 50 Ma. Similarly, the Palaeozoic formations of Dundas C-80 continued to subside following the Ellesmerian Orogeny and the Thumb Mountain was buried at >5,000m experiencing temperatures of 125°C. The Eurekan Orogeny at 25 Ma uplifted and eroded the formations to their present-day drilled depth. Since Dundas C-80 is located to the south of Apollo C-73 and the Eurekan Orogeny had a south-southwestern direction, it becomes apparent that it affected Apollo C-73 earlier than Dundas C-80, thus resulting in the 25 Ma difference between the two drillholes.

The oldest formation to enter the 'oil window' in Apollo C-73 is Eleanor River at 380 Ma and the youngest is Weatherall at 120 Ma. The Eleanor River exited from the 'oil window' at 320 Ma and the youngest formation to leave the same zone is Eids at 50 Ma. In Dundas C-80, the oldest formation to enter the 'oil window' is Irene Bay at 370 Ma and the youngest is the Beverley Inlet at 230 Ma. The Irene Bay left the above zone at 315 Ma, whereas the youngest formation to exit is Cape de Bray at 35 Ma.

Basinwide thermal subsidence alone cannot fully account for the relatively high degree of organic maturity, particularly in near-surface samples i.e. 0.5 to 0.6% Ro. Consequently, it is assumed that a heating event associated with periods of renewed rifting and associated igneous activity throughout time is in part responsible for elevated near-surface maturation levels.

During times of renewed rifting an efficient mechanism for surfaceward heat transfer is magmatic intrusion (Stephenson et al., 1987). This elevated heat flow plus thermal blanketing effects of relatively thick (1,000 m) but subsequently eroded Tertiary strata are thought to account for the high maturity of the near surface section. A similar mechanism is envisaged by Cardott and Lambert (1985) who have studied the thermal maturation of the Woodford shale, Anadarko Basin, Oklahoma and stated that "...if subsidence was caused by cooling, then maximum heat flow occurred at the beginning of increased subsidence". This effect has been modelled in this work through use of the relationship given by Royden (1986). By analogy, it is proposed here that enhanced thermal maturation of the near surface sediments occurred during and after the renewal of rifting in Cretaceous time. These Late Cretaceous-Early Tertiary sediments are thought to have been more deeply buried prior to uplift and erosion commencing at about time during the Eurekan Orogeny.

Since geohistory modelling evaluates the integrated effect of time and temperature on the maturation of organic matter in sediments, data on the history of subsidence and uplift and on the thermal history of the sediments is required. Near surface gradients average about 45°C/Km, while in the depth range 1.5 to 4.0 km the gradients vary between 20 and 30°C/Km. However, the depth range of the permafrost base is from zero (sub-sea) to 726 m and Jones et al., (1989) note that shallower BHT data can be unreliable. Jones et al., (1989) suggest either an unresolved temperature disturbance due to drilling or else due to disequilibrium gradients caused by the effects of coastal sea-level changes or Quaternary glaciation. The data used in the model for the Melville Island sedimentary successions, such as maximum depth of burial is consistent with stratigraphic observations and temperature profiles and agree with the results of Jones and Majorowicz (1987), indicating that the paleo- and present thermal gradients are similar (i.e. 20-30°C/Km) and that heat flow has varied by only about 15%

over the history of the Sverdrup Basin (Skibo, pers. commun., 1990).

CHAPTER XI

CHAPTER XI

INTRODUCTION

During the past twenty years the Geological Survey of Canada has developed a petroleum resource evaluation program with an emphasis on assessing the play level (Powell and Snowdon, 1983). Much of the organic petrological and organic geochemical work that has been done in Canadian sedimentary basins attempts to answer certain questions, such as the potential of the sedimentary succession to generate hydrocarbons, the nature of the hydrocarbon product, relationships between source rocks and reservoired hydrocarbons, the presence of migration and the timing of hydrocarbon generation and trap formation. This chapter is mainly concerned with the organic petrological characteristics of some well-known sedimentary basins in Canada, followed by a comparison between Sverdrup Basin in Canada's Arctic and the other sedimentary basins. These basins include: the Lower Cretaceous to Tertiary Beaufort-Mackenzie Basin, the Palaeozoic of the Williston Basin, Saskatchewan, the Mesozoic of southern Saskatchewan, the Palaeozoic and Mesozoic of Alberta, the Tertiary of the Queen Charlotte Islands, the Jeanne d'Arc Basin, east of Newfoundland, and the Scotian and Labrador Shelves. In addition, potential source-rocks of Devonian age from Ontario and the N.W.T., Canada will also be discussed.

11.1 BEAUFORT-MACKENZIE BASIN

The Upper Cretaceous to Tertiary sedimentary succession in this basin contains significant quantities of gas-condensate and light oil (Powell and Snowdon, 1983). It has been demonstrated by Snowdon (1980) and Snowdon and Powell (1982) that terrestrial organic matter enriched in plant resins is possibly the source of

naphthenic oils generated at maturity levels of <0.55% Ro and gas-condensate generated at reflectance levels of >0.55% Ro. The proportion of resinite in the organic matter reaches 10-15% and has been the source for significant quantities of condensate and oil. According to Snowdon (1980) the oils from the Mackenzie Delta are naphthenic and low in wax, contradicting the highly waxy character of oils expected from terrestrial sources. In addition, the gas generated in the Beaufort-Mackenzie Basin, at vitrinite reflectance levels of 0.45 - 0.60% Ro is not biogenic but thermogenic gas. A model for oil and gas-condensate generation from terrestrial organic matter was developed by Powell and Snowdon (1983), which incorporates the gas generation of Monnier et al., (1983). The results of Monnier et al., (1983) show that in the reflectance level of 0.55 to 0.65% there is at least a five-fold increase in gas yield, per unit weight of organic carbon, from Type III organic matter. Possible mechanisms for the formation of methane from Type III organic matter in the early stages of maturation include the loss of methoxy groups and disproportionation reactions in the kerogen structure (Powell and Snowdon, 1983).

11.2 LOWER PALAEOZOIC OF THE WILLISTON BASIN

A tremendous petroleum potential in excess of 5 billion bbls of oil equivalent is believed to be present in the Ordovician source rocks in the Canadian portion of the Williston Basin, southern Saskatchewan (Osadetz et al., 1989). Most of the source rocks are thermally immature and only a small fraction, a total of 193,000,000 bbls of oil is inferred to have migrated out of the source rocks.

Several intervals have been identified as potential source rocks in the Canadian portion of Williston Basin (Osadetz and Snowdon, 1986a, 1986b; Osadetz et al., 1989). The family of oils occurring primarily in Ordovician reservoirs has been

attributed to potential source rocks in the Winnipeg Formation (Williams, 1974) and to rich 'kukersitic' beds within the Yeoman Formation of the Bighorn Group.

The thickest potential source-rock intervals within the Winnipeg Formation occur in black, fissile and thinly-laminated shales. Organic matter consists of alginite (Gloeocapsomorpha prisca) (Zalessky, 1917) associated with acritarchs and chitinozoa, therefore, it is entirely marine in origin and hydrogen indices (HI) range from 368 to 924 mg HC/g Corg, characteristic of Types II and I organic matter.

In the Yeoman Formation, the source rocks occur as thin laminae of pale yellowish-brown, bituminous lime mudstones (Osadetz et al., 1989). Organic matter is Type I marine (exclusively of Gloeocapsomorpha prisca), the HI values are commonly over 800 mg HC/g Corg and the OI values are less than 20 mg CO_2/g Corg. The work of Osadetz et al., (1989) on the Canadian part of the Williston Basin indicates that burial depth alone was neither sufficient to generate oil on a regional scale nor the sole control on the thermal maturity of these source rocks.

The fundamental control on the hydrocarbon potential of Ordovician rocks in the Canadian part of the Williston Basin is due to the presence of an ancestral crustal structure, the present expression of which is called the Nesson Anticline. The pattern of thermal maturity and rate of hydrocarbon generation in Upper Ordovician kukersites indicates geothermal gradients of the order of 40°C/km at least since Late Mesozoic (Osadetz et al., 1989). These elevated geothermal gradients, which are similar to those currently observed by Majorowicz et al., (1986) in Palaeozoic rocks in the Williston Basin, are believed to have controlled the generation of hydrocarbons in a region which was insufficiently buried for generation of hydrocarbons to occur.

11.3 MESOZOIC OF SOUTHERN SASKATCHEWAN

The only sediments in the Mesozoic in Saskatchewan which are mature with respect to hydrocarbon generation occur in the Jurassic. The Vanguard, Gravelbourg and Watrous Formations in certain locations contain up to 10% hydrogen-rich kerogen consisting of bituminite, marine alginite, dinoflagellates, Botryococcus, cutinite and matrix bituminite (Stasiuk, 1988). Hydrogen indices and S2 values from Rock-Eval are moderate for the Vanguard (32 mg HC/g Corg and 14.32 wt%), Gravelbourg (274 and 4.90) and Watrous Formations (414 and 21.75), (op. cit., 1988).

None of the Cretaceous strata examined by Stasiuk (1988) is within the hydrocarbon generation zone. However, intervals containing hydrogen-rich, marine organic matter have been observed in the Joli Fou Formation (op. cit., 1988).

Numerous strata in the Cretaceous contain concentrations of up to 10% amorphous organic matter (bituminite Types II and I). Morphologically-intact, marine phytoplankton such as dinoflagellates, alginite, and zooplankton are commonly associated with amorphous kerogen and matrix bituminite in the Colorado Group. Terrestrial contributions are present in the form of Types III and IV organic matter, microspores and traces of resinite and cutinite (Stasiuk 1988). The origin of the natural gas in the Cretaceous in Saskatchewan is most likely biogenic, as reported for equivalent rocks in north-central Montana (Rice and Shurr, 1980). A three-stage model for the generation of biogenic gas was also proposed by Stasiuk (1988).

11.4 DEVONIAN SOURCE-ROCKS IN THE ALBERTA BASIN

The Upper Devonian Duvernay Formation is an organic-rich basinal carbonate

succession that has sourced most of the oil presently reservoired in Leduc reefs of east-central Alberta. It accumulated in deep water anoxic bottom conditions that allowed preferential preservation of organic material and slow sedimentation rates resulted in a rich source rock (Stoakes and Creaney, 1984). Rich source intervals occur as dark to black laminites interbedded with leaner bioturbated lime mudstones.

11.5 MESOZOIC OF THE WESTERN CANADA BASIN

Triassic rocks are active exploration targets in the Alberta Basin and Triassic reservoir rocks are the most prolific in terms of volume of recoverable oil per volume of rock in the entire Western Canada Basin (Podruski et al., 1988). However, relative to the other source rock-reservoir systems, for example the Devonian System, Triassic source rocks have limited hydrocarbon potential due to their restricted distribution.

Riediger et al., (1991) studied Triassic oils and potential Mesozoic source rocks in the Peace River Arch area of the Western Canada Basin. Good to excellent source rocks were identified in the Middle Triassic lower Doig Formation and the Lower Jurassic 'Nordegg' Member. Total organic carbon content in the Doig Formation ranges up to 9.5 wt % and in the 'Nordegg' Member up to 23.6 wt %. The basal Doig Formation contains mainly Type II organic matter, whereas the 'Nordegg' Member is characterized by Type I organic matter.

Lower to Middle Triassic outcrop samples showed variable maturity and hydrocarbon potential. Triassic strata range from mature to overmature but no clean correlations of extracts from Triassic outcrop units to reservoired hydrocarbons could be established. Recently, light oil has been discovered at the Brassy field, near Dawson Creek, British Columbia, thus confirming that liquid hydrocarbons can be found in the

area. Riediger et al., (1991) were able to assign the Triassic oils to two groups based on biomarker characteristics, oils from Group 1 being sourced by the Doig Formation and oils from Group 2 being sourced from the 'Nordegg' Member.

11.6 QUEEN CHARLOTTE ISLANDS

As part of a study to evaluate the level of organic maturation and source-rock potential of the Phanerozoic succession in the Queen Charlotte Islands, surface exposures on Graham Island and core and drillhole cuttings from exploratory drillholes were analyzed.

The Neogene Skonun Formation comprises more than 4,500 m of nonmarine and transitional marine strata (Higgs, 1989). On Graham Island the formation is mainly immature with respect to oil generation, whereas in Hecate Strait and Queen Charlotte Sound the formation varies from immature to overmature (Vellutini and Bustin, 1988). The source rock potential of the strata is probably poor to moderate. Generally, the organic matter is gas prone Type II or Type III with low hydrogen and production indices. Locally, there are intervals with Type I or Type II organic matter, with hydrogen indices up to 450 mg HC/g Corg, production indices up to 1.0, and total organic carbon values up to 10.0 wt % (Bustin et al., 1990). There is no apparent stratigraphic or lateral variation in source rock quality and total organic carbon contents are higher on Graham Island and in northern Hecate Strait than in Queen Charlotte Sound.

11.7 JEANNE D'ARC BASIN, EAST OF NEWFOUNDLAND

Until the present time, significant discoveries of offshore hydrocarbon accumulations have been made only on the Canadian portion of the North American

eastern continental margin. While the discoveries off the Nova Scotian and the Labrador coasts are mainly gas, the Jeanne d'Arc Basin is the site of many significant oil discoveries and has a relatively small proportion of gas (Grant et al., 1986a and b). The potentially commercial oil reserves in this basin reflect the favourable association of a mature, organic-rich, oil-prone source rock, good reservoir beds and trapping mechanisms, proper timing of trap formation and good migration pathways.

Geochemical studies conducted by the Geological Survey of Canada on the oils and sediments of the Jeanne d'Arc Basin have provided a good understanding of hydrocarbon generation and entrapment in that area. The work of Powell (1984); Grant et al (1986a and b); McAlpine et al., (1986); McAlpine and Grant (1986); Swift and Williams, (1980); von der Dick and Meloche (1986); and Creaney and Allison (1987) indicated that all the discovered oils have a common oil-prone source, defined as the Kimmeridgian-age Egret Member of the Rankin Formation. Evidence of significant hydrocarbon contributions from terrestrial, gas-prone organic material in potential source rocks within the Lake Callovian-Early Oxfordian Voyager Formation and the upper unit of the Tithonian Jeanne d'Arc Formation has been shown by Snowdon and Krouse (1986), Fowler (1988) and McAlpine et al., (1988).

Rock-Eval pyrolysis data show high S2/S3 values for the Egret Member indicating that it contains highly oil-prone Type II-I organic matter whereas the relatively lower values in the Voyager and Jeanne d'Arc Formations indicate a greater proportion of gas-prone Type III organic matter.

Most of the hydrocarbon discoveries have been made in the Upper Jurassic to Lower Cretaceous rift sequences and reservoir units include the Jeanne d'Arc, Hibernia, Catalina, Eastern Shoals, Avalon and Ben Nevis Formations. The oil has migrated long

distances vertically and it is evident from the vertical variations in maturity that more than one episode of oil migration has occurred in some areas (McAlpine, 1989). The main path for oil migration appears to be along faults and fractures that have opened sporadically in response to buildup of abnormally high fluid pressures. In much of the prospective area of the Jeanne d'Arc Basin the source rock is overpressured, while the majority of discovered hydrocarbons are in the overlying, hydrostatically pressured regime. The laterally continuous Fortune Bay Shale generally forms the caprock for the overpressure (McAlpine, 1989).

The majority of oil discoveries lie within the area underlain by the present-day mature zone and the gas-prone drillholes are within or proximal to the overmature zone. It has been suggested (McAlpine, 1989) that the Egret Member is the dominant hydrocarbon contributor in the basin and that the gas may be an overmature product of this source rock, rather than a normal product of the Voyager or Jeanne d'Arc potential source intervals. Because the structural framework of the Jeanne d'Arc Basin was essentially established prior to Late Cretaceous time, the present thermal maturation configuration is likely to have existed throughout the last 100 Ma, and therefore, oil generation typically began only about 100 Ma ago and that peak generation was not reached until about 50 Ma ago during the Early Tertiary.

The average estimate for the entire Rankin Formation source interval is 43 billion cubic metres or 271 billion barrels of oil generated. The calculations for the Egret Member yielded an average value of 34 billion cubic metres or 214 billion barrels, about 80% of the total (McAlpine, 1989). These figures do not take into account expulsion, migration and trapping inefficiencies and, of course, do not include potential contributions from the Voyager and Jeanne d'Arc Formations. Potential oil in place in the Jeanne d'Arc Basin could be as high as 6.5 billion cubic metres or 41 billion barrels.

A recovery factor of 30% would give recoverable reserves of 1.95 billion cubic metres or 12.3 billion barrels (McAlpine, 1989).

In conclusion, favourable structure, stratigraphy, geochemistry and timing account for the hydrocarbon accumulations presently trapped in the Jeanne d'Arc Basin. A rich, oil-prone source rock was deposited in Late Jurassic time near the end of a period of relative tectonic stability. Basin subsidence during the latest Jurassic and Early Cretaceous led to deposition of a thick sequence of sandstones and shales that formed potential reservoirs and seals. Structuring was virtually complete by the Late Cretaceous before significant hydrocarbon generation had begun. Subsequent burial beneath a layer of Tertiary shales provided the thermal conditions necessary to generate oil and gas. It appears that significant oil reserves remain to be discovered and that the Jeanne d'Arc Basin will continue to be a very attractive target for petroleum exploration.

11.8 SCOTIAN SHELF, OFFSHORE EASTERN CANADA

Several accumulations of condensate and light oil have been found in the Scotian Basin in sediments ranging in age from Late Jurassic to Late Cretaceous (Powell and Snowdon, 1979). The onset of the marginally mature zone (vitrinite reflectance = 0.5% Ro) occurs at an average depth of 2,220 m whereas the onset of the fully mature zone (vitrinite reflectance ~0.7% Ro) does not occur until an average depth of 4,200 m (Purcell et al., 1979). Two of the hydrocarbon-bearing structures (Primrose and West Sable) on the Scotian Shelf are associated with piercement salt domes. Rashid and McAlary (1977) have shown that sediments immediately overlying the Primrose diapir have a higher thermal maturation level than the contemporaneous sediments away from the salt. This is attributed to the high thermal conductivity of the salt which creates an anomalous zone of heat flux at the crest of the diapir. In the case

of the Primrose structure the effect has been sufficient to raise the maturation level of the immediately surrounding sediments to the oil-generating zone, but not to a level where cracking of oil to gas would occur. The remainder of the accumulations are not associated with piercement salt domes, although salt may be involved in structural developments at depth (Purcell et al., 1979).

The sediments in the thick, marginally mature zone contain predominantly terrestrially-derived organic matter which is not normally considered to be a hydrocarbon source at low levels of maturation (vitrinite reflectance ~0.6% Ro). The Verrill Canyon Formation occurs in the mature zone in the Sable Island area and locally contains amorphous organic matter which may have acted as a source for liquid hydrocarbons (Powell and Snowdon, 1979). The marginally mature zone, in which the sediments are dominated by terrestrial organic matter, is characterized by occurrences of gas, condensate and light oil (Purcell et al., 1979). This association is inconsistent with the oil and gas generation model, thus necessitating an extensive vertical migration.

11.9 LABRADOR SHELF, OFFSHORE EASTERN CANADA

Rashid et al., (1980) in a study of the hydrocarbon potential of the East Newfoundland and Labrador Shelf areas showed that the Mesozoic-Cenozoic sedimentary succession contains high concentrations of organic carbon (>3.0 wt %) derived mainly from a terrestrial source. Gas-prone, organic matter Type III is responsible for the generation of condensates found in thermally immature reservoirs in the Labrador Shelf. As Rashid et al., (1980) indicated, the condensates were generated in the mature to overmature zones of hydrocarbon generation and have migrated vertically over long distances.

11.10 MARCELLUS FORMATION AND KETTLE POINT FORMATION OIL SHALES, ONTARIO

Organic-rich black shales of Middle to Upper Devonian age occur in southwestern Ontario. Macauley et al., (1985) showed that the oil yield from these oil shales is directly proportional to the total organic carbon content (TOC), with an average yield of 4.5 litres of oil/tonne/% TOC. An understanding of the classification and level of thermal maturity of the Ontario oil shales is significant to the interpretation of source beds for the subsurface hydrocarbon accumulations beneath Lake Erie.

The Middle Ordovician Marcellus Formation contains organic matter of mainly marine and amorphous types (Macauley et al., 1985) as well as marine fauna, such as chitinozoa, graptolites and flora (Tasmanites algae, acritarchs and bituminite Type II), the latter having formed from the alteration of hydrogen-rich components (Goodarzi et al., in prep.). The lower organic-rich beds of the Marcellus Formation is typical of the thin, widespread Type II organic matter deposits which follow the cessation of blanket carbonates deposition. Other Middle Devonian deposits of this nature include the Erie Member, which overlies the Keg River platform in northeastern British Columbia, the Horn River bituminous shales overlying the Lonely Bay carbonate platform in the southern Northwest Territories, the spore-bearing shale overlying the Hume Formation and the Canol shale overlying the Kee Scarp reef development in the Norman Wells area, Northwest Territories (Williams, 1983).

Vitrinite reflectance in the Marcellus Formation is projected to be in the range of 0.30 to 0.57% Ro, based on the fluorescence properties of the Tasmanites algae and using the relationship developed by Teichmuller and Ottenjann (1977) between the fluorescence of Tasmanites and vitrinite (corpocollinite) for the Jurassic Posidonia oil

shales of West Germany. Since the reflectance of vitrinite in hydrogen-rich sediments is known to be suppressed (Hutton and Cook, 1980), the reflectance of the organic matter in the Marcellus Formation oil shale could be in the range of 0.40 to 0.67% Ro, therefore, it would be defined as marginally mature (Teichmuller and Ottenjann, 1977; Goodarzi et al., in prep.). Similar relationships have also been observed by Kalkreuth and Macauley (1987) and Macauley et al., (1985) in moderately mature oil shales from the Lower Carboniferous Alberta Formation, New Brunswick, and in oil shales and coals from the Pictou and Antigonish areas of Nova Scotia.

The hydrogen indices (HI) of the Marcellus oil shales are between 600-650 mg HC/g Corg, TOC ranges between 3.0 and 13.0 wt %, Tmax values range from 436 to 450°C and the production indices (PI) are within the range of 0.04 to 0.12 (Goodarzi et al., in prep.).

The Kettle Point Formation oil shales contain predominantly Type II marine organic matter (reasonably hydrogen-rich), mixed with terrestrial Type III organic matter. TOC content varies between 1.0 and 15.0 wt % and they are less mature than the Marcellus Formation oil shales.

Overall, the Marcellus oil shales are very similar in terms of thermal maturity to the Ordovician Collingwood oil shales, described by Macauley and Snowdon (1984) and Macauley et al., 1985) in the Collingwood and Manitoulin Island areas, but the Marcellus beds are much less mature than those of the Collingwood in the Toronto-Whitby area (Goodarzi et al., in prep.).

11.11 DEVONIAN OF MACKENZIE CORRIDOR, N.W.T.

The bituminous shales in the Middle Devonian Horn River Formation and the "Evie" (Lower Bituminous Member) in the Mackenzie Corridor region of the southern Northwest Territories, Canada, are both organic-rich rocks with a good source potential for hydrocarbon generation. The two units were deposited in a "normal" marine, partially reducing conditions and possibly restricted terrigenous supply (Feinstein et al., 1991). A detailed organic petrological study reveals some diagnostic differences between the two units. Both the "Evie" and the "Horn River" are characterized by a relatively high organic matter content, between 3 and 18 wt% TOC (Feinstein et al., 1988). The relatively high Hydrogen Index (377-640 mg HC/g Corg), and low Oxygen Index (6-25 mg CO_2/g Corg) values suggest that the organic matter in the samples is mainly of Type II and possibly Type I having a very good hydrocarbon-generation potential.

The organic matter of the "Evie" Member contains mainly large (>200 μm) and small (<20 μm) algae of the Leiosphaeridia-type lamalginite, some pollen and spores and moderate amount of clam shells, whereas the organic fraction of the Horn River Formation samples is composed mainly of liptodetrinite and fluorescing amorphous matrix and some inertinite fragments (Feinstein et al., 1991).

The hydrocarbon yield obtained from extraction (38-107 mg/g Corg carbon) suggests that the formations have the potential for hydrocarbon generation and that they have undergone sufficient maturation for actual generation to have commenced (Powell, 1978).

The organic-facies characteristics of the Horn River and the Evie correlate well with the stratigraphically analogous Canol and Bluefish Formations in the Norman Wells area to the north and the Pine Point area to the south (Goodarzi and Macqueen, 1990).

11.12 COMPARISON OF THE SVERDRUP BASIN TO OTHER SEDIMENTARY BASINS IN CANADA

When evaluating Canadian sedimentary basins, it is important to emphasize on the thresholds at which organic matter types begin to generate hydrocarbons. These variations in the threshold of hydrocarbon generation are due to differences in the activation energy of various types of organic matter (Powell and Snowdon, 1983). In sedimentary basins, such as the Sverdrup Basin, which has low maturation gradients, the above variations translate into large differences in depth at which the different types of organic matter begin to generate hydrocarbons. In addition, a great thickness of the sedimentary succession lies within the immature and marginally mature stage of hydrocarbon generation in basins with low maturation gradients. This is even more important in sedimentary basins with low geothermal gradients where the issues of source rocks and thermal maturity should not be grouped together.

Only certain types of organic matter can be the source for hydrocarbons at marginally mature levels (% Ro >0.50% but <0.70%) and the thickness of the marginally mature zone of hydrocarbon generation in the Sverdrup Basin varies between 1,000 m and 2,000 m. Therefore, in the Sverdrup Basin, which has low geothermal gradients, there may be substantial differences in the depth between the onset of threshold values of hydrocarbon generation.

Apart from minor carbonates in the Triassic of Sverdrup Basin, the entire Mesozoic succession is dominated by marine and non-marine clastics and some Cretaceous igneous rocks that have intruded mainly the Carboniferous succession. Oil-prone, sapropelic kerogen (Type I/II organic matter) is rarely dominant in the Canadian Arctic Basins, including Sverdrup, and is present in the Triassic Schei Point

Group only. Therefore, the organic matter in the Schei Point Group has been the source of the gas in the Hecla and Drake hydrocarbon fields as well as the source of smaller quantities of oil in the Sabine Peninsula area of Melville Island. The oil and gas generation model of Powell and Snowdon (1983) (Figure 5-1) could aid in understanding the genesis of hydrocarbons in the Sverdrup Basin. The above model shows that for conventional Type II organic matter deposited in a moderately euxinic depositional environment (i.e. clastic, Fe-rich) biogenic gas may be produced at reflectance levels of 0.40 - 0.55% and thermogenic gas beyond the 0.55% Ro level. The oil generated in Sverdrup Basin would be expected to be paraffinic to naphthenic and the gas condensate generated towards the overmature zone of hydrocarbon generation from cracking would be mainly paraffinic.

Terrestrial organic matter (mainly Type II) is the source for hydrocarbons in numerous Canadian sedimentary basins, including the Beaufort-Mackenzie, the Scotian and Labrador Shelves and the Cretaceous Deep Basin of Alberta (Powell and Snowdon, 1983). What varies considerably among the above basins is the level of maturation at which the hydrocarbons were generated. The work of Snowdon (1980) and Snowdon and Powell (1982) indicates that the terrestrial organic matter in the Beaufort-Mackenzie Basin, which is rich in resinite, has yielded naphthenic oil and gas condensate at relatively low levels of thermal maturity (<0.55% Ro). To the contrary, the gas condensate and minor oil found in the Scotian Shelf was formed in the mature zone of hydrocarbon generation, and the gas condensate in the Labrador Shelf was generated in the mature to overmature zones of hydrocarbon generation. In the Cretaceous Deep Basin of Alberta the gas has been produced in the overmature zone (Powell and Snowdon, 1983), whereas oil and gas reserves in the Devonian of Alberta have been derived from normal Type II organic matter (Deroo et al., 1977), as has the oil in the upper part of the Lower Cretaceous and in the Upper Cretaceous of the Alberta Basin.

The most important and unusual characteristic of the Sverdrup Basin is the presence of non-biogenic gas at much lower levels of thermal maturity than what would be expected in the normal hydrocarbon-generation model of Vassoevich et al., (1974). Based on the organic petrology of the Triassic Schei Point Group sediments, it is well established that the predominant type of organic matter in the sediments is liptinite derived from marine organisms such as dinoflagellates, Tasmanites algae, other algal cysts and amorphous fluorescing materials (Type I/II) with a small input from vitrinite (Type III). According to Tissot et al., (1978), the generation of hydrocarbons from algal material (Type I) commences at about 0.70% Ro which is 0.20% higher than that for vitrinite and exinite (Types III and II) because of the higher activation energy needed for the breakdown of the Type I structure. The frequent presence of bitumen staining in the Schei Point Group sediments is a further indication of the generation of hydrocarbons from these sediments, including the ones that are in the marginally mature zone of hydrocarbon generation, such as in the vicinity of the Sabine Peninsula, northern Melville Island.

The depositional environment strongly influences the composition and properties of the organic matter (Powell and Snowdon, 1980; 1983; Snowdon and Powell, 1982; Tissot and Welte, 1984). Sedimentology, organic petrology and geochemical data all confirm the marine origin of the organic matter in the Schei Point sediments (Goodarzi et al., 1989a) and indicate that they were deposited in a highly-reducing environment with an algal input. The similarities and differences between the Triassic source rocks in the Sverdrup Basin, the only well-documented source rocks of Triassic age in Canada, and the Upper Jurassic to Lower Cretaceous of the Jeanne d'Arc Basin in Canada's east coast are evident. The Egret Member in the Jeanne d'Arc Basin contains highly oil-prone Type I/II organic matter but the oil in the basin has migrated vertically over long distances in more than one episode.

The Lower Palaeozoic of the Williston Basin in southern Saskatchewan contains an admixture of Type I/II organic matter dominated by the algae Gloeocapsomorpha prisca. The generation of hydrocarbons did not commence until the Late Mesozoic when elevated geothermal gradients (~40°C/Km) were established (Osadetz et al., 1989). In addition, certain similarities, particularly on the type of organic matter, exist between the Triassic of the Sverdrup Basin and the Middle Ordovician of the Mackenzie Corridor in the Northwest Territories and the oil shales of the Middle Ordovician Marcellus Formation in southwestern Ontario. The same can be said about the Middle Triassic Doig Formation and the Lower Jurassic 'Nordegg' Member in the Alberta Basin. Both are characterized by Type I/II organic matter, high TOC content and exceptionally high hydrogen indices (up to 900 mg HC/g Corg) (Riediger et al., 1991). Unfortunately, Triassic source rocks in western Canada have a limited distribution and have not been studied extensively as other source rocks, for example the Devonian.

Finally, the timing of hydrocarbon generation in the Franklinian miogeosyncline is in complete contrast to the Devonian of western Canada where hydrocarbon generation in Devonian rocks did not occur until Late Cretaceous or Early Tertiary (Deroo et al., 1977). Oil in the Franklinian miogeosyncline was generated prior to the Lower Carboniferous Ellesmerian Orogeny but most of the traps were destroyed because of erosion associated with the orogeny. Any hydrocarbon accumulations were subsequently converted to bitumen, most likely by de-asphalting.

CHAPTER XII

CHAPTER XII CONCLUSIONS

The Sverdrup Basin has the necessary ingredients to be a prolific oil province because it contains organic-rich shales and siltstones in the Schei Point Group which, in northern Sabine Peninsula, have experienced a favourable maturation history. The Jameson Bay, Ringnes and Deer Bay shales are still immature or marginally mature at the very best. The Mesozoic of Melville Island shows some extreme variations in source richness and organic matter types, as illustrated by the pyrolysis plots. After a careful examination of the optical and Rock-Eval data for Mesozoic sediments in the study area, the following facts emerge:

1) The Cape Richards Member of the Hoyle Bay Formation containing marine liptinitic organic matter has high HI, TOC and S_2 values in the subsurface of the Hecla hydrocarbon field, thus indicating a high hydrocarbon potential west of the Sabine Peninsula. In addition, the parameters for the Eden Bay Member of the Hoyle Bay Formation and the Cape Caledonia Member of the Murray Harbour Formation, which also contain marine liptinite, are slightly higher in the Hecla than in the Drake hydrocarbon field, pointing to a higher source-rock potential for these formations in a westerly direction.
2) Due to the limited number of measurements in the Jameson Bay, Ringnes and Deer Bay Formations, no conclusive evidence can be drawn about their hydrocarbon potential, although it appears to be limited due to a higher input of terrestrial organic matter. The Ringnes and Jameson Bay shales would have a good gas-generating potential at favourable maturation levels.
3) Most of the Triassic Schei Point Group sediments in Melville Island are marginally mature, whereas the Jurassic Jameson Bay and Ringnes, are immature. In contrast, the Upper Palaeozoic sediments, although mature, contain too little

organic matter to have any potential for hydrocarbon generation in this area of the southern Sverdrup Basin. The Bjorne and Blind Fiord Formations have very little source-rock potential, whereas the Permian Van Hauen Formations have some potential for the generation of gaseous hydrocarbons.

4) The Hecla and Drake hydrocarbon fields have the potential for generation of diagenetic gases only from the Mesozoic section and catagenetic gases due to the maturation of bitumen in the Permian Van Hauen Formation. The main source-rocks in the area occur in the Schei Point Group, which is thermally immature to marginally mature, with the exception of the northern Sabine Peninsula where it is mature (i.e. North Sabine H-49, Roche Point J-43).

5) Low sedimentation and subsidence rates during the middle to early Upper Jurassic indicate that there was little paleotopographic relief on lands adjacent to the Sverdrup Basin. As a result, oil-prone source beds formed in the paleotopographic lows because of the development of anoxic bottom conditions. The main event that triggered hydrocarbon generation and expulsion was probably the drastic increase in the rate of subsidence during Albian time, resulting in the deposition of the very thick sections of shales and siltstones of the Christopher Formation.

6) In some ways the Sverdrup Basin is similar to the Franklinian miogeosyncline. Both contain carbonate and evaporite sequences which were deposited relatively early in the history of each basin.

Sedimentation in each basin was terminated by a major orogeny (Ellesmerian and Eurekan respectively) and both these orogenies involved halokinetic movement. Salt diapirism appears to be restricted to the Sverdrup Basin and is probably the single most important tectonic element with regard to the development of most of the hydrocarbon bearing structures.

REFERENCES

REFERENCES

Abraham, H., 1960 Asphalts and allied substances, vol. 1: Historical review and natural raw materials, Princeton, NJ, Van Nostrand, 370 pp.

Alpern, B., 1978 Optical properties of palynomorphs and petroleum potential, Proceedings of the 6th International Palynological Conference, Lucknow 1976-1977, vol. 1, p. 110-125.

_____ , 1980 Petrographie du Kerogene; In: Kerogen, insoluble organic matter from sedimentary rocks, Durand,B. (Ed.), Editions Technip, Paris, p. 339-384.

Baker, D.A., Illich, H., Martin, S. and Landin, R.R., 1975 Hydrocarbon maturation analysis of the Sverdrup Basin; In: Canada's continental margins and offshore petroleum exploration, C. Y. Yorath, E.R. Parker and D.J. Glass (Eds.), Canadian Society of Petroleum Geologists, Memoir 4, p. 545-556.

Balkwill, H.R., 1978 Evolution of Sverdrup Basin, Arctic Canada, American Association of Petroleum Geologists Bulletin, vol. 2, p. 171-187.

_____ , 1983 Geology of Amund Ringnes, Cornwall and Haig Thomas Islands, Arctic Canada; In: Current Research, Part B, Geological Survey of Canada, Paper 84-1B, p. 299-308.

_____ , and Roy, K.J. 1977 Geology, King Christian Island, District of Franklin, Geological Survey of Canada, Memoir 386.

_____ , and Haimila, N.E., 1978 K/Ar ages and significance of mafic rocks, Sabine Peninsula, Melville Island, District of Franklin; In: Current Research, Part C, Geological Survey of Canada, Paper 78-1C, p. 35-38.

_____ , and Fox, F.G., 1982 Incipient rift zone, western Sverdrup Basin, Arctic Canada, Canadian Society of Petroleum Geologists, Memoir 8, p. 171-187.

_____ , Wilson, D.G. and Wall, J.H., 1977 Ringnes Formation (Upper Jurassic), Sverdrup Basin, Canadian Arctic Archipelago, Bulletin of Canadian Petroleum Geology, vol. 25, no. 6, p. 115-144.

_____ , Hopkins, W.S., Jr. and Wall, J.H., 1982 Geology, Lougheed Island, District of Franklin, Geological Survey of Canada, Memoir 388.

Barker, C.E., 1983 Influence of time on metamorphism of sedimentary organic matter in liquid-dominated geothermal systems, western North America, Geology, vol. 11, p. 384-388.

Beauchamp, B., Oldershaw, A.E. and Krouse, H.R., 1987 Upper Carboniferous to Upper Permian 13 C-enriched primary carbonates in the Sverdrup Basin, Canadian Arctic: Comparisons to coeval Western North American ocean margins, Chemical Geology, vol. 65, p. 391-413.

Bertrand, R. and Heroux, H., 1987 Chitinozoan, graptolite and scolecodont reflectance as an alternative to vitrinite and pyrobitumen reflectance in Ordovician and Silurian strata, Anticosti Island, Quebec, Canada, American Association of Petroleum Geologists Bulletin, vol. 71, no. 8, p. 951-957.

Blackadar, R.G., 1964 Basic intrusions of the Queen Elizabeth Islands, District of Franklin, Geological Survey of Canada, Bulletin 97, 36 pp.

Bostick, N.H., 1979 Microscopic measurement of the level of catagenesis of solid organic matter in sedimentary rocks to aid exploration for petroleum and to determine former burial temperatures - A review, Society of Economic Paleontologists and Mineralogists, Special Publication 26, p. 17-43.

———, and Foster, J.N., 1975 Comparison of vitrinite reflectance in coal seams and in kerogen of sandstones, shales and limestones in the same part of sedimentary section; In: Colloque International, Petrographie de la matiere organique des sediments, B. Alpern (Ed.), Paris, p. 13-25.

———, Cashman, S.M., McCulloh, T.H. and Waddell, C.T., 1978 Gradients of vitrinite reflectance and present temperature in the Los Angeles and Ventura Basins, California; In: Symposium in Geochemistry: Low Temperature metamorphism of coal and clay minerals, Oltz, D.F., (Ed.), Society of Economic Paleontologists and Mineralogists, Pacific Section, p. 65-96.

Brooks, B. T., 1948 Active-surface catalysts in formation of petroleum, American Association of Petroleum Geologists Bulletin, vol. 32, p. 2269-2286.

Brooks, J., 1981 Organic maturation of sedimentary organic matter and petroleum exploration - A review; In: Organic maturation studies and fossil fuel exploration, Brooks, J. (Ed.), Academic Press, London, p. 1-38.

Brooks, J. D., and Smith, J.W., 1969 The diagenesis of plant lipids during the formation

of coal, petroleum and natural gas - II. Coalification and the formation of oil and gas in the Gippsland Basin, Geochimica et Cosmochimica Acta, vol. 33, p. 1183-1194.

Brooks, P.W., Fowler, M.G., and Macqueen, R.W., 1988 Biological marker and conventional organic geochemistry of oil sands/heavy oils, Western Canada Basin, Organic Geochemistry, vol. 12, p. 519-538.

_____, Embry, A.R., Goodarzi, F., and Stewart, K.R., 1991 Geochemical studies of the Sverdrup Basin (Arctic Islands). Part I: Organic geochemistry and biological marker geochemistry of Schei Point Group (Triassic) and recovered oils, Bulletin of Canadian Petroleum Geology, (in press).

Bundebarth, G. and Schopper, J.R., 1976 Heat flow caused by water migration along faults in dependence on petrophysical parameters, Proceedings of International Congress on Thermal Waters, Geothermal Energy and Volcanism of the Mediterranean Area, Athens, 1976, vol. 2, p. 41-49.

Burgess, J.D., 1974 Microscopic examination of kerogen (dispersed organic matter) in petroleum exploration; In: Carbonaceous Materials as Indicators of Metamorphism, Dutcher, R.R., Hacquebard, P.A., Schopf, J.M., and Simon, J.A. (Eds.), The Geological Society of America, Special Paper 153, p. 19-30.

Bustin, R.M., 1984 Coalification levels and their significance in the Groundhog coalfield, north-central British Columbia, International Journal of Coal Geology, vol. 4, p. 21-44.

_____ , 1986 Organic maturity of Late Cretaceous and Tertiary coal measures, Canadian Arctic Archipelago, International Journal of Coal Geology, vol. 6, p. 71-106.

_____ , Hills, L.V., and Gunther, P.R., 1977 Implications of coalification levels, Eureka Sound Formation, northeastern Arctic Canada, Canadian Journal of Earth Sciences, vol. 14, no. 7, p. 1588-1597.

_____ , Barnes, M.A., and Barnes, W.C., 1985 Diagenesis, Part 10: Quantification and Modelling of Organic Diagenesis, Geoscience Canada, vol. 12, no. 1, p. 4-21.

_____ , Link, C. and Goodarzi, F., 1989 Optical properties and chemistry of graptolite periderm following laboratory simulated maturation, Organic Geochemistry, vol. 14, no. 4, p. 355-364.

_____ , Vellutini, D., and Goodarzi, F., 1990 Petroleum source rock characteristics of the Tertiary Skonun Formation, Queen Charlotte Islands, Hecate Strait and Queen Charlotte Sound, British Columbia; In: Current Research, Part F, Geological Survey of Canada, Paper 90-1F, p. 87-93.

Cardott, B.J. and Lambert, M.W., 1985 Thermal maturation by vitrinite reflectance of the Woodford shale, Anadarko Basin, Oklahoma, American Association of Petroleum Geologists Bulletin, vol. 69, no. 11, p. 1982-1988.

Chandra, D., and Taylor, G.H., 1982 Thermally altered coals; In: Stach's Textbook of Coal Petrology, E. Stach, M-Th. Mackowsky, M. Teichmuller, G.H. Taylor, D. Chandra and R. Teichmuller (Eds.), Gebruder Borntraeger, Berlin-Stuttgart, p.

206-215.

Christie, R.L., and Kerr, W.M., 1981 Geological Exploration of the Canadian Arctic Islands; In: A century of Canada's Arctic Islands, 1880-1980. M. Zaslow (Ed.), Royal Society of Canada, p. 187-202.

Clark, S.P. Jr., 1966 Thermal conductivity; In: Handbook of Physical Constants, S.P. Clark, Jr. (Ed.), Geological Society of America, Memoir no. 97, p. 459-482.

Clausen, C.D. and Teichmuller, M., 1982 Die Bedeutung der graptolithen - Fragmente im Palaozoikum von Soest Erwitte fur Stratigraphie und Inkohlung, Fortschritte in der Geologie von Rheinland und Westfalen, vol. 30, p. 145-167.

Clementz, D.M., 1979 Effect of oil and bitumen saturation on source-rock pyrolysis, American Association of Petroleum Geologists Bulletin, vol. 63, p. 2227-2232.

Combaz, A., 1980 Les Kerogenes vus au microscope, In: Kerogen, Durand, B. (Ed.), Editions Technip, Paris, p. 55-89.

Connan, J. and Cassou, A.M., 1980 Properties of gases and petroleum liquids derived from terrestrial kerogen at various maturation levels, Geochimica et Cosmochimica Acta, vol. 44, p. 1-23.

Cook, A.C., 1980 The origin and petrology of organic matter in coals, oil shales and petroleum source rocks, A.C. Cook with contributions from A.J. Kantsler, University of Wollongong, New South Wales.

_____, 1986 The nature and significance of the organic facies in the Eromanga Basin; In: Contributions to the Geology and Hydrocarbon Potential of the Eromanga Basin, Gravestock, D.I., Moore, P.S., and Pitt, G.M. (Eds.), Geological Society of Australia, Special Publication No. 12, p. 203-219.

_____, Murchison, D.G., and Scott, E., 1972 A British meta-anthracitic coal of Devonian age, Geological Journal, vol. 8, p. 83-94.

_____, Hutton, A.C. and Sherwood, N.R., 1980 Classification of oil shales, Bulletin des Centres de Recherches Exploration-Production Elf-Aquitaine, vol. 5, no. 2, p. 353-381.

Cornelius, C., 1984 Geochemical aspects of heavy oil bitumen exploration, The Future of Heavy Crude and Tar Sands, Second International Conference, Unitar, New York, NY, p. 318-335.

Creaney, S., 1980a The organic petrology of the Upper Cretaceous Boundary Creek Formation, Beaufort-Mackenzie Basin, Bulletin of Canadian Petroleum Geology, vol. 28, p. 112-129.

_____, 1980b Petrographic texture and vitrinite reflectance variation of the Alston Block, North-East England, Yorkshire Geological Society Proceedings, vol. 42, (Part 4), p. 553-580.

_____, and Allison, B.H., 1987 An organic geochemical model of oil generation in the Avalon/Flemish Pass subbasin, east coast Canada, Bulletin of Canadian Petroleum Geology, vol. 35, no. 1, p. 12-23.

Crowther, P. R., 1981 The fine structure of graptolite periderm, Special Papers in Palaeontology, The Paleontological Association, London, vol. 26, p. 1-119.

Curiale, J., 1986 Original solid bitumens with emphasis on biological marker results, Advances in Organic Geochemistry, vol. 10, p. 559-580.

Damberger, H., 1968 Ein Nachweis der Abhangigkeit der Inkohlung von der Temperatur, Brennstoff-Chemie, vol. 49, p. 73-77.

Deroo, G., Powell, T.G., Tissot, B., and McCrossan, R.G., 1977 The origin and migration of petroleum in the Western Canadian Sedimentary Basin, Alberta, Geological Survey of Canada, Bulletin 262.

Dow, W., 1977 Kerogen studies and geological interpretations, Journal of Geochemical Exploration, vol. 7, p. 79-99.

Dowdle, W.L. and Cobb, W.M., 1975 Static formation temperature from well logs - An empirical method, Journal of Petroleum Technology, vol. 27.

Drummond, K.J., 1973 Canadian Arctic Islands; In: The future petroleum provinces of Canada - their geology and potential, McCrossan, R.G. (Ed.), Canadian Society of Petroleum Geologists, Memoir 1, p. 443-472.

Durand, B., and Monin, J.C., 1980 Elemental analysis of kerogens (C, H, O, N, S, Fe); In: Kerogen, B. Durand (Ed.), Editions Technip, Paris p. 113-142.

——, Alpern, B., Pittion, J.L. and Pradler, B., 1985 Reflectance of vitrinite as a control

of thermal history of sediments, Institut Francais du Petrole, Reference 33729, Project L31 07401, Geologie No. 77407.

Eglinton, T.I., Rowland, S.J., Curtis, C.D., and Douglas, A.G., 1986 Kerogen-mineral reactions at raised temperatures in the presence of water, Organic Geochemistry, vol. 10, p. 1041-1052.

Eisenack, A., 1931 Neue Mikrofossilien des Baltischen Silurs, Palaeontologie, vol. 14, p. 257-277.

Embry, A.F., 1982 Stratigraphic subdivision of the Heiberg Formation, eastern and central Sverdrup Basin; In: Current Research, Part B, Geological Survey of Canada, Paper 83-1B, Report 24.

———, 1983a Stratigraphic subdivision of the Heiberg Formation, eastern and central Sverdrup Basin; In: Current Research, Part B, Geological Survey of Canada, Paper 83-1B, p. 205-213, Report 24.

———, 1983b The Heiberg Group, western Sverdrup Basin, Arctic Islands; In: Current Research, Part B, Geological Survey of Canada, Paper 83-1B, p. 381-389.

———, 1984a The Schei Point and Blaa Mountain Groups (Middle-Upper Triassic) Sverdrup Basin, Canadian Arctic Archipelago; In: Current Research , Part B, Geological Survey of Canada, Paper 84-1B, Report 31.

———, 1984b Stratigraphic subdivision of the Roche Point, Hoyle Bay and Barrow Formations (Schei Point Group), Western Sverdrup Basin, Arctic Islands; In:

Current Research, Part B, Geological Survey of Canada, Paper 84-1B, p. 275-283.

———, 1984c The Wilkie Point Group (Lower-Upper Jurassic), Sverdrup Basin, Arctic Islands; In: Current Research, Part B, Geological Survey of Canada, Paper 84-1B, p. 299-308.

———, 1985a Stratigraphic subdivision of the Isachsen and Christopher formations (Lower Cretaceous), Arctic Islands; In: Current Research, Part B, Geological Survey fo Canada Paper 85-1B, p. 239-246.

———, 1985b New stratigraphic units, Middle Jurassic to lowermost Cretaceous successions, Arctic Islands; In: Current Research, Part 1B, Geological Survey of Canada, Paper 85-1B, p. 269-276.

——— and Klovan, J.E., 1976 The Middle-Upper Devonian clastic wedge of the Franklinian Geosyncline, Bulletin of Canadian Petroleum Geology, vol. 24, p. 485-639.

England, T., and Bustin, R.M., 1986 Thermal maturation of the Western Canadian Sedimentary Basin south of the Red Deer River: I) Alberta Plains, Bulletin of Canadian Petroleum Geology, vol. 34. no. 1, p. 71-90.

Epstein, A.G., Epstein, J.B., and Harris, L.D., 1977 Conodont color alteration - an index of organic metamorphism, United States Geological Survey Professional Paper 995, 27 pp.

Erkmen, U., and Bozdogan, N., 1980 Cambrian acritarchs from the Sosink Formation in

southeast Turkey, Revista Espanola de Micropaleontologia, vol. XIII, p. 47-60.

Espitalie, J.M., Madec, M. and Tissot, B., 1977 Source rock characterization method for petroleum exploration, 9th Annual Offshore Technology Conference, Houston, Texas, UTC 2935, p. 439-448.

——— , Madec, M., and Tissot, B., 1980 Role of mineral matrix in kerogen pyrolysis: influence on petroleum generation and migration, American Association of Petroleum Geologists Bulletin, vol. 64, p. 59-66.

——— , Makadi, J., and Trichet, J., 1984 Role of mineral matrix during kerogen pyrolysis, Organic Geochemistry, vol. 6, p. 365-382.

——— , Deroo, G. and Marquis, F., 1985 Rock-Eval pyrolysis and its applications, Institut Francais du Petrole Preprint 333578, 72 pp.

Falvey, D.A. and Deighton, I., 1982 Recent advances in burial and thermal geochemistry analysis, Australian Petroleum Exploration Association Journal, vol. 22, p. 65-81.

Feinstein, S., 1981 Subsidence and thermal history of southern Oklahoma aulacogen: implication for petroleum exploration, American Association of Petroleum Geologists Bulletin, vol. 65, p. 2521-2533.

——— , 1985 Coal ranks and the thermal history of the sedimentary succession in southern Israel, Unpublished Ph.D. thesis (in Hebrew with English abstract), Ben Gurion University of the Negev, Beer Sheva, Israel, 138 pp.

_____ , Brooks, P.W., Gentzis, T., Goodarzi, F., and Snowdon, L.R. 1988 Thermal maturity in the Mackenzie Corridor, Northwest and Yukon Territories, Canada, Open File Report #1944, 88 pp.

_____ , Williams, G.K., Snowdon, L.R., Brooks, P.W., Fowler, M.G., Goodarzi, F., and Gentzis, T., 1991 Organic geochemical characterization and hydrocarbon generation potential of Middle to Late Devonian Horn River bituminous shales, southern Northwest Territories, Canada, Bulletin of Canadian Petroleum Geology, (in press).

Fisher, M.J., Barnard, P.C., and Cooper, B.S. 1980 Organic maturation and hydrocarbon generation in the Mesozoic sediments of Sverdrup Basin, Arctic Canada, Proceedings of the Fourth International Palynological Conference, Lucknow, vol. 2, p. 581-588.

Florkin, M., 1969 Fossil shell 'Conchiolin' and other preserved biopolymers; In: Organic Geochemistry, Methods and Results, G. Eglinton, and M.T.J. Murphy (Eds.), p. 498-530.

Fortier, Y.O., 1948 Flights in 1947 over the region of the North Magnetic Pole and the Mainland between the Arctic Coast, Great Slave Lake and Hudson Bay, Northwest Territories, Geological Survey of Canada, Paper 48-23.

_____ , and Thorsteinsson, R., 1953 The Parry Islands Folded Belt in the Canadian Arctic Archipelago, American Journal of Science, vol. 251, p. 259-267.

Fowler, M.G., Brooks, P.W., Snowdon, L.R., and McAlpine, K.D., 1988 Petroleum

geochemistry of the Jeanne d'Arc Basin; In: Program with Abstracts; Geological Association of Canada/Mineralogical Association of Canada/Canadian Society of Petroleum Geologists Joint Annual Meeting, St. John's, May 23-25, 1988, p. A40.

Fox, F. G., 1983 Structure sections across Parry Islands Fold Belt and Vesey Hamilton Salt Wall, Arctic Archipelago, Canada; In: Seismic expression of structural styles, vol. 3, A. W. Bally (Ed.), American Association of Petroleum Geologists, p. 3.4.1-54 to 3.4.1-72.

———, 1985 Structural geology of the Parry Islands Fold Belt, Bulletin of Canadian Petroleum Geology, vol. 33, no. 3, p. 306-340.

Frebold, H., 1960 The Jurassic faunas of the Canadian Arctic: Lower Jurassic and lowermost Middle Jurassic ammonites, Geological Survey of Canada, Bulletin 59.

———, 1975 The Jurassic faunas of the Canadian Arctic: Lower Jurassic ammonites, biostratigraphy and correlation, Geological Survey of Canada, Bulletin 243.

Galwey, A.K., 1970 Reactions of alcohols and hydrocarbons on montmorillonite surfaces, Journal of Catalysis, vol. 19, p.330-342.

Goldstein, T.P., 1983 Geocatalytic reactions in the formation and maturation of petroleum, American Association of Petroleum Geologists Bulletin, vol. 67, p. 152-159.

Goodarzi, F., , 1982 A brief hydrocarbon potential study of south-east Turkey using organic petrography, Report to Turkish Petroleum Research Centre, Ankara,

Turkey.

———— , 1984 Organic petrology of graptolite fragments from Turkey, Marine and Petroleum Geology, vol. 1, p. 202-210.

———— , 1985a Reflected light microscopy of chitinozoa fragments, Marine and Petroleum Geology, vol. 2, p. 72-78.

———— , 1985b Dispersion of optical properties of graptolites with increased maturity in early Palaeozoic organic-rich sediments, Fuel, vol. 64, p. 1735-1740.

———— , 1987 Comparison of reflectance data from various macerals from subbituminous coals, Journal of Petroleum Geology, vol. 10, p. 219-226.

———— , and Murchison, D.G., 1978 Influence of heating rate variation on the anisotropy of carbonized vitrinites, Fuel, vol. 57, p. 273-284.

———— , and Norford, B.S., 1985 Graptolites as indicators of the temperature histories of rocks, Journal of the Geological Society of London, vol. 142, p. 1089-1099.

———— , and Williams, P.V.F., 1986 Composition of natural bitumens and asphalts from Iran, 2. Bitumens from the Poshteh Ghear Valley, Southwest Iran, Fuel, vol. 65, p. 17-27.

———— , and Higgins, A.C., 1987 Optical properties of scolecodonts and their use as indicators of thermal maturity, Marine and Petroleum Geology, vol. 14, p. 353-359.

_____, and Norford, B.S., 1987 Optical properties of graptolite epiderm - A review, Bulletin of the Geological Society of Denmark, vol. 35, p. 141-147.

_____, and Stasiuk, L.D., 1987a Graptolite preparation for reflected light microscopy, a technical note, Geological Survey of Canada, Paper 87-1A, p. 317-322.

_____, and Stasiuk, L.D., 1987b Amorphous kerogen: Bituminite in the Second White Speckled shale, southern Saskatchewan; In: Current Research, Part A, Geological Survey of Canada, Paper 87-1A, p. 349-352.

_____, and Norford, B.S., 1989 Variation of graptolite reflectance with depth of burial, International Journal of Coal Geology, vol. 11, p. 127-141.

_____, and Goodbody, Q.H., 1990 Petrology of Devonian coals from western Melville Island, Arctic Canada and its significance in paleoenvironmental interpretations, International Journal of Coal Geology, vol. 14, p. 175-196.

_____, and Macqueen, R.W., 1990 Optical/Compositional character of six bitumen species from Middle Devonian rocks of the Pine Point Pb-Zn property, Northwest Territories, Canada, Bulletin of Canadian Petroleum Geology, vol. 14, p. 197-216.

_____, Stasiuk, L.D., and Lindholm, K., 1988a Graptolite reflectance and thermal maturity of Lower and Middle Ordovician shales from Scania, Sweden, Geol. Forening Stockholm Forhandl., vol. 100, no. 3, p. 225-236.

_____, Brooks, P.W. and Embry, A.F., 1989a Regional maturity as determined by organic petrology and geochemistry of the Schei Point Group (Triassic) in Western

Sverdrup Basin, Canadian Archipelago, Marine and Petroleum Geology, vol. 6, p. 290-302.

——— , Gandhi, S.S., and Snowdon, L.R., 1989b Bitumen in a Lower Proterozoic dolomite hosting Pb-Zn-Cu occurrences, Artillery Lake, Northwest Territories; In: Current Research, Part C, Geological Survey of Canada, Paper 89-1C, p. 369-376.

——— , Snowdon, L.R., Gunther, P.R. and Jenkins, W.A.M., 1985 Preliminary organic petrography of Palaeozoic rocks from the Grand Banks, Newfoundland, Marine and Petroleum Geology, vol. 2, p. 254-259.

——— , Davies, G.R., Nassichuk, W.W. and Snowdon, L.R., 1987a Organic petrology and Rock-Eval analysis of the Lower Carboniferous Emma Fiord Formation in Sverdrup Basin, Canadian Arctic Archipelago, Marine and Petroleum Geology, vol. 4, p. 132-145.

——— , Davies, G.R., Nassichuk, W.W., and Snowdon, L.R., 1987b Exsudatinite in Carboniferous oil shale from Arctic Canada, Fuel vol. 66, p. 771-773.

——— , Gentzis, T., Feinstein, S. and Snowdon, L.R., 1988b Effect of maceral sub-types and mineral matrix on measured reflectance of subbituminous coals and dispersed organic matter, International Journal of Coal Geology, vol. 10, p. 383-398.

——— , Gentzis, T., Embry, A.F. Skibo, D., and Stewart, K.R., 1991 Evaluation of maturity and source rock potential in the Lougheed Island area of the central Sverdrup Basin, Arctic Canada, Norwegian Petroleum Society, special volume on 'Arctic Geology and Petroleum Potential'.

_____ , Fowler, M., Macauley, G., and Barker, J.F., in prep. Organic Petrology and Geochemistry of Organic-rich Beds within the Middle Devonian Marcellus Formation Southwestern, Ontario; In: Current Research, Geological Survey of Canada Paper.

_____ , Gentzis, T., Feinstein, S., Snowdon, L.R., Bustin, R.M., and Labonte, M., in prep. The effect of mineral matrix and seam thickness on reflectance of vitrinite in high- to low-volatile bituminous coals: An enigma.

Gormly, J.R., and Mukhopadhyay, P.K., 1983 Hydrocarbon potential of kerogen types of pyrolysis-gas chromatography; In: Advances in Organic Geochemistry, M. Bjoroy et al. (Ed.), John Wiley and Sons, Oxford, 1983, p. 597-606.

Grant, A.C., McAlpine, K.D., and Wade, J.A., 1986a The continental margin of eastern Canada - geological framework and petroleum potential; In: Future Petroleum Provinces of the World, M.T. Halbouty (Ed.), American Association of Petroleum Geologists, Memoir 40, p. 177-205.

_____ , _____ , _____ , 1986b Offshore geology and petroleum potential of eastern Canada, Energy Exploration and Exploitation, vol. 4, p. 5-52.

Gretener, P.E., 1981 Geothermics: using temperature in hydrocarbon exploration, American Association of Petroleum Geologists, Education Course Note Series 17, Tulsa, Oklahoma.

Guidish, T.M., Kendall, C.G., St. C., Lerche, I., Toth, D.J. and Yarzab, R.E., 1985 Basin evaluation using burial history calculations: An overview, American Association of Petroleum Geologists Bulletin, vol. 69, no. 1, p. 92-105.

Gutjahr, C.C.M., 1983 Introduction to incident-light microscopy of oil and gas source rocks, Geologie en Mijnbouw, vol. 62, no. 3, p. 417-425.

Hacquebard, P.A., and Donaldson, J.R., 1974 Rank studies of coal in the Rocky Mountains and Inner Foothills belt, Canada, Geological Society of America, Special Paper 153, p. 75-94.

Hamilton, J.K. and Varney, G.R., 1982 Cores from the Canadian Arctic Archipelago, Geology and Hydrocarbon occurrences, American Association of Petroleum Geologists/Canadian Society of Petroleum Geologists Core Conference Manual, 21 pp.

Hamrla, M., 1956 On the conditions of origin of the coal beds in the Karst region (Yugoslavia, engl. abst. p. 253-264) - Diss. Univ. Ljubljana.

Harrison, J.C., Goodbody, Q.H. and Christie, R.L., 1985 Stratigraphic and structural studies on Melville Island, District of Franklin; In: Current Research, Part A, Geological Survey of Canada, Paper 85-1A, p. 629-637.

Harwood, R.J., 1977 Oil and gas generation by laboratory pyrolysis of kerogen, American Association of Petroleum Geologists Bulletin, vol. 61, p. 2082-2102.

Haughton, S., 1859 Reminiscence of Arctic ice-travel in search of Sir John Franklin, Royal Dublin Society Journal, vol. 1, p. 183-250.

Henao-Londono, D., 1977 Correlation of producing formations in the Sverdrup Basin, Bulletin of Canadian Petroleum Geology, vol. 25, p. 969-980.

Heng, S., Collin, P.J., and Wilson, M.A., 1983 Hydrogenation of maceral concentrates from Bayswater coal: effect of temperature on the yield and mean chemical composition of the product, Fuel, vol. 62, p. 1359-1368.

Heywood, W.W., 1955 Arctic piercement domes, Bulletin of Canadian Institute of Mining and Metallurgy, vol. 48, p. 59-64.

Higgs, R., 1989 Sedimentological aspects of the Skonun Formation, Queen Charlotte Islands, British Columbia; In: Current Research, Part H, Geological Survey of Canada, Paper 89-1H, p. 87-94.

Hitchon, B., 1963 Geochemical studies of natural gas, Journal of Canadian Petroleum Technology, vol. 2, p. 60-76.

——— , 1984 Geothermal gradients, hydrodynamics and hydrocarbon occurrences, Alberta, Canada, American Association of Petroleum Geologists Bulletin, vol. 68, p. 713-743.

Hood, A., Gutjahr, C.C.M. and Heacock, R.C., 1975 Organic metamorphism and the generation of petroleum, American Association of Petroleum Geologists Bulletin, vol. 59, p. 986-996.

Hufnagel, H., 1977 Des Fluoreszenzvermogen der Dinoflagellaten-Cysten-ein, Inkohlungsparameter Geologisches Jahrbuch, D. 23, p. 59-65.

Hughes, J.D., and Cameron, A.R., 1985 Lithology, depositional setting and coal rank-depth relationships in the Jurassic-Cretaceous Kootenay Group at Mount Allan,

Cascade Coal Basin, Alberta, Geological Survey of Canada, Paper 85-11.

Huizinga, B.J., Tannenbaum, E., and Kaplan, I.R., 1987 The role of minerals in the thermal alteration of organic matter-IV: Generation of n-alkanes in laboratory experiments, Geochimica et Cosmochimica Acta, vol. 51, p. 1083-1097.

Hunt, J.M., 1963 Composition and origin of the Uinta Basin bitumens; In: Oil and gas possibilities of Utah re-evaluated, Crawford, A.L. (Ed.), Utah Geological and Mineralogical Survey, Bulletin 54, Paper 24, Salt Lake City, Utah Geological Society, p. 249-273.

———, 1979 Petroleum Geochemistry and Geology, W.H. Freeman and Company, San Francisco, 617 pp.

———, and McNichol, A.P., 1984 The Cretaceous Austin chalk of south Texas - a petroleum source rock; In: American Association of Petroleum Geologists Studies in Geology, J. G. Palacas (Ed.), vol. 18, p. 117-125.

———, Stewart, F. and Dickey, P.A., 1954 Origin of hydrocarbons in the Uinta Basin, Utah, American Association of Petroleum Geologists Bulletin, vol. 38, p. 1671-1698.

Hutton, A., 1986 Petrographic classification of oil shales, International Journal Coal Geology, vol. 8, no. 3, p. 203-231.

———, and Cook, A.C., 1980 Influence of alginite in the reflectance of vitrinite from Joadja, N.S.W., and some other coals and oil shales containing alginite, Fuel, vol. 59, p. 711-716.

International Committee for Coal Petrology, 1975 International Handbook of Coal Petrology, 3rd edition 1971, supplement to 3rd edition 1975, Centre Nationale de la Recherche Scientifique, Paris.

Issler, D., 1985 Calculation of organic maturation levels for offshore eastern Canada-implications for general application of Lopatin's method, Canadian Journal of Earth Sciences, vol. 21, p. 477-487.

Jacob, H., 1967 Petrologie von Asphaltiten und asphaltischen Pyrobitumina, Erdol und Kohle, Hamburg, vol. 20, no. 6, p. 292-400.

———, 1975 Mikroskopphotometrische Analyse naturlicher fester Erdolbitumina; In: Petrographie de la matiere organique des sedimentes, relations avec la paleotemperature et le potentiel petrolier, Alpern, B (Ed.), Editions Technip, Paris, p. 103-113.

———, 1976 Optische analyse disperser bitumina, Erdol und Kohle, Leinfenden, vol. 29, no. 6, p. 257.

———, 1983 Report on bitumens: International Committee for Coal Petrology, Meeting 1983, Oviedo, Spain.

———, 1985 Disperse solid bitumens as an indicator for migration and maturity in prospecting for oil and gas, Erdol und Kohle, vol. 38, p. 365.

———, 1989 Classification, structure, genesis and practical importance of natural solid oil bitumen ('migrabitumen'), International Journal of Coal Geology, vol. 11, no. 1, p.

65-79.

_____ , and Wehner, H., 1981 Mikroskopphotometrische Analyse disperser Festbitumina in Sedimenten: DGMK - Forschungsbericht vol. 232, 123 pp. Hamburg.

_____ , and Hiltmann, W., 1985 Disperse, feste, Erdolbitumina, als Migrations-und Maturitats-Indikatoren im Rahmen der Erdol-/Erdgas-Prospektion. Eine Modellstudie in NW Deutschland: DGMK-Forschungsbericht vol. 267, 54 pp.

_____ , and Hiltmann, W., 1988 Disperse, feste erdol bituminic als matarituts - Indikatoren in Rahmen der Erdol-Erdgas-Prospektion, Geologisches Jahrbuch, vol. 89, p. 3-37.

Jenkins, W.A.M., 1970 Chitinozoa, American Association of Stratigraphic Palynologists 1st Annual Meeting, Geoscience and Man, vol. 1, p. 1-21.

Johns, W.D., and Shimoyama, A., 1972 Clay minerals and petroleum-forming reactions during burial and diagenesis, American Association of Petroleum Geologists, vol. 56, p. 2160-2167.

Jones, R.W. and Edison, T., 1979 Microscopic observations of kerogen related to geochemical parameters with emphasis on thermal maturation; In: D.E. Oltz (Ed.), Low temperature metamorphism of kerogen and clay minerals; Symposium in Geochemistry, Pacific section, Society of Econom. Paleontologists and Mineralogists, p. 1-12, Los Angeles.

Jones, F.W., and Majorowicz, J.H., 1987 An investigation of the terrestrial heat flow of the Sverdrup Basin, Canadian Arctic Islands and its relation to hydrocarbon maturation and migration, Phase I: Geothermal Laboratory, Department of Physics, The University of Alberta, Edmonton, Alberta. Internal Report prepared for Energy, Mines and Resources, Institute of Sedimentary and Petroleum Geology, Calgary.

———, Majorowicz, J.A., and Embry, A,F., 1989 A heat flow profile across the Sverdrup Basin, Canadian Arctic Islands, Geophysics, vol. 54, p. 171-180.

Jones, G. H., 1981 Economic development - oil and gas; In: A Century of Canada's Arctic Islands, 1880-1980, M. Zaslow (Ed.), Royal Society of Canada.

Jones, J. M., and Murchison, D.G., 1963 The occurrence of resinite in bituminous coals, Economic Geology, vol. 58, p. 263-73.

Jones, J.M., Murchison, D.G., and Saleh, S.A., 1971 Variation of vitrinite reflectivity in relation to lithology; In: H. W. Gartner and H. Wehner (Eds.), Advances in Organic Geochemistry, Pergamon Press, New York, NY, p. 601-612.

Kalkreuth, W., and Macauley, G., 1987 Organic petrology and geochemical (Rock-Eval) studies on oil shales and coals from the Pictou and Antigonish areas, Nova Scotia, Canada, Bulletin of Canadian Petroleum Geology, vol. 35, no. 3, p. 263-295.

Kantsler, A.J., 1980 Aspects of organic petrology with particular reference to the exinite group of macerals; In: Oil Shale Petrology Workshop, Cook, A.C. and Kantsler, A.J. (Eds.), Wollongong, 1980, Keiraville Kopiers, p. 16-42.

Karweil, J., 1955 Die metamorphase der kohlen von standpunkt der physikclischen Chemie: Zeitschrift der Deutschen Geologischen Gesellschaft, vol. 107, p. 132-139.

———, 1975 The determination of paleotemperatures from the optical reflectance of coaly particles in sediments; In: Colloque International Petrographie de la matiere organique des sediments, B. Alpern (Ed.), Paris, 1973, p. 195-204.

Katz, B.J., 1981 Limitations of Rock-Eval pyrolysis for typing organic matter, American Association of Petroleum Geologists Bulletin, vol. 65, p. 944.

———, 1983 Limitations of Rock-Eval pyrolysis for typing organic matter, Organic Geochemistry, vol. 4, p. 145-199.

———, Pheifer, R.N., and Shunk, D.J., 1988 Interpretation of discontinuous vitrinite reflectance profiles, American Association of Petroleum Geologists Bulletin, vol. 72, p. 926-931.

Kemp, A.E.S., Oliver, G.H.J., and Baldwin, J.R., 1985 Low-grade metamorphism and accretion tectonics: Southern Uplands terrain, Scotland, Mineralogical Magazine, vol. 49, p. 335-344.

Kendrick, J.W., Hood, A., and Castano, J.R., 1978 Petroleum-generating potential of sediments from the Eatern Mediterranean and Black Seas; In: Initial reports of the Deep Sea Drilling project, vol. 42, Washington, D.C., J. I. Usher and P. Supko (Eds.), U.S. Government Printing Office, p. 729-735.

Khavari-Khorasani, G., 1975 The properties and structural ordering of some fossil

bitumens, Unpublished Ph. D. thesis, University of Newcastle-upon-Tyne, England, 350 pp.

_____, 1983 Structure of albertite from New Brunswick, Canada, Bulletin of Canadian Petroleum Geology, vol. 31, p. 123-126.

_____, 1984 Free hydrocarbon in Unita Basin, Utah, American Association of Petroleum Geologists Bulletin, vol. 68, p. 193-194.

_____, 1987 Novel development in fluorescence microscopy of complex organic mixtures: Application in petroleum geochemistry, Organic Geochemistry, vol. 11, no. 3, p. 157-168.

_____, and Murchison, D.G., 1978 Thermally metamorphosed bitumen from Windy Knoll, Derbyshire, England, Chemical Geology, vol. 22, p. 91-105.

_____, and _____, 1988 Order of generation of petroleum hydrocarbons from liptinitic macerals with increasing thermal maturity, Fuel, vol. 67, no. 8, p. 1160-1162.

Kidwai, M.A., 1986 Development of graptolite reflectance as an indicator of paleotemperature and thermal maturation, Unpublished M.S. thesis, Oklahoma State University, Stillwater, 71 pp.

Kirste, D., Fowler, M.G., Goodarzi, F. and Macqueen, R.W., 1989 Optical and compositional character and paleothermal implications of a diverse suite of natural bitumen from Middle Devonian carbonate rocks, Pine Point, Northwest Territories; In: Current Research, Part G, Geological Survey of Canada, Paper 89-1G, p.

51-55.

Konig, C., 1823 An account of the rock speciments collected by Captain Parry, during the Northern Voyage of Discovery, performed in the years 1819 and 1820, Quarterly Journal of Science XV, 1923 p. 11-220.

Kunstner, E., 1974 'Vergleichende Inkohlungsuntersuchungen unter besonderer Berucksichtigung mikrophotometrischer Reflecionsmessungen an Kohlen, Brandschiefern und kohlehaltigem Nebengestein' Freiberger Forschungschefte, C287 Erkundungsgeologie, 1974, p. 9-86.

Kurylowicz, L.E., Ozimic, S., McKirdy, D.M., Kantsler, A.J. and Cook, A.C., 1976 Reservoir and source rock potential of the Larapinta Group, Amadeus Basin, Central Australia, Australian Petroleum Exploration Association Journal, vol. 16, no. 2, p. 49-65.

Lam, H.L., Jones, F.W. and Lambert, C., 1982 Geothermal gradients in the Hinton area of west-central Alberta, Canadian Journal of Earth Sciences, vol. 19, p. 755-766.

Larter, S.R., 1984 Application of analytical pyrolysis techniques to kerogen characterization and fossil fuel exploration/exploitation; In: Analytical Pyrolysis - Methods and Applications, Voorhess, K. (Ed.), p. 212-275, Butterworths, London.

Lebkuchner, R.F., Orhun, F., and Wolf, M., 1972 Asphaltic substances in southeastern Turkey, American Association of Petroleum Geologists Bulletin, vol. 56, p. 1939-1964.

Leckie, D.A., Kalkreuth, W.D. and Snowdon, L.R., 1988 Source rock potential and thermal maturity of Lower Cretaceous Strata: Monkman Pan area, British Columbia, American Association of Petroleum Geologists Bulletin, vol. 72, no. 7, p. 820-838.

Lee, W.H.K., and Uyeda, S., 1965 Review of heat flow data; In: Terrestrial Heat, A.G.U. Geophysical Monogram, vol. 8, p. 87-190.

Legall, F.D., Barnes, C.R. and Macqueen, R.W., 1981 Thermal maturation, burial history and hotspot development, Palaeozoic strata of southern Ontario-Quebec, from conodont and acritarch colour alteration studies, Bulletin of Canadian Petroleum Geology, vol. 39, no. 4, p. 492-539.

Leventhal, J.L., 1982 Limitations of Rock-Eval pyrolysis to characterize kerogen, American Association of Petroleum Geologists Bulletin, vol. 66, p. 593.

Link, C., 1988 A reconnaissance of organic maturation and petroleum source potention of Phanerozoic strata in northern Yukon and northwestern District of Mackenzie, M.Sc. thesis, University of British Columbia, 260 pp.

Lopatin, N.V., 1971 Temperature and geological time as factors in coalification, Izvestija Akademi Nauk SSRS, Serija Geologica, vol. 3, p. 95-106 (in Russian, translated into English by N.W. Bostick, 1972).

Macauley, G., and Snowdon, L.R., 1984 A Rock-Eval appraisal of the Ordovician Collingwood oil shales, southern Ontario, Geological Survey of Canada, Open File Report OF1092, 12 pp.

——— , Snowdon, L.R., and Ball, F.D., 1985 Geochemistry and geological factors governing exploration (or exploitation) of selected Canadian oil shale deposits, Geological Survey of Canada, Paper 85-13, 65 pp.

——— , Fowler, M.G., Goodarzi, F., Snowdon, L.R., and Stasiuk, L.D., 1990 Ordovician oil shale - source rock sediments in the central and eastern Canada mainland and eastern Arctic areas, and their significance for frontier exploration; In: Geological Survey of Canada, Paper 90-14, 51 pp.

MacKenzie, D., 1981 The variation of temperature with time and hydrocarbon maturation in sedimentary basins formed by extension, Earth and Planetary Science Letters, vol. 55, p. 87-98.

Mackowsky, M-Th. 1982 Preparation of polished surfaces from particulate samples; In: Coal Petrology Stach, E., Mackowsky, M-Th., Teichmuller, M., Taylor, G.H., Chandra, D., Teichmuller, R. (Eds.) Gebruder Borntraeger, Berlin-Stuttgart, p. 296-299.

Macqueen, R.W., and Powell, T.G., 1983 Organic geochemistry of Pine Point lead-zinc ore field and region, Northwest Territories, Canada, Economic Geology, vol. 78, p. 1-25.

Majorowicz, J.A., and Jessop, A.M., 1981 Regional heat flow patterns in the Western Canadian Sedimentary Basin, Tectonophysics, vol. 74, p. 209-238.

——— , Jones, F.W., and Jessop, A., 1986 Geothermics of the Williston Basin in Canada in relation to hydrodynamics and hydrocarbon occurrences, Geophysics,

vol. 51, p. 767-779.

Manskaya, S.M., and Drozdova, T.V., 1968 Geochemistry of organic substances, Pergamon Press, Oxford.

Mayr, U. 1980 Stratigraphy and Correlation of Lower Paleozoic formations of Bathurst and adjacent smaller islands, Canadian Arctic Archipelago, Geologial Survey of Canada, Bulletin 306.

McAlpine, K.D., 1989 Mesozoic Stratigraphy, Sedimentary Evolution and Petroleum Potential of the Jeanne d'Arc Basin, Grand Banks of Newfoundland; In: Current Research Geological Survey of Canada, Paper 9-17, 39 pp.

———, and Grant, A.C., 1986 Petroleum geology of the Jeanne d'Arc Basin, offshore Newfoundland; In: Program with Abstracts, Canadian Society of Petroleum Geologists 1986 Convention, Calgary, June 1-4, 1986, 64 pp.

———, Bell,, J.S., Avery, M.P., Snowdon, L.R., and Brooks, P.W., 1986 Hydrocarbon generation in the Jeanne d'Arc Basin, offshore Newfoundland; In: Program with Abstracts, Geological Survey of Canada Forum, Activities on Oil and Gas in Canada, Calgary, February 11-12, 1986, 11 pp.

———, Fowler, M.G., Brooks, P.W., and Snowdon, L.R., 1988 Hydrocarbon generation and migration in the Jeanne d'Arc Basin: a case history; In: Program with Abstracts, Geological Association of Canada/Mineralogical Association of Canada/Canadian Society of Petroleum Geologists Joint Annual Meeting, St. John's, May 23-25, 1988, p. A81.

McCartney, J.T., 1952 A study of the Seyler theory of coal reflectance, Economic Geology, vol. 47, p. 202-210.

McGregor, D.C. and Camfield, M., 1982 Middle Devonian miospores from the Cape de Bray, Weatherall, and Hecla Bay formations of northeastern Melville Island, Canadian Arctic, Geological Survey of Canada, Bulletin 348.

McMillan, J.G., 1910 Geological Report; In: Report on the Dominion of Canada Government Expedition to the Arctic Islands and the Hudson Strait on board the D.G.S. Arctic (1908-09), by J. E. Bernier, Ottawa, Queen's Printer.

Middleton, M.F., 1982 Tectonic history from vitrinite reflectance, Geophysical Journal of the Royal Astronomical Society, vol. 68, p. 121-132.

Monnier, F., Powell, T.G. and Snowdon, L.R., 1983 Qualitative and quantitative aspects of gas generation during maturation of sedimentary organic matter - Examples from Canadian Frontier Basins, Advances in Organic Geochemistry, p. 487-495, Wiley, Chichester.

Moore, R.C., Lalicker, C.G., and Fischer, A.G., 1952 Invertebrate Fossils McGraw-Hill, New York, Chapter 22, p. 715-733.

Mukhopadhyay, P.K., Hagemann, H.W. and Gormly, J.R., 1985 Characterization of kerogens as seen under the aspect of maturation and hydrocarbon generation, Erdol und Kohle, vol. 38, no. 1, p. 7-18.

Murchison, D.G., 1976 Resinite: its infrared spectrum and coalification pattern, Fuel, vol.

55, p. 79-83.

——— , 1987 Recent advances in organic petrology and organic geochemistry: an overview with some reference to 'oil from coal', Coal and coal-bearing strata: Recent Advances, Scott, A.C., (Ed.), Geological Society Special Publication no. 32, p. 257-302.

——— , Cook, D.G., and Raymond, A.C., 1985 Optical properties of organic matter in relation to thermal gradients and structural deformation; In: Geochemistry of Buried Sediments, Eglinton, G., Curtis, C.D., McKenzie, D.P. and Murchison, D.G., (Eds.) p. 157-86, Royal Society of London.

Nassichuk, W.W., 1965 Pennsylvanian and Permian rocks in the Parry Islands group, Canadian Arctic Archipelago; In: Report of Activities: Field 1964, Geological Survey of Canada, Paper 65-1, p. 9-12.

——— , 1972 Sverdrup Basin; In: The Canadian Arctic Islands and the Mackenzie Region, Christie, R.L., Cook, D.G., Nassichuk, W.W., Trettin, H.P., and Yorath, C.J. (Eds.), XXIV International Geological Congress, Montreal, Field Excursion A66, p. 109-131.

——— , 1975 Carboniferous ammonoids and stratigraphy in the Canadian Arctic Archipelago, Geological Survey of Canada, Bulletin 237.

Nunn, J.A., Sleep, N.H., and Moore, W.E., 1984 Thermal subsidence and generation of hydrocarbons in Michigan Basin, American Association of Petroleum Geologists Bulletin, vol. 68, p. 296-315.

Oliver, G.J.H., 1987 Arenig to Wenlock regional metamorphism in the paratectonic Caledonides of the British Isles: A review; In: The Caledonian-Appalachian Orogen, Harris, A.L. and Fettes, D.J. (Eds.), Special Publication of the Geological Society of London, Blackwell Scientific Publications, Oxford.

Orr, W.L., 1981 Comments on pyrolytic hydrocarbon yields in source-rock evaluation, Advances in Organic Geochemistry, M. Bjoroy et al. (Eds.), John Wiley, Chichester, p. 775-787.

Osadetz, K.G., and Snowdon, L.R., 1986a Petroleum source rock reconnaissance of southern Saskatchewan; In: Current Research, Part A, Geological Survey of Canada, Paper 86-1A, p. 609-617.

_____, _____, 1986b Speculation on the petroleum source rock potential of portions of the Lodgepole Formation (Mississippian) of southern Saskatchewan; In: Current Research, Part B, Geological Survey of Canada, Paper 86-1B, p. 647-651.

_____, _____, and Stasiuk, L.D., 1989 Association of enhanced hydrocarbon generation and crustal structure in the Canadian Williston Basin; In: Current Research, Part D, Geological Survey of Canada Paper 89-1D, p. 35-47.

Ottenjann, K., Teichmuller, M. and Wolf, M., 1974 Spektrale Fluoreszenzmessungen an Sporiniten mit Auflicht - Anregung, eine mikroskopische Methode zur Bertimmung des Inkohlungsgrades gering inkohlter Kohlen, Fortschr Geol. Rheinland und Westfalen, vol. 24, p. 1-36.

_____, _____, and _____, 1975 Spectral fluorescence measurements of sporinites in

reflected light and their applicability for coalification studies; In: Petrographie de la matiere organique des sedimentes, relations avec la paleotemperature et le potentiel petrolier, Alpern, B (Ed.), p. 67-91, Centre National de la Recherche Scientifique, Paris.

Parry, W.E., 1819 Journal of a Voyage for discovery of a North-West Passage from Atlantic to the Pacific performed in years 1819-1820 in H.M.S. Hecla and Criper, London, John Murray.

Pearson, J., and Murchison, D.G., 1990 Influence of a sandstone washout on the properties of an underlying coal seam, Fuel, vol. 69, p. 251-253.

Peters, K.E., 1986 Guidelines for evaluating petroleum source rock using programmed pyrolysis, American Association of Petroleum Geologists Bulletin, vol. 70, p. 318-329.

Pitt, G.M., 1982 Geothermal gradients in the Eromanga/Cooper Basins; In: Eromanga Basin Symposium, Summary Papers, Moore, P.S. and Mount, T.J. (Compilers), Geology Society of Australia and Petroleum Exploration Society of Australia, Adelaide, p. 268-283.

——— , 1986 Geothermal gradients, geothermal history and the timing of thermal maturation in the Eromanga-Cooper Basins, Contributions to the geology and hydrocarbon potential of the Eromanga Basin, Special Publication - Geological Society of Australia, vol. 12, p. 323-351.

Podruski, J.A., Barclay, J.E., Hamblin, A.P., Lee, P.J., Osadetz, K.G., Procter, R.M., and

Taylor, G.C., 1988 Conventional oil resources of Western Canada (light and medium), Geological Survey of Canada, Paper 87-26.

Polak, E.J. and Ramsay, D.C., 1977 Canaway Ridge, Queensland, Geophysical Survey, 1973 Australian Bureau of Mineral Resources Geology and Geophysics, no. 1977/29 (Unpublished).

Potonie, H., 1950 Petrographische Klassifikation der Bitumina, Geologisches Jahrbuch, vol. 65, p. 551-572.

Powell, T.G., 1978 An assessment of the hydrocarbon source rock potential of the Canadian Arctic Islands, Geological Survey of Canada, Paper 78-12, 78 pp.

——— , 1984 Developments in concepts of hydrocarbon generation from terrestrial organic matter, Proceedings of the Beijing Petroleum Symposium, p. 1-36, Beijing, China.

——— , 1984 Hydrocarbon-source relationships, Jeanne d'Arc and Avalon basins, offshore Newfoundland, Geological Survey of Canada, Open File #1094, 12 pp.

——— , and Snowdon, L.R., 1979 Geochemistry of crude oils and condensates: offshore eastern Canada, Bulletin of Canadian Petroleum Geology, no. 27, p. 453-66.

———, and _____, 1980 Geochemical controls of hydrocarbon generation in Canadian sedimentary basins; In: Facts and Principles of World Petroleum Occurrence, A.D. Miall (Ed.), Canadian Society of Petroleum Geologists, Memoir 6, p. 421-446.

——— , and _____ , 1983 A composite hydrocarbon generation model-implications for evaluation of basins for oil and gas, Erdol und Kohle, vol. 36, no. 4, p. 163-170.

——— , Creaney, S., and Snowdon, L.R., 1982 Limitations of use of organic petrographic techniques for identification of petroleum source rocks, American Association of Petroleum Geologists Bulletin, vol. 66, p. 430-435.

——— , Foscolos, A.E., Gunther, P.R., and Snowdon, L.R., 1978 Diagenesis of organic matter and fine clay minerals: a comparative study, Geochimica et Cosmochimica Acta, vol. 42, p. 1181-1197.

——— and McKirdy, D.M., 1975 Geological factors controlling crude oil composition in Australia and Papua New Guinea, American Association of Petroleum Geologists Bulletin, vol. 59, p. 1176-97.

Price, L.C. and Barker, C.E., 1985 Suppression of vitrinite reflectance in amorphous rich kerogen - A major unrecognized problem, Journal of Petroleum Geology, vol. 8, no. 1, p. 59-84.

——— , Clayton, J.L. and Rumen, L.L., 1981 Organic geochemistry of the Bertha Rogers No. 1 well, Oklahoma, Organic Geochemistry, vol. 3, no. 3, p. 59-77.

Procter, R.M., Taylor, G.C., and Wade, J.A., 1984 Oil and Natural Gas Resources of Canada Geological Survey of Canada, Paper 83-31, 59 pp.

Purcell, L.P., Rashid, M.A., and Hardy, I.A., 1979 Geochemical characteristics of sedimentary rocks in Scotian Basin, American Association of Petroleum Geologists

Bulletin, vol. 63, p. 87-105.

Radke, M., Schaefer, R.G., Leythaeuser, D. and Teichmuller, M., 1980 Composition of soluble organic matter in coals: relation to rank and liptinite fluorescence, Geochimica et Cosmochimica Acta, vol. 44, p. 1787-1800.

Rashid, M.A., and McAlary, J.D., 1977 Early maturation of organic matter and genesis of hydrocarbons as a result of heat from a shallow piercement salt dome, Journal of Geochemical Exploration, vol. 8, p. 549-570.

_____, Purcell, L.P. and Hardy, I.A., 1980 Source rock potential for oil and gas of the East Newfoundland and Labrador Shelf areas; In: Facts and Principles of World Oil Occurrence, Miall, A.D. (Ed.), Canadian Society of Petroleum Geologists, Memoir 6, p. 589-608.

Raymond, A.C., and Murchison, D.G., 1988 Development of organic maturation in the thermal aureoles of sills and its relation to sediment compaction, Fuel, vol. 67, p. 1599-1608.

_____, and _____, 1989 Organic maturation and its timing in a Carboniferous sequence in the central Midland Valley of Scotland: comparisons with northern England, Fuel, vol. 68, p. 328-334.

Rice, D.D. , and Shurr, G.W., 1980 Shallow low-permeability reservoirs of northern Great Plains - assessment of their natural gas resources, American Association of Petroleum Geologists Bulletin, vol. 64, p. 969-987.

Riediger, C.L., Bustin, R.M., and Rouse, G.E., 1984 New evidence for the chronology of the Eurekan Orogeny from south-central Ellesmere Island, Canadian Journal of Earth Sciences, vol. 21, p. 1286-1295.

———, Goodarzi, F., and Macqueen, R.W., 1989 Graptolite as an indicator of regional maturity in Lower Palaeozoic sediments, Selwyn Basin, Yukon and Northwest Territories, Canada, Canadian Journal of Earth Sciences, vol. 26, p. 2003-2015.

———, Fowler, M.G., Brooks, P.W., and Snowdon, L.R., 1991. Triassic oils and potential Mesozoic source rocks, Peace River Arch area, Western Canada Basin, Organic Geochemistry, (in press).

Robert, P., 1971 Etude petrographique des matieres organiques insolubles par la mesure de leur pouvoir reflecteur, Contribution a l'exploration petroliere et a la connaissare des basins sedimentaires, Revue Institut Francais du Petrole, vol. 26, p. 105-136.

———, 1973 Analyse microscopique des charbons et des bitumens disperses dans les roches et mesure de leur pouvoir reflecteur, Application a l'etude de la paleogeothermie des bassins sedimentaires et de la genese des hydrocarbures (abs); In: Advances in Organic Geochemistry, International Meeting of Organic Geochemistry, Program and Abstracts, no. 6, p. 549-569.

———, 1980 The optical evaluation of kerogen and geothermal histories applied to oil and gas exploration; In: Kerogen, Durand, B. (Ed.), Editions Technip, Paris, p. 385-414.

——— , 1988 Microscopic study of organic matter and thermal evaluation of sedimentary basins; In: Organic Metamorphism and Geothermal history, Elf Aquitaine and D. Riedel Publishing Company, Boston, Lancaster, Tokyo.

Rogers, M.A., 1979 Application of organic facies concept to hydrocarbon source evaluation; In: Exploration, Supply and Demand, vol. 2, p. 23-30, Proceedings of the 10th World Petroleum Congress, Bucharest.

——— , McAlary, J.D. and Bailey, N.J.L., 1974 Significance of reservoir bitumens to thermal maturation studies, Western Canada Basin, American Association of Petroleum Geologists Bulletin, vol. 58, no. 9, p. 1806-1824.

Royden, L., 1986 A simple method of analyzing subsidence and heat flow in extensional basins; In: Thermal Modelling in Sedimentary Basins, J. Burrus (Ed.), Editions Technip, Paris, p. 49-73.

Sass, J.H., Blackwell, D.D., Chapman, D.S., Costain, J.K., Decker, E.R., Lawver, L.A. and Swanberg, C.A., 1971 Heat flow from the crust of the United States, Chapter 12; In: Physical properties of rocks and minerals, Tonlockian, Y.S., Judd, W.R. and Roy, R.F. (Eds.), vol. II-2, McGraw-Hill Cindas, Data series on material properties, p. 503-548.

Saxby, J.D. and Shibaoka, M., 1986 Coal and coal macerals as source rocks for oil and gas, Applied Geochemistry, vol. 1, p. 25-36.

Schwab, K.W., 1966 Microstructure of some fossil and resent scolecodonts, Journal of Palaeontology, vol. 40, p. 416-423.

Sclater, J.E. and Christie, P.A.F., 1980 Continental stretching and explanation of the post-Mid-Cretaceous subsidence of the central North Sea Basin, Journal of Geophysical Research, vol. 85, p. 3711-3739.

Sherwood, N.R. and Cook, A.C., 1986 Organic matter in the Toobeluc Formation, Geological Society of Australia Special Publication, no. 12, p. 255-265.

Shibaoka, M., 1978 Micrinite and exudatinite in some Australian coals and their relation to the generation of petroleum, Fuel, vol. 57, p. 73-78.

——— , and Bennett, A.T.R., 1977 Patterns of diagenesis in some Australian sedimentary basins, Australian Petroleum Exploration Association Journal, vol. 17, p. 58-63.

Skibo, D.N., Osadetz, K.G., and Goodarzi, F., 1990 Models of organic maturation and hydrocarbon potential: Application to Lougheed Island drillholes, Sverdrup Basin, Canadaian Arctic Islands; In: Current Research, Part D, Geological Survey of Canada Paper 90-1D, p. 201-211.

Snowdon, L.R., 1980 Resinite - A potential petroleum source in the Upper Cretaceous/Tertiary of the Beaufort-Mackenzie Basin; In: Facts and Principles of World Petroleum Occurrence, Miall, A.D. (Ed.), Canadian Society of Petroleum Geologists, Memoir 6, p. 421-446.

——— , 1986 The stable carbon isotope distribution of distillation fractions of three Canadian frontier crude oils, Bulletin of Canadian Petroleum Geology, vol. 34, no. 3, p. 379-383.

——— , and Roy, K.J., 1975 Regional organic metamorphism in the Mesozoic strata of the Sverdrup Basin, Bulletin of Canadian Petroleum Geology, vol. 23, p. 131-148.

——— , and Powell, T.G., 1982 Immature oil and condensate-modification to hydrocarbon generation model for terrestrial organic matter, American Association of Petroleum Geologists Bulletin, vol. 66, p. 775-788.

——— , and Krouse, H.R., 1986 The stable carbon isotope distribution of distillation fractions of three Canadian frontier crude oils, Bulletin of Canadian Petroleum Geology, vol. 34, no. 3, p. 379-383.

——— , Brooks, P.W. and Goodarzi, F., 1986 Chemical and petrological properties of some liptinite-rich coals from British Columbia, Fuel, vol. 65, p. 460-472.

Stach, E., 1982 The lithotypes of humic and sapropelic coals; In: E. Stach, M- Th. Mackowsky, M. Teichmuller, G.H. Taylor, D. Chandra and R. Teichmuller (Eds.), Coal Petrology Gebruder Borntraeger, Berlin-Stuttgart, p. 171-177.

Stainforth, J.G., 1984 Gippsland hydrocarbons - a perspective from the basin edge, Australian Petroleum Exploration Association Journal vol. 24, no. 1, p. 91-100.

Staplin, F.L., 1969 Sedimentary organic matter, organic metamorphism, and oil and gas occurrence, Bulletin of Canadian Petroleum Geology, vol. 17, p. 47-66.

Stasiuk, L.D., 1988 Thermal Maturation and Organic Petrology of Mesozoic Strate of Southern Saskatchewan, Unpublished, M.Sc. Thesis, The University of Regina, Saskatchewan, 178 pp.

Stefansson, V., and Bartlett, R.A., 1916 The last voyage of the Kalkluk, Flagship of Wilhjalmar Steffanson's Canadian Arctic Expedition of 1913-1916 as related by Her Master Robert A. Bartlett and here set down by Ralph T. Hale, P.T.O. Toronto, McClelland, Goodchild and Stewart 1916.

Stephenson, R.A., Embry, A.F., Nakiboglu, S.M., and Hasticoglu, M.A., 1987 Rift-initiated Permian - Early Cretaceous subsidence in the Sverdrup Basin; In: Sedimentary Basins and Basin Forming Mechanisms, C. Beaumont and A. Tankard (Eds.), Canadian Society of Petroleum Geologists, Memoir 12, p. 213-231.

Stoakes, F.A., and Creaney, S., 1984 Sedimentology of a Carbonate Source Rock: The Duvernay Formation of Central Alberta, Carbonates in Subsurface and Outcrop, 1984, Canadian Society of Petroleum Geologists Core Conference.

Stroganov, V.P., 1973 On the main phase of generation of gaseous and liquid hydrocarbons and conditions of formation of zones of oil and gas accumulation, Sov. Geol. vol. 9, p. 65-75.

Sverdrup, O., 1903 The second Norwegian Polar Expedition in the "Fram", 1898-1902; plus summary of Geological results by P. Schei, Geological Journal, vol. 22.

———, 1904 Newland. Four years in the Arctic regions translated from the Norwegian by E.H. Hearn. Longmans, Green and Co., 2 volumes.

Swift, J.H., and Williams, J.A., 1980 Petroleum source rocks, Grand Banks area; In: Facts and Principles of World Petroleum Occurrences, A.D. Miall (Ed.), Canadian Society of Petroleum Geologists, Memoir 6, p. 567-588.

Tannenbaum, E., Huizinga, B.J., and Kaplan, I.R., 1986 Role of minerals in thermal alteration of organic - II: A material balance, American Association of Petroleum Geologists Bulletin, vol. 70, p. 1156-1165.

Teichmuller, M., 1958 Metamorphisme du charbon et prospection du petrole: Revue de l'Industrie Minerale, Special Publication, p. 99-113.

———, 1974 Generation of petroleum-like substances, in coal seams as seen under the microscope; In: Tissot, B. and Bienner, F. (Eds.), Advances in Organic Geochemistry, p. 379-408, Editions Technip, Paris.

———, 1978 Nachweis Von Graptolithen - periderm im geschieferten Gesteinen mit Hilfe Kohlenpetrologischer Methoden, Monatshefte Neues Jahrbuch Geologie und Palaontologie, vol. 7, p. 430-447.

———, 1982 Origin of the petrographic constituents of coal; In: Stach's Textbook of Coal Petrology, E. Stach, M-Th. Mackowsky, M. Teichmuller, G.H. Taylor, M. Teichmuller, D. Chandra and R. Teichmuller, (Eds.), Gebruder Borntraeger, Berlin-Stuttgart, p. 269-272.

———, 1987 Recent advances in coalification studies and their application to geology; In: Coal and Coal-bearing strata: Recent Advances, Scott, A.C. (Ed.), Geological Society Special Publication, no. 32, p. 127-169.

———, and Teichmuller, R., 1950 Das Inkohlungsbild des niedersachsischen Wealdenbeckens. Zeitschrift der deutschen geologischen Gesellschaft, vol. 100, p. 498-517.

_____ , and Teichmuller, R., 1968 Geological aspects of coal metamorphism; In: D. Murchison and T. S. Westoll (Eds.), Coal and Coal-bearing Strata, Oliver and Boyd, Edinburgh, p. 233-267.

_____ , and Ottenjann, K., 1977 Art und diagenese von Liptiniten und lipoiden stoffen in einem Erdolmuttergestein auf Grund fluoreszenzmikroskopischer Untersochungen, Erdol und Kohle, vol. 30, p. 387-398.

_____ , and Teichmuller, R., 1979 Diagenesis of coal (coalification); In: Larsen, G. and Chillingar, G.V. (Eds.), Diagenesis of sediments and sedimentary rocks, New York, Elsevier, Developments in Sedimentology, vol. 25A, p. 207-246.

_____ , and _____ , 1981 The significance of coalification studies to geology - A review, Bulletin des Centres de Recherches Exploration-Production Elf-Aquitaine, vol. 5, p. 491-534.

_____ , and Teichmuller, R., 1982 Fundamentals of Coal Petrology; In: Stach's Textbook of Coal Petrology, E. Stach, M-Th. Mackowsky, M. Teichmuller, G.H. Taylor, D. Chandra and R. Teichmuller (Eds.), Gebruder Borntraeger, Berlin-Stuttgart, p. 55-66.

_____ , and Durand, B., 1983 Fluorescence microscopial rank studies on liptinites and vitrinites in peats and coals, and comparisons of results with Rock-Eval pyrolysis, International Journal of Coal Geology, vol. 2, p. 197-230.

Texaco Canada Resources Ltd., 1983 Melville Island - Northwest Territories, Canada: Line No. 7; In: Seismic expression of structural styles, vol. 3, A. W. Bally (Ed.),

American Association of Petroleum Geologists, p. 3.4.1-73 to 3.4.1-78.

Thorsteinsson, R. and Tozer, E.T., 1970 Geology of the Arctic Archipelago, Geological Survey of Canada, Economic Geology Report No. 1, Fifth Edition, p. 548-590.

Timofeev, P.P. and Bogolyubova, L.I., 1975 Relation of changes of organic and clay substances in deposits of the recent peat accumulation areas; In: Colloque International Petrographie de la matiere organique des sediments, B. Alpern (Ed.), Paris, p. 153-172.

Tissot, B.P., 1984 Recent advances in petroleum geochemistry applied to hydrocarbon exploration, American Association of Petroleum Geologists Bulletin, vol. 68, p. 545-563.

____, and Welte, D.H., 1984 Petroleum formation and occurrence, 2nd Edition, New York, Springer-Verlag, 669 pp.

____, Deroo, G., and Hood, A., 1978 Geochemical study of Uinta Basin, Formation of petroleum from the Green River Formation, Geochimica et Cosmochimica Acta, vol. 42, p. 1467-1485.

____, Pelet, R., and Ungerer, P., 1987 Thermal history of sedimentary basins, maturation indices and kinetics of oil and gas generation, American Association of Petroleum Geologists Bulletin, vol. 71, no. 12, p. 1445-1466.

____, Durand, B., Espitalie, J., and Combaz, A., 1974 Influence of nature and diagenesis of organic matter in formation of petroleum, American Association of

Petroleum Geologists Bulletin, vol. 58, p. 499-506.

——— , Demaison, G. Masson, P., Delteil, J.R. and Combaz, A., 1980 Paleoenvironment and petroleum potential of middle Cretaceous black shales in Atlantic basins, American Association of Petroleum Geologists Bulletin, vol. 64, p. 2051-2063.

Tozer, E.T., 1956 Geological reconnaissance, Prince Patrick, Eglinton, and western Melville Islands Arctic Archipelago, Northwest Territories, Geological Survey of Canada, Paper 55-5.

——— , 1961 Triassic stratigraphy and faunas, Queen Elizabeth Islands, Arctic Archipelago, Geological Survey of Canada, Memoir 316, p. 1-116.

——— , 1963 Southeastern Sabine Peninsula, Melville Island; In: Geology of the north-central part of the Arctic Archipelago, Northwest Territories (Operation Franklin), Geological Survey of Canada, Memoir 320, p. 645-655.

——— , 1970 Geology of the Arctic Archipelago, Mesozoic; In: Geology and Economic Minerals of Canada, R.J.W. Douglas (Ed.), Geological Survey of Canada, Economic Geology, Report 1, p. 574-583.

——— , 1973 Triassic assemblages (macrofossils); In: Norford B.S. et al. (Eds.), Biostratigraphic determinations of fossils from the subsurface of the Yukon Territory and the District of Franklin Keewatin and Mackenzie, Geological Survey of Canada, Paper 72-38, p. 18-19.

_____ , and Thorsteinsson, R., 1964 Western Queen Elizabeth Islands, Arctic Archipelago, Geological Survey of Canada, Memoir 332, p. 177-185.

Trettin, H.P., 1972 Franklinian Geosyncline; In: The Canadian Arctic Islands and the Mackenzie Region, Christie, R.L., Cook, D.G., Nassichuk, W.W., Trettin, H.P., and Yorath, H.P. (Eds.), XXIV International Geological Congress, Montreal, Field Excursion A66, p. 87-109.

Trettin, H. and Hills, C.V., 1966 Lower Triassic tar sands of northwestern Melville Island, Arctic Archipelago, Geological Survey of Canada, Paper 66-34.

_____ , and _____ ,1967 Triassic "tar sands" of Melville Island, Canadian Arctic Archipelago; Proceedings of the 7th World Petroleum Congress, Mexico City, vol. 3, p. 773-787.

Tschudy, R.N., and Scott, R.A., 1969 Aspects of palynology, John-Wiley and Sons, London, 469-474 pp.

van Gijzel, P., 1966 Die Fluoreszenz-Mikrophotometrie von Mikrofossillen Isen mit dem Zweistrahl-Mikroskopphotometer nach Berek, Leitz Mitt. F. Wiss, u Techn, 317, p. 206-214.

_____ , 1967 Autofluorescence of fossil pollen and spores with special reference to age determination and coalification, Leisde Geol. Meded., vol. 40, p. 263-317.

_____ , 1971 Review of the UV-fluorescence microphotometry of fresh and fossil exines and exosporia; In: Sporopollenin, J. Brooks, P.R. Grant, M. Muir, P. van Gijzel and

G. Shaw (Eds.), Academic Press, London, p. 659-685.

———, 1975 Polychromatic UV-fluorescence microphotometry of fresh and fossil plant substances with special reference to the location and identification of dispersed organic matter in rocks; In: Petrographie organique et Potentiel Petrolier, Alpern, B. (Ed.), Centre National de la Recherche Scientifique, Paris, 67pp.

van Hinte, J.E., 1978 Geohistory analysis - application of micropaleontology in exploration geology, American Association of Petroleum Geologists Bulletin, vol. 62, p. 201-222.

Vassoevich, N.B., Akramkhodzhaev, A.M., and Geodekyan, A.A., 1974 Principal zone of oil formation; In: Advances in Organic Geochemistry, Tissot, B. and Bienner, F. (Eds.), p. 309-314, Editions Technip, Paris.

Vellutini, D., and Bustin, R.M., 1988 Preliminary results on organic maturation of the Tertiary Skonun Formation, Queen Charlotte Islands; In: Current Research, Geological Survey of Canada, Paper 88-1E, p. 255-258.

von der Dick, H., and Meloche, J.D., 1986 Generation, migration and expulsion of hydrocarbons in the Hibernia field; In: Program and Abstracts, Canadian Society of Petroleum Geologists 1986 Convention, Calgary, June 1-4, 1988, p. 38.

Voss-Foucart, M.F., Vonze-Vignaux, T.Th and Jeuniaux, Ch., 1973 Systematic characters of some polychaetes (Annelida) at the level of the chemical composition of the jaws, Biochem. Syst., vol. 1, p. 119-122.

Waples, D.W., 1980 Time and temperature in petroleum formation: applications of Lopatin's method to petroleum exploration, American Association of Petroleum Geologists Bulletin, vol. 64. p. 916-926.

Watson, S.W., 1976 The sedimentary geochemistry of the Moffat shales: a carbonaceous sequence in the Southern Uplands of Scotland. Unpublished Ph.D. thesis, University of St. Andrews, Fife.

Welte, D.H., Schaefer, R.G., Radke, M. and Weiss, H.M., 1982 Association of American Petroleum Geologists: Abstracts, p. 123.

White, D., 1935 Metamorphism of organic sediments and derived oils, Bulletin of the American Association of Petroleum Geologists, vol. 18, p. 589-617.

Williams, G.K., 1983 What does the term "Horn River Formation" mean?, Bulletin of Canadian Petroleum Geology, vol. 31, no. 2, p. 117-122.

Williams, J.A., 1974 Characterization of oil types in Williston Basin, American Association of Petroleum Geologists Bulletin, vol. 58, p. 1243-1252.

Williams, P.V.F. and Goodarzi, F., 1981 Iranian bitumens, late stage alteration products of crude oil; In: Organic maturation studies of fossil fuel exploration, J. Brooks (Ed.), Academic Press, London, New York, p. 319-336.

Wood, D.A., 1988 Relationships between thermal maturity indicies calculated using Arrhenius equation and Lopatin method: Implications for petroleum exploration, American Association of Petroleum Geologists Bulletin, vol. 72, p. 115-135.

Wright, N.J.R., 1980 Time, temperature and organic maturation - the evolution of rank within a sedimentary pile, Journal of Petroleum Geology, vol. 2, p. 411-425.

Zalessky, M.D., 1917 On marine sapropelite of Silurian age formed by a blue-green alga, Izvestia Imperatorsko Academii Nauk, IV Ser., no. 1, p. 3-18.

Zierfus, H., 1969 Heat conductivity of some carbonate rocks and clayey sandstones, American Association of Petroleum Geologists Bulletin, vol. 53, p. 251-260.

APPENDIX I

Dundas C-80

Depth (m)	Org. Matter Type	% Ro max.	N	Depth (m)	Org. Matter Type	% Ro max.		N	
30.0	Vitr. *	0.91	3	1303.0	Bit. *	1.45		15	
63.0	"	0.74	50	1394.0	"	1.54		6	
94.0	"	0.86	50	1454.0	"	1.66		2	
97.0	"	0.88	50	1470.0	"	1.82		10	
166.0	"	0.79	25	1545.0	"	2.01		8	
194.0	"	0.79	33	1606.0	"	1.83	2.63	3	4
233.0	"	0.92	50	1697.0	"	1.54		7	
370.0	"	1.05	10	1879.0	"	2.03		12	
388.0	"	0.89	50	1939.0	"	2.30		17	
406.0	"	0.79	14	2000.0	"	2.16	2.86	7	15
415.0	"	0.84	20	2091.0	"	2.75		9	
464.0	"	0.85	27	2182.0	"	2.95		4	
476.0	"	1.0	50	2242.0	"	2.91		8	
518.0	"	0.74	6	2333.0	"	2.84		15	
588.0	"	0.75	5	2424.0	"	2.91	3.53	7	5
760.0	"	0.90	5	2485.0	"	2.80		50	
803.0	"	0.82	4	2576.0	"	3.11		9	
854.0	"	0.94	12	2667.0	"	3.11		30	
912.0	"	0.88	12	2712.0	"	2.31	3.19	25	8
994.0	"	1.14	30			3.88		10	
1151.0	"	0.93	4	2797.0	"	2.94	3.78	3	15
1394.0	"	1.12	8	2867.0	"	3.91		6	
2182.0	"	1.50	6	2882.0	"	3.24		25	
2712.0	"	1.80	15	2883.0	"	3.23		25	
3027.0	"	1.83	7	2884.0	"	3.03		25	
3051.0	"	1.93	5	2887.0	"	3.93		25	
3230.0	"	1.85	5	2900.0	"	3.09	3.93	15	14
3550.0	"	2.03	4	2970.0	"	2.88	3.61	3	9
				3051.0	"	2.90			4
				3106.0	"	2.78			4
				3136.0	"	2.72	3.56	16	2
						4.25			8
				3179.0	"	3.20			8
				3203.0	"	2.71	3.39	15	6
				3264.0	"	2.83	3.63	9	9
				3394.0	"	2.83	3.47	5	7
						4.07		5	
				3500.0	"	3.75		10	
				3606.0	"	3.31	3.77	6	4
						4.84		5	
				3835.0	"	4.14		6	
				3857.0	"	5.06		15	
				3912.0	"	3.87	4.96	5	2 5
				3954.0	"	4.43	5.35	5	5

* Vitr. - vitrinite
* Bit. - bitumen

Apollo C-73

Depth (m)	Org. Matter Type	% Ro max.	N	Depth (m)	Org. Matter Type	% Ro max.		N	
36.0	Vitr. *	0.83	27	12.0	Bit. *	1.24		5	
65.0	"	0.87	10	282.0	"	1.17		6	
70.0	"	0.74	13	552.0	"	1.29		5	
88.0	"	0.75	6	712.0	"	1.63		10	
106.0	"	0.83	17	1409.0	"	1.92		4	
149.0	"	0.75	8	1452.0	"	2.05		2	
173.0	"	0.75	12	1712.0	"	2.27		2	
191.0	"	0.73	17	1812.0	"	2.48		6	
207.0	"	0.83	9	1910.0	"	2.25		5	
221.0	"	0.97	12	2127.0	"	1.82	2.46	3	6
267.0	"	0.99	6	2160.0	"	2.25		7	
282.0	"	0.85	25	2270.0	"	2.45		8	
297.0	"	1.01	3	2352.0	"	2.20		33	
376.0	"	0.79	15	2415.0	"	2.37		13	
458.0	"	1.08	4	2449.0	"	1.89	2.52	2	21
503.0	"	0.92	8	2479.0	"	2.08	2.45	8	3
533.0	"	0.90	10	2512.0	"	2.34		16	
552.0	"	0.81	15	2545.0	"	1.92	2.49	6	6
630.0	"	0.94	10	2588.0	"	2.08		8	
712.0	"	0.96	21	2624.0	"	1.95	2.58	7	7
912.0	"	1.20	15	2664.0	"	1.80	2.42	2	8
945.0	"	1.24	15	2697.0	"	2.06	2.49	12	9
976.0	"	1.48	10	2727.0	"	2.00	2.40	14	6
1058.0	"	1.11	21	2758.0	"	2.08	2.43	2	9
1076.0	"	1.30	12	2788.0	"	2.26	2.80	21	4
1127.0	"	1.29	30	2818.0	"	2.01	2.52	6	7
1179.0	"	1.27	14	2830.0	"	3.15		25	
1236.0	"	1.47	5	2831.0	"	3.12		25	
1270.0	"	1.60	8	2832.0	"	3.20		16	
1320.0	"	1.33	7	2833.0	"	3.42		7	
1409.0	"	1.57	4	2834.0	"	3.20		17	
1452.0	"	1.54	6	2838.0	"	3.29		25	
1467.0	"	1.79	3	2879.0	"	3.21		37	
1512.0	"	1.69	18	2939.0	"	3.17		12	
1573.0	"	1.62	6	3000.0	"	3.34		8	
1612.0	"	1.49	10	3061.0	"	3.54		7	
1712.0	"	1.56	10	3121.0	"	3.99		10	
1752.0	"	1.75	3	3182.0	"	3.99		9	
1785.0	"	1.85	7	3303.0	"	3.73		16	
1812.0	"	1.80	9	3364.0	"	3.57		32	
1858.0	"	1.83	8	3424.0	"	3.70		9	
1910.0	"	1.75	5	3471.0	"	2.70		5	
1950.0	"	1.75	7	3545.0	"	2.72		4	
1955.0	"	1.62	8						
1994.0	"	1.62	4						

* Vitr. - vitrinite
* Bit. - bitumen

Apollo C-73 (continued)

Depth (m)	Org. Matter Type	% Ro max.	N	Depth (m)	Org. Matter Type	% Ro max.	N
2057.0	Vitr. *	1.75	6				
2080.0	"	1.90	7				
		2.40					
2100.0	"	1.80	3				
2103.0	"	1.75	6				
2160.0	"	1.80	5				
2194.0	"	1.82	13				
2236.0	"	1.77	12				
2270.0	"	1.70	5				

Hearne Point F-85

Depth (m)	Org. Matter Type	% Ro max.	N
57.0	Vitrinite	0.65	8
72.0	"	0.65	12
109.0	"	0.63	18
135.0	"	0.66	12
154.0	"	0.66	20
243.0	"	0.67	11
279.0	"	0.65	8
336.0	"	0.71	3
450.0	"	0.67	11
594.0	"	0.69	5
789.0	"	0.65	2
1008.0	"	0.72	3
1404.0	"	0.70	2

* Vitr. - vitrinite

Winter Harbour # 1

Depth (m)	Org. Matter Type	% Ro max.		N	Depth (m)	Org. Matter Type	% Ro max.		N	
61.0	Vitr. *	0.68		9	2490.0	Bit. *	1.48	2.14	3	12
148.0	"	0.69		6	2544.0	"	1.59	2.04	7	3
209.0	"	0.68		8	2609.0	"	1.57	1.93	2	2
254.0	"	0.71		13	2670.0	"	2.26		2	
297.0	"	0.73		25	2763.0	"	1.73	2.29	5	4
361.0	"	0.74		7	2848.0	"	1.71	2.09	3	7
464.0	"	0.71		6	2870.0	"	1.57	2.27	2	15
600.0	"	0.73		10	2930.0	"	1.78	2.30	4	4
679.0	"	0.70		8	2970.0	"	2.41		3	
836.0	"	0.71		7	3105.0	"	1.81		5	
978.0	"	0.75		7	3152.0	"	2.46		7	
1050.0	"	0.74		9	3268.0	"	2.06	2.99	3	5
1147.0	"	0.73		3	3370.0	"	2.14		4	
1264.0	"	0.76		8	3515.0	"	2.05	2.95	7	4
1357.0	"	0.73		7	3592.0	"	2.26	3.23	3	14
1654.0	"	0.88		3	3627.0	"	2.82		2	
1730.0	"	0.82		4	3657.0	"	2.58	3.15	4	4
1824.0	"	0.95		2						
2236.0	"	0.94		5						
2544.0	"	1.16		3						
2609.0	"	1.19		2						
3152.0	"	1.28		2						
3515.0	"	1.35		5						
3718.0	"	1.45		2						

Beverley Inlet G-13

Depth (m)	Org. Matter Type	% Ro max.		N	Depth (m)	Org. Matter Type	% Ro max.		N	
5.0	Vitr. *	0.83		18	1294.0	Bit. *	1.22		7	
554.0	"	0.90		10	1790.0	"	1.51		15	
1139.0	"	0.86		3	1910.0	"	1.67	2.11	20	12
1294.0	"	0.88		20	2020.0	"	1.69		6	
1400.0	"	0.92		17	2350.0	"	1.81	2.17	8	5
							3.05		3	
					2390.0	"	2.17	3.10	5	5
					2514.0	"	2.40		7	
					2750.0	"	1.50		10	
					3000.0	"	1.58		8	
					3047.0	"	1.87		6	
					3292.0	"	2.05		5	
					3530.0	"	2.07		4	
					3838.0	"	2.17	2.58	5	6
							3.20		4	
					3950.0	"	2.72	3.10	7	3

* Vitr. - vitrinite
* Bit. - bitumen

Zeus F-11

Depth (m)	Org. Matter Type	% Ro max.		N	
210.0	Bitumen	1.96	2.55	5	8
230.0	"	2.68		10	
255.0	"	2.85		12	
280.0	"	2.27	2.65	12	14
312.0	"	2.27	3.02	10	8
330.0	"	2.35	2.80	15	17
350.0	"	2.35	2.77	9	13
373.0	"	2.46	2.85	7	10
394.0	"	2.62		13	
430.0	"	2.95		17	
469.0	"	2.64		6	
481.0	"	3.05		11	
508.0	"	2.70		18	
531.0	"	2.48	2.96	30	26
552.0	"	2.42	3.03	35	10
557.0	"	2.49	2.89	28	30
560.0	"	2.35	3.14	15	12
578.0	"	2.97		14	
594.0	"	2.38		22	
610.0	"	2.30		11	
617.0	"	2.15	3.02	8	19
623.0	"	3.10		34	
630.0	"	2.85	3.65	17	28
633.0	"	2.94		33	
640.0	"	3.10		15	
652.0	"	3.0		9	
670.0	"	3.20		14	
684.0	"	3.07		6	
710.0	"	3.61		11	
730.0	"	3.18		13	
740.0	"	3.30		7	

Sabine Bay A-07

Depth (m)	Org. Matter Type	% Ro max.	N	Depth (m)	Org. Matter Type	% Ro max.		N	
530.0	Vitr. *	0.96	16	1365.0	Bit. *	1.51		12	
550.0	"	0.93	15	1455.0	"	1.59	1.87	25	7
1115.0	"	1.05	17	1470.0	"	1.55		6	
1190.0	"	1.19	14	1712.0	"	1.60	1.85	3	5
1470.0	"	1.10	3	1752.0	"	1.67	1.95	12	2
				1837.0	"	1.94		17	
				1925.0	"	2.0		14	
				1930.0	"	2.12		3	
				1970.0	"	2.10		4	
				2010.0	"	2.15		5	
				2040.0	"	2.35		4	
				2335.0	"	2.78		11	
				2570.0	"	2.90		4	
				2910.0	"	2.96	3.39	4	20
				3078.0	"	2.90	3.05	5	7
				3170.0	"	3.25	3.55	3	3
				3410.0	"	3.60	4.65	3	8

* Vitr. - vitrinite
* Bit. - bitumen

King Point West B-53

Depth (m)	Org. Matter Type	% Ro max.	N	Depth (m)	Org. Matter Type	% Ro max.		N	
30.0	Vitr. *	0.62	5	180.0	Bit. *	0.63		7	
57.0	"	0.61	7	470.0	"	0.58		10	
71.0	"	0.62	10	745.0	"	0.23		7	
120.0	"	0.63	6	1080.0	"	1.45		10	
140.0	"	0.59	3	1318.0	"	1.65		10	
180.0	"	0.63	7	1657.0	"	1.37		7	
200.0	"	0.60	10	1780.0	"	1.40		19	
230.0	"	0.65	8	1817.0	"	1.38		20	
280.0	"	0.64	7	1830.0	"	1.39		14	
340.0	"	0.65	9	1870.0	"	1.35		15	
428.0	"	0.60	13	1910.0	"	1.55		13	
440.0	"	0.60	15	1970.0	"	1.10		8	
470.0	"	0.58	10	1994.0	"	1.04		6	
520.0	"	0.60	8	2050.0	"	1.12		14	
543.0	"	0.59	6	2097.0	"	1.12		19	
730.0	"	0.68	5	2230.0	"	1.13		25	
760.0	"	0.69	12	2310.0	"	1.10		20	
780.0	"	0.73	11	2340.0	"	1.13		14	
990.0	"	0.78	18	2370.0	"	1.39		12	
1035.0	"	0.77	13	2470.0	"	1.50		15	
1080.0	"	0.88	14	2490.0	"	1.78		11	
1164.0	"	0.90	5	2540.0	"	1.30	1.23	5	7
1197.0	"	0.90	7	2570.0	"	1.27	1.62	9	6
1218.0	"	0.92	4	2590.0	"	1.13		10	
1260.0	"	0.97	3	2620.0	"	1.22		17	
1291.0	"	0.88	9	2650.0	"	1.26		21	
1318.0	"	0.98	4	2690.0	"	1.32	1.75	13	9
1360.0	"	0.98	5	2770.0	"	1.23	1.59	10	12
1410.0	"	0.95	9	2780.0	"	1.14	1.64	7	14
1460.0	"	1.05	7	2800.0	"	1.64		10	
1490.0	"	0.97	10	2970.0	"	1.66		5	9
1548.0	"	1.07	11	2997.0	"	2.95		10	
1577.0	"	1.15	8	3095.0	"	0.24	1.73	3	5
1657.0	"	1.03	5			2.75		7	
1680.0	"	1.07	3						
1718.0	"	0.93	13						
1740.0	"	1.0	6						
1760.0	"	0.94	8						
1780.0	"	1.17	17						
1817.0	"	1.03	16						
1890.0	"	1.12	12						
1910.0	"	0.98	5						

* Vitr. - vitrinite
* Bit. - bitumen

Richardson G - 12

Depth (m)	Org. Matter Type	% Ro max.	N	Depth (m)	Org. Matter Type	% Ro max.		N	
48.0	Vitr. *	0.55	10	2500.0	Bit. *	0.96		3	
136.0	"	0.58	9	2588.0	"	1.02		3	
185.0	"	0.58	5	2706.0	"	1.10		5	
191.0	"	0.59	14	2788.0	"	1.34	2.10	3	4
275.0	"	0.62	3	2818.0	"	1.10	1.95	2	3
279.0	"	0.46	3	2870.0	"	1.04		2	
517.0	"	0.55	12	2909.0	"	1.05		2	
600.0	"	0.70	16	3064.0	"	2.20		5	
694.0	"	0.66	3	3194.0	"	1.30		4	
755.0	"	0.64	5	3321.0	"	1.18		7	
815.0	"	0.43	8						
950.0	"	0.47	9						
976.0	"	0.74	3						
1050.0	"	0.45	7						
1088.0	"	0.74	4						
1100.0	"	0.40	14						
1144.0	"	0.43	6						
1147.0	"	0.52	8						
1155.0	"	0.72	4						
1220.0	"	0.64	17						
1260.0	"	0.69	6						
1341.0	"	0.55	5						
1347.0	"	0.53	20						
1360.0	"	0.54	15						
1382.0	"	0.71	5						
1400.0	"	0.53	13						
1489.0	"	0.83	10						
1550.0	"	0.60	11						
1624.0	"	0.83	3						
1973.0	"	0.83	4						
2167.0	"	0.93	3						
2345.0	"	0.98	3						
2910.0	"	0.68	9						
2975.0	"	0.63	10						
2982.0	"	0.85	5						
3088.0	"	0.74	3						
3100.0	"	0.83	4						
3157.0	"	0.54	7						
3234.0	"	0.82	7						
3267.0	"	0.54	6						
3358.0	"	0.55	8						

* Vitr. - vitrinite
* Bit. - bitumen

Towson Point F-63

Depth (m)	Org. Matter Type	% Ro max.		N	
12.1	Bitumen	0.33	0.77	2	2
103.0	"	0.82		6	
121.0	"	0.80		3	
133.0	"	0.45	0.86	5	2
679.0	"	0.30		4	
697.0	"	0.40	1.71	4	3
712.0	"	1.05		4	
761.0	"	1.47		4	
782.0	"	1.60		5	
803.0	"	2.08		2	
833.0	"	1.81		28	
876.0	"	1.39		4	
952.0	"	2.24		2	
1088.0	"	1.11	2.05	4	5
1142.0	"	1.45		17	
1176.0	"	0.98	1.93	2	2
1203.0	"	1.99		2	
1239.0	"	2.00		5	
1252.0	"	1.86		2	
1288.0	"	2.33		2	
1321.0	"	1.61		2	

Drake Point D-68

Depth (m)	Org. Matter Type	% Ro max.	N	Depth (m)	Org. Matter Type	% Ro max.	N
106.0	Vitr. *	0.50	3	1342.0	Bit. *	1.05	2
136.0	"	0.44	40	1630.0	"	1.07	3
265.0	"	0.42	22	1864.0	"	0.99	10
388.0	"	0.53	8	2915.0	"	1.08	6
427.0	"	0.42	7	3021.0	"	1.05	7
455.0	"	0.47	20	3091.0	"	1.07	7
482.0	"	0.56	32	3170.0	"	1.00	8
494.0	"	0.52	30	3236.0	"	1.12	11
515.0	"	0.47	25	3270.0	"	1.10	7
558.0	"	0.46	5	3324.0	"	1.08	11
612.0	"	0.54	3	3361.0	"	1.05	3
661.0	"	0.59	2	3403.0	"	1.07	7
709.0	"	0.48	4	3455.0	"	1.12	3
770.0	"	0.55	18	3506.0	"	1.02	3
797.0	"	0.62	39	3633.0	"	0.96	2
818.0	"	0.54	38	3679.0	"	0.97	4
842.0	"	0.59	21	3761.0	"	1.03	2
876.0	"	0.54	19	4061.0	"	1.05	2
955.0	"	0.52	7	4194.0	"	1.02	2
994.0	"	0.52	2	4336.0	"	1.18	2
1033.0	"	0.55	2	4630.0	"	4.43	3
1197.0	"	0.70	13	4655.0	"	4.99	19
1242.0	"	0.80	13	4667.0	"	6.79	19
1288.0	"	0.71	5	4682.0	"	6.20	12
1342.0	"	0.72	2	4697.0	"	5.89	14
1403.0	"	0.74	3	4718.0	"	5.80	15
1864.0	"	0.89	7	4742.0	"	6.28	10
2900.0	"	0.85	2	4770.0	"	5.33	6
2965.0	"	0.88	2	4855.0	"	6.22	8
3021.0	"	0.90	3	4900.0	"	6.83	16
3170.0	"	0.85	2	4936.0	"	6.68	11
3236.0	"	0.92	5	4985.0	"	2.90	6
3270.0	"	0.88	6	5012.0	"	3.20	6
3324.0	"	0.85	3	5067.0	"	3.50	8
3361.0	"	0.80	2	5100.0	"	2.70	3
3403.0	"	0.86	10	5152.0	"	2.52	6
3450.0	"	0.67	6	5252.0	"	1.88	26
3455.0	"	0.90	2	5291.0	"	1.66	5
3506.0	"	0.86	2	5364.0	"	1.58	5
3552.0	"	0.90	6				
3582.0	"	0.83	5				
3633.0	"	0.85	5				
3761.0	"	0.82	2				
3805.0	"	0.55	7				
3821.0	"	0.80	8				
3824.0	"	0.83	4				

* Vitr. - vitrinite
* Bit. - bitumen

Drake Point D-68 (continued)

Depth (m)	Org. Matter Type	% Ro max.	N	Depth (m)	Org. Matter Type	% Ro max.	N
3876.0	Vitr. *	0.86	2				
3950.0	"	1.31	6				
3970.0	"	0.81	2				
4018.0	"	0.80	3				
4061.0	"	0.90	5				
4112.0	"	0.93	2				
4115.0	"	1.25	5				
4200.0	"	0.85	6				
4239.0	"	0.86	2				
4400.0	"	1.62	4				
4505.0	"	1.80	7				
5035.0	"	1.74	5				
5202.0	"	2.05	4				

Chads Creek B-64

Depth (m)	Org. Matter Type	% Ro max.	N	Depth (m)	Org. Matter Type	% Ro max.		N	
227.0	Vitr. *	0.50	3	61.0	Bit. *	1.55		10	
415.0	"	0.54	23	94.0	"	1.24		25	
757.0	"	0.57	15	194.0	"	0.90	1.60	13	5
848.0	"	0.52	3	227.0	"	1.12		3	9
973.0	"	0.54	46	261.0	"	1.29		5	
1250.0	"	0.57	10	363.0	"	1.30		6	
1397.0	"	0.6	7	415.0	"	1.13		5	
1523.0	"	0.58	12	757.0	"	1.42		10	
2133.0	"	0.65	6	848.0	"	1.25		5	
2318.0	"	0.64	3	1151.0	"	0.96	1.53	27	5
2636.0	"	0.57	3	1333.0	"	1.21		5	
3280.0	"	1.07	8	1397.0	"	1.29		12	
3303.0	"	1.74	10	1421.0	"	1.35		15	
3606.0	"	0.90	10	1891.0	"	1.04		6	
3909.0	"	1.15	20	2057.0	"	1.23		3	
4000.0	"	1.15	17	2318.0	"	1.07		5	
4180.0	"	1.13	7	2976.0	"	1.11	1.66	14	
4370.0	"	1.20	20	3061.0	"	1.67		9	
4448.0	"	1.10	24	3212.0	"	1.82		7	
4485.0	"	1.28	12	3303.0	"	1.74	2.25	7	20
4550.0	"	1.57	9	3379.0	"	1.83	2.97	4	11
4818.0	"	1.35	20	3606.0	"	1.30		5	
				3909.0	"	1.50	1.95		
				3950.0	"	1.60		12	
				3966.0	"	1.97		11	
				4000.0	"	2.13		15	
				4061.0	"	2.23			
				4151.0	"	2.26		5	
				4180.0	"	1.58		12	

* Vitr. - vitrinite
* Bit. - bitumen

Chads Creek B-64 (continued)

Depth (m)	Org. Matter Type	% Ro max.	N	Depth (m)	Org. Matter Type	% Ro max.		N	
				4242.0	Bit. *	2.18		21	
				4333.0	"	1.80	2.25	16	20
				4448.0	"	2.23		17	
				4485.0	"	2.14			
				4568.0	"	2.24		25	
				4571.0	"	2.27		12	
				4572.0	"	1.85		12	
				4579.0	"	1.92	2.14	35	30
				4597.0	"	2.35		40	
				4679.0	"	2.50		10	
				4688.0	"	2.20		6	
				4718.0	"	2.06		25	
				4727.0	"	2.39		10	
				4748.0	"	2.25		20	
				4818.0	"	1.84	2.34	17	20
				4879.0	"	2.29		20	
				4970.0	"	2.48		20	

Hecla J-60

Depth (m)	Org. Matter Type	% Ro max.	N	Depth (m)	Org. Matter Type	% Ro max.		N	
106.0	Vitr. *	0.46	24	612.0	Bit. *	1.11		7	
212.0	"	0.44	3	679.0	"	1.11		7	
382.0	"	0.44	17	1467.0	"	1.18		4	
442.0	"	0.45	9	1873.0	"	1.41		4	2
503.0	"	0.50	12	2264.0	"	1.59		4	4
552.0	"	0.46	6	2503.0	"	1.35	1.80	16	2
584.0	"	0.47	9	2570.0	"	1.37		10	
597.0	"	0.53	14	2594.0	"	1.34		5	
612.0	"	0.46	3	2633.0	"	1.40	1.85	5	9
679.0	"	0.40	3	2661.0	"	1.95		15	
800.0	"	0.44	6 3	2721.0	"	1.47		11	
830.0	"	0.52	23	2773.0	"	1.39	1.80	16	2
833.0	"	0.53	7	2824.0	"	1.25		10	
850.0	"	0.50	10	2891.0	"	1.51	1.93	6	18
912.0	"	0.52	9	2942.0	"	1.22	1.94	2	7
958.0	"	0.52	22	2991.0	"	1.35	1.82	6	7
1000.0	"	0.46	15	3030.0	"	1.85		8	
1080.0	"	0.48	12	3115.0	"	1.28	2.01	9	6
1100.0	"	0.50	11	3224.0	"	1.42	1.96	23	6
1170.0	"	0.49	16	3273.0	"	1.43	2.03	13	2
1191.0	"	0.51	8	3324.0	"	1.37		13	
1324.0	"	0.54	5	3376.0	"	1.17		7	
1370.0	"	0.45	8	3509.0	"	1.33		13	
				3573.0	"	1.46		10	

* Vitr. - vitrinite
* Bit. - bitumen

Hecla J-60 (continued)

Depth (m)	Org. Matter Type	% Ro max.	N	Depth (m)	Org. Matter Type	% Ro max.		N
1467.0	Vitr. *	0.48	3					
2020.0	"	0.74	5					
2633.0	"	0.84	10					
2824.0	"	0.95	5					

Depot Island C-44

Depth (m)	Org. Matter Type	% Ro max.	N	Depth (m)	Org. Matter Type	% Ro max.		N
88.0	Vitr. *	0.52	8	370.0	Bit. *	0.21		5
109.0	"	0.47	8	394.0	"	0.25		7
124.0	"	0.50	2	457.0	"	1.0		10
190.0	"	0.43	7	520.0	"	0.95		8
200.0	"	0.44	5	550.0	"	0.88		6
358.0	"	0.47	9	575.0	"	1.08		5
461.0	"	0.48	7	684.0	"	0.23		6
575.0	"	0.50	10	710.0	"	1.17		4
679.0	"	0.48	5	770.0	"	0.92		7
695.0	"	0.46	4	930.0	"	0.93		15
750.0	"	0.52	15	1321.0	"	1.03		6
795.0	"	0.46	12	1395.0	"	0.93		5
1078.0	"	0.54	3	1420.0	"	1.10		4
1420.0	"	0.57	5	1425.0	"	0.27		12
1837.0	"	0.60	7	1478.0	"	1.15		17
2010.0	"	0.68	7	1785.0	"	0.30		9
2108.0	"	0.68	10	1878.0	"	0.35		8
2170.0	"	0.64	8	2050.0	"	1.18		7
2193.0	"	0.69	4	2075.0	"	1.16		6
2244.0	"	0.65	3	2110.0	"	1.20		4
2270.0	"	0.71	5	2130.0	"	1.22		8
2325.0	"	0.76	9	2270.0	"	1.24		10
2390.0	"	0.66	10	2310.0	"	1.38		6
				2442.0	"	1.36		3
				2480.0	"	2.02	2.98	14 17
				2497.0	"	3.60		9
				2527.0	"	3.65		7
				2550.0	"	2.48		11
				2570.0	"	2.33		8
				2590.0	"	3.54		17
				2610.0	"	3.70		14
				2630.0	"	3.40		15
				2631.0	"	3.40		15
				2632.0	"	3.40		15
				2633.0	"	3.40		15

* Vitr. - vitrinite
* Bit. - bitumen

Roche Point J-43

Depth (m)	Org. Matter Type	% Ro max.	N	Depth (m)	Org. Matter Type	% Ro max.	N
382.0	Vitr. *	0.36	17	356.0	Bit. *	0.20	8
415.0	"	0.45	22	382.0	"	0.19	6
448.0	"	0.40	3	415.0	"	0.18	7
457.0	"	0.46	7	482.0	"	0.14	4
482.0	"	0.42	11	615.0	"	0.15	5
518.0	"	0.39	2	666.0	"	0.12	4
557.0	"	0.55	6	763.0	"	0.16	2
615.0	"	0.54	5	812.0	"	0.18	2
1136.0	"	0.57	8	863.0	"	0.15	7
1193.0	"	0.56	7	1778.0	"	0.20	2
1255.0	"	0.61	6				
1309.0	"	0.55	20				
1363.0	"	0.57	3				
1394.0	"	0.65	4				
1424.0	"	0.53	4				
1509.0	"	0.56	3				
1633.0	"	0.78	6				
1684.0	"	0.78	4				
1778.0	"	0.64	4				
1830.0	"	0.72	19				
1897.0	"	0.69	5				
1952.0	"	0.77	6				
2009.0	"	0.75	8				
2063.0	"	0.72	2				
2112.0	"	0.78	4				
2163.0	"	0.98	2				
2215.0	"	0.93	5				
2269.0	"	0.93	7				
2333.0	"	0.88	2				
2500.0	"	0.85	7				
2549.0	"	1.01	16				
2597.0	"	1.04	26				
2645.0	"	0.97	3				
2706.0	"	0.95	4				
2774.0	"	1.02	5				
2830.0	"	1.04	3				

* Vitr. - vitrinite
* Bit. - bitumen

North Sabine H-49

Depth (m)	Org. Matter Type	% Ro max.	N
336.0	Vitr. *	0.45	5
370.0	"	0.45	5
506.0	"	0.46	10
557.0	"	0.46	12
624.0	"	0.47	6
648.0	"	0.40	6
724.0	"	0.45	2
954.0	"	0.53	7
1000.0	"	0.42	4
1060.0	"	0.47	6
1215.0	"	0.48	3
1288.0	"	0.41	7
1333.0	"	0.50	4
1400.0	"	0.42	10
1409.0	"	0.51	15
1527.0	"	0.54	9
1615.0	"	0.53	10
1617.0	"	0.50	8
1727.0	"	0.54	8
1775.0	"	0.49	9
1830.0	"	0.55	9
1991.0	"	0.54	8
2016.0	"	0.50	17
2100.0	"	0.55	5
2121.0	"	0.55	9
2200.0	"	0.57	7
2290.0	"	0.58	10
2471.0	"	0.56	8
2610.0	"	0.67	7
2680.0	"	0.62	10
2789.0	"	0.63	20
2854.0	"	0.70	18
2985.0	"	0.61	10
2991.0	"	0.77	6
3060.0	"	0.73	3
3134.0	"	0.77	8
3170.0	"	0.78	5
3292.0	"	1.0	5
3351.0	"	1.02	12
3442.0	"	1.50	5
3480.0	"	0.83	3
3483.0	"	1.27	7
3490.0	"	1.12	4
3497.0	"	0.84	4
3508.0	"	1.11	9
3587.0	"	1.25	6
3602.0	"	0.85	9

* Vitr. - vitrinite

North Sabine H-49 (continued)

Depth (m)	Org. Matter Type	% Ro max.	N
3604.0	Vitr. *	1.12	3
3607.0	"	1.48	6
3630.0	"	1.23	7
3645.0	"	1.40	6
3654.0	"	1.30	5
3820.0	"	1.07	8

Weatherall O-10

Depth (m)	Org. Matter Type	% Ro max.	N	Depth (m)	Org. Matter Type	% Ro max.	N
130.0	Vitr. *	0.51	5	1579.0	Bit. *	1.02	6
430.0	"	0.51	7	1620.0	"	1.08	10
997.0	"	0.60	10	1700.0	"	1.06	27
1238.0	"	0.60	16	1760.0	"	1.10	5
1272.0	"	0.64	12				
1351.0	"	0.72	6				
1384.0	"	0.73	5				
1579.0	"	0.74	8				
1760.0	"	0.74	3				
1840.0	"	0.84	10				
2110.0	"	0.86	3				
2144.0	"	0.86	2				

Eldridge Bay E-79

Depth (m)	Org. Matter Type	% Ro max.	N	Depth (m)	Org. Matter Type	% Ro max.	N
164.0	Vitr. *	0.73	3	606.0	Bit. *	1.54	6
458.0	"	0.69	2	800.0	"	1.63	10
606.0	"	0.72	2	1277.0	"	1.05	7
676.0	"	0.69	9	1352.0	"	1.17	3
703.0	"	0.66	13	1579.0	"	1.11	16
767.0	"	0.67	12	1586.0	"	1.23	17
				1627.0	"	1.82	21
				1673.0	"	2.39	9
				1678.0	"	1.67	2.30 4 5
				1724.0	"	1.45	22
				1860.0	"	1.98	25
				1930.0	"	1.87	16
				1973.0	"	1.80	33
				2012.0	"	1.48	10
				2045.0	"	1.88	41

* Vitr. - vitrinite
* Bit. - bitumen

Eldridge Bay E-79 (continued)

Depth (m)	Org. Matter Type	% Ro max.	N	Depth (m)	Org. Matter Type	% Ro max.			N	
				2082.0	Bit. *	1.40	2.14	3.34	5	23 8
				2130.0	"		1.42		12	
				2158.0	"		1.33	1.81	5	14
				2206.0	"		1.90		6	
				2242.0	"		1.44		13	
				2282.0	"		1.71	2.57	2	14
				2321.0	"		1.76	2.89	2	25
				2582.0	"		2.21		13	
				2742.0	"		2.22		9	
				2833.0	"		5.29		15	
				2864.0	"		3.80	5.24	3	10
				2894.0	"	2.10	2.66	4.05	2	5 2
				2933.0	"		2.60		2	
				2964.0	"		2.03		2	

Kitson River C-71

Depth (m)	Org. Matter Type	% Ro max.	N	Depth (m)	Org. Matter Type	% Ro max.		N	
42.0	Vitr. *	0.60	8	606.0	Bit. *	1.40	1.92	4	2
45.0	"	0.61	8	727.0	"	1.63		6	
100.0	"	0.76	12	891.0	"	2.27		2	
110.0	"	0.67	10	918.0	"	1.95		2	
135.0	"	0.81	7	970.0	"	1.96	2.57	2	2
146.0	"	0.87	14	1030.0	"	1.97		6	
545.0	"	0.88	6	1091.0	"	2.44		8	
606.0	"	1.13	13	1152.0	"	2.35		16	
667.0	"	1.07	6	1212.0	"	2.15		3	
727.0	"	1.30	22	1273.0	"	2.10		2	
				1515.0	"	2.75	3.13	5	14
				1636.0	"	2.66		4	
				1758.0	"	2.65	3.11	2	8
				1818.0	"	2.64		18	
				1879.0	"	2.91		7	
				1939.0	"	2.87		3	
				2000.0	"	2.93		12	
				2061.0	"	2.77		3	

* Vitr. - vitrinite
* Bit. - bitumen

Sherard Bay F-34

Depth (m)	Org. Matter Type	% Ro max.	N
95.0	Vitr. *	0.48	6
246.0	"	0.34	11
490.0	"	0.35	12
621.0	"	0.37	8
730.0	"	0.42	32
734.0	"	0.49	27
750.0	"	0.49	30
752.0	"	0.40	30
947.0	"	0.46	10
960.0	"	0.45	50
1051.0	"	0.45	15
1164.0	"	0.50	6
1227.0	"	0.49	7
1290.0	"	0.52	6
1317.0	"	0.56	3
1324.0	"	0.56	9
2630.0	"	0.73	3
2774.0	"	0.68	14
3000.0	"	0.60	12
3598.0	"	0.70	5
3669.0	"	0.63	3
3851.0	"	0.70	7
4610.0	"	0.90	7
4874.0	"	0.70	8
5212.0	"	0.93	10

Sherard Bay F-14

Depth (m)	Org. Matter Type	% Ro max.	N
42.0	Vitr. *	0.52	6
208.0	"	0.50	4
232.0	"	0.48	5
430.0	"	0.49	3
724.0	"	0.51	3
770.0	"	0.52	6
891.0	"	0.52	8
1020.0	"	0.57	7
1022.0	"	0.53	8
1024.0	"	0.57	10
1028.0	"	0.55	5
1047.0	"	0.60	10
1050.0	"	0.52	3
1110.0	"	0.59	17
1209.0	"	0.60	4
1270.0	"	0.52	6

* Vitr. - vitrinite

Marryatt K-71

Depth (m)	Org. Matter Type	% Ro max.	N
90.0	Vitr. *	0.47	10
108.0	"	0.47	6
274.0	"	0.46	11
850.0	"	0.55	3
953.0	"	0.55	3
1270.0	"	0.55	6
1537.0	"	0.55	8
1592.0	"	0.54	3
1640.0	"	0.57	2
1653.0	"	0.58	5
1701.0	"	0.53	2
3270.0	"	0.66	5
3690.0	"	0.64	3

Collingwood K-33

Depth (m)	Org. Matter Type	% Ro max.	N
45.0	Vitr. *	0.34	18
106.0	"	0.38	2
454.0	"	0.43	2
498.0	"	0.48	10
650.0	"	0.50	7
784.0	"	0.51	10
921.0	"	0.52	6
979.0	"	0.48	10
1000.0	"	0.51	13
1010.0	"	0.51	4
1112.0	"	0.48	2
1114.0	"	0.53	25
1124.0	"	0.53	12
1340.0	"	0.53	24
1347.0	"	0.52	22
1354.0	"	0.56	12
1388.0	"	0.56	6
1395.0	"	0.54	8
1476.0	"	0.52	10
1530.0	"	0.54	2
1552.0	"	0.54	9
1570.0	"	0.54	7
1636.0	"	0.68	7
1660.0	"	0.62	4
1675.0	"	0.67	5
1733.0	"	0.66	4
1766.0	"	0.70	2
1851.0	"	0.67	2
1905.0	"	0.66	15
1918.0	"	0.68	4

* Vitr. - vitrinite

Drake L-67

Depth (m)	Org. Matter Type	% Ro max.	N
139.0	Vitr. *	0.49	20
290.0	"	0.51	5
303.0	"	0.50	16
412.0	"	0.51	8
454.0	"	0.49	7
530.0	"	0.50	16
592.0	"	0.54	10
594.0	"	0.55	10
790.0	"	0.53	13
848.0	"	0.55	4
955.0	"	0.50	9
1170.0	"	0.56	5
1344.0	"	0.59	3
1800.0	"	0.53	6
2057.0	"	0.61	2
2330.0	"	0.62	4
2995.0	"	0.67	6
3130.0	"	0.70	8
3235.0	"	0.69	7

Drake Point K-79

Depth (m)	Org. Matter Type	% Ro max.	N	Depth (m)	Org. Matter Type	% Ro max.		N	
30.0	Vitr. *	0.51	20	90.0	Bit. *	1.05		11	
73.0	"	0.52	15	169.0	"	0.74	1.4	15	8
185.0	"	0.47	10	182.0	"	1.25		48	
267.0	"	0.51	8	191.0	"	0.80	1.62	10	12
282.0	"	0.55	12	203.0	"	1.42		8	
303.0	"	0.62	10	212.0	"	1.25		5	
367.0	"	0.46	8	221.0	"	1.21		25	
436.0	"	0.47	18	267.0	"	0.81		12	
497.0	"	0.45	6	303.0	"	0.82	1.33	12	7
579.0	"	0.47	11	333.0	"	1.48		14	
606.0	"	0.59	10	364.0	"	0.89	1.21	2	3
636.0	"	0.52	3	515.0	"	0.75	1.27	16	5
648.0	"	0.48	11	727.0	"	1.39		5	
727.0	"	0.52	9	758.0	"	0.71		3	
863.0	"	0.48	4	849.0	"	0.87	1.70	2	2
950.0	"	0.56	6	909.0	"	0.60	1.13	8	5
1009.0	"	0.52	16	976.0	"	1.58		7	
1121.0	"	0.61	25	1030.0	"	1.06		16	
1298.0	"	0.61	50	1090.0	"	0.83		4	
1300.0	"	0.54	50	1212.0	"	1.10	1.40	4	5
1302.0	"	0.49	50	1455.0	"	1.82		6	
1304.0	"	0.50	22	1515.0	"	1.34	1.71	5	3

* Vitr. - vitrinite
* Bit. - bitumen

Drake Point K-79 (continued)

Depth (m)	Org. Matter Type	% Ro max.	N	Depth (m)	Org. Matter Type	% Ro max.	N
1305.0	Vitr. *	0.48	44	1576.0	Bit. *	1.15	3
1306.0	"	0.49	50	1636.0	"	0.95	5
1307.0	"	0.52	50	1697.0	"	1.40	2
1308.0	"	0.58	48				
1333.0	"	0.50	7				
1475.0	"	0.65	6				
1530.0	"	0.61	10				
1563.0	"	0.63	6				

Drake F-76

Depth (m)	Org. Matter Type	% Ro max.	N
130.0	Vit. *	0.35	5
170.0	"	0.36	9
307.0	"	0.37	11
327.0	"	0.37	6
395.0	"	0.37	11
397.0	"	0.38	14
530.0	"	0.39	21
532.0	"	0.38	6
779.0	"	0.45	8
860.0	"	0.46	11
865.0	"	0.43	9
878.0	"	0.45	12
969.0	"	0.44	2
865.0	"	0.43	25
1012.0	"	0.54	10
1030.0	"	0.58	5
1124.0	"	0.55	4

* Vitr. - vitrinite
* Bit. - bitumen

Drake E-78

Depth (m)	Org. Matter Type	% Ro max.	N
28.0	Vitr. *	0.38	2
148.0	"	0.42	3
455.0	"	0.42	10
466.0	"	0.43	3
542.0	"	0.44	3
678.0	"	0.46	3
703.0	"	0.47	30
728.0	"	0.50	2
830.0	"	0.48	2
1000.0	"	0.51	2
1027.0	"	0.55	7
1042.0	"	0.54	3
1115.0	"	0.53	4
1164.0	"	0.54	3
1173.0	"	0.55	12
1265.0	"	0.53	23
1270.0	"	0.55	2
1300.0	"	0.59	2
1309.0	"	0.55	8

Drake B-44

Depth (m)	Org. Matter Type	% Ro max.	N
30.0	Vitr. *	0.48	7
60.0	"	0.43	12
170.0	"	0.51	3
303.0	"	0.48	30
325.0	"	0.50	5
379.0	"	0.45	3
451.0	"	0.44	16
466.0	"	0.41	10
476.0	"	0.48	7
566.0	"	0.47	8
620.0	"	0.48	10
628.0	"	0.43	21
770.0	"	0.49	8
831.0	"	0.49	14
850.0	"	0.50	20
915.0	"	0.60	10
917.0	"	0.49	7
948.0	"	0.49	10
964.0	"	0.64	12
970.0	"	0.52	6
1100.0	"	0.50	15

* Vitr. - vitrinite

Drake B-44 (continued)

Depth (m)	Org. Matter Type	% Ro max.		N
30.0	Vitr. *	0.48		7
1150.0	"	0.47		4
1162.0	"	0.60		8
1184.0	"	0.53		6
1265.0	"	0.55		7
1290.0	"	0.55		7
1292.0	"	0.72		12
1300.0	"	0.52		9
1302.0	"	0.53		4
1330.0	"	0.55	0.40*	8

* denotes suppressed value

Drake D-73

Depth (m)	Org. Matter Type	% Ro max.	N
135.0	Vitr. *	0.54	10
135.0	"	0.54	10
148.0	"	0.55	6
182.0	"	0.54	2
300.0	"	0.49	6
364.0	"	0.50	3
451.0	"	0.54	7
579.0	"	0.54	6
667.0	"	0.50	6
670.0	"	0.49	26
724.0	"	0.52	4
772.0	"	0.49	8
867.0	"	0.52	17
874.0	"	0.50	9
1036.0	"	0.53	10
1057.0	"	0.54	7
1181.0	"	0.54	2
1182.0	"	0.54	3
1194.0	"	0.56	2
1210.0	"	0.56	7
1300.0	"	0.65	5
1309.0	"	0.64	8
1320.0	"	0.64	3

* Vitr. - vitrinite

Drake F-16

Depth (m)	Org. Matter Type	% Ro max.		N
30.0	Vitr. *	0.41		6
197.0	"	0.41		2
276.0	"	0.41		6
409.0	"	0.44		15
547.0	"	0.46		8
556.0	"	0.47		10
588.0	"	0.46		14
791.0	"	0.45		30
797.0	"	0.45		8
915.0	"	0.46		14
1008.0	"	0.50		5
1050.0	"	0.52		7
1063.0	"	0.55		3
1143.0	"	0.54		2
1204.0	"	0.52		7
1209.0	"	0.55		4
1260.0	"	0.52		4
1290.0	"	0.55		12
1303.0	"	0.58		3
1307.0	"	0.54		5
1349.0	"	0.55		20
1360.0	"	0.55	0.42*	6
1397.0	"	0.58		2
1400.0	"	0.64		3
1402.0	"	0.73		5

* Vitr. - vitrinite

* denotes suppressed value

Drake P-40

Depth (m)	Org. Matter Type	% Ro max.	N
439.0	Vitr. *	0.37	37
471.0	"	0.47	5
492.0	"	0.45	16
510.0	"	0.50	18
530.0	"	0.48	50
534.0	"	0.47	10
545.0	"	0.46	5
560.0	"	0.49	3
563.0	"	0.52	2
734.0	"	0.50	6
736.0	"	0.45	4
741.0	"	0.47	2
752.0	"	0.49	3
778.0	"	0.51	5
810.0	"	0.51	10
828.0	"	0.49	5
830.0	"	0.47	2
847.0	"	0.48	3
859.0	"	0.52	6
927.0	"	0.55	4
958.0	"	0.58	4
970.0	"	0.59	10
1069.0	"	0.52	3
1144.0	"	0.61	4
1157.0	"	0.60	4
1160.0	"	0.59	8
1170.0	"	0.61	5
1176.0	"	0.54	3
1197.0	"	0.55	3

East Drake I-55

Depth (m)	Org. Matter Type	% Ro max.	N
397.0	Vitr. *	0.42	7
409.0	"	0.41	7
425.0	"	0.41	27
503.0	"	0.43	5
507.0	"	0.44	10
742.0	"	0.48	4
750.0	"	0.49	7
921.0	"	0.53	6
936.0	"	0.54	10
947.0	"	0.55	12
1024.0	"	0.60	7
1027.0	"	0.55	3
1033.0	"	0.55	20
1070.0	"	0.55	2
1081.0	"	0.55	6
1100.0	"	0.54	8

* Vitr. - vitrinite

East Drake I-55 (continued)

Depth (m)	Org. Matter Type	% Ro max.	N
1127.0	Vitr. *	0.56	11
1130.0	"	0.54	5
1152.0	"	0.54	9
1118.0	"	0.56	3
1167.0	"	0.54	2
1170.0	"	0.63	2

Hecla SW C-58

Depth (m)	Org. Matter Type	% Ro max.		N
340.0	Vitr. *	0.46		7
440.0	"	0.47		5
628.0	"	0.51		10
837.0	"	0.54		3
842.0	"	0.55		25
889.0	"	0.56		23
872.0	"	0.56		3
954.0	"	0.55		4
963.0	"	0.57		11
1000.0	"	0.55		3
1075.0	"	0.56		5
1088.0	"	0.54		4
1121.0	"	0.58		7
1133.0	"	0.59	0.45 *	3

* denotes suppressed value

Hecla West P-62

Depth (m)	Org. Matter Type	% Ro max.	N
227.0	Vitr. *	0.44	18
231.0	"	0.43	11
512.0	"	0.30	14
650.0	"	0.42	6
720.0	"	0.44	2
727.0	"	0.42	24
769.0	"	0.47	26
797.0	"	0.50	2
807.0	"	0.52	9
824.0	"	0.47	3
831.0	"	0.56	7
903.0	"	0.53	4
947.0	"	0.56	2
950.0	"	0.56	10
976.0	"	0.57	3
1000.0	"	0.54	7
1010.0	"	0.55	8

* Vitr. - vitrinite

NW Hecla M-25

Depth (m)	Org. Matter Type	% Ro max.	N
620.0	Vitr. *	0.41	7
684.0	"	0.44	10
800.0	"	0.47	6
936.0	"	0.51	2
1172.0	"	0.60	5
1175.0	"	0.68	10
1179.0	"	0.62	5

Hecla W. N-52

Depth (m)	Org. Matter Type	% Ro max.	N
321.0	Vitr. *	0.46	3
324.0	"	0.47	10
506.0	"	0.48	5
663.0	"	0.50	10
736.0	"	0.52	4
794.0	"	0.54	4
830.0	"	0.55	7
921.0	"	0.57	13
937.0	"	0.59	8

Hecla W. C-05

Depth (m)	Org. Matter Type	% Ro max.	N
39.0	Vitr. *	0.41	7
140.0	"	0.40	10
148.0	"	0.40	8
303.0	"	0.41	7
418.0	"	0.43	3
430.0	"	0.41	35
530.0	"	0.41	21
618.0	"	0.41	2
757.0	"	0.43	50
761.0	"	0.41	23
770.0	"	0.44	13
885.0	"	0.44	8
893.0	"	0.45	12
951.0	"	0.49	7
963.0	"	0.51	6
1012.0	"	0.48	8
1054.0	"	0.50	2
1145.0	"	0.50	3
1196.0	"	0.57	4
1209.0	"	0.58	3

* Vitr. - vitrinite

Hecla I-69

Depth (m)	Org. Matter Type	% Ro max.	N
50.0	Vitr. *	0.35	7
118.0	"	0.42	3
309.0	"	0.44	3
490.0	"	0.38	10
537.0	"	0.47	15
551.0	"	0.44	22
575.0	"	0.46	6
788.0	"	0.56	4
884.0	"	0.53	25
890.0	"	0.45	6
1020.0	"	0.56	7
1033.0	"	0.60	7
1207.0	"	0.61	10
1341.0	"	0.56	5
1358.0	"	0.68	8

Hecla F-62

Depth (m)	Org. Matter Type	% Ro max.		N
30.0	Vitr. *	0.44		12
106.0	"	0.43		15
157.0	"	0.47		18
257.0	"	0.47		9
318.0	"	0.51		12
403.0	"	0.53		4
530.0	"	0.48		6
633.0	"	0.48		13
693.0	"	0.54		16
778.0	"	0.54		6
815.0	"	0.55		5
848.0	"	0.63	0.43 *	2
893.0	"	0.57		7
950.0	"	0.62		10
967.0	"	0.63		7
1000.0	"	0.69		10
1003.0	"	0.63		5
1048.0	"	0.66		7
1071.0	"	0.65		4
1090.0	"	0.67		6
1112.0	"	0.72		8

* denotes suppressed value

* Vitr. - vitrinite

Hecla C-32

Depth (m)	Org. Matter Type	% Ro max.	N
30.0	Vitr. *	0.43	6
190.0	"	0.45	4
204.00	"	0.42	8
307.0	"	0.47	3
315.0	"	0.46	10
437.0	"	0.41	19
490.0	"	0.48	25
510.0	"	0.52	5
560.0	"	0.48	12
657.0	"	0.49	3
807.0	"	0.55	3
893.0	"	0.54	7
950.0	"	0.61	6
959.0	"	0.57	11
990.0	"	0.57	3
1015.0	"	0.58	17
1150.0	"	0.58	8
1200.0	"	0.58	2
1210.0	"	0.63	5

Marie Bay D-02

Depth (m)	Org. Matter Type	% Ro max.	N	Depth (m)	Org. Matter Type	% Ro max.		N	
20.0	Vitr. *	0.62	7	260.0	Bit. *	1.17		5	
30.0	"	0.42	14	303.0	"	0.90	1.48	2	4
42.0	"	0.39	35	337.0	"	1.40		10	
51.0	"	0.45	30	429.0	"	1.05		3	
78.0	"	0.45	25	558.0	"	0.88	1.12	3	4
100.0	"	0.40	10	590.0	"	0.82	1.50	12	9
120.0	"	0.51	14	610.0	"	0.77		50	
150.0	"	0.49	3	894.0	"	2.17		10	
170.0	"	0.55	30	924.0	"	2.24	2.49	15	4
208.0	"	0.46	3	954.0	"	2.52		15	
391.0	"	0.57	3	973.0	"	2.20	2.70	10	11
530.0	"	0.60	8	1003.0	"	2.31	2.59	8	6
558.0	"	0.60	6	1033.0	"	2.35	2.63	2	5
730.0	"	0.60	15	1061.0	"	2.44		43	
767.0	"	0.51	17	1085.0	"	2.37	2.94	6	18
792.0	"	0.55	29	1106.0	"	2.85		2	
830.0		0.58	13	1133.0	"	2.80		9	
				1151.0	"	2.73		4	
				1176.0	"	2.70		3	
				1197.0	"	2.97		35	
				1221.0	"	2.80		30	
				1254.0	"	2.79		20	

* Vitr. - vitrinite
* Bit. - bitumen

Sandy Point L-46

Depth (m)	Org. Matter Type	% Ro max.	N
64.0	Vitr. *	0.51	42
337.0	"	0.47	12
365.0	"	0.46	7
770.0	"	0.51	12
1239.0	"	0.62	24
1261.0	"	0.58	6
1300.0	"	0.49	10
1727.0	"	0.65	4
1870.0	"	0.58	10

Depth (m)	Org. Matter Type	% Ro max.		N	
337.0	Bit. *	1.05	1.21	4	4
394.0	"	1.05	1.23	5	5
424.0	"	1.04		6	
461.0	"	0.94		3	
485.0	"	1.03	1.27	5	8
530.0	"	1.06	1.32	2	2
576.0	"	1.04	1.43	4	3
606.0	"	1.07	1.50	6	3
758.0	"	1.14	1.42	3	4
894.0	"	1.49		14	
939.0	"	1.10		5	
985.0	"	1.19	1.53	5	2
1076.0	"	1.16	1.53	12	6
1121.0	"	1.24	1.55	7	2
1167.0	"	1.22	1.58	2	4
1261.0	"	1.13	1.49	14	4
1300.0	"	1.23	1.62	8	2
1327.0	"	1.13	1.56	1	6
1349.0	"	1.27	1.68	10	16
1455.0	"	1.28	1.65	2	5
1515.0	"	1.17	1.67	12	8
1549.0	"	1.18	1.73	9	15
1606.0	"	1.09	1.58	2	3
1727.0	"	1.27	1.48	9	9
1794.0	"	1.32	1.82	25	6
1810.0	"	2.00			
1870.0	"	1.93		7	
1909.0	"	2.20		9	
1970.0	"	1.93		4	
2015.0	"	1.72		15	
2042.0	"	1.40	1.81	3	7

* Vitr. - vitrinite

* Bit. - bitumen

Grassy I-34

Depth (m)	Org. Matter Type	% Ro max.	N	Depth (m)	Org. Matter Type	% Ro max.	N
472.0	Vitr. *	0.51	7	475.0	Bit. *	0.98	5
475.0	"	0.54	8	490.0	"	1.07	4
485.0	"	0.48	5	893.0	"	1.15	3
490.0	"	0.55	6				
581.0	"	0.49	16				
697.0	"	0.56	8				
727.0	"	0.58	9				
764.0	"	0.60	10				
770.0	"	0.58	5				
790.0	"	0.57	9				
792.0	"	0.68	7				
850.0	"	0.52	10				
878.0	"	0.58	4				
893.0	"	0.60	6				

* Vitr. - vitrinite

* Bit. - bitumen

APPENDIX II

Drake D-68

Depth (m)	Qty	Tmax	S1	S2	S3	PI	S2/S3	TOC	HI	OI	FORMATION/MEMBER
162	50.2	437	.01	.05	2.29	.17	.02	1.07	04	214	Christopher
270	51.4	434	.01	.25	2.17	.04	.11	1.25	20	173	Christopher
442	50.6	431	.09	4.38	4.58	.02	.95	8.73	50	52	Isachsen
544	50.5	433	.03	2.07	2.07	.02	1.00	2.92	49	70	Deer Bay
939	49.7	431	.08	1.12	1.12	.04	1.00	3.43	51	32	Ringnes
1043	50.8	432	.01	.41	.41	.03	1.00	.51	60	80	Jameson Bay
1090	51.3	428	.01	.31	.31	.02	1.00	.59	71	52	Jameson Bay
1289	51.9	432	.07	1.69	.42	.04	2.92	1.31	129	32	Cape Richards
1319	53.0	433	.16	5.35	.35	.03	15.28	1.25	428	28	Eden Bay
1331	51.2	428	.93	27.81	.76	.03	36.59	4.26	652	17	Eden Bay
1346	51.4	431	1.01	30.03	1.01	.03	29.73	4.57	647	22	Eden Bay
1396	50.2	433	.85	21.03	1.29	.04	16.30	3.76	559	34	Cape Caledonia
1547	50.8	432	.01	.23	.62	.04	.37	.39	58	158	Bjorne
3269	51.3	447	.23	.35	.25	.40	1.4	.55	63	45	Trold Fiord
3471	50.7	451	.61	.21	.33	.21	.63	.61	54	34	Van Hauen
3831	52.8	453	.41	.56	.22	.43	2.54	.84	66	26	Van Hauen
3973	50.1	458	.13	.23	.21	.36	1.09	.25	27	24	Van Hauen
4114	52.0	458	.42	.48	.19	.47	2.52	1.03	46	18	Van Hauen
4272	49.7	454	.20	.18	.18	.53	1.0	1.04	17	17	Van Hauen

Drake D-68 (continued)

Depth (m)	Qty	Tmax	S1	S2	S3	PI	S2/S3	TOC	HI	OI	FORMATION/MEMBER
4523	53.7	459	.13	.33	.18	.28	1.83	.76	43	23	Van Hauen
5034	50.6	389	.07	.28	.51	.34	.55	.83	18	11	Van Hauen

Chads Creek B-64

Depth (m)	Qty	Tmax	S1	S2	S3	PI	S2/S3	TOC	HI	OI	FORMATION/MEMBER
212	50.3	435	.05	1.11	0.83	.04	1.33	3.43	32	24	Christopher
445	51.9	434	.07	1.31	2.85	.05	.46	3.04	43	93	Christopher
660	51.3	400	.05	.05	1.73	.50	.02	2.01	02	86	Isachsen
747	51.6	435	.09	1.10	1.47	.08	.75	2.46	44	59	Deer Bay
929	51.9	432	.07	.26	.55	.22	.47	1.82	14	30	Awingak
1121	51.1	435	.90	11.74	1.01	.07	11.62	8.12	144	12	Ringnes
1206	51.7	433	.07	.50	.25	.12	2.0	.47	106	53	Jameson Bay
1256	101.1	431	.10	.64	.29	.14	2.20	.46	139	63	Jameson Bay
1279	49.5	434	.08	.70	.00	.10	-	.49	142	00	Jameson Bay
1301	100.1	433	.15	.96	.34	.14	2.82	.57	168	59	Jameson Bay
1367	50.7	435	.07	.35	.27	.17	1.29	.86	40	31	Barrow
1419	50.0	439	.30	4.44	.02	.06	222.00	1.43	310	01	Cape Richards
1436	50.2	432	1.33	36.01	.27	.04	133.40	4.88	453	07	Cape Richards
1439	101.6	431	1.76	32.20	.76	.05	42.36	4.88	659	15	Cape Richards
1486	49.8	435	.82	27.30	.26	.03	105.00	4.27	639	06	Eden Bay
1563	50.1	433	.59	16.28	.41	.03	39.70	2.83	575	14	Eldridge Bay
2068	50.0	432	.14	5.76	.34	.02	16.94	1.69	370	20	Bjorne
2341	50.5	436	.63	18.53	.29	.03	63.27	2.93	632	09	Bjorne
3197	49.4	449	.16	.18	.28	.47	0.64	.34	52	82	Van Hauen
3353	100.8	447	.26	.03	.26	.93	.11	.41	7	63	Van Hauen
3727	49.7	454	.50	.44	.06	.53	7.33	.92	47	06	Van Hauen

Hecla J-60

Depth (m)	Qty	Tmax	S1	S2	S3	PI	S2/S3	TOC	HI	OI	FORMATION/MEMBER
506	6.5	427	6.61	133.84	24.00	.05	5.57	73.94	181	32	Isachsen Coal
551	98.3	435	.19	2.43	4.63	.07	.52	3.10	78	149	Deer Bay
918	100.9	430	.33	3.32	1.38	.09	2.40	4.70	70	29	Ringnes
1063	100.0	427	.05	.58	.33	.08	1.75	.57	101	57	Jameson Bay
1136	100.3	429	1.47	21.37	.73	.06	29.27	3.90	547	18	Eden Bay

Depot Island C-44

Depth (m)	Qty	Tmax	S1	S2	S3	PI	S2/S3	TOC	HI	OI	FORMATION/MEMBER
217	100.7	430	.12	.79	1.50	.13	.52	.86	91	174	Deer Bay
333	100.7	433	.30	2.40	1.60	.11	1.50	3.55	67	45	Ringnes
415	101.9	424	.22	2.79	2.53	.07	1.10	5.69	49	44	Hiccles Cove
609	99.0	424	.09	.71	.40	.11	1.77	.66	107	60	Jameson Bay
628	99.1	412	.17	.10	.23	.65	.43	.35	28	65	Jameson Bay Core
688	99.3	429	.47	3.34	1.32	.12	2.53	3.56	93	37	Eden Bay
2450	99.5	423	.03	.03	.03	.50	1.00	.05	60	60	Ibbett Bay Core
2554	100.0	393	.51	.06	.22	.91	.27	3.20	01	06	Ibbett Bay
2651	100.3	360	.02	.27	.34	.07	.79	.42	64	80	Ibbett Bay Core

Roche Point J-43

Depth (m)	Qty	Tmax	S1	S2	S3	PI	S2/S3	TOC	HI	OI	FORMATION/MEMBER
457	99.4	404	1.88	19.03	2.75	.09	6.92	7.47	254	36	Christopher
1915	100.3	434	.69	15.75	1.23	.04	12.80	8.81	178	13	Ringnes
1945	100.5	437	.33	4.90	1.57	.06	3.12	4.13	118	38	McConnell
2094	99.1	436	.07	.66	.94	.10	.70	.63	104	149	Jameson Bay
2227	99.1	437	.11	.95	.54	.10	1.75	.57	166	94	Jameson Bay
2424	100.6	442	.03	.27	.64	.10	.42	.58	46	110	Barrow
2551	101.5	441	.32	2.14	.41	.13	5.21	.94	227	43	Cape Richards
2667	100.6	443	2.08	13.16	.90	.14	14.62	3.15	417	28	Eden Bay
2697	101.6	443	4.33	19.40	1.05	.18	18.47	5.26	368	19	Eden Bay
2815	99.3	442	.53	1.91	.70	.22	2.72	1.25	152	56	Cape Caledonia

North Sabine H-49

Depth (m)	Qty	Tmax	S1	S2	S3	PI	S2/S3	TOC	HI	OI	FORMATION/MEMBER
21	51.2	425	.11	.00	.60	-	-	1.33	00	45	Eureka Sound
372	50.4	425	.01	.59	.75	.02	.78	1.94	30	38	Kanguk
557	51.2	424	.07	.94	1.19	.07	.79	3.82	24	31	Kanguk
643	51.9	425	.09	1.07	1.30	.08	.82	3.85	27	33	Kanguk
995	50.1	432	.01	.33	1.21	.03	.27	1.66	19	72	Christopher
1286	50.0	435	.04	.72	.62	.05	1.16	2.39	30	25	Christopher
1399	51.5	438	.09	1.08	.33	.08	3.27	3.02	35	10	Christopher
1612	49.9	437	.18	1.16	.66	.13	1.75	2.78	41	23	Christopher
1773	50.9	440	.27	1.47	1.37	.16	.01	2.78	52	49	Christopher
2007	51.1	438	.21	2.32	1.03	.08	2.25	2.70	85	32	Isachsen
2099	51.2	439	.17	1.71	1.07	.09	1.60	3.07	55	34	Deer Bay
2190	50.8	439	.25	1.88	1.14	.12	1.65	2.34	80	48	Deer Bay
2292	51.2	442	.17	1.58	.91	.10	1.73	2.17	72	41	Deer Bay
2474	51.3	445	.19	3.64	.33	.05	11.03	3.25	112	10	Awingak
2611	51.7	440	.73	14.46	.42	.05	34.42	6.45	224	06	Ringnes
2678	50.6	444	.17	2.31	.17	.07	13.59	1.95	118	02	McConnell
2782	51.7	440	.05	.52	.05	.09	10.40	.53	98	09	Jameson Bay
2847	51.7	445	.09	.98	.01	.08	98.0	.29	112	01	Jameson Bay
2983	51.8	445	.11	1.19	.00	.08	-	.62	191	00	Jameson Bay
3059	51.8	443	.09	.96	.00	.09	-	.66	145	00	Maclean Strait

North Sabine H-49 (continued)

Depth (m)	Qty	Tmax	S1	S2	S3	PI	S2/S3	TOC	HI	OI	FORMATION/MEMBER
3129	51.0	444	.11	.64	.00	.15	-	.45	142	00	Barrow
3175	51.1	443	.13	.99	.00	.12	-	.65	152	00	Barrow
3288	50.2	445	.29	1.45	.01	.17	145.0	.89	162	01	Cape Richards
3349	50.2	447	.17	.85	.00	.17	-	.67	126	00	Cape Richards
3452	49.8	448	1.96	9.15	.32	.18	28.59	3.78	242	08	Eden Bay
3476	49.9	448	1.96	8.53	.46	.19	18.54	3.94	216	11	Eden Bay
3650	49.8	452	.02	.02	.08	.50	-	.30	06	00	Murray Harbour

Sherard F-34

Depth (m)	Qty	Tmax	S1	S2	S3	PI	S2/S3	TOC	HI	OI	FORMATION/MEMBER
98	100.6	430	.06	.33	2.30	.16	.14	1.82	18	126	Christopher
248	102.0	428	.06	.65	1.56	.09	.41	3.47	18	44	Christopher
500	98.1	432	.25	2.73	13.21	.08	.20	4.33	63	305	Christopher
623	98.0	439	.10	2.09	9.30	.05	.22	4.04	51	230	Christopher
749	102.0	432	.28	3.24	8.07	.08	.40	3.20	101	252	Isachsen
759	6.5	434	.76	32.00	28.92	.02	1.10	68.25	46	42	Isachsen Coal
980	6.1	424	2.45	54.09	28.52	.04	1.89	70.22	77	40	Awingak Coal
1070	101.5	426	.10	1.93	1.69	.05	1.14	4.81	40	35	Ringnes
1176	101.6	430	.17	1.13	.55	.13	2.05	.82	137	67	Jameson Bay
1248	101.1	423	.63	21.32	1.06	.03	20.11	3.85	553	27	Cape Richards
1292	100.5	424	.88	21.17	.96	.04	22.05	3.86	548	24	Eden Bay
1299	100.1	423	.88	21.49	.97	.04	22.15	3.94	545	24	Eden Bay
1308	100.5	425	.63	17.99	.97	.03	18.54	3.28	548	29	Eden Bay
2630	100.8	417	.34	.28	.55	.55	.50	.28	100	196	Blind Fiord
2674	101.9	426	.04	.07	.39	.40	.17	.32	21	121	Trold Fiord Core
2768	101.1	430	.05	.07	.50	.42	.14	.23	30	217	Trold Fiord
2989	100.4	434	.06	.15	.97	.30	.15	.55	27	176	Van Hauen
3224	101.0	435	.33	1.26	.49	.21	2.57	1.29	97	37	Van Hauen
3450	101.8	442	.11	.72	.37	.13	1.94	1.04	69	35	Van Hauen
3458	101.1	439	.14	.60	.61	.19	.98	1.10	54	55	Van Hauen

Sherard F-34 (continued)

Depth (m)	Qty	Tmax	S1	S2	S3	PI	S2/S3	TOC	HI	OI	FORMATION/MEMBER
3485	101.4	439	.28	.41	.89	.41	.46	1.03	39	86	Van Hauen
3548	101.5	440	.52	.10	.37	.84	.27	.96	13	48	Van Hauen
3599	101.6	460	.28	.38	1.00	.42	.38	1.11	34	90	Van Hauen
3674	100.2	444	.33	.62	.59	.35	1.05	1.23	50	47	Van Hauen
3845	99.2	438	.08	.18	.58	.31	.31	.46	39	126	Belcher Channel
4184	100.4	445	.10	.19	.39	.38	.43	.61	27	63	Canyon Fiord
4617	99.7	461	.00	.02	.07	.00	.28	.41	04	17	Canyon Fiord Core
4883	101.9	451	.05	.17	.58	.23	.29	.59	28	98	Canyon Fiord
5209	98.0	454	.08	.22	.25	.27	.88	1.03	21	24	Canyon Fiord Core

Sherard F- 14

Depth (m)	Qty	Tmax	S1	S2	S3	PI	S2/S3	TOC	HI	OI	FORMATION/MEMBER
45	99.5	433	.19	.71	4.02	.21	.17	2.14	33	187	Christopher
727	99.2	439	.18	3.96	6.37	.04	.62	3.43	115	185	Isachsen
773	100.5	437	.21	3.70	5.17	.05	.71	4.09	90	126	Awingak
894	99.6	436	.55	3.90	8.91	.12	.43	3.24	120	275	Awingak
1051	98.6	431	.46	4.98	3.56	.08	1.39	5.99	83	59	Ringnes
1160	102.1	426	.13	2.70	.39	.05	6.92	1.17	230	33	Jameson Bay Core
1182	101.5	436	.04	.22	.59	.15	.37	.45	48	131	Grosvenor Island Core
1209	100.2	428	.42	15.32	1.35	.03	11.34	3.23	474	41	Cape Richards
1270	100.6	430	.89	18.64	1.55	.05	12.02	3.88	480	39	Eden Bay

Collingwood K-33

Depth (m)	Qty	Tmax	S1	S2	S3	PI	S2/S3	TOC	HI	OI	FORMATION/MEMBER
1348	101.4	428	1.12	17.19	1.51	.06	11.38	6.96	246	21	Ringnes
1348	99.9	424	1.12	16.33	1.38	.06	11.83	6.82	239	20	Ringnes
1536	102.9	431	.11	1.40	.27	.07	5.18	.72	194	37	Jameson Bay
1536	98.8	433	.10	1.40	.18	.07	7.77	.75	186	24	Jameson Bay
1615	100.6	439	.06	.17	.45	.27	.37	.44	38	102	Barrow
1642	102.5	431	.12	.27	1.38	.32	.19	.66	40	209	Barrow
1642	99.0	430	.12	.23	1.10	.35	.20	.65	35	169	Barrow
1851	101.6	432	1.98	34.96	.60	.05	58.26	5.40	700	11	Eden Bay
1891	102.3	430	.43	8.21	.47	.05	17.46	1.62	506	29	Cape Caledonia
1892	98.9	437	.10	1.42	.29	.07	4.89	.57	249	50	Cape Caledonia Core

Drake K-79

Depth (m)	Qty	Tmax	S1	S2	S3	PI	S2/S3	TOC	HI	OI	FORMATION/MEMBER
197	5.4	435	2.40	45.18	21.11	.05	2.14	60.68	74	34	Hassel Coal
333	101.8	427	.33	4.04	2.08	.08	1.98	4.37	92	46	Christopher
582	99.2	435	.40	2.67	6.12	.13	.43	4.65	57	131	Christopher
709	100.9	437	.29	2.71	5.86	.10	.46	4.70	57	124	Isachsen
709	5.9	429	3.72	31.01	20.33	.11	1.52	50.84	60	39	Isachsen Coal
788	98.6	434	.32	2.45	4.21	.12	.58	3.18	77	132	Deer Bay
930	101.2	435	.27	2.08	4.11	.12	.50	3.40	61	120	Awingak
1127	101.5	433	1.07	18.60	3.74	.05	4.97	10.68	174	35	Ringnes
1182	101.6	437	.09	.63	1.00	.12	.63	.43	146	232	Jameson Bay
1285	102.2	427	.08	.53	.34	.13	1.55	.51	103	66	Jameson Bay
1297	101.7	429	.06	.11	.42	.37	.26	.40	27	105	Jameson Bay Core
1418	100.7	429	.11	.15	.56	.42	.26	.37	40	151	Barrow
1476	101.3	436	.53	15.24	.78	.03	19.53	3.00	508	26	Cape Richards
1545	101.2	430	1.53	36.91	.80	.04	46.13	5.70	647	14	Eden Bay
1564	99.6	430	1.13	28.87	.65	.04	44.41	4.23	682	15	Eden Bay
1615	100.3	433	.40	7.41	.51	.05	14.52	1.46	507	34	Cape Caledonia
1615	99.7	436	.28	3.18	.52	.08	6.11	1.13	281	46	Cape Caledonia

Drake L-67

Depth (m)	Qty	Tmax	S1	S2	S3	PI	S2/S3	TOC	HI	OI	FORMATION/MEMBER
945	99.3	433	1.82	5.19	1.68	.26	3.08	5.02	103	33	Ringnes
1012	101.4	432	.75	.65	.62	.54	1.04	.54	120	114	Jameson Bay
1057	101.7	432	.62	.87	.53	.42	1.64	.64	135	82	Jameson Bay
1101	101.9	434	.43	1.22	.25	.26	4.88	.67	182	37	Jameson Bay
1342	101.7	432	2.53	33.90	.96	.07	35.31	5.38	630	17	Eden Bay
1974	101.3	400	.18	.13	.33	.60	.39	.23	56	143	Blind Fiord
2947	101.7	437	.06	.03	.17	.75	.17	.17	17	100	Blind Fiord
3116	101.3	443	.03	.13	.09	.19	1.44	.23	56	39	Blind Fiord Core
3233	101.5	447	.27	.53	.17	.34	3.11	.64	82	26	Van Hauen Core

Drake F-76

Depth (m)	Qty	Tmax	S1	S2	S3	PI	S2/S3	TOC	HI	OI	FORMATION/MEMBER
164	99.7	435	.13	.78	4.25	.14	.18	2.71	28	156	Christopher
300	101.0	433	.17	1.24	7.92	.12	.15	2.41	51	328	Christopher
394	101.3	438	.13	1.45	7.50	.08	.19	3.29	44	227	Christopher
536	100.6	435	.30	3.17	7.23	.09	.43	3.29	96	219	Isachsen
870	100.8	431	.18	2.51	1.52	.07	1.65	4.22	59	36	Ringnes
930	99.3	434	.15	.47	.69	.24	.68	.42	111	164	Jameson Bay
1015	100.8	431	.11	.62	.41	.15	1.51	.53	116	77	Jameson Bay
1018	98.8	424	.14	1.92	.40	.07	4.80	.200	93	19	Jameson Bay Core

Drake E-78

Depth (m)	Qty	Tmax	S1	S2	S3	PI	S2/S3	TOC	HI	OI	FORMATION/MEMBER
33	99.3	420	.45	1.52	2.03	.23	.74	3.20	47	63	Christopher
151	100.3	430	.33	1.64	2.91	.17	.56	3.62	45	80	Christopher
470	101.6	433	.29	1.87	6.37	.13	.29	3.22	58	197	Christopher
545	100.0	438	.33	3.31	10.32	.09	.32	3.98	83	259	Christopher
682	100.0	441	.41	5.00	5.28	.08	.94	3.50	142	150	Isachsen
721	5.8	427	9.48	101.03	25.51	.09	3.96	74.70	135	34	Isachsen Coal
733	101.9	432	1.77	7.14	4.31	.20	1.65	4.25	168	101	Deer Bay
833	102.8	432	.93	4.78	5.13	.16	.93	3.58	133	143	Awingak
1006	100.9	435	.44	3.99	4.51	.10	.87	3.43	114	131	Ringnes
1121	100.8	432	.46	1.65	1.54	.22	1.07	.82	201	187	Jameson Bay
1167	102.1	432	.37	1.58	.47	.19	3.36	.63	250	74	Jameson Bay
1236	101.6	429	.05	.14	.77	.28	.18	.35	40	220	Grosvenor Island Core
1272	101.9	434	1.32	5.42	4.43	.20	1.22	3.48	155	127	Barrow
1303	99.4	433	1.36	5.49	4.14	.20	1.32	3.56	154	116	Barrow

Drake B-44

Depth (m)	Qty	Tmax	S1	S2	S3	PI	S2/S3	TOC	HI	OI	FORMATION/MEMBER
30	101.5	437	.12	.43	3.27	.22	.13	2.04	21	160	Christopher
167	100.0	435	.10	.59	1.78	.15	.33	2.65	22	67	Christopher
457	101.5	434	.22	1.99	6.77	.120	.29	3.39	58	199	Christopher
621	101.4	429	1.41	3.16	6.70	.31	.47	3.29	81	172	Isachsen
772	100.2	434	1.47	4.92	4.23	.23	1.16	3.39	145	124	Awingak
821	102.2	434	.76	4.26	4.14	.15	1.02	3.38	126	122	Awingak
903	100.6	430	.78	3.95	4.53	.17	.87	3.33	118	136	Ringnes
951	101.8	430	1.69	5.13	4.71	.25	1.08	3.94	130	119	Ringnes
1015	100.0	430	.12	.54	.93	.18	.58	.44	122	211	Jameson Bay
1061	101.3	426	.12	.64	.44	.16	1.45	.63	101	69	Jameson Bay
1151	101.4	434	.08	.37	3.11	.18	.11	.94	39	330	Barrow
1182	101.7	430	.14	1.56	.45	.08	3.46	.90	173	50	Cape Richards
1291	101.7	432	.83	23.75	1.04	.03	22.83	4.67	508	22	Eden Bay
1333	101.6	433	.36	.46	.58	.04	14.58	1.83	462	31	Cape Caledonia

Drake D-73

Depth (m)	Qty	Tmax	S1	S2	S3	PI	S2/S3	TOC	HI	OI	FORMATION/MEMBER
151	98.9	431	.16	.99	5.74	.14	.17	2.29	43	250	Christopher
303	100.3	432	.07	1.98	2.83	.03	.69	4.15	47	68	Christopher
454	101.5	440	.24	2.43	9.30	.09	.26	3.94	61	236	Christopher
673	101.9	435	.33	2.83	9.34	.10	.30	4.06	69	230	Isachsen
727	100.2	434	.20	4.73	3.75	.04	1.26	3.28	144	114	Isachsen
776	100.3	439	.15	2.85	5.66	.05	.50	3.13	91	180	Deer Bay
870	100.3	434	.12	3.16	4.90	.04	.64	3.20	98	153	Awingak
1042	98.6	435	.25	3.66	6.08	.06	.60	3.28	111	185	Ringnes
1061	102.0	431	.41	4.55	2.07	.08	2.19	5.31	85	38	Ringnes
1182	102.3	430	.08	.57	.34	.12	1.67	.51	111	66	Jameson Bay
1197	100.8	427	.07	.72	.33	.09	2.18	.54	133	61	Jameson Bay
1229	102.4	437	.04	.14	.77	.22	.18	.30	46	256	Grosvenor Island Core
1312	99.6	427	.66	9.75	.78	.06	12.50	2.25	433	34	Hoyle Bay

Drake F-16

Depth (m)	Qty	Tmax	S1	S2	S3	PI	S2/S3	TOC	HI	OI	FORMATION/MEMBER
545	99.3	433	.52	4.44	4.67	.10	.95	3.48	127	134	Isachsen
591	101.3	433	.28	2.21	5.92	.11	.37	3.02	73	196	Deer Bay
794	6.1	426	3.11	47.86	33.1	.06	1.44	63.63	75	52	Awingak Coal
918	100.4	434	1.07	5.02	1.39	.18	3.61	4.44	113	31	Ringnes
1015	102.1	432	.26	.77	1.21	.25	.63	.55	140	220	Jameson Bay
1045	101.1	430	.15	.70	1.26	.18	.55	.50	140	252	Jameson Bay
1064	101.1	429	.13	.54	.24	.20	2.25	.61	88	39	Jameson Bay Core
1143	99.8	435	.09	.08	.69	.56	.11	.38	21	181	Barrow Core
1209	101.2	431	.42	6.16	.40	.06	15.40	1.57	392	25	Cape Richards
1303	100.3	426	1.83	30.70	1.05	.06	29.23	4.93	622	21	Eden Bay
1400	100.3	431	.35	8.31	.57	.04	14.57	1.98	419	28	Eldridge Bay

Drake P-40

Depth (m)	Qty	Tmax	S1	S2	S3	PI	S2/S3	TOC	HI	OI	FORMATION/MEMBER
961	100.8	428	.11	.43	1.76	.20	.24	1.43	30	123	Maclean Strait Core
1148	101.6	422	1.69	38.11	1.49	.04	25.57	6.26	642	23	Eden Bay
1157	100.6	423	1.36	35.30	1.33	.04	26.54	5.74	623	23	Eden Bay

Drake I-55

Depth (m)	Qty	Tmax	S1	S2	S3	PI	S2/S3	TOC	HI	OI	FORMATION/MEMBER
409	102.1	433	.34	2.83	9.63	.11	.29	3.05	92	315	Christopher
506	99.2	441	.57	3.15	12.74	.15	.24	3.77	83	337	Christopher
745	101.6	435	.48	4.03	8.89	.11	.45	4.11	98	216	Awingak
924	102.4	431	.72	5.93	3.47	.11	1.70	6.78	87	51	Ringnes
939	101.2	429	.79	5.94	3.12	.12	1.90	6.66	89	46	Ringnes
1000	100.1	424	.09	.50	.67	.16	.74	.44	113	152	Jameson Bay
1030	99.2	429	.29	1.10	.84	.21	1.30	.71	154	118	Jameson Bay
1072	101.1	431	.21	1.10	.32	.16	3.43	.64	171	50	Jameson Bay
1121	99.8	428	.36	1.39	.78	.21	1.78	.62	224	125	Barrow
1170	100.8	434	.25	3.26	.44	.07	7.40	1.17	278	37	Hoyle Bay

Hecla C-58

Depth (m)	Qty	Tmax	S1	S2	S3	PI	S2/S3	TOC	HI	OI	FORMATION/MEMBER
839	99.7	419	21.74	20.82	1.14	.51	18.26	7.29	285	15	Ringnes
876	99.6	432	.54	4.07	1.18	.12	3.44	3.86	105	30	McConnell
957	101.4	433	.08	.72	.59	.10	1.22	.56	128	105	Jameson Bay
1006	102.3	431	.10	.65	.45	.14	1.44	.52	125	86	Jameson Bay
1018	101.7	428	.11	.21	.14	.34	1.50	.51	41	29	Jameson Bay Core
1091	101.6	432	.50	16.43	.86	.03	19.10	3.52	466	24	Cape Richards
1121	101.5	428	.84	24.31	.97	.03	25.06	4.15	585	23	Eden Bay
1139	99.6	431	.85	22.81	.68	.04	33.54	4.00	570	17	Eden Bay

Hecla P-62

Depth (m)	Qty	Tmax	S1	S2	S3	PI	S2/S3	TOC	HI	OI	FORMATION/MEMBER
515	99.0	436	.59	3.76	4.40	.14	.85	3.75	100	117	Awingak
664	102.5	434	.59	5.74	1.99	.09	2.88	5.75	99	34	Ringnes
727	98.7	431	.24	1.16	1.13	.17	1.02	.57	203	198	Jameson Bay
773	97.9	432	.13	1.17	.59	.10	1.98	.57	205	103	Jameson Bay
815	102.2	436	.07	1.18	.59	.06	2.00	.62	190	95	Jameson Bay
830	99.3	433	.14	.97	.46	.13	2.10	.54	179	85	Jameson Bay
948	99.4	426	2.88	68.73	2.59	.04	26.53	12.06	759	23	Cape Richards
985	100.9	428	1.51	30.44	1.11	.05	27.42	5.09	651	21	Eden Bay
1003	99.0	429	1.18	26.82	1.02	.04	26.29	4.83	604	23	Eden Bay
1018	102.4	431	1.26	22.89	.97	.05	23.59	4.13	605	31	Cape Caledonia

Hecla M-25

Depth (m)	Qty	Tmax	S1	S2	S3	PI	S2/S3	TOC	HI	OI	FORMATION/MEMBER
939	98.1	436	.45	1.63	.82	.22	1.98	.67	243	122	Jameson Bay
978	101.4	432	.09	.72	.28	.11	2.57	.56	128	50	Jameson Bay Core
1176	99.4	433	2.93	58.91	1.32	.05	44.62	8.90	775	14	Cape Richards

Hecla N-52

Depth (m)	Qty	Tmax	S1	S2	S3	PI	S2/S3	TOC	HI	OI	FORMATION/MEMBER
324	100.6	437	.24	2.26	3.37	.10	.67	2.19	103	153	Deer Bay
506	98.3	436	.67	3.70	3.05	.15	1.12	3.55	104	85	Awingak
664	99.3	434	.82	6.80	1.75	.11	3.88	5.79	117	30	Ringnes
736	102.3	433	.27	1.04	1.11	.21	.93	.69	150	160	Jameson Bay
797	101.0	430	.16	.98	.48	.14	2.04	.62	158	77	Jameson Bay
827	100.6	436	.05	.11	.51	.31	.21	.30	36	170	Maclean Strait Core
924	101.0	433	3.54	102.46	2.01	.03	50.97	13.49	759	14	Cape Richards

Hecla C-05

Depth (m)	Qty	Tmax	S1	S2	S3	PI	S2/S3	TOC	HI	OI	FORMATION/MEMBER
148	100.9	438	.10	1.91	10.46	.05	.18	3.45	55	303	Christopher
424	99.9	433	.12	3.12	6.40	.04	.48	2.98	104	214	Isachsen
445	5.1	433	3.52	106.47	30.19	.03	3.52	60.71	175	49	Isachsen Coal
621	102.0	435	.29	2.77	5.49	.09	.50	2.23	124	246	Awingak
760	100.3	430	.54	10.96	3.07	.05	3.57	5.99	182	51	Awingak
891	99.6	433	1.33	11.14	4.69	.11	2.37	8.17	136	57	Ringnes
954	101.0	433	.07	.53	.63	.12	.84	.44	120	143	Jameson Bay
1015	103.1	436	.22	.82	.59	.21	1.38	.56	146	105	Jameson Bay
1057	102.4	433	.07	.92	.58	.07	1.58	.60	153	96	Jameson Bay
1102	100.6	438	.06	.09	.50	.43	.18	.36	25	138	Grosvenor Island Core
1148	102.2	434	.13	1.32	1.08	.09	1.22	1.11	118	97	Barrow
1203	102.2	430	.88	23.28	.86	.04	27.06	3.90	596	22	Cape Richards
1212	100.1	433	2.50	67.37	1.71	.04	39.39	9.96	676	17	Cape Richards

Hecla I-69

Depth (m)	Qty	Tmax	S1	S2	S3	PI	S2/S3	TOC	HI	OI	FORMATION/MEMBER
46	101.2	433	.11	1.02	2.37	.10	.43	3.47	29	68	Christopher
485	99.6	434	.65	5.15	4.41	.11	1.16	4.15	124	106	Isachsen
1364	99.0	428	2.12	26.30	1.29	.07	20.38	5.02	523	25	Eden Bay

Hecla F-62

Depth (m)	Qty	Tmax	S1	S2	S3	PI	S2/S3	TOC	HI	OI	FORMATION/MEMBER
324	99.6	437	.33	4.31	5.94	.07	.72	4.98	86	119	Isachsen
406	102.3	436	.18	2.04	2.65	.08	.76	2.19	93	121	Deer Bay
697	101.4	433	1.59	11.02	4.18	.13	2.63	10.84	101	38	Awingak
788	99.6	436	.64	5.31	1.24	.11	4.28	8.75	60	14	Ringnes
818	98.4	435	1.55	7.20	1.72	.18	4.18	4.94	145	34	Jameson Bay
894	100.7	433	.11	1.00	.40	.10	2.50	.54	185	74	Jameson Bay
954	100.0	433	.19	.98	.34	.16	2.88	.57	171	59	Jameson Bay
997	101.8	433	.30	5.18	.46	.05	11.26	1.80	287	25	Barrow
1048	199.2	430	2.73	69.03	1.69	.04	40.84	10.38	746	16	Cape Richards
1079	99.5	427	1.74	53.54	1.03	.03	51.98	7.47	731	13	Eden Bay
1091	101.1	429	1.35	39.32	1.15	.03	34.19	6.41	620	17	Eden Bay
1100	99.3	432	1.26	34.88	.92	.03	32.91	5.36	650	17	Eden Bay

Hecla C-32

Depth (m)	Qty	Tmax	S1	S2	S3	PI	S2/S3	TOC	HI	OI	FORMATION/MEMBER
197	99.9	439	.09	1.25	8.56	.07	.14	2.49	50	343	Christopher
333	101.0	434	.14	1.88	9.98	.07	.18	3.41	55	292	Christopher
424	99.5	431	.16	3.16	4.54	.05	.69	3.27	96	138	Isachsen
515	102.9	435	.43	2.94	3.14	.13	.93	3.14	93	100	Deer Bay
806	100.1	434	.84	6.59	2.87	.11	2.29	7.16	92	40	Awingak
885	101.8	428	.37	5.97	2.02	.06	2.95	6.51	91	31	Ringnes
954	99.4	433	.05	.62	.68	.08	.91	.44	140	154	Jameson Bay
1000	97.6	431	.04	.61	.59	.06	1.03	.52	117	113	Jameson Bay
1036	100.7	430	.10	.80	.24	.11	3.33	.68	117	35	Jameson Bay Core
1160	103.3	435	1.95	87.41	2.04	.02	42.84	12.09	779	16	Cape Richards
1203	101.8	428	1.33	36.93	1.01	.03	35.56	5.71	646	17	Eden Bay
1212	100.8	435	3.58	80.83	2.10	.04	38.49	12.29	657	17	Eden Bay

Marie Bay D-02

Depth (m)	Qty	Tmax	S1	S2	S3	PI	S2/S3	TOC	HI	OI	FORMATION/MEMBER
18	99.8	424	.25	4.12	4.48	.06	.91	6.45	63	69	Ringnes
123	100.0	430	.08	.99	.78	.08	1.26	1.58	62	49	McConnell
921	99.8	469	.85	.08	.37	.92	.21	6.76	01	05	Ibbett Bay
1072	100.1	464	.65	.33	.29	.66	1.13	6.70	04	04	Ibbett Bay
1261	101.4	453	.38	.04	.30	.90	.13	1.29	03	23	Ibbett Bay Core

Sandy Point L-46

Depth (m)	Qty	Tmax	S1	S2	S3	PI	S2/S3	TOC	HI	OI	FORMATION/MEMBER
151	99.8	432	.65	2.54	6.09	.20	.41	2.28	111	267	Deer Bay
367	98.8	433	.59	1.88	3.92	.24	.47	1.86	101	210	Deer Bay
424	100.7	433	.39	2.62	4.60	.13	.56	3.23	81	142	Deer Bay
485	99.9	430	1.22	5.57	2.84	.18	1.96	6.33	87	44	McConnell
593	99.4	431	.13	.45	.22	.22	2.04	.51	88	43	Jameson Bay Core
678	99.4	429	.12	.65	.57	.16	1.14	.58	112	98	Jameson Bay
766	99.7	436	.24	8.86	.57	.03	15.54	2.10	421	27	Schei Point Core
771	102.4	431	.18	1.66	.40	.120	4.15	1.77	93	22	Schei Point Core
772	101.3	431	.15	.19	1.20	.44	.15	1.15	16	104	Schei Point Core
1245	6.9	438	8.69	142.89	4.92	.06	39.04	46.81	305	10	Trold Fiord

Grassy I-34

Depth (m)	Qty	Tmax	S1	S2	S3	PI	S2/S3	TOC	HI	OI	FORMATION/MEMBER
485	102.0	429	.24	2.00	1.54	.11	1.29	3.97	50	38	Ringnes
764	102.4	430	.10	2.19	.26	.04	8.42	1.18	185	22	Jameson Bay Core
785	100.7	432	.08	.09	.23	.50	.39	.37	24	62	Jameson Bay Core
854	101.7	424	.89	46.01	1.84	.02	25.00	8.52	540	21	Cape Richards
888	99.4	425	1.20	43.54	1.89	.03	23.03	7.98	545	23	Eden Bay

Drillhole	*Locality*	*Formation*	*Age*	*Lithology*	*% Ro, max*	*% Ro, min*	*BRO*	*Missing section (m)*
Apollo C-73	Melville Island	Cape Phillips	Silurian to Lower Devonian	Shale	3.90	2.65	1.25	3,800-4,300
Eldridge Bay E-79	Melville Island	Cape Phillips	Silurian	Shale	1.75	1.30	0.45	3,500-4,300
Marie Bay D-02	Melville Island	Ibbett Bay	Ordovician	Shale	3.50	2.75	0.75	5,800-6,600

APPENDIX III

CALCULATION OF ERODED SECTION

Under the login of Mgr. form, core

- Files were created for the input of the Kelly Bushing, subsea [(+) below, (-) above], and reflectance (Ro) values as expressed in percent.

- The % Ro values were then converted to logRo using the program LogRo under codename Linklog.

- The logRo vs. K.B. depth was computed into a plot file and the line of best fit as well as error lines were calculated.

- The specs for the plot were input from a file (specs) which could be altered for each drillhole, input data included the drillhole name and the scales for the x and y axis.

- A listing of the slope and y-intercept values for the line of best fit was given in the file lftout, generated for each plot.

- The logRo vs depth (K.B.) plot was then generated.

- The amount of eroded section can be calculated for each well using the zero maturity line of Ro = 0.20% and the equation $y = mx + b$ where m is the slope and b is the y-intercept (x - depth y - logRo).

- The amount of error can be determined from the plot using log 0.20 and the interception of the error curves.

- From these plots depth to the oil window can be determined using 0.5 - 0.7% Ro depending on the type of organic matter in the source rocks.

BURIAL PROGRAM

This computer program calculates and draws the burial history curves of a stratigraphic section.

One of the most important steps is the establishment of the chronostratigraphy of the drillhole because the burial plot gives the actual depth to any nominated chronostratigraphic boundary at any time in the past (after its deposition) relative to its present datum. The geological record at any particular site may be incomplete because of unconformities and hiatuses. However, such gaps which are caused by erosion, non-deposition and tectonism have been expressed within the graphic time-depth framework. Therefore, when inverting chronostratigraphy into burial, the geological history of any drillhole is continuous and complete with respect to time.

The second important step to establish is the temperature history of the drillhole. This can be achieved by vitrinite reflectance measurements on core and cuttings samples, using the method of Falvey and Deighton (1984).

The relationship between temperature gradient and Ro is:

$$T\ gr = 166 * \frac{\Delta (\log Ro)}{\Delta\ Depth}$$

Occasionally, two gradients had to be used, a shallow one and a deeper one.

The program calculates TTI values, which are then converted into Ro values using a modification of Lopatin's (1971) and Waples's (1980) methods. The observed Ro values are then compared to the calculated ones and if a match is not successful, the process is itterated until satisfactory match is achieved. At this stage the assumption of constant Tgr with depth will have to be either confirmed or reassessed.

The most readily identifiable cause of miss-match between theoretical and observed present day Ro values is variable paleo-heat flow. The assumption of constant paleo-heat flow may sometimes be unjustified and heat flow variations may have dramatic effects on maturation.